

2013

Characterisation, monitoring and dynamic modelling of a two-stage stabilisation pond system supporting reuse and recycling of dairy shed effluent

Julian Fyfe

University of Wollongong

Follow this and additional works at: <https://ro.uow.edu.au/theses>

University of Wollongong

Copyright Warning

You may print or download ONE copy of this document for the purpose of your own research or study. The University does not authorise you to copy, communicate or otherwise make available electronically to any other person any copyright material contained on this site.

You are reminded of the following: This work is copyright. Apart from any use permitted under the Copyright Act 1968, no part of this work may be reproduced by any process, nor may any other exclusive right be exercised, without the permission of the author. Copyright owners are entitled to take legal action against persons who infringe their copyright. A reproduction of material that is protected by copyright may be a copyright infringement. A court may impose penalties and award damages in relation to offences and infringements relating to copyright material.

Higher penalties may apply, and higher damages may be awarded, for offences and infringements involving the conversion of material into digital or electronic form.

Unless otherwise indicated, the views expressed in this thesis are those of the author and do not necessarily represent the views of the University of Wollongong.

Recommended Citation

Fyfe, Julian, Characterisation, monitoring and dynamic modelling of a two-stage stabilisation pond system supporting reuse and recycling of dairy shed effluent, Doctor of Philosophy thesis, School of Civil, Mining and Environmental Engineering, University of Wollongong, 2013. <http://ro.uow.edu.au/theses/4263>

2013

Characterisation, monitoring and dynamic modelling of a two-stage stabilisation pond system supporting reuse and recycling of dairy shed effluent

Julian Fyfe
University of Wollongong

Recommended Citation

Fyfe, Julian, Characterisation, monitoring and dynamic modelling of a two-stage stabilisation pond system supporting reuse and recycling of dairy shed effluent, Doctor of Philosophy thesis, School of Civil, Mining and Environmental Engineering, University of Wollongong, 2013. <http://ro.uow.edu.au/theses/4263>

UNIVERSITY OF WOLLONGONG

COPYRIGHT WARNING

You may print or download ONE copy of this document for the purpose of your own research or study. The University does not authorise you to copy, communicate or otherwise make available electronically to any other person any copyright material contained on this site. You are reminded of the following:

Copyright owners are entitled to take legal action against persons who infringe their copyright. A reproduction of material that is protected by copyright may be a copyright infringement. A court may impose penalties and award damages in relation to offences and infringements relating to copyright material. Higher penalties may apply, and higher damages may be awarded, for offences and infringements involving the conversion of material into digital or electronic form.

**UNIVERSITY OF
WOLLONGONG**



**CHARACTERISATION, MONITORING AND DYNAMIC
MODELLING OF A TWO-STAGE STABILISATION POND
SYSTEM SUPPORTING REUSE AND RECYCLING OF DAIRY
SHED EFFLUENT**

**A thesis submitted in fulfilment of the
requirements for the Award of the degree**

DOCTOR OF PHILOSOPHY

from

UNIVERSITY OF WOLLONGONG

by

JULIAN FYFE (BE HONS I, BA, ME RESEARCH)

SCHOOL OF CIVIL, MINING AND ENVIRONMENTAL ENGINEERING

FACULTY OF ENGINEERING

2013

CERTIFICATION

I, Julian Fyfe, declare that this thesis, submitted in fulfilment of the requirements for the award of Doctor of Philosophy, in the Faculty of Engineering, University of Wollongong, is wholly my own work unless otherwise referenced or acknowledged. The document has not been submitted for qualifications at any other academic institution.

Julian Fyfe

19 January 2014

ABSTRACT

Best practice handling of dairy shed effluent (DSE) in Australia and New Zealand currently uses two-stage stabilisation pond systems, comprising anaerobic and facultative ponds in series. One of the purported benefits of two-pond systems is the ability to contain and reuse the nutrients contained in the manure deposited at the dairy. Estimates of recoverable nutrient loads, however, are typically based upon coarse partitioning factors, and understanding remains limited regarding the complex array of physical, chemical and biological processes occurring in DSE ponds and their effects on nutrient forms and quantities. There is also very little information available on the impacts of placing pond systems within a partially closed effluent recycling loop in which effluent is recycled back to the dairy as flush water or reused via irrigation. This thesis aims to address the shortage of data related to the behaviour and performance of Australian (and New Zealand) DSE pond systems supporting recycling, which are distinct from systems elsewhere for their relatively small manure loads and more dilute influent. It does so through a detailed field-based study of a typical best practice system which treats effluent from a commercial pasture-based dairy farm with a milking herd of 300 cows. The field data are used to establish a foundation for dynamic modelling of these systems, leveraging knowledge from the more developed modelling fields of urban wastewater stabilisation ponds and activated sludge systems.

High resolution water quality monitoring, incorporating real time measurement at various locations in the system and seasonal profiling of the water column of each pond, produced a unique insight into temporal (including diurnal, seasonal and longer term) and spatial variation in the underlying conditions that both inform and respond to the natural treatment processes occurring in DSE ponds. Important observations included spatial uniformity of water quality in the anaerobic pond, biochemical and thermal stratification in the facultative pond, and persistent salt accumulation in both ponds.

A water balance analysis using wastewater flow and storage data and involving calibration and validation of detailed evaporation and seepage models generated high resolution data on the hydrology of pond system. An in-depth analysis of pond hydraulics and hydrodynamics used hydrological, meteorological, sludge accumulation, water quality and in-pond Lagrangian flow data to characterise the hydraulic regime of each pond. Some key insights were the loss of active treatment volume to accumulating sludge (at a rate of $0.0043 \text{ m}^3 \text{ kg}^{-1}$ total solids added or $0.88 \text{ m}^3 \text{ cow}^{-1} \text{ y}^{-1}$), the role of rising biogas bubbles in producing well-mixed conditions in the anaerobic

pond, the low frequency of short-circuiting (5% or less) and the potential presence of a hydraulic dead zone in the anaerobic pond, and the complexity of the hydraulics in the facultative pond despite very slow advective flow.

Data generated through an intensive flow-weighted wastewater sampling program was then used to characterise the influent to and effluents from the pond system and the dominant treatment and nutrient cycling processes in each stage of the system. This enabled effluent variability, biodegradability and constituent fractions and loading, as well as other aspects of pond function to be studied in more detail than had previously been possible, particularly the effects of sludge accumulation and struvite precipitation (related to salt accumulation caused by recycling). A mass balance analysis was also developed to quantify partitioning and removal of wastewater constituents and investigate actual and potential nutrient recovery rates. Contrary to conventional assumptions, nutrient partitioning to the sludge in the anaerobic pond was found to be lower than expected at just 18% for phosphorus (P) and 21% for nitrogen (N), and overall nutrient removal was actually higher in the facultative pond. Low effluent nutrient utilisation rates (47% N and 50% P) and problematic accumulation of potassium (K) helped to identify a new management strategy for pond systems supporting effluent recycling whereby the pond system is used to harvest stormwater to dilute recycled effluent and improve nutrient recovery rates.

The outputs from the monitoring and characterisation work represent a comprehensive set of qualitative and quantitative data unprecedented in Australia and internationally and provided the basis to developing a dynamic biokinetic model of the primary anaerobic pond using the Activated Sludge Anaerobic Digestion model (ASDM) in the BioWin simulation environment. The model was formulated with a simplified yet dynamic hydraulic regime, full hydrological accounting, and a comprehensive suite of process sub-models coupled with state variables to represent detailed fractionations of organic substrate, nutrients and salts. Model calibration achieved reasonable agreement between predicted and observed concentrations for total and filterable chemical oxygen demand (11% and 16% mean absolute percentage error, respectively), total suspended solids (11%), total volatile suspended solids (9%), total N (14%), ammonia N (11%), total P (10%), orthophosphate (12%), calcium (7%), magnesium (7%) and K (7%). It also exhibited sensible responses to the shock induced by desludging and produced predictions of biogas production which were used to estimate greenhouse gas emissions from the pond.

Following a sensitivity analysis, the model was used to run scenario simulations to examine the impacts on pond performance and nutrient recovery of a hydraulic dead zone, high organic loading, regular desludging and properly sealing the pond to prevent seepage losses. These simulations provided valuable insights for improving pond design, construction and management. Key outputs included a new design value for peak organic loading of $0.3 \text{ kg volatile solids m}^{-3} \text{ d}^{-1}$ and evidence to show that the anaerobic pond would be largely unaffected by the presence of a hydraulic dead zone and that nutrient recovery rates from pond desludging are highest when sludge and supernatant are extracted separately. The model has a number of limitations; most notably that it has not been validated on a second data set, relies on theoretical fractionations for some constituents and contains several empiricisms. Nonetheless it represents the first known attempt to apply a dynamic mechanistic modelling framework to DSE ponds and to livestock waste ponds more broadly.

ACKNOWLEDGEMENTS

Having spanned a decade, this thesis work has enlisted help of more than a few exceptional people. Firstly I would like to thank my supervisor Associate Professor Muttucumaru Sivakumar, whose advice, feedback, patience and support have been invaluable. I am also indebted to my original primary supervisor Dr Dharma Hagare who helped to secure the funding to support this PhD, and then, after leaving academia for several intervening years, returned to provide professional, academic and financial support through the final stages of the work.

This research was made possible with the funding support from the NSW Department of Infrastructure, Planning and Natural Resources (DIPNA), the Sydney Catchment Authority (SCA), the Faculty of Engineering at the University of Wollongong, the University of Western Sydney (UWS), the Civionics Research Centre at UWS, and Dairy Australia (DA). I am compelled to single out Guy van Owen, Shane Muldoon from the SCA, and Catherine Phelps from DA who believed in the value of the research enough to arrange the funding from their respective organisations. The SCA also provided significant in-kind support to the research in the form of field equipment, without which much of the monitoring would not have been possible, field assistance (thank you James Ray), meteorological data (through Robert Craig), monitoring advice (Martin Krogh), and liaison with farmers (Shane Muldoon).

The research could not have been as successful as it was without the open, friendly and incredibly accommodating cooperation of the owners and managers of the Sugarloaf Holsteins dairy farm. To Greg, Trish and Jason Maloney I am deeply indebted for the free access you granted me to your farm and the generosity you showed in not only allowing, but facilitating the monitoring activities that on occasion even caused disruption to farm operations. I must also acknowledge the same cooperation offered by other dairy farmers in the region who supported preliminary work for this thesis including Noel and Brad Snowden, Joe Chittick, Kelvin Menzies and Brian McEvilly.

The field and laboratory work for the thesis was conducted with assistance from a cast of many dedicated and willing University technical staff. Joanne George and Norm Gal, former lab technicians at the Faculty of Engineering Environmental Engineering Laboratories, provided help with acquiring lab equipment and consumables, developing lab methods, fabricating field equipment and undertaking field work in sometimes very unforgiving conditions. They also provided critical moral support and friendship when it

was needed most. Other brave technical staff who joined me on my trips to the farm site included Wendy Halford, Bob Rowland, Jason Knust and Rhys Sartori. I also received invaluable help with fabricating and repairing equipment from Keith Maywald and Stuart Rodd, and guidance with laboratory work from David Wexler, Nick Mackie and Greg Tillman. More general support and advice was generously provided by Ian Laird, Alan Grant, Ron Marshall and Ian Bridge.

This work was also ably supported by several honours and masters thesis students who agreed to rise with the birds to then put in many long hours in the field and the lab. To Marcia Dawson, Tie Ling, Asri Djatnika, Jane Smalley, Michael Douglas and Alex Jenkins, hopefully your successful thesis submissions were sufficient payoff for the contributions I asked of you all.

Research simply would not happen without computers and IT support. Big thanks go to Peter Turner, Leonie McIntyre and Des Jamieson for their always friendly, accommodating and effective assistance. I extend the same gratitude to Pam Burnham and Stacey Young for their help with managing expenses and the research accounts associated with the research. Academic and administrative support came from Associate Professor Long Nghiem and from Professor Brian Uy. Research, technical and theoretical help and advice was provided at by Dr Buyung Kosasih, Dr Alexandra Golab, Dr Phil Flentje, Dr Daniel Palamara and Dr Stuart Kahn.

Significant contributions to the research also came from outside the University of Wollongong and the funding bodies. The team at Greenspan Technology including Steve Bird, Clem, Marc Schmidt, Wayne Farrell, Peter Johnston, and Robert Briggs supplied an excellent customised monitoring system and displayed great generosity in responding to my requests for help to keep the system producing reliable data under challenging circumstances. Graham Lancaster and the team at EAL laboratories (Southern Cross University) did a fantastic job of analysing difficult wastewater and sludge samples and were very flexible with sample delivery and handling. Mark Fairlamb and his colleagues at EnviroSim Associates Ltd. were exceptionally responsive to my queries about the finer details of modelling using BioWin. Invaluable dairy-oriented technical advice and feedback was provided by Scott Birchall in his capacity as regional coordinator for Dairying for Tomorrow. My colleagues Peter Rickwood and Steve Mohr at the Institute for Sustainable Futures (ISF) provided scripts for processing some of my data in a way that I could not have done myself.

I must also acknowledge the unquestioning support given to me by ISF, my employer of the past six or so years that has graciously allowed me to work part time and take extended periods of leave to work on the thesis. In particular I am indebted to my supervisors Andrea Turner, Dr Damien Giurco and Dr Roel Plant, the manager Dr Carroll Graham and the director Professor Stuart White.

I extend my love and gratitude to members of my family who have been directly involved as well as giving ongoing support and. To my mother Crissy Fyfe, thank you for applying your hawk-like editing prowess to my thesis write-up. Thank you to my to-be mother-in-law Julie Fraser for her hard work in reviewing and extracting abbreviations and symbols from the thesis text. Thanks to my brother Jesse for helping install the first piece of monitoring equipment at the farm site, to my brother Lyndon for his printing and desktop publishing help and to my father Iain for his encouragement and motivational chats.

Lastly, and most importantly, thank you to my gorgeous children Araluen and Djarwyn Fraser who have had to put up with a father with a mildly unhealthy preoccupation with a thesis. And thank you, oh thank you, to my beloved partner Raen Fraser who has not only had to deal with editing and refining text, random lab and field tasks and all other manner of thesis-related requests from me, but has taken on the family responsibilities that I have had to shed in order to complete the thesis, as well as counselled me through the tougher times of the thesis experience. You have had to bear the same emotional burden I have for all these years; one that is like a feather ever-present on your shoulder, but at times weighs a thousand tonnes. This PhD is as much yours as it is mine, if not in name, in commitment and self-sacrifice.

LIST OF PUBLICATIONS

- Fyfe, J and Birchall, S 2013 (in press), 'Effluent recycling', in *Effluent and Manure Management Database for the Australian Dairy Industry*, Dairy Australia.
- Fyfe, J and Birchall, S 2013 (in press), 'Treatment and Storage Ponds', in *Effluent and Manure Management Database for the Australian Dairy Industry*, Dairy Australia.
- Fyfe, J, Hagare, D & Sivakumar, M 2013, Development of a dynamic model for sustainable management of dairy shed effluent using two-stage stabilisation pond system with effluent recycling, report prepared for Dairy Australia, University of Western Sydney, Kingswood, NSW.
- Fyfe, J & Sivakumar, M 2008, Performance and Water Quality Benefits of Dairy Shed Waste BMP in the Sydney Catchment, report prepared for the Sydney Catchment Authority, University of Wollongong, Wollongong.
- Fyfe, J, Sivakumar, M, Hagare, D & Jenkins, A 2007, 'Dynamic variation of supernatant quality in a dairy shed waste stabilisation pond system'. *Water Science and Technology*, vol.55, no.11, pp245–255.
- Fyfe, J, Smalley, J, Hagare, D & Sivakumar, M 2007, 'Physical and hydrodynamic characteristics of a dairy shed waste stabilisation pond system'. *Water Science and Technology*, vol.55, no.11, pp11–20.
- Fyfe, J & Hagare, D 2004, 'Dairy Shed Waste Management – A Critical Review of Best Management Practice in Australia', in *Environmental Change: Make it Happen*, Environmental Engineering Research Event, 6-9 December, Wollongong, pp230–240.

TABLE OF CONTENTS

CERTIFICATION	i
ABSTRACT	iii
ACKNOWLEDGEMENTS	vii
LIST OF PUBLICATIONS	xi
TABLE OF CONTENTS.....	xiii
LIST OF FIGURES	xxi
LIST OF TABLES	xxix
LIST OF PLATES	xxxv
NOTATION	xxxvii
Chapter 1.....	1
INTRODUCTION	1
1.1 THE AUSTRALIAN DAIRY INDUSTRY	1
1.1.1 Water Consumption	3
1.1.2 Fertiliser Use	3
1.2 DAIRY SHED EFFLUENT	4
1.2.1 DSE Management	5
1.3 RESEARCH GAPS.....	7
1.3.1 Treatment and Nutrient Partitioning and Losses in DSE ponds.....	7
1.3.2 Effluent Recycling.....	8
1.4 IMPLICATIONS	9
1.5 RESEARCH AIMS AND OBJECTIVES.....	10
1.6 RESEARCH SCOPE	12
1.7 THESIS OUTLINE	15
Chapter 2.....	17
LITERATURE REVIEW	17
2.1 EFFLUENT FROM AUSTRALIAN DAIRY FARMS - DSE	17
2.1.1 Dairy Water Usage and Effluent Flows	18
2.1.2 Raw DSE Characteristics.....	21

2.2	TREATMENT AND RECYCLING OF DSE.....	29
2.2.1	Solids Separation in Trafficable Solids Traps.....	31
2.2.2	Primary Anaerobic Ponds	34
2.2.3	Secondary Facultative Ponds	44
2.2.4	Insights from Investigations Into Other Modes of Treatment	50
2.2.5	Effluent Recycling.....	52
2.3	MODELLING DSE SYSTEMS	57
2.3.1	Modelling Effluent Generation.....	59
2.3.2	Modelling of Other Forms of DSE Treatment	60
2.4	MODELLING OF STABILISATION PONDS.....	62
2.4.1	First Order Reactor Theory Models.....	63
2.4.2	Biokinetic Models.....	65
2.4.3	Adaptations of Activated Sludge Models	71
2.4.4	Integrating Fluid Dynamics, Dispersion and Biokinetic Models.....	75
2.4.5	Thermal models.....	78
2.5	SUMMARY	79
2.5.1	Research gaps.....	81
Chapter 3	83
SITE SELECTION AND CHARACTERISATION	83
3.1	SELECTION PROCESS	83
3.2	FARM DESCRIPTION	84
3.2.1	Soil and Geology	85
3.2.2	Climate	85
3.2.3	Operations	87
3.3	WASTE MANAGEMENT SYSTEM	89
3.3.1	Dairy Shed Cleaning.....	90
3.3.2	Wastewater Treatment.....	92
3.3.3	Effluent Recycling and Reuse	94
3.4	MAPPING THE SITE AND THE SYSTEM	95

3.4.1	Topographical Surveys	95
3.4.2	Holding Yard, Solids Trap and Solids Storage Dimensions.....	96
3.4.3	Pond Mapping and Bathymetry.....	96
3.5	SYSTEM CONDITION, OPERATION AND MAINTENANCE	100
3.6	MONITORING AND SAMPLING REGIME	102
3.7	SUMMARY	105
Chapter 4.....		107
POND WATER QUALITY DYNAMICS.....		107
4.1	INTRODUCTION	107
4.2	MATERIALS AND METHODS	109
4.2.1	Real Time Monitoring.....	109
4.2.2	Supernatant Profiling	114
4.3	RESULTS.....	115
4.3.1	Anaerobic Pond	116
4.3.2	Facultative Pond.....	131
4.3.3	Dairy Water Supply.....	151
4.4	DISCUSSION	151
4.4.1	Temperature Dynamics	151
4.4.2	Thermal Stratification.....	153
4.4.3	pH as an Indicator of Biological Activity	153
4.4.4	Salt Accumulation and Struvite Precipitation.....	154
4.4.5	Dissolved Oxygen and Aerobic Treatment in the Facultative Pond	158
4.5	SUMMARY	159
Chapter 5.....		163
SYSTEM WATER BALANCE.....		163
5.1	INTRODUCTION	163
5.2	MATERIALS AND METHODS FOR MEASURED COMPONENTS.....	167
5.2.1	Anaerobic Pond Inflows and Outflows	167
5.2.2	Facultative Pond Outflows	170

5.2.3	Pond Liquid Volumes	171
5.2.4	Rainfall	171
5.3	ESTIMATION METHODS FOR UNMEASURED COMPONENTS	171
5.3.1	Effluent Irrigation, Effluent Recycling and Fresh Water Use	171
5.3.2	Stormwater Runoff	172
5.3.3	Evaporation	173
5.3.4	Seepage	186
5.4	MODEL CALIBRATION AND VALIDATION	191
5.4.1	Calibration by Water Balance Closure	191
5.4.2	Validation	200
5.4.3	Sensitivity Analysis	201
5.5	RESULTS AND DISCUSSION	203
5.5.1	Water and Recycled Effluent Usage at the Dairy	203
5.5.2	Wastewater Flows	206
5.5.3	Effluent Irrigation	207
5.5.4	Rainfall, Runoff and Evaporation	209
5.5.5	Seepage Losses and Infiltration	211
5.5.6	Final Pond System Water Balance	212
5.6	SUMMARY	216
Chapter 6	219
POND HYDRAULICS AND HYDRODYNAMICS	219
6.1	INTRODUCTION	219
6.1.1	Objectives, Scope, and Rational	220
6.2	HYDRAULIC CHARACTERISATION	221
6.2.1	Hydraulic Loading	221
6.2.2	Hydraulic Retention Times	222
6.2.3	Pond Geometries	224
6.2.4	Inlet-Outlet Configurations	227
6.3	SLUDGE ACCUMULATION IN THE ANAEROBIC POND	228

6.3.1	Methodology	229
6.3.2	Sludge Blanket Size and Shape	229
6.3.3	Active Sludge or Slurry Layer	233
6.3.4	Accumulation Rate	233
6.4	WATER QUALITY INDICATORS OF MIXING	236
6.4.1	Transverse Dispersion	236
6.4.2	Thermal Stratification and Hydraulic Efficiency	245
6.5	THEORETICAL ANALYSIS OF ADVECTIVE MIXING INPUTS	248
6.5.1	Inflow Power	248
6.5.2	Wind Shear Power	251
6.5.3	Power Exerted by Rising Biogas Bubbles (Anaerobic Pond)	253
6.5.4	Comparative Power Input	256
6.5.5	Energy Required for Effective Vertical Mixing	257
6.6	FIELD STUDY OF ANAEROBIC POND HYDRODYNAMICS	260
6.6.1	Methodology	261
6.6.2	Results	262
6.6.3	Discussion	271
6.7	SUMMARY	272
Chapter 7	275
WASTEWATER CONSTITUENT MONITORING AND MASS BALANCES	275
7.1	INTRODUCTION	275
7.2	MATERIALS AND METHODS	275
7.2.1	Sampling Regime	276
7.2.2	In-field Sample Handling	279
7.2.3	Laboratory Sample Preparation	280
7.2.4	Sample Analysis	281
7.3	RESULTS	285
7.3.1	Wastewater Characteristics	285
7.3.2	Anaerobic Pond Sludge Characteristics	296

7.3.3	Mass Flows.....	298
7.4	ANALYSIS AND DISCUSSION.....	304
7.4.1	Effects of Sludge Accumulation	304
7.4.2	Constituent Correlations	309
7.4.3	Load Distributions.....	311
7.4.4	Constituent Fractions and Wastewater Treatment Processes	313
7.4.5	Mass Balances and Pond Treatment Effects	316
7.4.6	Struvite Precipitation.....	325
7.4.7	Land Application and Nutrient Recovery	331
7.5	SUMMARY	334
Chapter 8	339
FORMULATION AND INITIALISATION OF A DYNAMIC MODEL OF THE ANAEROBIC POND		339
8.1	INTRODUCTION	339
8.2	KEY MODEL FEATURES.....	340
8.3	MODELLING PLATFORM	341
8.3.1	BioWin Wastewater Treatment Process Models	343
8.3.2	Adjusting Model Parameters for Simulation of DSE Treatment	343
8.3.3	New Evaporation Element	347
8.4	MODEL CONFIGURATION AND FLOW ROUTING	348
8.5	INFLUENT WASTEWATER CHARACTERISATION.....	350
8.5.1	Readily Biodegradable and Non-Biodegradable Soluble COD	354
8.5.2	Particulate and Colloidal COD	357
8.5.3	COD:VSS	364
8.5.4	Nitrogen.....	365
8.5.5	Phosphorus	367
8.5.6	Cations and Anions.....	368
8.5.7	Summary of Wastewater Constituent Fractions	368
8.6	ADDITIONAL TREATMENT PROCESSES.....	368

8.6.1	Degradation of 'Non-Biodegradable' Particulate COD.....	370
8.6.2	Decay of Endogenous Products	372
8.7	DATA PRE-PROCESSING.....	373
8.7.1	Wastewater Flows	374
8.7.2	Meteorology and Hydrology	375
8.7.3	Pond Temperatures.....	376
8.7.4	Influent Characteristics	377
8.8	SUMMARY	380
Chapter 9.....		383
ANAEROBIC POND MODEL CALIBRATION, SENSITIVITY ANALYSIS AND SCENARIO SIMULATIONS.....		383
9.1	INTRODUCTION	383
9.2	MODEL REFINEMENTS AND CALIBRATION	384
9.2.1	Controlling Gaseous Carbon Dioxide and Ammonia Losses	385
9.2.2	Settling and Sludge-Supernatant Flux	386
9.2.3	Hydrolysis of Very Slowly Biodegradable Material	390
9.2.4	Organic Nitrogen Fractionation	392
9.2.5	Non-Settleable Particulate P	392
9.2.6	Calibration Process.....	395
9.2.7	Model Outputs	396
9.2.8	Final Model Parameter Values.....	403
9.3	SENSITIVITY ANALYSIS	405
9.4	SCENARIO SIMULATIONS.....	409
9.4.1	Presence of a Dead Zone	410
9.4.2	High Organic Loading Rate.....	412
9.4.3	Regular Desludging.....	418
9.4.4	Low Seepage Losses	424
9.5	DISCUSSION	427
9.5.1	Insights into DSE Characteristics, Treatment and Modelling.....	428

9.5.2	Model Limitations.....	433
9.5.3	Model Expansion	438
9.6	SUMMARY	439
Chapter 10	443
CONCLUSIONS AND RECOMMENDATIONS.....		443
10.1	POND SYSTEM CHARACTERISTICS	443
10.1.1	Water Quality.....	443
10.1.2	Hydrology	444
10.1.3	Hydraulic Regimes.....	445
10.2	DEVELOPING A DYNAMIC BIOKINETIC MODEL OF THE ANAEROBIC POND.....	446
10.2.1	Formulation and Initialisation	446
10.2.2	Calibration and Sensitivity Analysis.....	447
10.2.3	Limitations	448
10.3	POND TREATMENT PROCESSES AND PERFORMANCE	448
10.3.1	The Role of Sludge	448
10.3.2	Anaerobic Pond Performance	449
10.3.3	Facultative Pond Processes and Performance.....	450
10.3.4	System Performance	451
10.4	IMPLICATIONS FOR DSE MANAGEMENT.....	451
10.5	RECOMMENDED FUTURE RESEARCH	453
10.6	CLOSING REMARKS	455
REFERENCES		457
APPENDICES.....		485
Appendix A	FIELD MONITORING EQUIPMENT AND SAFETY.....	487
Appendix B	INFILLING MISSING WASTEWATER FLOW DATA	497
Appendix C	WATER BALANCE MODEL FITTING CONSTRAINTS	501
Appendix D	INVESTIGATION OF DSE BIOCHEMICAL OXYGEN DEMAND CHARACTERISTICS	503

LIST OF FIGURES

Figure 1-1 Milk production in Australia plotted against indices of farms and cows milked (Dairy Australia 2012)	2
Figure 1-2 Topic map of the thesis content. Chapters that deal with particular topics are given in brackets. Dashed lines represent connections that are relevant beyond the topic of DSE stabilisation ponds.....	14
Figure 2-1 Trafficable solids trap (adapted from Haughton 2006).....	32
Figure 2-2 Conceptual model of sludge accumulation in livestock waste stabilisation ponds (Barth & Kroes 1985).....	42
Figure 2-3 Effluent constituent load estimation in OVERSEER (Wheeler, Shepherd & Power 2012).	60
Figure 2-4 Theoretical treatment efficiency of CM and PF reactors under first order kinetics. C = effluent substrate concentration; C_0 = influent substrate concentration.	64
Figure 2-5 The conceptual framework behind the Fritz, Middleton & Meredith (1979, p.2725) WSP model.....	67
Figure 2-6 The organic-inorganic P (a) and total P (B) models by Houngh and Gloyna (1984).	68
Figure 2-7 Hydraulic configuration of the AP model by Rajbhandari et al. (2007).....	71
Figure 2-8 Aerated FP supernatant and sediment reactor configuration used by Houweling et al. (2005) and (2008).	72
Figure 2-9 Facultative (Fac.) and maturation (Mat.) pond TSS concentrations (lines) predicted by the Gehring et al. (2010) model plotted against observed data.	74
Figure 2-10 Compartmental model configuration used by Alvarado et al. (2012).	75
Figure 2-11 Plot of DO concentrations predicted by the Beran & Kargi (2005) model against observed data.....	77
Figure 3-1 Map showing the study site location, nearby rainfall stations operated by the SCA and the location of the SILO data drill.	85
Figure 3-2 Monthly mean rainfall recorded at SCA stations 568070 (1974 – 2006) and 568113 (1978 – 2006) and by SILO (1889 – 2006) and monthly mean evaporation recorded at SCA station 568113 (1978 – 2006) and by SILO (1970 – 2006).....	87
Figure 3-3 Monthly mean daily minimum and maximum temperatures and solar radiation calculated from the SILO data drill.	88
Figure 3-4 Schematic diagram depicting the dairy and the waste management system at Sugarloaf Holsteins farm.	90
Figure 3-5 Plan view and cross-section elevation of the solids trap (not to scale).	96

Figure 3-6 Scale surface maps of (a) the anaerobic pond and (b) the facultative pond. Blue contour lines indicate pond liquid capacities.....	99
Figure 3-7 Polynomial curves fitted to pond liquid volume, liquid surface area and wetted area data plotted against liquid surface elevation. Left: anaerobic pond. Right: Facultative pond.....	100
Figure 3-8 Locations of influent/effluent/supernatant sampling points, multi-parameter probes (CTDP300 and CS304) deployments and the monitoring control trailer housing/supporting the central data logger, the autosamplers, the AWS and the MA.	104
Figure 4-1 Temperature variation over time measured approximately 60 cm below the liquid surface at three locations in the anaerobic pond (orange, blue and green lines). Air temperature is shown in grey.....	118
Figure 4-2 Variation of pH variation over time measured approximately 50 cm below the liquid surface and at three locations in the anaerobic pond (coloured lines). Readings from discrete samples of influent and effluent are denoted by black symbols.....	120
Figure 4-3 Variation in conductivity at approximately 60 cm (measured at three locations) and cumulative water flux from rainfall, runoff and evaporation (loss positive, gain negative) over time in the anaerobic pond.	124
Figure 4-4 Summer diurnal variation in water quality parameters 50-60 cm below the surface of the anaerobic pond.....	125
Figure 4-5 Winter diurnal variation of water quality parameters 50-60 cm below the surface of the anaerobic pond.....	127
Figure 4-6 Anaerobic pond temperature profiles. Lines pass through mean values. Error bars represent two standard deviations. Daily maximum air temperature (DMAT) is plotted in the shaded region of the plot.....	128
Figure 4-7 Anaerobic pond pH profiles.....	129
Figure 4-8 Anaerobic pond EC profiles.	130
Figure 4-9 Anaerobic pond ORP profiles.....	130
Figure 4-10 Temperature variation in the facultative pond measured at three different locations within the pond and in the flood wash tank. Ambient air temperature is shown in grey in the background. Measurement depths are given in the legend (note FWT depth = pond extraction depth).	133
Figure 4-11 Variation in pH in the facultative pond measured at three different locations within the pond and in the flood wash tank containing effluent from the pond for reuse. Readings from discrete samples of the supernatant (in-pond) and effluent are denoted by black symbols.....	135

Figure 4-12 Variation in conductivity and flux of fresh water over time in the facultative pond.....	137
Figure 4-13 Variation DO in the epilimnion of the facultative pond measured at two different locations.....	140
Figure 4-14 Variation in turbidity at the surface of the facultative pond measured by the MA. Readings from discrete samples of supernatant and pond effluent are denoted by black symbols.....	141
Figure 4-15 Diurnal variation in the epilimnion (upper 5-10 cm) of the facultative pond in late spring to early summer.	143
Figure 4-16 Diurnal variation in the hypolimnion of the facultative pond in late spring to early summer.	144
Figure 4-17 Winter diurnal variation in the epilimnion (upper 5-10 cm) of the facultative pond.....	145
Figure 4-18 Facultative pond temperature profiles plotted with corresponding DMATs.	146
Figure 4-19 Facultative pond pH profiles.....	147
Figure 4-20 Facultative pond EC profiles.	149
Figure 4-21 Facultative pond DO profiles.....	150
Figure 4-22 Facultative pond ORP profiles.	150
Figure 4-23 Monthly average daily minimum and maximum pond supernatant temperatures.....	152
Figure 4-24 EDS analysis of a sample of crystalline deposit.	157
Figure 4-25 X-ray diffractogram of crystalline deposits sampled from facultative pond (red line) plotted with a standard pattern for struvite.....	157
Figure 5-1 Schematic diagram of water balance components and flow and depth measurement locations.....	164
Figure 5-2 Rating curve for the flumes used to measure flow into and out of the anaerobic pond.....	169
Figure 5-3 Daily clear water albedo at solar noon over the water balance period.....	178
Figure 5-4 Fitted and simplified temperature profiles (July 2005 and January 2007, others not shown) for estimating VT	183
Figure 5-5 Observed and predicted hourly liquid surface elevation in the facultative pond over the evaporation calibration period. Note predicted elevations were reset to observed elevations following each of the three main rainfall events.....	194
Figure 5-6 Comparison between estimates from the evaporation equation calibrated to the Sugarloaf Holsteins stabilisation pond site and Penman Monteith estimates and Class A pan measurements recorded by SCA.	197

Figure 5-7 Turbidity correction curve for albedo (Fresnel albedo = 0.06).....	198
Figure 5-8 Frequency of wind direction and speed recorded over the monitoring period.	199
Figure 5-9 Observed and predicted liquid surface elevation in the facultative pond 5 October - 6 December 2006.....	201
Figure 5-10 Box-whisker plots of daily water and reclaimed effluent consumption at the dairy.....	204
Figure 5-11 Average monthly water and recycled effluent consumption. Error bars indicate 95% confidence intervals.	205
Figure 5-12 Example of flow data – inflow to and outflow from anaerobic pond 1 July 2006 – 15 July 2006.....	206
Figure 5-13 Box-whisker plot of daily peak flow entering and leaving the anaerobic pond drawn from days with complete data records and less than 1 mm rainfall. The red diamond symbols are the respective means.	207
Figure 5-14 Volume and pumping time of effluent irrigation events.	209
Figure 5-15 Monthly rainfall, embankment runoff and evaporation over the water balance period.	210
Figure 5-16 Comparisons between rainfall (left) and evaporation (right) data recorded in the present study, by the SCA weather station 568113, and in a SILO data drill.	211
Figure 5-17 Average flows entering and leaving the anaerobic and facultative ponds (20 January – 5 December 2006).....	216
Figure 6-1 Theoretical HRTs for (a) the anaerobic plotted against sludge volume, and (b) the facultative ponds plotted against liquid volume.....	223
Figure 6-2 Sludge and slurry levels in the anaerobic pond (a) over the period 8 December 2004 and 19 October 2005 prior to desludging and (b) over the period 30 October 2005 and 12 January 2007 following desludging.	231
Figure 6-3 Sludge surfaces mapped on 8 December 2004 and 12 January 2007. The red line and arrows indicate the cross-section used in Figure 6-2.	232
Figure 6-4 Sludge accumulation in the anaerobic pond plotted against time. The unfilled points were considered outliers and have not been included in the linear fit.	234
Figure 6-5 Conductivity contours ($\mu\text{S cm}^{-1}$) at the surface (top) and at depth (bottom) in the anaerobic pond for June, October 2005 and March 2006. Influent EC is given adjacent to the inlet on the left hand side of the surface contour plots. Average wind speed and direction are given in the bottom right corner of the surface plots. Note the change in inlet configuration after the October 2005 profiling event.	238

Figure 6-6 Conductivity contours ($\mu\text{S cm}^{-1}$) at the surface (top) and at depth (bottom) in the anaerobic pond for May, August 2006 and January 2007.	239
Figure 6-7 Conductivity contours ($\mu\text{S cm}^{-1}$) at the surface, mid-depth and the bottom of the facultative pond for July (top) and November 2005. Influent EC is given adjacent to the inlet on the bottom right of the surface contour plots. Average wind speed and direction are given in the bottom right corner of the surface plots.	241
Figure 6-8 Conductivity contours ($\mu\text{S cm}^{-1}$) at the surface, mid-depth and the bottom of the facultative pond for February (top) and April (bottom) 2006.....	242
Figure 6-9 Conductivity contours ($\mu\text{S cm}^{-1}$) at the surface, mid-depth and the bottom of the facultative pond for September 2006 (top) and January 2007 (bottom) 2006.	243
Figure 6-10 Vertical temperature gradients in the facultative pond (green lines) and air temperature (blue lines) in (a) summer, (b) autumn, (c) winter and (d) spring. ...	247
Figure 6-11 Histogram of energy imparted to the anaerobic pond by wash down inflow peaks (10 October 2005 to 5 December 2006).	250
Figure 6-12 Histograms of daily wind shear energy inputs: (a) anaerobic pond; (b) facultative pond (10 October 2005 to 5 December 2006).	253
Figure 6-13 Comparison of power exerted by natural mixing forces ranked by frequency.....	257
Figure 6-14 Drogue design used in field experiments.	262
Figure 6-15 Velocity field incorporating drogue trails from 13 of 16 experimental runs.	264
Figure 6-16 Plots of flow and drogue velocity with time for all experimental runs.	270
Figure 6-17 Conceptual models of the hydraulics and hydrodynamics of the pond system.	273
Figure 7-1 Percentage differences between facultative pond supernatant (reference) and recycled effluent. Error bars are 95% confidence intervals.	294
Figure 7-2 Chlorophyll-a concentration measured across the full depth of the supernatant and chlorophyll-a and algal biomass concentrations estimated for the euphotic zone.	296
Figure 7-3 Sludge solids and organic carbon by wet weight.....	298
Figure 7-4 Sludge nutrient and cation composition by wet weight.	299
Figure 7-5 Example of linear regressions used to estimate sludge constituent (total, total fixed, and total volatile solids and carbon) mass loading rates.....	303
Figure 7-6 Anaerobic (AE) and facultative (FE) pond effluent constituent concentrations over time (a) COD and FCOD; (b) TSS and TVSS; (c) TVDS and BOD ₅ ; (d) TP and DRP; (e) TN and NH ₃ -N.	306

Figure 7-7 Anaerobic (AE) and facultative (FE) pond effluent constituent concentrations over time (a) TDFS and K^+ ; (b) Ca^{2+} and Mg^{2+} ; (c) Na^+ and Cl^-	307
Figure 7-8 Wastewater constituent correlations: (a) EC vs TDS; (b) EC vs TDFS	309
Figure 7-9 Wastewater constituent correlations: (a) COD vs FCOD; (b) TVSS vs particulate and colloidal COD; (c) TP vs DRP; (d) TKN vs NH_3-N	310
Figure 7-10 Correlations between turbidity, TSS and chlorophyll-a in the facultative pond.....	311
Figure 7-11 Histograms of constituent loads: (a) TSS; (b) COD; (c) Organic N; (d) Particulate P.....	312
Figure 7-12 Histograms of soluble constituent loads: (a) TDFS; (b) FCOD; (c) K^+ ; (d) DRP.	313
Figure 7-13 Mass balances for aggregate solids and organic constituents in the anaerobic pond. Data labels are absolute values in $kg\ d^{-1}$	318
Figure 7-14 Mass balances for the major nutrients, cations and anions in the anaerobic pond.....	319
Figure 7-15 Mass balances for aggregate solids and organic constituents in the facultative pond. Data labels are absolute values in $kg\ d^{-1}$	322
Figure 7-16 Mass balances for the major nutrients, cations and anions in the facultative pond.....	324
Figure 7-17 Struvite supersaturation indices over time.....	327
Figure 7-18 Predicted and observed TDS concentrations in the anaerobic and facultative ponds.	330
Figure 7-19 Available (soluble) and organic/particulate N, P and K loads plotted as percentages of strategic pasture fertiliser demand. Fertiliser demand for the dedicated effluent application area is also expressed as a fraction of total pasture fertiliser demand.....	334
Figure 8-1 BioWin element configuration for the anaerobic pond model.....	349
Figure 8-2 Fractionation of organic matter (COD) in the BioWin activated sludge and anaerobic digestion models and dairy shed wastewater organic constituents (adapted from Melcer et al. (2003) and Henze (1992))......	352
Figure 8-3 Estimated non-biodegradable soluble COD (SUS) over time.....	355
Figure 8-4 Estimated influent SBS plotted against measured influent FCOD	355
Figure 9-1 Predicted anaerobic pond supernatant pH, CO_2 gas and effluent NH_3-N levels plotted with corresponding observed data.	386
Figure 9-2 Model and idealised sludge dewatering unit solids removal efficiency curves.	389

Figure 9-3 Number of days anaerobic digestion in the sludge is inhibited by low pH plotted against the sludge-supernatant exchange areal flux rate fS	390
Figure 9-4 Process model curves for hydrolysis of cellulosic material.	391
Figure 9-5 Observed and predicted total P concentrations from a simulation run based on the conventional BioWin P fractionation. Note again the zero concentrations resulting from zero outflow.	393
Figure 9-6 Predicted and observed anaerobic pond effluent COD and FCOD (top), TSS and TVSS (upper middle), TKN and $\text{NH}_3\text{-N}$ (lower middle), and TP and DRP concentrations (bottom). Predicted data are represented by lines while discrete points represent observed data. Each is colour coded in accordance with their corresponding labels.....	397
Figure 9-7 Predicted and observed anaerobic pond supernatant pH (top) and effluent Ca^{2+} and Mg^{2+} (middle), and K^+ and Cl^- (bottom) concentrations. Predicted data are represented by lines while diamond points represent observed data. Each is colour coded in accordance with their corresponding labels, except for observed pH data which have been coloured light blue for visibility.	398
Figure 9-8 Predicted and observed anaerobic pond sludge COD (top), pH (upper middle), TSS and TVSS (lower middle), TN and TP (bottom) concentrations. Predicted data are represented by lines while diamond points represent observed data. Each are colour coded in accordance with their corresponding labels.	401
Figure 9-9 Predicted biogas emissions from the sludge and supernatant.....	403
Figure 9-10 Supernatant and sludge reactor liquid volumes over time in the calibrated model simulation and the dead scenario simulation. Sludge volume was the same in both simulations.	411
Figure 9-11 Removal efficiencies before and after desludging from the calibrated model and dead zone scenario simulations.	412
Figure 9-12 Pond geometry used to simulate high loading scenario.	414
Figure 9-13 Predicted COD concentrations in the high organic loading rate scenario model (HOLR) and the base model (BM).	415
Figure 9-14 Comparison of sludge and effluent COD fractions between the high loading rate scenario and the base model outputs.....	417
Figure 9-15 Simulated average sludge and supernatant biomass concentrations from the high loading rate scenario and base models.	418
Figure 9-16 Predicted supernatant volumes (top), effluent COD and FCOD concentrations (middle) and supernatant biomass concentrations (bottom) from the three desludging scenario simulations.	421

Figure 9-17 Removal efficiencies under the desludging scenarios A, B and C compared with those of the base model.....	422
Figure 9-18 Predicted sludge volumes (top), COD and FCOD concentrations (middle) and biomass concentrations (bottom) from the three desludging scenario simulations.....	423
Figure 9-19 Nutrient loads extracted during the final desludging events of scenarios A, B and C.....	424
Figure 9-20 pH and acetoclastic methanogen biomass and acetate concentrations in the sludge and supernatant under the low seepage scenario.....	426
Figure 9-21 Nutrient ratios in the sludge, supernatant, mixed sludge and supernatant compared with a fertiliser regime appropriate to recent soil nutrient levels. The denominator of all ratios is total P.	433
Figure 9-22 Biogas flows estimated in the data pre-processing and predicted in BioWin.	438
FIGURE A-1 Anaerobic pond inlet sampling intake.	494
FIGURE B-1 Extract from the flume data interpolation results. Signal drop outs in the original data are indicated by the (mostly flat) sections of zero or very low readings.	499
FIGURE B-2 Histograms comparing distributions of daily flow data unaffected by the ground loop and infilled flow data: (a) Flume 1; (b) Flume 2.	499
FIGURE D-1 Examples of total and filterable BOD exertion curve fits. (a) Raw wastewater, (b) solids separated wastewater, (c) anaerobic pond effluent and (d) facultative pond effluent.	505
FIGURE D-2 Ultimate BOD estimates for each type of wastewater by sampling date.	506
FIGURE D-3 Ultimate filterable BOD estimates for each type of wastewater by sampling date.....	507

LIST OF TABLES

Table 1-1 Changes in the Australian and New Zealand dairy industries.....	3
Table 1-2 Nutrient surpluses and efficiencies on Australian dairy farms.	4
Table 2-1 Components of DSE	19
Table 2-2 Raw DSE characteristics recorded on dairy farms in the Southern Highlands and Shoalhaven dairying regions of NSW, Australia (data from the University of Wollongong).....	23
Table 2-3 Raw DSE characteristics. Coefficients of variation (CV) are given in parentheses. NR = not reported; TN = total nitrogen.	27
Table 2-4 Wastewater constituent ratios drawn from published data on raw and settled/screened DSE. Where data have been drawn from multiple farms, averages have been weighted according to the number of samples collected from each farm.....	29
Table 2-5 Solids separation efficiencies reported or assumed for solids traps.....	33
Table 2-6 Reported solids trap removal efficiencies. CVs given in parentheses.	33
Table 2-7 Summary of DSE AP effluent characteristics from published and unpublished data. CVs for wastewater constituents given in parentheses.....	36
Table 2-8 Reported removal efficiencies (%) for APs treating DSE.	40
Table 2-9 Sludge characteristics reported in the literature. CVs given in parentheses.	43
Table 2-10 Summary of DSE FP effluent characteristics from published and unpublished data. CVs for wastewater constituents given in parentheses. Italics denote either TKN in place of TN data or TON in place of NO ₃ -N data.....	47
Table 2-11 Reported removal efficiencies (%) for FPs treating DSE.	48
Table 3-1 Comparison of recent annual rainfall at the farm site and nearby rainfall stations.	86
Table 3-2 Fertiliser use and soil conditioning (Maloney 2007, pers. comm. 19 February).	89
Table 3-3 Milking equipment hygienic cleaning-in-place regime.....	91
Table 3-4 As constructed volumes, surface areas and theoretical loading rates of the anaerobic and facultative ponds.....	98
Table 3-5 Coefficients for polynomials fitted to facultative pond liquid volume, liquid surface area and embankment wetted area data.	101
Table 4-1 Approximate relative vertical sampling positions of the probe sensors and MA pump	112
Table 4-2 Pond profiling events.	115
Table 4-3 Descriptive statistics – aligned anaerobic pond temperature data.	117

Table 4-4 Correlation coefficients between temperature data recorded at the three anaerobic pond probe locations. Values in parentheses are sample sizes.	117
Table 4-5 Descriptive statistics – aligned anaerobic pond pH data.....	121
Table 4-6 Descriptive statistics – aligned anaerobic pond EC data.	123
Table 4-7 Correlation coefficients between EC data recorded at the three anaerobic pond probe locations. Figures in parentheses are sample sizes.....	123
Table 4-8 Temperature gradients recorded in the anaerobic pond profiles.....	128
Table 4-9 Descriptive statistics - aligned facultative pond temperature data.....	132
Table 4-10 Correlation coefficients between temperature data recorded at the four facultative pond probe locations. Figures in parentheses are sample sizes.....	132
Table 4-11 Descriptive statistics – aligned facultative pond pH data.	136
Table 4-12 Descriptive statistics – aligned facultative pond EC data.	138
Table 4-13 Correlation coefficients between EC data recorded at the four facultative pond probe locations. Figures in parentheses are sample sizes.....	138
Table 4-14 Descriptive statistics – non-zero daily DO concentrations.	141
Table 4-15 Temperature gradients recorded in the facultative pond profiles.	147
Table 4-16 Descriptive statistics from dairy water supply monitoring.....	151
Table 5-1 Measured and estimated water balance components.....	167
Table 5-2 Albedos adopted or recommended in the literature	175
Table 5-3 Calibration and validation outputs from the facultative and anaerobic pond water balance models.	195
Table 5-4 Results from the sensitivity analysis of the fitted evaporation and seepage parameters.....	202
Table 5-5 Average daily, morning and evening water and reclaimed effluent usage at the dairy (values in parentheses are standard deviations).....	203
Table 5-6 Daily wastewater flow statistics drawn from days with complete data records and less than 1 mm rainfall.	208
Table 5-7 Rainfall, runoff and evaporation estimates over the period 30 October 2005 to 5 December 2006.....	210
Table 5-8 Net seepage losses over the period 30 October 2005 to 5 December 2006	211
Table 5-9 Anaerobic pond water balance outputs for periods with contiguous data...	214
Table 5-10 Facultative pond water balance outputs for periods with contiguous data.	215
Table 6-1 Anaerobic and facultative pond geometries.....	225

Table 6-2 Sludge volume estimates, associated active treatment volumes and theoretical HRTs and average slurry layer depths (standard deviations given in parentheses).....	230
Table 6-3 Volumetric sludge accumulation rates.....	235
Table 6-4 Specific sludge accumulation rates measured in this study and reported elsewhere.	236
Table 6-5 Occurrence of different forms of stratification as defined by Gu & Stefan (1995) in the facultative pond.....	248
Table 6-6 Inflow power input statistics for the anaerobic and facultative ponds between 10 October 2005 and 5 December 2006. Figures in italics were calculated from non-zero data only.	250
Table 6-7 Wind power input statistics for the anaerobic and facultative ponds between 10 October 2005 and 5 December 2006.	252
Table 6-8 Estimated energy inputs and energy required to break down stratification observed during pond profiling.	259
Table 6-9 Summary of drogue motion, pond inlet flow and wind conditions for each drogue run.	268
Table 7-1 Numbers of influent, effluent, supernatant and sludge samples collected over the course of the study.....	279
Table 7-2 Analyses performed on samples collected in the field.	281
Table 7-3 Analyses performed at the University of Wollongong laboratories.	283
Table 7-4 Analyses of pond liquid samples performed by EAL.....	284
Table 7-5 Analyses of sludge samples performed by EAL.	285
Table 7-6 Average physical and aggregate solids and organic constituent concentrations for the anaerobic pond influent (AI) and effluent (AE).	286
Table 7-7 Major nutrient, cation and anion composition of the anaerobic pond influent (AI) and effluent (AE).	288
Table 7-8 Average physical and aggregate solids and organic constituent concentrations for the facultative pond supernatant (FS) and effluent (FE).	291
Table 7-9 Major nutrient, cation and anion composition of the facultative pond supernatant (FS) and effluent (FE).....	292
Table 7-10 Composition of sludge and slurry samples.	297
Table 7-11 Average constituent loading rates to the anaerobic and facultative ponds and in effluent recycled to flood washing over the year commencing 31 October 2005. Error bounds are 95% confidence intervals.	300
Table 7-12 Constituent loads applied to land over the year commencing 31 October 2005.....	301

Table 7-13 Accumulated anaerobic pond sludge constituent loads and long term accumulation rates. Error bounds given for accumulation rates are 95% confidence intervals.	302
Table 7-14 Estimated seepage loads of soluble constituents for the year commencing 30 October 2005.	304
Table 7-15 Average wastewater constituent ratios	315
Table 7-16 Pond system treatment efficiencies.	325
Table 8-1 Stabilisation pond treatment processes and corresponding BioWin process models. Process models and elements used in the final model are identified in bold text.	345
Table 8-2 Parameter values adopted at model initialisation and parameters identified as candidates for adjustment during calibration.	347
Table 8-3 Summary of BioWin elements used in the anaerobic pond model.	351
Table 8-4 Chemical formulae and theoretical oxygen demand for key organic components of manure.	353
Table 8-5 VFA characterisation of dairy shed wastewaters and manures.	358
Table 8-6 Manure solids composition reported in the literature.	360
Table 8-7 Summary of wastewater constituent fractions adopted for modelling.	369
Table 8-8 Stoichiometry of the process models for the biodegradation of very slowly degradable (hemicellulose and cellulose) COD and associated particulate bound N and P.	372
Table 8-9 Stoichiometry of the model for decay of endogenous products.	373
Table 8-10 Summary of data available for use in modelling.	374
Table 8-11 Alternative meteorological data sources and adjustment factors derived from regression analysis.	375
Table 8-12 Anaerobic pond temperature model parameters and coefficients of determination.	377
Table 8-13 Wastewater constituent linear regression model coefficients and statistics.	381
Table 9-1 Error measures for the model predictions of effluent quality.	400
Table 9-2 Error measures for the model predictions of sludge composition.	402
Table 9-3 Final adopted model parameters.	404
Table 9-4 Model parameters and their adjusted values included in the sensitivity analysis.	406
Table 9-5 Relative sensitivities for COD, FCOD, TVSS and TSS removal efficiencies. Relative sensitivities exceeding ± 0.25 are identified with shaded cells.	408

Table 9-6 Relative sensitivities for effluent nutrient and cation loads. Relative sensitivities exceeding ± 0.25 are identified with shaded cells.....	408
Table 9-7 Relative sensitivities for sludge COD, FCOD, TVSS and TSS loads.	409
Table 9-8 Average simulated effluent concentrations, effluent loads and removal efficiencies during periods when sludge accumulation was below the threshold for compromised settling efficiency.	416
Table 9-9 Volumes of sludge and effluent removed under the three regular desludging scenarios.	419
Table 9-10 Average yearly soluble COD and nutrient loads contained in seepage and effluent from the ideal seepage scenario and the base model simulations.	427
Table 9-11 Average predicted sludge and supernatant biogas production and GHG emissions.....	430
TABLE A-1 Automated weather station components and data collection.	489
TABLE A-2 Flow measurement equipment and data collection.....	490
TABLE A-3 Real time water quality monitoring equipment and data collection.....	491
TABLE A-4 YSI 556 multi probe system.....	492
TABLE A-5 Assessment of risks associated with field work activities.....	495
TABLE B-1 Rules for identifying data points affected by signal interference.	498
TABLE B-2 Samples affected by flow signal drop outs.....	500
TABLE C-1 Fitting constraints used in estimating evaporation and seepage parameters for the facultative pond.....	501
TABLE C-2 Fitting constraints used in estimating evaporation and seepage parameters for the anaerobic pond.	502
TABLE D-1 Parameter estimates for the modified BOD exertion model.	507
TABLE D-2 Ratios of standard wastewater parameters.	509

LIST OF PLATES

Plate 3-1 Left: afternoon milking procession to the dairy. Right: interior of the milking shed.....	89
Plate 3-2 Left: flood washing the main section of the holding yard (flood wash tank stands to the right of the dairy shed). Right: manual hosing of the eastern side of the yard is aided by a stream of reclaimed effluent flowing from a pipe attached to the shed support column at the top-left corner of the yard.....	92
Plate 3-3 Left: view of the waste stabilisation pond system from the dairy shed holding yard (the solids trap sits at the bottom of the yard behind the fence at the middle left of the photograph). Right: view of the trafficable solids trap holding fresh wastewater.....	93
Plate 3-4 Left: view of the anaerobic pond showing the outlet pipe. Right: View of the facultative pond with the effluent recycling pump and control box in the foreground and the buoy supporting to foot valve to the extraction line sits on the water surface to the right.	95
Plate 3-5 The monitoring control trailer: trailer and AWS (top left); autosamplers at rear (top right); datalogger and power box (bottom left); FIA and power supply (bottom right).	105
Plate 4-1 Interior of the monitoring support trailer housing the mini-analyser (blue cabinet) and its cleaning and calibration solutions. Right: power support to a CTDP300 multi-parameter probe installed in the anaerobic pond (the probe is suspended in the supernatant from the orange buoy).	111
Plate 4-2 Left: crystals collected from the flood wash tank photographed in a petri dish. Right: magnified 20 times under a microscope (right).....	156
Plate 4-3 SEM image of a sample of crystalline deposit.	156
Plate 5-1 Moulded PVC flumes used to monitor effluent flow. Left: Flume 1 attached to the anaerobic pond inlet. Right: Flume 2 attached to the anaerobic pond outlet (facultative pond inlet).	168
Plate 5-2 Effluent pumping line fitted with the electromagnetic flow detector. Note the circuit arrangement of the pipework to ensure full flow and sufficient straight lengths upstream and downstream of the meter.....	170
PLATE A-1 Column sampler (left) and in use collecting a sample from the anaerobic pond (right).	493

NOTATION

α	Albedo of the evaporating surface
$\alpha_0, \alpha_1, \dots$	Regression coefficients
α_d	Diffuse radiation albedo
α_f	Albedo for direct radiation
$\alpha_{f,d}$	Freznel albedo adjusted for diffuse radiation
α_i	Kinetic energy correction factor
β	Solar elevation (radians)
β_0, β_1, \dots	Regression coefficients
γ	Psychrometric constant
Δ	Slope of the temperature saturation water vapour curve
ΔM_j	Change in the stored (liquid) load of constituent j
ΔS_j	Change in the constituent sludge load
ΔV_{An}	Change in volume held in the anaerobic pond
ΔV_{Fac}	Change in effluent held in the facultative pond
ϵ_a	Atmospheric emissivity
ϵ_w	Emissivity of water
ϵ_X	Particulate COD destruction
θ	Arrhenius temperature adjustment constant
ϑ	Actual mean hydraulic residence time
ϑ_t	Theoretical HRT
κ	Von Karman's constant
λ	Latent heat of vaporisation
$\mu_{max,H}$	Maximum heterotrophic growth rate
ρ	Density
$\rho(z)$	Function describing the liquid density at depth z
ρ_a	Air density
ρ_g	Density of the gas in the biogas bubble
ρ_w	Water (liquid) density
σ	Stefan-Boltzman constant
τ_w	Wind shear stress
v	Constant
A	Pond liquid surface area
$A(z)$	Function describing the pond surface area at depth z

A_b	Biogas bubble surface area
AE	Anaerobic pond effluent
A_F	Surface area of the pond floor
A_{fac}	Facultative pond surface area
A_i	Cross-sectional area of the inlet
AI	Anaerobic pond influent
AOB	Ammonia oxidising biomass
AOB	Ammonia oxidising biomass
AP	Anaerobic pond
A_s	Plan area of the solids trap
AS	Activated sludge
ASDM	Activated Sludge/Anaerobic Digestion Model
$A_{w,An}$	Anaerobic pond wetted area
$A_{w,Fac,E}$	Facultative pond embankments wetted area
A_y	Plan area of the holding yard
$b_{H,An}$	Heterotrophic decay rate
BM	Base model
BMP	Best management practice
BOD	Biochemical oxygen demand (general terminology)
BOD ₅	5-day biochemical oxygen demand (laboratory test)
BOD _t	BOD at time t
BOD _{ult}	Ultimate BOD
b_{Xe}	Decay rate
b_{Xe}	Endogenous product decay rate
C_{An}	Concentration of total dissolved solids in the anaerobic pond supernatant
CBOD _{ult}	Ultimate biochemical oxygen demand
C_{Db}	Biogas bubble drag coefficient
C_{Dz}	Pond surface drag coefficient for wind measured at height z
C_{Fac}	Concentration of total dissolved solids in the facultative pond supernatant
CFD	Computational fluid dynamics
Chl-a	Chlorophyll-a
CM	Completely mixed
COD	Chemical oxygen demand
c_p	Specific heat of air at constant pressure

CSTR	Continuous stirred tank reactor
CV	Coefficients of variation
c_w	Specific heat of water
d	Dispersion number
d_0	Zero displacement height
D_b	Biogas bubble drag force
d_b	Effective diameter of the biogas bubble
DGAS	Dairy Greenhouse Gas Abatement Strategy
DMDAMP	Dry matter digestibility approximation of manure production
DMI	Dry matter intake
DO	Dissolved oxygen
DO _s	Saturated concentration of dissolved oxygen
DPI	Department of Primary Industries
DRP	Dissolved reactive phosphorus
DSE	Dairy shed effluent
D_x, D_y, D_z	Dispersion coefficients for the x,y and z directions
E_0	Open water evaporation
E_a	Drying power of the air
EAL	Environmental Analysis Laboratory
E _{An}	Evaporation from the anaerobic pond
EBPR	Enhanced biological phosphorus removal
EC	Electrical conductivity
$EC_{r,f}$	Electrical conductivity of the recycled effluent used in the flood wash
EDS	Energy-dispersive X-Ray Spectroscopy
E _{Fac}	Evaporation from the facultative pond
E_p	Potential evaporation
ESP	Exchangeable sodium percentage
e_z	Vapour pressure at height z
e_z^0	Saturation vapour pressure at height z
$f(u)$	Wind function
f_{BOD}	Correction for non-biodegradable biomass lysis COD
f_{BSA}	Acetic acid fraction of readily biodegradable COD
f_{BSC}	Complex fraction of readily biodegradable COD
f_{BSP}	Propanoic acid fraction of readily biodegradable COD
FCBOD ₅	5-day filterable carbonaceous biochemical oxygen demand

$\text{FCBOD}_{\text{ult}}$	Ultimate filterable carbonaceous biochemical oxygen demand
FCOD	Filterable chemical oxygen demand
FE	Facultative pond effluent
f_{EA}	Aerodynamic correction factor
f_{NSP}	Fraction of non-settleable particulate P
f_{NUS}	Fraction of soluble non-biodegradable N
FP	Facultative pond
f_s	Sludge-supernatant flux coefficient
f_T	Surface turbulence factor
f_{XBC}	Very slowly biodegradable (cellulosic) fraction of particulate COD
f_{XI}	Conventionally non-biodegradable fraction of particulate COD
f_{XICa}	Ca fraction of particulate non-biodegradable and very slowly degradable material
f_{XIL}	Lignin fraction of particulate/colloidal COD
f_{XIMg}	Mg fraction of particulate non-biodegradable and very slowly degradable material
f_{XIN}	N fraction of particulate non-biodegradable and very slowly degradable material
f_{XIP}	P fraction of particulate non-biodegradable and very slowly degradable material
f_{XSC}	Colloidal fraction of slowly biodegradable COD
f_{XSP}	Particulate fraction of slowly biodegradable COD
$f_{\alpha 2}$	Albedo turbidity correction factor
g	Acceleration due to gravity
g_{440}	Absorption at 440 nm
GHG	Greenhouse gas
GRG2	Generalized Reduced Gradient
H	Depth of liquid or sludge
h	Liquid surface depth or elevation
\hat{h}	Predicted liquid surface elevation
h_B	Elevation of the lowest point in the anaerobic pond basin
h_F	Elevation of the facultative pond floor
h_i	Height of the inlet above the pond surface
HOLR	High organic loading rate
HRT	Hydraulic residence time

I	Cumulative infiltration
I_i	Sensitivity index i
K_{BC}	Cellulosic material hydrolysis half saturation constant
k_d	Light attenuation coefficient
k_{HBC}	Maximum specific hydrolysis rate for cellulosic material
k_l	Hydraulic conductivity of the pond liner
k_s	Hydraulic conductivity of the waste seal
$k_{S,H}$	Heterotrophic half-saturation constant
L	Pond length
$L_{eff,j}$	Effluent mass loading of constituent j
$L_{inf,j}$	Influent mass loading of constituent j
L_l	Pond liner thickness
L_M	Mass of TDS from manure deposited and chemicals used at the dairy
$L_{seepage,j}$	Seepage mass loading of constituent j
M	Manure including faeces and urine
m	Number of viable data points in flow record for flume 2 on day x ;
MA	Greenspan flow injection Mini-Analyser
mAHD	Elevation (m) above the Australian Height Datum
MAP	magnesium ammonium phosphate hexahydrate
MAPE	Mean absolute percentage error
MEDLI	Model for Effluent Disposal Using Land Irrigation
MPS	Multi Probe System
N	Nitrogen
n	Count or sample size OR number of viable data points in flow record for flume 1 on day x
NGGI	National Greenhouse Gas Inventory
N_{OS}	Concentration of soluble biodegradable N
NTU	Nephelometric turbidity units
n_w	Refractive index of water
NZ	New Zealand
OHO	Ordinary heterotrophic organisms
ORP	Oxidation-reduction potential
OUR	Oxygen uptake rate
P	Rainfall
PAO	Phosphorus accumulating organism

PAR	Potassium adsorption ratio
Pe	Peclet number
PF	Plug flow
P_{Fac}	Rainfall entering the facultative pond
P_i	Inflow power
P_j	Model parameter j
PM	Penman-Monteith
PW_0	Peak daily inflow
Q	Change in heat stored in water body
q	Specific flux
$Q1_{x,i}$	Stage or flow recorded in flume 1 at interval i on day x
$Q1_{y,i}$	Stage or flow recorded in flume 1 at interval i on day y
$Q2_{x,j}$	Stage or flow recorded in flume 2 at interval j on day x
$Q2_{y,j}$	Stage or flow recorded in flume 2 at interval j on day y
Q_{biogas}	Volumetric biogas production
Q_{CH4}	Volumetric methane production
r	Angle of refraction
R_{0L}^*	Net long-wave radiation
R_a	Extra-terrestrial short-wave radiation
RBCOD	Readily biodegradable chemical oxygen demand
R_e	Pond embankment runoff
$R_{e,An}$	Stormwater runoff from the anaerobic pond embankments
R_j	Net mass of constituent j converted, removed or added through physical, biological or chemical processes
R_{Lin}	Incoming long-wave radiation
R_{Lout}	Outgoing long-wave radiation
R_n	Net radiation
R_s	Stormwater runoff from the solids trap
R_s	Runoff from the solids trap
$R_{S,in}$	Incoming short-wave radiation
$R_{S,in,d}$	Diffuse component of incoming shortwave radiation
R_{S0}	Clear sky radiation.
R_{Sout}	Outgoing short-wave radiation
RTD	Residence time distribution
R_y	Stormwater runoff from the holding yard

S'	Seepage expressed as rate of change in liquid surface elevation
SA	Sludge accumulation rate
S_{An}	Seepage from the anaerobic pond
SAR	Sodium adsorption ratio
SBR	Sequencing batch reactor
S_{BS}	Readily biodegradable COD
S_{BSA}	Acetic acid COD
S_{BSC}	Complex readily biodegradable COD
S_{BSP}	Propanoic acid COD
S_c	Function or group of functions describing process kinetics affecting the constituent
SE	Sludge-supernatant flux
SEM	Scanning electron microscope
S_{Fac}	Seepage from the facultative pond
$S_{Fac,E}$	Seepage through the facultative pond embankments
$S_{Fac,F}$	Seepage through the facultative pond floor
SM	Soil moisture
$SMA_{AT,n}$	Mean of the current and previous $n - 1$ daily air temperature records
SS	Settleable solids
$SS_{x,y}$	Sum of squares of the differences for day to be interpolated x and comparison day (with complete flow record) y
S_{US}	Soluble non-biodegradable COD
T	Pond temperature
t	Elapsed time
T_a	Air temperature
TC	Total Carbon
TDP	Total dissolved phosphorus
TDS	Total dissolved solids
$TFSS$	Total fixed suspended solids
$ThOD$	Theoretical oxygen demand
TIS	Tanks in series
TKN	Total kjeldahl nitrogen
t_m	Average time milking herds spends at the dairy
TN	Total nitrogen
TON	Total oxidised nitrogen

TP	Total phosphorus
TPP	Total particulate phosphorus
T_{REF}	Reference temperature
TS	Total solids
TSS	Total suspended solids
T_t	Liquid temperature at time t
TVS	Total volatile solids
TVSS	Total volatile suspended solids
T_w	Water (liquid) temperature
T_z	Temperature at depth z
u	Wind speed
U_{bT}	Biogas bubble terminal velocity
UD3	User defined variable 3
UOW	University of Wollongong
u_s	Surface water velocity
u_x, u_y, u_z	Fluid velocities in the x,y and z directions
u_z	Wind speed measured at height z
V_{An}	Volume of the anaerobic pond
V_b	Biogas bubble volume
VFA	Volatile fatty acid
V_{Fac}	Volume of the facultative pond
v_i	Inflow velocity
VS	Volatile Solids
VSD	Volatile solids destruction
V_z	Liquid volume at depth z
W	Pond width
W_0	Wastewater inflow
W_e	Effluent leaving the anaerobic pond
W_f	Fresh water used for hosing and cleaning
W_i	Irrigated effluent
W_r	Recycled effluent used to wash down the dairy
W_r	Recycled effluent
$W_{r,f}$	Flood wash volume
$W_{r,f}$	Recycled effluent released from the flood wash tank
$W_{r,y}$	Recycled effluent pumped directly onto the holding yard
WSP	Waste stabilisation pond

X_{BC}	Very slowly biodegradable cellulosic material COD
X_e	Endogenous products COD
X_I	Conventionally non-biodegradable particulate COD
X_{IL}	Non-biodegradable lignin COD
X_{IN}	Very slowly biodegradable and non-biodegradable particulate nitrogen
X_{IP}	Very slowly biodegradable and non-biodegradable particulate phosphorus
X_{OP}	Particulate biodegradable organic phosphorus
XRD	X-ray diffraction
X_S	Slowly biodegradable COD
X_{SP}	Slowly biodegradable particulate COD
Y_{CH_4}	Specific methane yield
Y_H	Heterotrophic yield
z	Depth of the supernatant OR height of wind speed measurement
z_{0m}	Momentum roughness height
z_{0v}	Vapour transfer roughness length
z_1	Height of wind speed measurement
z_2	Height of vapour pressure measurement
z_e	Euphotic depth
Z_{OHO}	Heterotrophic biomass COD
Z_{PAO}	Phosphorus accumulating organism biomass COD
z_s	Secchi depth

Chapter 1

INTRODUCTION

Effluent from Australian dairy sheds is dilute, yet potent wastewater generated by the wash down of the dairy parlour and holding yard to remove manure accumulated during the milking of a dairy herd. To farmers facing financial pressures of low farm gate prices the management of dairy shed effluent (DSE) represents a time consuming distraction from their primary concern, milk production. To regulators and consumers who expect environmentally responsible milk production it is a potential source of pollution. The common currency between these two divergent but not mutually exclusive perspectives is the nutrient content of the effluent. Water quality, the prime indicator of environmental performance of dairy farms, is typically characterised in rural areas according to concentrations of nitrogen (N) and phosphorus (P) for the role of those nutrients in eutrophication and associated degradation of waterways. For farmers, the content of N and P in the effluent stream represents the main economic driver for investing in effluent management facilities as it can effectively substitute for a sizeable fraction of the demand for increasingly expensive fertilisers. In this way the containment and recovery of nutrients represents the common goal of effluent management amongst the various stakeholders in the dairy industry. Yet the design and modelling of best management practice DSE systems has been framed in relatively simple terms since their inception, limiting the quantification of the nutrient throughputs and general performance of these systems to very coarse terms. As such, optimisation of the design and management tends to be a process of trial and error for farmers and consultants to resolve, leaving the means to accessing the benefits that accrue from more refined waste management practices, including more efficient nutrient recovery, unexplored, untested and undocumented.

This thesis attempts to shed light on the inner workings of a widely endorsed and adopted form of DSE management – treatment and storage in a two-stage stabilisation pond system with recycling of effluent as flush water and to irrigation – to build a platform from which a more effective approach to handling this carbon and nutrient rich resource can be developed.

1.1 THE AUSTRALIAN DAIRY INDUSTRY

Dairy is one of Australia's most vital rural industries in terms of economic activity and productivity. In the 2011/2012 financial year the industry produced 9.5 billion litres of milk, with a farmgate value of production of \$4.0 billion, placing it as the third largest

industry in the rural sector (Dairy Australia 2012). Some 50,000 people are employed on dairy farms and manufacturing plants, and the flow-on economic activity generated in rural centres is estimated to be equivalent to a regional economic multiplier of 2.5. It is also a significant export industry, with 38% of its product being traded overseas, making up 7% of world dairy trade (Dairy Australia 2013). Deregulation, culminating at the full domestic price deregulation in mid-2000, forced many dairy farmers out of the industry and the remainder to increase their milk production by intensifying their operations. So while the number of dairy farms has steadily declined, the number of cows being milked in Australia and total milk production increased with a peak in 2001-02 (see Figure 1-1). The number of cows and hence milk production has significantly reduced since 2002 due to widespread and extended drought across Eastern Australia. This has caused many farms to reduce their herd or even cease operations. However production appears to be on the rise again with easing of the drought since 2009.

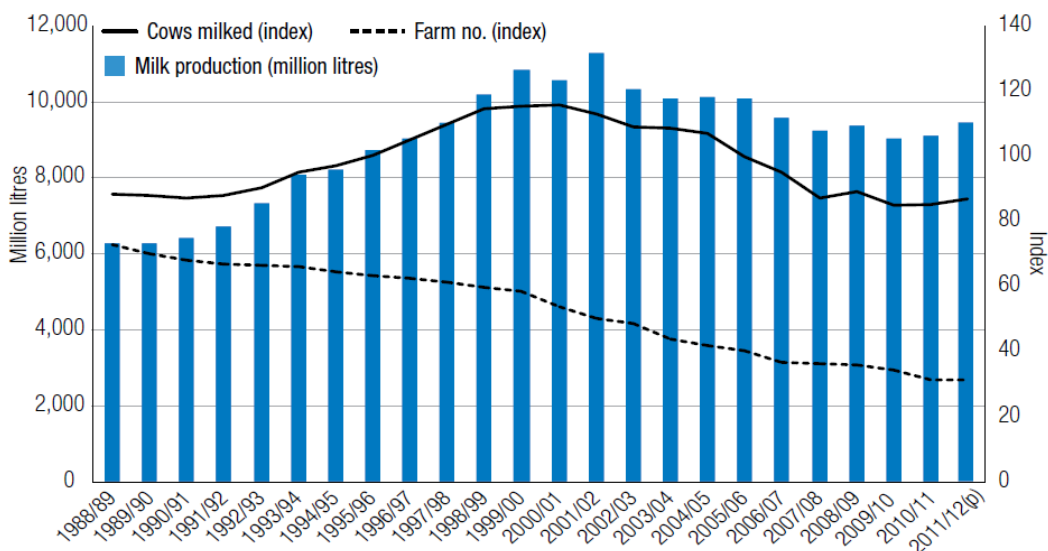


Figure 1-1 Milk production in Australia plotted against indices of farms and cows milked (Dairy Australia 2012)

Dairying in Australia is predominantly pasture-based, with approximately 70-75% of cattle food sourced from grazing under normal climatic conditions (Dairy Australia 2012). Feed lot operations make up a very small minority of dairy farms, and the climate in Australian dairying regions does not require the herd to be housed indoors over the winter. Also expansive land allows for ample feed production, limiting need to import feed. Hence farm and herd management practices are more closely aligned with New Zealand (NZ) practices than those encountered in Europe and the United States (ABARE & MAF 2006). The dairy industry in neighbouring NZ has also been undergoing a similar intensification trend since the mid-1970s as shown in Table 1-1.

Table 1-1 Changes in the Australian and New Zealand dairy industries.

	<i>Number of farms/herds</i>		<i>Herd size</i>		<i>Average annual milk production (L cow⁻¹ y⁻¹)</i>	
	<i>1979/80</i>	<i>2011/12</i>	<i>1979/80</i>	<i>2011/12</i>	<i>1979/80</i>	<i>2011/12</i>
Australia	21,994	6,770	85	240	2,848	5,926
New Zealand	16,506	11,798	124	393	2,930	4,128

1.1.1 Water Consumption

Dairy farming is one of Australia's most water-intensive industries. In 2004/05 the sector consumed around 2,276 GL of water, constituting 19% of agricultural demand in Australia (Khan et al. 2010). The vast majority of this goes to irrigation of pasture and fodder crops (Rogers & Alexander 2000), with some 56% of farms relying on irrigation to support production (NLWRA 2008). The next major use is stock water, while dairy shed operations and cleaning constitute just 1% of total water demand on a typical dairy farm (Rogers & Alexander 2000). A wide-reaching survey of Victorian farms found average water use at the dairy shed was about 4 ML yr⁻¹, or 42 L cow⁻¹ d⁻¹. Extrapolating using 2012 cow numbers (Dairy Australia 2012), this amounts to around 25 GL per year across Australia, which is on par with the annual demand of a large Australian inland town.

Benchmark figures for Australian dairies range from 205 L water per litre of milk produced (Rogers & Alexander 2000) to over 1500 L water per litre milk (Khan et al. 2010). The high variability in these figures is related to the range of irrigation practices, with some farms being fully irrigated (particularly in the Murray dairy region in Victoria, NSW and SA), while rainfall supplies a much larger portion, if not all of pasture demand for those in coastal regions. Much of the water used on dairy farms is self-extracted, although water is also sourced from irrigation providers, town mains supplies and effluent reuse (Khan et al. 2010). Being almost entirely pasture-based, dairying in Australia is highly prone to climate variability, with drought conditions dramatically reducing productivity as noted earlier.

1.1.2 Fertiliser Use

The dairy industry is estimated to be responsible for between 25-30% of total fertiliser demand in Australia (IPNI 2013) and up to 50% of all fertiliser applied to Australian pastures (Australian Government 2013). The effect of deregulation on the industry has led to intensified farming practices, with increased stocking rates and higher per cow milk production, creating an even greater reliance on imported nutrients. Over the past

20 years dairy farmers have increased their nitrogen fertiliser use between 4 and 10 times, now using around 180,000 tonnes per year (Gourley 2012). Fertiliser use varies greatly between farms and across the dairying regions, with average urea-based fertiliser use ranging from 93 to 216 kg/ha (IPNI 2013).

High rates of fertiliser use appear to be over-compensation for Australia's typically nutrient deficient soils. A broad reaching and comprehensive study of farm nutrient balances across Australia revealed that Australian dairy farms exhibit low nutrient efficiencies (nutrient exports expressed as a fraction of imports), with most farms studied having substantial surpluses of all the major nutrients (Gourley et al. 2012). High level results from the study are summarised in Table 1-2.

Table 1-2 Nutrient surpluses and efficiencies on Australian dairy farms.

<i>Nutrient</i>	<i>Median surplus (kg/ha)</i>	<i>Median efficiency (%)</i>
Nitrogen	193	26
Phosphorus	28	35
Potassium	74	20

1.2 DAIRY SHED EFFLUENT

Dairy shed effluent (DSE), otherwise known as dairy farm or farm dairy effluent or dairy shed waste, is the wastewater generated on dairy farms by the washing down of milking facilities and surfaces in the milking parlour, hygienic cleaning of milking equipment, and hydraulic flushing of holding yards, feed pads, and other concrete-lined stock containment areas. Treated effluent from solids separation facilities, stabilisation ponds and other treatment technologies also falls under the umbrella term of DSE, as does contaminated run-off from stock containment facilities.

The waste load generated on a typical farm is equivalent to that from a small community, but with lower volumes of water used to convey the waste, DSE is significantly more concentrated. The manure load that is deposited at the dairy shed and holding yards ranges from 6% to 15% of total manure generated by the herd (Birchall, Dillon & Wrigley 2008; Bolan et al. 2009). However, growth in herd sizes produces concomitant growth in overall manure loads, including that which becomes DSE. In addition, in both Australia and NZ there is a growing trend towards feeding herds on feed pads, many of which are connected to the same DSE management system that services the dairy (around 50% in Australia) (Watson & Watson 2012; Bolan et al. 2009). In net terms this means that DSE systems play an increasingly

important role in preventing pollution and capture a larger fraction of the farm nutrient budget.

1.2.1 DSE Management

Management of DSE generally encompasses the minimisation, collection, handling, storage and treatment of the wastewater for the purposes of effluent reuse by land application and effluent recycling as flush water. It also covers the management of the various by-products from the effluent management processes including manure solids from solids separation facilities and sludge from primary ponds. The stated objectives of DSE management are typically pollution control to satisfy regulatory obligations and protect catchment water quality, and resource efficiency and recovery which provides an economic incentive for adopting best management practice (BMP). It is anticipated that control of carbon emissions will increasingly become a key consideration in the design and implementation of DSE management systems.

In Australia, BMP is predicated on the retention of all waste products within the farm boundaries. Disposal of effluent, treated or otherwise, directly into waterways is effectively prohibited under the various state laws. Hence land application has become the primary means of effluent disposal under BMP guidelines, which essentially describe measures to ensure that adopting this form of disposal does not merely transform DSE from a point source to a diffuse source of water pollution. In NZ BMP is similar to Australian BMP in terms of technology, having gradually shifted from two-stage pond systems discharging directly to waterways to application to land since the 1990s (Houlbrooke 2008). Direct discharges to waterways do, however, still occur as legacy or consented activities (Houlbrooke 2008; Bolan et al. 2009).

BMP will often dictate specific approaches to accommodate localised conditions. However in broad terms the main options described in BMP guidelines are:

- effluent reuse by direct application to land with or without short term (up to several days) storage capacity;
- land application with pond storage (one or more in series) to hold effluent over the wettest period (months) of the year;
- partially closed effluent recycling system incorporating treatment and storage in stabilisation ponds (typically two or more in series), recycling effluent as flush water and effluent reuse by land application.

Solids separation may also be incorporated as preliminary treatment to all of the above options.

On account of the control they provide over land application rates and timing, there has been a widespread shift towards pond systems in Australia. A recent survey of 800 dairy farmers in the eight major dairying regions of Australia found that 75% of farms used a pond system to manage their waste stream, up from 54% in 2000 and 73% in 2006 (Watson 2006; Watson & Watson 2012). Of these, 65% had systems comprising two or more ponds, up from 52% in 2006. The trend towards adopting pond systems has been consistent across all major dairying regions, and is particularly evident amongst farms with larger herds. Conventional DSE pond systems are designed primarily to provide storage until the effluent is ultimately applied to land, although secondary and tertiary ponds provide the additional benefit of enabling the use of conventional irrigation equipment for effluent reuse. They may consist of one anaerobic pond alone or a series of ponds starting with an anaerobic primary pond and either facultative, anaerobic, aerobic or maturation secondary and tertiary stages.

Recycling of effluent is generally adopted for the water saving benefits associated with substituting fresh water used for flushing of the holding yard, which is more common amongst farms in dry regions (e.g. western Victoria, Rogers & Alexander (2000)) and those dependent on (expensive) town water supplies. Generally used in combination with two or more ponds to maximise effluent quality, recycling also reduces the storage requirements of pond systems by reducing net inflow, making it advantageous to farms in high rainfall areas. And if effluent irrigators are located a sizeable distance from the dairy shed, the reduced irrigation pumping needs can provide energy cost savings (DairyCatch 2006). Recycling is a relatively new addition to BMP and little is known about rates of adoption and performance. A survey of over 1600 dairy farms in the state of Victoria found that only around 18% of farms recycled their effluent back to the dairy (Calligan 2010). However, there is evidence to suggest that recycling is increasingly being incorporated into both new systems and system upgrades informed by BMP. In the NSW Southern Highlands region that since 2003 received considerable government support for BMP system upgrades, 4 farms out of the 9 farms with multiple pond systems capable of recycling effluent used the effluent for flushing the dairy (Sydney Catchment Authority 2010). The Resource Not Waste project in South Australia documented leading BMP systems across the state to promote the benefits of adopting BMP. Thirteen of the sixteen case study farms recycled effluent for flush water (DairySA 2008).

1.3 RESEARCH GAPS

As the fraction of manure captured in DSE rises on Australian and NZ dairy farms, the imperative to ensure management systems meet performance expectations and to quantify and improve nutrient recovery rates continues to grow. With pond systems being the dominant form of DSE management, there is a need to expand our understanding of these systems beyond coarse aggregate indicators such as total volatile solids, total P and total N so that optimisation can move beyond rough guides and rules of thumb. There is also value in developing a more sophisticated understanding of the treatment processes that determine the performance of a pond system and the fate of the nutrients captured within it.

1.3.1 Treatment and Nutrient Partitioning and Losses in DSE ponds

In particular there has been limited research into understanding, let alone predicting, the quantities, forms, partitioning and transformations of nutrients both entering and leaving DSE ponds. Pond systems are known to reduce the loads of total N and P in DSE, and this is generally attributed to sedimentation of the organically-bound fractions and volatilisation of ammonium. Yet despite the importance attached to harnessing effluent nutrients in the case made to farmers for implementing DSE BMP, there has been little to no research related to:

- quantification of actual nutrient removal;
- the role of pond biology or chemistry in nutrient cycling and removal;
- the forms and relative loads of the nutrients in the sludge of the primary pond and the effluent that leaves a pond system;
- the influence of pond nutrient dynamics on nutrient recovery through land application of effluent and sludge.

There are numerous published and unpublished studies that characterise raw DSE and DSE from treatment/storage ponds (for example Hickey, Quinn & Davies-Colley 1989; Sweeten & Wolfe 1994; Longhurst, Roberts & O'Connor 2000; Sukias et al. 2001; Skerman, Kunde & Biggs 2006). There have also been a number of studies that have looked more closely at DSE pond function such as Mason (1996), Sukias et al. (2003), Dawson (2003) and Fyfe (Fyfe 2004). Much of this research, however, has been undertaken in NZ with a focus on system effluent quality and as a result considers only secondary facultative pond performance. Moreover, it has not generated more advanced models of nutrient cycling that might inform effluent application planning. There is also useful data available from studies undertaken in the US, but much of it is

now out-dated, and fundamental differences in herd management, particularly feed regimes and confinement, complicate the translation to the Australian context.

The most powerful tool available for designing and testing DSE management systems available in Australia, MEDLI (Gardner et al. 1996; Gardner et al. 1998; Vieritz et al. 1998), contains a model that applies a dynamic mass balance to pond systems holding effluent for subsequent land application. However, the technical manual states that ‘no attempt has been made to model the chemical interactions within the pond nor the effects of temperature on these reactions’ (Casey & Atzeni 1998, pp.4–16). Moreover, ‘sludge accumulation rates and the concentrations of nutrients and salt in the sludge are yet to be validated under Australian conditions’. Previous observations of net increases in the plant available (soluble) nutrient fraction (ammonia and orthophosphate) in operational primary DSE ponds (Dawson 2003; Fyfe 2004) suggest that the current descriptions of the nutrient content of pond effluent are incomplete, particularly for the purposes of determining its role as a fertiliser substitute.

Only 20% of farmers actually test the nutrient concentrations of their effluent before applying it to land (Watson & Watson 2012). This alone suggests that better appreciation of nutrient partitioning between pond sludge and effluent would be a valuable contribution to BMP. Indeed with accurate data and modelling, prediction of effluent nutrient loads could be achievable and design tools such as the Dairy Pond calculator (Skerman 2004a), the Effluent Toolkit (McDowell & Birchall 2010) and MEDLI can be validated and/or improved (Skerman 2004c). Moreover, a more complete depiction of pond effluent nutrient fractionation would facilitate strategic land application schedules that are more closely integrated with fertiliser regimes, thereby optimising pasture uptake, and minimising soil accumulation, losses via runoff and drainage, and subsequent degradation of catchment water quality.

1.3.2 Effluent Recycling

Despite increasing adoption of effluent recycling for yard flush water, very limited attention has been paid to monitoring and evaluation of such installations, in Australia or elsewhere. Blockages of pumps and pipework caused by crystalline deposits of mineral struvite ($\text{MgNH}_4\text{PO}_4 \cdot 6\text{H}_2\text{O}$) have been reported since the 1970s (Booram, Smith & Hazen 1975; Westerman, Safley & Barker 1985; Westerman, Safley & Barker 1990). There is also potential for rising salinity to negatively impact on pond biological function and crops and soils receiving land applied effluent. The Dairy Australia *Effluent and Manure Management Database* (Birchall, Dillon & Wrigley 2008) makes brief reference to effluent recycling, noting that struvite precipitation is caused by

accumulation of salts within these partially closed loop systems, with the rate of accumulation primarily being determined by the ratio of fresh water to recycled effluent. However, besides some laboratory simulations and experiments (Hill, McCaskey & Hamilton 1981; Georgacakis & Samantouros 1986) and a couple of theoretical modelling exercises predicting salinity levels during continuous operation of livestock flush water recycling (Atzeni, McGahan & Casey 1995; Mason & Flowerday 2005) there has been no published literature on the factors and conditions that promote salt accumulation and struvite precipitation in such systems. Accumulation of salts and nutrients in DSE recycling systems has in fact previously been identified as a research priority for DSE management in Australia (Hubble 2002).

1.4 IMPLICATIONS

An enhanced understanding of DSE stabilisation pond systems and the nutrient value of effluents and sludges will help to address farm-wide nutrient inefficiencies by facilitating strategic and beneficial land application. While effluent and sludge contain useful concentrations of nutrients, other constituents such as suspended solids, salts and pathogens can have negative impacts on soil and water quality when application rates are excessive. Moreover the relative fractions of each nutrient are not agronomically balanced in pond effluent and sludge, which can lead to over- or under-supply of one or more nutrients (typically P and potassium) even when the land application rate is appropriate to the net budget of another nutrient.

Hence it is not uncommon for the touted fertiliser value of effluent to be squandered as, in the absence of informed guidance, farmers opt to apply effluent and/or sludge to a readily accessible, dedicated (even sacrificial) paddock that eventually becomes saturated with nutrients and exhibits only a limited pasture yield response to the effluent (Gourley, Powell, et al. 2007; Dougherty & Stein 2009; Silver, Whitelaw & Malone-McGrath 2009). Indeed, 37% of farms apply DSE to 10% or less of the total farm area, despite effluent typically capturing around 10% of the total manure nutrients (Watson & Watson 2012). This overloading is compounded as stock access to the area is limited to avoid exposure to freshly applied effluent, thereby constraining or even removing one of the key nutrient removal pathways that would otherwise help maintain an equilibrium with nutrient inputs. The presence of an overloaded effluent/sludge application area has implications for farm productivity as it reduces the amount of land that is available for grazing. It also poses stock health and environmental risks.

In the short-term, effluent that is applied to land during or shortly before a rainfall event is prone to entrainment in surface run-off (Fyfe 2004; Houlbrooke, Horne, Hedley,

Hanly & Snow 2004) and sub-surface drainage (Houlbrooke, Horne, Hedley & Hanly 2004; Houlbrooke, Horne, Hedley, Hanly, Scotter, et al. 2004; Houlbrooke et al. 2008) contributing to degradation of surface waters and groundwater. Longer-term build-up and mineralisation of organically bound N and P in the soil profile creates a pool of labile phosphates and mobile N species that contributes to nutrient losses to waterways via runoff and drainage (Holford, Hird & Lawrie 1997; Lawrie 1998; Houlbrooke, Horne, Hedley, Hanly & Snow 2004). Soil structure may be compromised by accumulating sodium (Na) and K, which magnify the dispersive properties of clays (NSW DEC 2004).

Another issue related to mismanaged effluent application to land is the potential for metabolic disorders caused by imbalances in soil nutrients (Bolan et al. 2009). Excess soil K can cause luxury uptake in pasture, which increases the K intake of grazing animals and suppresses the animals' uptake of magnesium (Mg) and calcium (Ca) (Wang, Magesan & Bolan 2004). Mg deficiency can lead to hypomagnesaemia or 'grass staggers', while Ca deficiency increases the risk of hypocalcaemia or 'milk fever'. Both disorders can reduce milk yield and create serious health problems in the herd. The high alkalinity of DSE may also contribute to alkalosis.

Thus, when effluent application is managed poorly, a valuable section of the farm can become a source of diffuse pollution and in the worst cases, unviable for grazing.

A key recommendation from a recent Australia-wide analysis of farm nutrient balances to improve nutrient efficiencies on farms is to implement more strategic effluent applications (Gourley et al. 2010). Developing an understanding of nutrient loads in DSE products is critical to developing a whole-of-farm nutrient budget which aids decision-making with regards to grazing, cropping and fertiliser use (Rogers & Alexander 2000) and helps to increase nutrient efficiency. Moreover, it also helps to make the case for investment in effluent management facilities, which when accounting for nutrient benefits, can be shown to have a return period of 4 to 7 years (Dairy Australia 2009). As pointed out by Jacobs & Ward (2007a), a better appreciation of the benefits of effluent reuse is required to encourage more sustainable effluent reuse practices, and key to this is a more complete understanding of the fate of nutrients in DSE pond systems.

1.5 RESEARCH AIMS AND OBJECTIVES

The central aim of this thesis is to expand current understanding of the behaviour and performance of DSE stabilisation pond systems to facilitate better design, operation

and integration with farm nutrient budgeting. Five specific objectives were identified to help achieve this aim:

1. Undertake a review of the literature related to DSE and its handling and treatment in stabilisation ponds, current approaches to modelling DSE ponds, and leading edge approaches used in modelling stabilisation ponds more generally.
2. Design and implement a comprehensive field and laboratory data collection program on a typical Australian working (commercial) dairy farm.
3. Examine DSE pond hydrology, water quality dynamics, hydraulic characteristics and hydrodynamic behavior, treatment performance and wastewater constituent mass flows using the data collected under objective two.
4. Develop and calibrate a dynamic mechanistic DSE pond model.
5. Use the model developed under objective four to undertake scenario analyses and develop recommendations for alternative approaches to pond design, construction, modelling and management.

Objective one establishes the research context for this thesis, but also sets out to bridge the knowledge gap that exists between design, monitoring and modelling of DSE pond systems and the more advanced field of urban wastewater stabilisation pond research. The second objective was a necessary precursor to the subsequent objectives and addresses a significant data shortage in relation to monitoring of Australian DSE pond systems. Objective three sought to produce a detailed and unprecedented (at least in Australia) analysis of DSE pond characteristics, behaviour and performance.

The generation and analysis of the data underpins objective four, the development of a modelling platform to facilitate a move towards detailed, dynamic analyses of the fate of carbon, nutrients and salts in DSE management systems. This highlights another gap in existing research – the availability of a sufficiently detailed and comprehensive data set upon which to build and calibrate a dynamic model. As stated by Sah et al. (2012), dynamic biokinetic modelling of stabilisation pond systems is constrained not by analytical or computational methodologies but by the availability of the data required to calibrate such models. Indeed, while there are some high quality and detailed published data sets, invariably they lack at least one essential component required for modelling. For example Sweeten & Wolfe (1994) undertook detailed, long-term monitoring of DSE pond influent and effluent characteristics on three dairy farms, but data on in-pond water quality conditions, hydrology, sludge and in-pond conditions are

limited. Mason (1996) undertook rigorous monitoring of a facultative pond in NZ, but again the focus lay with effluent characteristics.

This brings us to the modelling objectives of the thesis. Firstly, as identified in the literature review, there are no precedents of dynamic modelling of the physical, chemical and biological processes that drive treatment in DSE stabilisation ponds. There are, however, numerous examples of dynamic models of stabilisation ponds treating other forms of wastewater (predominantly urban) ranging from the early facultative pond models based on idealised reactor hydraulics of Fritz et al. (1979), to the fully integrated biokinetic and computation fluid dynamic model of Sah et al. (2011). Building on the findings of the literature review, the fourth thesis objective sought to apply the knowledge of wastewater treatment process modelling developed in other wastewater treatment fields to the relatively unexplored territory of DSE treatment. The final objective pertains to employing the model to explore issues of practical relevance to the management of DSE using pond systems.

1.6 RESEARCH SCOPE

As depicted in Figure 1-2, the research described in this thesis was multi-faceted in order to satisfy the objectives outlined above. The initial literature review under objective one was a comprehensive investigation of the state of knowledge in the various fields that are pertinent to the research topic and draw them together to form a coherent basis for the field work and modelling components of the research. The content of the literature review chapter however, does not represent the extent of the literature reviewed for the thesis in its entirety. Several of the chapters that follow have their own discrete literature review components.

Data collection for objective two involved developing and managing an intensive field surveying, monitoring and sampling program on an independent, commercially run dairy. First the bathymetry of the stabilisation ponds was established by a topographical survey. Supernatant water quality and depth, effluent flow and meteorological conditions were all monitored in real time using automated, logged field sensors. Wastewater/effluent entering and leaving each pond was regularly sampled for laboratory analysis of wastewater constituents including aggregate solids and organic constituents, and the major nutrients, cations and anions. Water quality profiling of the ponds to gauge spatial variation was undertaken seasonally, together with sampling and depth measurements of the sludge in the primary pond. An additional discrete piece of field work was an experimental study of the hydrodynamics

of the primary pond that involved tracking the movement of 'drogues' as they moved with the flow through the pond.

The data collected from the field monitoring and sampling program informed analyses of the system water balance and constituent mass flows under objective three. The water quality monitoring and the hydrodynamics study were primarily undertaken to inform the modelling component of the research, although the findings from each demanded their own chapters in this thesis. The water quality data were used to investigate the prevailing conditions and processes occurring within the ponds, while the results of the hydrodynamics study were combined with various analyses of pond construction, dispersion and energy inputs to develop a conceptual model of the pond hydraulic regime. These, together with the water balance and nutrient partitioning analyses, guided the modelling component of the research.

The scale of the field work component of the research demanded that a pragmatic approach to the modelling objectives (four and five) be adopted. Rather than build a numerical model from scratch, existing capability in activated sludge modelling was adapted to the specific application of the anaerobic pond. The development of a model of the facultative pond was ruled out of the scope of this thesis. The anaerobic pond model was implemented using the BioWin software package (EnviroSim Associates Ltd. 2007) and required the development of a detailed fractionation of influent aggregate wastewater constituents, identifying DSE-specific values for key kinetic and stoichiometric parameter values, and augmentation with additional process equations. The model was calibrated using the wastewater and sludge sampling data, and the outputs were used to gauge the greenhouse gas intensity of handling effluent in anaerobic ponds. The model was also subjected to a rigorous sensitivity analysis.

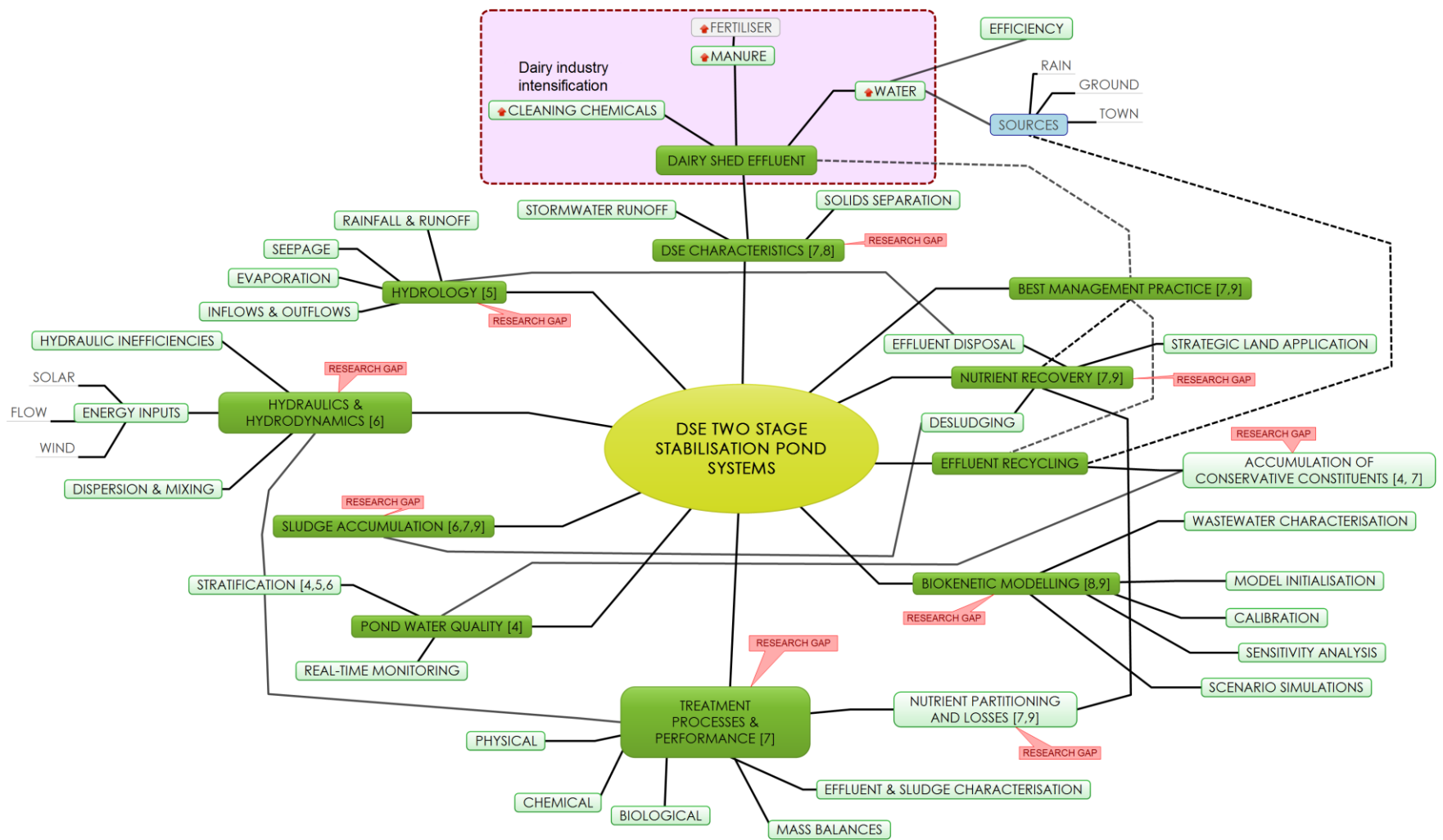


Figure 1-2 Topic map of the thesis content. Chapters that deal with particular topics are given in brackets. Dashed lines represent connections that are relevant beyond the topic of DSE stabilisation ponds.

To satisfy objective five the calibrated model was reconfigured to examine pond performance under different scenarios related to anaerobic pond function including the presence of a hydraulic dead zone, increasing the organic loading rate, annual desludging and reducing seepage losses. The outputs from the four simulations were analysed to determine the implications for treatment efficiency and nutrient losses and recovery of each scenario, demonstrating the utility of the model for optimising pond design and management.

1.7 THESIS OUTLINE

The scope of work described above has been divided into eight chapters. The first, Chapter 2, presents the literature review that outlines the research context of the chapters that follow. Chapter 3 describes the process of selecting an appropriate site at which to base the field work component of the research and the overall design of the monitoring and sampling program adopted for the site. Chapters 4 to 7 describe the different aspects of the field work component of the research, each comprising its own discrete methodology, results and discussion sections. Chapter 4 presents the acquisition, analysis and interpretation of the real time and water quality profiling data. The data and modelling used to develop the water balance of the pond system are presented in Chapter 5. Chapter 6 examines the hydraulics and hydrodynamics of the two ponds and includes the write-up of the drogue tracking field experiments. Chapter 7 explores treatment performance and nutrient partitioning based on the wastewater sampling data and the results from the water balance. Chapter 8 details the initialisation of the anaerobic pond model, including the fractionation, parameter identification and augmentation tasks as well as input data pre-processing. Model calibration, sensitivity analysis and scenario simulations are presented in Chapter 9. Conclusions and recommendations arising from the research are given in Chapter 10.

Chapter 2

LITERATURE REVIEW

This chapter reviews the literature related to the design, performance, characterisation and modelling of waste stabilisation pond systems with specific reference to the treatment of DSE. First an overview that details typical flows and composition of DSE is provided to give a sense of the loading that DSE pond systems receive. The implications of sampling method on data variability and reliability are also considered. This is followed by a review of research related to the main forms of DSE treatment used in Australia, namely solids separation in trafficable solids traps and anaerobic and facultative stabilisation ponds. A mix of various alternative, experimental modes of treatment is also canvassed to extract useful insights that may be applied to this study. In addition, research into the implications of effluent recycling for use as flush water at the dairy is covered. In particular the research on salt accumulation and the occurrence of and the conditions that promote struvite precipitation are reviewed.

The review then shifts focus to modelling of DSE treatment systems. First, existing models used in Australia to assist design of DSE systems are reviewed with specific focus on stabilisation ponds. Consideration is then given to modelling of waste generation on dairy farms and treatment of DSE by alternative technologies. The final section of the review looks closely at the various models that have been developed to explain and predict performance of stabilisation ponds treating other forms of wastewater, specifically sewage ponds. Focusing on models capable of dynamic simulation as opposed to those based on assumptions of steady state conditions, the review encompasses dedicated mechanistic 'biokinetic' models, models that attempt to reflect pond hydraulics with compartmental reactor arrangements, adaptations of biokinetic models developed in other fields (e.g. activated sludge modelling), and models that draw together dynamic models of pond hydraulics and biogeochemical processes.

2.1 EFFLUENT FROM AUSTRALIAN DAIRY FARMS - DSE

Australian dairy farms are generally pasture-based and therefore do not confine or house the herd for extended periods. Hence the majority of DSE is generated following milking when the accumulated manure from confining the herd in the holding yard and the milking parlour is hosed or flushed away and the milking machine and milk vats are cleaned. Wastewater flows from the dairy shed thus occur in discrete bursts two or three times a day, depending on the milking regime of the farm. The manure contained

in this wastewater amounts to between 6 and 15% of the total manure production of the herd, depending on the set-up and efficiency of the milking process (Birchall, Dillon & Wrigley 2008; Bolan et al. 2009). Similar herd management and milking practices are prevalent in New Zealand (NZ) (Bolan et al. 2009).

Enclosed or covered feed pads, however, are becoming an increasingly common feature on Australian pasture-based farms (Watson & Watson 2012) as operators seek to maintain milk production during periods of pasture shortage (drought), or to increase the rate and quality of milk production with supplemental feed (Birchall, Dillon & Wrigley 2008). Some feed pads are dry scraped with the collected manure solids handled separately to the DSE. The majority though are hydraulically flushed and drain to the dairy effluent management system (Watson & Watson 2012), creating additional wastewater slugs at a frequency and concentration that will vary with the amount of time the herd spends on the pad (Davison & Andrews 1997). Loafing or stand-off pads designed to protect pastures on soils prone to pugging in high rainfall areas are typically dry-scraped to remove accumulated manure and typically do not contribute to the loading of a DSE management system. In NZ flushed feed pads and winter housing facilities that drain to DSE systems are also becoming more common (Bolan et al. 2009).

The primary components of dairy shed and feed pad effluent are water and cow excreta, but typically a range of other contaminants will be present as listed in Table 2-1. The following sections review published data on dairy effluent volumes and characteristics. Since feed pad usage is less established and more variable than milking practices, less is known about the nature of feed pad effluent streams. Hence the information presented in the following sections focuses primarily on DSE, although many of the same principles will apply to feed pad effluent.

2.1.1 Dairy Water Usage and Effluent Flows

On Australian dairy farms the majority of water consumed at the dairy and the feed pad is used for cleaning purposes; hence wastewater volumes are closely aligned with water usage. A significant portion is also used for chilling the milk, although it is common for this water to be recirculated back into the cleaning supply. Hygiene standards dictate the use of fresh water for cleaning of milking machinery, milk vats and all surfaces in the milking area including cups, teats, floors, fencing and cows. Fresh water is typically sourced from nearby creeks, rivers, channels, springs, bores, dams, rainwater tanks or in some cases town water supply (McDonald 2005). At the end of the milking session concrete holding yards are also washed down to remove

accumulated manure, using hand held hoses, fixed high-pressure hydrants and hoses, and/or a flood wash system. Flood wash systems provide significant labour savings, but they also use larger volumes of water which require larger wastewater collection, holding and treatment facilities. Since, however, holding yards are not in the immediate vicinity of the milk storage, the use of recycled treated effluent to wash down these areas is generally permitted, providing scope for substantial fresh water savings (Rogers & Alexander 2000; McDonald 2005).

Table 2-1 Components of DSE

<i>Constituent</i>	<i>Source</i>
Water	Hosing and flushing of milking parlour, holding yards and feed pads; milking machine and milk vats sanitation; stormwater runoff (where not diverted)
Manure (mixed faeces and urine)	Cattle
Manure residues including organic matter, nutrients, salts, pathogens	Recycled effluent
Milk	Spillages, cleaning of milking machine and milk vats
Feed	Milking stall bales
Soil and other debris (including sand, gravel)	Cattle hooves
Salts	Manure, recycled effluent, milking machine cleansing
Detergents, disinfectants	Milking machine cleansing
Veterinary chemicals	Treatment of cattle

While the configuration and capacity of the milking facility and the herd size are often nominated as key determinants of total water use and wastewater volumes (Loehr 1984), the correlation between these factors has been found to be relatively poor (Brewer, Cumby & Dimmock 1999; McDonald 2005; Calligan 2010) due to the large array of other factors that influence dairy water consumption. Much of the variability in water demand and wastewater flows between farms is related to differing degrees of recycling, reuse and other efficiency measures employed (DPI 2009). Wastewater flowrates also tend to be highly variable due to the differing nature and timing of the various end uses at the dairy. During milking wastewater flow is relatively low and intermittent as hoses are used in short bursts to keep the milking area clean. The flow peaks after milking is finished when the majority of cleaning, including washing of milking machines, is performed. If a flood wash system is used to flush the holding yard, the peak wastewater flow can be as high as 1.8 m³/s (Birchall, Dillon & Wrigley 2008).

Very few studies have actually set out to quantify water use let alone wastewater flows in Australian dairies. Calligan (2010) collated and analysed water consumption data collected between 2001 and 2009 from some 1500 dairy farms in Victoria. Overall mean water consumption at the dairy shed was found to be $42.4 \text{ L cow}^{-1} \text{ d}^{-1}$ but showed enormous variability ranging from 1 and $385 \text{ L cow}^{-1} \text{ d}^{-1}$. Consumption varied significantly by region and dairy type while effluent generation was only significantly different between dairy types. An earlier survey of 114 Victorian dairy farms found daily dairy shed water consumption varied between 3.7 and 138 and averaged $32 \text{ L cow}^{-1} \text{ d}^{-1}$ (Rogers & Alexander 2000). As much as 70% of this demand came from hosing/flushing manure from dairy pits and holding yards. In an analysis of total effluent released into natural waters across NZ, Flemmer & Flemmer (2008) used an average wastewater generation estimate of $50 \text{ L cow}^{-1} \text{ d}^{-1}$, a figure which has been used or cited repeatedly in NZ DSE-related publications including Mason (1996), Wilcock et al. (1999), Longhurst et al. (2000), DEC (2006) and Bolan et al. (2009) without reference to the data from which it was generated.

The only known published study that has actually set out explicitly to measure flows from a DSE system in Australia or NZ was that undertaken by Sukias, Tanner & Nagels (2003). Tipping buckets installed at the outflow from secondary facultative ponds on 5 different farms in the Waikato region of NZ produced a mean flow, after rainfall gains and evaporation and seepage losses, of $38 \text{ L cow}^{-1} \text{ d}^{-1}$. In a separate study, Sukias et al. (2003) recorded effluent flows from an anaerobic pond into a facultative pond averaging $15 \text{ m}^3 \text{ d}^{-1}$ or $44 \text{ L cow}^{-1} \text{ d}^{-1}$ (not correcting for other hydrological gains/losses) and peaking in late summer. In a study of the performance of constructed wetlands receiving treated DSE from an anaerobic pond, Geary & Moore (1999) recorded outflows from the pond of $6 - 10 \text{ m}^3 \text{ d}^{-1}$, which equated to approximately $55 - 90 \text{ L cow}^{-1} \text{ d}^{-1}$.

Dairy water usage and wastewater flows on dairy farms in the US differ substantially from Australian and NZ data due to different herd and manure management practices. For example figures presented by Van Horn et al. (1994) indicated that water used for flushing manure and cleaning the dairy parlour and milking equipment on a typical US farm was at the time around $355 \text{ L cow}^{-1} \text{ d}^{-1}$. Presumably this level of water consumption allows for much longer periods of herd confinement through the day (or permanent confinement). A dairy water use and effluent characterisation study undertaken in Texas, US by Sweeten & Wolfe (1994) measured water consumption for manure removal and sanitation across 11 farms with herds of between 150 and 1500 head over a period of almost 2.5 years. Average daily consumption was $150 \text{ L cow}^{-1} \text{ d}^{-1}$

and ranged between 47 to 262 L cow⁻¹ d⁻¹. Again the higher water use was related to the longer times the herd spent in confinement (estimated to be around 4 hours per day), although water used to clean cows before milking is also a factor. A survey of 20 farms in the major dairying regions of England and Wales found that 'dirty water' flows including flows from feed 'clamps' and manure heaps as well as manure flush waters were of similar magnitude and variability to effluent flows reported in Australia, ranging from 7.5 L cow⁻¹ d⁻¹ to 167 L cow⁻¹ d⁻¹.

The overriding theme from this review appears to be that dairy water use and effluent generation is not simply a function of the herd size or other variables. Rather it is determined by an array of factors including the many and varied characteristics of the dairy, the milking and cleaning methods of the dairy operators, and environmental factors including climate and water source. Indeed variability in water use would be a significant factor behind the variability in effluent characteristics noted in the following section.

2.1.2 Raw DSE Characteristics

Being essentially a slurry of cow manure, DSE is a moderately strong form of organic wastewater with high oxygen demand and particulate solids load. Due to the enriched nutrient (N, P and K) content of improved pasture that dairy herds graze, it also tends to have elevated nutrient concentrations. The quantity and composition of DSE tend to be highly variable both between individual farms and over time on a particular farm (Hubble & Phillips 1999; Longhurst, Roberts & O'Connor 2000; Dawson 2003; Fyfe 2004; Hawke & Summers 2006). Differences in waste characteristics between farms are attributable to the unique site conditions, herd breeds and sizes, cow live weights, pasture and feed supplements, milk production scale and intensity, milking practices, feed pad usage, and water sources and consumption of individual dairy farms. The variability of DSE composition over time on a given farm is due to the inconsistent nature of the factors that influence the volume and constituent loading of the waste stream. These determinants vary from day to day and over the course of a season and include (McDonald 2005):

- herd size;
- time spent on holding yards, milking and on feed pads;
- manure characteristics related to cattle breed, age, live weight, milk production and feed type and level;
- stress experienced by the herd during milking;

- distance travelled between the paddock and the dairy;
- type of wash down system and other water uses;
- milking machine and milk vat capacities and cleaning methods;
- quantity of recycled effluent used in flushing;
- solids separation;
- rainfall and use of stormwater diversion.

2.1.2.1 Australia

There is very little published material from Australia documenting DSE characteristics. A widely referenced set of data is that produced by Wrigley (1994) from sampling DSE from a number of farms in Victoria. However, with increasing herd sizes, changing milking and effluent management practices, amongst other sector-side shifts, these data can now be considered out-dated. More recently (in 2006), raw DSE samples were collected from sumps being pumped out to land on 21 different farms in the Gippsland region of Victoria for analysis of nutrient content (McDonald 2013, pers. comm. 18 January). Average concentrations for total N, P, K and sulphur (S) were 517, 99, 519 and 61 mg L⁻¹, respectively. The data exhibited significant variability, with coefficients of variation ranging between 0.58 and 0.71. However, in the absence of information about the sampling methodology or the farm system, no inferences can be made as to the source of the variability.

Research involving the author undertaken through the University of Wollongong (UOW) between 1999 and 2003 produced numerous data sets on DSE characteristics, the ranges of which are presented in Table 2-2. Samples were collected at various times from eight commercial dairy farms in the Southern Highlands and Shoalhaven dairying regions of NSW. The variability between farms, even of similar herd sizes, is clearly apparent. There appears to be a pattern of lower and more concentrated effluent flows on farms that apply effluent directly to land, which would be related to the limited capacities of the pump-out sumps of those systems. Dairies with pond systems can be more liberal with water use, allowing two farms to implement flood washing of the holding yard.

Table 2-2 Raw DSE characteristics recorded on dairy farms in the Southern Highlands and Shoalhaven dairying regions of NSW, Australia (data from the University of Wollongong).

<i>Farm</i>	<i>A</i>			<i>B</i>			<i>C</i>			<i>D</i>			<i>E</i>			<i>F</i>			<i>G</i>		
Cows milked	125			125			220			160			180			130			240		
Milking time (h d ⁻¹)	3			6			3.5			Not estimated			4			2.75			3		
Water use (L d ⁻¹)	4500			7000			6000			11000			Not estimated			9500			8000		
Effluent management system	Direct application to land			Direct application to land			Direct application to land			Solids trap, single holding pond, land application			Solids trap, two ponds, land application			Solids trap, two ponds, two wetlands, discharge to creek			Two ponds, recycled flush water, land application		
Flood wash	No			No			No			Yes			No			No			Yes		
Sampling period	1999 - 2001			2001			2001			1999			2003			1999			2003 - 2004		
	<i>n</i>	<i>Min</i>	<i>Max</i>	<i>n</i>	<i>Min</i>	<i>Max</i>	<i>n</i>	<i>Min</i>	<i>Max</i>	<i>n</i>	<i>Min</i>	<i>Max</i>	<i>n</i>	<i>Min</i>	<i>Max</i>	<i>n</i>	<i>Min</i>	<i>Max</i>	<i>n</i>	<i>Min</i>	<i>Max</i>
pH	8	7.9	8.5	3	7.8	7.8	3	7.4	9.0	3	7.8	8.6	2	8.1	8.3	2	7.9	8.1	5	8.3	8.7
EC (μS cm ⁻¹)	4	1446	4860	3	1828	5950	3	2240	4380	0			2	4540	4930	0			5	1389	3617
TS (mg L ⁻¹)	6	4529	16962	3	9566	15962	3	5260	11420	1	8031		2	21591	27506	0			5	5981	10378
TVS (mg L ⁻¹)	5	2543	8306	3	7012	10031	3	2643	6704	1	5625		2	12437	14431	0			5	3413	6534
TSS (mg L ⁻¹)	5	2913	10200	1	1789		0			3	1433	3140	2	15600	17733	2	2220	3360	4	2580	6800
TVSS (mg L ⁻¹)	0			0			0			0			0			0			2	2213	2625
COD (mg L ⁻¹)	8	5357	12447	3	10660	>15000	3	4513	13550	4	2830	9080	2	11225	22050	2	3470	3960	5	3366	15840
BOD ₅ (mg L ⁻¹)	7	914	4000	2	2735	3757	3	768	4247	3	467	1519	2	4414	4642	3	777	2417	5	931	3541
TKN (mg N L ⁻¹)	7	309	1133	3	481	972	2	327	559	1	247		2	546	709	1	269		2	235	457
NH ₃ -N (mg N L ⁻¹)	6	90	508	2	182	407	2	99	165	1	120		2	152	349	1	142		2	32	81
TP (mg P L ⁻¹)	7	38	160	4	39	221	3	17	118	3	27	39	2	126	136	1	76		2	58	147

n = number of samples analysed for the particular parameter/constituent; EC = electrical conductivity; TS = total solids; TVS = total volatile solids; TSS = total suspended solids; TVSS = total volatile suspended solids; COD = chemical oxygen demand; BOD₅ = 5-day biochemical oxygen remand; TKN = total kjeldhal nitrogen, NH₃-N = ammonia-N; TP = total P.

Also apparent in the data is the significant variability observed at each farm. While this is in part caused by the temporal variability of the waste streams, it is also an artefact of technical difficulties associated with both collecting representative samples in the field and representative sub-sampling for laboratory analysis. As noted by Longhurst et al. (2000), the unpredictable nature of fluctuations in wastewater flow makes obtaining representative composite samples of the waste stream problematic. An unbalanced composite sample can result in over- or under-representation of hosing, milking equipment washing or flood wash flows, each of which can have substantially different compositions. Where effluent was applied directly to land, samples could be collected by placing a vessel under the spray from the travelling irrigator. This produced reasonably consistent samples from event to event on account of the mixing that occurred in the collection sump and the homogenisation effect by the macerating pump. The same effect was noted by Longhurst et al. (2000).

Effluent flowing to a pond system, however, was much more problematic to sample. Various methods were trialled over the course of the research including:

- manual flow weighting of grab samples based on visual approximation of flow,
- diversion of a sidestream to a large collection vessel for subsequent sub-sampling, and
- pumping small volumes at regular intervals.

The approach to testing the above methods was not systematic, so the reliability of each method cannot be quantitatively assessed. None of the methods, however, appeared to offer significant improvements to reproducibility. Better designed sidestream diverters could be developed that proportionally capture a small fraction of the flow during a flow event to produce a large composite sample, but would require customising to each site sampled, and it would be difficult to control the volume of samples collected. Properly flow weighted composite sampling using automatic samplers would also improve sampling reproducibility. It would not, however, eliminate sampling imbalances altogether, as the timing of sampling cannot be programmed to coincide with changes in the wastewater source. Moreover it would be prone to blockages from the very coarse particulate material in the effluent. Automated sampling would be more appropriate to effluent that has passed through a solids trap or sedimentation basin (see section 2.2.1), either of which would help to equalise the flow and reduce the particulate loading.

In the laboratory, replicates of solids analyses sometimes exhibited considerable variability due to the difficulty of capturing a representative distribution of particulates, even from a well-mixed sample. Extracting sub-samples for subsequent dilution using wide-mouthed pipettes while the sample was being stirred or pouring sample for dilution into a measuring cylinder immediately after stirring was found to reduce replicate variability. Sample homogenisation was critical for all other particulate fractions, but had to be performed on a large, thoroughly mixed sub-sample to maximise reproducibility.

2.1.2.2 International

Accessible published data on DSE characteristics from international sources is also limited and becoming out-dated as intensification and other trends change the nature of herd management and dairy operations. The most comparable to Australian conditions is that generated from pasture-based dairy farms in New Zealand. Longhurst et al. (2000) collated and reviewed data on DSE characteristics from a variety of sources in NZ (refer to Table 2-3), making a similar observation to that made in the previous section that variability in solids and other constituents is a function of water usage relative to the manure load deposited at the dairy. They also identified a rising trend in DSE N concentrations in data from different dairying regions of NZ, which they attributed to increasing N fertiliser usage. Seasonal variation observed in DSE nutrient content was reported to be correlated with pasture growth cycles and fertiliser use, as well as being indicative of the digestibility of nutrients in the pasture. Beyond seasonal fluctuations, temporal and spatial variability in DSE nutrient concentrations were considered to be related to solids content and therefore water usage.

Ellwood & Mason (2003) reported data obtained from collecting 10 samples of raw DSE from a NZ dairy milking 500 cows. Wastewater flow was reported to be 'relatively constant', which allowed the researchers to produce reasonably consistent composite samples from series of grab samples (see Table 2-3). A shift, however, from manure removal using flushing only to combined scraping and flushing resulted in much higher concentrations of all constituents. Temporal variability is clearly evident in the raw DSE composition data produced by Di et al. (1998) from a study into the impacts of land application of DSE. The data, which are summarised in Table 2-3, were of similar magnitudes to Australian data and showed similar variability to that observed in the UOW data. At least two other NZ studies have reported raw DSE composition data, including those by Hawke & Summers (2003) and Monaghan & Smith (2004) who were studying the impacts of land application of DSE on soil properties and drainage water

quality, respectively. The DSE analysed by Hawke & Summers (2003) appears to have been very dilute due to high water usage at the dairy. As observed in the UOW data, the Monaghan & Smith (2004) data collected from a single farm exhibits considerable variability, again most likely related to water usage.

Table 2-3 summarises the data from the NZ studies as well as data from a selection of studies conducted in the United States (US) and the United Kingdom (UK). Herd management, dairy operation and water use tend to be quite different on European and American dairy farms, particularly in the US where herds are often confined for much, if not all of the day. Nonetheless, wastewaters made up predominantly of manure should exhibit similar traits if not concentrations to Australian DSE streams, particularly where water usage relative to manure production is similar to levels typically found in Australian dairies. Summaries of the US and UK studies are given below.

As part of a monitoring exercise to gauge the performance of pond systems treating DSE in Texas, US, Sweeten and Wolfe (1994) collected and characterised raw wastewater samples from three commercial dairy farms. Wastewater samples were obtained from flows from the milking shed, which incorporated wastewater from cow watering as well as manure flushing and sanitation. Wastewater characteristics differed considerably between the farms, highlighting the differing management practices in place at the three dairies. Temporal variation in raw DSE samples collected at each farm was also significant. Despite the large numbers of samples collected from each farm, variability was very high in most wastewater parameters. Coefficients of variation for TS, COD, TN, TP and K ranged between 52-73%, 69-74%, 57-151%, 65-202% and 51-217%, respectively. Explanations for the high temporal variability were not given, but it is likely to be related to fluctuations in water use at the dairy since at least one of the dairies was said to be manually flushed. While automatic samplers were used to sample the DSE streams, it is unclear whether the samples were weighted using measurements from the flumes installed to monitor flows. Hence it is also possible that sampling methods may have introduced bias to DSE characteristics.

Table 2-3 Raw DSE characteristics. Coefficients of variation (CV) are given in parentheses. NR = not reported; TN = total nitrogen.

<i>Reference</i>	<i>Sweeten & Wolfe (1994)</i>	<i>Cumby et al. (1999)</i>	<i>Di et al. (1998) and Silva et al. (1999)</i>	<i>Longhurst et al. (2000)</i>	<i>Ellwood & Mason (2003)</i>	<i>Monaghan & Smith (2004)</i>	<i>Wood et al. (2007)</i>
Country	US	UK	NZ	NZ	NZ	NZ	UK
Number of farm sites	3	20	1	Various	1	1	1
Number of samples	48, 35, 36	20 × 3	5	NR	10	3	NR
Cows milked	281, 809, 540	48 - 200	NR	NR	500	NR	400
Wastewater flow (L d ⁻¹)	59460, 93359, 58860	500 - 16700	NR	NR	NR	NR	25000
pH	7.6 (0.08)	6.9 (0.15)	8.3 (0.04)		8.4 (0.02)		
EC (μS cm ⁻¹)	3999.8 (0.73)						
TS (mg L ⁻¹)	5767.5 (0.65)	10833 (0.97)	13400 (0.65)	400 - 52000			6144 (0.48)
TVS (mg L ⁻¹)	3736.2 (0.75)						
COD (mg L ⁻¹)	6719.9 (0.74)	13383 (0.97)			9616 (0.27)		6690 (0.47)
BOD ₅ (mg L ⁻¹)		6593 (1.13)			3386 (0.27)		2811 (1.12)
TN (mg N L ⁻¹)	304.2 (1.16)	550 (1.26)	363 (0.55)	181 - 506	434 (0.39)	428 (0.64)	540 (0.55)
NH ₃ -N (mg N L ⁻¹)	280.1 (1.22)	457 (0.94)	95 (0.51)	26 - 132	112 (0.47)	197 (0.41)	366 (0.61)
TP (mg P L ⁻¹)	61.7 (1.84)	277 (1.13)	40 (0.42)	21 - 82	80 (0.39)	111 (0.78)	89 (0.42)
K (mg L ⁻¹)	383.9 (1.63)	783 (1.14)		164 - 705			

‡ Data presented are weighted averages from multiple data sets.

⊕ Total kjeldahl nitrogen.

* Due to ambiguity in the published data, concentrations may be soluble or total K.

Cumby et al. (1999) collected raw wastewater samples from 20 dairy farms in the major dairying regions of England and Wales to gauge the feasibility of treating DSE so as to reduce pollution risks associated with land application. They observed significant variability between farms and between seasons for all wastewater constituents analysed including TS, COD, BOD₅, N, P and K. Even normalised to a per cow basis, TS exhibited considerable variability, ranging from 0.05 to 2.05 kg cow⁻¹ d⁻¹. However constituents did show strong correlation with TS concentrations, demonstrating again the influence of the water to manure ratio to DSE composition. It was noted that potassium (K) concentrations were particularly high, posing a risk of hypomagnesaemia (electrolyte imbalance in grazing cows) if applied to pasture at rates appropriate to other nutrients. N and P concentrations were also high compared with corresponding Australian and NZ data. Feed, fertiliser and milking regimes were not reported, but it is likely that the UK herds generally had higher nutrient intake rates.

Table 2-4 gives average wastewater constituent ratios drawn from the key DSE data sources. For comparison purposes it includes DSE streams subjected to solids separation (refer to section 2.2.1). The ratios that characterise the organic content of wastewater (TVS:TS, COD:TVS and BOD₅:COD) show reasonable consistency between DSE samples collected in Australia, the US and the UK. The similarity in the fundamental make-up of DSE suggests that it is reasonable to draw comparisons between DSE generated in Australia and overseas. As such, some key observations from the US studies and one of the UK studies are discussed below. Nutrient ratios (TN:TP and TN:K) show greater variability, which would be related to differences in the feed supplied to the milking herd. On pasture-based farms DSE nutrient content will depend on fertiliser regime as mentioned earlier and the mix of forages, grains and other supplements. On farms operating as partial or total mixed ration systems, it depends on the type and digestibility of the imported feed. The use of recycled effluent as flush water will affect the N:K (and P:K) ratio as K, being highly soluble and non-reactive, can accumulate over time in a partially closed recycling system (see section 2.2.5).

Table 2-4 Wastewater constituent ratios drawn from published data on raw and settled/screened DSE. Where data have been drawn from multiple farms, averages have been weighted according to the number of samples collected from each farm.

<i>Source</i>	<i>Country</i>	<i>TVS:TS</i>	<i>COD:TS</i>	<i>COD:TVS</i>	<i>BOD₅:COD</i>	<i>N:TP</i>	<i>K:P</i>
<i>Raw DSE</i>							
UOW	AUS	0.61	1.1	1.7	0.26	5.9	
McDonald (2013, pers. comm. 18 January)	AUS					5.2	5.2
Di et al. (1998)	NZ					9.2	
Longhurst et al. (2000)	NZ					3.9	5.4
Ellwood & Mason (2003)	NZ				0.42	6.8	
Hawkes & Summers (2003)	NZ					2.6	1.7
Monaghan & Smith (2004)	NZ					3.9	
Sweeten & Wolfe (1994)	US	0.65	1.2	1.8		5.6	6.6
Cumby et al. (1999)	UK				0.47	2.0	2.8
Wood et al. (2007)	UK				0.42	6.0	
<i>Screened/settled DSE</i>							
UOW	AUS	0.59	0.7	1.2	0.22	5.8	
Safley & Westerman (1992a)*	US	0.75	1.0	1.3			
		0.68	1.1	1.6			
Safley & Westerman (1992b)	US	0.73	1.1	1.6		4.2	
Sweeten & Wolfe (1994)	US	0.61	1.2	2.0			
Wilkie et al. (2004)	US	0.62	1.0	1.6		5.3	0.8

* Data from DSE passed through a settling tank only and settling tank and mechanical screen.

2.2 TREATMENT AND RECYCLING OF DSE

With land application being the ultimate destination for DSE on practically all dairy farms in Australia, treatment (not storage) of DSE is applied for two purposes:

1. Reducing the solids load to avoid blockages of pumps, pipes and irrigation equipment
2. Reducing solids, organic material, pathogens and odours for recycling as flush water

The typical commercial Australian dairy farm operates within tight financial constraints with very few employees and farm investment focused on infrastructure more directly related to milk production. As such, more advanced treatment systems have not gained traction in the industry. The exception may be feed lot style farms that have a greater DSE burden but less land available for spreading manure solids, effluent and sludge.

Waste stabilisation pond (WSP) systems therefore remain the dominant means of treating and handling DSE in Australia. In NZ where discharge of effluent to waterways still occurs (albeit as a controlled or discretionary activity (Bolan et al. 2009)), there has been, at least in the past, a greater focus on treating DSE to reduce the pollution potential of the wastewater – that is to bring down the oxygen demand and pathogen and nutrient content as much as practicable so that with dilution its impact on receiving waterways is minimal. (Note that while there has been a significant shift towards land application driven by regional councils in New Zealand, research into pond systems has tended to consider their performance in relation to discharging effluent to waterways.) It is perhaps this fundamental difference in the rationale behind the adoption of stabilisation ponds that might explain why there has been a great deal more research into pond performance and improvement undertaken in NZ than in Australia.

Australian and New Zealand stabilisation pond treatment systems typically comprise two ponds in series – a primary anaerobic pond (AP) followed by a secondary facultative pond (FP). Single pond systems are generally used for storing DSE over the wettest part of the year to allow land application when it is least susceptible to nutrient losses via runoff, drainage and leaching. Unless they are also used for producing recycled flush water, which is uncommon in Australia, they can be classified as holding rather than treatment ponds. A common feature of pond treatment systems (and many direct application and single pond systems) in Australia is the use of solids separation facilities that provide preliminary treatment to reduce the solids load of effluent entering the primary pond.

This section reviews published material on the three main components of DSE treatment systems. Literature on other modes of treatment is also covered to extract observations and findings that may be transferable to pond treatment. Research into the impacts of effluent recycling as flush water (not irrigation water) on pond function and performance is canvassed in the final sub-section. Note that this review was intentionally confined to research related to treatment of DSE. There are various studies available that investigate treatment of manure slurries from other livestock such as swine and poultry using technology of similar design to that applied to DSE. However it has been demonstrated under controlled conditions that fundamental differences in manure characteristics result in critical differences in treatment (pond) system performance indicators such as the rate of salt build-up, removal of COD, TS and TVS, mineralisation of organic N and accumulation of sludge (Hill, McCaskey &

Hamilton 1981). As such it was felt that references to treatment of other waste types would be unhelpful or even misleading.

2.2.1 Solids Separation in Trafficable Solids Traps

Since DSE on Australian farms tends to have relatively low solids content (<2%), sedimentation tends to be the most appropriate approach to solids removal (Birchall, Dillon & Wrigley 2008). On account of their simplicity and relatively low cost, trafficable solids traps are a common form of solids separation system. They comprise a small concrete-lined settling basin with a weeping weir or screen at the outlet (see Figure 2-1) that allows for rapid partitioning of coarse (manure) solids from the wastewater. Accumulated solids are extracted from the trap using a front end loader or rear scraper (Haughton 2006); hence the term trafficable. Larger earthen sedimentation basins are recommended for large hydraulic loads such as where stormwater runoff is intentionally drained to the effluent management system (Birchall, Dillon & Wrigley 2008). Mechanical solids separation systems such as stationary, rotating, conveyor and vibrating screens, screw and belt presses, and centrifuges are widely used in the US and Europe where manure slurries often exhibit much higher solids concentrations (see for example Wilkinson 1979; Westerman et al. 1985; Safley & Westerman 1992b; Chastain, Vanotti & Wingfield 2001; Møller, Sommer & Ahring 2002; Møller, Lund & Sommer 2000). Reviews of the application of mechanical separation technologies to dairy and other manure slurries have been undertaken by Van Horn et al. (1994), Zhang & Westerman (1997) and Hjorth et al. (2010). The following review focuses on solids traps and similar separation facilities as these are the more common forms of solids separation found on Australian dairy farms. Moreover, the DSE pond system that is the subject of data collection in this study utilises a solids trap for pre-treatment.

The main benefit of solids separation upstream of pond systems is the reduction in poorly biodegradable material that slows the rate of sludge accumulation and improves solids removal efficiency in the primary pond (Hill, McCaskey & Hamilton 1981; Skerman 2004c). Partitioning of solid material, however, creates an additional waste stream that must also be applied to land, requiring solids handling facilities and equipment including a front end loader, an impermeable storage area that drains to the effluent treatment system, and a manure or slurry spreader for distribution. Solids traps and sedimentation basins must also be emptied of accumulated solids on a regular basis. The frequency of emptying depends on the size of the facility, but solids traps tend to require weekly to monthly emptying while sedimentation basins would typically be designed to be emptied every one or two months (Dairy Effluent Guidelines Steering

Committee 2006). According to industry guidelines for South Australian dairies, solids traps become impractical on dairies with more than 300-400 milkers and using flood wash, or with 500 or more milkers and hose washing (Dairy Effluent Guidelines Steering Committee 2006). Other than reducing DSE particulate loads, the main effects of solids separation relate to changes in the balance between readily biodegradable and poorly biodegradable material and to the ratios between N, P and K (Westerman et al. 1985).

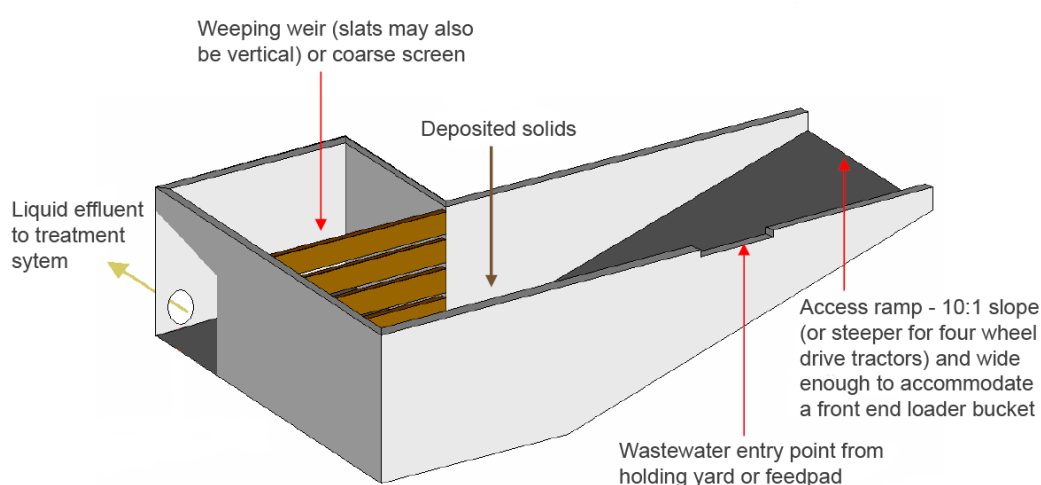


Figure 2-1 Trafficable solids trap (adapted from Haughton 2006).

While published materials on the design of solids traps are readily available in Australia, there is very little published material on actual measured performance either from an operational perspective or with regards to the effect on the effluent being treated or the solids being removed. Based on data from monitoring a solids trap on a demonstration dairy farm, volumetric solids removal of $0.9 \text{ m}^3 \text{ cow}^{-1} \text{ yr}^{-1}$, equivalent to about 75% separation efficiency, was suggested in older guidelines for the NSW industry (NSW Dairy Effluent Subcommittee 1999). Birchall et al. (2008) presents a table of anticipated volumes of solids captured in solids traps for different milk yields and herd holding time based on 50% retention of solids; however no basis for the data is provided. Separation efficiencies assumed or reported in the main design guides and tools are presented in Table 2-5. While the research behind the assumptions for other solids separation facilities including sedimentation basins are reviewed in Birchall et al. (2008) and in the documentation for DairyBAL (McGahan et al. 2009), no basis for the figures in Table 2-5 are supplied for solids traps.

Table 2-5 Solids separation efficiencies reported or assumed for solids traps.

<i>Source</i>	<i>Separation efficiency (%)</i>				
	<i>TS</i>	<i>TVS</i>	<i>TN</i>	<i>TP</i>	<i>K</i>
Dairy Pond (Skerman 2004a)	55	55	20	20	15
DairyBAL (McGahan et al. 2009)	55	55	25	20	15
Dairy Australia database (Birchall, Dillon & Wrigley 2008) Effluent toolkit (McDowell & Birchall 2010)	50	55	30	35	15

Limited sampling of influent and effluent from solids traps was undertaken as part of the research conducted at UOW referred to in section 2.1.2.1. The removal efficiencies presented in Table 2-6 were calculated from concentrations rather than on a mass load basis and the sample numbers are small. Some confidence in the data from two of the farms can be gained from the fact that changes to EC levels were minimal, which indicates that the sampling has not significantly biased the results. The data show reasonable consistency between sites and suggest that existing design tools and guidelines may over-estimate the extent of partitioning of solids and nutrients that occurs in actual systems.

Table 2-6 Reported solids trap removal efficiencies. CVs given in parentheses.

<i>Farm</i>	<i>UOW</i>				<i>Chastain, Vanotti & Wingfield (2001)</i>	<i>Meyer et al. (2004)</i>
	<i>D</i>	<i>E</i>	<i>F</i>	<i>G</i>		
Samples	1	2	2	1	1	4 [⊕]
EC		2	-2			4 (0.80)
TS		36	30	31	23	59 (0.11)
TVS		35	34	34	27	58 (0.16)
TSS		39	42			
TVSS			45			
COD		23	30	25		
BOD ₅	29		16			
TKN	4	24		0	3	
NH ₃ -N	4	15		5	0	
TP		10			15	

[⊕] Four sampling events collecting multiple influent and effluent sub-samples.

Only two published studies on solids separation facilities resembling Australian solids traps could be found in the literature. The first examined a facility that took the form of two trafficable solids traps in series and received mechanically screened flush water from a freestall barn housing 54 cows fed a total mixed ration (Chastain, Vanotti & Wingfield 2001). The raw wastewater was highly concentrated, partly due to the presence of bedding material and waste feed, meaning that the screened effluent was of similar composition (TS 14959 mg L⁻¹, TKN 729 mg N L⁻¹, TP 190 mg P L⁻¹) to a strong raw wastewater stream from an Australian dairy. Reported removal efficiencies given in Table 2-6 were estimated from constituent concentrations in the composite samples of influent and effluent streams from just one sampling event. Despite the two basins, the removal efficiencies were lower than anticipated in design documentation (Table 2-5), although this could in part be related to the removal of settleable material by the screen. Laboratory settling tests on the raw wastewater, however, suggested that settling alone could not achieve the same degree of removal as combined screening and settling. This indicates that the screen removed mostly coarse, poorly settleable particulates.

Higher TS removal of 50-60% was observed by Meyer et al. (2004) from a facility comprising two parallel sedimentation basins with long weeping weirs forming the side walls of the basins. With average TS concentration around 1.5% particle size analysis revealed that the weeping weir efficiently removed coarse particles, reducing the fraction of TS captured by 1- and 2- mm screens from 23% in the influent to 2% in the effluent. The TS fraction passing through the 0.125-mm screen increased from 31% in the influent to 81% in the effluent. The high solids removal efficiency would in part be related to the longer detention time of the basins (which held up to 8 to 12 weeks worth of accumulated manure), but more so due to the presence of bedding in the raw wastewater, which was estimated to make up more than 50% of the TS load. Electrical conductivity was found to be unaffected by solids separation. Analyses of a sub-set of samples indicated that ammonia-N, soluble P, K, Ca, Mg, Na and Cl were also largely unaffected. Interestingly, there was also no significant difference between influent and effluent concentrations of organic N, which corroborates the low N removal efficiencies encountered in the UOW work (Table 2-5).

2.2.2 Primary Anaerobic Ponds

The conventional approach to sizing the treatment component of anaerobic DSE ponds in Australia is based on a volumetric volatile solids (VS) loading rate incorporating adjustment for ambient temperature (Birchall, Dillon & Wrigley 2008; Arthy & Biggs

2005; Skerman 2004c; NSW Dairy Effluent Subcommittee 1999). Referred to as the rational design standard, the method was originally standardised in the US (ASAE 2004). The pond is divided into active treatment and sludge accumulation volumes, with the active volume being determined by the VS loading to the pond estimated using one of the approaches described in section 2.3.1. The allowance made for sludge depends on land availability and the preferred number of years between desludging events, and is calculated using an assumed sludge accumulation rate usually taken from Barth & Kroes (1985). The surface area is then a function of the adopted depth and batter slopes. New Zealand design guidelines opt for a BOD rather than VS loading approach, giving geographically (climate) specific limiting rates to be applied in conjunction with allowances for rainfall (in excess of evaporation) (DEC 2006). Note that while in many cases single holding ponds behave like APs, the basis of their design (storage rather than treatment volume) and manner in which they are operated (periodic pumping out of supernatant) are quite different from APs designed for treatment purposes. Hence the following review prioritised published material related to ponds that overflow to secondary ponds.

Data on DSE APs produced in Australia are limited to a handful of studies, most of which were not concerned with performance or behaviour. Geary & Moore (1999) monitored a small (280 m³) AP treating about 7.5 m³ d⁻¹ of effluent from a dairy milking 110 cows (data presented in Table 2-7); however this was solely for the purpose of gauging the performance of constructed wetlands immediately downstream of the pond. In a 2001 cross-sectional survey of 110 DSE management systems in South West Victoria, samples were collected from primary, secondary and tertiary ponds for analysis of nutrient content (Kane 2004, pers. comm. 7 October). The data from the 60 ponds that were part of a two- or three-stage system are summarized in Table 2-7. In the absence of information relating to pond dimensions, loading and management, there is little that can be inferred from the data, other than to say that variability was significant with standard deviations being greater than 50% of the corresponding mean for most constituents. There was also significant variability in TKN:TP (0.9-22.8) and K:TP (1.8-16.9) ratios, indicating that physical settling and biological treatment processes in APs do not have a normalising effect on the nutrient composition of the liquid fraction of DSE.

Table 2-7 Summary of DSE AP effluent characteristics from published and unpublished data. CVs for wastewater constituents given in parentheses.

Reference	Country	Sites	VSLR [#] (g m ⁻³ d ⁻¹)	Sample (n [*])	pH	TS (mg L ⁻¹)	TVS (mg L ⁻¹)	COD (mg L ⁻¹)	TN (mg N L ⁻¹)	NH ₃ -N (mg N L ⁻¹)	TP (mg P L ⁻¹)
Geary & Moore (1999)	AUS	1	170	E (NR)					227 (0.29)	126 (0.47)	59 (0.18)
Kane (2004)	AUS	60		S (60)	7.4 (0.04)				437 (0.84)	258 (0.77)	80 (0.48)
Dawson (2003) [‡]	AUS	2	50	E (3)	7.7 (0.01)	3880 (0.06)	1499 (0.13)	2592 (0.36)	283 (0.41)	216 (0.23)	46 (0.17)
			34	E (2)	7.7 (0.06)	2783 (0.31)	1327 (0.30)	2343 (0.45)	176 (0.40)	130 (0.34)	31 (0.49)
McDonald (2013)	AUS	61		(61)					535 (0.72)		122 (1.04)
Skerman et al. (2006)	AUS	11	6-77	S (11)	7.6 (0.06)				220 (0.74)		46 (0.50)
Mason (1996)	NZ	1	100	E (12)	7.3 (0.02)			884 (0.23)	172 (0.05)	143 (0.14)	25 (0.13)
Longhurst (2000)	NZ	13		NR					180		29
Westerman et al (1985)	US	NR		S (37-44)		5200 (0.48)			440 (0.34)	295 (0.24)	90 (0.44)
Barth and Kroes (1985)	US	4	12-50	S (NR)					179		48
Safley and Westerman (1992a)	US	1	41	S (108-166)	7.7 (0.02)	5300 (0.60)	2777 (0.11)	2820 (0.75)	388 (0.35)	265 (0.29)	
Safley and Westerman (1992b)	US	1	120	S (106-112)	7.4 (0.02)	4003 (0.52)	2090 (0.14)	3846 (1.37)	518 (0.67)	316 (0.15)	129 (0.45)
Sweeten and Wolfe (1994) [‡]	US	1	63	E (42)	7.6 (0.08)	2088 (0.46)	966 (0.57)	1480 (1.01)	172 (0.16)	161 (0.15)	53 (1.77)
		1	90	E (41)	7.6 (0.06)	3551 (0.79)	1865 (1.01)	3619 (1.34)	193 (0.61)	182 (0.66)	35 (0.51)
McGarvey et al (2004)	US	1		S (NR)	8.0				348	245	
McGarvey et al (2005) [◇]	US	2		E (8)	7.3 - 7.50			800 - 3200	90 - 315	63 - 267	22 - 62

VSLR = Volatile solids loading rate; E= Effluent; S = supernatant.

[#] Loading rates based on total pond capacity. Where not provided in the reference, VSLR was estimated using influent TVS and average water consumption, or milking time (2 hours if unknown) and herd size assuming manure VS of 4.4 kg VS cow⁻¹ d⁻¹ for Australian herds (Skerman 2004c) or 3.0 kg VS cow⁻¹ d⁻¹ for NZ herds (DEC 2006).

^{*} Ranges indicate some samples were not analysed for all constituents.

[‡] Data from two separate sites presented.

[◇] Standard deviations not given, hence ranges presented.

A similar survey of DSE pond effluent was conducted in the Gippsland region of Victoria in 2006 (McDonald 2013, pers. comm. 18 January). Lack of information about the farm and DSE system limits the utility of the data, but comparison with the data produced by Kane (2004, pers. comm. 7 October) indicated that concentrations were higher on average for all nutrients. Again though, variability was considerable, particularly for TP which had a coefficient of variation of 1.04. N:P ratios varied between 1.7 and 13.4, while K:P ratios ranged from 0.6 to 19.1. Skerman et al. (2006) sampled supernatants from pond systems on 20 farms in south-east Queensland. Samples were collected from pump-out ponds only, however, which meant that data for primary ponds was only available for the 11 single pond systems. The supernatant characteristics of primary holding ponds were, however, reasonably similar to those in the Victorian study, if slightly more dilute (see Table 2-7). The degree of variability was also quite similar to the Victorian data. The survey also collected information on the size and average live weight of the herd, milking time, flush water usage and pond volume; however analysis of the data (performed by this author) found no reasonable correlation between any of these factors and supernatant constituent concentrations.

One of the components of the UOW DSE research program referred to in section 2.1.2.1 was a characterisation study of two two-stage (AP plus FP) DSE stabilisation pond systems (Dawson 2003) and was a pre-cursor to the research presented in this thesis. The newer of the two systems was more heavily loaded (see Table 2-7), receiving raw wastewater from a 240-head herd producing about 23 L cow⁻¹ d⁻¹ milk. The second system received effluent from a solids trap pre-treating wastewater from a 200-head herd with similar milk production. Periodic sampling from the respective APs indicated that both the strength and variability of influent was substantially reduced by the equalising treatment effects of the ponds. The newer AP was larger and deeper (~2.6 total depth compared with ~2 m) and received more dilute influent due to the use of large volumes of recycled effluent; yet the pond produced slightly more concentrated effluent and accumulated sludge more rapidly than the older AP, demonstrating the importance of understanding loading rates when analysing pond effluent characteristics. Effluent from the newer pond also exhibited significantly higher concentrations of ammonia-N and lower organic N concentrations than the incoming wastewater, which was attributed to the settling and mineralisation of organic N and accumulation due to effluent recycling. The pH in both APs was consistently around 7 despite influent pH levels being above 8. Vertical profiling of the pond supernatants revealed that temperature, pH and EC varied little with depth in both ponds.

In evaluating methane emissions from a DSE AP in NZ, Craggs, Park & Heubeck (2008) measured in-pond temperatures as well as VS effluent concentrations. Temperatures in the supernatant (15 cm depth) and in the sludge (pond floor) were similar over the course of the monitoring period, although the sludge exhibited a lag in warming and cooling. Theoretical VS removal (VS loading was based on an assumed manure load) was 59%, producing an average effluent VS concentration of 563 mg L^{-1} . AP effluent data reported by Mason (1996) was mainly presented to demonstrate the performance of a downstream facultative pond, although it was noted that the AP achieved upwards of 80% BOD_5 removal. Sukias et al. (2003) also presented limited AP effluent data in a study of a FP. Longhurst et al. (2000) collated various data on the nutrient composition of AP effluent, reporting average TN and TP concentrations of $116 - 230 \text{ mg N L}^{-1}$ and $26 - 31 \text{ mg P L}^{-1}$, respectively. Longhurst et al. (2000) stated that the majority of AP nutrients are held in the sludge, which may be the case at any one instant, but may not be the case when considered as a function of time.

Most other published research related to DSE APs has been conducted in the US. A review by Westerman et al. (1985) presented typical nutrient content of AP liquid and noted that the ratio of N to P tends to drop in DSE treated in ponds due to settling of P to the sludge while the K:N ratio increases with (conservative) K staying in solution. Barth and Kroes (1985) also presented nutrient concentrations for primary ponds treating DSE but made no specific observations related to the data.

Sweeten & Wolfe (1994) monitored the influent and effluent from three primary ponds treating DSE, two of which were operated purely as treatment ponds in a treatment train while the other was used as the single holding pond prior to land application. One of the two treatment ponds exhibited strong treatment performance, with COD and TSS removal efficiencies averaging 77% and 71%, respectively (see Table 2-7), and COD:TS and VS:TS ratios were both considerably reduced. An explanation for the poorer performance of the other treatment pond was not provided, but was likely related to inflows of runoff from open lots in addition to milking shed wastewater (runoff on the other farm was directed to a tertiary holding pond). Indeed Mukhtar et al. (2004) found that mixed sludge and supernatant samples from ponds that receive runoff from dry lots tended to have higher TS, TKN and K concentrations than those that didn't. Loading to the two treatment ponds comprised mostly ammonia-N, causing TKN removal rates (34% and 28%) to be almost entirely associated with ammonia losses. P removal was as high as 38% in one pond, but negligible in the other. Accordingly, changes in the N:P and K:P ratios were not consistent between the ponds.

Mukhtar et al. (2004) sampled (mixed) sludge and supernatant from APs on 12 dairy farms in Texas (US) to gauge the effects of various management practices on pond solids and nutrient content. Systems receiving recycled flush water or dry lot runoff and those with fewer pond cells produced effluent with lower solids and nutrient concentrations and lower sludge accumulation rates. Larger herds and the use of bedding material were also found to produce poorer effluent quality. A similar study by Ullman & Mukhtar (2007) compared the composition of sludge-supernatant samples from APs treating effluent from dry lot and hybrid type dairy operations in Texas. While not given as an explanation, it is likely that the sampling approach (mixing supernatant and sludge) contributed to the high variability recorded in compositional analyses, as the relative proportions of sludge and supernatant would vary with the sludge level in each pond. Seasonality related to changing feed rations was also noted as a source of variability that was not addressed in the sampling approach. Focusing on the influence of differences in wastewater sources, the paper presented little information on pond performance, although it was noted that pH levels were always close to neutral and never observed to be below 7.1.

Table 2-7 summarises the data from the studies described above that sampled pond supernatant or effluent (as opposed to mixed sludge and supernatant). While there is considerable variability in some of the data, particularly nutrient concentrations, the relative consistency in the TS, TVS and COD data suggest that the effects of settling and digestion of organic material in APs are reasonably predictable. pH shows particularly low variability, indicating the strong buffer capacity of DSE, but also consistency in physico-chemical conditions. Variability in effluent nutrient concentrations and ratios is likely to be closely associated with influent variability, although factors such as climate, underlying soil type, sludge levels and the use of recycled effluent for flush water would also be at play. Comparisons of coefficients of variation (CV) between cross-sectional studies sampling from multiple sites and longitudinal studies monitoring the one pond indicate that variability in effluent/supernatant composition is higher between farms than it is over time on a single farm.

2.2.2.1 Treatment efficiency

Table 2-8 summarises reported removal efficiencies for DSE APs. Removal of organic material, as COD indicated by COD, TVS and TVSS, is generally high at between 70% and 90% (except for the second Sweeten & Wolfe (1994) site which received runoff inflows). Analysis of the reported influent and effluent data indicates that settling and

biological treatment reduces the TVS:TS ratio in DSE by 20-25%. The COD:TS ratio tends to rise through APs, although the proportion is much more variable. The inclusion of inorganic salts causes removal of TS to be more moderate. Nutrient removal is highly variable. Ammonia-N actually increased in two of the ponds, which would indicate mineralisation occurring at a faster rate than combined volatilisation and microbial uptake (assuming nitrification does not occur in APs). To the author's knowledge, no published study has undertaken a mass flows analysis of nutrients in an anaerobic DSE pond; hence there is very little upon which to base interpretation of treatment efficiency data. One of the only known studies to quantify a nutrient pathway in a DSE pond was actually concerned with emissions rather than treatment. Using measurements of atmospheric ammonia gas concentrations by open path differential optical absorption spectroscopy together with tracer ratio flux experiments, Rumburg et al. (2008) determined ammonia volatilisation losses from a DSE AP amounted to about 24% of the total (theoretical) N loading to the pond. However, the authors made the point that the very limited understanding of N processes in such ponds, particularly ammonification and bacterial uptake of ammonia-N was a significant impediment to predicting volatilisation fluxes.

Table 2-8 Reported removal efficiencies (%) for APs treating DSE.

Constituent	Safley and Westerman (1992a)	Safley and Westerman (1992b)	Sweeten and Wolfe (1994)		Dawson (2003)	
			Site 1	Site 2	Site 1	Site 2
TS	82	64	62	26	53	82
TVS	87	74	72	40	70	85
TSS			71	24	88	93
TVSS			75	-12		
COD	91	70	77	10	81	82
TKN	78	28	34	7	87	89
NH ₃ -N	55	-36	35	27	-282	73
TP		25	38	4	55	74

2.2.2.2 Microbiology

McGarvey et al. (2004) characterised the microbiological make-up of the supernatant of a primary pond treating settled DSE, finding *Firmicutes*, which includes many ruminant bacteria genera, to be the most populous identifiable phylum. In a subsequent study, McGarvey et al. (2005) compared the supernatants from stagnant (unmixed) and mechanically circulated (mixed) primary ponds of similar size and receiving very similar waste loading. The study found that circulation made no difference to effluent organic

matter content, nutrient concentrations, gross microbiology or other physicochemical parameters. Elevated purple sulfur bacteria counts in the circulated pond, however, were thought to be caused by the destratifying and homogenisation effect of circulation and were believed to result in reduced odour-related VOC emissions.

2.2.2.3 Sludge accumulation and characteristics

Despite being a major feature of primary ponds treating DSE, relatively little research has been published on the characteristics, handling, treatment or otherwise of pond sludge. It would appear that DSE pond sludge is viewed as little more than a sink for nutrients and potential cause of pond failure – its role in pond treatment performance has not been closely investigated. Nordstedt & Baldwin (1975) measured sludge levels along a central transect of a DSE pond treating effluent from the milking parlour, cow washing and holding areas of dairy milking 600-800 cows on four occasions over 4.5 years. The accumulation rate was estimated to be 15-17% of the pond capacity per year. Their sampling allowed them to detect discrete strata of lighter sludge above denser digested sludge after 40 months of operation, both of which increased in depth over time. Sludge texture and appearance varied with distance from the outlet, changing from manure-like material closer to the inlet to darker, finer textured material further away. TS were found to generally increase with depth, but not consistently down the length of the pond. VS decreased with distance from the inlet and with depth, indicating the effects of anaerobic digestion. Effluent VS concentrations were observed to increase towards the end of the study as sludge accumulated near the outlet structure.

Barth & Kroes (1985) measured sludge accumulation and analysed sludge and supernatant composition (see Table 2-9) in four APs treating DSE. Long-term accumulation rates ranged between 0.0037 to 0.0056 (average 0.0455) m³ kg⁻¹ TS added, while long term VS destruction was approximately 55%. Their data revealed that Ca in sludge was significantly higher than in supernatant, while the reverse was the case for Mg. As would be expected for highly soluble species, K and Na were found to be in similar concentrations in the sludge and supernatant. Based on their observations, Barth & Kroes (1985) proposed a model for sludge dynamics in livestock waste stabilisation ponds (see Figure 2-2). The model divides accumulating sludge into an active sludge layer undergoing anaerobic digestion overlying an inert layer comprising poorly biodegradable material and fixed solids. The inert layer begins to form once anaerobic digestion is properly established and becomes increasingly dense with time due to compaction. Initially sludge accumulation is more rapid as anaerobic

digestion becomes established. Once the system stabilises and VS destruction is more consistent, the rate of sludge accumulation slows and continues to decline very gradually over time due to destruction of more slowly degradable material and compaction. The active layer is relatively constant in size (ignoring seasonal fluctuation) until the inert sludge level begins to compromise the treatment efficiency of the active sludge and supernatant above it. The point of failure was estimated to be when inert sludge occupied about 70% of the pond.

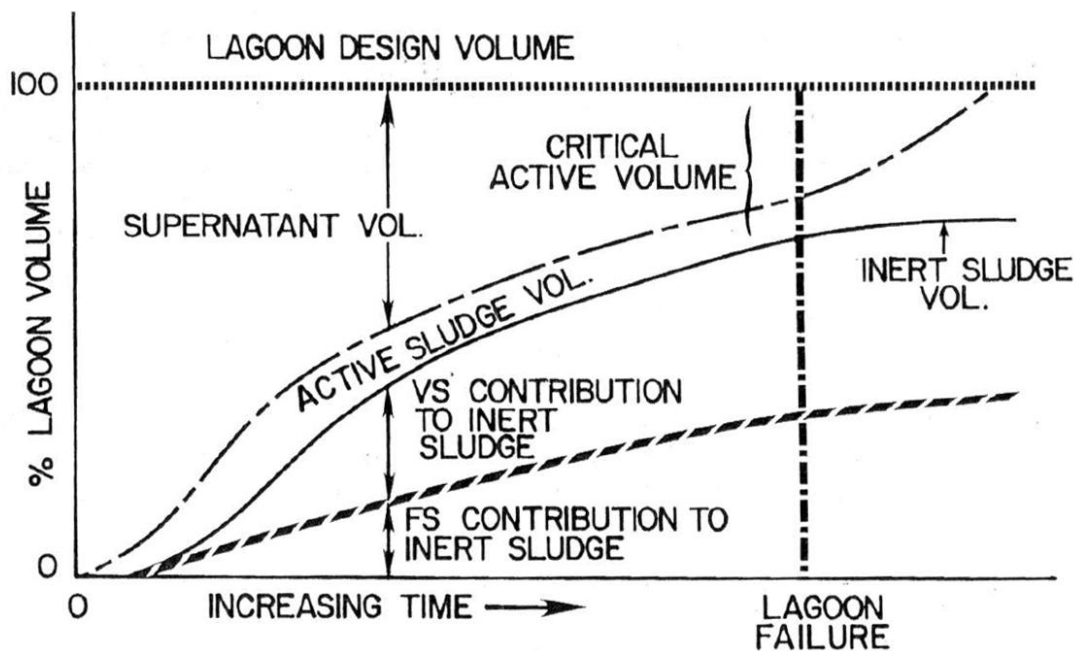


Figure 2-2 Conceptual model of sludge accumulation in livestock waste stabilisation ponds (Barth & Kroes 1985).

Collecting samples of the entire sludge-supernatant column from two DSE APs using a clear polycarbonate column sampler, Dawson (2003) observed similar strata to those described above – discrete layers of digested sludge, active sludge and supernatant. The size of the active sludge layer varied between 0.2 and 0.7 m and was largest in the centre of the pond. The characteristics of the denser digested sludge are presented in Table 2-9. The only other recently published article directly related to DSE pond sludge found in the literature was that by Mukhtar et al. (2004), which examined the effects of management practices on sludge levels (data not presented for the same reason given earlier). In their survey of 12 Texan farms, they found that sludge accumulation was higher in systems using recycling effluent for flush water and systems allowing runoff from dry lots to flow into the ponds.

A number of studies have characterized AP sludge as part research into the effects on pasture (Ward & Jacobs 2008b) and forage crop productivity (Ward & Jacobs 2008a), N mineralisation rates (Zaman et al. 1998) and plant uptake and leaching of nutrients (Cameron et al. 1996) following application of pond sludge to land. None of these studies, however, linked the sludge characteristics to pond function or performance. Table 2-9 summarises the available data from the various studies. Despite the consistency in the dry matter (TS) content, there is considerable variability in a number of the other constituents, particularly, total carbon (TC), TN and TP.

2.2.2.4 Biogas production

Anaerobic digestion in primary DSE ponds generates significant quantities of methane-containing biogas, which has prompted a number of studies investigating the harvesting of biogas for energy generation. Safley & Westerman (1988) monitored biogas production from several pond systems treating different manure wastewaters, including one loaded with DSE at about $0.02 \text{ kg VS m}^{-3} \text{ d}^{-1}$. Gas production depended on high total organic acid concentrations and temperature and was therefore highly seasonal. Methane production also displayed considerable spatial variability, which may have been related to the pattern of solids deposition.

Table 2-9 Sludge characteristics reported in the literature. CVs given in parentheses.

	<i>Barth & Kroes (1985)</i>	<i>Dawson (2003)</i>	<i>Ward (2010)</i>	<i>Zaman et al. (1998)</i>	<i>Cameron et al. (1996)</i>	<i>Longhurst, Roberts & O'Connor (2000)</i>
Sites	4	1	2	1	1	1
Samples	NR	1	4	1	2	NR
pH		7	7.3 (0.02)	7.2	6.65	
EC ($\mu\text{S cm}^{-1}$)	1170-3295	5087	5865 (0.31)		2064	
TS (%)		8.7	8.3 (0.06)	7.6	5.65	21.0
TC (% TS)			26 (0.02)	15	12	
TN (mg N L^{-1})	2546	3204	980 (0.23)	1320	1527	2400
NH ₃ -N (mg N L^{-1})	328		72 (0.30)	145	143	
TP (mg P L^{-1})	1143	562.0	245 (0.25)			250
K (mg L^{-1})	700		604 (0.11)		637	500

Safley & Westerman (1992a) measured areal biogas production of $0.22 \text{ m}^3 \text{ m}^{-2} \text{ d}^{-1}$ from a pond treating settled and screened wastewater from a 200 head dairy herd. The methane content of the biogas was relatively high compared with gas from other

digesters (averaging 80%) and increased as pond temperature decreased. The negative correlation between biogas methane concentration and pond temperature was confirmed in another study by Safley & Westerman (1992b). Average methane concentration was lower at 69%, but the methane yield ($0.39 \text{ m}^3 \text{ CH}_4 \text{ kg}^{-1} \text{ VS added}$) and specific yield ($0.53 \text{ m}^3 \text{ CH}_4 \text{ kg}^{-1} \text{ VS destroyed}$) were both relatively high. The high productivity was attributed to the long solids retention time and effective upstream screening of non-biodegradable lignin particulates. Heating of supernatant over the winter was found to make a significant difference to methane yield.

Slightly lower methane production was observed in the more recent study by Craggs et al. (2008) (yield $0.29 \text{ CH}_4 \text{ kg}^{-1} \text{ VS added}$, specific yield $0.36 \text{ m}^3 \text{ CH}_4 \text{ kg}^{-1} \text{ VS destroyed}$). Methane output was strongly seasonal and appeared to stop altogether for a brief period in winter. Output was lower than that from a piggery pond that was also monitored in the study, which was thought to be related to the higher proportion of poorly biodegradable material in the DSE and verifies the assertion made earlier regarding differences between ponds treating different wastewaters.

2.2.3 Secondary Facultative Ponds

On account of the high organic loading of raw DSE, FPs are generally used as secondary treatment after APs. Often mistakenly referred to as aerobic ponds, DSE FPs are characterised by the contrast between aerobic conditions in the upper 10-15 cm of the supernatant generated by algal photosynthesis and surface re-aeration, and anaerobic or anoxic conditions below. In Australia secondary FPs are operated as holding ponds, varying in depth over time as the pond is gradually filled by overflow from the AP and periodically pumped out to land. They are typically sized to meet minimum storage needs according to a monthly soil moisture balance of the land application site (Skerman 2004a; McDowell & Birchall 2010). The minimum surface area is advised to be within a range specified for areal BOD_5 loading rate of between 30 and $50 \text{ kg BOD}_5 \text{ ha}^{-1} \text{ d}^{-1}$ (Birchall, Dillon & Wrigley 2008). Calculation of an appropriate surface area then requires assumptions relating to the treatment efficiency of the AP and, if present, the solids trap preceding the AP. If not predetermined (and therefore prescribing a surface area to meet the minimum storage requirement), depth is then a function of surface area and batter slopes. Areal BOD loading is the primary design parameter used in NZ guidelines, with an upper limit of $84 \text{ kg BOD}_5 \text{ ha}^{-1} \text{ d}^{-1}$ and allowing for 70% BOD removal in the primary AP (DEC 2006). A pond depth of 1.2 m is prescribed, and allowance must be made for rainfall in excess of evaporation losses on the 30 wettest days of the year.

Research in Australia related to FPs treating/holding DSE has, like that related to APs, mostly been limited to determining the effluent nutrient composition. The Victorian (Kane 2004, pers. comm. 7 October; McDonald 2013, pers. comm. 18 January) and Queensland (Skerman, Kunde & Biggs 2006) studies described in section 2.2.2 all collected samples from secondary ponds in addition to AP samples, average concentrations of which are presented in Table 2-10. The data clearly demonstrate that FP supernatant quality can vary enormously between farms. Detailed characterisation of supernatant from one FP on a Victorian farm was undertaken in a number of studies conducted at the same site to determine the impacts of irrigating the effluent to pasture and forage crops (Jacobs & Ward 2007a; Jacobs & Ward 2007b; Jacobs & Ward 2007c; Jacobs & Ward 2008; Jacobs, Ward & Kearney 2008). The data, compiled in Table 2-10, showed relative consistency over time (between studies), as did data collected by Fyfe (2004) who sampled effluent from a FP on a 130-head farm in NSW over a 10-month period. Comparison between these longitudinal data and the data from the cross-sectional studies suggests that as with APs, farm and milking operations have a greater impact on pond characteristics than do seasonality and other temporal factors.

FPs have been the subject of a number of detailed studies conducted in NZ, presumably because in the past they represented the final stage of treatment before disposal to a waterway. Hickey et al. (1989) sampled FP effluent from 11 pond systems designed according to contemporary national guidelines. The study compared intra- and inter-farm variability, showing that variation over time on a particular farm could be comparable to variability between different farms for a number of constituents including BOD₅, coliforms, DRP, nitrate and DO. While there was reasonable similarity in median values of BOD₅, pH and DRP from different farms, central tendencies of other constituents such as conductivity, suspended solids (SS), ammonia-N and TP varied considerably between farms. Analysis of statistical power indicated that ten samples from a given site should be sufficient to accommodate temporal variability for most constituents. Seasonality in the data was relatively weak. Neither temperature fluctuations nor influent variability associated with seasonal milking and influent loading had significant bearing on effluent quality. Theoretical influent loading and retention times (both based on cow numbers) appeared to have little bearing on effluent quality, and it was remarked that actual measurement of inflows would likely have produced better correlation between influent and effluent quality.

Mason (1996) undertook a detailed study of a single FP treating anaerobically treated effluent from a dairy milking up to 490 cows at the peak of the season. Relatively low

COD removal (30%) combined with higher BOD₅ reduction (55%) meant that COD:BOD₅ ratio increased through the pond. The larger fractions of both COD and BOD₅ were associated with poorly biodegradable particulate matter. Because of high effluent ammonia-N and low nitrate concentrations, nitrification was not considered to be a significant process in the pond. Volatilisation was considered to be the main N removal pathway as averaged N removal expressed in terms of surface area (0.75 g m⁻² d⁻¹) fell within expected ranges for ammonia volatilisation rates. Algal uptake was thought to be the main P cycling process, as indicated by low TP removal together with higher reductions in DRP.

Sukias et al. (2001) sampled supernatant from six FPs that were constructed to updated design standards requiring allowances for rainfall. Sampling from the upper 40 cm of the liquid column near each pond outlet, indicated that 68% BOD₅ was in particulate form and most suspended material was organic (80%). No distinct seasonality was observed in effluent quality; however BOD, suspended solids and N were all negatively correlated with free liquid depth in the upstream AP. The ponds generally produced better effluent quality than observed in the Hickey et al. (1989) study, which was attributed to improved design standards, but variability and associated poor effluent quality still remained a problem. Less than desirable BOD₅ removal was attributed to sustained oxygen demand from the slow break down of poorly degradable material.

There is surprisingly little published material on secondary DSE ponds from the US. Two of the pond systems monitored by Sweeten & Wolfe (1994) incorporated a secondary pond. Both caused significant reductions in TS, TVS, TSS, TVSS and COD, and produced effluent concentrations for these and other constituents similar to those presented in Table 2-10. An important distinction was made between the two secondary ponds in the study in that one was classified as an anaerobic lagoon while the other was simply termed a second stage lagoon. This may explain the dramatic difference in their impact on nutrient concentrations. N and P reductions in the second AP of the first farm were moderate at around 30% and of similar proportions to those observed in the primary pond. On the other farm N and P reductions in the secondary pond were significantly higher than in the upstream primary pond and compared with the corresponding reductions on the other farm. The paper did not, however, provide an analysis that compared the performance of the two pond systems.

Table 2-10 Summary of DSE FP effluent characteristics from published and unpublished data. CVs for wastewater constituents given in parentheses. Italics denote either TKN in place of TN data or TON in place of NO₃-N data.

<i>Reference</i>	<i>Country</i>	<i>Sites</i>	<i>Specific volume (m³ cow⁻¹)</i>	<i>Sample (n)</i>	<i>pH</i>	<i>TSS (mg L⁻¹)</i>	<i>COD (mg L⁻¹)</i>	<i>TN (mg N L⁻¹)</i>	<i>NH₃-N (mg N L⁻¹)</i>	<i>NO₃-N (mg N L⁻¹)</i>	<i>TP (mg P L⁻¹)</i>
Dawson (2003)	AUS	1	13.7	E (3)	8.4 (0.02)	348 (0.19)	1618 (0.34)	89 (0.59)	63 (0.54)		19 (0.10)
		1	6.8	S (2)	7.8	278 (0.74)	1095 (0.06)	83 (0.36)	51 (0.11)		19 (0.49)
Fyfe (2004)	AUS	1	8.6	E (6)	7.7 (0.02)	304 (0.42)	958 (0.32)	166 (0.24)	114 (0.23)	6.4 (0.01)	34 (0.09)
Kane (2004)	AUS	52		S 52	7.7 (0.04)			196 (0.91)	119 (0.83)	1.7 (1.27)	47 (0.82)
McDonald (pers. Comm. 2013)	AUS	79		S (79)				286 (0.94)			107 (1.92)
Skerman et al. (2004)	AUS	7	12.2	S (7)	8.3 (0.05)			175 (0.56)			22 (0.34)
Jacobs	AUS	1		S (30)	8.1 (0.02)			163 (0.17)	117 (0.27)		29 (0.22)
Hickey	NZ	11	9.1	S (76)	7.9 (0.02)	227 (0.09)			63 (0.15)	0.2 (0.36)	
Mason (1996)	NZ	1	4.7	E (13)	7.9 (0.01)	226 (0.31)	618 (0.21)	129 (0.09)	100 (0.16)		24 (0.14)
Sukias et al. (2001) [‡]	NZ	6		S (57)		105 - 307		46 - 134	26 - 106	0.1 - 0.4	
Sukias et al. (2003)	NZ	1	4.4	S (8)		104		61	41	0.7	
Bolan et al. (2004)	NZ	1	3.8	E (10)		85 (0.26)	453 (0.17)		95 (0.13)	15.0 (0.01)	24 (0.09)
Sweeten & Wolfe (1994)	US	1	8.3	E (45)	7.8 (0.04)	480 (0.77)	650 (0.37)	117 (0.36)	117 (0.23)	4.7 (0.66)	39 (2.03)
		1	15.7	E (7)	7.9 (0.04)	831 (1.11)	394 (0.49)	72 (0.53)	118 0.00	4.2 (0.41)	3

[‡] Standard deviations not given, hence ranges of median values by farm presented.

2.2.3.1 Treatment efficiency

As with DSE APs, there are very few studies that have attempted to gauge the treatment efficiency of DSE FPs, even in NZ where several studies have been dedicated to characterising the effluent from FPs. As shown in Table 2-11, removal of solids and organic material is less effective in secondary ponds, mainly due to the fact that remaining organic material after anaerobic treatment is poorly biodegradable (Mason 1996; Sukias et al. 2001). Nutrient removal, like in APs, is variable although quite high in many instances. Reported increases in nitrate concentrations confirm that nitrification does occur in secondary ponds even if only to a limited extent (see below). Total N and Ammonia-N removal can be quite high, but the relative influence of volatilisation and nitrification-denitrification is not clear.

Table 2-11 Reported removal efficiencies (%) for FPs treating DSE.

<i>Constituent</i>	<i>Sweeten & Wolfe (1994)</i>		<i>Mason (1996)</i>	<i>Dawson (2003)</i>		<i>Sukias et al. (2003)</i>
	<i>Site 1</i>	<i>Site 2</i>		<i>Site 1</i>	<i>Site 2</i>	
TS	21	58		22	55	
TVS	30	71		24	54	
TSS	43	58	38	39	52	80
TVSS	45	80				80
COD	56	89	30	38	58	
TN	32	63	25	68	71	64
NH ₃ -N	28	36	30	71	76	72
NO ₃ -N	-202	-446				
TP	26	90	6	59	60	

2.2.3.2 Algal photosynthesis and stratification

The contrasting aerobic conditions at the surface and anaerobic conditions at depth in FPs are an artefact of algal photosynthesis being confined to an upper euphotic zone. The extent of the irradiated zone in DSE FPs, however, is limited by high levels of dissolved organic matter and turbidity. Mason (1996) reported algal cell counts in DSE FP effluent within ranges expected of other FPs (1.2×10^5 - 3.98×10^6 cells mL⁻¹). Estimates of potential oxygen produced by algal photosynthesis based on solar radiation and typical algal growth and oxygen production rates indicated that algal photosynthesis should have been able to more than satisfy oxygen demand from incoming wastewater. However, incomplete destruction of BOD and lack of nitrification were viewed as symptoms of a shallow euphotic zone constrained by light attenuation.

Sukias et al. (2001) also reported chlorophyll-a concentrations comparable to concentrations in sewage FPs. Chlorophyll-a was positively correlated with total, volatile and fixed suspended solids and organic N, indicating that algae constituted a significant portion of suspended material. In summer the upper 10-20 cm of the ponds monitored in the study exhibited diurnal patterns related to algal photosynthesis with DO reaching 200% saturation and pH approaching 9 on sunny afternoons. As would be expected, conditions in the hypolimnion below were consistently anaerobic. Algal biomass, however, was relatively low compared with that in sewage ponds and was confined to the upper 10-15 cm due to low available carbon and high light attenuation. Thermal stratification, which was observed to occur from mid-morning on sunny days but was weak on cloudy, windy ($> 10 \text{ m s}^{-1}$) days, was thought, however, to help maintain a viable algae population by creating a discrete euphotic zone that did not mix with liquid below except under high winds.

2.2.3.3 Nitrification-denitrification and N removal

While the heavily reducing conditions of anaerobic ponds effectively preclude the growth of nitrifying biomass, the introduction of oxygen from algal photosynthesis in facultative ponds presents the potential for nitrification. In addition, anaerobic conditions below the surface could facilitate denitrification of nitrate or nitrite that is formed. However low nitrate and high ammonia-N concentrations reported in various studies (refer to Table 2-10) indicate that nitrification rates are low and that denitrification keeps pace with nitrification that does occur. As pointed out by Craggs et al. (2000), the temporal nature and limited depth penetration of photosynthetic aeration provides little opportunity for slow-growing nitrifying biomass to establish, particularly when it must compete with heterotrophic biomass for DO. To evaluate the enhanced nitrification potential offered by the installation of biofilm support surfaces combined with mechanical aeration in DSE FPs, Craggs et al. (2000) incubated biofilms supported on plastic growth media in full scale FPs under different aeration regimes (continuous, night only, turbulent and quiescent) and at three depths. Under controlled laboratory conditions they then measured ammonia-N uptake of biofilm samples harvested from the pond. Preliminary testing confirmed that suspended biomass on its own exhibits very poor nitrification potential due to low nitrifier biomass. Biofilm cultivated under continuous aeration produced the strongest nitrification potential, although night only aeration during the summer produced comparable potential due to daytime photosynthetic aeration. A lack of correlation between biofilm mass and nitrification indicated that even with the boost of aeration and support media, nitrifier activity was likely to be limited by competition with heterotrophic bacteria in DSE FPs.

Sukias et al. (2003) conducted field experiments to test nitrification rates in mechanically aerated DSE FPs. Using a geomembrane to segment a full-scale pond in halves (each receiving the same influent), they observed effective conversion of ammonia-N to nitrate in the aerated section (continuously and night only) compared with that in the non-aerated section. They did not offer an explanation as to why total N removal was the same for both sections of the pond, although it was likely due to a lack of anoxic denitrification sites in the aerated section. Similar low concentrations of organic N in both sections of the pond suggested algal uptake was not a significant pathway under aerated or unaerated conditions. Inorganic N in the non-aerated pond effluent was almost all ammonia-N, while that in the aerated pond was composed entirely of oxidised forms. The reduction in ammonia-N in the unaerated pond was greater than the concomitant increase in total oxidised N (TON), suggesting ammonia-N removal also occurred via volatilisation. The study demonstrated that nitrification is unlikely to occur without mechanical aeration due to photosynthetic oxygen being confined to the upper layer of the pond when slow-growing nitrifier biomass needs to attach to the pond floor to establish a critical mass and not be washed out.

2.2.4 Insights from Investigations Into Other Modes of Treatment

The focus of this thesis is treatment using stabilisation ponds; however, valuable insight may be gained from studies involving wastewater characterisation, laboratory experiments and field trials to investigate treatment using other approaches. This section presents a review of a number of studies that have characterised DSE for the purposes of developing alternative treatment technologies and pilot studies of alternative technologies.

Ellwood & Mason (2003) examined ratios of organic material to nutrients in raw DSE to evaluate the potential for biological nutrient removal (BNR), producing insights that are transferrable to stabilisation ponds. They found that while the total organic load was theoretically more than sufficient for BNR, only a small fraction was in the form of volatile fatty acids (VFAs) that could support biological P removal or denitrification. Inorganic carbon in the form of alkalinity was also low for nitrification-denitrification. Hence either significant reductions in the particulate fractions of N and P through sedimentation or hydrolysis of particulate material to produce biodegradable substrates would be required to support BNR. Importantly, reduced water consumption that resulted in more concentrated effluent did not appear to dramatically alter the ratios between constituents.

The findings of the abovementioned characterisation prompted a study into the potential for pre-fermentation of DSE to support BNR (Mason & Mulcahy 2003). Batch experiments produced yields of up to 0.39 g VFA as COD per g BOD₅ from raw DSE, demonstrating the potential for VFA production in anaerobic ponds. COD concentrations were not analysed, but based on a COD:BOD₅ ratio of about 3 determined for raw DSE from the same farm in the previous study (Ellwood & Mason 2003), this would amount to just under 15% of total COD. This figure agrees well with the 15% yield obtained from screened dairy manure in similar experiments run by Yanosek, Wolfe & Love (2003) to test the potential of pre-fermentation to provide VFAs as a carbon source for enhanced biological P removal (EBPR). Güngör et al (2009) compared the VFA yield of the liquid fraction of mechanically separated (diluted) dairy manure with that of supernatant from a settling basin receiving the liquid fraction of mechanically separated DSE. Batch experiments showed that the dilute manure had a substantially higher potential yield than the settled supernatant (0.73 compared with 0.015 g VFA as COD g⁻¹ TSS). This was mainly attributed to the high proportion of inert organic material in the supernatant, as attested to by the lack of destruction of the volatile fraction of suspended solids. Beck et al. (2007) employed pre-fermentation to mineralise organic N and produce VFAs to support biological N removal in a sequencing batch reactor (SBR). They showed that close to 100% ammonia-N removal could be achieved using low aeration levels (DO < 1.1 mg L⁻¹) that favoured nitrification by ammonia oxidising biomass, avoiding nitrification by nitrite oxidising biomass and thereby reduced aeration energy and subsequent VFA demand in the denitrification stage.

Wilkie et al. (2004) undertook regular daily composite sampling of screened and settled effluent from a dairy in Florida, US, over a 1-year period for the purpose of characterising the waste to aid the application of fixed film anaerobic digestion technology. The milking herd averaged 359 cows and was permanently confined, producing around 500 m³ d⁻¹ of wastewater from hydraulic flushing of the freestall barns and the milking parlour with fresh (not recycled) water. Solids separation was estimated to remove 47% of TS and 60% of volatile solids (VS). The VS removed was found to have lower COD:VS ratio than the effluent, while the dissolved fraction of the effluent had the highest COD:VS ratio. This indicated that COD was concentrated in poorly settleable and soluble organic matter. Methane production from fixed film digestion of the effluent was reported to comprise up to 80% of the yield from whole manure, suggesting that most of the material removed in solids separation is poorly degradable.

Tie & Sivakumar (2007b) analysed various forms of DSE (from the one farm) including raw wastewater, effluent from a solids trap (see section 2.2.1), the same effluent passed through a 2-mm screen (in the lab post field sampling), and effluent from an AP to investigate the potential of applying and simulating treatment by anaerobic digestion. In developing analytical techniques for measuring VFAs and total reducing sugars, they found that concentrations of soluble COD and VFAs were higher in screened and unscreened solids trap effluent than in the raw wastewater. This, however, is likely to have been related to field sampling methods since the raw wastewater was a grab sample while the solids trap effluent was a 24-hour composite sample collected using an auto-sampler. Nonetheless, readily biodegradable sugars and VFAs comprised only 30-40% of soluble COD and around 10% of total COD, indicating that slowly or poorly biodegradable material makes up a significant proportion of soluble and particulate COD.

McGarvey et al. (2007) produced valuable insights into bacteria populations and nutrient removal arising from aerobic (25 °C) and anaerobic (37 °C) treatment in laboratory reactors fed once a day with manure screened then mixed with water to achieve TS 4%. The treatment reactors fed storage tanks, the contents of which were compared also with raw wastewater held in a storage tank. Significant reductions in TS, BOD were achieved under both treatment modes. Anaerobic treatment reduced sulphur and sulphate concentrations while ammonia-N and TN were reduced under aerobic treatment through mineralisation of proteins and urea, and nitrification. Denitrification occurred in subsequent storage under anoxic conditions. Aerobic treatment caused notable changes in the type of bacteria present in the wastewater, with oxygenation giving rise to higher *Proteobacteria* and reduced *Firmicutes* (obligate anaerobes) populations. Subsequent anoxic storage resulted in the *Firmicutes* population becoming re-established. Anaerobic treatment and subsequent storage resulted in less marked changes to influent phyla, presumably due to conditions reflecting those in the rumen of the cattle.

2.2.5 Effluent Recycling

There are two modes of effluent recycling employed in DSE management: through irrigation to pasture and crops and as flush water for cleaning holding yards, feed pads and other confinement areas. Land application is typically the ultimate destination for DSE in Australia, providing a means of 'disposing' of effluent without discharging directly to water bodies and offers the benefits of nutrient reuse. There has been extensive research into the impacts and benefits of land application of treated DSE and

pond sludge (e.g. Jacobs & Ward 2007a; Jacobs & Ward 2007c; Jacobs & Ward 2008; Jacobs, Ward & Kearney 2008; Ward & Jacobs 2008a; Ward & Jacobs 2008b; Bolan, Horne & Currie 2004; Cameron et al. 1996; Di et al. 1998; Di & Cameron 2000; Silva, Cameron & Hendry 1999; Zaman et al. 2002; Zaman et al. 1998). None of these studies, however, consider the effects of pumping effluent to land on the performance of pond systems, hence they will not be discussed in detail here.

Recycling effluent for use as flush water is typically employed to conserve water, particularly on dairies (or feedpads) utilising flood wash systems and where fresh water is scarce or expensive. It is typically used in conjunction with a two-stage pond system, although it is possible to use effluent from a single holding pond. Such recycling systems are always only partially closed since effluent irrigation is required to accommodate the fresh water used in plate coolers, for sanitation of milking equipment and in the cleaning of the milking parlour surfaces. Effluent recycling for flush water has direct implications for stabilisation pond treatment as it creates a feedback loop for conservative wastewater constituents including non-biodegradable organic material and soluble non-reactive mineral species such as K, Na and chloride. The replacement of fresh water with recirculated effluent in yard flushing causes the concentrations of conservative constituents to continually increase as the rate of dilution and removal is substantially reduced (Roberto & Sweeten 1985). Accumulation of conservative constituents can impair biological treatment, accelerate corrosion, promote scaling of pipes and fittings and lead to a general decline in effluent quality over time that could eventually lead to operational problems.

2.2.5.1 Accumulation of conservative species

Mason & Flowerday (2005) undertook modelling to investigate rates of dissolved salts accumulation in a partially closed DSE recycling system with a single pond at different ratios of fresh water to recycled effluent. The model assumed the pond to be completely mixed and considered two modes of pond operation: fixed volume in which excess wastewater flows out of the system, and variable volume storage in which wastewater accumulates in the pond. As it was a theoretical exercise, hydrology and effluent irrigation were not incorporated into the model. However, it demonstrated that salt accumulation occurs at a faster rate in smaller, variable volume systems, with concentrations in a 1500-m³ system exceeding a nominal limit of 3500 mg L⁻¹ (based on salinity considerations for ultimate land application of effluent) in less than 50 post-milking wash down events at fresh water fractions less than 0.5. The modelling also showed how flowthrough systems eventually reach a steady state condition, which at a

fresh water fraction of greater than 0.5 kept salinity at reasonable levels for land application.

Only a handful of published studies have monitored pond system performance and effluent quality under partially closed recycling. Rising EC trends in laboratory scale two-stage pond systems treating DSE and piggery wastewater and recirculating the treated effluent were reported by Hill et al. (1981). EC levels reached 3500-4000 $\mu\text{S cm}^{-1}$ in both ponds of the DSE system within 3 years of operation at moderate volatile solids loading rates (40-80 g VS m^{-3}) and a ratio of fresh water to recycled effluent of 0.25 (Hill, Hamilton & McCaskey 1980). The rate of salt build-up, however, was considerably lower than that observed in the ponds treating piggery wastewater due to the differing animal diets. TKN and ammonia-N concentrations also rose over time, although appeared to be levelling off towards the end of the study, perhaps as the system approached a steady state as COD appeared to do within about 40 weeks of operation. Georgacakis & Samantouros (1986) studied intentionally accelerated salt accumulation in laboratory-scale APs treating piggery wastewater, reporting that mixed salts of manure origin had a much reduced impact on biological activity than did chloride-based salts added at similar loads, which was attributed to antagonistic effects between salt, particularly cation, species. Salt levels (as EC) rose above 30 mS cm^{-1} before biological activity declined. The highest reported EC in an Australian DSE system supporting effluent recycling seen by this author is 9.2 mS cm^{-1} with much of the salt load coming from bore water (Jacobs & Ward 2008; Ward 2012, pers. comm. 5 June), indicating that effluent recycling should not generally pose a problem for pond biological activity.

Data presented by Westerman, Safley & Barker (1990) showed rising trends in supernatant orthophosphate and K in a poultry manure pond system and elevated average EC levels amongst 6 of 8 pond systems treating recycled flush waters from piggery, poultry and beef operations. Ammonia-N concentrations exhibited seasonality, peaking in spring and summer pattern, but did not increase over time. Mukhtar et al. (2004) found that effluent recycling increased the salinity and ammonia content of mixed pond contents. Sludge N, P and K levels were also higher on average in ponds receiving recycled flush waters, although the differences were not statistically significant. Güngör et al. (2009) attributed poor fermentation VFA yield from supernatant from a settling basin treating mechanically separated DSE to the accumulation of inert organic material associated with using recycled effluent for manure flushing. Despite 84% of the suspended solids of the wastewater being volatile,

fermentation achieved only very low destruction of TSS and did not measurably reduce the volatile fraction.

2.2.5.2 Struvite precipitation

Salt accumulation from effluent recycling eventually causes the formation of crystalline deposits that constrict and eventually block pumps, pipework and fittings (Hopkins 2002). The crystals typically take the form of magnesium ammonium phosphate ($\text{MgNH}_4\text{PO}_4 \cdot 6\text{H}_2\text{O}$), otherwise known as struvite, which precipitates out of solution when continuous recycling of effluent pushes the concentration of dissolved ionic species to supersaturation. In simple batch tests using centrifuged swine pond supernatant, Westerman, Safley & Barker (1985) observed the formation of crystalline deposits at Mg and orthophosphate concentrations as low as 15 and 30 mg/L, respectively, both of which are substantially lower than concentrations typically found in DSE systems. The common incidence of spontaneous struvite precipitation has prompted research into intentional or controlled precipitation from dairy manure wastewaters (e.g. Uludag-Demirer, Demirer & Chen 2005; Uludag-Demirer et al. 2008; Qureshi et al. 2006) as well as swine manure wastewaters (e.g. Beal, Burns & Stalder 1999; Nelson, Mikkelsen & Hesterberg 2003; Suzuki et al. 2002) and liquors from anaerobic digestion of activated sludge (e.g. Battistoni et al. 1997; Munch & Barr 2001; Battistoni et al. 2001; Türker & Çelen 2007).

Speciation of the components that form struvite is pH dependent, with competing equilibrium effects of hydrogenated phosphates, Mg hydroxo- and phosphate complexes and ammonia gas determining the ultimate solubility of the precipitate (Uludag-Demirer, Demirer & Chen 2005; Doyle & Parsons 2002; Wang et al. 2006; Ohlinger, Young & Schroeder 1998). Since phosphate ions are most active above pH 7, struvite is least soluble and most likely to precipitate under alkaline conditions up to a limit of about pH 11 (Doyle & Parsons 2002; Wang et al. 2006). The optimum pH will depend on the molar ratios and broader make-up of the solution but is generally around 9 for manure wastewaters (Wrigley, Webb & Venkitachalm 1992; Nelson, Mikkelsen & Hesterberg 2003; Wang et al. 2006). Data presented in 2.1.2 shows that raw DSE is generally alkaline, while carbon dioxide uptake by photosynthetic algae in DSE FPs can push pH towards the optimum range for struvite precipitation. Struvite is less likely to form in the more neutral environment of DSE APs. Temperature also affects struvite precipitation, with solubility decreasing with lower temperatures (Le Corre et al. 2009; Hanhoun et al. 2011), indicating that spontaneous precipitation is most likely to occur in a DSE pond system over winter.

Alkaline conditions combined with high P and Ca conditions can also lead to precipitation of Ca phosphates, particularly hydroxylapatite (Valsami-Jones 2001; Harris et al. 2008), yet scale found in manure wastewater systems has largely been reported to be struvite. Mg and carbonate ions are known to inhibit phosphate precipitation, as are low-molecular-weight organic acids (Valsami-Jones 2001). Indeed Battistoni et al. (1997) attributed the precipitation of struvite ahead of hydroxylapatite in anaerobic digester supernatant to the inhibition effect of Mg and bicarbonate ions. Westerman et al. (1985) suggested that struvite tends to be the main precipitation product in manure wastewaters on account of instability of Mg-organic matter complexes relative to similar Ca complexes and the higher solubility of Mg carbonates leaving Ca to preferentially precipitate with carbonate. Interestingly, however, Harris et al. (2008) found that at pH greater than 9, addition of Mg aided precipitation of Ca phosphate by preventing precipitation of Ca carbonate.

Struvite precipitation occurs most where liquid comes into contact with surfaces and in high energy (turbulent) environments; hence the preferential deposition observed in pipe bends and pumps. Field tests recirculating poultry pond supernatant demonstrated deposits form preferentially on metal fittings (particularly metal footvalves) and pump components (impellers and discharge ports), but also forms in PVC and PE pipes. Booram et al. (1975) contended that contact with rough, metallic surfaces was the critical determinant to preferential crystal growth. Loewenthal et al. (1994), however, produced a chemical equilibrium model that demonstrated how struvite precipitation is triggered by small drops in pressure at pump inlets and pipe bends that cause degassing of CO₂ and an associated rise in pH. Struvite precipitation may be divided into two stages: the initial formation of crystals, or nucleation, and crystal growth (Doyle & Parsons 2002). Analysing experimental and modelling data, Ohlinge et al. (1999) concluded that preferential struvite deposition was primarily a function of mixing energy on the basis that nucleation was a reaction-controlled process governed by saturation state, which is relatively uniform in a liquid, while the crystal growth rate was transport-limited and therefore a function of local mixing energy. They highlighted that acceleration of crystal growth through turbulent mixing from aeration was far more influential to preferential deposition than accelerated induction from localised shifts in thermodynamic properties, in particular reduced solubility under elevated pH caused by CO₂ liberation. Ohlinge et al. (1999) also found that crystal growth on surfaces was a function of the mixing energy induced by local turbulence and/or additional nucleation sites associated with the surface roughness of a material more than the type of

material. Doyle et al. (2002) on the other hand found that crystal growth was a function of both material type and roughness.

2.2.5.3 Pathogens

The use of recycled effluent near (but not directly on) milking facilities raises concerns about pathogen risks and hygiene; however a number of studies have shown the risk to be low. In their laboratory study of ponds treating recirculated effluent, Hill, McCaskey & Hamilton (1981) found that despite the recirculation of effluent, pathogen destruction appeared to be effective with all traces of *Salmonella* introduced via inoculation eliminated within 32 weeks after an initial growth period. Janzen & Bishop (1983) compared bacterial counts in fresh and recycled flush waters before and during flushing of animal holding pens, finding that while there were higher counts in the recycled water before it was used, the use of treated effluent did not make a measurable difference to pathogen numbers in the resulting wastewater. Ramsey & Megehee (1988) collected swab samples from the floor of a dairy holding lot following flushing with fresh water and recycled effluent from the third cell in a treatment pond series. They found no statistically significant differences (based on a total of 32 observations) in microbial counts or numbers of enteric indicator bacteria between water- and effluent-flushed surfaces. In addition, four hours of exposure to sunlight significantly reduced counts of the microorganisms analysed. Sampling of cow teats also found no added microorganisms from the use of recycled effluent.

2.3 MODELLING DSE SYSTEMS

Modelling of conventional DSE systems in Australia and NZ is largely confined to design applications. There are two sets of design calculator type tools currently in circulation: the dairy calculator series that includes Dairy Flood Wash, Dairy Solids Trap, Dairy Pond and Dairy Effluent produced by the Queensland Department of Primary Industries and Fisheries (Skerman 2004c) and the Dairy Effluent Toolkit originally developed by the Victorian Department of Primary Industries (McDowell & Birchall 2010). With respect to treatment by solids separation and stabilisation ponds, these tools only consider the effects on the nutrient composition of the effluent by way of assigning coarse factors to estimated influent loads that represent partitioning to the sludge in a primary pond and loss of N via ammonia volatilisation. It was recognised in a paper presenting the Dairy Calculator series that the tool required validation against data from working systems in Australia and that there existed significant research gaps in relation to reliable Australian data on the 'decomposition of solids in effluent systems, waste partitioning between separated solids, pond sludge and liquid effluent'

(Skerman 2004c). A study by Skerman et al. (2006) set out to validate the Dairy Pond calculator and found that the model produced poor predictions of effluent nutrient composition.

A more sophisticated modelling platform used for optimising effluent storage and land application areas for handling effluent from sewage treatment plants, feedlots and piggeries as well as dairies is the Model for Effluent Disposal Using Land Irrigation, or MEDLI (Vieritz et al. 1998). MEDLI comprises a range of static, steady state, dynamic sub-models (daily time step) including waste estimation, pretreatment partitioning, pond water and constituent mass balances, soil water and nutrient balances, soil salinity, pasture and crop growth (for nutrient uptake), groundwater transport, and aerosol pathogen dispersion. The pretreatment module reduces effluent solids and nutrient loads by user-specified fractions. The water and mass balances of the pond module accommodate dilution by rainfall and concentration by evaporation, sludge accumulation, recirculation of constituents via effluent recycling and associated salt accumulation and hydraulic and soluble constituent losses to seepage. Nutrients (N, P and K) are considered in total fractions only and sedimentation and ammonia volatilisation are the only treatment processes considered, although nutrients are also lost to seepage. Volatilisation is a function of surface area and concentration adjusted by a proportionality constant while settling fractions are used to estimate partitioning of nutrients to sludge. It is unclear how nutrient loads lost to seepage are calculated. The technical manual explicitly states that 'No attempt has been made to model the chemical interactions within the pond nor the effects of temperature on these reactions' (Casey & Atzeni 1998). The extant version of MEDLI was released in 1998 (although a new version is under development). Nonetheless it currently remains the most powerful DSE modelling tool available in Australia.

The salt accumulation model formulated by Mason & Flowerday (2005) referred to earlier was essentially a dynamic mass balance of inert salts (as total dissolved solids) and as such did not consider treatment dynamics in the pond. The only known example of modelling of treatment occurring in a DSE system was that performed by Fyfe (2004) who developed simple temperature-dependent first order kinetic models (see section 2.4.1 below) of removal of oxygen demand, solids and nutrients in a system comprising a conventional two-stage pond system followed by two wetland cells. The two stabilisation ponds were treated as lumped complete mix reactors, while the wetland models considered the two cells as a lumped plug flow reactor. The reactor models incorporated adjustments to accommodate changes in flow related to the hydrology of the system. While reasonable agreement was achieved with observed data, the models

provided very limited insight into the actual treatment processes occurring in the ponds/wetlands.

In addition to the models pertaining to DSE treatment in stabilisation ponds described above there are a number of examples of modelling of alternative treatment approaches which are reviewed below. First, though, the various approaches to predicting DSE production and composition are explored.

2.3.1 Modelling Effluent Generation

DSE composition is typically estimated based on the manure load captured at the dairy (and the feedpad if connected to the effluent management system) and the volume of water used to flush the manure load. Manure loads may be drawn from typical characteristics such as those published by ASAE (2003) or NRCS (2008) that are expressed in terms of animal body weight, while the fraction captured at the dairy or feedpad is based on the percentage of time the herd spends on the area. This is the approach used in the MEDLI model, which uses manure composition data presented by van Horn et al. (1994) scaled according to animal liveweight. In recognition of the variability of manure produced under different conditions, typical analyses are being superseded by regression models that predict manure composition using milk yield, dry matter intake (DMI), body weight and dietary composition as per Nennich (2005) and ASAE (2005). Birchall et al. (2008) warn that being derived from data drawn from US farming systems, equations based on DMI and feed nutrient concentrations are difficult to apply to grazed herds for which dietary parameters are difficult to determine. Accordingly, the Effluent Toolkit uses equations from Nennich et al. (2005) that use milk yield as the only independent variable.

To estimate likely loading to a pond system, the Dairy Pond calculator uses average daily TS and VS production rates (5.2 and $4.4 \text{ kg cow}^{-1} \text{ d}^{-1}$, respectively) that were derived using the DairyBal model (McGahan et al. 2009) for typical farm systems in Queensland, Australia (Skerman 2004c). The DairyBAL model adopts a dry matter digestibility approximation of manure production (DMDAMP) approach to estimating manure composition. TS excreted in manure are estimated as the non-digestible portion of the combined DMI from pastures, forages and supplements. Manure fixed solids (FS) and nutrients (N, P, K) are considered proportional to the ash or nutrient content of the feed with allowances made for quantities going to milk production while VS are the difference between manure TS and FS. Critically, the DairyBAL model is yet to be validated against field data from a working Australian dairy farm (McGahan, Ouellet-Plamondon & Watts 2010).

The NZ dairy farm nutrient budgeting model OVERSEER also uses dietary intake as the basis for estimating DSE loads. The approach, summarised in Figure 2-3, explicitly avoids using typical data on effluent composition and wastewater flow on account of the high variability described in section 2.1.2 (Wheeler, Shepherd & Power 2012).

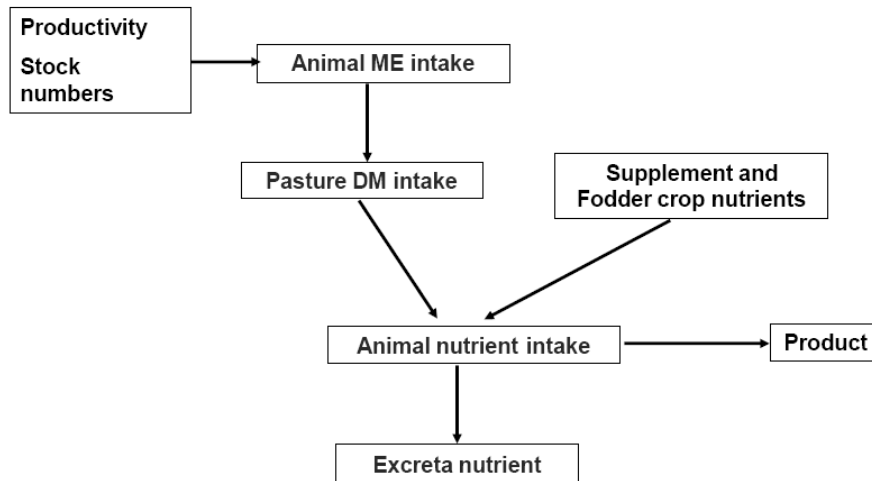


Figure 2-3 Effluent constituent load estimation in OVERSEER (Wheeler, Shepherd & Power 2012).

Methods for estimating manure and effluent loads have also been developed as part of greenhouse gas emission accounting and abatement assessment methodologies. The Dairy Greenhouse Gas Abatement Strategy (DGAS) calculator is an industry-endorsed analytical tool that adopts Australian National Greenhouse Gas Inventory (NGGI) algorithms (DCCEE 2009) to estimate on-farm emissions (Christie et al. 2012). Manure volatile solids are estimated from dry matter intake (which may be calculated from average liveweight, liveweight gain and metabolic rate using an empirical formula) including additional intake for milk production, dry matter digestibility and ash content. Manure N is divided into faeces and urine loads. Faeces N is determined from crude protein intake and digestibility together with a function of metabolisable energy and dry matter intake. Urine N is essentially the balance between total crude protein intake, faecal N and N retained by the animal.

2.3.2 Modelling of Other Forms of DSE Treatment

The paucity of DSE modelling precedents is not confined to stabilisation pond treatment. While there have been numerous studies into alternative treatment modes (see section 2.2.4), very few have attempted modelling the processes involved. There are several examples of modelling anaerobic digestion of raw dairy manure (e.g. Hill, Taylor & Grift 2001; Page et al. 2008); however since the focus of this study is flushed manure they are not reviewed here. Wood et al. (2007) applied a simple first model

equation with a term for bed adsorption to predict BOD_5 removal in downflow reed beds treating raw and aerated DSE from a 400-head milking herd in the UK. The model predictions showed good agreement with observed data and was used to estimate the required area for a full-scale treatment system. However it provided no insight into the inner workings of the reed bed or the impact on other constituents. Otherwise, published research employing modelling to investigate DSE treatment has largely come from a team based at Virginia Tech in the US and is summarised below.

Whichard (2001) complemented lab-scale tests of treatment of pretreated (solids separation) flushed dairy manure in an anoxic/aerobic sequencing batch reactor (SBR) configured for N removal with simulations of the same process using the BioWin activated sludge model simulation package (EnviroSim Associates Ltd. 2007). To inform the modelling, Whichard (2001) conducted experiments to determine critical activated sludge model parameters such as heterotrophic growth and decay rates. The modelling was designed to determine an optimum influent loading regime for the SBR, finding that denitrification was most effective when influent step feed volumes were incrementally reduced with each sub-cycle from an initial loading of 40%. In recognition that modelling a delicately balanced SBR system could be prone to inaccuracies from parameter error, sensitivity analysis was performed using eight criteria applied to 11 key parameters. The analysis revealed that many of the kinetic and stoichiometric parameters had little bearing on the outcome of simulations provided they were within typical ranges used in activated sludge modelling (despite the wastewater being DSE). However, the heterotrophic maximum specific growth rate and half-saturation constant, the autotrophic yield, autotrophic half saturation constant, and the oxygen concentration used in the autotrophic switching function did exert minor influence on simulation outcomes. Hydrolysis was also thought to be influential where settling was not efficient.

Exploring the potential for enhanced biological P removal (EBPR) of DSE, Yanosek et al. (2003) undertook a sensitivity analysis using a BioWin model of an SBR to identify critical parameters related to EBPR. Assigning up to 15% of soluble and colloidal COD in the influent DSE to volatile fatty acid (VFA) COD based on results from fermentation experiments, the modelling showed that effluent orthophosphate was largely unaffected by changes to heterotrophic growth parameters (since there was already sufficient carbon from VFAs). Phosphate removal was also insensitive to autotrophic growth parameters due to growth conditions being inadequate to support autotrophic organisms. Six critical parameters related to phosphorus accumulating organism (PAO)

growth were identified and ranges for corresponding parameter values within which EBPR could be sustained were reported on.

Beck et al. (2007) also used BioWin to simulate biological N removal in an SBR, in this instance treating liquid fraction of mechanically separated dairy manure. Examining the potential for using nitrification of ammonia-N (oxidation to nitrite under low oxygen conditions) followed by denitrification using VFAs from pre-fermented wastewater as an energy source, modelling was performed to predict an initial operating strategy for a pilot SBR. Poor performance of the pilot system necessitating increasing of the solids retention and aeration times indicated the presence of a nitrification inhibitor. This was confirmed by experimentation with dilution of fermenter supernatant and prompted a modelling sensitivity analysis to determine which ammonia oxidising biomass (AOB) parameters could be adjusted to calibrate the model to the observed data (Beck 2007). When inhibition functions were subsequently applied to the AOB maximum specific growth rate and half saturation coefficient, the simulation outputs still differed from the pilot plant data. The discrepancies could be remedied by reducing the BioWin default hydrolysis rate, which was thought to be reflective of inhibition from CuSO_4 from a cattle foot bath.

2.4 MODELLING OF STABILISATION PONDS

While dynamic process modelling of DSE treatment has been focused on other technologies, contemporary modelling of sewage stabilisation ponds is highly advanced, with cutting edge models incorporating comprehensive chemical and biological process models as well as simulating fluid dynamics. In a review of stabilisation pond design and modelling, Shilton (2001) identified four categories of approaches:

- loading rates,
- empirical equations,
- models based on reactor theory, and
- mechanistic models.

The loading rate approach to pond design is essentially a benchmarking methodology linking wastewater constituent loading quantified according to the sector from which it is drawn to pond size (area or volume). Despite offering only qualitative links to predicted effluent quality and variability, this is the approach used for designing stabilisation ponds treating DSE in Australia and New Zealand as outlined in sections 2.2.2 and 2.2.3.

Empirical equations have in the past been derived in attempts to explain or predict pond performance (see for example Ellis & Rodrigues 1995b). However their utility is limited by the selection of variables included in the model and the fact that empirical models rarely translate well outside the conditions under which they were derived. Moreover, most empirical models consider only static variables and are not designed for dynamic analyses. Hence they warrant no further discussion in this review.

Taking the approach pioneered in chemical reaction engineering, reactor theory models use idealised flow regimes to simplify pond hydraulics and lump the effects of the multitude of treatment processes into a first order kinetic model. These types of models represented a move towards a more mechanistic understanding of pond performance, but they remained essentially empirical in that the few model parameters were fitted to observed data and could not be generalised to allow for different design configurations, wastewater types, hydrology, biology and so on. Mechanistic models, also referred to as biokinetic models, also make use of the simplified hydraulics of reactor theory but simulate pond function using an array of equations that describe fundamental physical, biological and chemical processes occurring in the pond. Attempts to improve on the simplistic hydraulics of biokinetic (and first order) models have involved compartmentalisation of the pond liquid body into arrangements of smaller interconnected reactors. Another category of pond modelling has emerged in recent years, which uses adaptations of sophisticated and more established biokinetic models developed for other applications such as activated sludge or water quality modelling. Such adaptations typically adopt a compartmentalisation approach to represent pond hydraulics. As modelling of the treatment processes has evolved with greater access to increasingly powerful personal computing, so has modelling of fluid dynamics. This has inevitably led to the emergence of a sixth modelling category that merges biokinetic models and computational fluid dynamics.

2.4.1 First Order Reactor Theory Models

Modelling based on reactor theory assumes that the pond flow regime approximates one of the two idealised hydrodynamic states – completely mixed (CM) and plug flow (PF). A second gross assumption is that the multitude of processes that effect removal of organic matter or pathogens can be distilled to a single first order reaction. Under a CM model, constituents in the incoming wastewater are assumed to instantaneously mix with the contents of the pond reactor (Shilton & Sweeney 2005). Every molecule of wastewater has an equal probability of leaving the reactor at any given time, but also of remaining in the reactor for the duration of the theoretical hydraulic retention time.

Effluent leaving a complete mix reactor thus has the same constituent concentrations as does the liquid in the reactor itself. Application of first order CM models typically involves empirically determining a rate constant for consumption of a selected substrate such as BOD₅ or COD (e.g. Ellis & Rodrigues 1995a; Torres et al. 1997).

Under the idealised PF hydrodynamic regime, a discrete volume of wastewater is assumed to move incrementally through the reactor without mixing with wastewater that enters before or after it. A PF model is the theoretical equivalent of an infinite series of complete mix reactors. All wastewater is held in the reactor for the entire duration of the hydraulic retention time (Marchand 1997), making PF reactors theoretically more efficient than CM reactors of the same size. Figure 2-4 shows the difference in treatment performance between CM and PF reactors at different first order reaction rates.

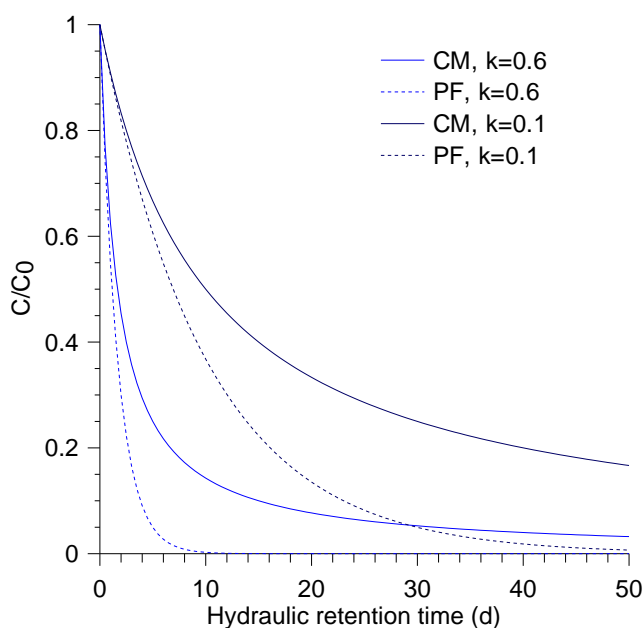


Figure 2-4 Theoretical treatment efficiency of CM and PF reactors under first order kinetics. C = effluent substrate concentration; C_0 = influent substrate concentration.

2.4.1.1 Non-deal (dispersed) flow

Empirically derived reaction first order rate coefficients for CM and PF models based on theoretical retention times effectively lump into one parameter not only the complexity of treatment, but also the various hydraulic inefficiencies that may be present in a pond. Dispersed flow reactor models represent an attempt to derive separate parameters for treatment and hydraulics and are used to reflect departures from the plug-flow regime described above caused by axial dispersion of the substrate (Shilton & Sweeney 2005). As such they are characterised by the dispersion

coefficient, d , which is meant to account for the mixing effects of diffusion and advection such that when d is 0 the expression simplifies to a plug flow model and when d approaches infinity, the model becomes complete mix. Thus, d is a simple quantification of the extent of mixing and is determined by tracking the passage of a known quantity of a non-reactive substance (tracer) through a reactor.

Polprasert & Bhattarai (1985) asserted that the dispersed flow model better reflected the hydraulic conditions of WSPs than ideal reactor models, demonstrating the point by applying the model to total and faecal coliform removal. However, mixing in large, exposed reactors such as stabilisation ponds is subject to a host of hydraulic and environmental vagaries, meaning that a singular value for d must somehow represent an array of dynamic complexities such as (Shilton 2001):

- inflow jetting and plunging,
- short-circuiting,
- dead zones,
- stratification,
- recirculation,
- upwelling and overturn,
- flow, wind-induced and other turbulence

Moreover, estimation of the dispersion coefficient using a tracer study is subject to a range of limitations, most notably that the outcome reflects only a single snapshot of a dynamic system that may change substantially as internal and external driving forces such as temperature and thermal stratification, wind, inflow and biological activity change over time (Ferrara & Harleman 1981). This may explain why despite numerous studies describing tracer experiments to determine WSP dispersion coefficients, very few (one example being Soares & Bernardes (2001)) have taken the next step and applied the dispersed flow model to predict treatment performance.

2.4.2 Biokinetic Models

The shift towards mechanistic approaches to modelling of stabilisation pond performance was pioneered by Fritz, Middleton & Meredith (1979). Drawing from diverse fields including wastewater treatment, microbiology, limnology and water quality, they formulated a sophisticated suite of process models to represent biological processes mediated by bacteria and algae as well as a number of physical and chemical processes occurring in a FP. The pond was divided into a CM supernatant reactor and a hydraulically static sludge (detritus) reactor to simulate treatment effects

on twelve constituents using numerical methods to solve a set of simultaneous differential equations. Environmental forcing from air temperature, wind shear and solar radiation was also incorporated into the model, as was the pond hydrology. Bacterial growth was based on a soluble COD substrate monod function with dissolved oxygen (DO) and nutrient limitation. Algal growth took the same functional form but with CO_2 as substrate and additional terms to model responses to insolation and temperature. Organic N and P were subject to first order hydrolysis. Inorganic forms were utilised by algae and bacteria, and ammonia-N could be nitrified (denitrification was not considered). The model did not consider particulate substrate, thus settling was only applied to biomass detritus, which, once settled (according to first order kinetics), became a source of ammonia-N and inorganic carbon (C) and P via benthic regeneration. The absence of particulate influent COD required influent soluble COD to be inferred from total COD, which proved to be a limitation of the model. Simulations predicted diurnal DO and pH fluctuations associated with algal photosynthesis, although it was recognised that distribution of DO through the entire water column may have influenced other model parameters related to DO. Lack of data on sludge accumulation and biokinetics, and nitrification and denitrification in stabilisation ponds were identified as being impediments to accurate modelling of WSPs.

Ferrara and Harleman (1980) formulated a somewhat simpler dynamic biokinetic model for a FP that incorporated processes of settling, precipitation and biologically-mediated transformations between organic and inorganic forms of C, N and P. Mineralisation, settling of all organic constituents, and lumped P losses to precipitation and adsorption were modelled using first order kinetics. Algae and bacteria were lumped as organic carbon in a monod type equation for organism growth. Ammonia-N was not subject to nitrification, yet denitrification was included as a first order reaction. DO was not included as a state variable. Seepage losses were lumped into other rate constants. Overall it may be argued that in lumping so many processes into single equations, the model retains a high degree of empiricism. Nonetheless it represents an important development in the move towards mechanistic modelling of stabilisation ponds.

Houng and Gloyna (1984) undertook modelling of P removal in two laboratory scale pond systems incorporating anaerobic, facultative and polishing ponds. Each pond was divided into a CM supernatant reactor and a hydraulically static sludge reactor as depicted in Figure 2-6. In a two phase model, organic P could be settled to the sludge to be decomposed or mineralised in the supernatant. Inorganic P could undergo synthesis to organic P in the supernatant or sludge, and be precipitated/settled to or released from the sludge. A fraction of precipitated/settled P was made unavailable for

release. An alternative model that considered P as a total fraction only was also formulated as per (b) in Figure 2-6. All processes were modelled as first order reactions, although release from the sludge was a function of the concentration difference between the sludge and supernatant as opposed to just the sludge concentration. The modelling showed that P release from sediments was highest in the AP followed by the FP (the aerobic environment of the polishing pond was thought to prevent release), while microbial uptake was greatest in the facultative and polishing ponds due to algal growth.

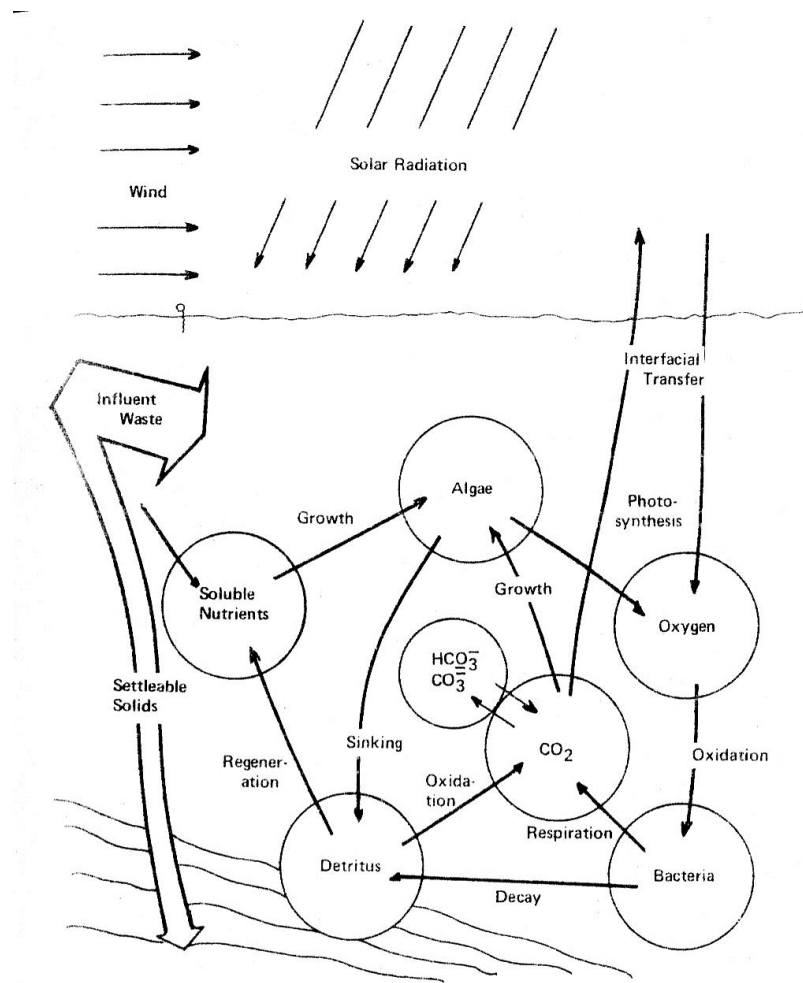


Figure 2-5 The conceptual framework behind the Fritz, Middleton & Meredith (1979, p.2725) WSP model.

In extending the model developed by Fritz, Middleton & Meredith (1979), Colomer and Rico (1993) changed the primary substrate state variable to BOD, modified the nitrification equation to temperature- and pH-dependent monod form, and added process models for ammonia volatilisation, denitrification and P precipitation, among other improvements. The model was calibrated to a data set sourced from the literature, and comparisons with outputs from the Fritz, Middleton & Meredith (1979)

model suggested that the modifications improved the predictive power of the model, while sensitivity analysis showed that aside from retention time, the most influential parameters in the model included the Arrhenius constant for temperature adjustment, bacterial synthesis efficiency, the aerobic substrate decomposition rate constant, and the algal maximum growth rate, oxygen yield and light extinction constants.

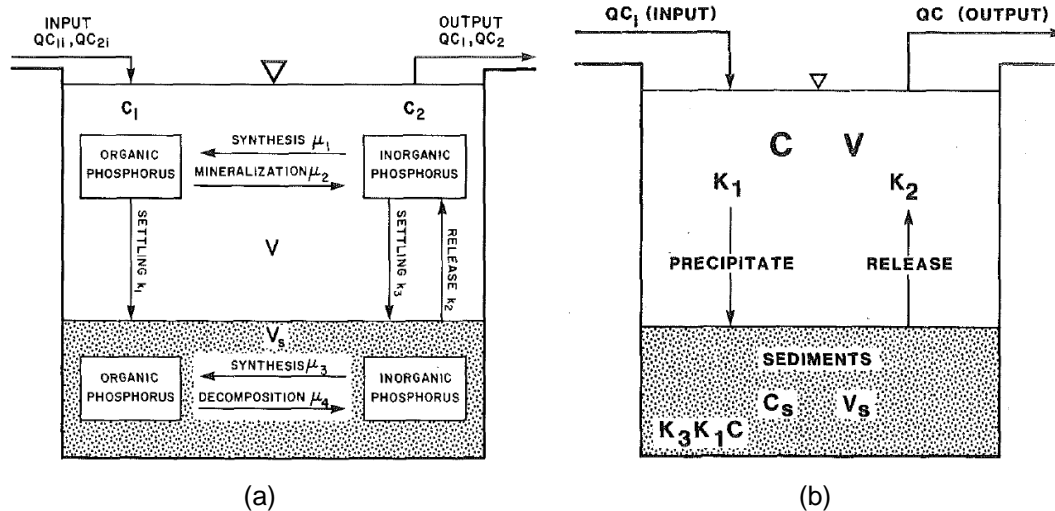


Figure 2-6 The organic-inorganic P (a) and total P (B) models by Houngh and Gloyna (1984).

Xian-Hua, Yi & Xia-Sheng (1994) presented a stabilisation pond model that used monod expressions for algal and bacterial growth and first order equations for 'all other biochemical reactions such as biodecay, biolysis and organism settling'. Nitrification-denitrification was neglected altogether, and settling and sediment decomposition were lumped into a single expression. Reincorporation of constituents from the sludge was also ignored as the laboratory-scale ponds used to calibrate the model were too small to effect sedimentation, yet settling of algae and bacteria made up a significant fraction of the mass carbon balance. The paper presented very little information related to the calibration and validation of the model, instead focusing on the steady state simulation mass balance outputs.

Senzia et al. (2002) developed a model of a primary FP specifically for predicting N transformations. Using organic N, ammonia-N and nitrate as state variables, they adopted the same hydraulic regime and many of the equations for N used by Fritz, Middleton & Meredith (1979) and Colomer et al. (1993). Microbial uptake of ammonia-N and nitrate, however, used organic N as a surrogate for biomass in a monod expression that lumped algae and bacteria together. Denitrification was modelled as first order reaction with an Arrhenius temperature dependency. An analysis of N loads following the various pathways showed that sedimentation of non-biomass organic N

was the main removal pathway (9.7% of influent N), while denitrification removed 4% of incoming N. Contrary to many other studies, volatilisation losses were found to be negligible due to neutral pH levels, and effluent ammonia-N concentration was higher than the influent concentration, in part due to high mineralisation rates. Almost 40% of incoming N did not undergo any transformation.

Kayombo et al. (2000) developed a single state variable model to predict DO concentrations in FPs that incorporates production from algal growth (modelled by a monod function combined with light and pH dependency functions), and consumption by oxidation of organic matter and lumped, temperature-dependent respiration and excretion of algae. Surface re-aeration was assumed to have negligible effect on DO levels, but model predictions reasonably reflected DO concentrations observed over 16 days in primary and secondary FPs. The process equations of this DO model were to form part of a broader model that simulates removal of organic matter (as COD) in FPs (Mashauri & Kayombo 2002). The COD model includes additional terms for bacterial growth, sedimentation of algal and bacterial cells and inorganic carbon regeneration from anaerobic sludge, and borrows much from the work of Fritz, Middleton & Meredith (1979). Model predictions of effluent COD were of the right magnitude but did not correlate well with daily fluctuations due to inability to explain variability associated with environmental forcing. Predictions of algal and heterotrophic biomass were very good; however the analysis of mass flows appeared to give inexplicably imbalanced results.

A (primary) FP model developed in France took the common approach of dividing the pond vertically into two zones, but considered three microbial populations: (micro)algae and aerobic bacteria in the upper layer and sulphate-reducing bacteria in the bottom layer (Dochain et al. 2003). Monod growth kinetics were employed for the microorganisms with algae and aerobic bacteria consuming soluble organic carbon and the sulphate-reducing bacteria utilising particulate substrate. The initial model included state variables for oxygen, carbon dioxide and hydrogen sulphide, although in order to reduce the number of parameters to be identified, the state variable carbon dioxide and associated process equations were discarded. The model was calibrated and validated against DO data from single days in three different seasons based on adjustment of two critical parameters. Dochain et al. (2003) stated unambiguously that the model was burdened with a large number of parameters that required identification, although they did not present a sensitivity analysis to explore the leverage the various parameters exerted on the model.

2.4.2.1 Compartmental biokinetic models

A common feature amongst the biokinetic models described above is the division of the pond into discrete reactors representing the supernatant and the sludge. There are also examples of WSP models in which the concept of hydraulic discretisation has been applied to the supernatant so as to approximate the complex fluid dynamics within a pond. Such 'compartmental' or 'finite stage' models comprise a network of idealised reactors of different volumes connected by flow exchanges to represent the total liquid volume. Early compartmental models were predicated on simpler first order kinetics and steady state conditions but still required identification of multiple hydraulic parameters related to reactor sizes and exchange flows (e.g. Preul & Wagner 1988). More recently, compartmental models have incorporated biokinetic models, with some reactor configurations being calibrated against experimental data from dispersion studies.

A logical extension of the sludge-supernatant discretisation used in most of the models described above is the division of pond supernatant into vertical layers to simulate stratification. This was the approach taken by Soler et al. (2000) in developing a model for a 13.5-m deep sewage stabilisation pond operated in batch mode. The model comprised two interconnected CM reactors representing the division of the supernatant into an upper epilimnion and a hypolimnion below. The size of each reactor and hydraulic flow between them was dependent on the depth of the thermocline which was determined using a separate thermal model. Influent was only loaded to the epilimnion reactor. Material exchanges between the reactors consisted of first order settling of particulate material, hydraulic transfer of substrate and nutrients caused by deepening of the thermocline and regeneration of soluble nutrients from the sediments to the hypolimnion. Process models in the reactors largely took the form of those described by the Fritz, Middleton & Meredith (1979), except equations for algae, DO and nitrate were not included in the hypolimnion reactor and a first order equation for denitrification was added to the epilimnion reactor. The predictive power of the model was only assessed through t-tests to compare the mean values of outputs with mean experimental values; thus the dynamic capability of the model could not be determined.

Rajbhandari et al. (2007) adopted a compartmental approach to hydraulics in developing one of the few known biokinetic models of an AP. The model comprised a series of columns made up of reactors for bulk liquid and active sediments and non-reactive vessels for inert sediments as per Figure 2-7. Each liquid reactor was considered completely mixed through the effect of rising biogas bubbles. The number

of columns in series was determined from the inverse of the pond dispersion number, which was estimated experimentally for laboratory scale ponds and from an empirical equation for field scale ponds. The bulk liquid and active sediment model components were considered to be entirely anaerobic, utilising monod kinetics to simulate growth of methanogens and sulfidogens and first order kinetics to simulate settling of particulate matter, hydrolysis and microbial decay, and a surface area mass transfer model to simulate exchange of soluble components between sediments and liquid. The reactors did not vary in volume in response to accumulation of sediments, which the authors conceded was a limitation of the model. The model exhibited good predictive performance for removal of COD and sulphate when compared to experimental data from both laboratory scale and full scale ponds. The main limitations of the biokinetics were stated to be the omission of inhibition effects pH, VFA and sulphide.

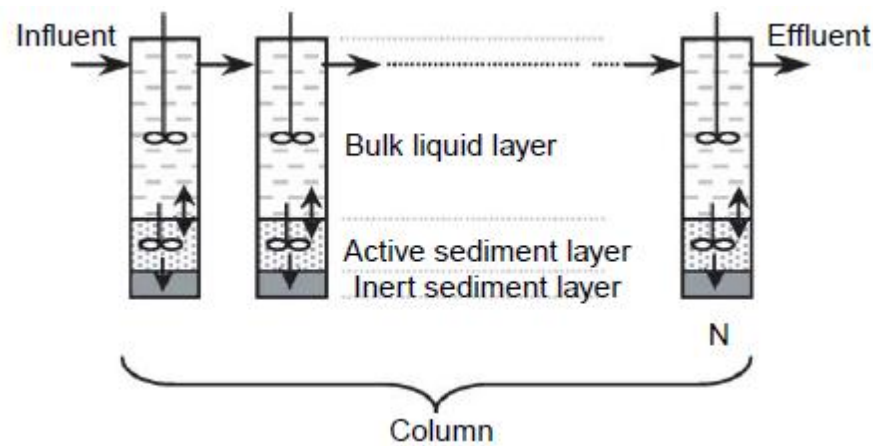


Figure 2-7 Hydraulic configuration of the AP model by Rajbhandari et al. (2007).

2.4.3 Adaptations of Activated Sludge Models

A number of researchers have taken the approach of adapting established biokinetic models developed for other types of wastewater treatment plants to simulate treatment in stabilisation ponds. In particular, the biokinetics of activated sludge (AS) models have been adopted, simplified and sometimes augmented with pond-specific reactions to simulate the conditions that occur in different stabilisation pond configurations. The main advantage of taking this approach is that AS models are highly developed, and the various commercial and other implementations available contain arrays of sophisticated physico-chemical and biological reaction equations with calibrated kinetic and stoichiometric parameters, most of which can be readily applied to stabilisation ponds. AS models also incorporate growth and decay of multiple types of bacteria consuming different substrates at varying rates and therefore represent a more sophisticated treatment of bacterial biology than most dedicated pond biokinetic

models. They do not, however, consider growth of algal biomass, which some researchers have addressed by adding process equations to the base AS model. And since AS models are based on CM reactors, adaptations to simulate ponds typically take a compartmental approach to representing pond hydraulics.

Houweling et al. (2005) modelled a series of four aerated FPs using a commercial implementation (GPS-X) of the Activated Sludge Model 2d (ASM2d, see Henze 2000). Each pond was represented by a pair of aerated and unaerated CM reactors representing the supernatant and sludge in each pond, respectively, as depicted in Figure 2-8. Sedimentation to the sludge was simulated by a hydraulic flow regulated by a mass partitioning (solids separation) unit. Settled constituents were returned to the supernatant via a recycle flow. The AS model (with biological P removal deactivated) was augmented with equations and stoichiometry for the anaerobic growth of methanogenic organisms and conversion of inert particulate COD to soluble substrate. However the addition of algal processes, which are central to FP functionality but are not accommodated in ASM2d, was not considered.

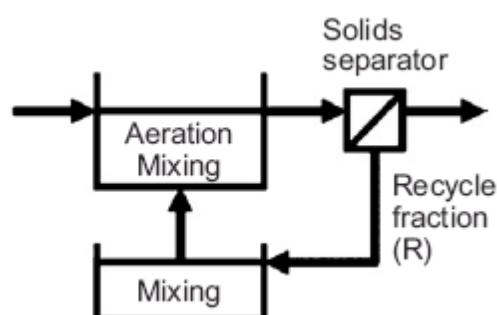


Figure 2-8 Aerated FP supernatant and sediment reactor configuration used by Houweling et al. (2005) and (2008).

The same configuration was used again in a subsequent study by Houweling et al. (2008), although unlike the earlier model which adopted a constant aeration rate, DO concentrations were entered into the model as a dynamic input. The sludge recycle flow was also a dynamic input, defined by a linear function of the measured aeration flow in the pond which was adjusted to aid calibration. The efficiency of the solids separator was set to reflect observed effluent TSS concentrations. All parameters used in the model were set to the source model defaults except for the specific growth rate of nitrifying biomass, which was again adjusted in the calibration process. Overall the model predicted nitrification dynamics well in calibration and validation, and the two reactor configuration - coined the 'simple hydraulic model-complex biokinetic model' -

was considered an adequate representation of sludge-supernatant interaction. The implications of neglecting algal processes, however, were not raised.

Houweling et al. (2007) examined the impact on nitrification rates of introducing baffles into short-circuiting aerated stabilisation ponds using a compartmental model configured to reflect the mixing regime of the pond. Biokinetic processes were modelled with ASM2d combined with a simplified death-regeneration nitrification model that simulated nitrifying biomass growth without DO dependency. The base model reactor network included an 'initial volume' of 4 CM reactors in series that received the influent, a large CM reactor representing the main supernatant body and a small plug-flow reactor made up of 16 CM reactors in series to represent short-circuiting. The number of reactors in each series and the fraction of the pond volume assigned to them were established by calibrating against residence time distributions (RTDs) derived from tracer studies. The effect of installing a baffle to prevent short-circuiting was simulated by removing the short-circuit chain of CM reactors, while installation of baffles to promote PF conditions was simulated with one long series of CM reactors. They managed to calibrate the base model to effluent ammonia-N concentrations by adjusting the nitrifying biomass growth rate, but noted that a shortcoming of the model configuration was that it did not account for the effects of substrate decomposition in the sludge and associated exchanges of soluble constituents with the supernatant.

Using a commercial implementation of Activated Sludge Model 3 (ASM3 in SIMBA), Gehring et al. (2010) developed a compartmental model to simulate treatment of landfill leachate in pilot scale facultative and maturation ponds. The base AS model was expanded with algal process models including solar radiation-mediated growth on ammonia-N and nitrate, and respiration. Ionic equilibrium equations for ammonia/ammonium and carbonate/carbon dioxide were also added, along with expressions for wind-assisted gas transfer between the air and the pond surface. Each pond was divided vertically into three CM reactors to reflect stratification. Flow through the system was held constant, but the manner in which the flow was routed through the three reactors was not elaborated on. The model appeared to predict FP effluent characteristics reasonably well, but there were notable discrepancies in the maturation pond predictions (see for example Figure 2-9) that were not addressed in the discussion of the results.

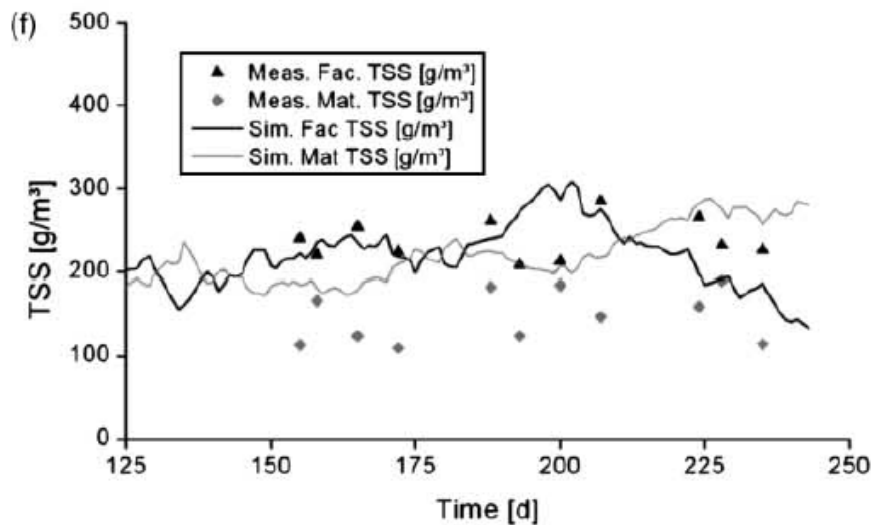


Figure 2-9 Facultative (Fac.) and maturation (Mat.) pond TSS concentrations (lines) predicted by the Gehring et al. (2010) model plotted against observed data.

Alvarado et al. (2012) used a computational fluid dynamics (CFD) model of a tertiary maturation pond calibrated against tracer response data to develop a compartmental hydraulic configuration to link with the Activated Sludge Model 1 (ASM1) (see Henze 2000). Using the velocity profile generated by the CFD model (that ignored wind, temperature and vertical diffusion effects to reduce computational load), tanks in series analysis and estimates of diffusion, a compartmental network of 25 CM reactors and 30 exchange fluxes was formulated. The final configuration (shown in Figure 2-10) comprised a primary flow through zone, which was assigned 13 CM reactors in series, an intermediate zone comprising a large CM reactor and several smaller reactors to redirect flow, and a recirculation zone made up of two large CMs and smaller reactors handling exchange flows. The synthetic RTD curve produced by the compartmental model was very similar to both experimental and CFD-derived RTD curves. By contrast, the synthetic RTD produced by a simple tanks-in-series (TIS) model of the same pond was notably different. The compartmental and TIS models were both coupled with ASM1 to demonstrate the effects of misrepresenting pond hydraulics on biokinetic modelling outputs. The over-simplification of pond hydraulics in the TIS model caused autotrophic biomass to be washed out of the reactor, resulting in very different predictions of effluent ammonia concentrations to those produced by the compartment model. It was concluded that care must be taken when using biokinetic models with simplified hydraulics to avoid adjusting biokinetic parameters to overcome hydraulics-related shortcomings.

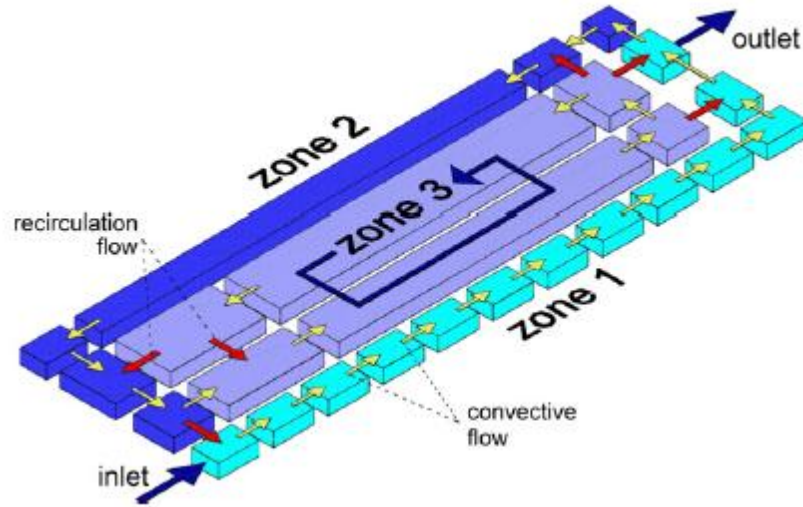


Figure 2-10 Compartmental model configuration used by Alvarado et al. (2012).

2.4.4 Integrating Fluid Dynamics, Dispersion and Biokinetic Models

Three-dimensional mass transport (mixing) in a fluid is a function of fluid velocity and molecular and turbulent diffusion and is governed by the advection-dispersion partial differential equation (Cussler 2009):

$$\frac{\partial C}{\partial T} = u_x \frac{\partial C}{\partial x} + u_y \frac{\partial C}{\partial y} + u_z \frac{\partial C}{\partial z} - \frac{\partial}{\partial x} \left(D_x \frac{\partial C}{\partial x} \right) - \frac{\partial}{\partial y} \left(D_y \frac{\partial C}{\partial y} \right) - \frac{\partial}{\partial z} \left(D_z \frac{\partial C}{\partial z} \right) + S_c \quad (1.1)$$

where

C = Constituent concentration;

u_x, u_y, u_z are fluid velocities in the x,y and z directions;

D_x, D_y, D_z are dispersion coefficients for the x,y and z directions;

S_c =function or group of functions describing process kinetics affecting the constituent.

The terms in equation 2.1 that incorporate dispersion coefficients represent mixing caused by turbulence and/or molecular diffusion. The terms incorporating velocity describe advective transport related to fluid motion in the pond. The term on the right hand side of the equation comprises the various equations that would form a biokinetic model. This form of the equation assumes that dispersion from turbulence dominates

and discounts molecular diffusion (or lumps it with dispersion). At very low velocities under laminar flow, diffusion and dispersion are analogous. However, at most non-zero velocities, dispersion becomes independent of diffusion and is instead proportional to velocity (Cussler 2009). Hence in an open system such as a pond in which there is continuous flow and currents and eddies associated with inflows, wind and convection are likely to occur, dispersion, particularly that associated with turbulence is likely to dominate. Where in the past modellers have had to rely on gross simplification, simplistic parametersation or a compartmental approach to address the hydraulic inefficiencies and dispersion described by the left hand side of equation 2.1, the ubiquity of powerful personal computers has enabled formulation of models that discretise the pond liquid body and employ sophisticated numerical methods to solve mass transport and biokinetic equations simultaneously.

A paper by Moreno-Grau et al. (1996) presents what would be the earliest known attempt to merge biokinetics with mass transport in a WSP model. They developed a longitudinal one dimensional fluid flow and dispersion model (the x-axis components in equation 2.1) to reflect the dispersed plug flow conditions in long, narrow and shallow ponds treating raw sewage. The biokinetic component considered growth of bacterial, algal and zooplankton biomass as well as macrophytes for a planted WSP (free water surface wetland) using monod kinetics. Respiration, decay and sedimentation were each modelled separately as first order reactions. The sub-models of Fritz et al. (1979) were adopted for benthic regeneration and surface re-aeration. COD was used as the organic substrate and was divided into settleable and non-settleable refractory and degradable fractions. There were also state variables for ammonia and organic N, soluble and total P, DO and total and faecal coliforms. The dispersion coefficient, which was universal for all constituents, was defined as a function of fluid velocity and depth and Manning's roughness. A finite difference numerical method was employed to solve the system of partial differential equations. Of the 85 model parameters listed, apparently only two were calibrated with the rest being drawn from the literature producing remarkably good agreement between predicted and observed COD, DO and chlorophyll-a concentrations.

In their model of a FP, Beran & Kargi (2005) took the abovementioned approach one step further by adding a second (vertical) dimension to the diffusion component. Reasoning that the inlet and outlet were evenly distributed along the pond width, causing the mixing to approximate plug flow, they discretised the pond to apply a Crank Nicholson numerical solution scheme to the governing mass transport equation - equation 2.1 without y and z velocity terms and the y dispersion term. Flow through the

pond was treated as open channel flow, using Manning's equation and the continuity equation to determine mean velocity in the pond. The longitudinal dispersion coefficient, which was universal for all wastewater parameters and presumably attempted to account for turbulence-related dispersion rather than molecular diffusion, was estimated by aligning observed and predicted supernatant concentrations measured along the length of the pond at the commencement of the monitoring and assuming a hydraulic retention time of one day. Sedimentation was incorporated by applying a settling velocity to biomass (but not incoming suspended material). Once sediments had reached the lower layers of the mesh, they were exempted from longitudinal advection and dispersion. They were still, however, subject to anaerobic decomposition, and resulting soluble compounds could be returned to the water column via a mass transfer diffusion model, coefficients for which were constituent-specific. The biokinetic model incorporated bacterial and algal growth, and a DO model responsive to photosynthesis, respiration, nitrification and surface reaeration. Many of the model parameters, were drawn from the studies described above as well as water quality and limnological models. The model was calibrated to data collected from the field by adjusting a total of eight biokinetic parameters along with the longitudinal dispersion coefficient. Beran & Kargi's model appeared to perform exceptionally well, producing time series predictions that agreed closely with observed data (see Figure 2-11) and exhibiting convincing diurnal variation, and spatial distributions of algae, bacteria and DO that align well with theory. The added z dimension, although not hydraulically active, facilitated the simulation of vertical gradients in DO and wastewater constituents that had not previously been achieved.

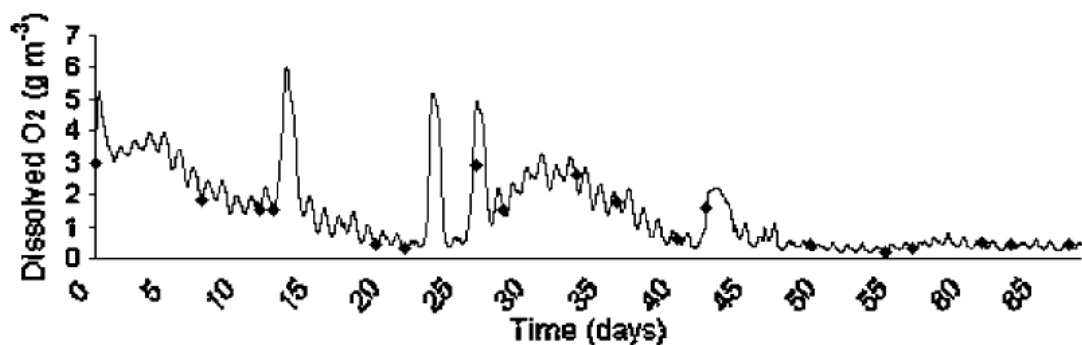


Figure 2-11 Plot of DO concentrations predicted by the Beran & Kargi (2005) model against observed data.

2.4.4.1 Coupling CFD and biokinetic models

The most powerful models now in development are those which leverage computational fluid dynamics (CFD) code to predict fluid velocities and turbulent dispersion, and link it with comprehensive biokinetic models. CFD may be described as the application of 'computer-based methods for solving the linked partial-differential equation set that governs the conservation of energy, momentum and mass in fluid flow' (Shilton 2001). On account of the intensive computing power required, CFD has only been applied to WSP modelling since the mid-1990s. On its own, CFD has been used in numerous studies investigating pond flow patterns and hydraulic phenomena. The influence of pond hydraulics on treatment efficiency has been explored with the aid of CFD by incorporating simple first order treatment equations for faecal coliforms (e.g. Shilton & Harrison 2003b) and BOD (e.g. Vega et al. 2003; Abbas, Nasr & Seif 2006).

It has been only very recently, however, that a CFD model has been coupled with a sophisticated biokinetic model. Sah et al. (2011) developed a model of a FP that integrated CFD with a comprehensive suite of treatment process models centred on growth and decay of bacteria and algae. Sedimentation, however, was excluded on the basis that TSS loading to a newly established secondary FP would be very low, and P was not included as a state variable. Ammonia volatilisation was also omitted as it was thought to have little bearing on N removal. Bacterial growth and associated processes were modelled with ASM1 while a constructed wetland model was used for anaerobic bacteria. The IWA river water quality model RWQM1 (Reichert et al. 2001) was used to simulate algal processes. The model was used to run simulations of the pond with and without baffles to promote plug flow and under continuous and intermittent wind blowing across or against the liquid flow. Due to a lack of available and sufficiently comprehensive data, model calibration could not be undertaken and was identified as a future research priority. Indeed, collecting the full suite of data required to calibrate such sophisticated models would appear to present a greater challenge than model specification.

2.4.5 Thermal models

The temperature-dependence of the various treatment processes that occur in WSPs is well established. Thus it is important that WSP models attempting to predict seasonal variation incorporate temperature either as a dynamic input or sub-model (Sah, Rousseau & Hooijmans 2012). Fritz et al. (1980) developed a dedicated model to predict bulk liquid temperature based on a thermal balance of incoming and outgoing flows and radiation, and evaporation losses. Outputs from the model were used to set

pond temperatures in the Fritz, Middleton & Meredith (1979) biokinetic model. Moreno-Grau et al. (1996) incorporated a similar heat budget sub-model into their 1-dimensional WSP model. Neither of these thermal models, however, considered stratification, both treating the pond contents as a completely mixed whole.

Thermal stratification inhibits vertical advection and mixing, thereby reducing active treatment volumes and creating gradients in biomass density and concentrations of wastewater constituents (Kellner & Pires 2002). With regards to WSP treatment modelling, stratification is often handled by discretising the pond into layers (e.g. Soler et al. 2000; Gehring et al. 2010), which does not necessarily allow for differences in temperature. The 2D model by Beran & Kargi (2005) predicted algal biomass stratification, but it is not clear whether this was related to solar radiation alone or if temperature gradients were also simulated. Gu & Stefan (1995) modified a 1-dimensional dynamic lake water quality driven by daily weather parameters to simulate thermal stratification in a tertiary WSP. Incorporating the hydrodynamic mixing effects of an inflow jet, the model successfully predicted large diurnal and seasonal swings in temperature gradients, and it was recommended that the model be linked with biological and chemical kinetic models to predict effluent quality. There does not appear, however, to be any publications since that describe an attempt to undertake this.

Sweeney et al. (2005) expanded a previously isothermal CFD model of a WSP to incorporate a thermal balance similar to those described above applied to each discrete element of the CFD grid. The accuracy of predictions was limited by the omission of wind shear, but the model showed that stratification was highly transient and spatially variable in the large pond, which would have implications for hydraulic and treatment efficiency. The integrated CFD-biokinetic model by Sah et al. (2011) managed to simulate stratification in temperature as well as DO, algal biomass and other components by incorporating a heat flux sub-model that appears to have been applied to the discretised CFD grid in full. Simulations demonstrated that cross winds readily break down stratification and generate recirculation flows. Under the specific boundary and forcing conditions simulated, COD removal was very similar whether the pond was stratified or exposed to wind.

2.5 SUMMARY

DSE is characterised by its strong organic loading, coarse particulate material and unpredictable hydraulic loading that makes it difficult to sample representatively. Influenced by a range of factors, DSE composition and particularly nutrient content can

vary significantly between farms and over time within a given farm. Its treatment in Australian and New Zealand contexts generally comprises two-stage stabilisation pond systems, which may be preceded by solids separation, most commonly in a trafficable solids trap. The very limited research into the performance of solids traps suggests that their efficiency may not be as high as anticipated in design guidelines and tools. Research into the behaviour and performance of DSE stabilisation ponds in Australia has been limited to a handful of studies designed to quantify the nutrient loads contained in their supernatant.

Primary anaerobic ponds have been the subject of limited research overseas which has been mostly targeted at aspects of their function other than their internal treatment processes such as biogas and ammonia emissions. Hence there is very little data available on the dynamic processes that take place within these ponds or the associated partitioning and transformations of wastewater constituents. Sedimentation and associated accumulation and digestion of sludge are known to be behind the reasonably effective removal/degradation of organic material, yet there have been no studies that have attempted to quantify mass loads of anything other than volatile solids accumulating in sludge. Secondary facultative ponds are better understood, mostly thanks to a number of detailed studies undertaken in New Zealand. Characterised by their diurnal fluctuations related to thermal stratification and algal photosynthesis, there exists a reasonable bank of data that provides a sense of effluent/supernatant quality and variability, as well as the factors involved in the decomposition of the poorly biodegradable organic substrate that remains after anaerobic pond treatment of DSE. There is very little known, however, about the prevalence or relative influence of the processes that are known to affect nutrients in FPs as applied to DSE ponds.

Effluent recycling for use as flush water is a common feature amongst dairy farms seeking to be water efficient. This review identified a small number of overseas studies that were primarily interested in the dynamics of these partially closed recycling systems, particularly the accumulation of inert constituents. None of these, however, have involved monitoring of a real world DSE system, let alone in Australia. Pathogen risks have been explored in at least two studies and found to be minor. The formation of struvite deposits causing blockages in pumps and pipes, however, is a common occurrence in effluent recycling systems handling manure wastewaters. There is an enormous bank of knowledge related to struvite precipitation that has in the main been developed through research into the prospects for recovery of the mineral in engineered reactors. Less is understood in relation to the incidence and extent of

struvite precipitation in WSPs (DSE or otherwise) and its role in ammonia and P removal.

Models of DSE handling and treatment in Australia have been developed for sizing ponds, predicting nutrient loads for land application and accounting of greenhouse gas emissions. Manure production models that are used to predict effluent constituent loads also have yet to be validated against Australian data. Models of pond treatment rely on coarse partitioning factors that do not appear to be supported by data collected from Australian pond systems. More sophisticated modelling of DSE treatment has been performed in a number of US studies, but these have focused on sequencing batch reactor approaches to DSE treatment.

Modelling of stabilisation ponds treating sewage is far more advanced with numerous examples of dynamic models, mostly formulated to simulate facultative ponds, of various levels of complexity in terms of both biokinetics and hydraulics. A number of studies have opted to leverage the more advanced models developed for activated sludge modelling, taking a compartmental approach to simulating pond hydraulics. Models have also been developed to examine temperature and stratification dynamics, while others have linked pond-specific biokinetic models to 1D or 2D mass transport models. Computational fluid dynamics is also increasingly being employed to assist with or even perform simulations of pond treatment. Perhaps the most comprehensive WSP model to date is one which merges three biokinetic models, albeit with a reduced set of processes and state variables, with a CFD model that incorporates a thermal sub-model. The model is so advanced, however, that producing a suitably comprehensive data set against which to calibrate it presents an enormous challenge in itself.

2.5.1 Research gaps

The previous remark related to data and model calibration brings us to the key research gap in relation to modelling of DSE pond systems. While existing models may be simplistic, this is just as much a limitation of data availability as it is a lack of model development. The generation of a sufficiently comprehensive data set that includes information on prevailing in-pond conditions, environmental forcing and critical hydraulic and mass flows was therefore the primary focus of the research presented in the forthcoming chapters. In addition to this, this thesis addresses the following research gaps identified in this literature review:

- development of a mass flows analysis of key wastewater constituents in a DSE stabilisation pond system;
- identification of key treatment processes that determine DSE pond effluent quality;
- development of a dynamic, mechanistic model to simulate a DSE pond;
- generation of a data set that can provide the basis for calibrating a biokinetic model of a DSE pond.

Chapter 3

SITE SELECTION AND CHARACTERISATION

Central to this study was the collection of real-world data from an operational dairy farm. This chapter describes the process and rationale behind the selection of an appropriate site upon which to focus the research. Also presented is a general description of the farm site and its operations along with a more detailed characterisation of the farm's waste management system, including its design, configuration, components, operation and maintenance. Finally, the approach taken to monitoring the site conditions and the waste management system is explained.

3.1 SELECTION PROCESS

The primary aim of this research was to develop a stronger understanding of DSE stabilisation pond function and the impacts on pond systems when treated effluent is recycled at the dairy. Thus the fundamental requirement for selecting a farm site was that the DSE management system incorporated a two-stage (or more) stabilisation pond treatment system and effluent recirculation. Additional key criteria for selection of a research site included:

- an operational and commercially-viable dairy farm with a full-scale and functional waste management system and a medium to large size herd that represents the current and future direction of dairying in Australia;
- a stabilisation pond system that, at the commencement of the research, complied with Australian best practice standards in terms of design, construction and present working condition;
- a farm that was located within a manageable distance from the research base (the University of Wollongong);
- a farm owner/operator that was co-operative and accommodating; and
- a site that was readily accessible to allow regular site visits and amenable to installation of automated monitoring and sampling systems.

Proximity to the University of Wollongong determined the pool of dairy farms that was to come under consideration for site selection. A number of dairying regions were within a commutable distance from the University including southern Illawarra (Dapto, Albion Park, Jamberoo, Kiama, Gerringong and Gerroa), northern Shoalhaven (Berry, Kangaroo Valley) and the Southern Highlands (Robertson, Bowral, Mittagong, Moss Vale). On account of the author's previous research work in the area (see Fyfe 1999;

Fyfe 2004), the majority of the farms considered as research site candidates were located within the Southern Highlands region. In addition, the assistance offered to local farmers by the Sydney Catchment Authority through the Primary Industries Program (and previously by the Department of Land and Water Conservation through the Catchment Protection Scheme) had ensured that most farms in the Southern Highlands had adopted best practice waste management. Nonetheless, at least four dairy farms from the other regions that had adopted best practice waste management were factored into the selection process.

Initially, a farm located just north of the town of Gerringong on the South Coast was selected as the research site. However preliminary investigations revealed that the primary pond was on the verge of failure due to excessive sludge accumulation. Desludging of the pond was not a priority for the farm manager at the time (the farm was experiencing severe drought conditions), thus an alternative site had to be found. This came in the form of a farm called 'Sugarloaf Holsteins' located in the northeast of the Southern Highlands dairying region. This farm had relatively new milking and waste management facilities and a receptive and cooperative owner-operator. Consultation with the owner and a subsequent site investigation confirmed that the farm satisfied all the key site selection criteria.

3.2 FARM DESCRIPTION

Sugarloaf Holsteins was established in 1862 and at the time of the study was the oldest continuously-run family operated dairy farm in Australia. It is located within the upper Nepean catchment in the Kangaloon district of the Southern Highlands of NSW, Australia (refer to Figure 3-1). The farm dairy is situated at latitude 34.5336 °S and longitude 150.5493 °E, approximately 680m above sea level. The immediate surroundings of the farm comprise cleared agricultural land on undulating terrain. However the protected catchment areas of Avon and Wingecarribee dams sit a few kilometres to the northeast and southwest of the site, respectively. At the commencement of the study, the farm ran a 300-cow milking herd that grazed improved pasture (pasture that is sown with a mixture of introduced grasses and legumes, and fertilised on a regular basis) and was milked twice a day on a rotary dairy.

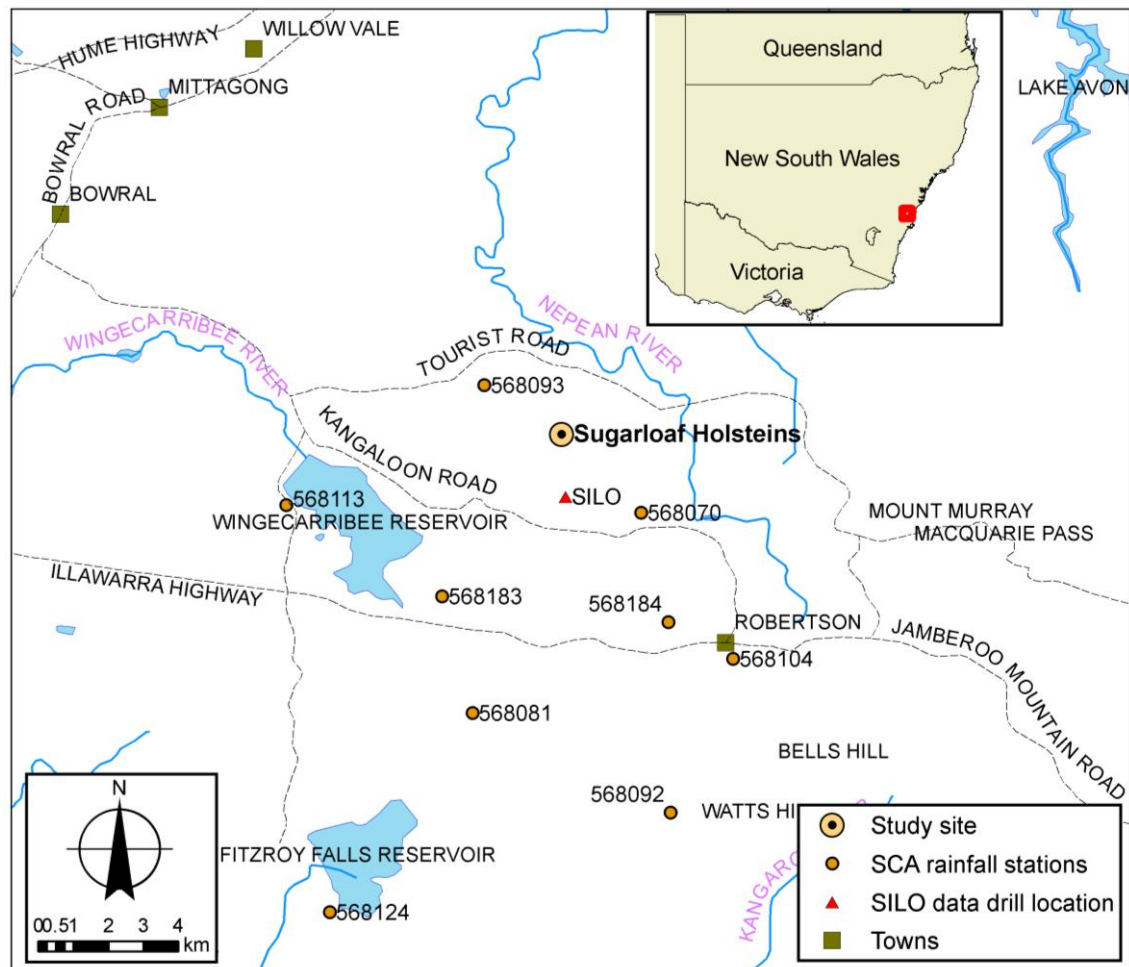


Figure 3-1 Map showing the study site location, nearby rainfall stations operated by the SCA and the location of the SILO data drill.

3.2.1 Soil and Geology

The main soil type on the farm is a deep fertile volcanic red clay loamy soil classifiable as red kraznozem (Charman & Murphy 1991; Hazelton 1992; Stace 1968) or red ferrosol (Isbell 2002; Peverill, Reuter & Sparrow 1999). The predominant underlying geology of the farm is Robertson basalt, although the lower northern paddocks extend into the Wildes Meadow soil landscape (Wianamatta Group – Bringelly Shale) which sits atop the Hawkesbury Sandstone shelf (Hazelton 1992).

3.2.2 Climate

Historical rainfall records kept by the current farmer and his predecessors indicate a long-term average of about 1300 mm per year (Maloney 2007, pers. comm. 19 February). The average annual rainfall recorded between 1974 and 2006 at the nearest SCA rainfall station (station 568070, located approximately 2.9 km southeast of Sugarloaf Holsteins – see Figure 3-1) was 1282 mm. According to the farmer, rainfall

had been below average in most years since 1990 and the farm had been suffering drought conditions from 2002 onwards (Maloney 2007, pers. comm. 19 February). Indeed, records from the SCA rainfall station show that 12 out of the 17 years between 1990 and 2006 (including the last 7 years continuously) recorded falls below the long-term average.

On average, rainfall is detected at station 568070 on 143 days of the year, with almost 13 days a year recording more than 25 mm. It is important to recognise, however, that rainfall events in the region tend to be highly localised, causing notable spatial variation in rainfall records. Table 3-1 presents annual rainfall recorded over the period 2003 to 2006 at the farm site by the farmer and at the nearest operational SCA rainfall stations. The relative positions of the stations given in the table may be viewed in Figure 3-1. The data reveals marked differences across relatively small distances, which highlights the importance of using on-site rainfall measurements when undertaking a site water balance analysis. Also of note is that the station nearest to the site (568070) does not produce the closest matching records. The recent records would suggest that station 568113 is perhaps more representative of climate conditions at the farm site.

Table 3-1 Comparison of recent annual rainfall at the farm site and nearby rainfall stations.

<i>Site or station</i>	<i>Station operator</i>	<i>Latitude (°S)</i>	<i>Longitude (°E)</i>	<i>Annual rainfall (mm)</i>			
				<i>2003</i>	<i>2004</i>	<i>2005</i>	<i>2006</i>
Sugarloaf Holsteins		34.5336	150.5493	848	661	879	641
568070	SCA	34.5542	150.5694	1152	955	1130	851
568113	SCA	33.4478	150.4783	837	654	857	719
568183	SCA	34.5756	150.5183	946	725	996	794

The nearest historical (pan) evaporation data comes from SCA station 568113, with records commencing in 1978. Annual pan evaporation often exceeds annual rainfall, with the long-term average between 1979 and 2006 being 1350 mm. Mean monthly rainfall from stations 568070 and 568113 is depicted in Figure 3-2 together with mean monthly evaporation from 568113. Site 568113 has considerably lower rainfall than site 568070 in every month of the year. For the sake of comparison, the equivalent figures based on long-term synthetic data from a SILO Data Drill (SILO 2008; - historical data are interpolated between Australian Bureau of Meteorology weather stations as described in Jeffrey et al. 2001) from the nearest 5-degree geographical grid point to the farm (refer to Figure 3-1) are also presented in Figure 3-2. On average rainfall exceeds evaporation in up to 7 months of the year. In the spring and summer months

the soil moisture losses caused by evaporation are not countered by commensurate rainfall, requiring irrigation to make up the deficit and maintain healthy pastures and crops.

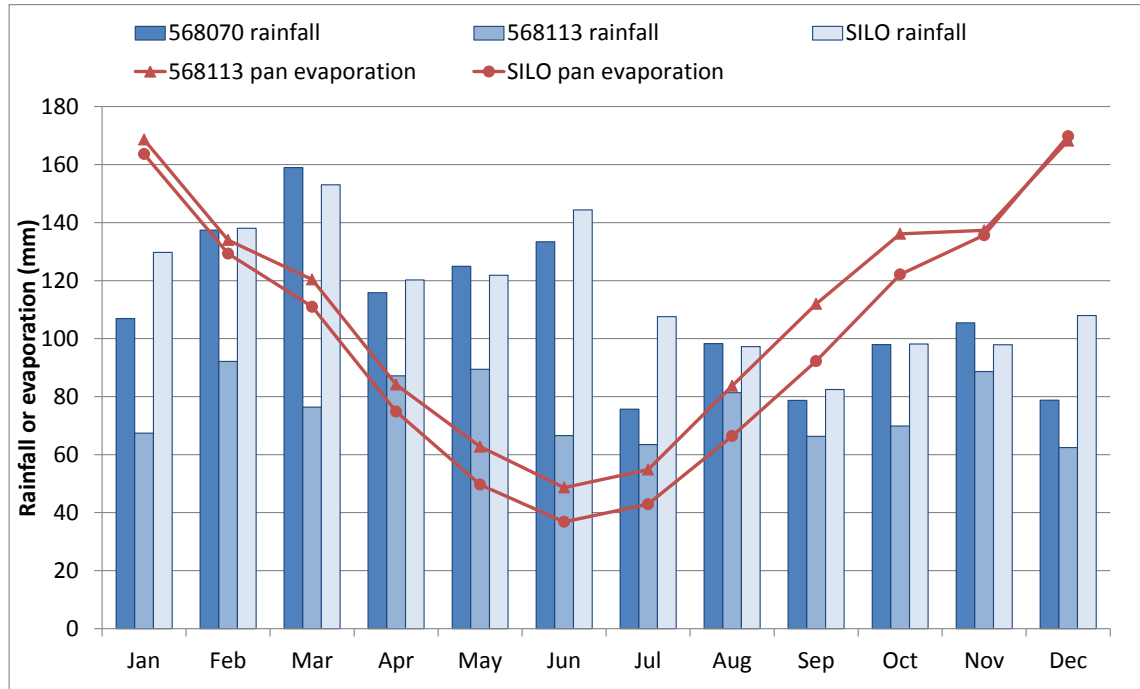


Figure 3-2 Monthly mean rainfall recorded at SCA stations 568070 (1974 – 2006) and 568113 (1978 – 2006) and by SILO (1889 – 2006) and monthly mean evaporation recorded at SCA station 568113 (1978 – 2006) and by SILO (1970 – 2006).

Other long-term historical meteorological data are not available from SCA stations and the nearest Australian Bureau of Meteorology station is over 10 km away. Hence the best record of typical climate for the site was deemed to be that drawn from the SILO extract. Average daily temperatures and solar radiation by month are presented in Figure 3-3. Mean maximum temperature ranges from just over 10 °C in winter to 23.3 °C in January. On average, daily maximum temperature exceeds 30 °C four times a year. Minimum temperature averages just 2.6 °C in July and drops below freezing an average of almost 9 days a year. As expected, solar radiation is closely correlated with temperature, typically peaking in January/February.

3.2.3 Operations

As the name of the farm suggests, the Holstein cow is the stock breed of the farm; however Jersey cows were introduced to the herd in October 2005 to increase the fat and protein content of the raw milk. Over the study period, there were on average 300 cows being milked twice daily, producing over 5000 litres of milk per day (18 L per cow

per day). The total herd, which included the milkers, between 100 and 180 dry cows, 50 replacement calves, and cows on agistment, averaged around 500 head over the study period. The average live weight of the Holstein milking cows was 500-550 kg, while the Jerseys, which made up one third of the milking herd, had an average weight of 400 kg. Plate 3-1 shows the milking herd making its way to the dairy for the afternoon milking.

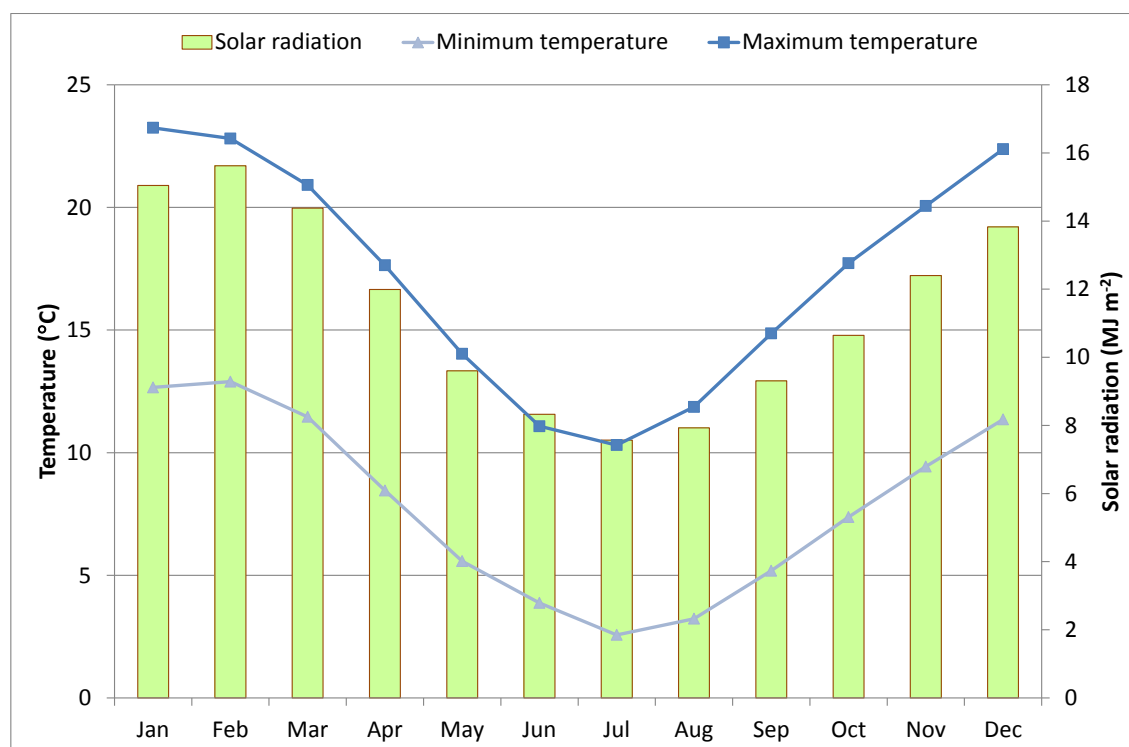


Figure 3-3 Monthly mean daily minimum and maximum temperatures and solar radiation calculated from the SILO data drill.

The herd is generally pasture-fed, although drought conditions had forced greater importation of oaten cereal hay to provide adequate feed for the herd since 2002. The extents of the farm cover 160 ha, 90% of which is improved ryegrass and clover pasture. A twenty four hectare area of the farm is irrigated with groundwater between October and May and the pasture is fertilised/conditioned according to the regime given in Table 3-2. Ryegrass and cereal are harvested for silage in spring (when in sufficient supply) to be stockpiled and fermented for 6 weeks. Corn and sorghum crops are sown in spring and early summer for autumn forage feed on a rotational basis. Milking cows also consume between 4 and 8 kg of supplementary bale feed (16% protein pellets) per day during milking, depending on their time of lactation (0-100, 100-200 or 200-300 days).

Table 3-2 Fertiliser use and soil conditioning (Maloney 2007, pers. comm. 19 February).

Fertiliser / Soil conditioner	Frequency/timing	Rate	Comments
Phosphorus (super)	Spring and autumn	22 kg P ha ⁻¹ yr ⁻¹	Sometimes mixed with potash
Nitrogen (urea)	Up to every two months on newly sown pastures	57 kg N ha ⁻¹ yr ⁻¹	Frequency dependent on finances and rainfall
Potassium (potash)	Spring and autumn	31 kg K ha ⁻¹ yr ⁻¹	Sometimes mixed with super
Lime	Every 5 years	2.5 t ha ⁻¹ yr ⁻¹	Dependent on pH levels and pasture growth
Organic (poultry manure)	Spring and autumn	7.5 m ³ ha ⁻¹ yr ⁻¹	

The milking parlour is equipped with a 50 stall rotary platform, a milking machine with an automated cleaning process, and one 15,500 L milk vat. The rotary platform and associated milking equipment are pictured in Plate 3-1. Fresh water for the plate cooler system and hygienic cleaning and hosing is supplied to the dairy from the nearby Doudles Folly Creek and from natural springs. Spent plate cooler water is recirculated into the fresh water supply tank. At the time of this study average fresh water demand at the dairy was approximated by the farmer to be 11,000 L⁻¹ d.

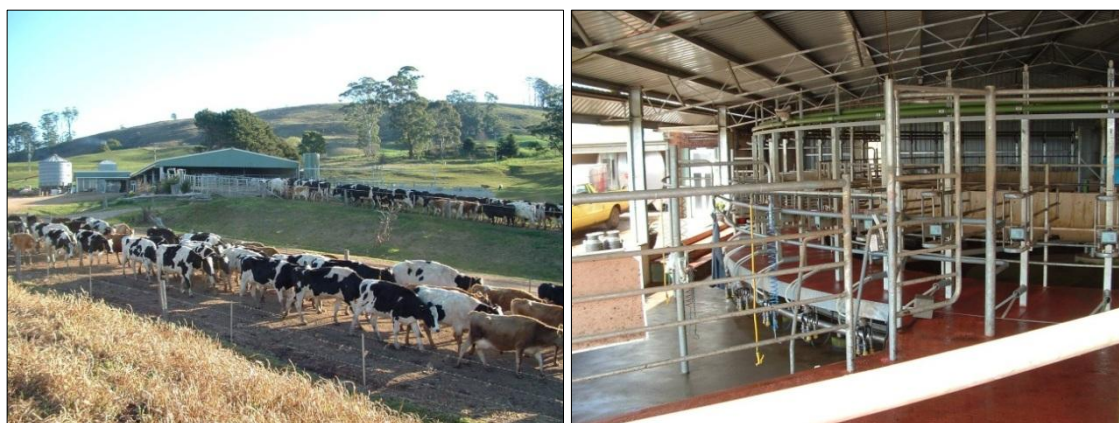


Plate 3-1 Left: afternoon milking procession to the dairy. Right: interior of the milking shed.

3.3 WASTE MANAGEMENT SYSTEM

The waste management system at Sugarloaf Holsteins (herein referred to as ‘the system’) was constructed in conjunction with an upgrade to the milking shed. The new shed and the waste system commenced operation on 1 August 2002. The design for the system was provided by the (former) NSW Department of Agriculture and was based on the standards outlined in the NSW Guidelines for Dairy Effluent Resource

Management (NSW Dairy Effluent Subcommittee 1999). The system, depicted in Figure 3-4, comprises a conventional two-stage dairy shed waste stabilisation pond system (two ponds in series) with a trafficable solids trap for wastewater pre-treatment. Effluent from the pond system is recycled for hydraulic flushing of the holding yard. Excess effluent is reused by pumping to land via a travelling irrigator.

The system receives the wastewater generated by the cleaning processes described in section 3.3.1 below. Runoff from the roof of the shed does not enter the waste drainage system. Stormwater runoff from the holding yard can be diverted from the wastewater treatment system by sliding a barrier across the entry canal to the solids trap, although being a manual operation this is not always attended to during a rainfall event.

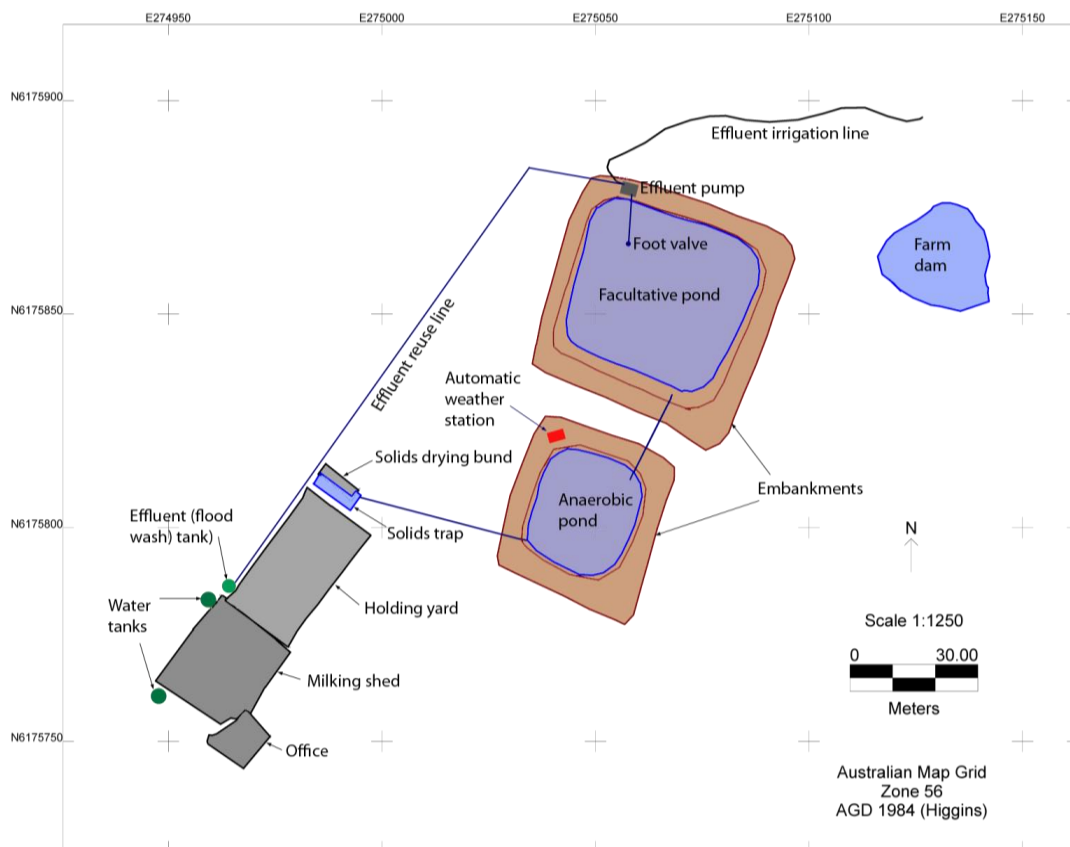


Figure 3-4 Schematic diagram depicting the dairy and the waste management system at Sugarloaf Holsteins farm.

3.3.1 Dairy Shed Cleaning

During the milking process the milking platform is hosed down with fresh warm water using 12 mm hoses fitted with trigger nozzles. At the completion of milking the rotary platform and the shed floor are hosed down with fresh water (not heated) using high-volume 25 mm hoses fitted with fire-fighting nozzles. The milking machine and milk

vats are automatically cleaned by a cleaning-in-place system using acid and alkaline washes on a rotational basis, as summarised in Table 3-3. Occasionally chlorine is added to the wash water for additional disinfection.

Table 3-3 Milking equipment hygienic cleaning-in-place regime.

<i>Equipment</i>	<i>Wash</i>	<i>Frequency</i>	<i>Wash cycles</i>	<i>Water</i>		<i>Active ingredients</i>
				<i>Volume (L per wash)</i>	<i>Temperature</i>	
Milking machine	Acid	Once every three milkings	Pre-rinse	400	Warm	
			Chemical wash	400	Hot (>82 °C)	7-10 mL per 10 L water of 1152 g/L phosphoric acid and 30 g/L non-ionic detergent
			Rinse	400	Cold	
	Alkaline	Twice every three milkings (rotating with acid wash)	Pre-rinse	400	Warm	
			Chemical wash	400	Hot	30 mL per 10 L water of 399 g/L NaOH
			Rinse	400	Cold	
Milk vats	Acid	Once every four days	Pre-rinse	400	Warm	
			Chemical wash	400	Hot (>82 °C)	As per milking machine acid wash
			Rinse	400	Cold	
	Alkaline	Once every four days (alternating with acid wash)	Pre-rinse	400	Warm	
			Chemical wash	400	Hot	As per milking machine alkaline wash
			Rinse	400	Cold	

The holding yard is cleaned after each milking session by hydraulic flush (flood wash) using recycled (treated) effluent from the pond system (see section 3.3.3 below). Recycled effluent is held in a tall 15 m³ fibreglass tank at the north-western corner of the yard to provide sufficient head for effective flushing. It is released in a surge through a single 300 mm outlet fitted with a butterfly valve and a rudder to control the flow rate and direction (see Plate 3-2). The potential head (4 m) and yard slope were designed to generate a rapid wave that effectively removes accumulated dirt, excreta and other debris. No risers were installed to assist the wash down, although an additional fixed pipeline releases treated effluent at a slower rate (governed by the capacity of the effluent pump) to aid cleaning the eastern side of the yard which is

mostly manually hosed down with fresh water (see Plate 3-2). Additional cleaning of the yard is performed using fresh water from 25 mm hoses fitted with fire-fighting nozzles (high pressure, low volume). Water usage is covered in detail in Chapter 5.



Plate 3-2 Left: flood washing the main section of the holding yard (flood wash tank stands to the right of the dairy shed). Right: manual hosing of the eastern side of the yard is aided by a stream of reclaimed effluent flowing from a pipe attached to the shed support column at the top-left corner of the yard.

3.3.2 Wastewater Treatment

Wastewater generated by the various cleaning processes drains to a conventional two-stage anaerobic-facultative stabilisation pond system. The system, pictured on the left in Plate 3-3, was constructed when the new dairy shed was built; however while the shed has a milking capacity of 500 head, the original design of the wastewater system appears to have been based on a milking herd of only 170 cows. A review of the original system design reveals that the design capacity of trafficable solids trap was appropriate despite the significant underestimation of the herd size. The sizing of the stabilisation ponds followed the principles of NSW best practice guidelines available at the time (NSW Dairy Effluent Subcommittee 1999), but no longer meets current best practice standards.

3.3.2.1 Trafficable solids trap

To prevent large manure solids and other coarse particulates such as feed grains, grass and stones reaching the stabilisation pond system, the wastewater first passes through a trafficable solids trap located adjacent to the bottom (northern) end of the holding yard. Entering the trap through a channel atop the northern wall (visible on the right of the photograph of the trap in Plate 3-3), wastewater seeps through a 25-30-mm mesh metal grate at the eastern end of the northern (left-hand) wall, leaving behind a watery mass of screened solids. Based on calculations performed using the Dairy

Solids Trap design tool (Skerman 2004b), the trap's 25,000 L volume is adequate for handling the wastewater load from the 300 head herd that was being milked at the time of the study, theoretically providing an emptying interval of six weeks or more. However if the herd size was to reach the milking shed capacity of 500 head, the trap would become impractical, requiring very frequent emptying (more than once a week).



Plate 3-3 Left: view of the waste stabilisation pond system from the dairy shed holding yard (the solids trap sits at the bottom of the yard behind the fence at the middle left of the photograph). Right: view of the trafficable solids trap holding fresh wastewater.

Accumulated manure solids were removed from the solids trap basin using a tractor fitted with a loader bucket. When the study commenced the trap was being emptied every few weeks when the level of solids began to encroach upon the trap's capacity to hold the liquid from a flood wash. In response to ongoing problems with screen blockages, the farmer started emptying the trap weekly in January 2006. The design of the solids trap facility incorporated a bunded drying bay that drained via weepholes directly back into the solids trap (seen atop the northern wall in the picture in Plate 3-3), which was intended for holding manure solids emptied from the trap until they were spread to land using a dry manure spreader. However over the course of the study it remained only partially constructed and was not in use, with manure solids instead being stockpiled on open ground behind the entry to the trap.

3.3.2.2 Stabilisation ponds

Screened/settled wastewater drains from the solids trap via a 150 mm PVC stormwater pipe to a deep primary (anaerobic) stabilisation pond designed to provide settling of particulate matter not captured in the solids trap and anaerobic fermentation to reduce the organic loading of the wastewater and stabilise the settled sludge. The primary effluent leaves the pond through a 150 mm pipe fitted with a T-junction that draws supernatant from approximately 50 mm below the surface (see Plate 3-4). Secondary

biological treatment is provided by a facultative pond (pictured in Plate 3-4) which also acts as an effluent storage. Effluent is pumped directly from this pond for recycling as flush water for the dairy holding yard, thus the pond plays an important role both in providing adequate treatment for wastewater reclamation and as a holding pond during wet weather.

Both the primary and secondary ponds are earthen basins excavated on sloping terrain immediately downhill from the dairy. Stock is generally excluded from the ponds and their immediate surrounds, although calves are occasionally allowed to graze the pond embankments to keep them from becoming overgrown with kikuyu grass. Kikuyu overgrowth into the pond had in the past been removed using an excavator arm fitted to a tractor. There had been no pond sludge management measures undertaken prior to the commencement of this study.

As stipulated in the NSW Dairy Effluent Subcommittee (1999) guidelines, sizing of the stabilisation ponds was based on the provision of adequate effluent storage capacity to ensure land application only occurred in the two months of the year when evaporation exceeds 90th percentile rainfall. However the design failed to incorporate a number of key considerations that feature in current best practice documentation (Birchall, Dillon & Wrigley 2008) including allowances for sludge accumulation, rainfall and runoff contributions. The liner for both ponds consisted of track rolled in-situ clay soil. Tests were not performed to determine the hydraulic conductivity of the liners, but the water balance analysis described in Chapter 5 indicates that the permeability of the liners in one (anaerobic) or both of the ponds exceeded the limit recommended by Birchall, Dillon & Wrigley (2008).

3.3.3 Effluent Recycling and Reuse

Treated effluent from the secondary pond is recycled through the flood wash system. The release of effluent held in the flood wash tank tips a float switch, triggering a centrifugal pump that transfers effluent from the pond to the tank. Effluent is extracted from the pond through a brass foot valve suspended from a buoy approximately 30-40 cm below the water surface and about 12 m from the water's edge. A valve in the polypipe extraction line can be manually switched to divert pumped effluent to a small travelling irrigator, facilitating periodic reuse of excess effluent by application to land to provide renewal of the pond liquid and prevent overfilling of the pond. A white plastic depth marker indicates the allowable high water level to aid in the farmer deciding when to irrigate effluent. The effluent pump is pictured in Plate 3-4 together with its control and electrical boxes (mounted on the post in the foreground), the foot valve

buoy (on the water surface to the right), and the pond high water mark (visible through the gap between the two pipes connected to the pump).



Plate 3-4 Left: view of the anaerobic pond showing the outlet pipe. Right: View of the facultative pond with the effluent recycling pump and control box in the foreground and the buoy supporting to foot valve to the extraction line sits on the water surface to the right.

The design of the pond and reuse system specified a land application area of 7.77 ha to allow for safe disposal of effluent in 9 out of 10 years. The limited reach of the travelling irrigator meant that at the time of the field monitoring, effluent could only be applied within a 3.2 ha paddock. However, plans were in place to connect the effluent pump line to the main irrigation line to shandy the effluent with groundwater and distribute it over 24 ha of pasture.

3.4 MAPPING THE SITE AND THE SYSTEM

Topographical surveys of the site were undertaken to map the key features of the site and the relief contours of the stabilisation pond basins. The data from the surveys were digitised to produce a site schematic and to generate three dimensional grids of the pond surfaces for calculating their working volumes.

3.4.1 Topographical Surveys

Key features of the dairy and the effluent management system were mapped during initial site investigations using a sub-metre geographic positioning system (Trimble XR Pro receiver). Several more detailed topographical surveys were undertaken over the course of the monitoring program to map the pond system and sampling/monitoring locations more accurately. Two permanent traverse station points were established to form a line of reference for combined radiation and coordinate contour surveying techniques. The traverse stations were selected on the basis of visibility and proximity to the features being surveyed and were geo-referenced using the geographic

positioning system (GPS). A Leica TN 400N electronic total station and a wandering reflector target and staff were used to perform the surveys. In most instances, points sighted using the total station were simultaneously recorded using the GPS in order to provide a check for the survey data and for broader mapping purposes. The surveying data, including coordinates (Australian Map Grid 1984, Zone 56) and elevations (with respect to the Australian Height Datum), are presented in Appendix E.

3.4.2 Holding Yard, Solids Trap and Solids Storage Dimensions

The holding yard has dimensions of approximately 34 m × 19 m and a surface area of 646 m², most of which drains directly into the solids trap. The dimensions of the solids trap are presented in Figure 3-5. The combined surface areas of the solids trap and the bunded solids storage draining to the pond system total approximately 74 m².

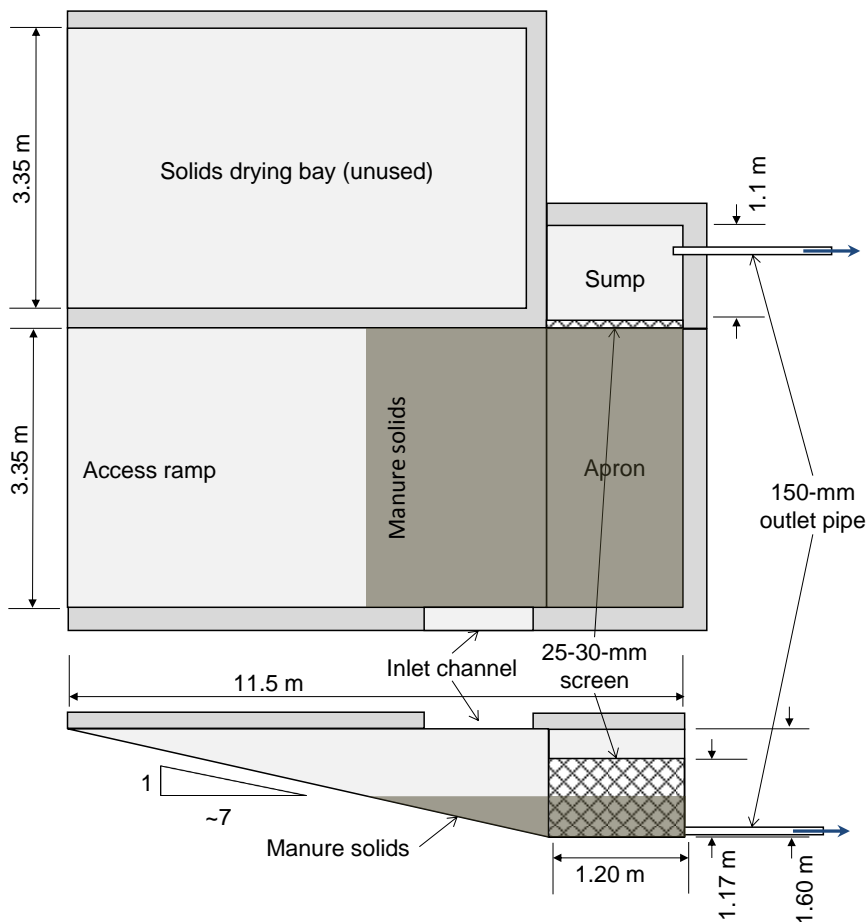


Figure 3-5 Plan view and cross-section elevation of the solids trap (not to scale).

3.4.3 Pond Mapping and Bathymetry

The topography of the pond embankments was surveyed first by profiling cross sections of crests on each side of the pond, and then by following distinct contour lines

around the pond embankment and water perimeters. The relief of the pond basins was surveyed by lowering a target staff into the supernatant to the floor of the pond from an aluminium dinghy. The dinghy was manoeuvred around the pond water surface by using a rope secured across the breadth of the pond. Using the GPS unit as a guide, the target operator would move to points in an approximate grid over the pond basin. The depth of the supernatant and the sludge was also recorded at each survey point within the pond using a column sampling device similar to that described by Pearson et al. (1987).

Data recorded by the GPS were uploaded and processed using the custom software supplied with the device (Pathfinder Office 2.51). Data gathered from the topographical surveys were digitised in Microsoft Excel for subsequent processing and mapping in Surfer Version 8.05 (Golden Software, Inc. 2004). Three dimensional grids of the pond basins were generated using the krigging (linear variogram) technique of spatial data interpolation. The grids were then used to create surface plots of the ponds and to estimate the volume and surface areas of the basins. Pond liquid and sludge volumes were calculated as 'negative fill' in the Surfer 'grid volume' computation.

The layout of the dairy and the effluent management system is depicted in Figure 3-4. Table 3-4 presents the measured volumes, surface areas and depths of the two ponds. Figure 3-6 presents the surface plots of the anaerobic (primary) pond and facultative (secondary) pond. The total capacity of the anaerobic pond was calculated to be 1,285 m³, which corresponds to a loading rate of 0.067 kg VS m⁻³ d⁻¹ under the following assumptions:

- TS and VS production of 5.2 and 4.4 kg cow⁻¹ d⁻¹, respectively (Skerman 2004a);
- the milking herd spends on average 2.75 hours per day at the dairy (Maloney 2007, pers. comm. 19 February);
- 50% VS removal in the solids trap (Birchall, Dillon & Wrigley 2008);
- 5 years sludge accumulation at 0.00455 m³ kg⁻¹ TS .

Even under a conservative activity ratio of 0.75 this loading rate is well below the upper limit of 0.17 kg VS m⁻³ d⁻¹ recommended by Birchall et al. (2008). The maximum depth at the centre of the pond was measured at 4.8 m, while the total liquid surface area is 590 m².

Table 3-4 As constructed volumes, surface areas and theoretical loading rates of the anaerobic and facultative ponds.

	<i>Units</i>	<i>Anaerobic pond</i>	<i>Facultative pond</i>
Liquid capacity	m ³	1285	2297
Maximum depth	m	4.8	2.3
Surface area (at capacity)	m ²	590	1484
Loading rate	kg VS m ³ d ⁻¹	0.067	
	kg BOD ₅ ha ⁻¹ d ⁻¹		36

The holding capacity of the facultative pond based on the high water indicator (Australian Height Datum, AHD, 666.5 m) was calculated from the gridded data to be 2297 m³. This does not provide enough storage to contain effluent over wet-weather months in a 90th percentile rainfall year (storage requirement of 3043 m³ based on rainfall data used in the design). The surface area of the facultative pond is, however, theoretically adequate to satisfy its treatment objectives. Assuming an anaerobic pond effluent BOD loading of 0.17 kg BOD₅ cow⁻¹ d⁻¹, the theoretical loading rate to the facultative pond is 36 kg BOD₅ ha⁻¹ d⁻¹, which is within the loading range recommended by Birchall, Dillon & Wrigley (2008).

3.4.3.1 Relating pond volume, surface area and wetted area to liquid depth

To assist the analysis of the water and mass balances, empirical functions were derived to allow liquid volume, surface area and wetted area in the ponds to be calculated directly from liquid depth (expressed as elevation in mAHD). Polynomial equations of the form given in equation 3.1 below were fitted to the volume and surface and wetted area data generated using the 'grid volume' command in Surfer 8 (Golden Software, Inc. 2008).

$$y = \beta_0 + \beta_1 h + \beta_2 h^2 + \beta_3 h^3 + \beta_4 h^4 + \beta_5 h^5 \quad (1.1)$$

where

y = volume (m³), surface area (m²) or wetted area (m²);

$\beta_0, \beta_1 \dots$ = regression coefficients;

h = elevation of liquid surface (mAHD) – 660.

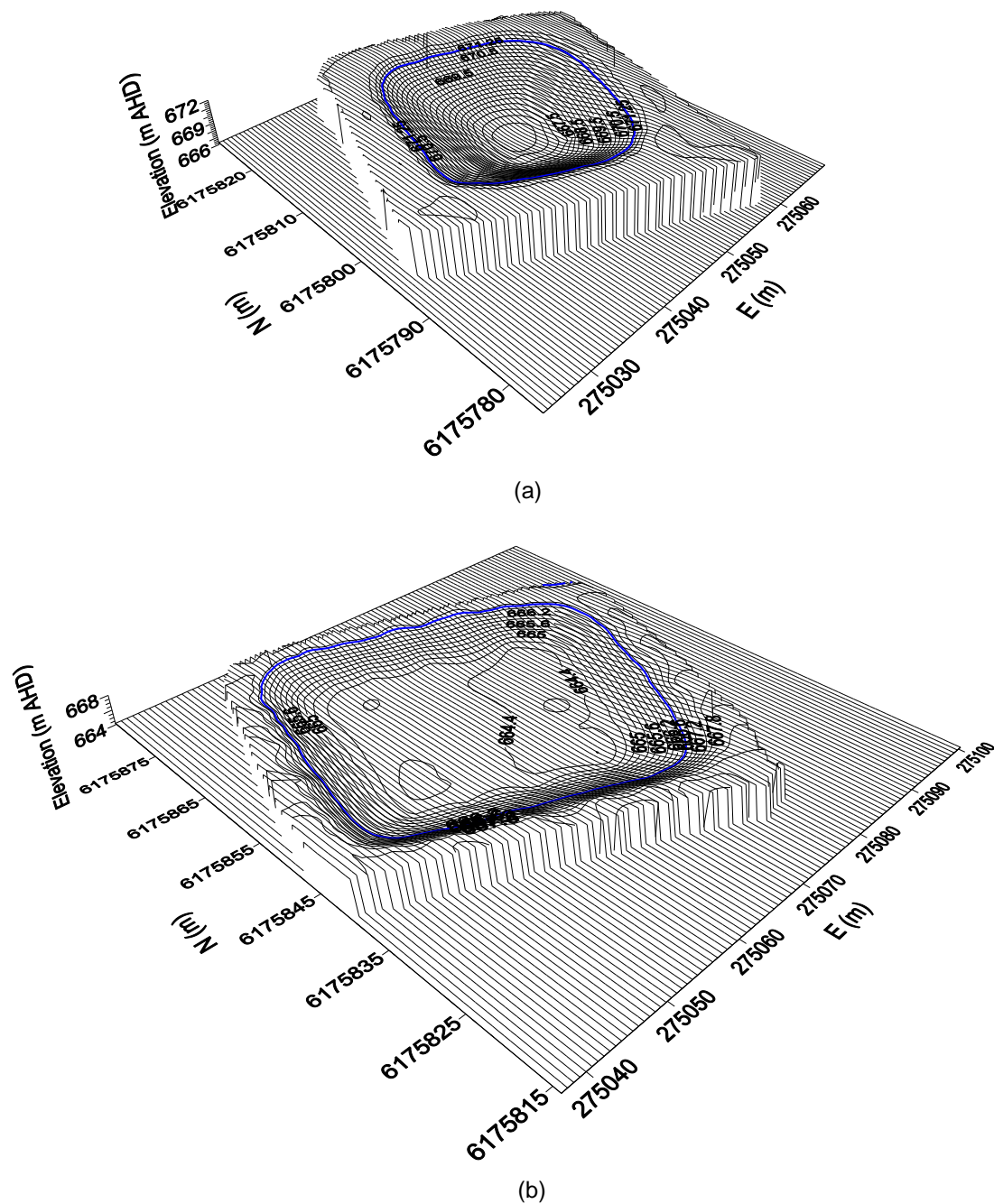


Figure 3-6 Scale surface maps of (a) the anaerobic pond and (b) the facultative pond. Blue contour lines indicate pond liquid capacities.

Figure 3-7 presents plots of the synthesised data against depth together with the fitted polynomial functions for each pond. The regression coefficients are given in Table 3-5. Note that the numbers of significant figures are necessarily large as rounding error would be substantial when applying coefficients of such large magnitude. The subtraction of 660 from liquid surface elevation data was applied to help limit such rounding errors. The embankment wetted area curve was prepared to assist seepage and runoff calculations later in the thesis. The data used in the curves were calculated

by subtracting the wetted area of the pond 'floor' - the area enclosed by the contour at 664.5 mAHD (636 m²) - from total wetted area.

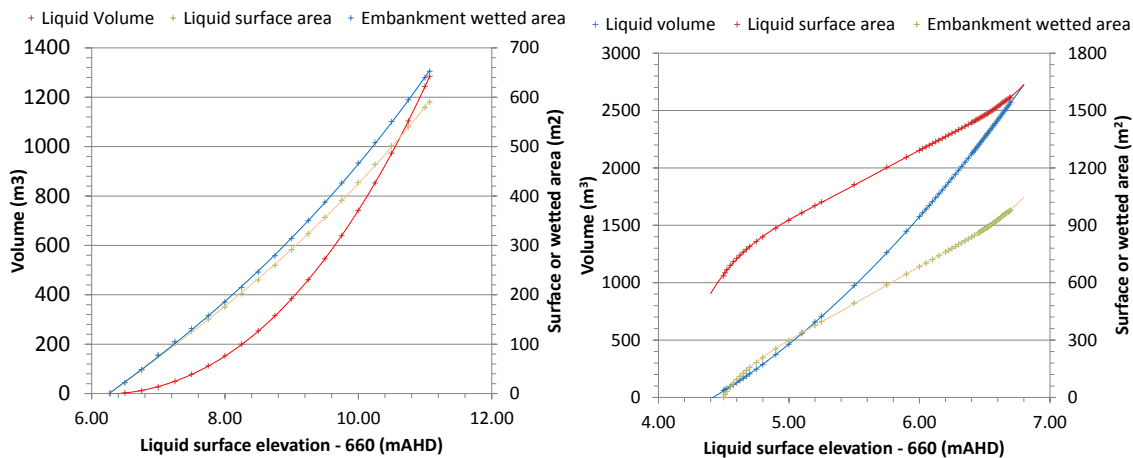


Figure 3-7 Polynomial curves fitted to pond liquid volume, liquid surface area and wetted area data plotted against liquid surface elevation. Left: anaerobic pond. Right: Facultative pond.

3.5 SYSTEM CONDITION, OPERATION AND MAINTENANCE

At the initial site investigation it was observed that the effluent management system was in mostly good shape and had been operating without any major problems since it came on line. The only issue that affected the operation of the system was that the screen in the solids trap had been sized and installed incorrectly. This had resulted in regular overtopping of the screen (allowing raw wastewater to enter the inlet to the anaerobic pond) and unnecessary difficulties associated with emptying the trap. The screen was reoriented and raised to prevent overtopping in December 2004. Eventually, however, in early January 2006 (in the midst of the monitoring program) the screen support structure failed causing the screen to collapse. The screen was widened and replaced with a reinforced support structure on 12 January 2006.

Operation of the effluent management system requires four manual activities:

- release of the flood wash;
- emptying and cleaning of the solids trap;
- distribution/disposal of materials from the solids trap; and
- initiating effluent irrigation.

Table 3-5 Coefficients for polynomials fitted to facultative pond liquid volume, liquid surface area and embankment wetted area data.

<i>Polynomial term*</i>	<i>Coefficients</i>		
Anaerobic pond	Volume	Surface area	Wetted area
β_0	$8.04606650678739 \times 10^2$	$-8.01924114231767 \times 10^2$	$-6.49775150782877 \times 10^2$
β_1	$-1.58397564491959 \times 10^2$	$1.95650108120768 \times 10^2$	$1.41166181229088 \times 10^2$
β_2	$-1.28682287374915 \times 10^1$	$-1.66265473045908 \times 10^1$	$-1.09909301601711 \times 10^1$
β_3	2.80823508180856	$9.33126562530560 \times 10^{-1}$	$8.01985291207075 \times 10^{-1}$
Facultative pond	Volume	Surface area	Embankment wetted area
β_0	$1.62674592022395 \times 10^3$	$-4.03656358220926 \times 10^5$	$-4.00374623911597 \times 10^5$
β_1	$-1.53155830833835 \times 10^3$	$3.56215853052397 \times 10^5$	$3.52765660012999 \times 10^5$
β_2	$2.89955671439442 \times 10^2$	$-1.25509515502573 \times 10^5$	$-1.24296612547629 \times 10^5$
β_3	-6.02669372683158	$2.20894011460859 \times 10^4$	$2.18755772665631 \times 10^4$
β_4		$-1.93995341187901 \times 10^3$	$-1.92098357721464 \times 10^3$
β_5		$6.80124689824879 \times 10^{-1}$	$6.73370624231174 \times 10^{-1}$

The flood wash is activated by manually opening the valve to the tank; hence the quantity of effluent released can be varied by the operator to suit the conditions. After the early troubles with the screen in the solids trap the farmer agreed to empty and clean the trap on a weekly basis to ensure that overtopping did not occur. Solids extracted from the trap were stockpiled over the course of the research but not distributed (on the farm) or disposed of by other means. While effluent irrigation was generally planned for dry days in the summer months, its timing was often dictated by the supernatant level in the secondary pond. This sometimes led to irrigation occurring in months of higher rainfall and low evaporation, although rarely actually during wet weather.

System maintenance is performed on an as-needed basis rather than according to a schedule. Kikuyu grass on the pond embankments is kept down by allowing calves to occasionally graze the area. Prior to the commencement of the study, however, the farmer used a tractor excavator to remove kikuyu grass that was spreading across the supernatant surface around the anaerobic pond inlet. Running repairs were made on the effluent pump and the travelling irrigator when necessitated by break-downs. Given the age of the system, desludging of the anaerobic pond should not have been needed

until after the monitoring program had been completed. However, sludge measurements made on 9 June 2005 (see Chapter 6) revealed that sludge was occupying approximately 56% of the pond. Following advice to desludge the pond, the farmer arranged to hire a sludge tanker to pump out and distribute the sludge on-farm between 26 and 31 October 2006. Approximately 660 m³ of effluent and sludge were removed in the desludging.

3.6 MONITORING AND SAMPLING REGIME

In order to generate the data set needed to build a dynamic model of the stabilisation pond system, a customised real time monitoring and sampling regime was devised for the field site. Being situated remote from the University, the monitoring system site had to be robust, have the capacity to store long series of data and be controllable via telemetry. It also had to run on solar power due to the lack of proximity to grid power connections.

Treatment performance of a pond system is primarily determined by the loading rate, which is a function of hydraulic loading, influent concentration and the active volume of the pond. Accordingly, flow was monitored in real time at the key wastewater transfer points including the anaerobic pond inlet and outlet, the facultative pond pump and the flood wash tank as described in Chapter 5. Concentrations of wastewater constituents including nutrients, organic material, solids and cations were determined from 24-hour composite samples collected by automatic samplers as recommended by Pearson et al. (1987). Samples were collected from the anaerobic pond inlet and outlet, the flood wash tank and the facultative pond supernatant. Details of the sample collection, handling and analysis procedures are given in Chapter 7. The physical capacity of the ponds was determined as described in section 3.4.1; this, however, is not a true indication of the active treatment volume due to:

- sludge accumulation in the anaerobic pond;
- fluctuations in the volume of effluent held in the facultative pond;
- stratification; and
- hydraulic inefficiencies.

To account for sludge accumulation, the monitoring regime incorporated seasonal measurements of sludge depth as described in Chapter 6. The liquid level in both ponds was monitored in real time using pressure sensors (see Chapter 5). Stratification was gauged through seasonal profiling of the pond water columns using measurements of temperature and other water quality parameters as detailed in

Chapter 4. The profiling data were complemented with real time monitoring of water quality parameters performed using robust self-logging multi-parameter field probes deployed at several locations in each pond, together with a telemetrically controllable flow injection mini-analyser (MA) for high accuracy measurements of the facultative pond supernatant (see also Chapter 4). The data from this continuous monitoring was also intended to provide insight into the dynamics of pond supernatant conditions. The characterisation of hydraulic inefficiencies presented a more difficult challenge, which is addressed in detail in Chapter 6.

Most pond treatment processes are temperature-dependent; hence air and pond supernatant temperatures were measured in real time. To quantify hydrologic inputs and outputs, meteorological data were collected using an automatic weather station (AWS) incorporating a rainfall gauge, anemometer, wind vane, humidity sensor and pyranometer to go with the air temperature sensor. Data gathered from wastewater flow and meteorological measurements were recorded by a central logger which also controlled the wastewater sampling and could be manipulated through telemetric connection. The logger was housed in a central monitoring control trailer (pictured in Plate 3-5) which also housed the MA, the autosamplers, batteries and other miscellaneous equipment, and to which the AWS was mounted. Figure 3-8 depicts the dairy and pond system (to scale), and the locations of wastewater sampling points, probe deployments and the monitoring control trailer. A summary of the monitoring equipment deployed at the site is given in Appendix A together with a summary of the risk assessment of the field monitoring activities.

The monitoring regime was designed to generate an unprecedented suite of data from a real world, Australian best practice dairy shed waste management system. While there exists a number of published and unpublished data sets on DSE characteristics and DSE treatment performance (Hickey, Quinn & Davies-Colley 1989; Mason 1996; Sukias et al. 2001; Bolan, Wong & Adriano 2004; Skerman, Kunde & Biggs 2006; Geary & Moore 1999; Sweeten & Wolfe 1994; Cumby, Brewer & Dimmock 1999), they either focus on one pond only or a different treatment mode attached to a pond system, consider only pond effluent characteristics (making no mention of influent), have multiple farm subjects and thus fail to give adequate detail of any one farm, or do not properly quantify hydraulic loads. Moreover none of the published studies appear to have undertaken flow-weighted sampling, which is important in estimating wastewater loading and material balance. This is particularly so when examining highly variable influent wastewaters such as DSE. The Sweeten & Wolfe (1994) study may be the exception, although this originated in the US where farm management practices differ

substantially from Australian practices. Hence, the unique and detailed data presented herein provides a strong foundation for the modelling component of this thesis. It will also be useful to future research and development of best practice in the field of DSE management.

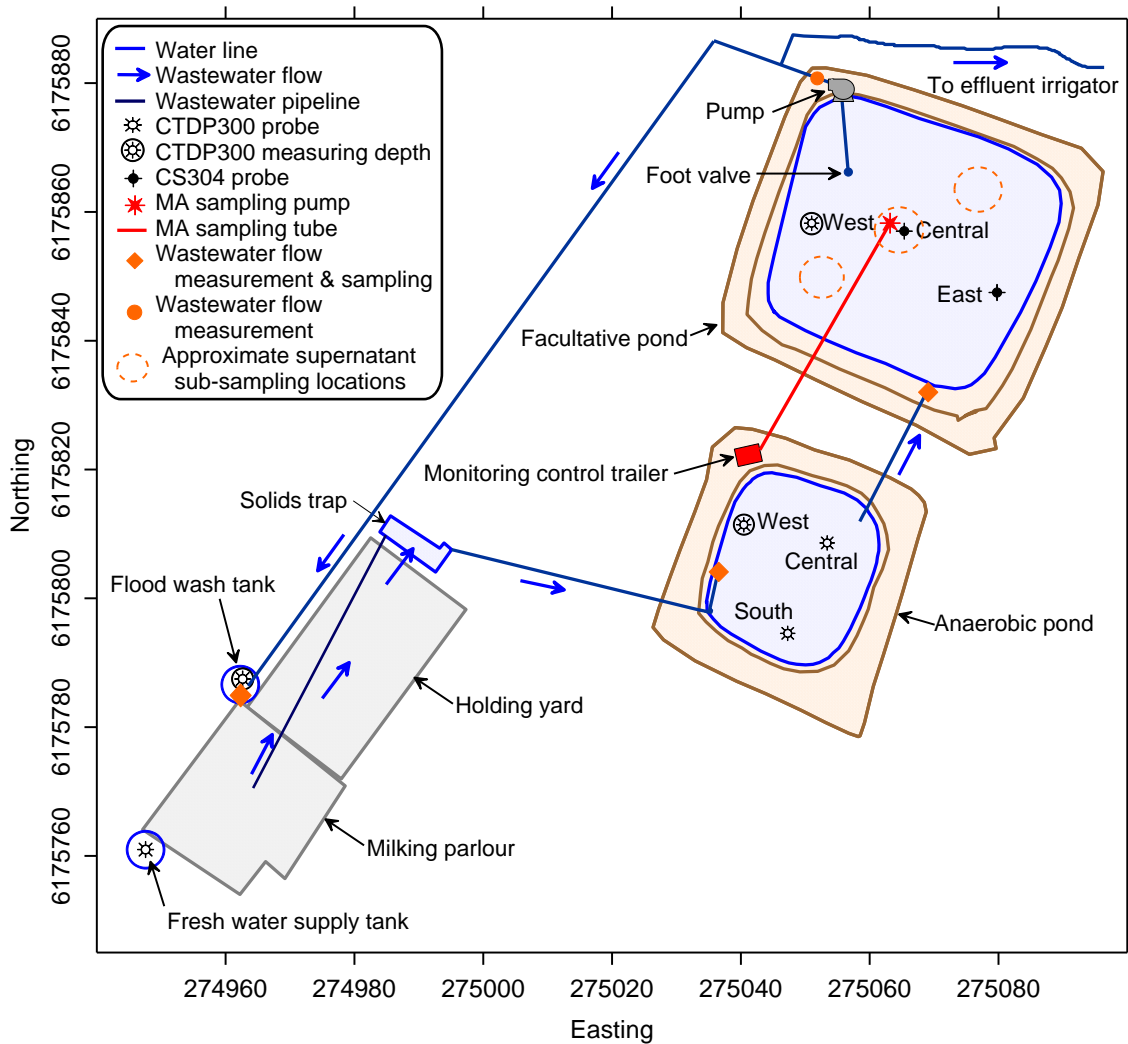


Figure 3-8 Locations of influent/effluent/supernatant sampling points, multi-parameter probes (CTDP300 and CS304) deployments and the monitoring control trailer housing/supporting the central data logger, the autosamplers, the AWS and the MA.



Plate 3-5 The monitoring control trailer: trailer and AWS (top left); autosamplers at rear (top right); datalogger and power box (bottom left); FIA and power supply (bottom right).

3.7 SUMMARY

The selection of an appropriate operational dairy farm as the subject of the study was a critical preliminary phase of the research. The site chosen was Sugarloaf Holsteins, a large farm with a long and proud history of milk production. The farm was selected from a range of potential sites in accordance with a set of key criteria including the type and standard of waste management system, proximity to the University and the cooperativeness of the farm owner-operators. The local climate could be described as temperate, receiving around 1300 mm of rainfall annually, and in recent years prone to drought. The farm facilities and operations are typical of modern Australian dairy farming practices. The large herd is milked twice daily on a rotary platform milking machine and fed mainly on improved pasture supplemented by protein pellet bale feed and, where necessary as dictated by drought conditions, imported hay.

The effluent management system is a conventional two-stage stabilisation pond system (an anaerobic pond followed by a facultative pond) with preliminary solids separation that treats wastewater for recycling at the dairy and reuse by irrigation to land. The system meets current best practice guidelines on most fronts including solids trap

capacity and waste loading. The storage capacity of the secondary pond, however, is small by today's standards as its design was based on out-dated calculation techniques. Effluent recycled from the facultative pond is automatically pumped to a holding tank for hydraulic flushing of the holding yard. Excess effluent is irrigated to a relatively small nearby paddock when the supernatant level in the facultative pond starts to approach the pond's capacity. This irrigation is not scheduled but is generally planned to avoid wet weather. The management of irrigated effluent does not currently meet best practice standards and certainly does not provide for optimum nutrient recovery.

Once the site had been selected and characterised, a comprehensive real time monitoring and sampling regime customised to the research objectives and the nature of the site was devised. The data generated from the monitoring program is unprecedented in the field in terms of rigour and detail and provides a platform for the modelling component of this thesis and should prove highly valuable to researchers and practitioners working in the field of DSE management.

Chapter 4

POND WATER QUALITY DYNAMICS

A thorough understanding of the water quality dynamics that both characterise and influence the behaviour of the pond system provides a firm basis for developing realistic conceptual and mathematical models of the system. Physico-chemical water quality parameters such as temperature, pH and conductivity can be used to shed light on the nature the dominant physical, chemical and biological treatment processes that drive stabilisation pond systems as well to diagnose the functional state of those processes. This chapter explores in detail the temporal and spatial variation of water quality parameters in the supernatant and sludge of the anaerobic and facultative ponds at the Sugarloaf Holsteins dairy farm. The objective of this component of the research was to investigate temporal and spatial variation of water quality parameters within the pond system across the full seasonal cycle using high-resolution data collected in real time. The insights gained from this monitoring were to inform the modelling components of the thesis described in following chapters.

4.1 INTRODUCTION

Characterisation and monitoring of supernatant and effluent is a fundamental component of any research on waste stabilisation ponds (WSPs) (Pearson, Mara & Bartone 1987). Stabilisation pond monitoring typically involves periodic or more regular sampling and analysis of supernatant and/or effluent, which provides a series of snapshots of information about the system under scrutiny. The data are often used to determine seasonal and longer patterns and trends in the operation and performance of a pond system and for design and modelling purposes. There are also examples of pond systems being subject to brief periods of intense sampling for the purpose of scrutinising diurnal variation of in-pond conditions (e.g. Kayombo et al. 2002; Sund et al. 2001; Tadesse, Green & Puhakka 2004; Craggs et al. 2000; Aneja et al. 2001).

Fewer studies, however, have made use of high-frequency sampling and analysis of supernatant or effluent over a prolonged period. Long-term, continuous monitoring can provide a detailed picture of diurnal, day-to-day and seasonal variation in pond conditions through collection of high resolution data. It also reduces or eliminates bias introduced by data outliers that are more likely to occur when samples are collected less frequently and are therefore more prone to stochastic variability and sampling and calibration error. That is, high resolution data from continuous monitoring enables a

firmer distinction between random noise and actual trends or patterns in the measurement signal.

Another important aspect to developing a deterministic appreciation of stabilisation pond functionality is the spatial variation in physico-chemical parameters. Stabilisation ponds are prone to physical and thermal stratification, which are both characterised by changes in water quality with depth (Paterson & Curtis 2005; Paing *et al.* 2000). Physical stratification is the formation by sediment deposition of a stagnant sludge blanket below the water column. Primary ponds receiving dairy shed wastewaters are particularly prone to this form of stratification due to the high solids load of the influent associated with the roughage content of a milking herd's diet (Nordstedt & Baldwin 1975). Physical stratification can substantially reduce the hydraulic retention time (HRT) of the pond, but it also has implications for the treatment processes of the pond as the sludge undergoes anaerobic digestion which affects the physico-chemical conditions in the water column above.

Thermal density stratification of the water column results from heating of the surface by solar radiation (Paterson & Curtis 2005). A steep temperature gradient (referred to as the thermocline) forms between the warm and less dense surface layer and the cooler, denser water below. Being temperature-driven, thermal stratification exhibits both diurnal and seasonal variation, being more pronounced during the day in warmer months. It is broken down overnight when the surface temperature drops more rapidly than that of the water below (Tadesse, Green & Puhakka 2004), or simply by wind action (Sweeney *et al.* 2005). Stratification has significant implications for performance and modelling as it stifles diffusive and advective mixing and promotes short-circuiting (Shilton 2001; Tadesse, Green & Puhakka 2004).

In relation to characterising and monitoring DSE stabilisation ponds, a number of studies have involved collection and analysis of grab samples of supernatant or effluent for wastewater characterisation including those undertaken overseas by Hickey *et al.* (1989) Sweeten and Wolfe (1994), Mason (1996), Sukias *et al.* (2001), Bolan *et al.* (2004) and, in Australia, Skerman *et al.* (2006). Sukias *et al.* (2001) complemented their sample time series data from several DSE facultative ponds with detailed water column profiling and diurnal variation monitoring. Sukias *et al.* (2003) also presented results from monitoring the vertical profile and diurnal variation in a DSE facultative pond.

The abovementioned studies tended to either be relatively short (less than one year), take a cross-sectional approach to the analysis (examining inter-farm variability rather than variation within a particular pond system) or involve infrequent or intermittent sampling. This component of the present study set out explicitly to collect high-resolution water quality data over the course of at least one year to rigorously examine both spatial and temporal aspects of in-pond variation.

4.2 MATERIALS AND METHODS

The water quality monitoring program involved two components:

1. Continuous real time monitoring in the supernatant of the anaerobic and facultative ponds
2. Seasonally-based profiling of the water column in both ponds

Short term (diurnal) fluctuations, seasonal patterns and longer term trends were tracked using data from the real time water quality monitoring. Simultaneous monitoring of water quality parameters at various locations and depths within the ponds would also facilitate analysis of spatial variability. The purpose of supernatant profiling was to examine the incidence and nature of stratification in the ponds at various times of the year, with consideration given to diurnal and transverse variability.

4.2.1 Real Time Monitoring

Monitoring of water quality parameters in the supernatant of both ponds was performed in real time on a continuous basis over a period of just over two years between November 2004 and February 2007. Self-logging multi-parameter probes were deployed at various locations in the pond system to record basic water quality parameters including temperature, pH, electrical conductivity (EC) and dissolved oxygen (DO). A flow-injection auto-analyser was also permanently deployed on site to provide laboratory-standard analysis of the same parameters in the facultative pond.

The primary goal of real time monitoring of pond supernatant was to facilitate identification of both short term (diurnal) fluctuations and longer term (seasonal and greater) trends in pond functioning. The deployment of probes at different locations and depths within the ponds was intended to provide time series data to supplement the cross-sectional data gathered from the supernatant profiling in relation to spatial variation within the pond (see section 4.2.2 below).

To monitor the inputs and outputs to the system, additional probes were installed in the flood wash tank holding reclaimed effluent from the facultative pond and in the holding tank that supplied fresh water to the dairy.

4.2.1.1 Deployment of monitoring equipment

Temperature, pH and EC were measured at three locations in the anaerobic pond using Greenspan CTDP300 multi-parameter probes (Greenspan Technology, Australia). Two probes were suspended from buoys attached to ropes strung across the water surface; one approximately midway between the inlet and the outlet (herein anaerobic pond probe 'Central'), the other in the South-eastern quadrant of the pond (anaerobic pond probe 'South'). The third probe was attached to a galvanised steel pole driven into the floor on the western side of the pond again with the sensors located between 50 and 60 cm below the surface (anaerobic pond probe 'West'). Mounting the probe to a fixed support enabled the pressure sensor of the CTDP300 model to be used to gauge supernatant depth in addition to the water quality parameters.

A CTDP300 probe was also fixed to a pole driven into the floor of the western side of the facultative pond to measure changes in supernatant depth, temperature, pH and EC (facultative pond probe 'West'). On the eastern side of the facultative pond, a Greenspan CS304 probe measuring temperature, pH, EC and DO was suspended in the upper 10-15 cm from a buoy (facultative pond probe 'East'). Recycled effluent from the facultative pond was monitored using a CTDP300 probe installed at the bottom of the flood wash tank at the dairy. Depth readings from this probe (Flood Wash Tank or FWT) also allowed for measurement of the volume of effluent used in each flood wash. A sixth probe (CTDP300 model from 24 November 2004 to 18 August 2005 then CS304 model from 18 August 2005 to) was suspended just above the bottom of the holding tank supplying fresh water to the dairy to monitor the quality of the water used in the dairy washing processes. All probes were supported by independent solar power systems as pictured on the right of Plate 4-1.

To complement the data from the multi-parameter probes in the facultative pond, a Greenspan flow injection Mini-Analyser (MA) (Greenspan Technology, Australia) was installed in the monitoring control trailer to provide laboratory-grade measurement of temperature, pH, oxidation-reduction potential (ORP), conductivity, DO and turbidity by flow injection analysis. Supernatant from the upper 10-15 cm of the facultative pond was transferred via polyethylene tube to the MA from a submersible diaphragm pump suspended from a buoy in the centre of the facultative pond. The MA unit as installed in

the MCT is pictured in Plate 4-1. The MA was later replaced with a CS304 probe (facultative pond probe 'Central') due to repeated sampling and sensor failures.

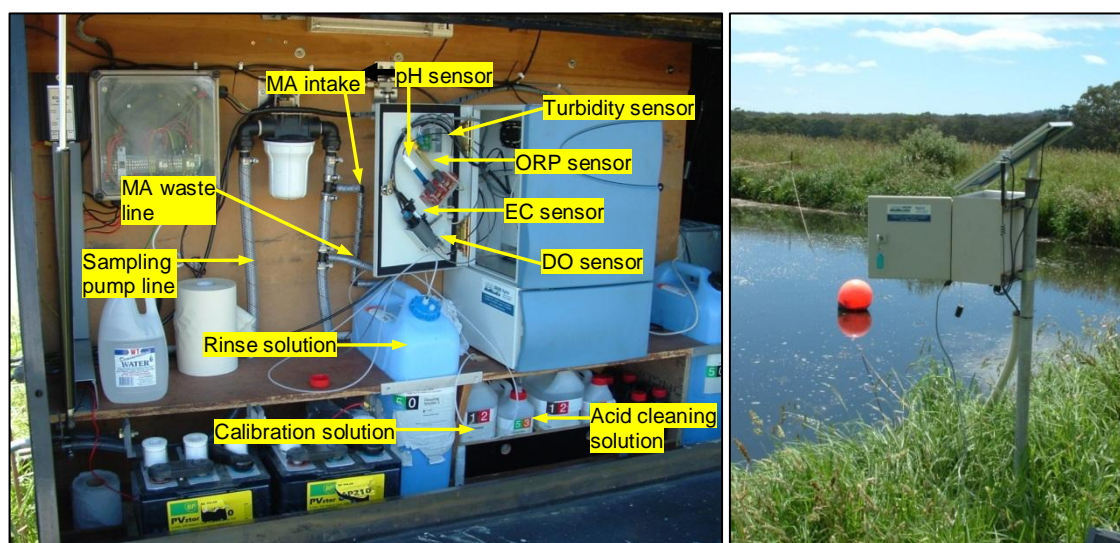


Plate 4-1 Interior of the monitoring support trailer housing the mini-analyser (blue cabinet) and its cleaning and calibration solutions. Right: power support to a CTDP300 multi-parameter probe installed in the anaerobic pond (the probe is suspended in the supernatant from the orange buoy).

The locations of the various probes and the MA housing and sampling pump and are depicted in Figure 3-11 in Chapter 3. Table 4-1 summarises the relative sampling depths of the probe sensors and the MA sampling pump.

4.2.1.2 Sampling frequency

All probes except the CDTP300 in the flood wash tank were programmed to record readings of all parameters at 30 minute intervals. A scanning frequency of 5 minutes was used to detect and record changes in parameters greater than predetermined trigger values, which were generally set at 1.0 °C, 0.5, 250-500 $\mu\text{S}/\text{cm}$ and 1.0 mg/L for temperature, pH, EC and DO, respectively. These values were considered to represent significant changes within the expected range of typical readings for the probes based on preliminary data collected prior to installation. Trigger values used for pressure on the three probes measuring depth depended on the depth of the probe deployment.

The recording interval on FWT probes was much less frequent so as to allow high frequency logging during the release of the flood wash and the subsequent refilling of the tank. Thus the scan interval was typically set to 30-60 seconds and the depth trigger value was set to 0.01-0.02m to pick up the rapid changes in water level that occur when the flood wash is released. Initially the MA was programmed to pump and

analyse sample every 30 minutes, but on account of the resulting rapid consumption of cleansing solutions, the program was modified to sample every 30 minutes during the day and every 3 hours overnight. The sampling pumping routine allowed for complete flushing of the line with fresh sample prior to the sample being drawn into the MA.

Table 4-1 Approximate relative vertical sampling positions of the probe sensors and MA pump

Deployment	Reference point	Approximate vertical sensor sampling position (m)				
		Temperature	EC	pH	Pressure	DO
Anaerobic pond						
West	Pond floor	0.73	0.70	0.79	0.84	
	Water surface	-0.59	-0.62	-0.53	-0.49	
Central	Water surface	-0.58	-0.61	-0.52	NA ^a	
South	Water surface	-0.58	-0.61	-0.52	NA ^a	
Facultative pond						
West ^b	Pond floor	0.59	0.56	0.65	0.69	
MA ^c /Central	Water surface	-(0.05 - 0.1)	-(0.05 - 0.1)	-(0.05 - 0.1)		-(0.05 - 0.1)
East	Water surface	-(0.05 - 0.1)	-(0.05 - 0.1)	-(0.05 - 0.1)		-(0.05 - 0.1)
FWT (recycled effluent)	Bottom of the tank	0.13	0.1	0.19	0.23	NA
Dairy water supply tank	Bottom of the tank	0.25	0.10	0.25	0.28	0.25

^a Depth was not recorded as the probes were floating rather than fixed to a stationary support

^b Position relative to the pond floor only as water depth was variable

^c The MA also measured ORP and turbidity in samples from 0.1 m below the surface

4.2.1.3 Calibration and maintenance

The probes and the MA were maintained and calibrated as regularly as practicable on a remote field site. The probes, designed specifically for long-term deployment, were recalibrated every 3 to 6 months under a rotational program whereby spare probes were kept aside so that probes could be replaced immediately upon being removed for recalibration in the laboratory. Calibrations were performed in accordance with the manufacturer's guidelines using standard solutions for pH and EC (APHA 2005), and a graduated plastic column filled with water for pressure. CS304 DO sensors were calibrated in air with correction for atmospheric pressure after being allowed to stabilise for at least 3 hours.

The MA was programmed to pump both acid solution (2.5% HNO₃) and distilled water through its internal lines after each analysis, and to self-calibrate once a day at 12:30 am using a single solution (pH 4, EC 2040). However the suspended solids and

microorganism content of the facultative pond supernatant caused the MA to frequently break down, either through sample line blockages or sensor fouling. Additional periodic manual cleaning, maintenance and recalibration of the MA were performed to keep it operational and producing reliable data. Manual calibrations of pH, EC, ORP and turbidity were performed with standard solutions as per APHA (2005).

Data recorded by the probes and the MA were downloaded at least once a month using a laptop computer in regular rotation to avoid exceeding the limit of the on-board memory of each device.

4.2.1.4 Data screening

Being deployed in the field for months at time, water quality sensors were susceptible to fouling, drift and declining accuracy. Occasionally probes were deployed with inaccurate sensor calibrations, particularly when calibrations were performed in the field, which could go unnoticed until the next data download. Where it was clear from comparison with other data that a sensor had produced inaccurate data during a rotational deployment – typically indicated by large offsets or unusually high variability – the inaccurate data were omitted from plotting and statistical analyses. With the exception of data from the dairy water supply tank probe, data from the multi-parameter probes were screened in large time-contiguous blocks such that the data from an entire period of a particular probe's deployment was removed rather than individual or groups of data points being selectively removed.

The data from the dairy water supply probes contained only one distinct block of unusable data from a malfunctioning EC sensor. Otherwise the main issues with the data from the water supply was associated with the water level very occasionally dropping below the position of the sensors in the tank and random infrequent interference with pH readings of an unknown source, characterised by unusually large and sudden jumps or drops (0.5 pH units or more) followed by a return to previous levels over the course of a few minutes or hours. Where water depth data were available, water supply tank data were first screened by removing all readings taken when the water depth relative to the probe was less than zero. A second filter was then applied to pH and EC data that removed any points that fell outside the range $MA_{30} \pm 3 \times \sigma_{MA}$, where MA_{30} is the 30-day centred moving average and σ_{MA} is the standard deviation of the moving average time series. This essentially provided time-sensitive outlier bounds that allowed for seasonality and trends in the time series data.

Bad data produced by the MA were easily identified as they were generally caused by blockages in the pump lines that resulted in either sample failing to reach or be drawn away from the sensors, or a bad calibration. Screening was performed manually by examining the data and cross referencing against documentation of technical problems encountered with the MA.

4.2.2 Supernatant Profiling

Profiling of the supernatant column involved logging simultaneous measurements of temperature, EC, pH, ORP and DO over a range of depths using a YSI 556 MPS (YSI Inc., USA) multi-parameter probe. Measurements were taken at 5, 10, 25, 50 cm depths and then at 50-cm increments down to the sludge or pond floor and were recorded using the probes on-board data logger. The probe was lowered into the supernatant from a dinghy which was manoeuvred around the ponds with the assistance of rope fixed to fence posts on opposing embankments. Profile measurements of the anaerobic pond supernatant were typically taken at 9 locations in an approximate square grid. On the larger facultative pond, profiling would comprise between nine and sixteen measurement locations, depending on observed amount of variation (less points for less variation), the time available, and weather conditions.

At each measurement location, supernatant depth was read off markings on a column sampler (refer to Appendix A for details). In the absence of permanent fixtures to guide the sampling, profiling locations were selected by eye and were therefore not consistent between runs. Accordingly profiling locations were surveyed using either a Leica TN400N electronic total station with a reflective target placed atop of the column sampler when supernatant depth was being recorded, and/or a Trimble Pro XR sub-metre GPS unit. Profiling runs were undertaken a total of six times on each pond at various times in the year that would reveal season-induced change. The dates and seasons of when the profiling runs were undertaken are listed in Table 4-2.

Since water quality readings were logged manually, little was required in the way of data screening. The main data processing tasks were to calculate averages where multiple readings were taken at the one sampling location/depth, and to align readings with depth measurements and topographical survey data.

Table 4-2 Pond profiling events.

<i>Anaerobic pond</i>		<i>Facultative pond</i>	
<i>Date</i>	<i>Season</i>	<i>Date</i>	<i>Season</i>
9 June 2005	Early Winter	21 July 2005	Winter
19 October 2005	Spring	23 November 2005	Late Spring
1 March 2006	Early Autumn	1 February 2006	Summer
22 May 2006	Late Autumn	26 April 2006	Autumn
21 August 2006	Late Winter	4 September 2006	Early Spring
12 January 2007	Summer	11 January 2007	Summer

4.3 RESULTS

Data collected through the continuous real time monitoring were used to investigate seasonal and long-term trends in pond water quality. Subsets of the data were extracted to examine diurnal patterns in pond water quality at different times of the year. Variability with depth in the ponds was examined using the profiling data. Consideration was also given to the implications of variability across profiling locations, although this is addressed in greater detail in section 4.1 of Chapter 6. The water quality data from the continuous monitoring and seasonal profiling are provided in Appendix G. Analyses of the various water quality data also considered the various environmental factors that influence water quality (and potentially cause interference with measurement) and the level of agreement between data collected at the three different monitoring locations in the pond. Meteorological data used in the analyses were drawn from the data presented in Appendix H.

Real time water quality data collected from the anaerobic pond included temperature, pH and conductivity. DO was also measured in the anaerobic pond using a CS304 probe for the first half of 2005 (see section 4.3.1.2 for a sample of the data), but as would be expected DO levels never moved above zero. The same parameters were monitored in real time in the facultative pond along with turbidity and ORP. The set of probes deployed at any given time for real time monitoring was dependent on the working condition of the probes available and the current calibration rotation. As described earlier, where a significant problem with the calibration or the accuracy of a monitoring device has affected the quality of the data (sensor fouling was a common problem, particularly in the facultative pond), the data have either been omitted from the results presented, or are identified as being compromised.

The MA proved to be particularly prone to clogging of the pump and sampling line and rapid fouling of sensors by suspended solids, precipitants and attached growth. Due to the inevitable delays between a breakdown and its detection and subsequent rectification in the field, there are numerous gaps in the data produced by the MA. By 16 November 2006 the MA had become dysfunctional and on 6 December 2006 it was removed from service to be replaced with a CS304 probe (facultative pond probe 'Central') on 14 December 2006.

4.3.1 Anaerobic Pond

4.3.1.1 Seasonal and long-term variation in the anaerobic pond

Temperature

Figure 4-1 shows temperature levels in the anaerobic pond over the entire monitoring period. The coloured lines represent temperature data recorded at each probe location that have been smoothed using a centred weighted moving average equivalent to approximately one day's data either side of an observation. A smoothing period of 1 day provided maximum clarity (by removing noise) while retaining sufficient information to indicate variability. The same scheme has been applied to all time series plots used to present the continuous monitoring results herein. An equivalent 1-day moving average has also been applied to the hourly ambient air temperature data (grey line).

The data reveals a remarkable consistency between the temperature readings taken at three different probe locations (West, Central and South). The plots are almost indistinguishable from each other suggesting that temperature can be considered to be uniform across the length and breadth of the pond, at least at ~0.6 m depth. The seasonality of in-pond temperature is also clearly visible. The heat storage effects of the supernatant and sludge are evident when the in-pond temperature remains higher than the air temperature following peaks in air temperature. As observed by Safley & Westerman (1992a) and Safley & Westerman (1992b), in-pond temperatures fluctuate much less than ambient air temperatures. Note too that temperature readings do not appear to be affected by sludge encroachment on the probe sensors as was the case with both pH and conductivity (see below), indicating that sludge does not interfere with temperature measurements, and importantly, differences between sludge and supernatant temperatures are small.

Descriptive statistics calculated from the temperature data from each probe and the three probes combined are presented in Table 4-3. For the purposes of comparison, the raw (not smoothed) data from each probe were aligned by date and time and

timestamps without a reading from all three probes were removed from the calculations. Hence the common sample size (n) for the three probes. Since the three probe locations produced very similar outputs, statistics were also produced from their combined data. Table 4-4 gives the correlation coefficients between aligned data from each of the probe locations, again demonstrating the consistency between the probe measurements. Data alignment by timestamp was required for pairwise correlation analyses, hence the differing sample sizes.

Table 4-3 Descriptive statistics – aligned anaerobic pond temperature data.

<i>Statistic</i>	<i>West</i>	<i>Central</i>	<i>South</i>	<i>Combined</i>
n	30839	30839	30839	92517
Minimum (°C)	5.87	5.62	5.78	5.62
Median (°C)	16.88	16.79	16.91	16.86
Maximum (°C)	26.87	27.06	27.35	27.35
Mean (°C)	16.52	16.37	16.53	16.47
Standard deviation (°C)	4.94	4.92	4.98	4.95

Table 4-4 Correlation coefficients between temperature data recorded at the three anaerobic pond probe locations. Values in parentheses are sample sizes.

<i>Probe location</i>	<i>West</i>	<i>Central</i>	<i>South</i>
West	1 (40,080)		
Central	0.998 (33,002)	1 (34,935)	
South	0.998 (33,531)	0.998 (32,699)	1 (39,239)

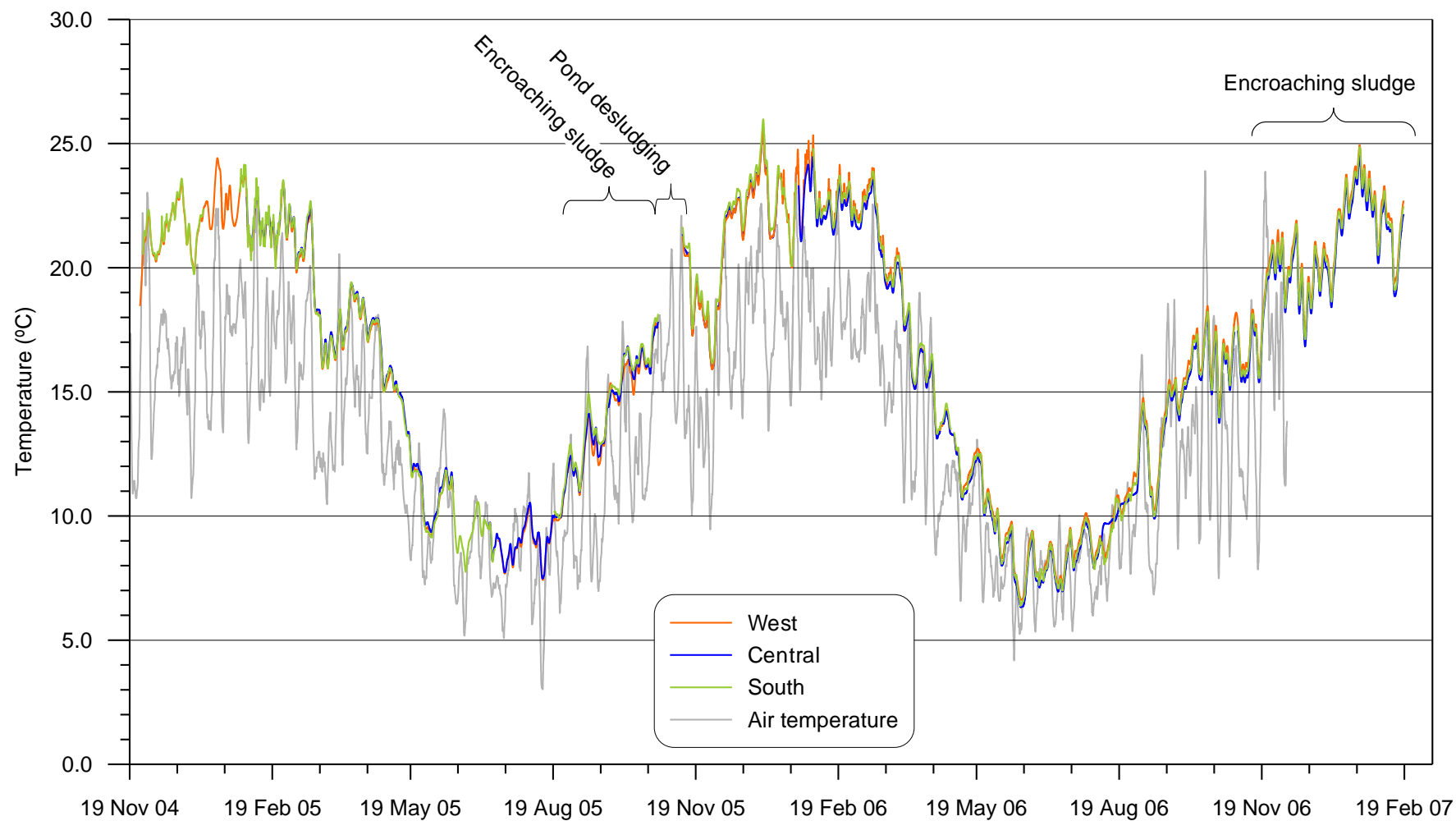


Figure 4-1 Temperature variation over time measured approximately 60 cm below the liquid surface at three locations in the anaerobic pond (orange, blue and green lines). Air temperature is shown in grey.

pH

There was reasonable consistency in pH readings between the probes in the anaerobic pond, with levels ranging between 6.9 and 7.8 as shown in Figure 4-2. The pH range is similar to anaerobic pond supernatant reported by Skerman et al. (2006) and Safley & Westerman (1992a), effluent pH levels observed by Mason (1996) and sludge pH measured by Ward & Jacobs (2008b; 2008a). There were small differences between the probe locations, although this variation is within the margin of error associated with sensor accuracy range (± 0.2). Moreover the differences are clearly offsets related to sensor calibration as the three time series generally exhibit very similar movements and trends and tend to 'switch places' when probes are replaced or recalibrated. The similarity in pH dynamics at the different locations in the pond is also indicative of an overriding spatial uniformity in supernatant chemistry. The descriptive statistics from the data aligned by date and time presented in Table 4-5 show close agreement in the pH ranges and averages between the three locations. The changing offsets in calibration do, however, cause correlation coefficients between the monitoring locations to be poor (data not presented).

The individual data points marked by symbols in Figure 4-2 represent measurements conducted on discrete wastewater samples collected at the pond inlet and outlet (see Chapter7). There is a considerable offset between the effluent data and the continuous data, which is an artefact of the strong alkalinity of the wastewater. Influent to the pond has an alkalinity of around 1500 mg/L as CaCO_3 and pH of about 8.0 - 8.1 (see Chapter7). Lowering of pH through anaerobic ponds containing high sludge levels has been observed elsewhere (e.g. Pena, Mara & Sanchez 2000) and is caused by anaerobic digestion processes taking place in the sludge. Firstly the fermentation of the organic matter generates acetic acid and higher order volatile fatty acids, which readily ionise to increase the concentration of ionised hydrogen. The acidifying effect of volatile acids that are not immediately consumed by methanogens is to some extent counteracted by the alkalinity of the wastewater. Indeed it is the alkalinity of the influent that provides the buffer capacity that prevents the pond from becoming acidic and causing anaerobic digestion to become inhibited. In addition to the generation of organic acids, carbon dioxide generated during fermentation of organic compounds and then through methanogenesis combines with water to form carbonic acid. Effluent leaving the pond is no longer exposed to this continuous stream of carbon dioxide, causing the equilibrium to shift away from dissociated carbonic acid and the pH to rise over the hours between sample collection and analysis.

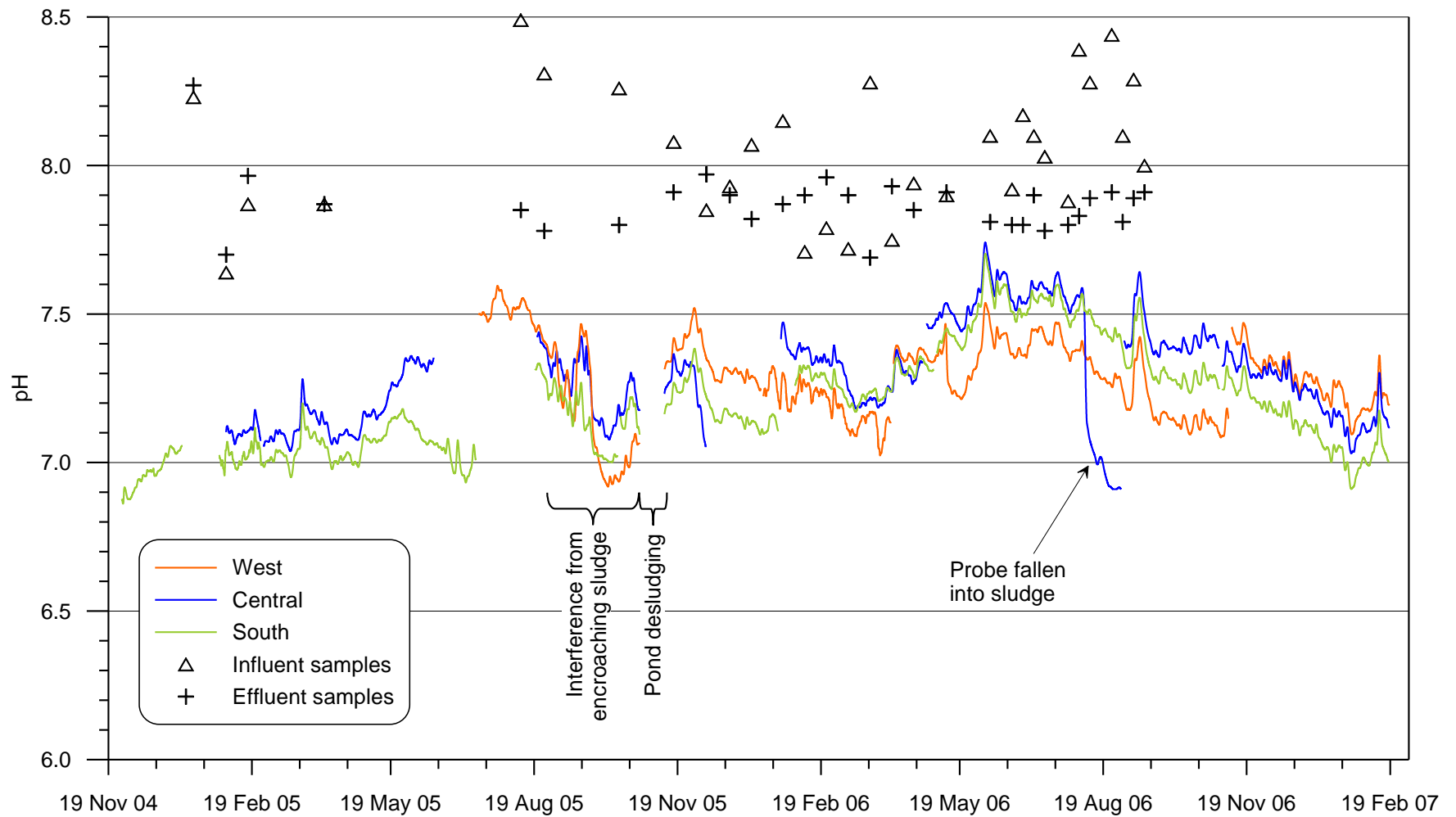


Figure 4-2 Variation of pH variation over time measured approximately 50 cm below the liquid surface and at three locations in the anaerobic pond (coloured lines). Readings from discrete samples of influent and effluent are denoted by black symbols.

Table 4-5 Descriptive statistics – aligned anaerobic pond pH data.

<i>Statistic</i>	<i>West</i>	<i>Central</i>	<i>South</i>	<i>Combined</i>
n	23039	23039	23039	69117
Minimum	6.9	6.9	6.9	6.9
Median	7.3	7.3	7.3	7.3
Maximum	7.6	7.8	7.7	7.8
Mean	7.3	7.3	7.3	7.3
Standard deviation	0.1	0.2	0.2	0.2

Overall there appears to be a trend of supernatant pH rising over autumn and winter when sludge digestion activity slows with lower temperature, and falling in negative correlation with rising temperatures as acidogenesis and acetogenesis picks up again. That pH appears to respond to the biological activity of the sludge suggests that the sludge blanket acts as a form of regulating agent that helps to maintain uniform supernatant conditions across the pond.

Electrical conductivity

Figure 4-3 shows a persistent trend of increasing EC levels over time recorded by all three probes in the anaerobic pond. The rising salinity is an artefact of the reclamation of effluent for flush water whereby conservative (non-reactive) ionic species accumulate with each flood wash when there is not adequate dilution from fresh water or removal via land irrigation. EC levels exceeded $4000 \mu\text{S cm}^{-1}$ for much of the 6 months following desludging in October 2005. Levels of this magnitude are notably higher than values reported in published research (e.g. Mason 1996; Sweeten & Wolfe 1994), but are not uncommon in Australian DSE anaerobic (primary) ponds (see for example Skerman, Kunde & Biggs 2006)

The dashed black line plotted against the (descending) secondary y-axis in Figure 4-3 represents cumulative water added from rainfall and runoff (positive) or lost to evaporation as a percentage of pond capacity. Rising EC tends to be accompanied by increasing water losses from evaporation, while disruptions to the general upward trend in EC are consistently associated with influx of fresh water from rainfall. EC levels in the anaerobic pond peaked around November 2005 immediately after desludging of the pond. It would appear that there are factors at play other than dilution/concentration by rainfall/evaporation that determine supernatant salinity since over the period November 2005 to June 2006 EC levels plateaued despite rising evaporation losses.

Then between September 2006 and February 2007, evaporation losses were again dominant but the concomitant rise in EC levels tapers off from mid-November 2006. Conversely, the period May to July 2006 saw a significant reduction in EC levels associated with relatively small but frequent fresh water inputs from rainfall and runoff, to both ponds (with effluent recycling proving the feedback loop from the facultative to the anaerobic pond) and mass export via irrigation from the facultative pond.

Generally there was close agreement between the three monitoring locations as evidenced by the similar central tendencies and degrees of dispersion exhibited by the three aligned data sets (Table 4-6) and correlation coefficients greater than 0.7 (Table 4-7). There also is good alignment between the continuous monitoring data and the discrete effluent sample measurements. Influent data also correlates with the supernatant data except for on a few occasions when rainfall runoff from the holding yard diluted the wastewater, which suggests that that the salt load contained in recycled flush water from the facultative pond is the main determinant of influent salinity.

The noise in the data over the period early September to late October 2005 was caused by encroachment of the sludge blanket into the upper metre of the liquid column. As explained in the pond profiling below (section 4.3.1.3), the sludge was characterised by slightly lower pH and EC relative to overlying supernatant. Following desludging, the noise in EC mostly dissipates, although data recorded by the West probe exhibits sharp and sustained drops during summer months. Immediately following desludging of the pond, the inlet pipe was reconfigured to reduce peak inflow velocity, putting the West probe directly in the path of incoming wastewater. The drops in EC are thought to be the result of less saline influent enveloping the West probe. Going by the very close agreement in the EC levels measured by the other two probes, the spatial extent of this poorly mixed zone appears limited. That this constrained mixing is limited to summer suggests that it may be related to differences in temperature and density that cause influent to displace rather than mix with surrounding supernatant when it hits the pond surface. Pond mixing and hydrodynamics are explored in detail in Chapter 6.

Table 4-6 Descriptive statistics – aligned anaerobic pond EC data.

<i>Statistic</i>	<i>West</i>	<i>Central</i>	<i>South</i>	<i>Combined</i>
n	30565	30565	30565	91695
Minimum ($\mu\text{S cm}^{-1}$)	1953	2570	2603	1953
Median ($\mu\text{S cm}^{-1}$)	3616	3669	3760	3678
Maximum ($\mu\text{S cm}^{-1}$)	4951	4783	5049	5049
Mean ($\mu\text{S cm}^{-1}$)	3660	3707	3793	3720
Standard deviation ($\mu\text{S cm}^{-1}$)	415	457	416	433

Table 4-7 Correlation coefficients between EC data recorded at the three anaerobic pond probe locations. Figures in parentheses are sample sizes.

<i>Probe location</i>	<i>West</i>	<i>Central</i>	<i>South</i>
West	1 (40,080)		
Central	0.7149 (32,728)	1 (34,390)	
South	0.7670 (33,531)	0.8398 (32,154)	1 (39,239)

The large drop in the Central probe readings in June 2006 is thought to have been caused by a sludge ‘eruption’. Sludge eruptions were a frequent but irregular occurrence, observable at the surface as circular expanding masses of dark particulate matter up to several metres in diameter. Similar eruptions in primary DSE ponds have been observed by Nordstedt & Baldwin (1975) and were used by McGrath & Mason (2004) as a basis for estimating biogas production. The cause of these eruptions is related to the escape of accumulating biogas bubbles entrapped within the sludge blanket, convection currents caused by temperature gradients that form between confined zones of heightened fermentation activity and surrounding less biologically active sludge. It is possible that one of these eruptions occurred immediately below the Central probe causing sludge to temporarily envelop the conductivity sensor. A few months later, the same probe became detached from its support buoy and fell into the sludge blanket, causing a significant departure in its EC measurements from those of the other two probes.

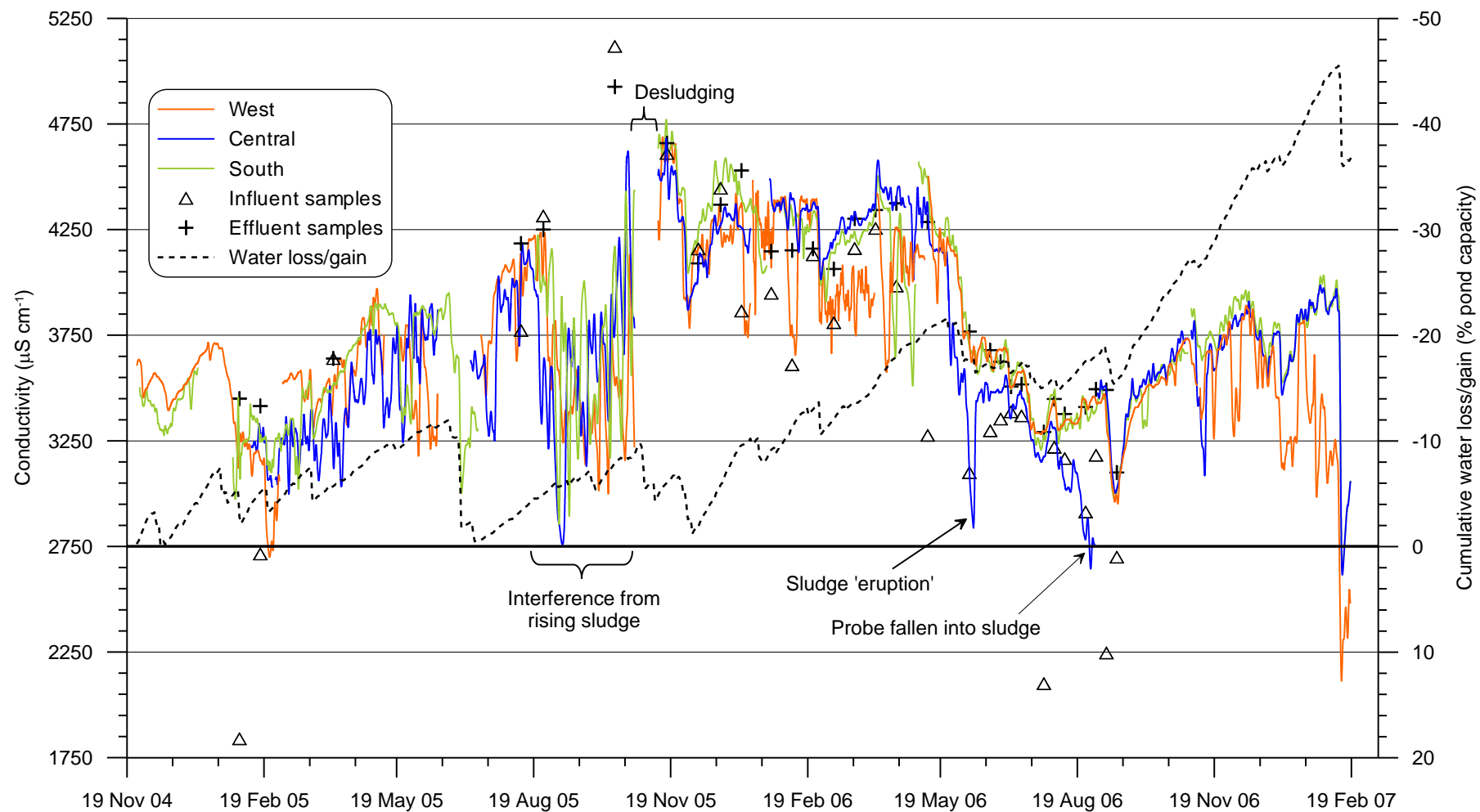


Figure 4-3 Variation in conductivity at approximately 60 cm (measured at three locations) and cumulative water flux from rainfall, runoff and evaporation (loss positive, gain negative) over time in the anaerobic pond.

4.3.1.2 Diurnal variation in the anaerobic pond

With readings taken every half hour or so, data from the continuous monitoring were of sufficient resolution to discern patterns in diurnal fluctuations in water quality parameters. Figure 4-4 presents raw temperature, DO, pH and EC data (no smoothing) for a 15-day interval in the height of summer of 2005 when ambient and internal pond temperatures show the widest diurnal variability. Overnight temperatures in the supernatant are higher than corresponding ambient temperatures, demonstrating the heat storage capacity of the pond and/or that biological activity is contributing heat to the pond. Heavily reducing conditions prevail due to the high oxygen demand of the organic load, leaving no traces of dissolved oxygen.

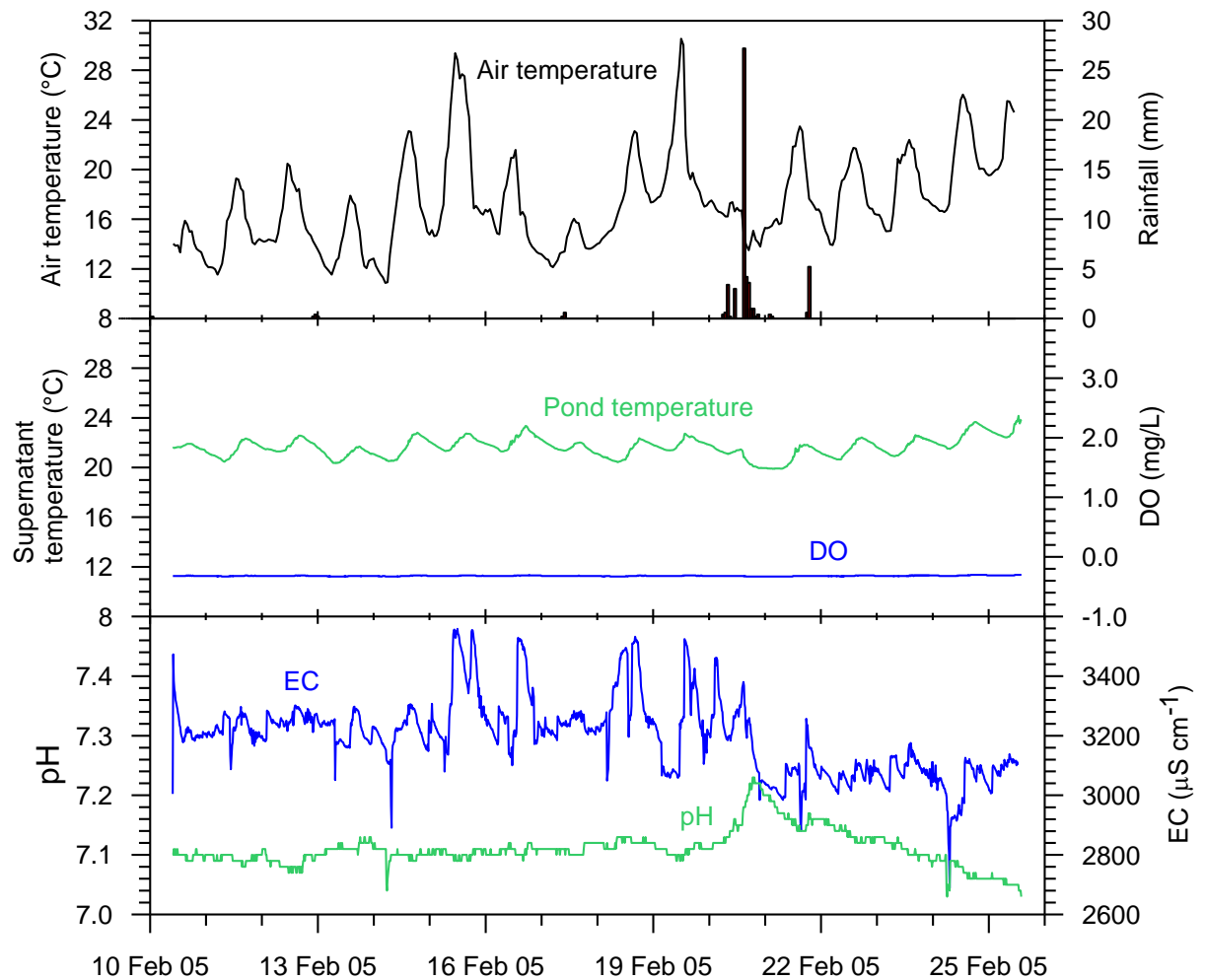


Figure 4-4 Summer diurnal variation in water quality parameters 50-60 cm below the surface of the anaerobic pond.

The concentration of free ionic species (EC) displays no distinct diurnal pattern or correlation with temperature. Inspection of corresponding inflow data (not presented here) revealed that the fluctuations in EC were not related to dilution by influent either. There is no discernible diurnal pattern to pH, although the peak in pH on 21 February 2005 coincides with a rainfall event, which may have mitigated acidification of the supernatant by digestion products. The following decline towards 7.0 was likely related to increased anaerobic digestion activity prompted by the rising pond temperature.

The same plot using data from June 2005 when temperatures reached their yearly low reveals a positive correlation with a lag of up to several hours between pH and temperature (Figure 4-5). This is somewhat counterintuitive as pH would be expected to decrease with the stimulation of digestion activity provided by higher temperature. However, at such low temperatures, digestion activity would be mild and pH would be more susceptible to temperature-induced shifts in the bicarbonate system and to mass transfer losses of carbon dioxide and ammonia. The scale of the temperature-related variability is within 0.1 pH units, which is within the margin of accuracy of the pH sensors and is unlikely to have significant bearing on other aspects of pond functionality, particularly so close to neutral pH. It is also worth noting that the smaller rainfall events (compared with the main event in the summer time series) appeared to have no impact on pH. Again DO levels are held fast at zero and the small peaks and troughs in the EC data do not correspond with temperature fluctuation or time of day. EC values were higher than they were in the summer due to accumulation of salts from effluent recycling. The DO measurements in Figure 4-4 and Figure 4-5 were made 50-60 cm below the surface of the pond. Vertical profiling of the pond (section 4.3.1.3) showed that there was no evidence of stratification that would warrant monitoring diurnal variation closer to the surface.

4.3.1.3 Anaerobic pond supernatant profiles

Temperature profiles measured in the anaerobic pond are plotted in Figure 4-6 together with the maximum air temperature recorded on the day of the profiling event. The profiles show that temperature gradients in the supernatant were generally mild, but increased with larger differentials between air and supernatant temperatures. The error bars attached to each plot give an indication of the variability in the nine (or more) measurements that comprise the average for a given depth in a profile, representing one standard deviation either side of the mean. All profiling runs were commenced mid-morning as the rise in ambient temperature began to accelerate, which meant that in case of temperature,

variability was a function of temporal rather than spatial factors. Hence the larger error bars closer to the surface.

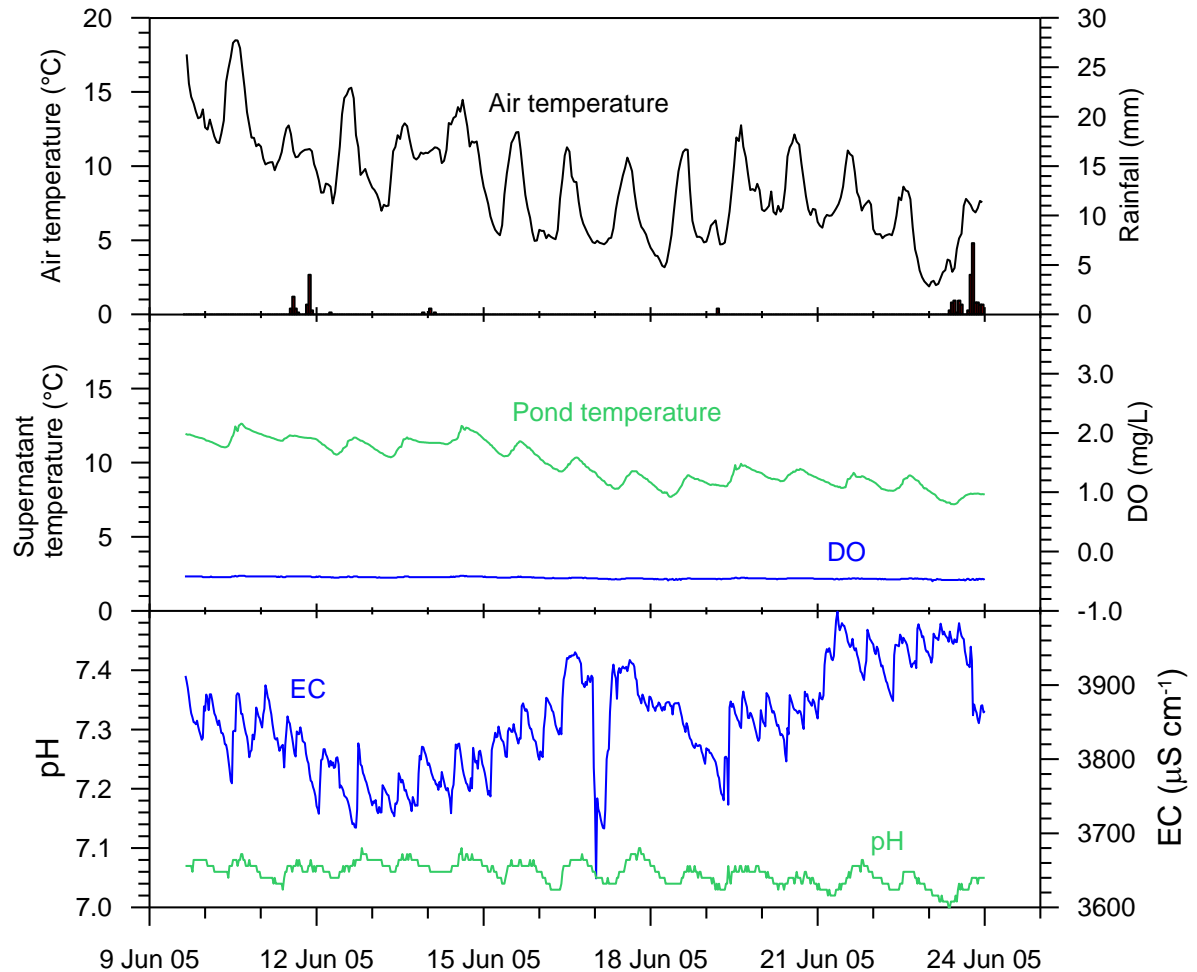


Figure 4-5 Winter diurnal variation of water quality parameters 50-60 cm below the surface of the anaerobic pond.

Table 4-8 shows that the largest observed temperature gradient between the surface and mid-depth (taken to be 50 cm in this case) was $6.4\text{ }^{\circ}\text{C m}^{-1}$, recorded by the last profile of the January 2007 run, which was measured between 1:18 and 2:30 pm. Characterising thermal stratification as a temperature gradient of $1.0\text{ }^{\circ}\text{C m}^{-1}$ or greater (Abis & Mara 2006), then the pond was also stratified on the winter (August) 2006 run, demonstrating that stratification can occur at any time of the year. Gradients did peak just above $1\text{ }^{\circ}\text{C m}^{-1}$ on two other occasions, but fleetingly. Importantly there was little evidence of thermal stratification between the sludge and the supernatant. All profiles included at least one measurement taken from the sludge. Only the January 2007 profile shows any distinction

between sludge and supernatant temperatures, with the sludge being 1°C cooler than the supernatant immediately above it.

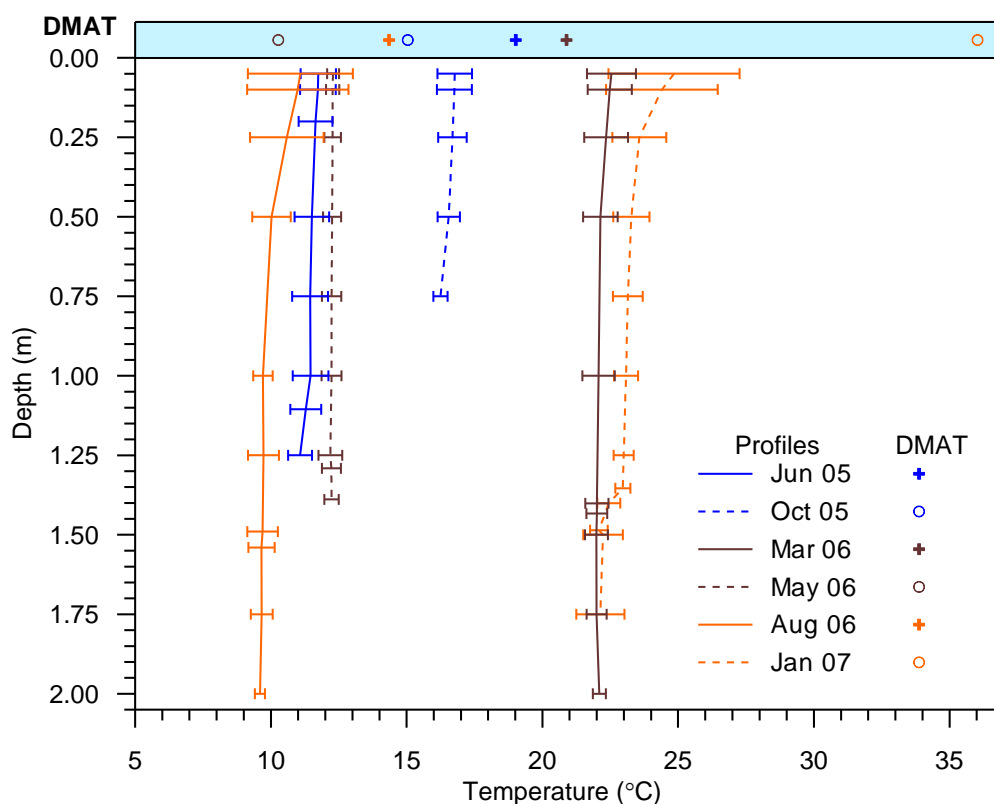


Figure 4-6 Anaerobic pond temperature profiles. Lines pass through mean values. Error bars represent two standard deviations. Daily maximum air temperature (DMAT) is plotted in the shaded region of the plot.

Table 4-8 Temperature gradients recorded in the anaerobic pond profiles.

Profiling event	n	Temperature gradient ($^{\circ}\text{C m}^{-1}$)		
		Minimum	Maximum	Average
June 2005	11	0.1	1.0	0.5
October 2005	16	0.0	1.2	0.5
March 2006	9	0.1	1.6	0.9
May 2006	9	-0.1	0.5	0.1
August 2006	9	0.0	5.2	2.4
January 2007	9	0.6	6.4	3.5

Profiles of pH and EC are presented in Figure 4-7 and Figure 4-8, respectively. Changes in pH and EC across sampling events mostly align with the continuous monitoring results,

particularly the EC data which peaks in October 2005. Sharp decreases observed at depth in both parameters were found to correspond with the height of sludge blanket. In the overlying supernatant, however, there was very little movement in pH or EC with depth. The profiles are almost identical in shape to those recorded by Paing et al. (2000), affirming that pH or EC measurements can be used to reliably determine pond sludge levels. Note that the depth of supernatant above the sludge layer receded significantly between June and October 2005 due to rapid sludge accumulation. Aside from variation in the depth at which the parameters drop in response to the presence of sludge, the respective shapes of the pH and EC profiles were consistent between sampling events. Variability associated with sampling location (indicated by the error bars) is minimal - less than ± 0.02 for pH and less than $\pm 25 \mu\text{S}/\text{cm}$ for EC. Variability was slightly greater between readings taken at different locations (at the same depth) in the sludge, presumably due to reduced diffusion in the semi-solid material. DO levels in the anaerobic pond are not presented simply because they were never observed to rise above zero, which is to be expected from a properly functioning anaerobic pond. Indeed the heavily reducing conditions of the pond are evident in the ORP profiles in Figure 4-9 which were always well below -100 mV.

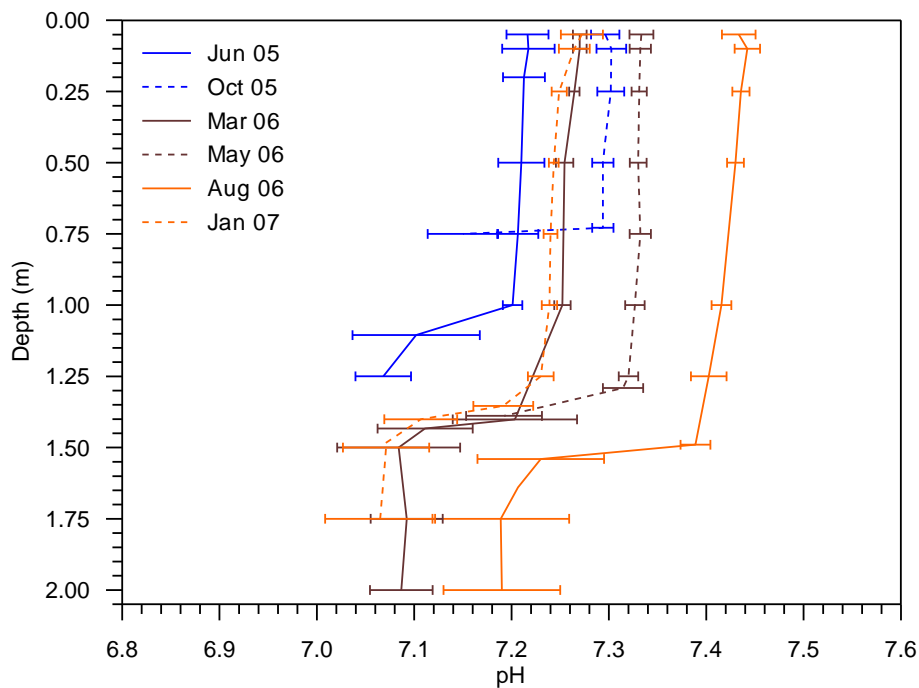


Figure 4-7 Anaerobic pond pH profiles.

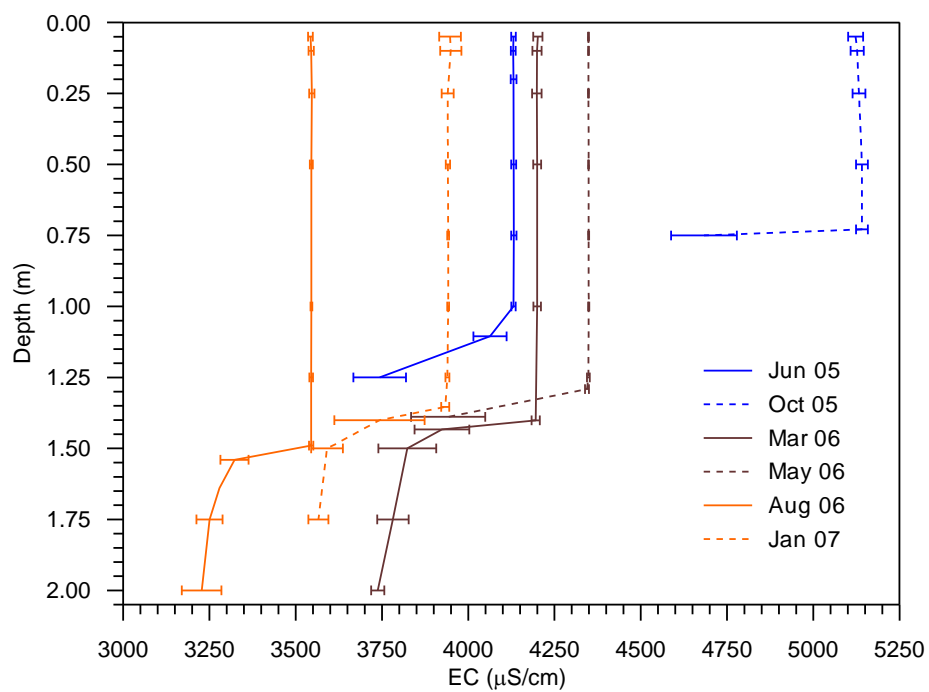


Figure 4-8 Anaerobic pond EC profiles.

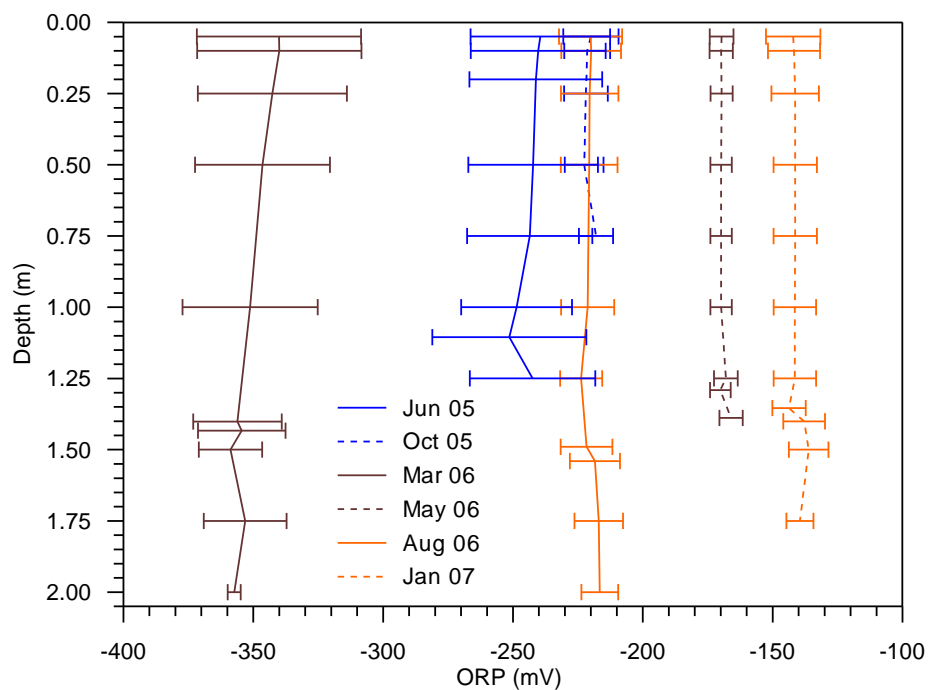


Figure 4-9 Anaerobic pond ORP profiles.

4.3.2 Facultative Pond

4.3.2.1 Seasonal and long-term variation temperature in the facultative pond

Temperature

Temperature readings from the various monitoring points in the facultative pond and the flood wash tank holding recycled effluent did not show the same degree of consistency displayed by the probes in the anaerobic pond (see Figure 4-10). This is primarily related to differences in the depths at which the probes were deployed as evidenced by the results of the supernatant profiling described in section 4.3.2.3. The sampling depth of the West probe varied, but was always at least 60 cm below the surface, causing temperatures to be consistently lower than those recorded at the other locations. The MA, the Central probe (which replaced the MA in December 2006) and the East probe all sampled from between 5-15 cm below the surface of the supernatant, which was subject to heating from insolation. Hence the dramatic peaks and troughs in the warmer months similar to those observed in the air temperature data. The peaks and variability in the data from the MA, however, are notably more pronounced, which may be due to a number of factors including:

- MA samples were extracted from a slightly shallower depth than the East and Central probes;
- the East and Central probes were subject to greater shading by their support buoys;
- supernatant was pumped out of the pond to the MA through black tubing that was prone to heating by the sun.

The MA sampling routine was programmed to perform extensive flushing of the sampling line at each sampling event. Nonetheless it is likely that some heating of the sample did occur as it was pumped through the sampling tube. Accordingly, MA temperature data were not used in subsequent analyses and modelling of the facultative pond.

Deployed deep in an opaque fibreglass tank, the FWT probe recorded relatively consistent temperatures through the day. The effluent held in the tank was drawn from 40-60 cm below the pond surface making it slightly warmer than the supernatant sampled by the deeper-positioned West probe, particularly in summer. The variability of temperature with depth is also evident in the descriptive statistics of the temperature data from the

facultative pond supernatant. Table 4-9 presents statistics from facultative pond temperature data aligned by date and time from the three main probes (West, East and FWT) that were installed over most of the monitoring period, and the same statistics when the data alignment incorporates the Central probe that had a much shorter data set. The probes deployed at the surface (East and Central) recorded higher mean and median temperatures and exhibited greater variability due to larger diurnal swings. The correlation coefficients presented in Table 4-10 show that the West and FWT probe data are the most closely correlated on account of the reduced variability at depth. The East probe has a stronger correlation with the FWT probe presumably on account of the closer vertical proximity of the sampling depth.

Table 4-9 Descriptive statistics - aligned facultative pond temperature data.

<i>Statistic</i>	<i>Not including Central probe</i>			<i>Including Central probe</i>			
	<i>West</i>	<i>East</i>	<i>FWT</i>	<i>West</i>	<i>East</i>	<i>FWT</i>	<i>Central</i>
n	24991	24991	24991	10649	10649	10649	10649
Minimum (°C)	5.15	5.00	5.72	5.15	5.00	5.72	-0.90
Median (°C)	13.40	16.05	14.68	13.84	16.60	15.01	17.80
Maximum (°C)	22.13	38.40	24.71	21.61	35.30	24.68	49.10
Mean (°C)	13.08	16.08	14.59	13.59	16.86	15.08	19.19
Standard deviation (°C)	3.97	5.93	4.32	3.79	5.91	4.13	9.00

Table 4-10 Correlation coefficients between temperature data recorded at the four facultative pond probe locations. Figures in parentheses are sample sizes.

<i>Probe location</i>	<i>West</i>	<i>East</i>	<i>FWT</i>	<i>MA/Central</i>
West	1 (41,065)			
East	0.83 (38,062)	1 (50,466)		
FWT	0.97 (27,366)	0.89 (26,441)	1 (101,697)	
Central	0.54 (15,865)	0.79 (15,052)	0.63 (11,532)	1 (16,360)

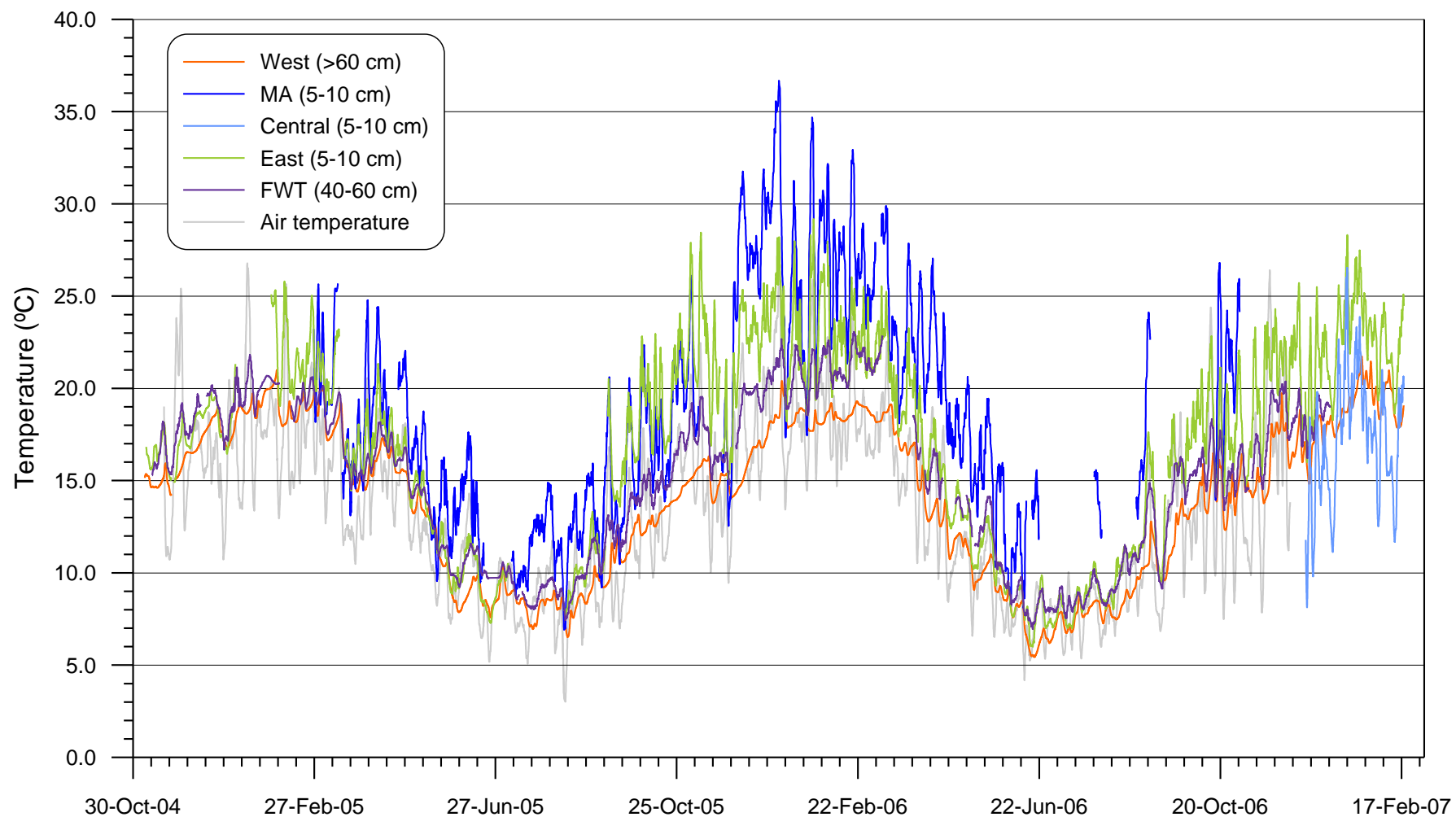


Figure 4-10 Temperature variation in the facultative pond measured at three different locations within the pond and in the flood wash tank. Ambient air temperature is shown in grey in the background. Measurement depths are given in the legend (note FWT depth = pond extraction depth).

pH

Inconsistency between probes was also evident in the facultative pond pH data (see Figure 4-11). This inconsistency is partly attributable to problems caused by failing sensors (particularly in pre-2006 data) and fouling of the sensors by attached biological growth as well as crystalline deposits (see EC results below) in cooler months. However, as with temperature, variability between the probes is also an artefact of the sampling depth. Production of CO₂ from algal respiration at the surface of the pond causes pH levels to rise, an effect that is diurnal as it depends on sunlight. Thus pH can be expected to vary substantially in the pond epilimnion, particularly in the warmer, sunnier months of the year.

The high turbidity of the supernatant (see 'Turbidity' section below) limits light penetration and photosynthesis at depth, thus pH readings taken within the hypolimnion would be expected to be lower and more consistent. This behaviour is borne out in the data: the MA, and the Central and East probes generally recorded higher, noisier pH levels while the FWT and West probes, producing lower, more stable readings. The same is evident in the descriptive statistics given in Table 4-11. Note that the increase in the aligned data sample size *n* obtained by the omission of the MA and Central probe data (which constitute the smallest data set due to less frequent sampling and problems with the MA sensor) does not significantly alter the statistics for the other three probes.

The mean and median pH values at the four sampling locations were all between 7.9 and 8.2, which agree with published data on DSE facultative ponds (Hickey et al. 1989; Mason 1996; Sukias et al. 2001). Again the alkalinity of dairy shed wastewater is evident as without the acidifying effect of anaerobic digestion, the pH returns to the level it was prior to entering the anaerobic pond. The range of pH measured in the epilimnion (MA, Central and East) is also similar to that reported in the only study known to have looked specifically at diurnal pH variability in DSE facultative ponds (Sukias et al. 2001).

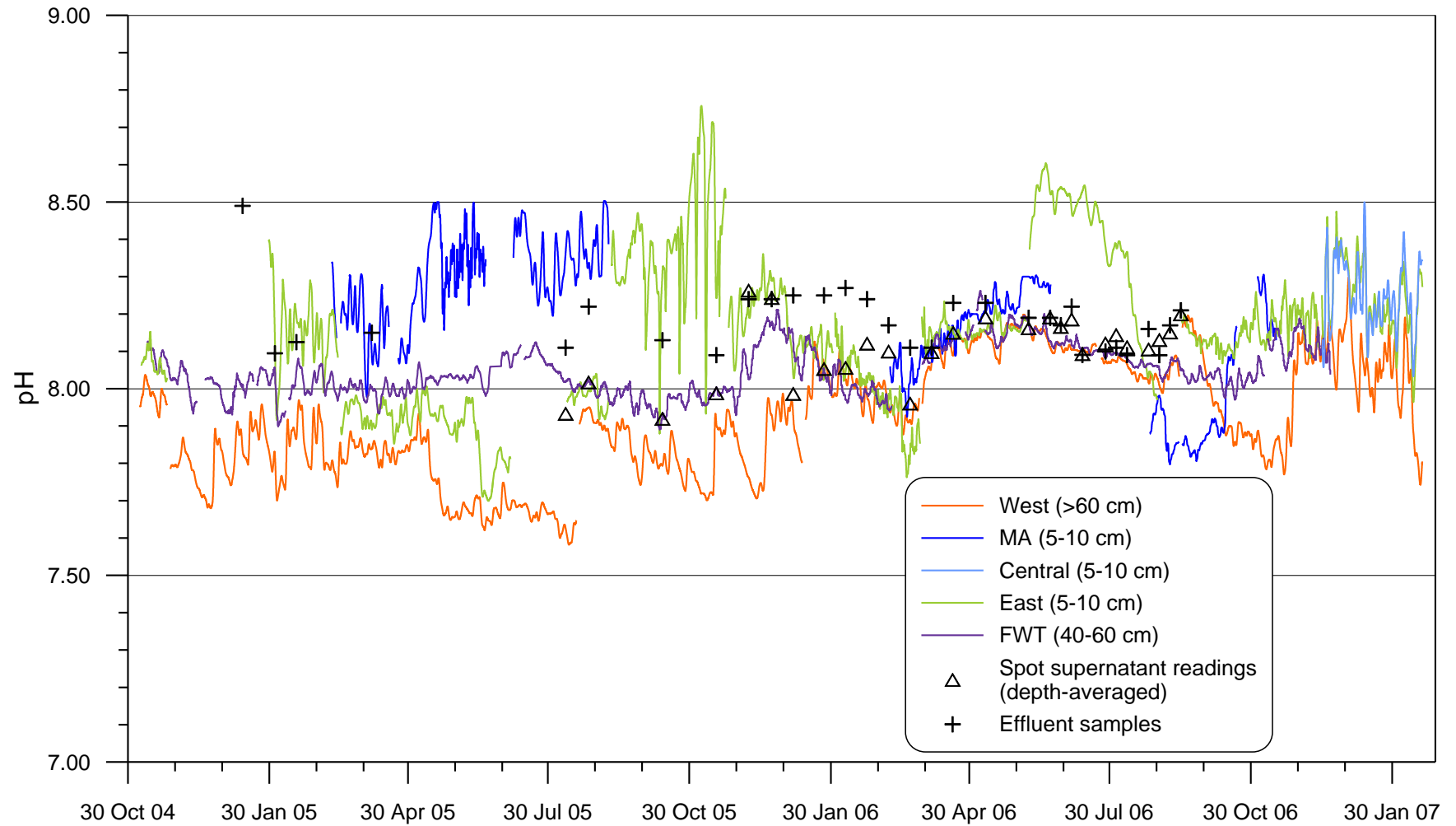


Figure 4-11 Variation in pH in the facultative pond measured at three different locations within the pond and in the flood wash tank containing effluent from the pond for reuse. Readings from discrete samples of the supernatant (in-pond) and effluent are denoted by black symbols.

Table 4-11 Descriptive statistics – aligned facultative pond pH data.

<i>Statistic</i>	<i>West</i>	<i>MA/Central</i>	<i>East</i>	<i>FWT</i>
n	6887	6887	6887	6887
Minimum	7.6	7.6	7.7	7.8
Median	7.9	8.2	8.1	8.0
Maximum	8.3	8.6	8.7	8.3
Mean	7.9	8.2	8.1	8.0
Standard deviation	0.2	0.2	0.2	0.1

Agreement between the continuous data and discrete effluent and supernatant sampling data was generally good, particularly from early 2006 onwards. In-pond supernatant measurements were taken at approximately 25 cm depth while effluent samples were pumped out from the flood wash tank, which was filled from supernatant drawn from about 50 cm below the surface of the pond. There was particularly strong consistency both between sampling techniques and between probes during the autumn/winter period from March through to September 2006 when algal growth would have been at its seasonal ebb. The pH of discrete effluent samples was often higher than corresponding supernatant pH, which may have been caused by degassing of CO₂ during pumping.

Electrical conductivity

Figure 4-12 presents EC levels recorded at the four sampling locations in the facultative pond together with cumulative flux of fresh water from rainfall, runoff and evaporation expressed as a percentage of pond capacity on the secondary y-axis (evaporative losses considered positive to reflect their concentrating effect on EC). Also plotted on the secondary y-axis are effluent irrigation volumes, expressed as a negative percentage of pond capacity since irrigation effectively removes salt from the system. Incidents related to supernatant conductivity and its measurement are identified on the x-axis monitoring timeline. Statistics from the data aligned by timestamp are presented in Table 4-12 and correlation coefficients for each location pairing are given in Table 4-13.

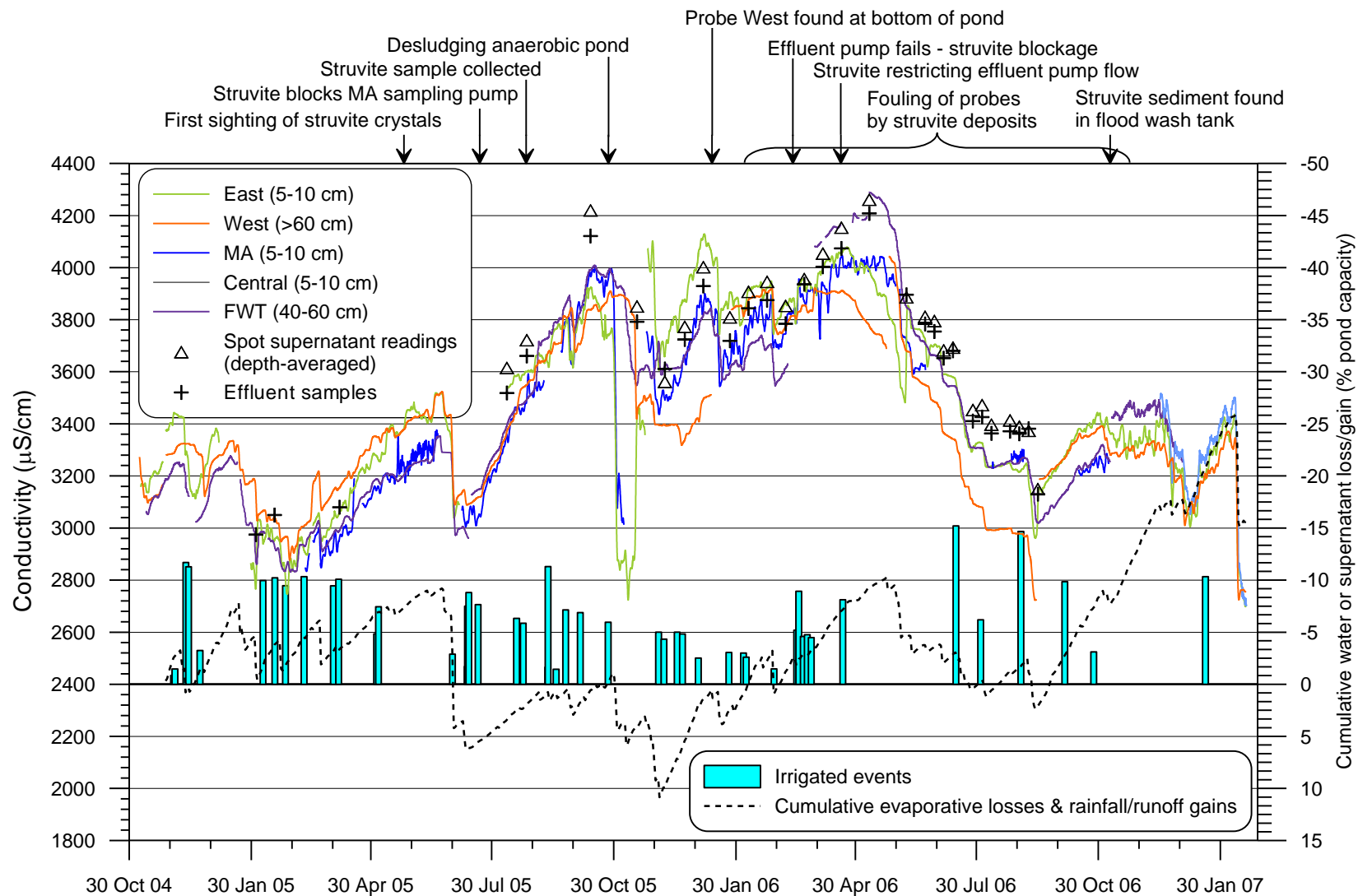


Figure 4-12 Variation in conductivity and flux of fresh water over time in the facultative pond.

Table 4-12 Descriptive statistics – aligned facultative pond EC data.

<i>Statistic</i>	<i>Not including MA/Central data</i>				<i>Including MA/Central data</i>		
	West	MA/Central	East	FWT	West	East	FWT
n	9780	9780	9780	9780	25701	25701	25701
Minimum ($\mu\text{S cm}^{-1}$)	2900	2658	2773	2898	2631	2631	2748
Median ($\mu\text{S cm}^{-1}$)	3505	3558	3685	3613	3581	3581	3571
Maximum ($\mu\text{S cm}^{-1}$)	4147	4151	4316	4297	4316	4316	4297
Mean ($\mu\text{S cm}^{-1}$)	3550	3532	3610	3580	3542	3542	3537
Standard deviation ($\mu\text{S cm}^{-1}$)	285	341	331	365	342	342	360

Table 4-13 Correlation coefficients between EC data recorded at the four facultative pond probe locations. Figures in parentheses are sample sizes.

<i>Probe location</i>	<i>West</i>	<i>East</i>	<i>Recycle</i>	<i>MA/Central</i>
West	1 (41,065)			
East	0.78 (38,057)	1 (50,436)		
Recycle	0.84 (27,362)	0.78 (26,433)	1 (101,642)	
Central	0.83 (14,972)	0.92 (14,194)	0.91 (10,635)	1 (15,306)

As in the anaerobic pond, there is a consistent upward trend in EC levels related to effluent recycling, with levels peaking considerably higher than published data from similar DSE facultative ponds (Hickey et al. 1989; Sweeten et al. 1994; Mason 1996; Sukias et al. 2001). The elevated conductivity, however, is not unusual for Australian DSE pond systems that support effluent recycling (Skerman, Kunde & Biggs 2006; Jacobs & Ward 2007a; Jacobs, Ward & Kearney 2008; Jacobs & Ward 2007c) and poses a relatively low risk to soil structure and to pasture growth, especially given the relatively low Na and chloride concentrations (see Chapter 7) (ANZECC & ARMCANZ 2000; NSW DEC 2004). Data from the four monitoring locations and the discrete sampling show good agreement both in terms of measure and trend. Table 4-13 shows that in the absence of influent plumes and accumulating sludge, the correlations between the monitoring locations were stronger than those for conductivity in the anaerobic pond, even despite the fact that the probes in the facultative pond were deployed at different depths.

The movements in EC levels largely reflect the dynamics of water gains/losses, showing that the accumulation of salts is amplified by extended dry periods and dislocated by dilution from rainfall/runoff events. However the magnitude of the decline in conductivity levels between May and August 2006 does not correspond to other drops caused by rainfall/runoff events, suggesting that accumulation and dilution are not the sole factors at play in determining effluent salinity. The removal of salt loads via effluent irrigation would also be expected to help reduce salinity, but only when accompanied by fresh water additions. Larger irrigation events extracting around 10% of pond capacity did seem to result in small reductions in EC, or at least dampen the rate of salt accumulation, as fresh water used at the dairy provides gradual, if very limited dilution. Irrigation events followed by rainfall events, however, had the greatest impact on EC, as demonstrated by the more substantial drops in July, August and September 2006.

Another potential cause of the decline in EC levels in mid-2006 is precipitation of mineral salts. Offsets between readings from the West probe and the other sampling points gradually increased over the autumn and winter of 2006, as did differences between continuous in-pond measurements and readings taken from discrete samples. This was caused by the formation of crystals on the in-pond probe sensors, interference from which was found in laboratory testing to cause reduce conductivity readings by 5-10%. The form and nature of the crystalline deposits are explored further in section 4.4.4.

The EC data also provide indications of the extent of mixing in the pond. The largest abrupt change to EC levels occurred when inflow to the pond stopped due to desludging of the anaerobic pond in October 05. This caused an immediate response (significant drop) in MA and the East probe EC readings made close to the surface, but responses from the West and Flood wash tank probes (positioned at depth) were delayed by several days and were less dramatic. This would indicate that mixing in the pond is constrained vertically by stratification (refer to section 4.3.2.3) and/or transversally by lack of dispersion.

Dissolved oxygen

DO was recorded in the facultative pond by the East probe, the MA and the Central probe that replaced the MA in December 2006. The raw DO data presented in Figure 4-13 shows that DO readings were the least consistent of the parameters in terms of agreement between sampling locations. This would in part be on account of the highly dynamic nature and spatial variability of the relationship between algal photosynthesis

and bacterial respiration. It is also likely that different types of sensors used in the CS304 probes and the MA produce differing response rates to changes in DO concentration. Fouling of DO sensors was also a problem for the East and Central probes that were not regularly cleaned like the MA.

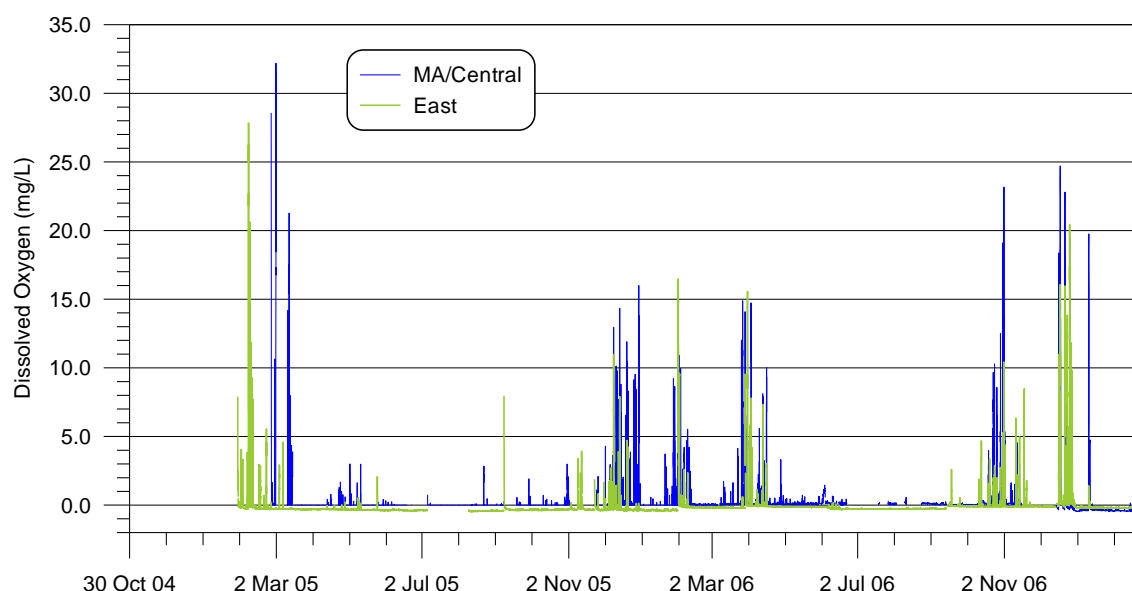


Figure 4-13 Variation DO in the epilimnion of the facultative pond measured at two different locations

All sampling locations did, however, reveal a clear pattern of DO reaching supersaturation levels intermittently between late spring and early autumn, and remaining close to zero the remainder of the time. The predominance of zero concentrations render descriptive statistics drawn from the raw data meaningless. Table 4-14 thus presents statistics for daily non-zero data, which show that while daily peaks could produce highly saturated conditions (DO over 30 mg L^{-1}), the average peak was less than 5 mg L^{-1} . Averaged over the entire day DO concentrations remained very low, demonstrating the high oxygen demand created by residual organic matter the supernatant. Note that the much higher number of non-zero days and lower daily average DO for the MA/Central data is most likely due to the greater sensitivity of the MA DO sensor, which allowed it to detect lower DO concentrations.

Extreme daytime DO saturation has previously been observed in DSE facultative ponds (Sukias et al. 2001) and primary facultative ponds treating sewage (Dochain et al. 2003). The seasonality of the peaks (see Figure 4-13) indicates that DO is mostly introduced to the supernatant by algal photosynthesis – if surface re-aeration was dominant then DO would peak throughout the year. It also shows that algal growth only

becomes prolific enough to sustain aerobic conditions in the pond during the warmer months of the year in the temperate climate of the region.

Table 4-14 Descriptive statistics – non-zero daily DO concentrations.

	<i>MA/Central</i>	<i>East</i>
n	357	76
Average (mg L^{-1})	0.6	1.6
Standard deviation (mg L^{-1})	1.4	2.2
Minimum peak (mg L^{-1})	0.01	0.02
Maximum peak (mg L^{-1})	32.2	27.8
Average peak (mg L^{-1})	2.3	3.8
Standard deviation of peak (mg L^{-1})	4.8	5.0

Turbidity

Turbidity measurements were made on samples from drawn from the upper 5-10 cm of the pond. The raw (unsmoothed) data presented in Figure 4-14 show good agreement between the MA data and data from discrete supernatant and effluent samples analysed in the laboratory (refer to Chapter 7). There appears to be better alignment between the MA and effluent data, which is due to the difference in sampling methods for the two discrete samples. Effluent samples were drawn from approximately 50 cm below the surface while the supernatant samples were composite samples of the entire water column.

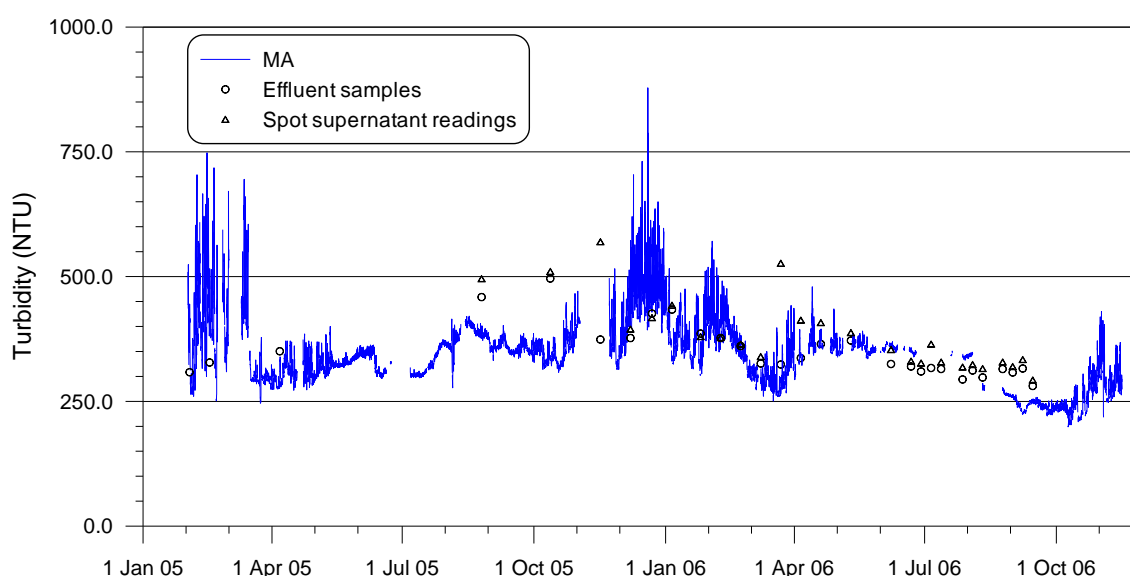


Figure 4-14 Variation in turbidity at the surface of the facultative pond measured by the MA. Readings from discrete samples of supernatant and pond effluent are denoted by black symbols.

Average turbidity over the monitoring period was 343 NTU (standard deviation 66 NTU). The time series in Figure 4-14 suggests there is a base level of turbidity below this average which is reflective of the poorly settleable material remaining in the effluent from the anaerobic pond. Peaks above this level over spring and summer would be caused by propagation of algal cells. The relationship between turbidity and algae is further examined in section 4.3.2.2 below and in Chapter 7 (section 4.2).

4.3.2.2 Diurnal variation in the facultative pond

Figure 4-15 shows the range of diurnal variation in the epilimnion of the facultative pond as it comes to life following the period of low biological activity during winter and early spring. While surface temperatures are already climbing well into the twenties, the algal population initially remains subdued due to the inertia of winter inactivity. Until this time, turbidity and pH oscillate around 250 NTU and 8.1 respectively, while ORP struggles to rise above 0 mV. Once algal photosynthesis takes hold from 24 October 2006, DO is produced at a rate exceeding the oxygen uptake rate, thus generating increasingly large DO peaks that eventually surpass saturation levels, similar to the supersaturated DO peaks observed by Sukias et al. (2001). At the same time turbidity, pH and ORP levels all begin to climb, reaching peaks above 400 NTU, 8.3 and 150 mV, respectively.

These results demonstrate that DO, turbidity, ORP, pH and EC are all heavily influenced by algal activity, which is stimulated by solar radiation and warmer temperatures. DO is directly linked with algal growth as increased photosynthesis generates more oxygen. Turbidity is correlated with algal population as algal cells flocculate to create light blocking particulate matter. ORP is increased, at a slight lag, by the presence of free oxygen, while increasing pH (also lagged) is a result of photosynthesis removing carbon dioxide from the supernatant. The roles of temperature and solar radiation in driving algal activity are evident through their correlations with the abovementioned parameters. Importantly, there is no clear correlation between DO levels and wind speed, further indicating that algal photosynthesis is the dominant factor behind aeration of the epilimnion. The overall upward trends in turbidity, pH and ORP, as well as in the peaks of DO, show the cumulative effect of the growing algal biomass population. Elevated daytime DO and ORP levels could also potentially support nitrification (Qureshi et al. 2008), although the nightly descent to reducing conditions and the absence of attachment surfaces within the (intermittently) aerated epilimnion place considerable constraints on nitrifier

growth (Craggs et al. 2000; Sukias et al. 2003). EC was generally steady with very minor drops caused by rainfall on 3 and 8 November 2006.

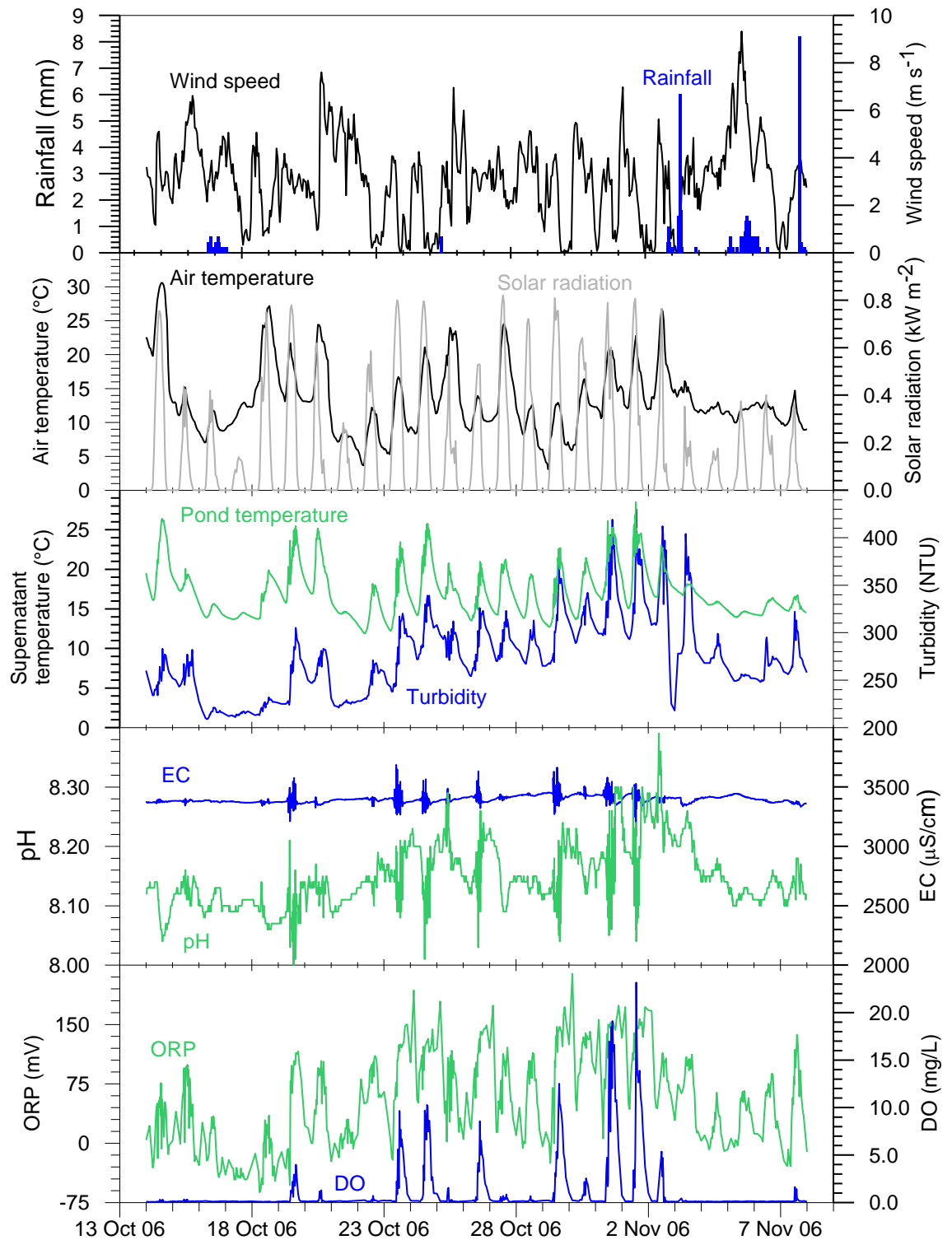


Figure 4-15 Diurnal variation in the epilimnion (upper 5-10 cm) of the facultative pond in late spring to early summer.

Figure 4-16 is a plot of temperature, pH and EC recorded at depth over the same period. The depth of the probe sensors is also plotted to demonstrate that the varying depth (between 0.45 and 0.65 m) did not have a material effect on the water quality parameters. The graph shows that temperature stays significantly lower than surface temperatures (Figure 4-15) and that pH is notably lower and does not show the same diurnal pattern as it does at the surface. EC levels recorded at depth are close to surface levels and exhibit a similar absence of a recurring diurnal pattern.

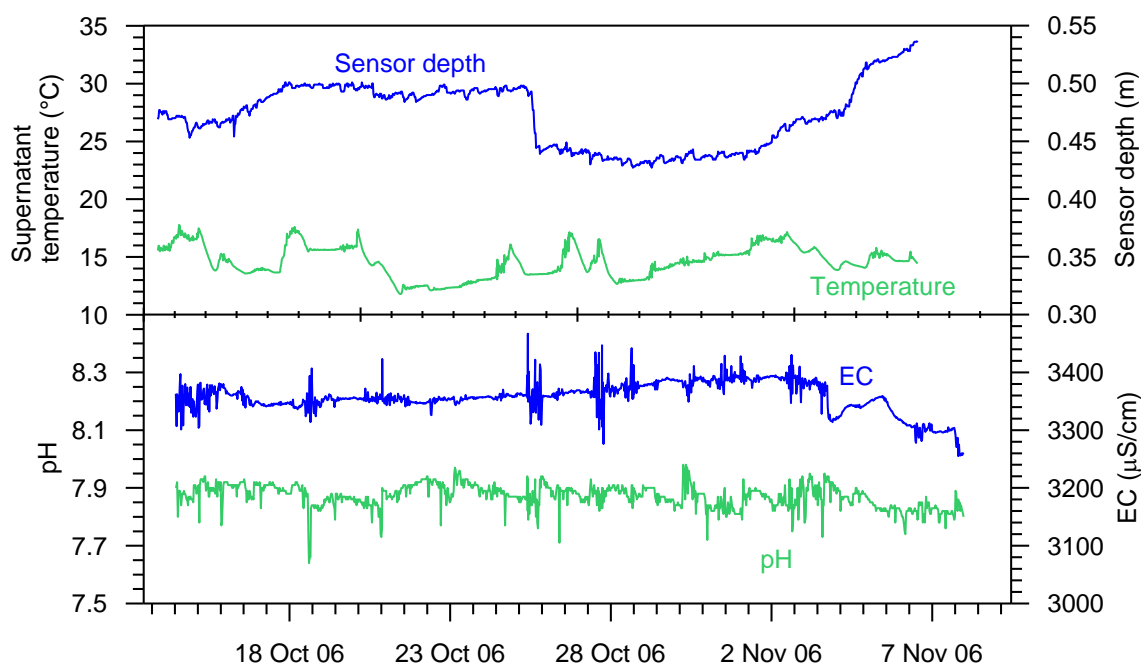


Figure 4-16 Diurnal variation in the hypolimnion of the facultative pond in late spring to early summer.

Figure 4-17 shows diurnal fluctuations that are typical of winter conditions when minimum ambient temperatures approach zero. The difference to warmer months is most notably indicated by the complete lack of DO, despite wind approaching 5 m s^{-1} on numerous occasions. Other parameters still exhibit faint diurnal swings, but the timing of the peaks differs to periods when algal activity dominates. ORP peaks above 50 mV in the early hours of the morning, suggesting the presence of electron acceptors. It should be noted here that given the typically slow response rate of ORP sensors, peaks and troughs in ORP are likely to have been higher than measured under the limited exposure time of the MA sampling regime. It is possible that DO being drawn from the air at low temperatures while microbial activity ebbs is enough to create mildly oxidising conditions. The DO satisfies a portion of the oxygen uptake rate, but not enough to result in accumulation of DO. Peak ORP is high enough to support nitrification (Qureshi et al. 2008), but without DO, oxidation of ammonia cannot

proceed. Troughs in pH levels coincide with peak temperatures, suggesting that microbial respiration (producing CO_2) is the dominant biological process during the day in winter. Fluctuations in turbidity do not appear to correlate with other diurnal patterns, further suggesting the algae population is dormant.

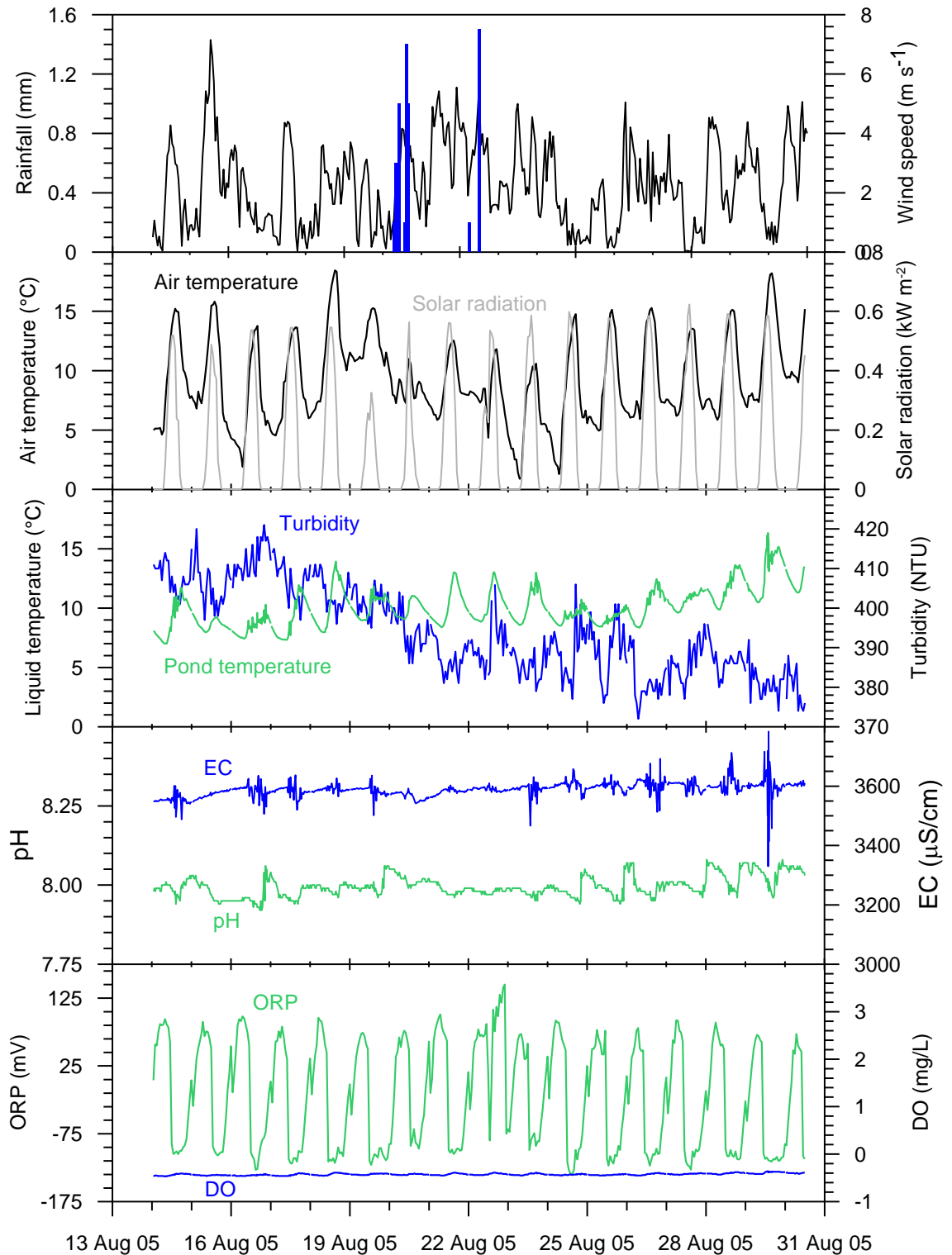


Figure 4-17 Winter diurnal variation in the epilimnion (upper 5-10 cm) of the facultative pond.

4.3.2.3 Facultative pond supernatant profiles

Average temperature profiles from the six profiling runs in the facultative pond are presented in Figure 4-18. The difference to the anaerobic pond is immediately clear in the formation of a thermocline whenever there is a large positive differential between the air temperature and the supernatant temperature at the lower depths. The wide error bars at the surface also indicate that the facultative pond is more prone to diurnal swings in air temperature, but the influence appears to dissipate significantly below 50 cm. As a result the pond could be classified as thermally stratified on all profiling events, with average temperature gradients - presented in Table 4-15 - consistently greater than $1\text{ }^{\circ}\text{C m}^{-1}$. The minimum observed gradients show that on the July (winter) and November (spring) 2005 events, the pond was initially unstratified, but soon became stratified as the day proceeded and the ambient temperature rose.

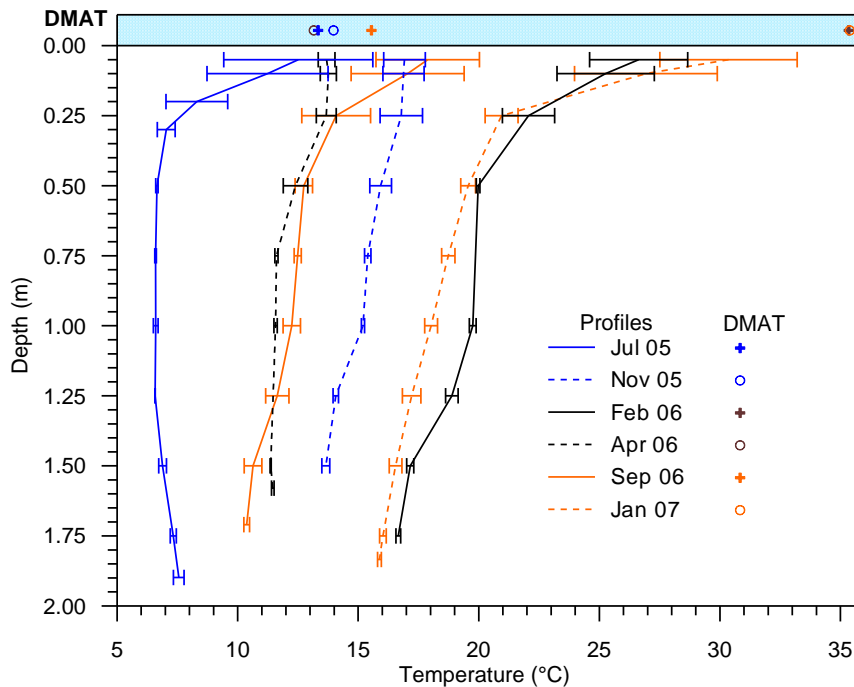


Figure 4-18 Facultative pond temperature profiles plotted with corresponding DMATs.

Figure 4-19 plots the profiles of pH in the facultative pond, four out of six of which show the same pattern of relatively constant pH levels between 0.25 and 1 m depth underlain by approximately linear gradients to the bottom of the pond. The stable pH above is a manifestation of the wastewater's alkalinity, while the slight upward inflections in the upper 25 cm would be the result of algal activity. The lower pH levels at depth appear to be related to the production of VFAs and CO_2 at the bottom of the pond where organic material undergoes fermentation in the anaerobic conditions. The gradients are indicative of the limited extent of fermentative activity and are more pronounced at

warmer temperatures due increased biological activity. The main departures from this trend occurred in autumn (April 2006) and summer (January 2007). The lack of gradient in the April 06 profile appears to be an artefact of turnover, whereby thermal instability results in vertical mixing of the water column. Thermal instability and turnover occurs when surface liquid becomes cooler than underlying liquid, generating vertical convection currents (Shilton & Harrison 2003a) that mix the water column and produce uniform water quality profiles. Accordingly the same lack of gradient is also evident in the April 2006 EC profile.

Table 4-15 Temperature gradients recorded in the facultative pond profiles.

Profiling event	n	Temperature gradient ($^{\circ}\text{C m}^{-1}$)		
		Minimum	Maximum	Average
July 2005	14	1.0	15.2	8.5
November 2005	16	0.6	3.8	2.2
February 2006	15	3.6	10.8	7.2
April 2006	9	2.4	4.1	3.0
September 2006	16	2.6	13.0	7.7
January 2007	13	6.1	20.5	16.6

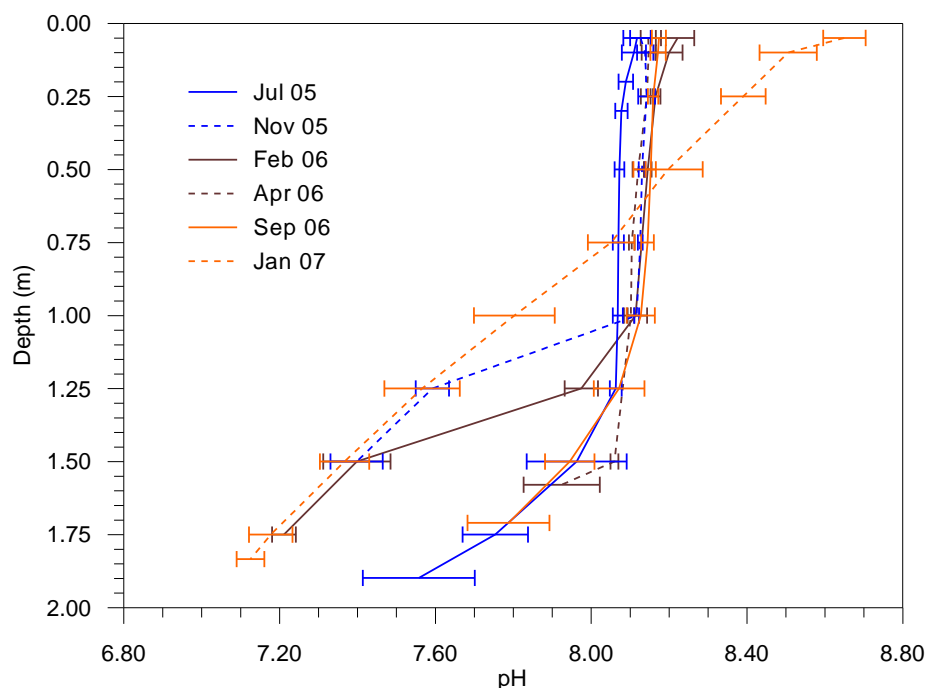


Figure 4-19 Facultative pond pH profiles.

The continuous gradient in pH down the entire profile recorded in January 2007 is the result of the contrasting biological processes occurring at the surface and the bottom of

the pond, which were both stimulated by unusually hot temperatures (maximum around 35 °C) and high solar radiation (over 32 MJ m⁻² for the day). The bottom half of the pond was characterised by the same gradient observed at other times of the year, while at the surface heightened consumption of CO₂ by rapidly growing algae caused pH to rise above 8.7. The key difference between the January 2007 profiling event and the other summer profiling event (February 2006) appears to have been the temperature and solar radiation over the preceding 24 hours. In January 2007, the temperature on the previous day peaked just above 25 °C and solar radiation totalled almost 31 MJ m⁻², whereas in February 2006, the temperature on the day previous reached just 17 °C and total solar radiation was only about 10 MJ m⁻². This again is suggestive of the cumulative nature of algal productivity touched upon in section 4.3.2.2 and shows the dynamic nature of water quality changes within the pond.

The EC profiles plotted in Figure 4-20 present almost a mirror image of the shape of the pH profiles in Figure 4-19. In all but one case (April 2006), EC is relatively constant down to about one or so metres below the surface, below which EC rises to levels similar to those observed in the anaerobic pond. The offsets between each of the profiles are related to accumulation and concentration of salts caused by effluent recycling and evaporation, respectively, and the counter effects of effluent irrigation and rainfall.

It is suggested that the gradients below 1 m are caused by the combined effects of solution chemistry and hydrodynamics. With pH levels above 8.0, high alkalinity and Ca concentrations, and supersaturation conditions (see Chapter 7), the upper 1 m of the water column is likely to be prone to spontaneous precipitation of Ca carbonate, particularly as growing algae remove carbon dioxide from solution (Stumm & Morgan 1981). Indeed algal-driven precipitation would explain the suppressed EC levels in the upper 15 cm of the pond in January 2007 when extreme conditions produced very high algal activity. Precipitation of mineral phosphates is also likely where conditions are alkaline and supersaturated (see section 4.4.4 below). At the bottom of the pond, the lower pH associated with fermentation of organic compounds and the lack of algal activity significantly reduces the potential for precipitation, keeping reactive ionic species in solution. Thus the EC gradient would appear to be directly linked to the pH gradient. This differentiation in solution chemistry of the upper and lower regions of the pond may also be both causative of and amplified by more saline and therefore denser influent from the anaerobic pond plunging through the upper layer to the bottom of the facultative pond.

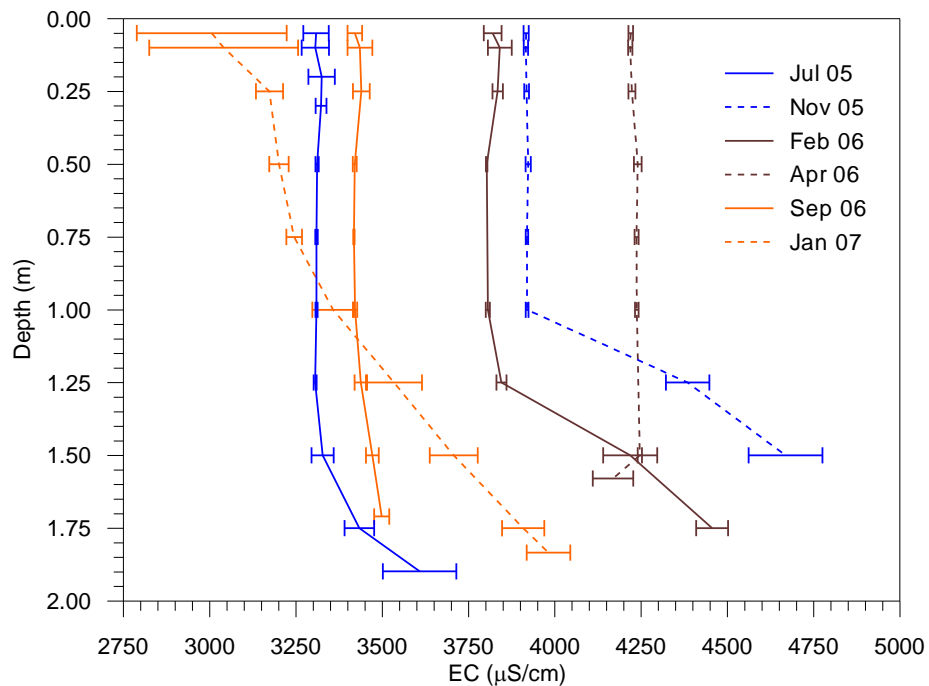


Figure 4-20 Facultative pond EC profiles.

DO profiles plotted in Figure 4-21 corroborate the seasonality of oxygenation seen in the real time monitoring data. The cumulative nature of algal growth alluded to earlier would appear to be behind the higher DO measured in January 2007 compared with February 2006. The turbidity and colour of the influent wastewater allow only a shallow euphotic zone (estimated to be ~5 cm in Chapter 7), which confines active algal biomass to the upper reaches of the supernatant column. As a result, DO concentrations were consistently negligible beyond a depth of 50 cm. Similar DO gradients were observed by Tadesse et al. (2004) in an advanced pond system treating tannery wastewater of comparable strength.

ORP profiles (Figure 4-22) also showed little to no vertical gradient in the cooler months but a steep gradient from the surface in the summer, again highlighting the influence of algal photosynthesis. Also of note are the strong and seemingly permanent reducing conditions (around -200 mV) present below the epilimnion. Surface ORP was negative on four of the profiling events, contradicting the continuous data collected by the MA that exhibited consistent diurnal swings from reducing conditions at night to oxidising conditions in the day. This, however, was most likely a limitation of the sampling approach. The sensor was very slow to respond to large changes in ORP (particularly from large negative values to positive ones). On account of the cold conditions making the exercise very uncomfortable, the ORP sensor was not allowed sufficient time to equilibrate when taking surface readings outside of summer. The

choice was made at the time of sampling to allow the other, more responsive sensors to equilibrate, but to accept compromised readings of surface ORP. Hence only the ORP measurements made below 25 cm depth can be considered true reflections of supernatant conditions.

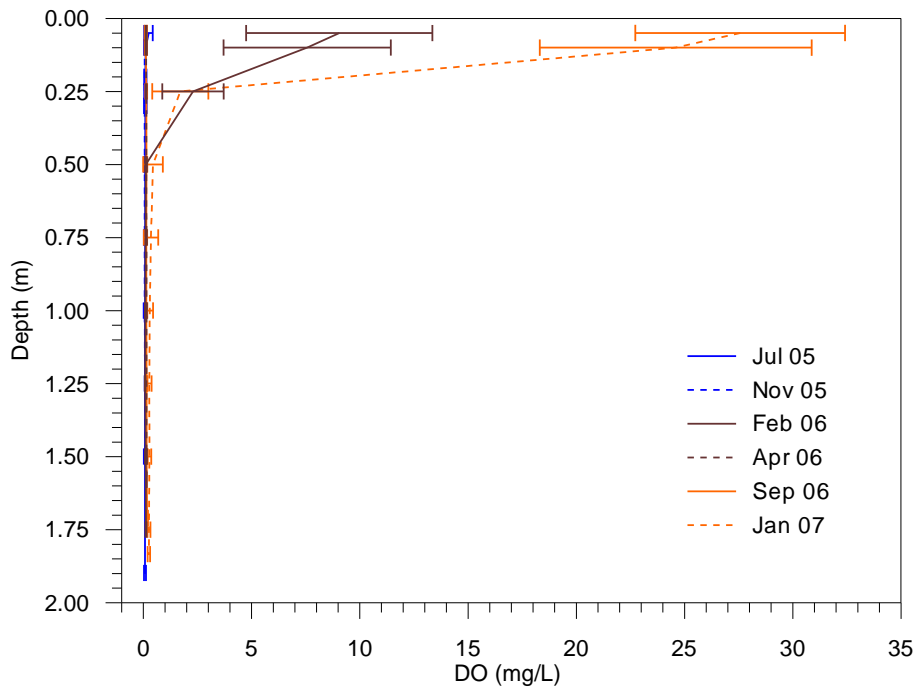


Figure 4-21 Facultative pond DO profiles.

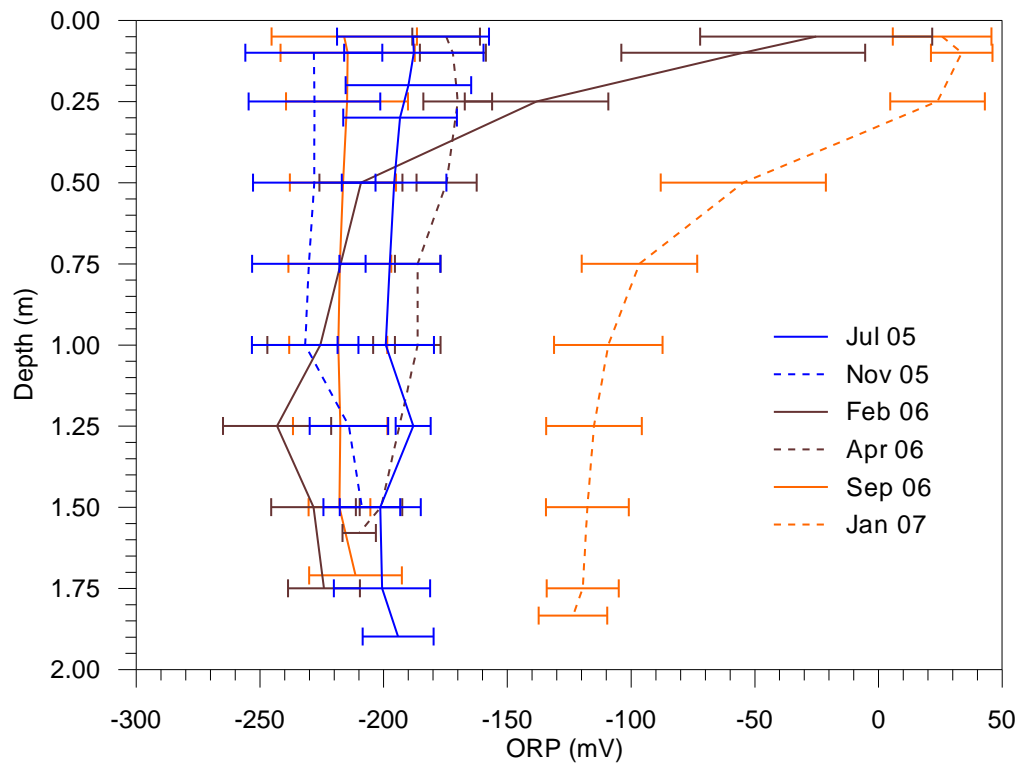


Figure 4-22 Facultative pond ORP profiles.

4.3.3 Dairy Water Supply

The descriptive statistics from the data recorded by the probes deployed in the dairy water supply tank are given in Table 4-16. The data show that the fresh water used at the dairy is generally pH neutral, low in salts and close to saturated with dissolved oxygen.

Table 4-16 Descriptive statistics from dairy water supply monitoring

	Temperature °C	pH	EC µS/cm	DO mg/L
Readings	40623	38416	31953	15743
Minimum	8.7	5.46	45	0.0
Median	19.3	6.96	86	8.6
Maximum	29.5	7.97	134	11.3
Mean	18.5	6.91	87	8.2
Standard deviation	4.3	0.36	14	1.9

4.4 DISCUSSION

4.4.1 Temperature Dynamics

Figure 4-23 shows average daily minimum and maximum supernatant temperatures in the two ponds. The difference between the ponds is clear. Firstly temperature is higher at depth in the anaerobic throughout the year, but daily swings are only slightly greater in amplitude. In the facultative pond, temperatures are higher at the surface than at depth between September and March. Over the cooler months, daily maximum temperatures are generally higher at the surface, but minimum temperatures drop as low or lower than minimum temperatures at depth. Diurnal swings at the surface are consistently larger than at depth and become exaggerated in summer.

Continuous temperature measurements were only made at 60 cm depth in the anaerobic pond. Profiling of the supernatant column showed that the pond can become mildly stratified, thus estimates were made of likely surface temperatures (represented by the red dashed lines in Figure 4-23) based on gradients determined from the temperature profiles and month-to-month relativities of temperature gradients in the facultative pond. The estimates indicate that even in summer differentiation between surface and depth temperatures is limited. Two factors would be behind this. Firstly the sludge may act as a heat bank, if not a heat generator, which would help maintain

slightly higher temperatures overnight and over winter. Second, mixing of the water column by rising biogas prevents the surface of the pond from becoming superheated as occurs in the facultative pond. As such, the solids load of the influent effectively acts as a regulating agent that constrains both the upper and lower temperature bounds of the supernatant. Conversely, on account of thermal stratification of the supernatant and the lack of sludge, the facultative pond is prone to large diurnal swings and day-to-day variation at the surface, and lower minimum temperatures generally.

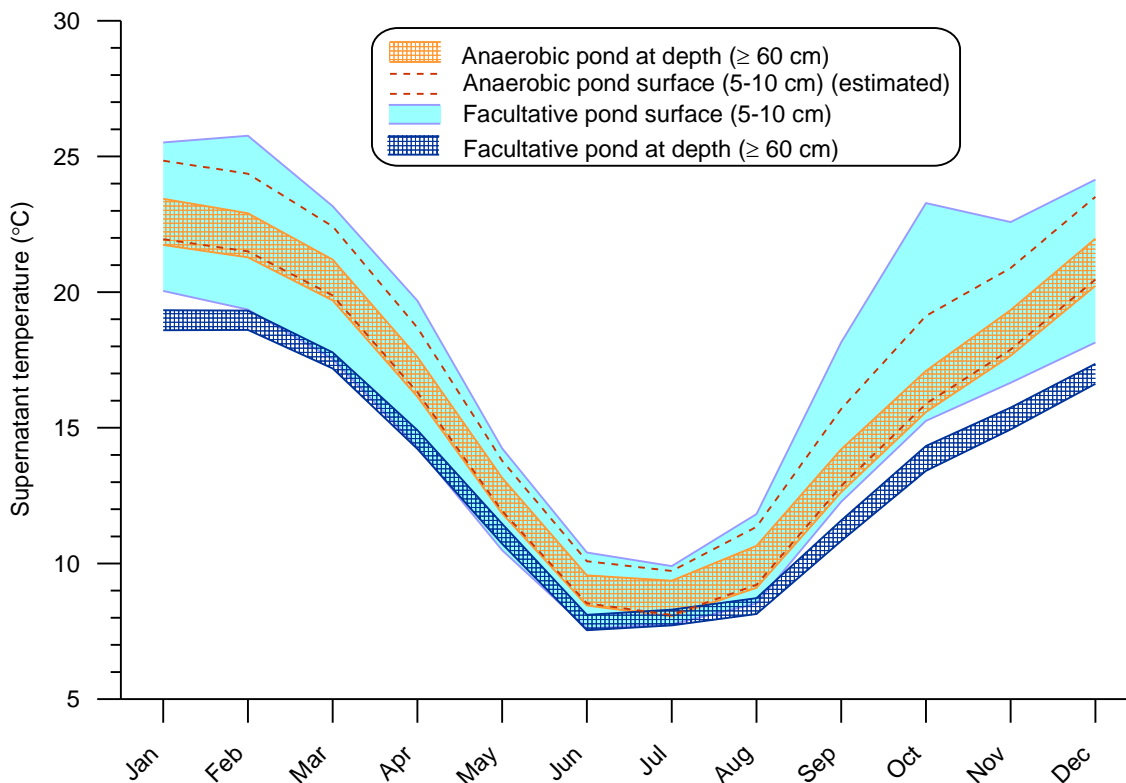


Figure 4-23 Monthly average daily minimum and maximum pond supernatant temperatures.

This behaviour has implications for modelling biological and chemical treatment processes, which all have some degree of temperature dependence. Thus it is important that not only is the seasonal component to temperature accommodated in a dynamic model of pond treatment, but that daily extremes in temperatures are considered. This is particularly the case for the facultative pond that undergoes large swings which could cause shifts between algal and bacterial activity and associated fluctuations in pH, DO and ORP, all of which influence supernatant chemistry and also feedback to the dominant microbial-mediated processes.

4.4.2 Thermal Stratification

Another temperature-related characteristic that will be important to the formulation of the wastewater treatment model is thermal stratification of the facultative pond, which was evident on all but one profiling events. The sole unstratified profile was recorded in autumn, coinciding with pond turnover. The continuous temperature data also reflected stratified conditions in the daytime over much of the year, and in the warmer months, sustained stratification overnight. Unlike natural water bodies and WSPs treating less concentrated wastewaters, the high turbidity of DSE ponds limits penetration of solar radiation to a very thin upper layer. The 'well-mixed epilimnion' is accordingly very shallow, with the thermocline starting from the first profiling measurement at 5 cm depth. This has significant implications for modelling, requiring either thermodynamically controlled fluid dynamics or at least a division of reactor space. However, gradients in the pH and EC profiles indicated a degree of vertical diffusion of dissolved species which must be allowed for through diffusion coefficients or inter-reactor exchanges.

The anaerobic pond on the other hand, exhibited only mild thermal stratification even on very warm days. And despite the formation of temperature gradients, other water quality parameters did not exhibit variability with depth in the supernatant, suggesting that there is no need to consider vertical variation in modelling wastewater treatment. Similar observations were reported by Dawson (2003) who undertook profiling of two DSE anaerobic ponds. There was, however, a clear, albeit slight, water quality distinction between the supernatant and the sludge. The lower pH of the sludge is indicative of greater acidogenesis and CO₂ production arising from the concentration of particulate organic material, while the lower EC would be due to the higher solids concentration impairing conductance. The lack of a gradient in water quality parameters rising from the liquid-sludge interface would further indicate effective vertical mixing in the supernatant. The incidence and effects of stratification are explored further in Chapter 6.

4.4.3 pH as an Indicator of Biological Activity

Raw DSE is characterised by a mildly basic pH, high alkalinity and strong buffer capacity (refer to Chapter 4). These characteristics establish the underlying supernatant chemistry, but it is clear from the data that supernatant pH is a function of the dominant biological processes occurring in each pond. Despite, or more likely because of the buffer capacity, the pH of the anaerobic pond consistently hovered around 7. Acidogenesis and the formation of CO₂ by anaerobic digestion put downward

pressure on pH. In the warmer months when anaerobic digestion is most active, pH remains steady over the course of the day while in winter there was evidence of diurnal peaks correlated with temperature. This suggests that the alkalinity of the influent establishes a floor below which pH generally does not descend. That the supernatant pH was consistently lower than the influent pH even in winter demonstrates that anaerobic digestion continues throughout the year despite the supernatant temperature dropping well below 10 °C in the winter. Again the sludge blanket appears to be acting as a regulating agent, in this case maintaining an upper bound to pH in the pond. Indeed the presence of sludge could be identified by the drop in pH, demonstrating that it is a source of acidity that counteracts the influent alkalinity.

The facultative pond was characterised by two extremes – pH similar to influent levels at 8 or above from the surface to about 1 m depth and levels closer to those seen in the anaerobic pond at the bottom of the pond. pH in the upper layer was subject to diurnal fluctuations superimposed on top of the underlying alkaline pH. During the summer, pH peaks in the day in concert with consumption of carbon dioxide by algae, but in winter pH swings were reversed with troughs coinciding with peak temperature as bacterial respiration (CO₂ production) became dominant. Anaerobic conditions at depth are conducive to fermentation, causing pH to drop below 8, even approaching 7 when microbial activity peaks with high summer temperatures.

These dynamic characteristics are central to the functionality of the ponds and must be accommodated in the modelling, particularly given the influence pH appears to have on precipitation and dissolved salt concentrations (see below). pH must therefore either be set to the correct level within the different regions of the ponds, or if it is to be a dependent variable itself, pH should be used as a key indicator of the appropriateness of the model both in terms of supernatant chemistry and the effects of dominant biological processes.

4.4.4 Salt Accumulation and Struvite Precipitation

Conductivity monitoring in both ponds revealed a persistent upward trend in supernatant salinity as would be expected in a system in which salts are concentrated by the combined effects of recirculation of effluent, continuous addition of salts from manure and cleaning chemicals and evaporation. As detailed in Chapter 2, a handful of monitoring and modelling studies related to salt accumulation in partially closed DSE systems have been undertaken elsewhere. However the real-time monitoring of salt accumulation presented in this chapter is the first of its kind in Australia, as is the analysis that relates salt levels to hydrology and other factors.

An operational concern related to salt accumulation is the formation of crystalline deposits in pumps, pipes and fittings that lead to blockages and system down time, which could potentially result in pond failure should a blockage arise when the storage pond is close to or at capacity. Indeed, this scenario almost did eventuate on two occasions over the course of this study. On 14 March and 20 May 2006, blockages in the gland of the effluent recycling pump caused by crystalline deposits rendered the pump unusable and had to be removed by disassembling the pump and dissolving the crystals in diesel fuel. As mentioned in section 4.3.2.1, crystalline deposits were also found to be forming on monitoring equipment deployed in the facultative pond over autumn and winter in both monitoring years, causing interference with sensors and blocking sampling pumps and lines. On 8 November 2006 a layer several centimetres deep (about 0.3-0.4 m³) of loose crystals was uncovered on the bottom of the flood wash tank. As detailed in Chapter 2, the form of scale typically seen in manure flush water systems is magnesium ammonium phosphate (NH₄MgPO₄·6H₂O), or struvite. The form of the crystalline deposits encountered in the present study was confirmed as being struvite as outlined in section 4.4.4.1 below.

It is also suspected that precipitation of struvite and potentially other mineral salts may actually have dampened the rate of accumulation of dissolved salts in the pond system. The average ratio of fresh water to recycled effluent used at the dairy was 0.36 (Chapter 4). According to modelling performed by Mason & Flowerday (2005), salt levels in a 1500-m³ variable volume pond system loaded with waste from milking herd of 300 cows would reach 3500 mg L⁻¹ (starting from 1600 mg L⁻¹) within 100 days (dairy shed wash downs using 15 m³ d⁻¹ blended water and effluent) at this ratio. While the anaerobic pond would add substantial buffer to the present system, this simulated rate is considerably faster than was observed in this case, which would suggest that other processes such as precipitation may be at play. The role of struvite precipitation in the pond system is explored further in section 4.6 of Chapter 7.

4.4.4.1 Analysis of crystalline deposits

Samples of crystalline deposits attached to the MA sampling pump were taken on 25 August 2005 and again the following year on 5 April 2006 for identification by scanning electron microscopy (SEM), energy-dispersive X-Ray Spectroscopy (EDS) and X-ray diffraction (XRD). A sample of the crystals found in the flood wash tank was also retained for the same analyses and are pictured in Plate 4-2.



Plate 4-2 Left: crystals collected from the flood wash tank photographed in a petri dish. Right: magnified 20 times under a microscope (right).

Crystal samples were rinsed with distilled water to remove organic and other residues and dried at room temperature in a desiccator. Sub-samples were crushed using a mortar and pestle, although SEM analyses were also performed on whole crystals. Plate 4-3 presents an SEM image showing the dominant struvite crystals with traces of an amorphous substance that had formed on the surface of the crystals.

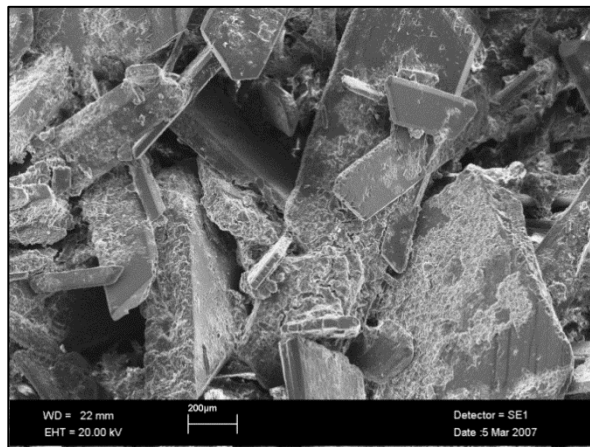


Plate 4-3 SEM image of a sample of crystalline deposit.

Figure 4-24 presents an output from EDS analysis which confirms the crystalline material contains mostly Mg and P. The amorphous material on the surface of the crystals was found to contain high levels of Ca and P (EDS output not presented), suggesting a Ca phosphate precipitate. Traces of K and chloride detected in many analyses would likely to have been residue from the supernatant.

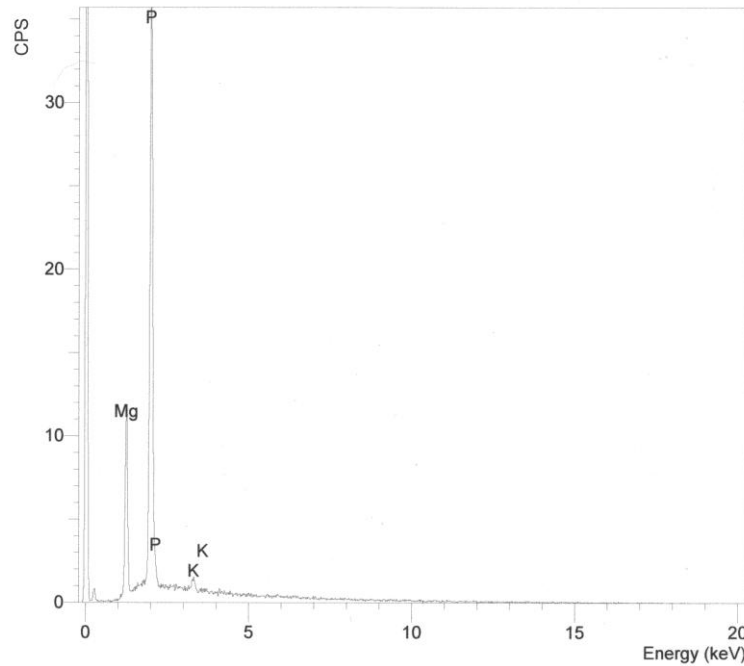


Figure 4-24 EDS analysis of a sample of crystalline deposit.

XRD was performed using a GBC diffractometer with a graphite monochromator and CuK α radiation (wavelength 1.54 angstroms). Data were collected using Traces™ software with search matches performed using the 2003 PC-PDF (powder diffraction file). Figure 4-25 presents an XRD trace of one of the crystal samples that shows good agreement with a standard struvite pattern.

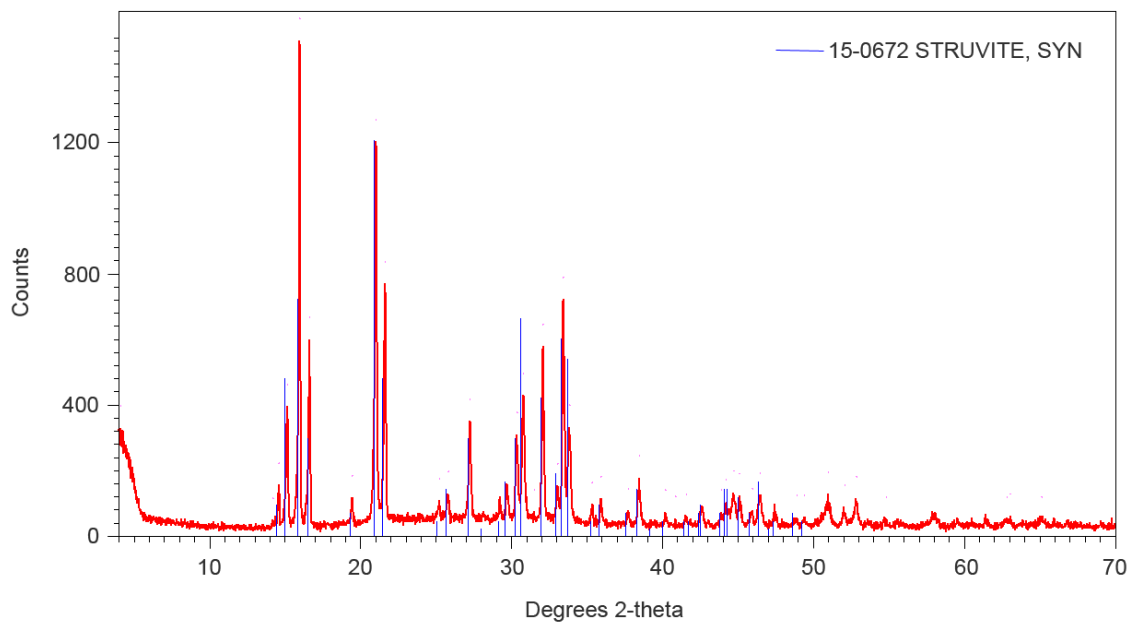


Figure 4-25 X-ray diffractogram of crystalline deposits sampled from facultative pond (red line) plotted with a standard pattern for struvite.

4.4.5 Dissolved Oxygen and Aerobic Treatment in the Facultative Pond

It is clear from the data that DO is present in the epilimnion of the facultative pond at high, or even saturation concentrations during summer, and to a lesser extent in spring and autumn. Aerobic conditions, together with associated elevated pH and ORP levels are likely to result in very different biological and chemical treatment to that which would prevail below the depth to which diffusing DO penetrates (about 50 cm). Indeed the contrasting forms of biological and chemical treatment that occur at depth and at the surface result in the formation of pH and EC gradients that under very warm conditions can span the entire depth of the pond. Under most conditions, however, these gradients tended to span the region between the bottom of the pond and a depth of 1.0 to 1.25 m, with the supernatant above exhibiting relatively constant pH and EC. The gradients in pH and EC therefore appear to be stemming from fermentative activity concentrated at the bottom of the pond and carbon dioxide and VFAs diffusing upwards. Only when highly stimulated algal activity rapidly consumes CO_2 and generates DO at a rate that exceeds the OUR of the supernatant do gradients begin to extend downward from the surface as per the January 2007 profiling event. The slope of the pH gradient is determined by the differential between algal consumption and upward diffusion of dissolved CO_2 . The DO gradient is a function of downward diffusion of DO and the OUR, producing the non-linear (summer) curves in Figure 4-21. EC increases with depth as the decline in pH reduces precipitation of mineral salts.

This behaviour of the facultative pond presents a complex modelling challenge. At the very least, the pond will need to be divided into two separate reactors; one incorporating an algal growth model that produces DO to represent the upper region of the pond and the second reflecting the anaerobic processes that dominate the lower region. A third reactor may be required to represent the 'middle ground' between the two extreme. The complexity arises in sizing the reactors appropriately and simulating diffusion exchanges between the layers that produce the gradients in water quality parameters. A superior option would be to discretise the entire pond as in a mass transport model capable of simulating diffusion similar to that constructed by (Beran & Kargi 2005). However, the intermittent nature of pumping out of the pond and the associated variation in liquid volume would add considerable complexity to what is already a complicated numerical model. Similarly, integrating biological and chemical process models into a CFD model of the pond as per (Sah et al. 2011) could present a powerful but very complex solution.

4.5 SUMMARY

High-resolution real-time monitoring and periodic spatially-defined sampling of the supernatant of the pond system was undertaken to characterise the water quality dynamics in each pond. The study revealed a number of important characteristics of the system.

Firstly temperature variation is distinctly different between the two ponds. Regulated by limited penetration of solar radiation due to the high turbidity and the biological activity of the sludge blanket, the anaerobic pond largely exhibited uniform, relatively constrained diurnal swings across its breadth and depth. The facultative pond on the other hand was thermally stratified for much of the year, with a thermocline extending from very close to the surface and temperatures at the surface displaying exaggerated diurnal swings. Below 60 cm depth temperature variation in the facultative pond was more constrained, exhibiting diurnal swings of similar magnitude to those observed in the anaerobic pond.

The sludge in the anaerobic pond also influenced the pH of the supernatant, helping to bring it down from influent levels of around 8 to near neutral. The alkalinity of the influent is likely to have prevented the pond becoming acidic when anaerobic digestion activity peaked in summer. In the facultative pond the alkalinity of the wastewater is evident, with pH oscillating around 8. A gradient in the pH from the bottom up to about 1 m depth arising from fermentative activity at the bottom was evident across all seasons while at the surface pH exhibited daytime peaks due to algal consumption of CO₂ in warmer months and night time peaks in the winter due to heterotrophic respiration. pH profiles are mirrored by EC profiles. Precipitation stimulated by the higher pH, alkalinity and Ca levels as well as uptake of CO₂ by algae suppresses EC levels in the upper 1 m of the water column, while below 1 m the increasing influence of fermentation with depth and sinking influent keeps supernatant EC closer to influent levels.

Salt accumulation was an ever-present dynamic in both ponds due to effluent recirculation, as evidenced by rising EC levels in the real time data and large offsets in the supernatant profiles from both ponds. Accumulating salts produced supersaturation conditions, which combined with pH levels of 8 and above in the facultative pond, look to have resulted in precipitation of struvite and potentially trace amounts of other mineral salts such as Ca phosphates. The ever-changing concentration of dissolved inorganic species would suggest that the pond system cannot be adequately modelled assuming steady state conditions.

The organic loading to the anaerobic pond eliminated any trace of DO that may have been in the influent or introduced by surface re-aeration. ORP in the pond was consequently heavily reducing (well below -100 mV) throughout the liquid profile and in the sludge. The facultative pond exhibited strong seasonal and diurnal patterns in DO, which appeared to be exclusively related to algal photosynthesis. Over the winter algal activity was too low to produce DO at a rate exceeding the heterotrophic OUR of the supernatant. From late spring to early autumn algal growth on warm sunny days was substantial, creating supersaturated peak DO concentrations close to the pond surface and corresponding peaks in turbidity (biomass) and ORP. Algal growth was correlated with both pond temperature and incoming solar radiation, with lulls occurring during periods of consecutive days of low minimum temperatures and low peak solar radiation. Due to a very shallow euphotic zone, DO production was confined to the upper 5-10 cm of the liquid. Downward penetration of DO by diffusion was limited to approximately 50 cm by the high OUR of the supernatant.

The elevated daytime DO and ORP levels in the upper reaches of the facultative pond supernatant could potentially promote nitrification; however anoxic or anaerobic conditions arising from rapid overnight consumption of DO and the complete absence of DO in winter together with a lack of aerated surfaces to facilitate attached growth present substantial barriers to sustaining a viable nitrifier population. Despite the lack of algal growth to produce DO in the winter months, ORP still peaked around 50 mV. The timing of the peak, however, was notably different to algae-induced peaks, occurring very early in the morning when temperature and biological activity were at a minimum. It is suggested that the peaks may have been related to surface re-aeration that did not overcome the supernatant OUR but was enough to register the presence of electron acceptors.

All the above characteristics must be considered when undertaking modelling of wastewater treatment processes occurring in the ponds. Simulations using models of both ponds should be dynamic so as to capture diurnal and seasonal variation and longer-term trends. In the case of the anaerobic pond, the lack of diurnal and spatial variation allows for a relatively simple modelling framework, requiring differentiated but interconnected the supernatant and sludge phases and allowance for seasonal variation driven by temperature. The facultative pond requires a more complex approach that accommodates:

- diurnal swings in temperature, DO, ORP and pH that vary in magnitude with season;

- vertical stratification of the supernatant into zones characterised by
 - algal photosynthesis in the daytime over the warmer months and bacterial respiration at night and during the day in winter (which both drive the diurnal fluctuations near the surface),
 - anaerobic, fermentative conditions at the bottom of the pond, and
 - a transition zone between the surface and bottom layers;
- changing volumes of and mass exchanges between the different zones;
- precipitation of struvite and other mineral salts.

The results from this component of the research also show that water quality parameters can be effectively used to characterise and diagnose the dynamic performance of a stabilisation pond system. Turbidity, DO, ORP and pH all provide helpful (positively correlated) indicators of algal activity in the facultative pond. pH can also provide insight into the state of the anaerobic pond, with lower levels relative to the pH of the alkaline influent indicating greater fermentative activity. EC, meanwhile, provides a good measure of the impact effluent recycling is having on the system. EC and pH can both also be used to gauge the depth of the sludge blanket in the anaerobic pond.

Chapter 5

SYSTEM WATER BALANCE

Integral to understanding and modelling a wastewater management system is an appreciation of the liquid loading/additions and extractions/losses to and from the system. Primarily, these influence the hydraulics and hydrodynamics of the system, which determine the hydraulic residence time (HRT) of the system. The HRT informs the system's treatment efficiency and its storage capacity. Quantification of liquid inputs and outputs is also critical to developing a mass balance of wastewater constituents entering and leaving the system. This chapter details the development of a water balance across the stabilisation pond system. This involved processing, verifying and correcting wastewater inflows and outflows, accounting for rainfall and runoff contributions, and developing and validating a method for estimating system evaporation and seepage losses using the residual of the water balance. The process also enabled analysis of wastewater flow patterns, deduction of water usage patterns at the dairy and quantification of the hydrology of the pond system.

5.1 INTRODUCTION

The key inputs and outputs to be considered in a water balance of a DSE pond system include fresh water used at the dairy for cleaning and hosing, effluent recycled for hydraulic flushing of the holding yard, effluent irrigated to land, the waste material collected at the dairy, rainfall and runoff, evaporation and seepage. The amount of fresh water used at the dairy determines the concentration of the influent wastewater while the volume of recycled effluent used at the dairy relative to freshwater usage influences the rate at which conservative inert waste constituents (salts) accumulate within the system. Rainfall and runoff additions dilute the supernatant in both ponds as well as inflows to the anaerobic pond, and reduce the storage capacity of the facultative pond. Evaporation losses concentrate supernatant in both ponds but effectively add storage capacity to the facultative pond. Seepage losses reduce the amount of effluent available for irrigation and reclamation and remove soluble species from the system, potentially polluting underlying groundwater.

The approach taken to developing a water balance of the system was similar to those described by Cumba & Hamilton (2002) and Cothren et al. (2001). As depicted in Figure 5-1, the system comprises two ponds, hence a separate balance was developed for each.

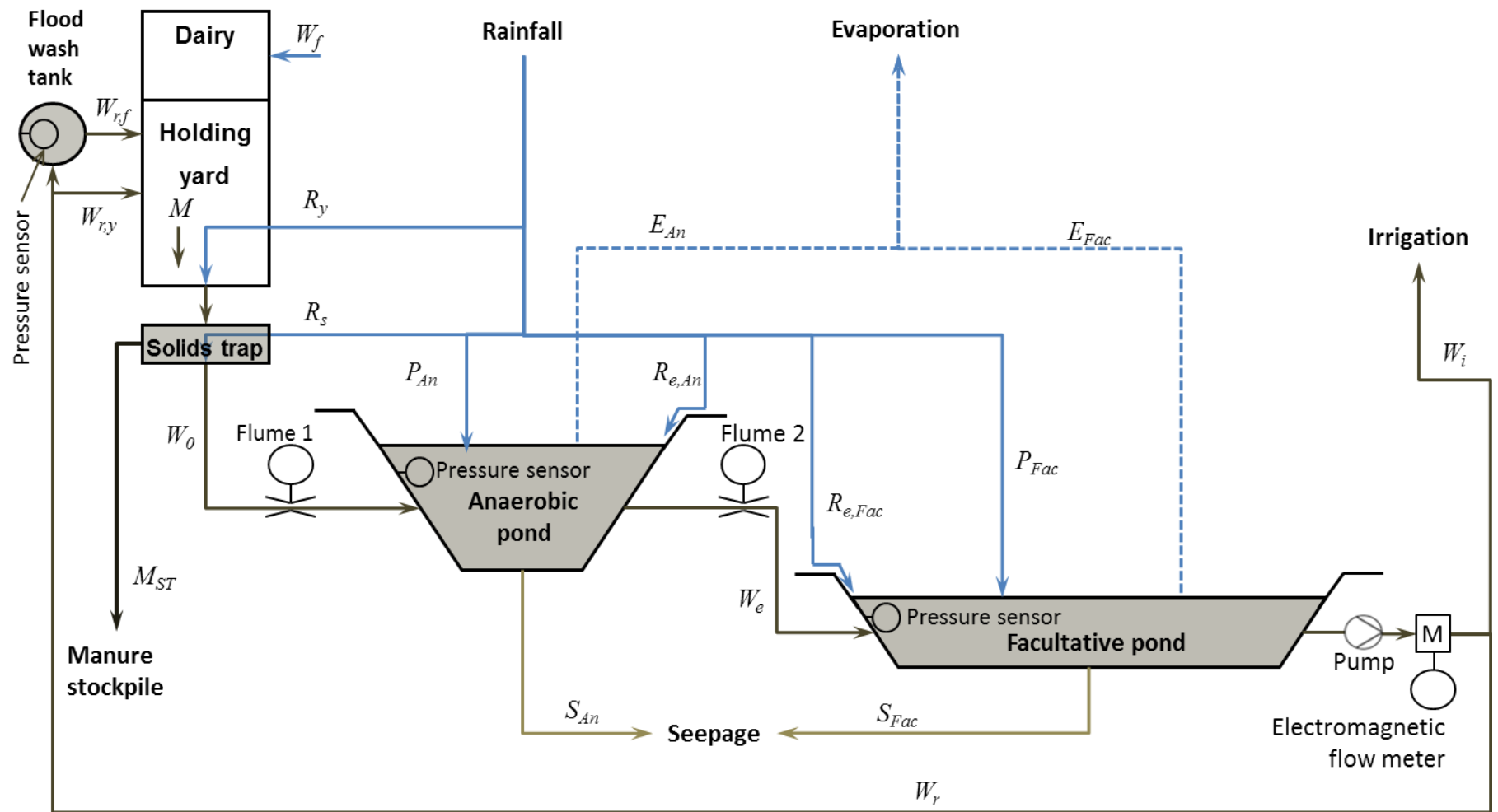


Figure 5-1 Schematic diagram of water balance components and flow and depth measurement locations.

The water balance for the anaerobic pond is expressed

$$W_f + W_r + M - M_s + P_{An} + R_y + R_s + R_{e,An} - W_e - E_{An} - S_{An} = \Delta V_{An} \quad (5-1)$$

where

W_f = fresh water used for hosing and cleaning;

W_r = recycled effluent (from the facultative pond);

M = raw manure deposited in the dairy and on the holding yard;

M_s = manure captured in the solids trap;

P_{An} = rainfall entering the anaerobic pond;

R_y = stormwater runoff from the holding yard;

R_s = stormwater runoff from the solids trap;

$R_{e,An}$ = stormwater runoff from the anaerobic pond embankments;

W_e = effluent leaving the anaerobic pond;

E_{An} = evaporation from the anaerobic pond;

S_{An} = seepage from the anaerobic pond; and

ΔV_{An} = change in the anaerobic pond combined liquid and sludge volume.

It is assumed that the volume of the suspended solids that pass through the solids trap and become part of the influent to the anaerobic pond (W_0) is negligible. While sediments come to occupy a significant volume of the pond over time (refer to Chapter 6), they remain relatively dilute (<10% dry matter – see Chapter 7), which means that the actual solid material contributes very little volume. Thus in this water balance analysis sludge is not differentiated from liquid.

While the solids trap is not 100% efficient at removing particulate material, it is assumed that the difference in volume between raw manure solids and manure solids captured in the solids trap would be negligible compared with the total inflow volume. It is also assumed that the difference between the water content of raw manure and manure solids captured and removed from the solids trap is negligible such that the volume of water held in the two forms of solids may be considered equal. This means that M and M_s may be considered equal, allowing the two terms to be cancelled out in equation 5-1. The four other components of the inflow to the anaerobic pond, W_f , W_r , R_y and R_s , are combined into one waste stream as they pass through the solids trap to

the inlet of the pond. Hence in the analysis of the anaerobic pond, the terms are collapsed into a single wastewater inflow figure W_0 . Equation 5-1 then becomes

$$W_0 + P_{An} + R_{e,An} - W_e - E_{An} - S_{An} = \Delta V_{An} \quad (5-2)$$

Recycled effluent pumped from the facultative pond comprises two streams such that

$$W_r = W_{r,f} + W_{r,y} \quad (5-3)$$

where

$W_{r,f}$ = recycled effluent used for the flood wash;

$W_{r,y}$ = recycled effluent pumped directly onto the holding yard

Since the anaerobic pond has a gravity outfall, changes in liquid/sludge volume tend to be very small and should average to zero over time.

The facultative pond water balance is expressed

$$W_e + P_{Fac} - W_r - W_i - E_{Fac} - S_{Fac} = \Delta V_{Fac} \quad (5-4)$$

where

W_i = irrigated effluent;

P_{Fac} = rainfall entering the facultative pond;

E_{Fac} = evaporation from the facultative pond;

S_{Fac} = seepage from the facultative pond; and

ΔV_{Fac} = change in the facultative pond liquid volume.

All terms in the above equations are expressed in units of $\text{m}^3 \text{d}^{-1}$, but may also be expressed in terms of pond water surface elevation as metres above the Australian Height Datum (mAHD). Where possible the individual or combined components of the water balance equations were measured; however a number of components could not be measured directly and had to be inferred from other data or estimated through a modelling approach. Table 5-1 identifies which components were measured and those that were estimated together with the measurement or estimation method used. Details of the measurement techniques are given in section 5.2 while modelling approaches are detailed in section 5.3.

Table 5-1 Measured and estimated water balance components.

<i>Component</i>	<i>Name/Description</i>	<i>Measurement or estimation method</i>	<i>Chapter section</i>
<i>Measured components</i>			
W_0	Raw wastewater flow and runoff from the yard and solids trap	Flume	5.2.1
W_e	Anaerobic pond effluent	Flume	5.2.1
$W_i + W_{r,f} + W_{r,y}$	Combined irrigated effluent and recycled effluent for flood wash and direct pumping	Electromagnetic flow meter	5.2.2
$W_{r,f}$	Flood wash (recycled effluent)	Flood wash tank shape and liquid depth	5.2.2
P_{An}, P_{Fac}	Rainfall	Tipping bucket rain gauge	5.2.4
$\Delta V_{An}, \Delta V_{Fac}$	Anaerobic and facultative pond volumes	Pond bathymetry and liquid depth	5.2.3
<i>Estimated components</i>			
W_i	Irrigated effluent	Inspection of measured data	5.3.1
$W_{r,y}$	Recycled effluent pumped directly onto the holding yard	Inspection and comparison of measured data	5.3.1
$W_{r,f}$	Recycled effluent for flood wash	Calculation	5.3.1
W_f	Fresh water used for hosing and cleaning	Calculation	5.3.1
R_y, R_s	Stormwater runoff from the holding yard and solids trap	Calculated from rainfall and surface area	5.3.2
$R_{e,An}, R_{e,Fac}$	Stormwater runoff from the pond embankments	Soil moisture balance model	5.3.2
E_{An}, E_{Fac}	Evaporation from the anaerobic and facultative ponds	Modified Penman combination equation with parameters fitted by closure of the water balance	5.3.3
S_{An}, S_{Fac}	Seepage from the anaerobic and facultative ponds	Filter cake and Darcy's law infiltration models, respectively, with parameters fitted by closure of the water balance	5.3.4

5.2 MATERIALS AND METHODS FOR MEASURED COMPONENTS

5.2.1 Anaerobic Pond Inflows and Outflows

Flows into and out of the primary anaerobic pond (W_0 and W_e) were gauged using long-throated V-shaped flumes fitted to the openings of the inlet (Flume 1) and outlet (Flume 2) pipes, respectively (refer to Figure 5-1). Milltronics 'Probe' ultrasonic level monitors (Siemens Milltronics Process Instruments Inc., Canada) were mounted directly above the throat of the flume (see Plate 5-1) and connected to a central CR10X data logger

(Campbell Scientific Inc., US) to measure and record stage. Stage measurements were taken every 10 seconds and converted into flow rates using a polynomial rating curve. Flow rate readings were totalised to calculate and record cumulative volumetric flow through the flume every 5 minutes. Instantaneous stage and flow rate readings were also recorded by the logger every 5 minutes. The data logger program containing the code for the flow measurement algorithm is presented in Appendix E. Stage, flow rate and volume data collected from each flume (anaerobic pond inflow and outflow) is presented in Appendix I.



Plate 5-1 Moulded PVC flumes used to monitor effluent flow. Left: Flume 1 attached to the anaerobic pond inlet. Right: Flume 2 attached to the anaerobic pond outlet (facultative pond inlet).

The stage-discharge relationship used to quantify flow through the flumes was initially derived theoretically using the principles outlined in Bos (1989). This flume rating was then tested and refined using both manual flow readings (time taken to fill a 20-L bucket) and readings taken from a dedicated HVFlo flow meter incorporating ultrasonic doppler velocity measurement and ceramic pressure transducer stage measurement (Measuring & Control Equipment Co. Pty. Ltd., Australia). The HVFlo meter was deployed immediately upstream of the flume attached to the anaerobic pond inlet for a period of two months. A polynomial function was fitted to the validation flow data to derive a 'real-world' rating curve that was very similar to the original theoretical rating. The measured data plotted in Figure 5-2 exhibits a degree of noise but the fitted

polynomial is very similar to the original theoretical rating. The initial theoretical curve, the measured flow rates and the final fitted rating curve are presented in Figure 5-2.

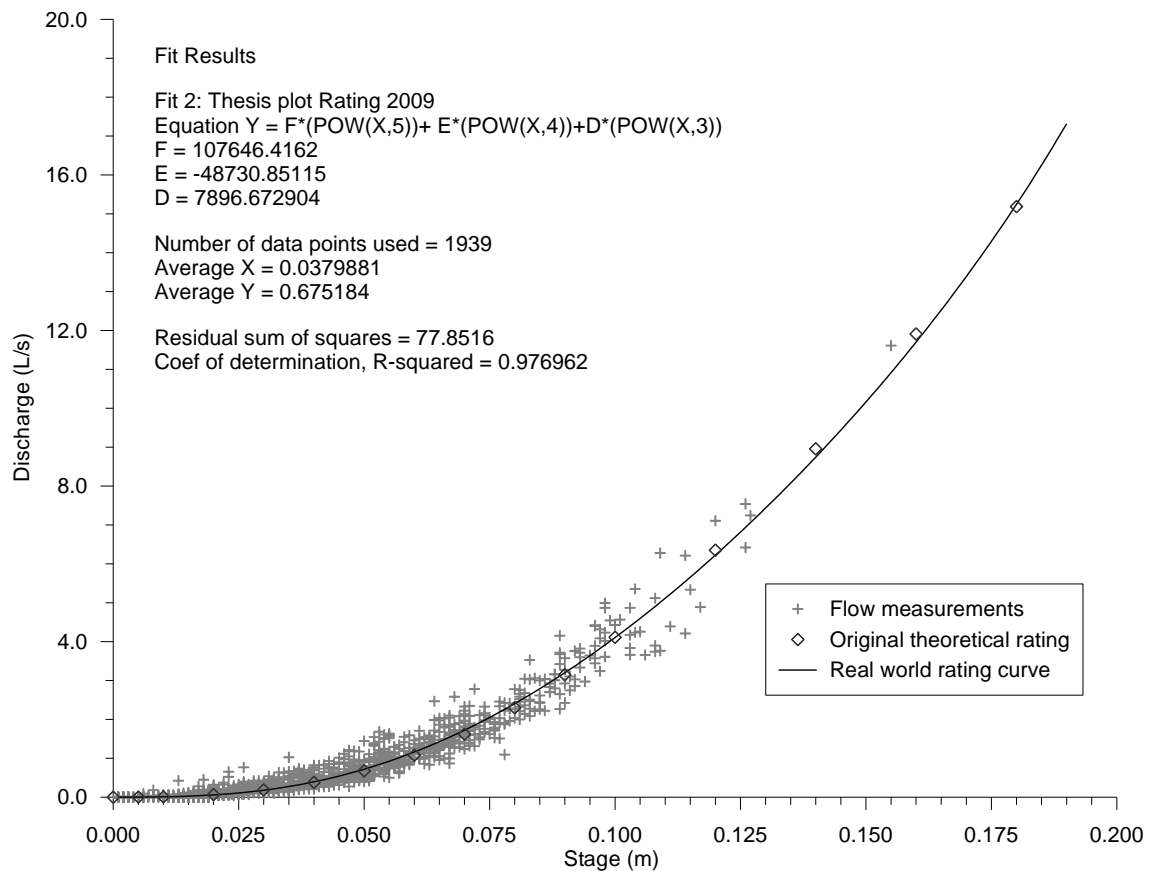


Figure 5-2 Rating curve for the flumes used to measure flow into and out of the anaerobic pond.

5.2.1.1 Missing data

Due to a technical problem with the power supply causing the signal from the ultrasonic level meters to drop out intermittently, the flow data collected between October 2005 and 5 June 2006 contained numerous blocks of false zero readings. Around 37% of flume 1 data and 19% of flume 2 data collected during the period were affected. However most signal drop outs occurred at night during flow lulls, thus a method was developed to ‘infill’ the missing data using other data in the time series. The infilling method is described in detail in Appendix B and is shown to have produced sensible synthetic data. Nevertheless it must be emphasised here that synthesised data have not been used in either the calibration or the validation of the water balance, which were all performed on data not affected by signal drop outs. Note though that the flume flow data presented in Appendix I does contain synthesised data, which is denoted by ‘T’ in the ‘Synthesised?’ column.

5.2.2 Facultative Pond Outflows

Effluent pumped from the facultative pond to the flood wash tank, directly onto the holding yard, and to irrigation ($W_{r,f} + W_{r,y} + W_i$) was measured using a single 100-mm Emflux 2020 electromagnetic flow detector (Combined Instrument Systems Pty. Ltd., Australia) connected between the pump and a ball valve switch that directs effluent to either the dairy recycle line or to the irrigator. The electromagnetic meter maintained its own log of cumulative flow, but was also linked to the central datalogger to record instantaneous flow rates and cumulative volumes at 5-minute intervals as per the flume data collection algorithm. The electromagnetic meter installation after the piping rearrangement is pictured in Plate 5-2.

Effluent used for flood washing ($W_{r,f}$) was measured on its own using the pressure sensor of a Greenspan CTDP300 multi-parameter probe (FWT probe described in Chapter 4) deployed to detect and log changes in the depth of liquid held in the flood wash tank. The probe was secured at the bottom of the tank and set to scan every 30 seconds for sudden changes in depth greater than 0.1 m that would indicate the release of a flood wash. The volume of effluent used in a flood wash was calculated from the total change in liquid depth recorded for the event multiplied by the cross-sectional area of the cylindrical tank.

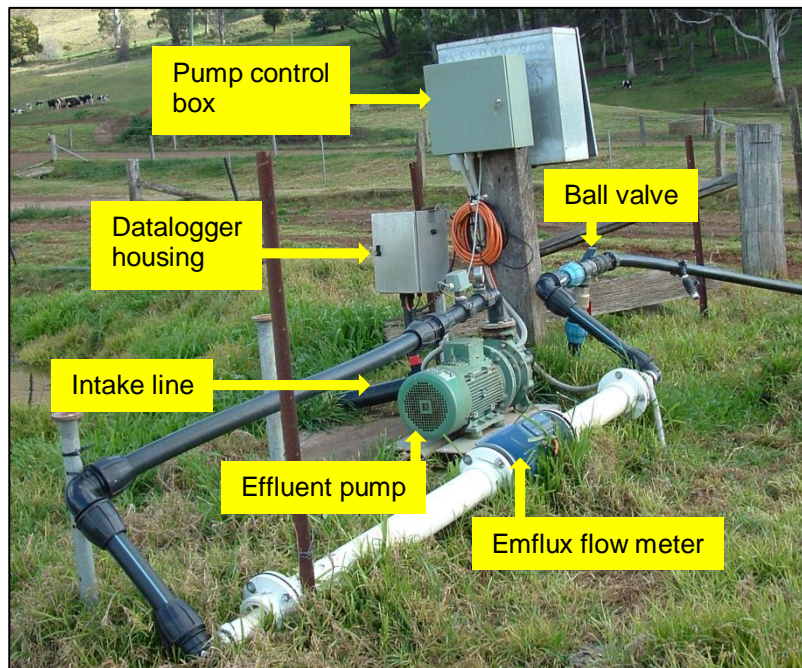


Plate 5-2 Effluent pumping line fitted with the electromagnetic flow detector. Note the circuit arrangement of the pipework to ensure full flow and sufficient straight lengths upstream and downstream of the meter.

5.2.3 Pond Liquid Volumes

The depth of supernatant held in both ponds was also monitored in real time using CTD300 pressure sensors. The West probes in each pond (see Chapter 4) were fixed to poles driven into the floor of each pond and set to take recordings of depth every 30 minutes. Pond liquid volumes, surface areas and wetted areas were calculated by inserting liquid surface elevation data into the polynomial functions for volume given in Chapter 3 (section 4.3.1). Having a gravity outfall, the anaerobic pond exhibited only very small changes in volume whereas the facultative pond volume fluctuated significantly with the timing and length of effluent irrigation events. The liquid surface elevation data are provided in Appendix I.

5.2.4 Rainfall

Rainfall (P) was measured using a 0.2-mm tipping bucket rain gauge attached to the site automatic weather station (AWS) which recorded every bucket tip and summed the data by hour and by day. The hourly data are presented in Appendix H. Volumetric contributions to the ponds (P_{An} , P_{Fac}) were determined by multiplying recorded rainfall by the pond surface area. Surface area in the anaerobic pond (A_{An}) was assumed to be constant, but the surface area of the facultative pond (A_{Fac}) was a function of depth as described by the corresponding polynomial equation given in Chapter 3.

5.3 ESTIMATION METHODS FOR UNMEASURED COMPONENTS

Comprehensive measurement of all flows entering and leaving the system was not feasible, hence a number of water balance components had to be calculated or inferred from other data, or modelled using established methodologies. Calibration of unknown model parameters was achieved through closure of the water balance as described in the following section (5.4). As pointed out by Parker, Auvermann & Williams (1999), inaccuracies in evaporation estimates can have a considerable effect on seepage estimates (and vice versa) based on a water balance approach. Accordingly, considerable effort was applied to adapting modelling methods to reflect the specific conditions of the site.

5.3.1 Effluent Irrigation, Effluent Recycling and Fresh Water Use

Effluent irrigation events were characterised by extended periods of pumping (usually overnight) at a slightly higher flow rate than observed during recycle pumping due to the fall to the land application paddock; hence irrigation volumes (W_i) could be discerned from close inspection of the flow data from the electromagnetic flow meter on the facultative effluent pumping line. Volumes of recycled effluent used for flood

washing were monitored as described in the previous section, allowing effluent pumped directly onto the yard ($W_{r,y}$) to be calculated as the difference between the total effluent pumped from the pond over the course of each post-milking wash down event and the volume of effluent used in the flood wash (as per equation 5-2). Where it was clear that no effluent was pumped directly onto the yard (indicated by pumping and tank refill timing and duration being equal for a given wash down event), the data from the electromagnetic flow meter and the pressure sensor in the flood wash tank were cross checked against one another.

Fresh water consumption at the dairy (W_f) was approximated from other flows at the dairy in a rearrangement of equation 5-3 applied to days without rain and associated stormwater runoff from the yard. The resulting data were used to generate the fresh water use statistics presented in section 5.5.1. During rainfall events, stormwater runoff from the yard and solids trap could not be distinguished from fresh water flow, thus the outputs from the final water balance (5.5.6) do not differentiate these components.

5.3.2 Stormwater Runoff

Stormwater runoff from the holding yard was captured by the flume measuring flow into the anaerobic pond and did not need to be estimated for purposes of the water balance. Runoff from the pond embankments was estimated using a soil moisture model that was an adaptation of the initial loss and continuing loss method for runoff estimation described in the Australian Rainfall and Runoff guide (Pilgrim 1998). Soil on the pond embankments was treated as a 10 mm deep reservoir losing infiltrating rainfall at a rate of 2.5 mm per hour. The algorithm for calculating soil moisture was

$$\begin{aligned}
 SM_t &= SM_{t-1} + P - 2.5 \text{ where } 0 \geq SM_{t-1} + P - 2.5 \geq 10 \\
 SM_t &= 10 \text{ where } SM_{t-1} + P - 2.5 > 10 \\
 SM_t &= 0 \text{ where } SM_{t-1} + P - 2.5 < 0
 \end{aligned}
 \tag{5-5}$$

where

SM_t = soil moisture at time t (mm);

Embankment runoff ($R_{e,t}$) occurred when rainfall in a given hour (P_t) exceeded both the deficit in the soil reservoir from the previous time step and the continuing infiltration losses.

$$R_{e,t} = P_t - (10 - SM_{t-1}) \quad (5-6)$$

Treating the soil as a reservoir allowed estimation of runoff on a continuous basis rather than by discrete storm events. The adopted depth of the soil reservoir is equivalent to the 10-mm ‘initial loss rate’ recommended by Pilgrim et al. (1998) for NSW while the infiltration rate is equivalent to the recommended ‘continuing loss rate’. In keeping with the principles of initial and continuing loss rates, infiltration losses were not applied to the soil moisture balance in the first four hours of a rainfall event, or until SM exceeded 10 mm.

Runoff depth expressed in m was then converted to a volumetric figure for each pond by multiplying it by the respective catchment areas of each pond. The anaerobic pond catchment area ($E_{c,An}$) was constant and was determined through the pond bathymetry survey (see Chapter 3) to be 206 m². The catchment area of the facultative pond ($E_{c,Fac}$) was adjusted according to the surface area of the liquid held in the pond:

$$E_{c,Fac} = 1710 - A_{Fac} \quad (5-7)$$

5.3.3 Evaporation

Measurement and estimation of evaporation from open water bodies such as stabilisation ponds is a field replete with inconsistencies and uncertainties. There is a wide range of techniques to choose from including measurement using evaporation pans, lysimeters and eddy correlation, and estimation using energy and water budgeting, or more commonly bulk transfer or combination equations. Ultimately a modified form of the Penman-Monteith (PM) combination method was adopted as the data required can be collected using a standard weather station with low maintenance needs. A term for heat storage was included in the PM formulation to account for the large diurnal and seasonal swings in the temperature of the water body. Adjustments were also made to the radiation and aerodynamic components to account for site specific considerations. The general form of the equation was

$$E_o = \frac{1}{\lambda} \left[\frac{\Delta(R_n - Q) + 3600\rho_a c_p (e_z^0 - e_z)/r_a}{\Delta + \gamma} \right] \quad (5-8)$$

where

E_o = open water evaporation (mm h⁻¹);

λ = latent heat of vaporisation (MJ kg⁻¹);

Δ = slope of the temperature saturation water vapour curve (kPa °C⁻¹);

R_n = net radiation flux (MJ m⁻² h⁻¹);

Q = change in heat stored in water body (MJ m⁻² h⁻¹);

ρ_a = air density (kg m⁻³);

c_p = specific heat of air at constant pressure

$$= 1.013 \times 10^{-3} \text{ MJ kg}^{-1} \text{ K}^{-1};$$

e_z^0 = saturation vapour pressure at height z (kPa);

e_z = vapour pressure at height z (kPa);

r_a = aerodynamic resistance (s m⁻¹);

γ = psychrometric constant (kPa °C⁻¹).

The estimation of the radiation, heat storage and aerodynamic components of the equation is elaborated on in the forthcoming sections.

5.3.3.1 Radiant energy flux

The flux of radiant energy in the pond supernatant was calculated from the balance of incoming and outgoing short- and long-wave radiation.

$$R_n = R_{S_{in}} - R_{S_{out}} + R_{L_{in}} - R_{L_{out}} \quad (5-9)$$

where

R_n = net radiation;

$R_{S_{in}}$ = incoming short-wave radiation;

$R_{S_{out}}$ = outgoing short-wave radiation;

$R_{L_{in}}$ = incoming long-wave radiation;

$R_{L_{out}}$ = outgoing long-wave radiation;

and all units are MJ m⁻² h⁻¹.

$R_{S_{in}}$ was measured on-site while the other components were modelled.

Short-wave radiation

Net short-wave radiation R_S^* was calculated as

$$\begin{aligned} R_S^* &= R_{S_{in}} - R_{S_{out}} \\ &= (1 - \alpha)R_{S_{in}} \end{aligned} \quad (5-10)$$

where

α = albedo of the evaporating surface.

Incoming short-wave radiation was recorded by the site AWS; the data are presented in Appendix H. The albedo of a water surface varies with solar elevation, cloud cover, wave action, turbidity and temperature. At most solar zenith angles, albedo lies within the range of 0.05-0.15 (Ward & Robinson 2000); although at very large solar zenith angles albedo can approach 1.0 (Sturman & Tapper 1996). Despite large potential for daily and seasonal variation, albedo is often treated as a constant in combination method calculations. Values adopted for open water bodies typically range between 0.04 and 0.09 (ASCE 1996; Brutsaert 2005; Ladson 2008). A selection of values suggested or adopted in various publications is given in Table 5-2.

Table 5-2 Albedos adopted or recommended in the literature

<i>Albedo</i>	<i>Reference</i>	<i>Water body</i>	<i>Location</i>
0.12	Parker, Auvermann & Williams (1999)	Clear ground water and farm effluent in plastic pans*	Texas, USA
0.08	McJannet et al. (2008)	River system	Murray Darling basin, Australia
	Maidment(1993)	Open water	
	Valiantzas (2006)	Open water	
0.06	McVicar et al. (2007)	Open water	China
0.05	Grayson (1996)	Open water	All of Australia
0.23	Craig (2006)	Farm dams using FAO 56 reference crop combination method (Allen et al. 1998)	Queensland, Australia

*Evaporation estimates consistently underestimated measured evaporation suggesting the adopted albedo was too high

Stefan et al. (1983) derived an empirical relationship between albedo and suspended solids concentration and incoming radiation (as a surrogate for solar elevation). In a water balance study on piggery ponds, Cumba & Hamilton (2002) fitted a linear function to short-wave radiation to estimate net radiant energy flux. The fitted slope

suggested that the fraction of R_{S_in} reflected was indeed much higher than typical open water albedo values.

In recognition that albedo is a function of solar elevation, the albedo for direct radiation α_f was first calculated dynamically using Fresnel's equation:

$$\alpha_f = 0.5 \left[\frac{\sin^2 \left(\frac{\pi}{2} - \beta - r \right)}{\sin^2 \left(\frac{\pi}{2} - \beta + r \right)} + \frac{\tan^2 \left(\frac{\pi}{2} - \beta - r \right)}{\tan^2 \left(\frac{\pi}{2} - \beta + r \right)} \right] \quad (5-11)$$

where

β = solar elevation (radians);

r = angle of refraction (radians)

$$= \sin^{-1} \left[\frac{\sin \left(\frac{\pi}{2} - \beta \right)}{n} \right];$$

n = refractive index of water = 1.33.

Fresnel albedo is an estimate of albedo for clear water under direct radiation unaffected by factors such as turbidity and wind (Cogley 1979). R_{S_in} , however, comprises both direct and diffuse radiation, which causes actual albedo to be higher than α_f at low solar elevations and lower than α_f at higher elevations (Nunez, Davies & Robinson 1972). The albedo of water for diffuse radiation is considered to be constant at between 0.06 and 0.10 (Cogley 1979). To account for the reflection of the diffuse component of R_{S_in} , α_f was adjusted to reflect the diffuse component of R_{S_in} as per Jacobs et al. (2008).

$$\alpha_{f,d} = f_{\alpha 1} \alpha_f + (1 - f_{\alpha 1}) \alpha_d \quad (5-12)$$

where

$\alpha_{f,d}$ = fresnel albedo adjusted for diffuse component of R_{S_in} ;

$$f_{\alpha 1} = 1 - \frac{R_{S_in,d}}{R_{S_in}};$$

$R_{S_in,d}$ = diffuse component of R_{S_in} ;

α_d = diffuse radiation albedo = 0.08.

Diffuse radiation was estimated as functions of the ratio of hourly R_{S_in} to extraterrestrial shortwave radiation and solar elevation according to the method used by Spitters, Toussaint & Goudriaan (1986) and Jacobs & van Pul (1990):

$$\frac{R_{S_in,d}}{R_a} = 1 \quad \text{for} \quad \frac{R_{S_in}}{R_a} \leq 0.22 \quad (5-13a)$$

$$\frac{R_{S_in,d}}{R_a} = 1 - 6.4 \left(\frac{R_{S_in}}{R_{S0}} - 0.22 \right)^2 \quad \text{for} \quad 0.22 \leq \frac{R_{S_in}}{R_a} \leq 0.35 \quad (5-11b)$$

$$\frac{R_{S_in,d}}{R_a} = 1.47 - 1.66 \frac{R_{S_in}}{R_{S0}} \quad \text{for} \quad 0.35 \leq \frac{R_{S_in}}{R_a} \leq K \quad (5-11c)$$

$$\frac{R_{S_in,d}}{R_a} = R \quad \text{for} \quad K < \frac{R_{S_in}}{R_a} \quad (5-11d)$$

where

R_a = extra-terrestrial shortwave radiation ($\text{MJ m}^{-2} \text{d}^{-1}$)

$$R = 0.847 - 1.61 \sin \beta + 1.04 \sin^2 \beta;$$

$$K = \frac{1.47 - R}{1.66}$$

R_a was calculated as per the algorithm described by Allen et al. (1998) for hourly or shorter periods. Figure 5-3 shows clear water albedo calculated daily at noon over the water balance period. The base seasonality is evident in the lower envelope while the noise is caused by increased albedo under cloudy conditions.

Finally, to account for the effect of turbidity on albedo, an exponential function of turbidity of the form used by Stefan et al. (1983) was added to the diffuse radiation-adjusted albedo.

$$\alpha = \alpha_{f,d} + f_{\alpha 2} \left[1 - \exp \left(- \frac{\text{Turbidity}}{100} \right) \right] \quad (5-14)$$

The turbidity correction factor $f_{\alpha 2}$ was fitted as described in section 5.4.1.

Long-wave radiation

Net long-wave radiation includes incoming radiation emitted by clear sky atmosphere and outgoing radiation from the water surface, both of which are mediated by cloud cover (which includes re-emitted atmospheric and water surface radiation) (ASCE 1996; Oke 1992; Brutsaert 2005). Net long-wave radiation R_{0L}^* over a cloudless period is expressed as (Oke 1992; Dingman 1994; Brutsaert 2005; Johnson & Sharma 2007):

$$\begin{aligned}
 R_{0L}^* &= R_{L_{in}} - R_{L_{out}} \\
 &= \epsilon_a \sigma T_a^4 - [\epsilon_w \sigma T_w^4 + (1 - \epsilon_w) \epsilon_a \sigma T_a^4] \\
 &= \epsilon_w \epsilon_a \sigma T_a^4 - \epsilon_w \sigma T_w^4
 \end{aligned} \tag{5-15}$$

where

ϵ_a = atmospheric emissivity;

T_a = air temperature (K);

ϵ_w = emissivity of water = 0.97;

σ = Stefan-Boltzman constant = $4.903 \times 10^{-9} \text{ MJ m}^{-2} \text{ K}^{-4} \text{ d}^{-1}$;

T_w = water (liquid) temperature (K).

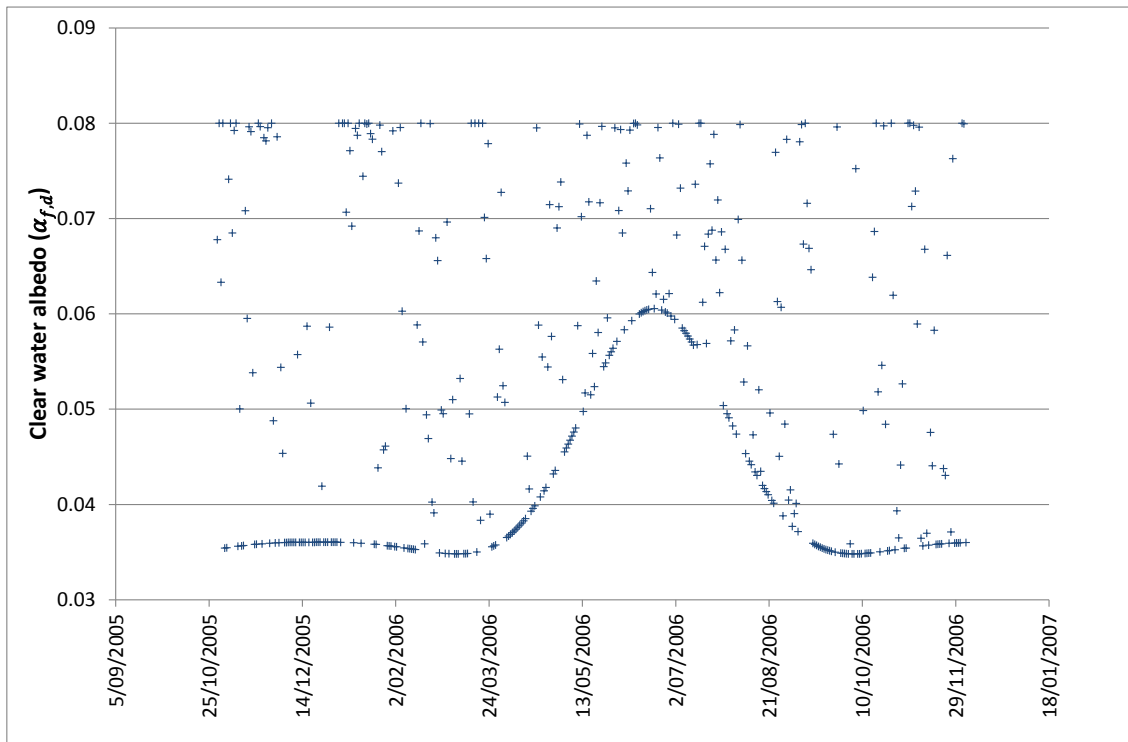


Figure 5-3 Daily clear water albedo at solar noon over the water balance period.

Air temperature was recorded by the AWS (see Appendix H). Emissivity has previously been modelled using temperature (Idso & Jackson 1969) and vapour pressure (Brutsaert 1975). The equation used in this case, however, was developed by Idso (1981) and incorporated the theory of water dimer in utilising both temperature and vapour pressure:

$$\epsilon_a = 0.70 + 5.95 \times 10^{-5} e_z \exp\left(\frac{1500}{T_a}\right) \quad (5-16)$$

The effect of cloud cover on net long-wave radiation was accounted for with a 'cloudiness' function f_c such that

$$R_L^* = f_c R_{0L}^* \quad (5-17)$$

The cloudiness function generally takes the form of a linear function of the ratio of observed to clear sky radiation:

$$f_c = a \frac{R_S}{R_{S0}} + b \quad (5-18)$$

where

R_{S0} = clear sky radiation;

a, b = empirical constants.

Clear sky radiation was estimated from extra-terrestrial radiation:

$$R_{S0} = R_a(0.75 + 2 \times 10^{-5}Z) \quad (5-19)$$

where

Z = elevation above sea level = 674 m;

Various values for the cloudiness function coefficients a and b are provided in the literature. Jegede et al. (2006) used a value of 1 for a and did not make use of an intercept term. Similarly Ward & Trimble (2004) suggest coefficients of $a = 1.0$ and $b = 0$ for humid areas. For a semi-humid environment they recommend $a = 1.1$ and $b = -0.1$, while for arid areas they suggest $a = 1.2$ and $b = -0.2$. Craig (2006) adopts the cloudiness function described in Allen et al. (1998) in which $a = 1.35$ and $b = -0.35$. Noting that cloudiness function coefficients are best locally calibrated, Meyer et al. (1999) derived coefficients ($a = 0.92$ and $b = 0.08$) for the cloudiness function by back calculation and regression using data from Griffith, NSW. The regression fit was, however, relatively poor and it is questionable as to whether these values can be applied elsewhere. Given the climate of the region in which the site is situated, the coefficients for a semi-humid environment suggested by Ward & Trimble (2004) were adopted. Cloud cover for night time calculations was drawn from the cloudiness

function result calculated 2-3 hours before sunset following the approach recommended by Allen et al. (1998).

Where net long-wave radiation could not be calculated due to missing water temperature data, an expression for net emittance based on vapour pressure was applied to air temperature to calculate net long-wave radiation as per ASCE (1996), Allen et al. (1998), Craig (2006) and Dodds, Meyer & Barton (2005).

$$R_L^* = f_c (0.34 - 0.14\sqrt{\epsilon_a}) \sigma T_a^4 \quad (5-20)$$

When this formula was applied, f_c was calculated using the Allen et al. (1998) cloudiness function coefficients.

5.3.3.2 Heat storage component

Contributions to evaporation from changes in stored energy are often ignored in evaporation estimation using combination methods, generally because of lack of data and/or reasoning that they amount to a negligible fraction of the total energy budget. Certainly when considering losses over an entire year, energy losses to and gains from storage should effectively cancel out. However heat storage could potentially play a significant role in net evaporation losses from stabilisation ponds over shorter timeframes. Grayson (1996) states that ‘ignoring heat storage effects will render the [combination] method inaccurate...where high turbidity creates a shallow, hot layer of water’. In addition, heat stored from radiation absorption during the day supports continued evaporation throughout the night (Oke 1992). Similarly, heat transferred to depth by conduction and thermal convection over the summer contributes to sustained evaporation in autumn through the release of stored energy as latent heat flux (Shuttleworth 1993). In the anaerobic pond, anaerobic digestion of the sludge might also contribute heat to the water body which in turn may be transferred to latent heat flux.

Facultative pond

The change in stored energy in the water body was calculated from the volume and average temperature of the water body at the beginning and the end of the time step (Dingman 1994):

$$Q = \frac{c_w \rho_w V}{A} (T_t - T_{t-1}) \quad (5-21)$$

where

Q = change in heat stored in water body ($\text{MJ m}^{-2} \text{h}^{-1}$);

c_w = specific heat of water ($\text{MJ kg}^{-1} \text{°C}^{-1}$);

ρ_w = liquid density (kg m^{-3});

V = liquid volume (m^3);

A = liquid surface area (m^2);

T_t = liquid temperature at time t (°C).

The volume used in the equation 5-21 will not necessarily be the total liquid volume since incoming radiation will be adsorbed or reflected by the dissolved organic matter, suspended sediment, bacteria and algae (Parker, Auvermann & Williams 1999). This is particularly the case for the facultative pond which exhibits thermal stratification during the day. To better approximate the heat stored in the facultative pond, water quality profile data presented in Chapter 4 were examined to determine a typical shape of the temperature profile. Exponential decay functions of the form presented in equation 5-22 (below) were fitted to temperature data from six profiling runs plotted against liquid volume (above the temperature reading).

$$T_d = \gamma_2 e^{(-\varphi V_d)} + \gamma_1 V_d + \gamma_0 \quad (5-22)$$

where

T_d = temperature at depth d (°C);

V_d = liquid volume at depth d (m^3);

$\varphi, \gamma_2, \gamma_1, \gamma_0$ = fitted constants.

Each temperature function was then integrated to determine the area under the curve, which corresponds to VT (at time t or $t-1$) in equation 5-23.

$$\begin{aligned} VT &= \int_0^V (\gamma_2 e^{(-\varphi V_d)} + \gamma_1 V_d + \gamma_0) dV_d \\ &= -\frac{\gamma_2}{\varphi} e^{(-\varphi V)} + \frac{1}{2} \gamma_1 V^2 + \gamma_0 V + \frac{\gamma_2}{\varphi} \end{aligned} \quad (5-23)$$

The values for VT so derived provided a basis for developing a method to dynamically estimate VT using temperature measurements made at just two depths as opposed to

a full set of profiling measurements. Liquid temperature in the facultative pond was continuously measured at the surface and in the hypolimnion (see Chapter 4 and Appendix G). To obtain estimates of VT from these data, a simplified representation of the area under the profile curves defined by equation 5-23 was developed that assumed a linear gradient from the surface to a nominal ‘thermocline depth’ d_t and constant temperature from this depth to the bottom of the pond as per the two examples given in Figure 5-4. This simplification may be expressed as the sum of the areas of the triangle and rectangle pairs marked by dashed lines in Figure 5-4:

$$VT = 0.5(V - V_{d_t})(T_s - T_{d_t}) + VT_h \quad (5-24)$$

where

T_s = temperature measured at the pond surface.

The depth d_t was determined to be approximately 0.15 m by minimising the sum of squares between VT estimates based on integration of six fitted seasonal profile curves (equation 5-23) and corresponding estimates made with equation 5-24. Continuous temperature data could then be used in conjunction with equation 5-24 to estimate stored heat in the facultative pond on an hourly basis.

Anaerobic pond

Temperature in the anaerobic pond did not display the same variability with depth as that in the facultative pond, presumably due to greater mixing of the supernatant (see Chapter 6). As such, changes in temperature recorded at approximately 0.5 m were considered an adequate reflection of changes in heat storage of the bulk supernatant, after adjustment for sludge accumulation, allowing the continuous data to be inserted directly into equation 5-21.

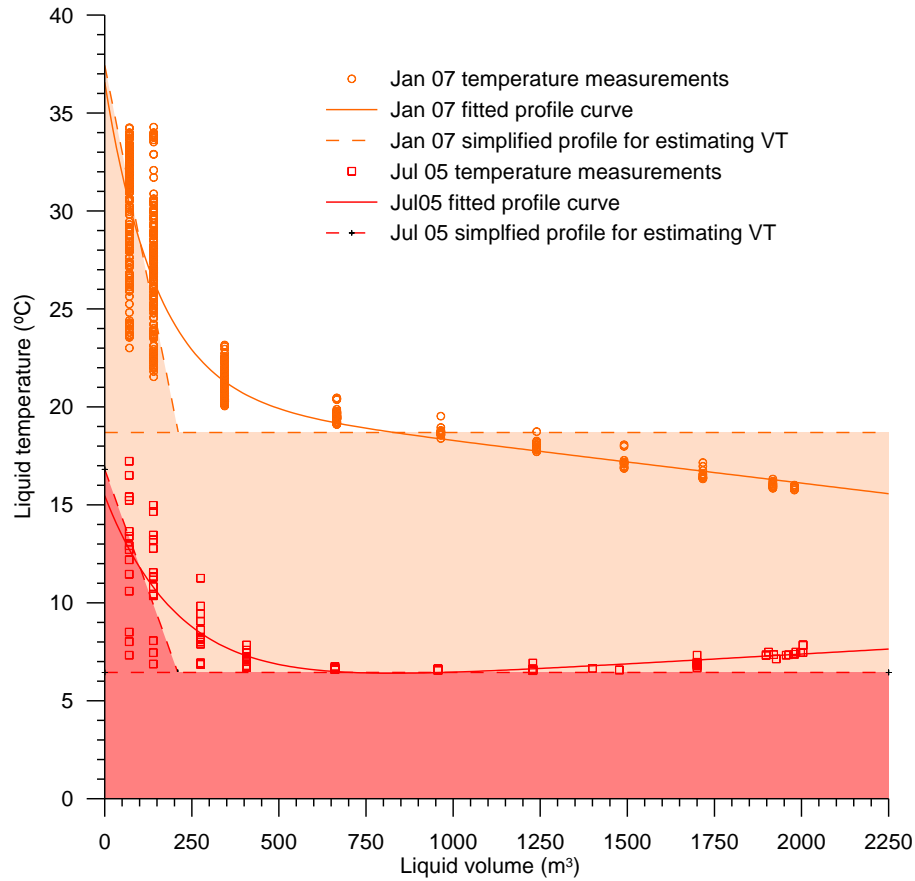


Figure 5-4 Fitted and simplified temperature profiles (July 2005 and January 2007, others not shown) for estimating VT.

5.3.3.3 Aerodynamic component

The PM equation describes evaporation from a reference crop and assumes latent heat loss via diffusion of water vapour is regulated by the surface resistance of the crop as well as aerodynamic resistance. In open water applications, the free water surface is considered to have a surface resistance of zero, leaving an aerodynamic component (the second group of terms in the numerator of equation 5.8) that describes the drying power of the air in terms of aerodynamic resistance only. A generalised expression for aerodynamic resistance under conditions of neutral atmospheric stability may be derived from the principles of turbulence similarity (Jensen, Allen & Burman 1990; Brutsaert 2005):

$$r_a = \frac{\ln\left(\frac{z_2 - d_0}{z_{0v}}\right) \ln\left(\frac{z_1 - d_0}{z_{0m}}\right)}{\kappa^2 \bar{u}} \quad (5-25)$$

where

κ = the von Karman's constant = 0.41;

\bar{u} = mean wind speed at height (m s^{-1})

z_1 = height of wind speed measurement (m);

z_2 = height of vapour pressure measurement (m);

d_0 = zero displacement height (m)

= 0 for open water (ASCE 1996);

z_{0m} = momentum roughness height

= 0.0001 (m);

z_{0v} = vapour transfer roughness length (m).

The momentum roughness height for open water is a dynamic parameter and depends on wave height, which in turn is a function of wind speed (Wiernga 1993). For the purposes of this analysis and to facilitate comparisons with other published data, a constant value of 0.0001 m that represents open water under relatively smooth conditions (Sethuraman & Raynor 1975; Wiernga 1993; Brutsaert 2005) was adopted. It is also generally assumed that on open water, z_{0v} is approximately equal to z_{0m} (ASCE 1996). Since wind speed and humidity measurements were made at the same height, equation 5-25 simplifies to

$$r_a = \frac{\ln\left(\frac{z_1}{z_{0m}}\right)^2}{\kappa^2 \bar{u}} \quad (5-26)$$

Jensen et al. (1990), however, reported that the above form of the aerodynamic resistance term required unrealistically high values for momentum roughness to produce reasonable estimates of evaporation, presumably due to the assumption of neutral atmospheric conditions. Accordingly, a generalised form derived by Thom & Oliver (1977) that provides allowance for atmospheric buoyancy was adopted.

$$r_a = \frac{4.72 \ln\left(\frac{z_1}{z_{0m}}\right)^2}{(1 + 0.54 \bar{u})} \quad (5-27)$$

There are, however, a number of other factors that undermine the direct application of resistance theory to atmospheric diffusion from open water including:

- wind and humidity measurements were made on the anaerobic pond embankment, which has substantially different roughness characteristics from the water surface;
- equation 5-27 assumes an atmospheric boundary layer in equilibrium requiring a minimum fetch length along the liquid surface, which would be of the order of several hundred metres for the height at which the wind speed measurements were made (ASCE 1996);
- the embankments surrounding the ponds would cause wake interference, which together with the transition between land and water surface, would form an internal boundary layer that dislocates the idealised logarithmic wind profile (see Wiernga 1993; Condie & Webster 1997);
- bubbles from biogas generated in the anaerobic pond are likely to create additional turbulence at the air-liquid interface.

Rather than attempt to model each of these effects, a task well beyond the scope of this research, an empirical correction factor similar to the ‘stability correction factor’ used by Jacobs et al. (2008) was included in the aerodynamic component of equation 5-8:

$$E_o = \frac{1}{\lambda} \left[\frac{\Delta(R_n - Q) + f_{EA} 3600 \rho_a c_p (e_z^0 - e_z) / r_a}{\Delta + \gamma} \right] \quad (5-28)$$

where

f_{EA} = aerodynamic correction factor.

Dynamic calculations of ρ_a and e_z^0 were made using equations given in Maidment (1993). Wind speed and vapour pressure were collected by the AWS (see Appendix H). This leaves two unknown parameters to be determined for the evaporation estimation method, namely the aerodynamic correction factor f_{EA} and the turbidity correction coefficient $f_{\alpha 2}$ described in section 5.3.3.1, both of which were arrived at through the calibration process described in section 5.4.1.

5.3.3.4 Calculating volumetric evaporation losses

Hourly evaporation (E_o) in metres was converted to volumetric loss by multiplying by surface area of the pond.

$$E = E_o A \quad (5-29)$$

where

E = Evaporation (m^3);

A = Liquid surface area.

Surface area was taken to be constant in the anaerobic pond ($A_{An} = 590 \text{ m}^2$) while the facultative pond surface area (A_{fac}) was calculated dynamically using the polynomial function formulated in Chapter 3. Evaporation losses from wastewater passing through the solids trap were assumed negligible on account of the relatively small surface area and its low hydraulic residence time. Evaporation losses from the captured manure solids were not considered since manure solids were already discounted from the water balance (refer to section 5.1).

5.3.4 Seepage

Seepage was the only component of the water balance that did not involve some form of field measurement and consequently had to be determined through closure of the water balance. Water balance studies of animal waste ponds such as those by Ham & DeSutter (1999) and Cumba & Hamilton (2002) have adopted Darcy's equation to describe specific flux based on an assumed or back-calculated coefficient of permeability.

$$q = k_l \left(\frac{H}{L_l} + 1 \right) \quad (5-30)$$

where

q = specific flux (m h^{-1});

k_l = hydraulic conductivity of the pond liner (m h^{-1});

H = liquid depth (m);

L_l = depth of the pond liner (m).

Flux is assumed to be uniform across the pond and seepage flow is then calculated as the product of flux and the pond wetted area, with an appropriate adjustment of H to reflect the reduced depth at the pond embankments.

It has been demonstrated, however, that earthen ponds holding animal wastes effectively 'self-seal' over time as solids settling out of supernatant clog soil pores and fissures (e.g. Rowsell, Miller & Groenevelt 1985), even when constructed on coarse (silty, sandy) soils. Tyner & Lee (2004) derived a two-layer 1-dimensional steady state model that assumed a unit gradient in the unsaturated soil liner below the low conductivity waste seal to simulate leachate flux from an animal waste pond. The modelling demonstrated that flux is ultimately governed by the hydraulic conductivity and depth of the waste seal rather than the corresponding characteristics of the liner.

Cihan, Tyner & Wright (2006) proposed and tested a model for infiltration through waste seals based on filter cake theory whereby flux is initially determined by soil characteristics, but as waste solids settle atop the soil and move into soil pores to form a seal, flux is increasingly controlled by the properties of the seal. Flux mediated by the waste seal, which is equivalent to the change in cumulative infiltration over time, is expressed

$$q = \frac{dI}{dt} = k_s \left(\frac{H}{L_s} + 1 \right) \quad (5-31)$$

where

I = cumulative infiltration (m);

k_s = hydraulic conductivity of the waste seal (m h^{-1})

$< k_l$;

t = elapsed time (d).

The thickness of the seal may be expressed as a linear function of cumulative infiltration; that is, the depth of waste accumulated in the soil matrix (Tyner, Wright & Lee 2006):

$$L_s = Iv \quad (5-32)$$

where v is a constant that reflects the concentration and clogging effect of the solids entrained in the infiltrating liquid. Substituting into equation 5-32, rearranging and integrating gives cumulative infiltration over time (Cihan, Tyner & Wright 2006):

$$I = \sqrt{2Ht \left(\frac{K_s}{v} \right)} \quad (5-33)$$

Cihan, Tyner & Wright (2006) tested the model by monitoring leaching through silt loam soil monoliths overlain by liquid dairy manure waste. They observed that flux dropped rapidly over the initial 2 days of waste loading as the pressure head was increasingly taken up by the seal formed by the waste. Once the waste seal was established, the underlying soil became unsaturated and cumulative infiltration was directly proportional to the square root of elapsed time as per equation 5-33. Cihan, Tyner & Wright (2006) expanded the model testing to swine waste and to a range of soil textures, as well as to data from other studies. They found that the model was generally applicable but underpredicted infiltration in coarse textured soils that have greater difficulty forming seal.

Equation 5-33 models the gradual slowing of infiltration through a growing waste seal over time. Differentiating produces a time-dependent expression of flux that accounts for the cumulative sealing effect of infiltration:

$$\frac{dI}{dt} = q = \sqrt{\frac{Hk_s}{2tv}} \quad (5-34)$$

At the commencement of the field monitoring, the pond system had been in operation for nearly 2.5 years, over which time the seal formed by sediments would have been well and truly established. Total seepage is calculated by multiplying flux by wetted area, which varies with location in the pond and with liquid depth. To accommodate this, seepage was expressed as an integral:

$$\begin{aligned} dS_{An} &= q dA_{w,An} \\ &= \sqrt{\frac{k_s}{2tv}} H^{\frac{1}{2}} \frac{dA_{w,An}}{dh} dh \end{aligned} \quad (5-35)$$

where

S_{An} = seepage from the anaerobic pond ($\text{m}^3 \text{d}^{-1}$);

h = liquid surface elevation - 660 (mAHD);

$A_{w,An}$ = anaerobic pond wetted area.

Inserting the derivate of the anaerobic pond wetter area polynomial from Chapter 3:

$$dS_{An} = \sqrt{\frac{k_s}{2tv}} H^{\frac{1}{2}} (3\beta_3 h^2 + 2\beta_2 h + \beta_1 c) dh \quad (5-36)$$

where

h_B = surface elevation of the lowest point of the pond basin - 660 = 6.276 mAHD;

$\beta_3, \beta_2, \beta_1$ are coefficients for the anaerobic pond wetted area polynomial defined in Chapter 3.

The anaerobic pond has a gravity outflow, thus for the purposes of seepage estimation the liquid surface elevation may be considered constant and equation 5-36 may be expressed as an integral:

$$\begin{aligned} \int dS_{An} &= \sqrt{\frac{k_s}{2tv}} \int_{h_B}^h (h - h_B)^{\frac{1}{2}} (3\beta_3 h^2 + 2\beta_2 h + \beta_1 c) dh \\ &= \sqrt{\frac{k_s}{2tv}} \int_{6.276}^{11.071} (h - h_B)^{\frac{1}{2}} (3\beta_3 h^2 + 2\beta_2 h + \beta_1 c) dh \end{aligned} \quad (5-37)$$

Integrating yields

$$S_{An} = \frac{1017}{\sqrt{2t}} \sqrt{\frac{k_s}{v}} \quad (5-38)$$

k_s/v was treated as a single parameter in the implementation of the algorithm in the same manner as Cihan et al. (2006).

In the facultative pond, liquid depth H varies with time in a manner that cannot be expressed as a mathematical function, preventing formulation of an equivalent version of equation 5-35. Unlike the anaerobic pond, however, the facultative pond did not exhibit measurable sediment accumulation, suggesting that flux would actually be governed by equation 5-31. In this case seepage is calculated by multiplying specific flux by wetted area. To account for the sloping faces of the embankments, the pond surface area was divided into two: the level floor that was enclosed by the contour at 664.5 mAHD (see Figure 3-9 in Chapter 3) and the embankments, the wetted area of which was calculated from liquid surface elevation using the polynomial function given in Chapter 3. The expression for seepage through the embankments as a function of liquid depth was derived as follows:

$$\begin{aligned}
\int dS_{Fac,E} &= \int k_l \left(\frac{H}{L_l} + 1 \right) dA_{w,Fac,E} \\
&= \frac{k_l}{L_l} \int_{h_F}^h (h - h_F + L_l) (5\beta_5 h^4 + 4\beta_4 h^3 + 3\beta_3 h^2 + 2\beta_2 h + \beta_1) dh
\end{aligned} \tag{5-39}$$

Integration yields:

$$\begin{aligned}
S_{Fac,E} &= \frac{5}{6} \beta_5 h^6 + \frac{4}{5} \beta_4 h^5 + \frac{3}{4} \beta_3 h^4 + \frac{2}{3} \beta_2 h^3 + \frac{1}{2} \beta_1 h^2 \\
&\quad + (L_l - h_F) (\beta_5 h^5 + \beta_4 h^4 + \beta_3 h^3 + \beta_2 h^2 + \beta_1 h)
\end{aligned} \tag{5-40}$$

where

$S_{Fac,E}$ = seepage through the facultative pond embankments ($\text{m}^3 \text{d}^{-1}$);

$A_{w,Fac,E}$ = facultative pond embankments wetter area (m^2);

h_F = elevation of the pond floor – 660 = 4.5 mAHD;

$\beta_5, \beta_4, \beta_3, \beta_2, \beta_1, \beta_0$ are coefficients for the facultative pond wetted area polynomial defined in Chapter 3.

Seepage through the pond floor was expressed

$$S_{Fac,F} = k_l \left(\frac{h - h_F}{L_l} + 1 \right) A_F \tag{5-41}$$

where

$S_{Fac,F}$ = seepage through the facultative pond floor ($\text{m}^3 \text{d}^{-1}$)

A_F = surface area at elevation 664.5 m

$$= 635.7 \text{ m}^2$$

Liquid depth in the pond was measured by the pressure sensor on a Greenspan CTDP300 probe deployed at a fixed depth in the pond (probe facultative West in Chapter 4). Liquid depth measured by the probe and corresponding surface areas and volumes are presented in Appendix I. Liner thickness L_l was assumed to meet the minimum standard prescribed in the Dairy Australia guidelines (Birchall, Dillon & Wrigley 2008) of 0.3 m.

5.4 MODEL CALIBRATION AND VALIDATION

The modelling approaches described in section 5.3 introduce three unknown parameters to the water balance for each pond. Two of these came from the modified Penman equation for evaporation – the turbidity correction coefficient and the aerodynamic correction factor – while the third was related to the hydraulic conductivity of the liner or waste seal of the ponds. The following section describes the determination of these parameters through a process of fitting the outputs of the evaporation and seepage models to achieve closure of the water balance. The model calibrations were then validated against data from different periods in the monitoring time series. Finally a sensitivity analysis was applied to test the impact of varying the assumed runoff model parameters on the evaporation and seepage models and the overall water balance outputs.

5.4.1 Calibration by Water Balance Closure

With three parameters to determine, closure of the water balance for each pond to calibrate their respective evaporation and seepage components was an iterative process of parameter fitting, elimination and deduction using the most complete and reliable measured data sets available. The process thus had to be tailored to the specific contents of each pond data set, both of which contained significant periods with missing or erroneous data arising from temporary equipment failures.

5.4.1.1 Facultative pond

Closing the facultative pond water balance involved aligning predicted pond liquid surface elevation with observed data over a period during which system inputs and outputs were minimal and associated data were reliable. Between 12 midnight 29 October and 6 pm 11 November 2005 inflows to the facultative pond ceased due to desludging of the anaerobic pond. In addition, there were no effluent irrigation events with outflows that were limited to pumping effluent to the dairy, and the flow and meteorological data collected over the period were neither disrupted nor error prone. That the period was during spring was also advantageous as daily evaporation would be variable but relatively low, giving adequate information to calibrate the evaporation parameters and at the same time minimising its impact on the estimation of the seepage parameter (Ham 2002b).

Measurements of pond depth recorded at hourly intervals by the fixed Greenspan CDTP300 probe located on the western side of the pond (refer to Figure 3-8) were translated to liquid surface elevation to be used as the basis for the calibration. The

calibration was performed by simultaneously adjusting the albedo turbidity correction factor f_{a2} , the aerodynamic correction factor f_{EA} and hydraulic conductivity k_l to match predicted and observed liquid surface elevation predicted in a least squares fitting process. Predicted elevation was calculated as

$$\hat{h}_t = \hat{h}_{t-1} + \frac{P_{Fac,t} + R_{e,Fac,t} - W_{e,t} - E_{Fac,t} - S_{Fac,t}}{A_{Fac,t}} \quad (5-42)$$

where

\hat{h}_t = predicted liquid surface elevation (mAHD);

t = time step (h).

Water surface elevation was chosen as the basis for the calibration as the precision of the probe was not sufficient to detect the small increments in depth caused by evaporation and seepage alone. The fit, therefore, was guided by the overall trend in elevation and less prone to bias from inaccuracies in short term variation and noise. However, fitting the water balance model to liquid surface elevation data meant that influence of the relatively small evaporation and seepage components on a normal least squares calculation would be overwhelmed by that of effluent flows. Seepage was assumed to vary little over time, hence little could be done to address this imbalance for fitting k_l . But in order to place more emphasis on evaporation in a least squares fitting process, the squares of the model residuals were weighted to accentuate times when evaporation would be high.

$$\sum_{t=1}^n \frac{E_{p,t} - MIN(E_p)_{t=1...n}}{\bar{E}_{p,t=1-n} - MIN(E_p)_{t=1...n}} \cdot (h_t - \hat{h}_t)^2 \quad (5-43)$$

where

E_p = potential evaporation (mm h^{-1})

= evaporation calculated as described in 5.3.2 without turbidity and aerodynamic adjustments

To eliminate any potential bias caused by error associated with rainfall measurement and runoff estimation, hourly time steps that recorded more than 1 mm of rainfall were precluded from the calibration fit. A total of 125 mm of rain fell during the calibration period mainly in three discrete events, as indicated by the red bars in Figure 5-5 below. The removal of the corresponding hourly data points reduced the effective number of

data points used in the calibration from 330 to 307 (7%). Fitting the parameters was performed using central differencing in the Generalized Reduced Gradient (GRG2) Algorithm of the Solver component of Microsoft Excel. Parameter constraints and initial values used to guide the solution are given in Appendix B.

Figure 5-5 presents predicted and observed liquid surface elevation from the calibration fit. The parameter estimates and outputs derived from the calibration fit are presented in Table 5-3 together with corresponding values from the literature. The standard error of 1.2 mm d^{-1} amounts to 46% of average combined evaporation and seepage and is higher than the equivalent figure derived by Craig (2006) (0.36 mm d^{-1}) who was quantifying evaporation (only) from a farm dam under more controlled conditions. Daily errors relative to outflows averaged 11%, but expressed as a fraction of changes in pond volume averaged 7%. Predictions of the liquid level relative to the starting level averaged within $\pm 6\%$. The resulting value for k_l ($2.8 \times 10^{-7} \text{ m h}^{-1}$) is an order of magnitude lower than the average hydraulic conductivities determined for manure ponds with well-compacted liners (Ham 2002a; Cumba & Hamilton 2002). It is also lower than the upper limit of $3.6 \times 10^{-6} \text{ m h}^{-1}$ recommended for DSE pond liners (Birchall, Dillon & Wrigley 2008). This is somewhat surprising given that the pond liner comprises in-situ ferrosol soil that was probably subject to only rudimentary compaction. Ferrosol soils are known for their high infiltration and effective drainage – their typical range for saturated hydraulic conductivity at 1 m depth is reported to be about 0.1 m h^{-1} (McKenzie et al. 1999). It is unlikely that such low permeability could be achieved with the in-situ liner, especially given that the anaerobic pond exhibited very high seepage losses as shown in the following section.

However refitting the calibration starting at the upper limit for k_l and adjusting the constraints on the parameters to force lower evaporation estimates (capping the stability correction factor at unity and increasing the upper limit of the albedo to 0.23, the typical value for land crops) made little difference to the outcome, with seepage tending towards zero and evaporation remaining the dominant loss mechanism. Another explanation for the low apparent liner permeability could be that seepage from the anaerobic pond is infiltrating into the facultative pond, which is explored further in section 5.5.5.

The average noon albedo derived from the calibration shows that the turbidity of the supernatant substantially increases the amount of incoming radiation that is reflected compared with clear water. While the correction function in this instance used turbidity data rather than suspended solids as per Stefan et al. (1983), the two measures of

turbidity exhibit very close to a 1:1 relationship in the facultative pond (see Chapter 7), meaning that the correction factor is closely comparable to that derived by Stefan et al. (1983). The aerodynamic correction factor was found to be greater than 1, indicating that the transition from land to water surfaces and the wake effects of the embankments generate more turbulence than might be observed on open water with extensive fetch. The contribution of the aerodynamic term to evaporation (25%), however, was within the range generally reported over open water and other wet surfaces (Brutsaert 2005), while adjusted aerodynamic resistance was close to the typical value of 125 s m^{-1} noted by Ward & Robinson (2000). Heat storage had the effect of reducing overall evaporation over the calibration period as a portion of incoming radiant energy was retained by the supernatant.

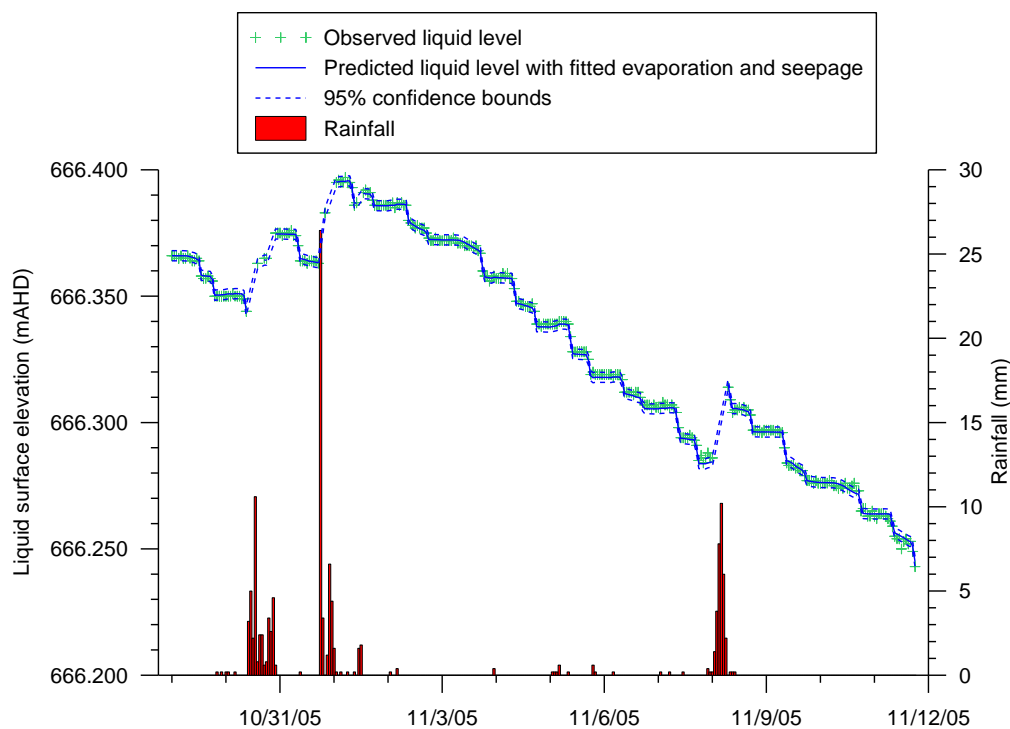


Figure 5-5 Observed and predicted hourly liquid surface elevation in the facultative pond over the evaporation calibration period. Note predicted elevations were reset to observed elevations following each of the three main rainfall events.

As a final check, daily evaporation estimates were compared to estimates using the Penman Monteith method and Class A pan measurements recorded at the nearby SCA weather station 568113. Figure 5-6 shows the evaporation estimates exhibit similar magnitude and fluctuations to the SCA data, suggesting that the methods and calibration adopted here are sound.

Table 5-3 Calibration and validation outputs from the facultative and anaerobic pond water balance models.

Model output	Units	Calibration		Validation		Typical or reported values
		Facultative pond	Anaerobic pond	Facultative pond	Anaerobic pond	
Observations, n	h or d	307 h	103 d	1469 h	61 d	
Calibration season		Spring	Winter	Spring	Spring	
Albedo turbidity correction factor, $f_{\alpha 2}$		0.116	0.116	0.116	0.116	0.11 (Stefan et al. 1983)
Aerodynamic term correction factor, f_{EA}		2.05	3.74	2.05	3.74	
Soil liner hydraulic conductivity, k_l	m h ⁻¹	2.8×10^{-7}		2.8×10^{-7}		Ferrosol soil 1.2-2.4 m d ⁻¹ (McKenzie et al. 1999). Manure wastewater ponds with compacted soil liners 6.5×10^{-6} (Ham 2002a), $< 3.6 \times 10^{-6}$ (Cumba & Hamilton 2002) Recommended pond liner 3.6×10^{-6} (Birchall, Dillon & Wrigley 2008)
Waste seal hydraulic conductivity parameter, k_s/v	m d ⁻¹		7.6×10^{-4}		7.6×10^{-4}	Compacted loam soils 1.7×10^{-6} to 5.8×10^{-4} m h ⁻¹ (Cihan, Tyner & Wright 2006)
Root-mean-square error of combined evaporation and seepage estimates	m ³ d ⁻¹	1.75	1.74	3.1	2.8	
	mm d ⁻¹	1.2	2.9	2.2	4.8	≤ 1 mm d ⁻¹ (Craig 2006)
Mean of absolute error expressed as a fraction of effluent flow	%	11	6	16	9	
Average daily evaporation	m ³ d ⁻¹	3.8	2.2	5.5	3.1	2.6; 1.5; 3.75 mm d ⁻¹ ϕ (PM estimates from SCA station 568113)
	mm d ⁻¹	2.7	3.7	4.0	5.2	
Radiation contribution to evaporation	%	84	44	75	52	
Heat storage contribution to evaporation	%	-8	-10	-4	6	

<i>Model output</i>	<i>Units</i>	<i>Calibration</i>		<i>Validation</i>		<i>Typical or reported values</i>
		<i>Facultative pond</i>	<i>Anaerobic pond</i>	<i>Facultative pond</i>	<i>Anaerobic pond</i>	
Aerodynamic contribution to evaporation	%	24	66	29	43	~25 (Brutsaert 2005)
Average noon albedo		0.173	0.174	0.157	0.165	
Median aerodynamic resistance	s m ⁻¹	144	56	120	56	~125 (Ward & Robinson 2000)
Average daily seepage	m ³ d ⁻¹	0.05	2.5	0.05	2.5	Ponds lined with properly compacted in-situ soil ~1.0 mm d ⁻¹ (Ham & DeSutter 1999; Ham 2002b; Ham 2002a). Ponds with variable compacted in-situ soil liners 0.1 – 10 mm d ⁻¹ (Simpkins et al. 2002). Unlined pond 5-11 (Parker, Eisenhauer, Schulte & Martin 1999; Parker, Eisenhauer, Schulte & Nienaber 1999).
	mm d ⁻¹	0.03	4.3	0.03	4.2	

† SCA data listed in order corresponding to facultative pond calibration, anaerobic pond calibration and validation periods.

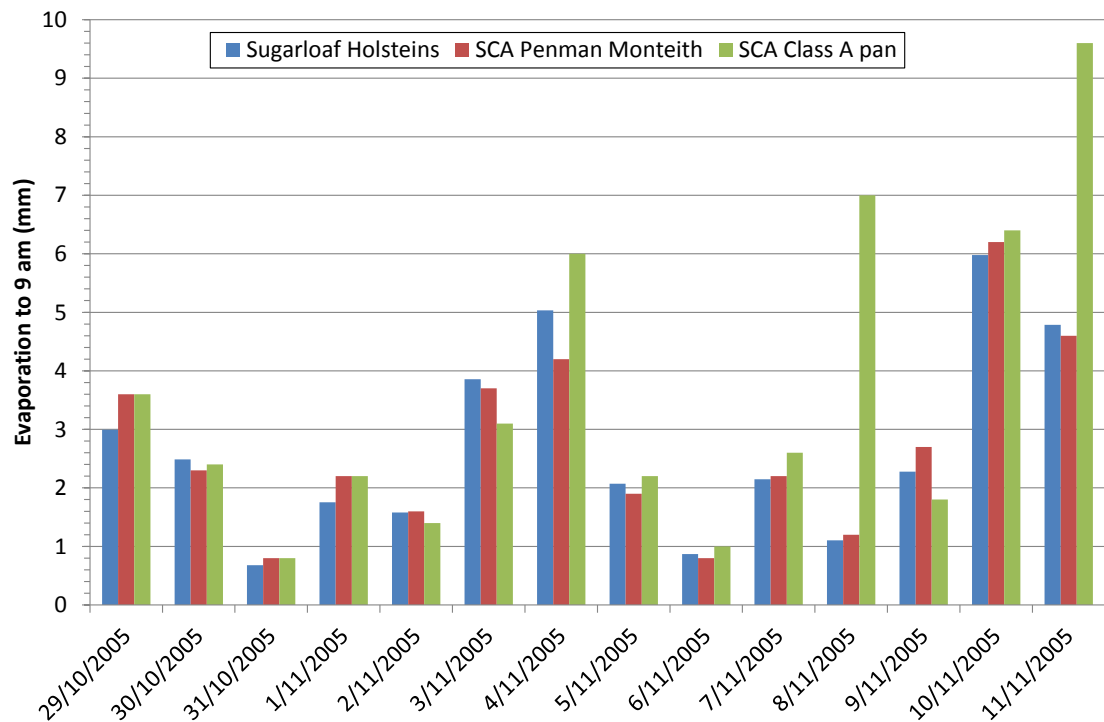


Figure 5-6 Comparison between estimates from the evaporation equation calibrated to the Sugarloaf Holsteins stabilisation pond site and Penman Monteith estimates and Class A pan measurements recorded by SCA.

5.4.1.2 Anaerobic pond

The different characteristics of the anaerobic pond necessitated deriving evaporation and seepage parameters distinct from those fitted to the facultative pond data. The fitted function for the albedo turbidity correction, however, approaches an upper limiting asymptote at around 600 NTU (see Figure 5-7), which suggests that the higher turbidity of the anaerobic pond should have no additional effect on albedo. In addition, turbidity was not measured continuously in the anaerobic pond but was observed in periodic sampling data to be relatively stable. Hence the turbidity correction factor derived for the facultative pond was applied directly to a time-averaged turbidity of 560 NTU. This meant that only two parameters - aerodynamic correction factor and the seepage constant k_s/ν (equation 5-38) – needed to be fitted to the conditions of the anaerobic pond.

The overflow outlet of the anaerobic pond ensured that liquid could not accumulate in the pond, and hourly variation in liquid depth was confined to a very small band that was not conducive to teasing out the seepage and evaporation components that are small in relation to the influent and effluent flows. Thus to gain a more distinguishable signal to the calibration fitting process, the water balance model of the anaerobic pond

was run at a daily timestep. Analysing the larger timestep allowed fitting of seepage and evaporation directly, using a rearrangement of equation 5-2:

$$E_{An} + S_{An} = W_0 + P_{An} + R_{e,An} - W_e - \Delta V_{An} \quad (5-44)$$

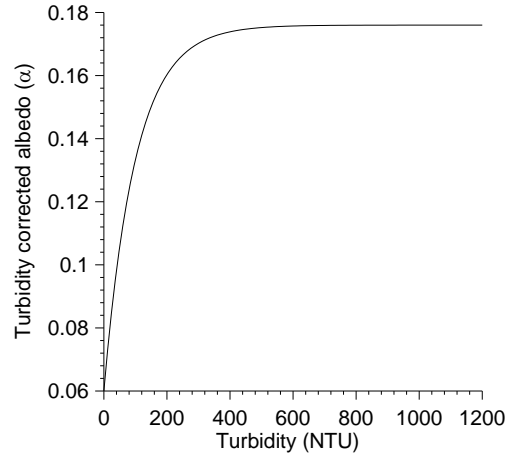


Figure 5-7 Turbidity correction curve for albedo (Fresnel albedo = 0.06).

The model was fitted by adjusting f_{EA} and k_s/v so as to minimise the square differences between the values calculated using each side of equation 5-44. The data selected for the calibration was a contiguous time series that spanned the winter of 2006 (8 June to 20 September) and provided sufficient data points to use a daily timestep. Winter was the preferred season as the radiation component of evaporation would be lower, leaving the aerodynamic component to be more dominant. Data for each of the terms in equation 5-44 can be found in Appendices H and I.

Initial attempts at fitting the parameters were confounded by the tendency for the aerodynamic adjustment factor to move towards unrealistically high estimates before any change was made to the seepage parameter, indicating that the fit needed initial estimates that were closer to the actual values. Thus to obtain an initial seepage parameter estimate, a preliminary fit was derived using days exhibiting potential aerodynamic evaporation (aerodynamic adjustment factor set to 1) below the 10th percentile. This approach was adapted from Glanville et al. (2001) who limited their water balance estimates of seepage from earthen manure storages to data sequences displaying low humidity and wind speed (and thus low evaporation). The preliminary k_s/v estimate was considered a lower bound for the subsequent full model fit under the assumption that, as is generally the case, actual evaporation would be lower than pan evaporation (ASCE 1996). For the full model fit, the aerodynamic factor was set to 1 to be fitted simultaneously with k_s/v . Initial parameter values and parameter constraints used to guide the fit are summarised in Appendix B.

The results from the final calibration fit are presented in Table 5-3. The fitted aerodynamic correction factor is higher than the factor derived for the facultative pond, causing the aerodynamic resistance to be unusually low and the contribution to evaporation from the aerodynamic component to be high. There are a number of factors that are likely to contribute to this including:

- the potential for biogas bubbles escaping from the supernatant to promote the diffusion of water vapour into the atmosphere through upward advection;
- the increased turbulence over the liquid surface that would be caused by the approaching wind run and the wake effect from the embankment;
- heightened oasis effect on the anaerobic pond due to its smaller surface area;
- fluid motion created by the inlet jet.

Figure 5-8 shows that wind predominantly came from the south and southwest over the monitoring period. Depending on whether the direction was more southerly or westerly, this prevailing wind would approach the pond uphill or downhill, respectively, to then strike the pond embankment and generate turbulent eddies as it passed over the water surface. Sitting below the anaerobic pond to the northeast, the facultative pond would be partially shielded from this wind.

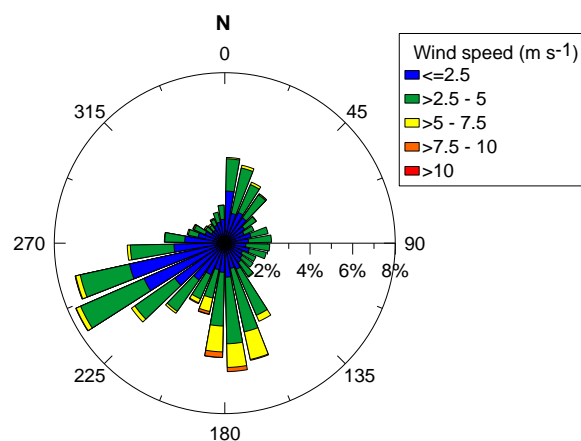


Figure 5-8 Frequency of wind direction and speed recorded over the monitoring period.

Referring to Table 5-3, the root-mean-square error of the fit was very similar to that of the facultative pond fit at $1.74 \text{ m}^3 \text{ d}^{-1}$ while the mean absolute error amounted to 6% of average effluent flow. The value for k_s/ν derived in this study (0.66 m d^{-1} or $7.6 \times 10^{-4} \text{ m h}^{-1}$) is at the top end of the range of values determined by Cihan, Tyner & Wright (2006) for infiltration of dairy waste both through compacted loam soil columns and actual pond basins. However it is much closer to the value predicted by Cihan, Tyner &

Wright's (2006) empirical equation based on pond total solids concentration (TS), which from Chapter 7 was 3010 mg L⁻¹:

$$\begin{aligned}\frac{k_s}{v} &= 2.37 \times 10^{-5} \exp\left(\frac{TS}{0.21}\right) \\ &= 5.65 \times 10^{-6} \text{ cm s}^{-1} \\ &= 2.0 \times 10^{-4} \text{ m h}^{-1}\end{aligned}\tag{5-45}$$

The average seepage loss rate of 4.3 mm d⁻¹ is higher than the typical rate 1.0 mm d⁻¹ from various livestock waste ponds with well-compacted in-situ soil (Ham & DeSutter 1999; Ham 2002b; Ham 2002a). It is, however, comparable to the rates estimated by Simpkins et al. (2002) for ponds lined with compacted in-situ soil (0.1 - 10 mm d⁻¹) and lower than losses from an unlined feedlot storage pond observed by Parker, Eisenhauer, Schulte & Nienaber (1999) (8.7 mm d⁻¹) and simulated by Parker, Eisenhauer, Schulte & Martin (1999) (5 - 11.1 mm d⁻¹). The pond in the present study was lined only with in-situ ferrosol soil that was compacted by track rolling. Thus while the estimates for k_s/v and seepage loss rate are high, they are not necessarily outside reasonable bounds. However the large difference in seepage rates between the anaerobic and facultative ponds again suggests that seepage from the anaerobic pond may be intruding into the facultative pond.

5.4.2 Validation

In order to test the generalisability of the evaporation and seepage parameters determined in the calibrations described above, fitted parameters were applied to water balances for periods outside the calibration windows. The most reliable and complete water balance data for the facultative pond was collected between 5 October and 6 December 2006. Figure 5-9 shows good agreement between predicted and observed liquid surface elevation. Importantly the validation period is characterised by consistent inflows and associated rises in the liquid surface level, unlike the calibration period during which there was no inflow to the pond. In addition, rainfall events have not been factored out of the water balance in the validation. Mean absolute error, calculated as a fraction of daily effluent flow, was 16%. Total daily evaporation to 9 am estimated by the SCA using the Penman Monteith method over the validation period was 229 mm. The corresponding total calculated for the facultative pond was 249 mm. Other key outputs from the validation of the facultative pond water balance model are presented in Table 5-3.

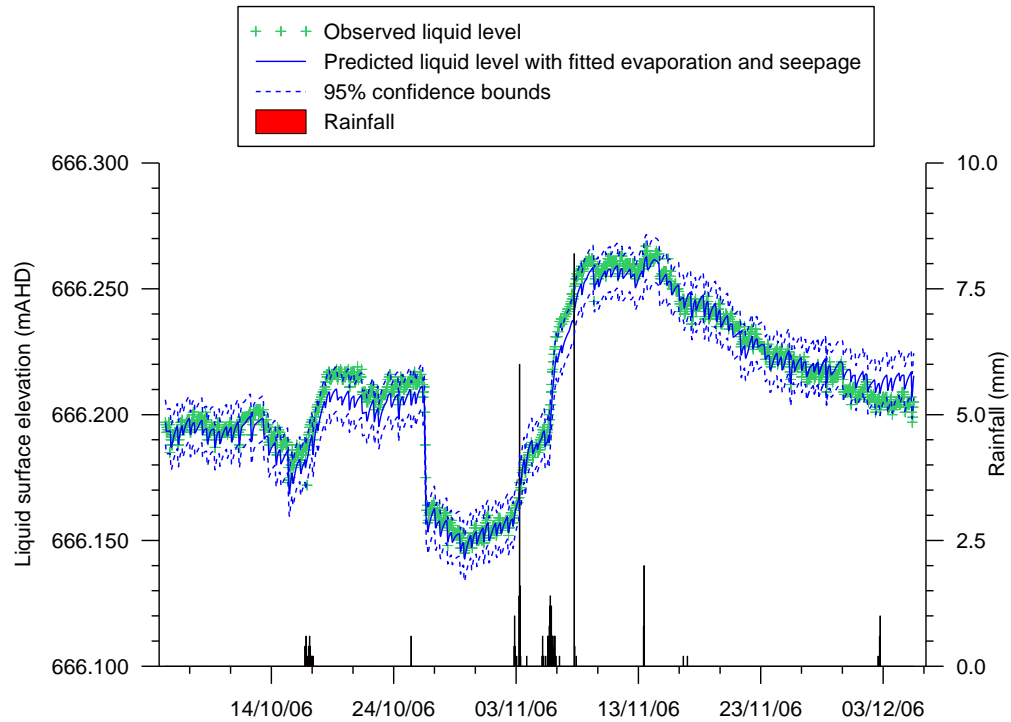


Figure 5-9 Observed and predicted liquid surface elevation in the facultative pond 5 October - 6 December 2006.

The anaerobic pond evaporation and seepage parameters were validated on data from the same period used for the facultative pond validation. The discrepancy between measured inflows and predicted outflows from the pond at the end of the 3-month period is 10.6 m^3 , or 0.5% of total outflow, which indicates there is no systematic error in the evaporation or seepage models. The key outputs from the validation of the anaerobic pond seepage and evaporation components are given in Table 5-3.

5.4.3 Sensitivity Analysis

Sensitivity analyses were performed to gauge the influence of the fitted evaporation and seepage parameters on model outputs and the overall water balance. Parameters were adjusted one at a time by $\pm 20\%$ and the relevant model outputs entered into the stability function:

$$\text{Relative sensitivity} = [\Delta(I_i)/I_i]/(\Delta P_j/P_j) \quad (5-46)$$

where

I_i = sensitivity index i ;

P_j = parameter j .

Two indices were assessed, namely model predictions of either evaporation or seepage, and the change to total predicted outflows. The results presented in Table 5-4 show that evaporation predictions are most sensitive to the aerodynamic term correction factor while predicted seepage from the facultative pond is highly sensitive to the hydraulic conductivity parameter, mainly due to the very small seepage flows. However, the impacts of the three parameters on the overall water balance outputs are relatively small since evaporation and seepage losses combined constitute around 20% of total outflows. The main concern related to the estimation of the model parameters and model uncertainty is therefore the accuracy of the apportionment of the water balance residual between evaporation and seepage.

Sensitivity analysis was also performed on the two pond embankment runoff parameters since both were based entirely on assumptions drawn from the literature. The relative sensitivities of runoff predictions were well above 50% for both ponds. Due to the very small contributions of runoff to the water balance, however, the impact of the parameters on the estimates of seepage and evaporation was negligible, with relative sensitivities below 5% for both ponds.

Table 5-4 Results from the sensitivity analysis of the fitted evaporation and seepage parameters.

	Units	$f_{\alpha 2}$		f_{E_A}		k_s/v or k_l	
Parameter change	%	20	-20	20	-20	20%	-20%
<i>Anaerobic pond</i>							
Parameter value		0.139	0.093	4.49	2.99	9.08×10^{-4} m h ⁻¹	6.06×10^{-4} m h ⁻¹
Change in predicted seepage or evaporation	%	2.1	2.1	9.8	9.8	9.5	10.6
Evaporation/seepage model relative sensitivity	%	10	-10	49	-49	48	-53
Change in total outflows	%	0.2	0.2	1.0	1.0	0.8	0.9
Water balance relative sensitivity	%	1.1	-1.1	5.1	-5.1	4.1	-4.5
<i>Facultative pond</i>							
Parameter value		0.139	0.093	2.46	1.64	3.33×10^{-7} m h ⁻¹	2.22×10^{-7} m h ⁻¹
Change seepage or evaporation	%	2.5	2.5	5.9	5.9	38.9	38.9
Evaporation/seepage model relative sensitivity	%	13	-13	29	-29	194	-194
Change in total outflows	%	0.5	0.5	1.2	1.2	0.1	0.1
Water balance relative sensitivity	%	2.5	-2.5	5.8	-5.8	0.3	-0.3

5.5 RESULTS AND DISCUSSION

The water balance model was applied to the period between 30 October 2005 when reconfiguration of the flow metering allowed all effluent flows from the facultative pond to be captured, and 5 December 2006 when the flow monitoring system was decommissioned. Results from the key measured and estimated components of the water balance are presented below.

5.5.1 Water and Recycled Effluent Usage at the Dairy

Average figures for fresh water and reclaimed effluent consumption over the period 30 October 2005 to 5 December 2006 are presented in Table 5-5. All figures are derived using days/mornings/evenings with no missing data and less than 1 mm rainfall. A day was defined as the 24 hours from 3 am in order to capture all morning and evening flows. Morning was defined as the 11 hours between 4 am and 3 pm, while the afternoon was from 3 pm to 2 am. This represented a reasonably similar distribution of hours before and after morning and evening peak flows. The two hours between 2 and 4 am were ignored to allow for the shorter daytime gap between morning and evening flows (as compared to overnight) whilst retaining the same number of hours as the basis for comparison. The summation of morning and evening flows does not, therefore, equate to total daily flow. Also, due to the lag associated with flows moving through the solids trap to the anaerobic pond inlet flume, fresh water estimates sometimes produced negative numbers. The different sample sizes (n) are a result of excluding periods with negative fresh water estimates.

Table 5-5 Average daily, morning and evening water and reclaimed effluent usage at the dairy (values in parentheses are standard deviations).

<i>Period</i>	<i>n</i>	<i>Recycled effluent + fresh water</i>	<i>Fresh water</i>	<i>Flood wash</i>	<i>Effluent pumped directly onto the yard</i>
		$\text{m}^3 \text{d}^{-1}$			
Daily (starting 3 am)	302	28.20 (7.20)	10.28 (5.23)	14.78 (4.59)	2.93 (4.16)
Morning milkings (4 am – 3 pm)	283	16.11 (5.67)	5.62 (2.71)	7.71 (3.40)	2.79 (4.00)
Evening milkings (3 pm – 2 am)	285	12.38 (4.31)	5.34 (4.18)	6.82 (3.10)	0.22 (0.71)

The data exhibit good agreement with the farm owner's estimates of daily usage, which were 22 m^3 of fresh water every two days and around half the tank (7.5 m^3) of reclaimed effluent each flood wash. On average, more water and effluent is consumed

during and after morning milkings than evening milkings. This corresponds to the shorter time the herd spends at the dairy in the evenings, which the operators estimate to be around 2 hours as compared to 3 to 3.5 hours in the morning (Maloney 2007, pers. comm. 19 February). Direct effluent pumping was used inconsistently, being employed on only 227 out of the 699 milking events analysed.

Total consumption data exhibits considerable variability, ranging from 11.6 to 74.5 m³ d⁻¹. Box plots of water/effluent consumption given in Figure 5-10 show that most variability appears to come from fresh water consumption. Figure 5-11 shows that there may be some seasonality behind the variability in total water usage, although the differences from month to month are generally not statistically significant. There is also an apparent but again not statistically significant rising trend from June 2006 in recycled effluent (flood wash and direct pumping) volumes. If the trend is real, then it may be related to improved pump performance following removal of struvite scale that eventually caused the pump to fail in March and May 2006. Based on the average consumption figures, the ratio of recycled effluent to fresh water is 1.7; that is, fresh water constitutes 36% of total water use at the dairy shed.

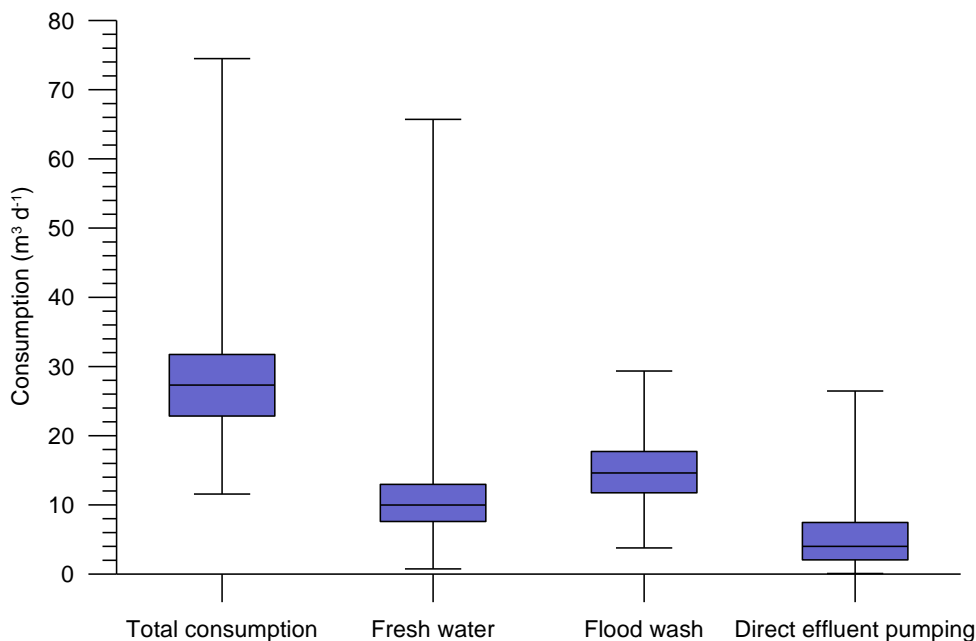


Figure 5-10 Box-whisker plots of daily water and reclaimed effluent consumption at the dairy.

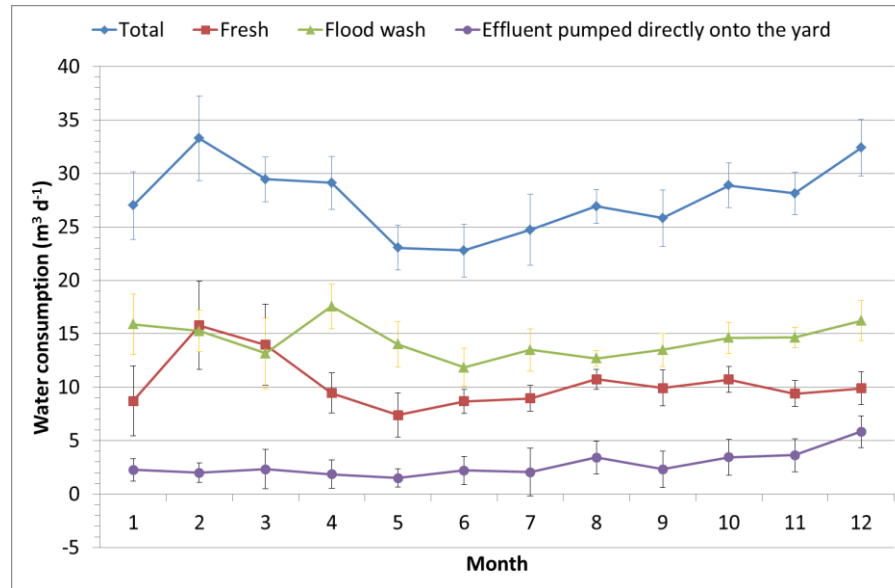


Figure 5-11 Average monthly water and recycled effluent consumption. Error bars indicate 95% confidence intervals.

5.5.1.1 Comparisons with industry benchmarks

Compared with industry benchmarks, overall water/effluent consumption is relatively high at Sugarloaf Holsteins. Mean total daily consumption ($27.9 \text{ m}^3 \text{ d}^{-1}$) sits in the third quartile ($20.0 - 30.2 \text{ m}^3 \text{ d}^{-1}$) reported for the 182 rotary type dairies surveyed as part of a comprehensive review of dairy shed waste use in the state of Victoria (Calligan 2010). According to the industry guide based on the abovementioned study, consumption is equivalent to 'reasonable' consumption for a herd of 400 cows (DPI 2009). Expressed on a per cow basis, daily consumption remains high at $94 \text{ L cow}^{-1} \text{ d}^{-1}$, which is well above the average of $47 \text{ L cow}^{-1} \text{ d}^{-1}$ for rotary dairies reported by Rogers & Alexander (2000) and approaching the 95th percentile in the more recent survey (Calligan 2010). This is also substantially higher than the NZ benchmark of $50 \text{ L cow}^{-1} \text{ d}^{-1}$ referred to by Mason (1996), Bolan et al. (2009) and Flemmer & Flemmer (2008).

Fresh water usage, however, makes up only 36% of total consumption at $10.3 \text{ m}^3 \text{ d}^{-1}$ or $34 \text{ L cow}^{-1} \text{ d}^{-1}$. This is mostly used for hosing out the parlour and washing machinery and vats. When compared with data on the same uses from Victorian rotary dairies, fresh water consumption may be classified as 'reasonable', being well below the 75th percentile of $14.0 \text{ m}^3 \text{ d}^{-1}$. The combined averages of flood wash and direct effluent pumping calculated from all days on which wastewater flows occurred was $17.7 \text{ m}^3 \text{ d}^{-1}$, which places it in the 50 to 75% range for rotary dairy flood wash consumption.

5.5.2 Wastewater Flows

Wastewater flows into and out of the anaerobic pond are characterised by two daily peaks that follow the conclusion of the morning and evening milking sessions. Figure 5-12 presents flow data recorded in the first two weeks of July 2006. The timing of the peaks exhibits strong consistency as they generally follow the milking regime. The size and shape of the peaks, however, are more erratic and are primarily determined by the size of the flood wash, the amount of solids held in the solids trap and the state of the solids trap screen. Peak inflow to the anaerobic pond could be as high as 15 L s^{-1} when a sizeable flood wash volume was released into the solids trap soon after it had been emptied and the screen cleared of blockages. The equalisation effect of the anaerobic pond is clear from the shorter and wider peaks of the outflow. The flow buffering effect of the pond is also evident in the box plots of daily peak inflow and outflow data presented in Figure 5-13. Both the average size and the variability of peak flows are considerably reduced by the pond.

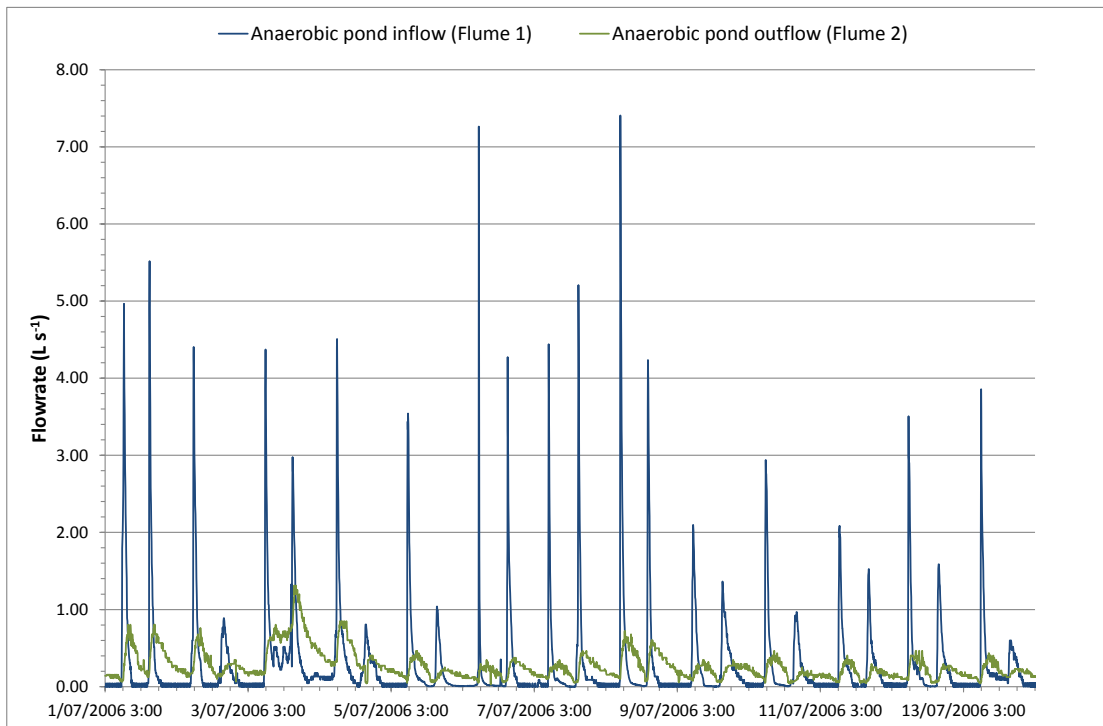


Figure 5-12 Example of flow data – inflow to and outflow from anaerobic pond 1 July 2006 – 15 July 2006.

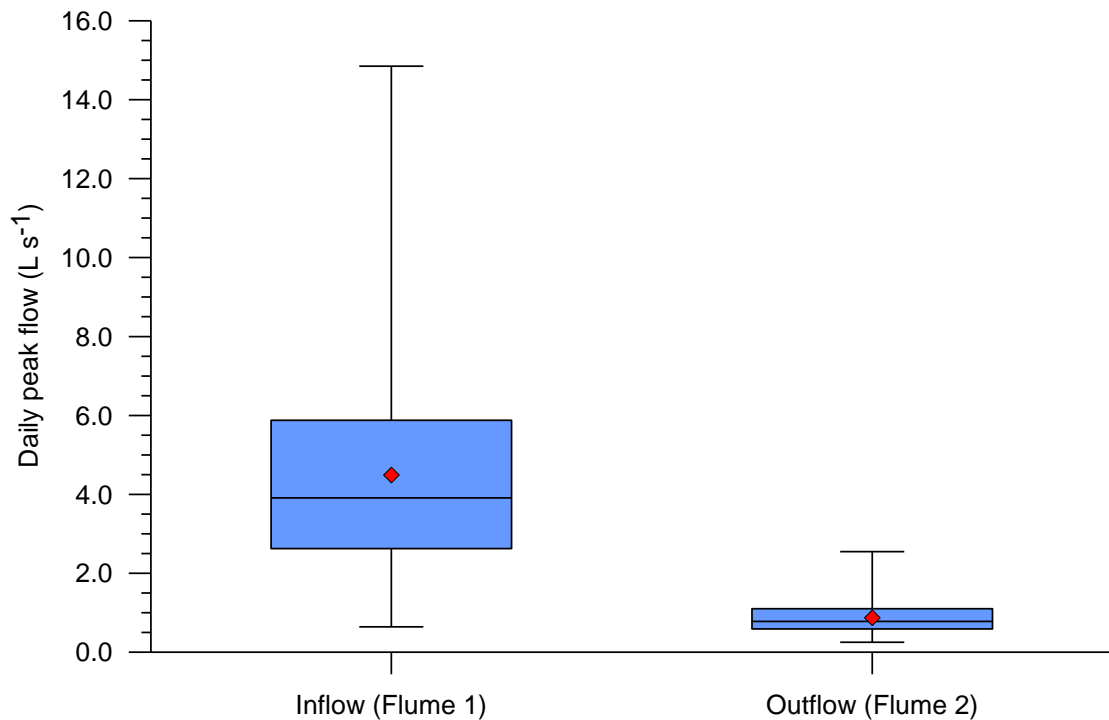


Figure 5-13 Box-whisker plot of daily peak flow entering and leaving the anaerobic pond drawn from days with complete data records and less than 1 mm rainfall. The red diamond symbols are the respective means.

Table 5-6 presents daily flow statistics for the anaerobic pond inlet and outlet and the facultative pond pump. The figures are drawn from all days with a complete data record and less than 1 mm rainfall, and include days with zero flow except for the period when the anaerobic pond outlet was not flowing following desludging. The small discrepancy between the water use estimate in section 5.5.1 and anaerobic pond inflow is an artefact of different sample sizes but well within the error bounds of the analysis. Facultative pond effluent pumping includes effluent used for cleaning the yard and irrigation. The effects of evaporation and seepage losses are evident in the reduction in daily flow through the anaerobic and facultative ponds. All median flows are slightly lower than corresponding means, which together with high 95th percentile values indicate positively skewed distributions. Note that the exaggerated difference between the irrigation and total facultative pond effluent mean and median flows is due to the irregularity and magnitude of irrigation events.

5.5.3 Effluent Irrigation

Effluent was applied to land periodically over the monitoring period as shown in Figure 5-14. The raw data are provided in Appendix I. The irrigation events recorded in the first half of the monitoring period are considerably smaller in volume than later events due to partial blockage of the pump by struvite deposits. The pump was cleaned out on

16 March 2006, with a cluster of irrigation events in the following fortnight. The pump was cleaned again, this time more thoroughly, sometime before 24 May 2006. A number of irrigation events occurred in the following winter months in an effort to reduce the high liquid level in the facultative pond, an artefact of the impaired irrigation capacity caused by the struvite earlier in the summer. The impact of the struvite is evidenced by the time required to pump the smaller volumes of effluent in the period to May 2006. The average pumping flowrate dropped from 2.73 L s^{-1} in October 2005 to as low as 0.75 L s^{-1} on 27 February 2006. Following the second cleaning of the pump, the flowrate approached 6 L s^{-1} .

Table 5-6 Daily wastewater flow statistics drawn from days with complete data records and less than 1 mm rainfall.

Statistic	Anaerobic pond		Facultative pond		
	Inflow	Outflow*	Recycled to dairy	Irrigated	Total
n	317	308*	317	317	317
Mean ($\text{m}^3 \text{ d}^{-1}$)	27.9	24.7	17.4	6.7	24.1
Standard deviation ($\text{m}^3 \text{ d}^{-1}$)	7.3	8.1	6.9	27.9	27.7
5 percentile ($\text{m}^3 \text{ d}^{-1}$)	17.7	14.7	8.2	0.0	8.5
Median ($\text{m}^3 \text{ d}^{-1}$)	27.3	23.2	16.9	0.0	17.7
95 Percentile ($\text{m}^3 \text{ d}^{-1}$)	38.3	39.3	28.9	47.0	58.7

* Also the inflow to the facultative pond.

* Days of zero flow following desludging not included.

The total volume of effluent irrigated to land over the monitoring period was 2685 m^3 , which equates to an annual application rate of 2.44 ML y^{-1} or 75 mm yr^{-1} based on the area of the application paddock. Total effluent leaving the facultative pond, including the fraction that is recycled back to the dairy, was 9.0 ML y^{-1} , which places the farm in the third quartile of the rotary dairies surveyed by Calligan (2010). The effluent load amounts to $82.1 \text{ L cow}^{-1} \text{ d}^{-1}$, which is considerably higher than outflows from similar sized dairies in New Zealand ($28.7 - 44.8 \text{ L cow}^{-1} \text{ d}^{-1}$) reported by Sukias et al. (2003). However, when effluent generated is considered only that which leaves the system through irrigation, annual effluent production sits in the bottom 5% of Victorian rotary dairies and is well below New Zealand counterparts at $22.8 \text{ L cow}^{-1} \text{ d}^{-1}$, emphasising the benefits of effluent recycling in terms of water consumption and effluent disposal.

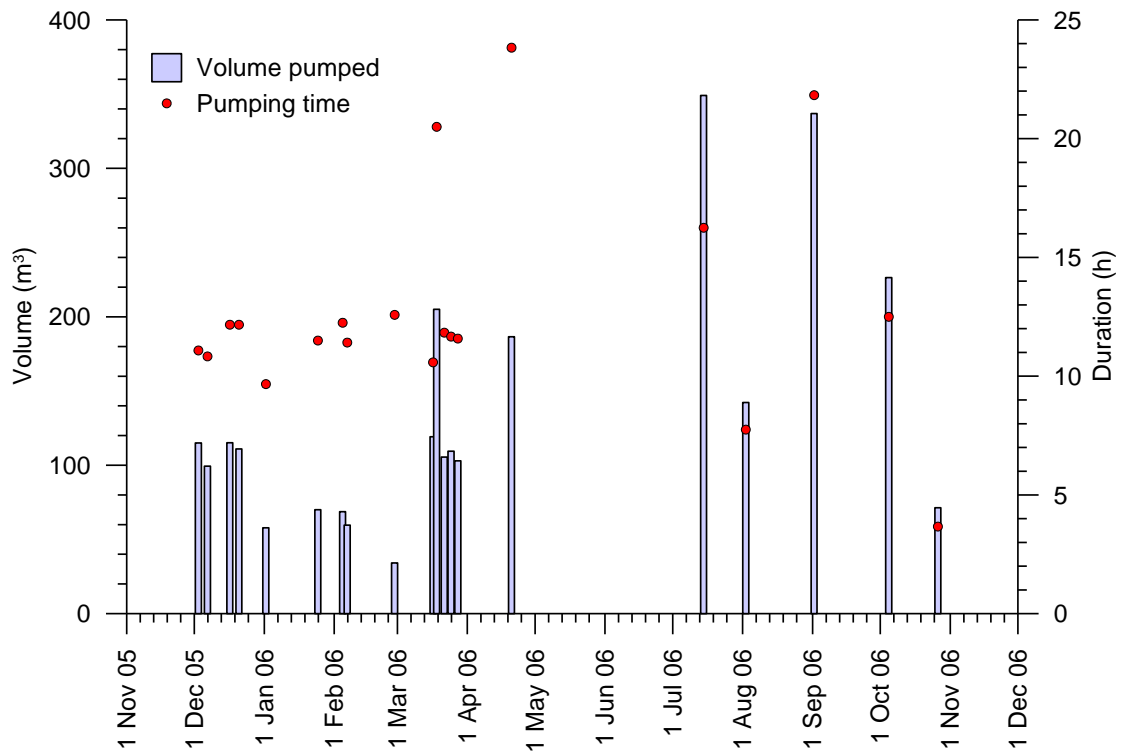


Figure 5-14 Volume and pumping time of effluent irrigation events.

5.5.4 Rainfall, Runoff and Evaporation

Total rainfall, embankment runoff and evaporation to 9 am recorded for each pond over the water balance period are given in Table 5-7. The measured hourly rainfall data and modelled evaporation data may be viewed in Appendix H while the runoff data are given in Appendix I. Note that runoff figures reported in mm represent the depth on the embankments, not the liquid depth contribution to the ponds, thus comparisons with runoff should only be made in volumetric terms. Total evaporation was considerably higher than combined rainfall and runoff (in m³) in both ponds, resulting in net liquid losses to the atmosphere. As shown in Figure 5-15, evaporation exceeded rainfall in most months of the year. Evaporation from both ponds was greater than both the SCA Penman-Monteith estimates and the SILO lake evaporation estimates, highlighting the value of using an estimation method that accurately reflects site conditions and the wastewater. This also corroborates the findings of Parker, Auvermann & Williams (1999) who observed evaporation losses from liquid from manure effluent ponds to be 8.3 to 10.7% higher than losses from clear water. Higher evaporation rates are in part related to elevated liquid temperatures caused by the particulate matter in the effluent. However, in the case of the ponds they are primarily associated with elevated aerodynamic losses caused by the formation of an internal air flow boundary layer arising from the abrupt change in surface roughness between the pond surface and the

surrounding land (Webster & Sherman 1995). In the anaerobic pond, turbulence at the liquid surface created by biogas bubbling further promote aerodynamic losses, which together with higher bulk liquid temperatures cause evaporation to be higher than in the facultative pond.

Table 5-7 Rainfall, runoff and evaporation estimates over the period 30 October 2005 to 5 December 2006.

	<i>Anaerobic pond</i>		<i>Facultative pond</i>	
	mm	m ³	mm	m ³
Rainfall	913	519	913	1283
Runoff from pond embankments	157*	38	157*	30
Evaporation	1497	849	1174	1602

* Depth of runoff on the embankment, not the pond liquid surface.

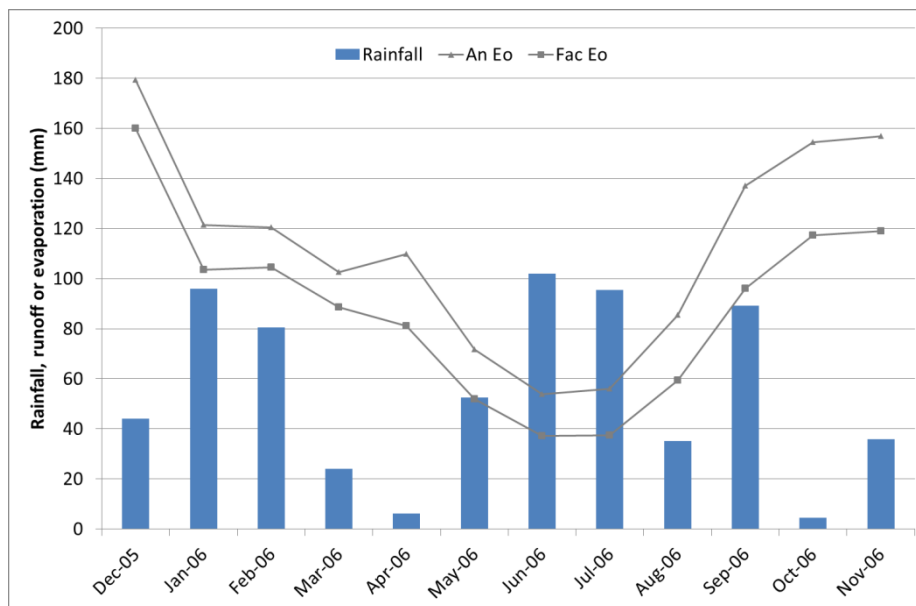


Figure 5-15 Monthly rainfall, embankment runoff and evaporation over the water balance period.

Figure 5-16 compares data from the present study with corresponding data from the nearby SCA weather station that best reflects historical rainfall patterns at the farm (station 568113) and from a SILO data drill from the nearest 5-km grid point location (SILO 2008). Rainfall measured by the AWS rainfall gauge agrees well with records kept by the farmer (Sugarloaf Holsteins gauge) and those from the SCA station. The SILO data drill was located to the southeast of the site which appears to have a different local rainfall pattern. Class A pan evaporation data from the SCA site were only complete up to 30 September 2006. Evaporation estimates for both ponds were

below SCA pan evaporation but higher than corresponding Penman-Monteith estimates confirming the evaporation estimates are within plausible bounds. Conversely, the pond evaporation estimates bounded the SILO shallow lake and pan evaporation estimates.

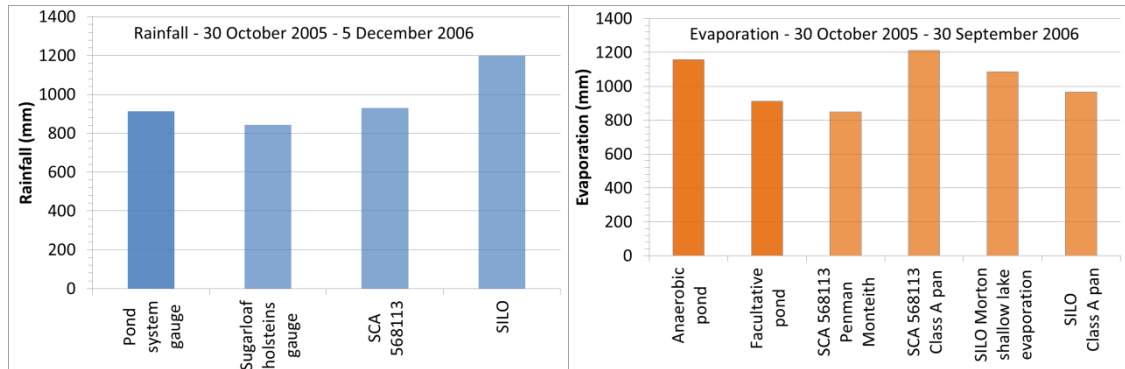


Figure 5-16 Comparisons between rainfall (left) and evaporation (right) data recorded in the present study, by the SCA weather station 568113, and in a SILO data drill.

5.5.5 Seepage Losses and Infiltration

Total and average net daily seepage losses are presented in Table 5-8. The hourly seepage data from which Table 5-8 is drawn are provided in Appendix I. The term net is applied here as seepage from the facultative pond is two orders of magnitude lower than that from the anaerobic pond, which suggests that there may be unaccounted for subsurface inflows into the facultative pond. The anaerobic and facultative ponds were constructed at the same time and should have been subject to similar compaction methods in the process of forming a 'liner' from the in-situ clay soil. It is unlikely, therefore, that there should be such a large discrepancy in seepage from the two ponds. The anaerobic pond is situated uphill relative to the facultative pond such that most of the pond floor sits at a higher elevation than the facultative pond liquid surface. There is a distinct likelihood that some fraction of the seepage leaving the anaerobic pond flows directly towards the facultative pond and intrudes into the liquid body, which would explain the low apparent seepage losses from the facultative pond.

Table 5-8 Net seepage losses over the period 30 October 2005 to 5 December 2006

	<i>Total</i>	<i>Daily average</i>
	m ³	mm d ⁻¹
Anaerobic pond	1045	4.4
Facultative pond	20	0.04

There are a number of other factors that could also help explain the large differences in seepage rates between the two ponds including:

- the embankments on the northern and eastern sides of the anaerobic pond appear to have been formed from excavated soil that may have been drawn predominantly from the upper region of the soil profile. They may therefore contain a lower clay content than the facultative pond floor, much of which would be situated further down the soil profile.
- scouring of the anaerobic pond liner from inflow and desludging.

It is also likely that there is a degree of misattribution of liquid losses between evaporation and seepage; however the effect should be relatively small since close attention was paid to placing sensible bounds on the fitted parameters.

Total seepage losses from the anaerobic pond over the monitoring period were greater than evaporation losses. Average daily seepage was high relative to properly lined ponds that have been found to exhibit leakage rates of around 1.0 mm d^{-1} (Ham 2002a), but not unreasonable for an earthen pond with a poorly compacted native soil liner. In this context apparent seepage from the facultative pond again appears unusually low averaging less than 0.1 mm d^{-1} , adding weight to the hypothesis that seepage from the anaerobic pond is infiltrating the facultative pond.

5.5.6 Final Pond System Water Balance

Over the water balance period, there were three discrete time windows during which wastewater flow and meteorological data were not collected, resulting in gaps in the overall water balance:

1. 11:00 am 30 November to 10:00 am 1 December 2005
2. 1:00 pm 1 May to 10:00 am 3 May 2006
3. 1:00 pm 20 September to 11:00 am 25 September 2006

Table 5-9 and Table 5-10 summarise the collated outputs from the corresponding four contiguous data sets for the anaerobic and facultative ponds, respectively. Comparisons between observed and predicted changes in pond volume show reasonable agreement. Percentage errors, calculated as the difference between observed and predicted change in volume as a fraction of total effluent flow, are all below 10%. Note that the error could not be calculated for the first data set from the anaerobic pond as the probe measuring depth in the pond was removed from service

when pond desludging was commenced and was not returned until the water level had returned to normal levels on 13 November 2005.

The anaerobic pond water balance shows good agreement between inflows and outflows for the large majority of the data. The 17% imbalance calculated between 1 November 2005 and 20 January 2006 was related to the combined effect of inexplicably high effluent flows, infilling for missing data, and slight drift in the readings of the pressure sensor measuring the liquid level. Almost all of the error was generated in the second half of November when effluent started flowing again after desludging and in the first two and a half weeks of January 2006. The drift in the liquid depth data was most noticeable in the last two days of November and between 31 December 2005 and 10 January when the problem was detected and the probe replaced.

The liquid depth measurement error was compounded by poor quality flow data recorded over the last two weeks of November 2005 and the first 2-3 weeks of January 2006. Flow rates measured in the outlet flume in these two episodes were substantially higher than observed over the rest of the water balance period. The elevated flow data measurements coincided with drop-outs in the stage measurement signal that encompassed entire milking sessions and required the fabrication of entire peaks in the interpolation process described in Appendix B. It is therefore possible both that

- a) the elevated flow data were inaccurate, another symptom of the ground loop that caused the signal drop-outs, and
- b) the synthesised peaks for the effluent flows generated in the interpolation were too high.

The 7% error calculated for October/November 2005 in the facultative pond is almost exclusively associated with discrepancies between measured/estimated rainfall/runoff and corresponding changes in liquid level. There would also be error associated with neglecting losses (or gains) associated with manure solids, although this is likely to be so small as to be inconsequential. The error between May and September 2006 is partly due to downward sensor drift evident in the pond depth data.

Table 5-9 Anaerobic pond water balance outputs for periods with contiguous data.

	<i>Units</i>	<i>29 Oct to 30 Nov 2005</i>	<i>1 Dec 2005 to 20 January 2006</i>	<i>20 January to 1 May 2006</i>	<i>3 May to 20 Sep 2006</i>	<i>25 Sep to 5 Dec 2006</i>	<i>SUM</i>	<i>SUM 20 January 2006 onwards</i>
Days	d	32	50	101	140	71	395	312
Influent								
Fresh wastewater and runoff	m ³	195	481	1303	1575	789	4342	3667
Recycled effluent wastewater	m ³	743	1053	1807	2013	1243	6860	5064
Rainfall	m ³	126	74	74	220	25	519	318
Pond embankment runoff	m ³	18	4	9	7	0	38	16
Total in	m³	1083	1612	3193	3815	2057	11760	9064
Effluent		-1165*	-1716	-2745	-3276	-1663	-10564	-7684
Seepage	m ³	-88	-137	-270	-358	-175	-1029	-803
Evaporation	m ³	-66	-148	-227	-195	-213	-849	-635
Total out	m³	-1319	-2001	-3243	-3829	-2051	-12442	-9122
SUM (Predicted change in volume)	m³	-236	-389	-50	-14	6	-683	-58
Observed change in volume	m³	-	-91	9	-10	12	-	11
Absolute error	m³	-	296	59	4	6	-	69
Error as fraction of total outflow	%	-	-17	-2	-0.1	-0.4	-	-1

*Incorporates sludge and effluent outflows.

Table 5-10 Facultative pond water balance outputs for periods with contiguous data.

	<i>Units</i>	<i>1:00 29 Oct to 11:00 30 Nov 2005</i>	<i>10:00 1 Dec 2005 to 7:00 20 January 2006</i>	<i>8:00 20 January to 13:00 1 May 2006</i>	<i>10:00 3 May to 13:00 20 Sep 2006</i>	<i>11:00 25 Sep to 12:00 5 Dec 2006</i>	<i>SUM</i>	<i>SUM 8:00 20 January 2006 onwards</i>
Days	d	32	50	101	140	71	395	312
Influent	m ³	835	1716	2745	3276	1663	10234	7684
Rainfall	m ³	341	176	190	522	58	1287	770
Runoff	m ³	18	6	7	10	0	40	17
Total in	m³	1194	1897	2942	3807	1721	11561	8470
Effluent								
Recycled	m ³	-743	-1053	-1807	-2013	-1243	-6860	-5064
Irrigated	m ³	0	-497	-1069	-830	-297	-2693	-2196
Seepage	m ³	-2	-3	-5	-7	-3	-20	-16
Evaporation	m ³	-132	-297	-471	-325	-381	-1606	-1178
Total out	m³	-877	-1849	-3353	-3175	-1925	-11179	-8453
SUM	m³	317	48	-411	632	-204	382	17
Observed change in volume	m³	262	-233	-251	436	-251	-37	-66
Absolute error	m³	55	281	160	196	47	419	83
Error as fraction of total outflow	%	7	18	-6	7	3	4	2

Average flows into and out of the pond system are plotted in Figure 5-17. On account of uncertainty surrounding the flow data recorded between November 2005 and January 2006, average flows for both ponds were calculated using data collected from 20 January 2006 onward, which amounts to 79% of the available data. Influent makes up a larger fraction of the total inflow to the anaerobic pond (96%) than that to the facultative pond (91%). This difference in inflows is partially offset by the larger rainfall and runoff inflows to the facultative pond arising from its larger surface area. The effect of surface area is also evident in evaporation losses which are much higher in the facultative pond at 14% of total outflows compared with 7% in the anaerobic pond. Seepage losses, however, are much higher from the anaerobic pond (9% total outflow compared to 0.2%) due to the lack of an effective liner or leakage from compromised sections of the liner.

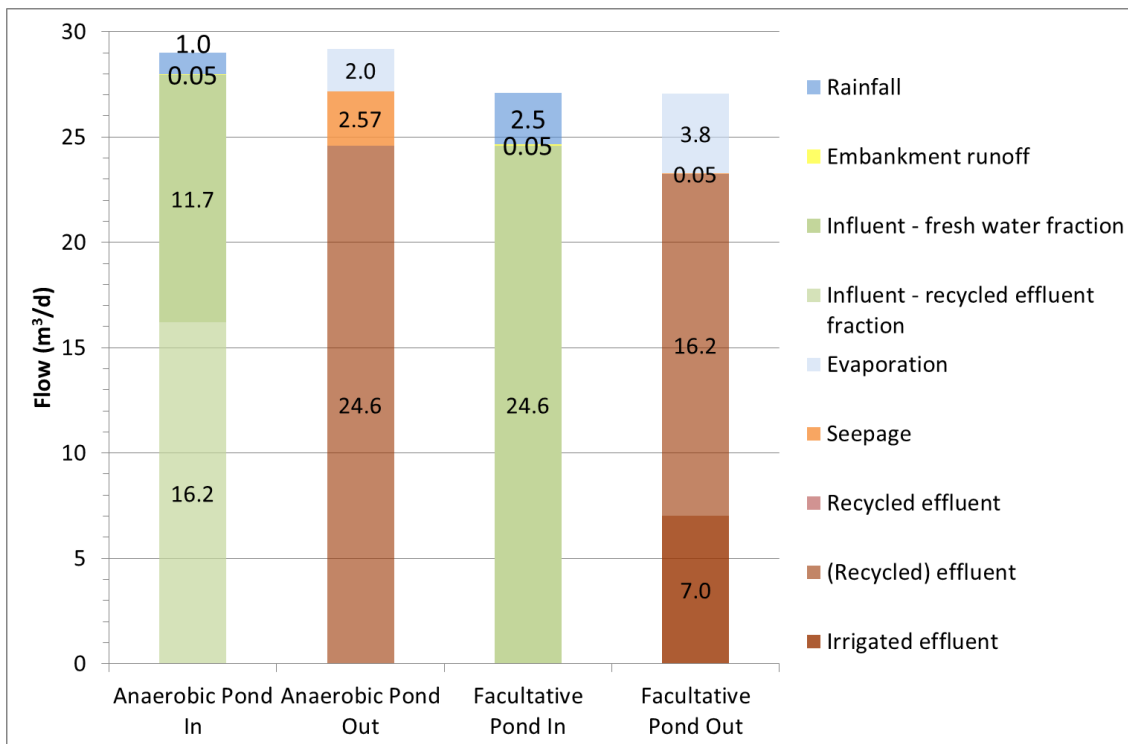


Figure 5-17 Average flows entering and leaving the anaerobic and facultative ponds (20 January – 5 December 2006).

5.6 SUMMARY

This water balance analysis has produced a detailed account of the hydrology of the pond system, quantifying wastewater inflows and outflows as well as rainfall and runoff inputs, and evaporation and seepage losses. The formulation of the water balance involved:

- collection and processing of flow and meteorological data;
- modelling runoff, evaporation and seepage;
- apportioning flows between end uses.

The outputs from the analysis are later used to inform the wastewater treatment modelling described later in Chapters 8 and 9.

Evaporation and seepage were the main unknown quantities of the water balance and were estimated using various modelling approaches sourced from the literature. Five model parameters (three for the facultative pond and two for the anaerobic pond) had to be quantified through a process of calibration by closure whereby the unmeasured residual in the water balance was apportioned between evaporation and seepage by fitting predicted changes in liquid depth or volume to observed data. The standard errors of the calibration fits were large relative to the parameter estimates. The calibrated models produced mostly sensible parameter values and predictions that showed reasonable agreement with other local and published data. Moreover, the models were validated using data from a different period, producing very good agreement between predicted and observed data despite the anaerobic pond validation being applied in a different season and the facultative pond validation period incorporating inflows where the calibration period had not.

The modelling outputs showed that evaporation and seepage losses amounted to 7% and 9%, respectively, of total inflow to the anaerobic pond over the water balance period (29 October 2005 to 5 December 2006). Corresponding losses from the facultative pond were 19% and 0.3%, respectively. Evaporation estimates for both ponds were higher than estimates based on conventional combination methods. This is attributed to particulate matter causing high liquid temperatures and the formation of an internal boundary layer over the pond surface from the land-to-water transition of air flow. Evaporation from the anaerobic pond was particularly high on account of biogas-induced turbulence at the water surface and high bulk liquid temperatures. Seepage from the anaerobic pond was higher than from ponds constructed with well compacted liners, but comparable to losses observed or estimated from other earthen ponds. There is, however, significant uncertainty surrounding the seepage estimates for the facultative pond that arises from indications of seepage from the anaerobic pond infiltrating the facultative pond and causing apparent seepage from the facultative pond to be unusually low. In the absence of other field measurements that could confirm or reject this hypothesis, the seepage estimates for the facultative pond are herein classified as 'net seepage'.

The breakdown of water usage at the dairy showed that while water use per cow is relatively high compared to published data and industry benchmarks, the use of recycled effluent for flood washing the yard results in highly efficient use of fresh water. Over the course of the monitoring period, fresh water usage was $34 \text{ L cow}^{-1} \text{ d}^{-1}$, or 3.7 ML yr^{-1} , constituting 36% of total usage at the dairy. Both fresh and recycled water use showed considerable variability, some of which could be related to seasonality or trends, although statistically speaking these indications could be coincidental. At 2.44 ML y^{-1} , effluent irrigation barely kept pace with net fresh water contributions to the system, despite the low fresh water usage at the dairy and evaporation losses being greater than rainfall inputs for most of the year. The low rate of irrigation was in part caused by the issues with pump impairment, and it would be advisable that the facultative pond is emptied more effectually in future if the system is to perform sustainably.

The model calibration process, followed by model validation, highlighted the difficulties and complexities associated with field data collection and dealing with interactions of different streams in an earthen stabilisation pond system that is used for storing effluent as well as treating it. Despite a significant amount of data to work with, relying on water balance closure to determine several unknown parameters and quantify two separate flows is problematic and it is advised that at least one of the parameters for seepage or evaporation is determined by experimental means. The most straightforward parameter to quantify would be the hydraulic conductivity of the soil liner or the corresponding modified form of this parameter used for a waste sealed seepage.

Chapter 6

POND HYDRAULICS AND HYDRODYNAMICS

Central to the modelling of wastewater treatment in stabilisation ponds is an appropriate approximation or simulation of the flow regime, which requires an understanding of the hydraulic characteristics, internal hydrodynamics and associated propensity for dispersion. This chapter examines the relative influence of the key variables that influence the hydraulics of the Sugarloaf Holsteins stabilisation pond system. It also revisits water quality data from Chapter 4 for indications of pond mixing and describes monitoring and experimental work undertaken to quantify sludge accumulation in the anaerobic pond to and characterise the internal hydrodynamics of the anaerobic pond.

6.1 INTRODUCTION

DSE ponds are not typically mechanically mixed, relying instead on naturally forced advection and diffusion to promote internal mixing. Thus for wastewater treatment modelling purposes they cannot be considered ideal completely mixed reactors. Conversely, being simple, relatively square basins without baffles or other structures to direct the flow and limit dispersion of constituents, they cannot be considered ideal plug flow reactors either. Hence they sit somewhere between the two theoretical ideal mixing regimes, with an array of complex internally and externally driven hydrodynamics causing varying degrees of dispersion or mixing.

There has been very little research dedicated to characterising the hydraulics and hydrodynamics of stabilisation ponds built to the specifications required for the treatment of DSE. DSE ponds typically have long residence times to accommodate the high organic loading of the influent wastewater and to provide sufficient storage to hold incoming wastewater, rainfall and runoff during periods of high rainfall when effluent cannot be irrigated to land (Birchall, Dillon & Wrigley 2008). They also have unique hydraulic loading regimes as dictated by the operation of the dairy and the nature of the hydraulic flushing facilities. A critical feature of anaerobic ponds is the ever-growing sludge blanket, which gradually reduces the active liquid treatment volume and contributes to turbulent mixing through the continuous release of biogas bubbles (Pescod 1996). In part due to the reduction in the solids load effected by preceding anaerobic ponds, facultative ponds are prone to thermal stratification (see Chapter 4), which inhibits vertical mixing. However with typically larger surface areas than anaerobic ponds, they are more exposed to wind-induced mixing (Shilton & Sweeney

2005). The hydrology of DSE pond systems is also important to the hydraulic regime. Reductions in residence time caused by intrusion of rainfall and runoff are counteracted by continuous losses to evaporation, while seepage losses reduce outlet flows by providing an alternative exit route that is distributed across the entire pond basin. The impacts of such hydrologic features are not limited to wastewater residence time, extending also to the concentration, dilution and even dispersion of wastewater constituents within the liquid body.

The impacts of these hydraulic and hydrologic features on the hydrodynamics on the pond system and the associated implications for wastewater modelling are the subject of this chapter.

6.1.1 Objectives, Scope, and Rational

The central aim of the research described in this chapter was to develop an understanding of the pond system hydraulic characteristics and hydrodynamic behaviours that could be used to inform and interpret the wastewater treatment modelling described in Chapters 8 and 9. A key objective was to characterise the pond system in terms of its hydraulic loading and design with direct reference to theory and practice documented in the literature. The second objective was to leverage relevant data gathered from the field monitoring program to corroborate the theoretical understanding of the system. Section 6.2 describes the hydraulic characterisation of the ponds while section 6.4 revisits the physicochemical profiling data presented in Chapter 4 to look at dispersion in the pond supernatant. Section 6.5 builds on the theoretical foundation of section 6.2 and the observations from 6.4 in presenting a theoretical analysis of the environmental forcing that promotes mixing within the pond system. Section 6.3 examines the nature of sludge accumulation in the primary pond using sludge depth measurements also collected during the pond profiling.

The third objective of this research component was to conduct field experimental work to characterise the hydraulics and hydrodynamics of the system. Stabilisation pond hydraulic efficiency is often investigated using tracer studies. However, a number of factors precluded performing such an experiment on the pond system at Sugarloaf Holsteins including the risk to herd health, the difficulties associated with tracer recirculation caused by effluent recycling and rapid fouling of in-situ sensors, amongst others. An alternative to collecting data in the field is to simulate the hydrodynamic behaviour of the system using computational fluid dynamics (CFD) modelling. In order for a CFD model to produce meaningful outputs, however, it needs to be calibrated and

verified against real world data such as that from a tracer studies (Shilton 2001), which as mentioned above was not feasible for this project.

Another approach to characterising the hydrodynamics of water bodies is drogue tracking, which has been previously adapted to stabilisation ponds by Shilton and Kerr (1999) and Barter (2003). The simplicity and applicability to the site conditions of drogue tracking presented an ideal means of generating both quantitative and qualitative data on pond hydrodynamics. Section 6.6 describes the experimental methodology and the results of a drogue tracking study conducted on the anaerobic pond. The final section (6.6.3) of the chapter synthesises the various findings from the research in terms of the implications for wastewater treatment modelling.

6.2 HYDRAULIC CHARACTERISATION

The extent of mixing within a pond is to a large degree determined by its hydraulic design. The hydraulic loading, geometry, shape and the positioning and configuration of the inlet and outlet are all highly influential to pond hydrodynamics (Persson & Wittgren 2003; Agunwamba 2006; Shilton & Sweeney 2005). The effects of each design component are interdependent and can create complex flow patterns including recirculation, mixed zones, dead zones and short-circuiting. This section examines the key characteristics of the pond system to obtain an understanding of the likely hydrodynamic behaviours in each pond.

6.2.1 Hydraulic Loading

The hydraulic loading at the headworks of the system follows the farm milking regime which consists of two milking sessions a day and generates two variable and largely discrete batches of wastewater each day. These batch loads are characterised by relatively low flow (around $0.2\text{--}0.5\text{ L s}^{-1}$) during milking when intermittent hosing of surfaces is performed, a number of small surges (several hundred litres each) from dumping of milking equipment wash and rinse waters, and a large surge ($5\text{--}10\text{ m}^3$) of wastewater generated by flood washing of the holding yard. The wastewater surges are dampened to a varying extent before entering the anaerobic pond by the solids trap. Flow equalisation in the solids trap depends on the extent of clogging of the weeping wall screen with greater clogging resulting in more flow dampening, as well as the occurrence of overtopping due to excessive build-up of captured solids which reduces dampening. Inflow to the pond generally occurs over two blocks of several hours, the exact length of each depending on the total load and the fraction delivered by the flood wash, as well as the rate at which wastewater can pass through the solids

trap. That the total load to the pond occurs over only a fraction of the day has implications for turbulent mixing associated with the inlet jet, short circuiting and the general flow pattern of the pond.

Loading to the facultative pond is also defined by peaks associated with the dairy wash down but dramatically attenuated by the anaerobic pond. Flow into the facultative pond tends therefore to be continuous and does not cease between wash down events as it can to the anaerobic pond. Conversely, however, flow out of the pond occurs only in discrete bursts of pumping (as opposed to gravity driven overflow) that occur each milking when refilling the flood wash tank or pumping directly onto the yard, and when effluent is irrigated to land. As such the volume of liquid held in the pond, and its surface area, vary over time. This makes for more quiescent conditions in the pond and is a factor in the enormous variability in the theoretical HRT.

6.2.2 Hydraulic Retention Times

One of the key factors that determine pond treatment efficiency is the hydraulic retention time (HRT). While the internal hydrodynamics can cause the actual HRT of a pond to differ from the theoretical value, the theoretical HRT indicates the treatment potential. The highly variable hydraulic loading to the system described above causes the HRT in both ponds to be non-stationary. In addition sludge accumulation gradually reduces the supernatant volume and thereby the HRT in the anaerobic pond. The facultative pond acts as a holding pond; thus its volume fluctuates with the rate of pumping for effluent recycling and irrigation. Both ponds are also subject to hydraulic gains from rainfall events that can range from small, gradual additions to large, rapid intrusions, as well as continuous losses to evaporation and seepage as shown in Chapter 4.

To provide a sense of the variability that DSE ponds might exhibit in treatment performance, Figure 6-1 presents plots of theoretical HRTs under typical operating conditions: the anaerobic pond containing 25-75% sludge, and the facultative pond holding a liquid volume between the 5th and 95th percentiles of actual observed liquid volumes (not 5%-95% capacity). HRTs were calculated using average, 5th percentile and 95th percentile daily flow data (24 hours from 3 am). Inflow- and outflow-based HRTs are presented to give an indication of the differences made by hydrological losses and storing effluent. The plots show that variability in flow can potentially cause variability in HRT of more than 50%, which is comparable to the variation caused by fluctuations in supernatant volume caused by sludge accumulation (anaerobic pond) and irrigation (facultative pond). In the anaerobic pond instantaneous HRT based on

inflow can depart from the average by almost 100% and can drop below 10 days at high sludge and flow. Rainfall, evaporation and seepage exaggerate the variability by almost 50%.

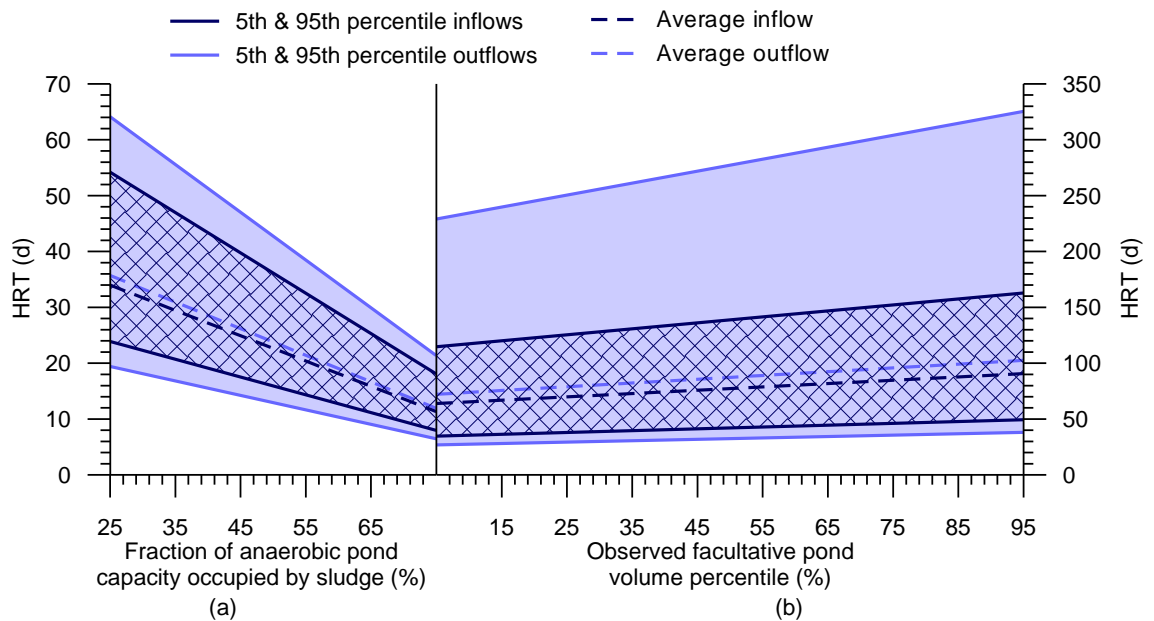


Figure 6-1 Theoretical HRTs for (a) the anaerobic plotted against sludge volume, and (b) the facultative ponds plotted against liquid volume.

Unless there is a problem with equipment such as pump failure that would cause water or recycled effluent consumption at the dairy to be low for an extended period, flows through the anaerobic pond tend to vary stochastically with no consistent correlation with previous flows. Actual HRT is therefore more likely to tend towards that based on average flow, which means that sludge volume is the primary determinant of HRT. At low sludge levels the longer HRT provides a significant buffer against high flows. As the sludge level increases the range of variability decreases but the shorter HRT means that fluctuations in inflows and rainfall events become increasingly influential on treatment efficiency, particularly in winter when biological processes ebb.

The facultative pond is designed to provide storage capacity to the system, accumulating supernatant for weeks or months at a time between irrigation events. This together with the variability in recycling outflows (to yard washing) results in instantaneous (outflow) HRTs in the order of hundreds of days, dwarfing the variability caused by fluctuating inflow and liquid volume. Such extended HRTs would help to effect more complete breakdown of the slowly biodegradable material typically found in DSE. The typical operating range for liquid storage ($1700 - 2450 \text{ m}^3$) causes HRT to vary by around 30%, with the shortest HRTs still being over 20 days. Thus despite

being large flows (on a relative scale) occurring over short periods, irrigation events are unlikely to draw down the pond volume enough to cause wash out of microbial biomass and associated reductions in biological treatment efficiency. If extraction was to occur from the photosynthetically active and very shallow epilimnion, then wash out of algal biomass could occur; however the foot valve on the extraction line is located 40-60 cm below the surface which should ensure most liquid is drawn from the hypolimnion.

The potential for truncated HRTs in the anaerobic pond and extended HRTs in the facultative pond suggests that steady state modelling of this system based on average flow data may not adequately predict system performance. Modelling of hydraulic loading should therefore be dynamic, incorporating variability associated with inflows and outflows and hydrology. In addition, it is also important to incorporate the dynamics of the liquid volume in each pond. Liquid volume in the anaerobic pond should decline as a function of sludge level while in the facultative pond volume must be able to vary with the effluent extraction rate.

6.2.3 Pond Geometries

Table 6-1 presents the geometries of the anaerobic pond at full capacity and when sludge occupies approximately 50% of the pond, and of the facultative pond at full capacity and at the median liquid level observed for the period over which liquid depth was monitored (25 November 2004 to 19 January 2007). The irregular shape of the pond means that dimensions are at best approximate. Horizontal dimensions were measured between the liquid edges at the centre of opposing pond embankments. Floor elevation, average liquid depth and volume were determined using bathymetric data (see Chapter 3 and section 6.3.1) digitised in Surfer (Golden Software, Inc. 2008). Also presented in Table 6-1 are estimates for the dispersion number (d), Peclet number (Pe) and hydraulic efficiency. Dispersion numbers were estimated using an equation derived by Fisher (1967; cited in Persson & Wittgren 2003):

$$d = \frac{0.304[\sqrt{\vartheta_t v W}(W + 2h)^{1.5}]}{(Lh)^{1.5}} \quad (6-1)$$

where

d = dispersion number;

ϑ_t = theoretical HRT (d);

W = pond width (m);

h = average pond depth (m);

L = pond length (m).

Peclet numbers (Pe) were based on a formula produced by Nameche & Vassel (1998) using regression analysis of data from dispersion studies conducted on 11 full scale stabilisation ponds.

$$Pe = 0.31 \frac{L}{W} + 0.055 \frac{L}{h} \quad (6-2)$$

The hydraulic efficiency (also referred to as effective volume) of each pond was calculated using the equation derived by Thackston, Shields & Schroeder (1987) who analysed data from 12 pond dispersion studies.

$$\frac{\vartheta}{\vartheta_t} = 0.84[1 - e^{(-0.59L/W)}] \quad (6-3)$$

where

ϑ = actual mean HRT (d).

Table 6-1 Anaerobic and facultative pond geometries.

	<i>Units</i>	<i>Anaerobic pond</i>		<i>Facultative pond</i>	
		<i>Capacity</i>	<i>~50% sludge</i>	<i>Capacity</i>	<i>Median liquid level</i>
Length, L	m	27		41	40
Width, W	m	24		38	37
L:W		1.1:1		1.1:1	1.1:1
Minimum floor elevation	mAHD	666.28	669.17		664.20
Liquid surface elevation	mAHD	671.07		666.52	666.33
Average liquid depth, h	m	2.18	0.79	1.55	1.44
Liquid volume	m ³	1285	630	2297	2022
Distance from inlet to outlet	m	27			36
Predicted dispersion number, d		1.1	2.9	3.3	3.3
Predicted Peclet number, Pe		1.0	2.2	3.5	3.7
Predicted hydraulic efficiency, ϑ/ϑ_t		0.41		0.39	0.40

Both ponds have a low length to width ratio, making them more prone to eddies, recirculation and other hydrodynamics that cause dispersion (Nameche & Vasel 1998; Persson 2000), and also more likely to develop dead space (Mangelson & Watters 1972). CFD modelling performed by Wood et al. (1995) to examine the hydrodynamics of agricultural waste ponds demonstrated the predisposition of ponds with low length to width ratios to short-circuiting and recirculation patterns. This would certainly be the case for the anaerobic pond as jetting from the inlet would encourage circulatory flow encompassing the whole pond that would help transport influent directly to the outlet (Shilton & Sweeney 2005).

The depth of the active liquid volume in the anaerobic pond varies with sludge accumulation, while in the facultative pond depth varies with irrigation rates. Mangelson & Watters (1972) and Thackston, Shields & Schroeder (1987) found that increasing depth relative to pond width resulted in greater dispersion, increased dead space and reduced actual HRT. Data presented by Pena, Mara & Sanchez (2000) indicated that while the absolute mean HRT increased in an anaerobic pond after desludging, relative to theoretical HRT based on active liquid volume, mean HRT decreased. On the other hand, Pearson, Mara & Arridge (1995) found that varying the depth of facultative ponds made little difference to treatment performance. As suggested by Thackston, Shields & Schroeder (1987), it would appear that for a given length to width ratio (and inlet-outlet arrangement) there is an optimum range for pond depth, below which short-circuiting becomes a problem and above which hydraulic inefficiencies negate benefits afforded by additional volume. Both ponds in this study tend to operate within the range 0.6 – 2.5 m recommended by Thackston, Shields & Schroeder (1987), suggesting that on the whole, the fluctuations in depth should not cause actual HRTs to depart radically from the theoretical values.

Dispersion numbers provide a measure of the extent of mixing, with values greater than three indicating a complete mix flow regime (Sperling & Chernicharo 2005). Based on the Fisher (1967) estimates of d , the anaerobic pond may be classified as completely mixed when sludge occupies a significant fraction of the pond, while the facultative pond would also generally be completely mixed. The Peclet number is the inverse of the dispersion number, with smaller values indicating greater dispersion. According to the findings of Nameche & Vasel (1998), adopting a complete mix regime to model BOD removal by a first order decay reaction in the anaerobic pond (Peclet number between 1.0 and 2.2) would result in maximal prediction errors of around 10%, compared with 15-20% error adopting a plug flow regime. The Peclet numbers of the

facultative pond indicate non-ideal partially mixed conditions, which when represented by either ideal flow regime, produce errors in BOD of up to 15%.

The low predicted values for the hydraulic efficiency again suggest that the ponds are more likely to be prone to short-circuiting or dead zones. The anaerobic pond estimate is comparable to values determined for a similar shaped anaerobic pond (ignoring volume lost to sludge) by Pena et al. (2000) using dispersion experiments. Persson & Wittgren (2003) argue that this aspect of the pond hydraulics is in fact more influential on treatment performance than the degree of mixing. Short-circuiting and dead zones are examined further in section 6.6.

It should be noted here that the hydraulic properties described are typically applied to rectangular shaped ponds. It is unclear the effect the irregularity of the pond basins would have on the hydraulic performance of this system as there is no known published research that compares different pond bathymetries. However it is suggested that the contoured shapes of the pond basins and rounded corners of the anaerobic pond should limit the formation of dead zones, while the large surface area to volume ratios should promote wind-induced mixing.

6.2.4 Inlet-Outlet Configurations

The arrangement and configurations of the inlet and outlet are highly influential to stabilisation pond hydrodynamics and treatment efficiency (Mangelson & Watters 1972; Wood et al. 1998; Agunwamba 2006; Shilton 2001). The inlets to both ponds were perched above the supernatant while the positioning and structures of the outlets adhered to recommended design principles described by Agunwamba (2006) and Shilton & Sweeney (2005). Over the course of the study the anaerobic pond had two inlet configurations. The original configuration was an open pipe poised about 6 cm above the liquid surface in the south western corner. The inlet was modified in October 2005 when a U-bend and a 90° elbow redirecting inflow to the western side of the pond were added to improve the reliability of the flume measurements by dampening peak flow velocity. The outlet of the anaerobic pond was a T-pipe with one opening above the liquid surface and the opposing intake extending some 60-70 cm below the surface. The original and reconfigured anaerobic pond inlet positions can be viewed in the December 2004 and January 2007 plots of Figure 6-3 (section 6.3.2), respectively.

According to the findings of Shilton (2001) who conducted laboratory investigations of the effects of inlet and outlet positioning, the positioning of the outlet in the opposing corner and its submerged intake may help to limit short-circuiting but would have little

bearing on the prevailing flow pattern. Marchand (1997) measured and simulated a pond with an inlet-outlet configuration similar to that of the anaerobic pond of this study. His results indicated the presence of dead zones in the corners opposing the inlet and outlet, short-circuiting and recirculation. The inlet-outlet arrangement and length to width ratio of the anaerobic pond are also similar to the design of an anaerobic pond subjected to dispersion experiments by Pena et al. (2000), who found that this design promoted mixing. Compared with a design where the inlet was essentially on the same side of the pond, the diagonally opposed inlet-outlet arrangement was found to distribute tracer more widely and evenly through the pond. That the inlet of the pond in the present study pours influent into the supernatant from above the surface adds a vertical component to the inflow velocity which may also promote localised turbulent mixing, but is unlikely to alter the general flow pattern of the pond (Shilton & Sweeney 2005). The differential between inlet and outlet elevations should also help minimise short-circuiting (Agunwamba 2006).

The facultative pond inlet-outlet arrangement is shown in Figure 6-7 (section 6.4.1.2). The inlet sits approximately 1.0 m above the pond high water mark and for most of the monitoring period influent poured onto exposed embankment above the water line and cascaded gently into the supernatant. With its momentum dramatically diminished, inflow would have had little influence on the internal hydrodynamics of the pond. Effluent is extracted from the northern corner of the pond about 40-50 cm below the surface. This positioned the pump intake towards the bottom of the thermocline (see Chapter 4), which would limit stratification-induced short-circuiting whereby influent passes directly to the outlet without mixing with the underlying supernatant.

6.3 SLUDGE ACCUMULATION IN THE ANAEROBIC POND

The high concentrations of suspended particulate matter typically found in both raw and pre-treated (screened) DSE cause primary stabilisation ponds to be prone to rapid accumulation of sediments. The continuous growth of the sludge blanket displaces supernatant and gradually erodes treatment efficiency by reducing the HRT. This fundamental trait of DSE ponds is widely recognised but not particularly well characterised, with most data in published literature based on theoretical analysis rather than actual field measurements. This section details the physical characterisation of the sludge blanket and quantification of the rate of its growth. The data generated was used to inform the wastewater modelling described in Chapters 8 and 9 but may also be used to validate current design assumptions regarding sludge accumulation rates and minimum desludging frequencies.

6.3.1 Methodology

Initial measurements of sludge depth were made during the topographical survey of the anaerobic pond (Chapter 3). Measurements were made using the column sampler described in Appendix A. The assembled sampler was lowered from a dinghy to the pond floor to capture a sample of the full undisturbed sludge and liquid column. The sampler was then raised so as to gauge the depth of sludge by visually inspecting its contents. This was repeated at 59 locations in the pond, the exact position of each being recorded by sighting a reflector placed atop the sampler from a theodolite situated on the embankment.

Repeated measurements of sludge depth were made on each of the six water quality profiling runs performed on the anaerobic pond described in Chapter 6, at a minimum of 9 locations in the pond on each run. Adopting the approach taken by Nelson & Jimenez (2000), each set of sludge depth measurements was used to create interpolated surfaces for mapping using the Surfer 8 surface mapping software (Golden Software, Inc. 2008). Sludge volumes were calculated as 'negative fill' in the Surfer 'grid volume' computation using average sludge depth as the lower surface.

It should be noted here that there was no measurable accumulation of sludge in the facultative pond (greater than a depth of 10 cm) observed during any of the profiling runs, hence the focus in this section on the anaerobic pond.

6.3.2 Sludge Blanket Size and Shape

At the time of the initial topographical survey, accumulated sludge had already significantly curtailed the active liquid volume of the anaerobic pond, reducing it by 51% to 634 m³. The anaerobic pond was partially desludged on 26 October 2005 when the sludge blanket occupied approximately 66% of the pond. According to the sludge accumulation model described by Barth & Kroes (1985), the pond was on the verge of failure. Indeed the remaining active treatment volume (385 m³) was well below the ideal volume (831 m³) based on the observed daily volatile solids loading to the pond (see Chapter 7) and the design loading rate for the region (Birchall, Dillon & Wrigley 2008). This would explain the declining effluent quality leading up to desludging noted in Chapter 7 (section 4.1). Table 6-2 provides a summary of sludge volumes recorded over the course of the study and associated free liquid volumes and theoretical HRTs. Note that in August 2006 the sludge volume appears to decrease. This is related to the bulking effect of desludging which is discussed in section 6.3.4. The survey data from

which sludge volumes were estimated are presented together with the water profiling data in Appendix G.

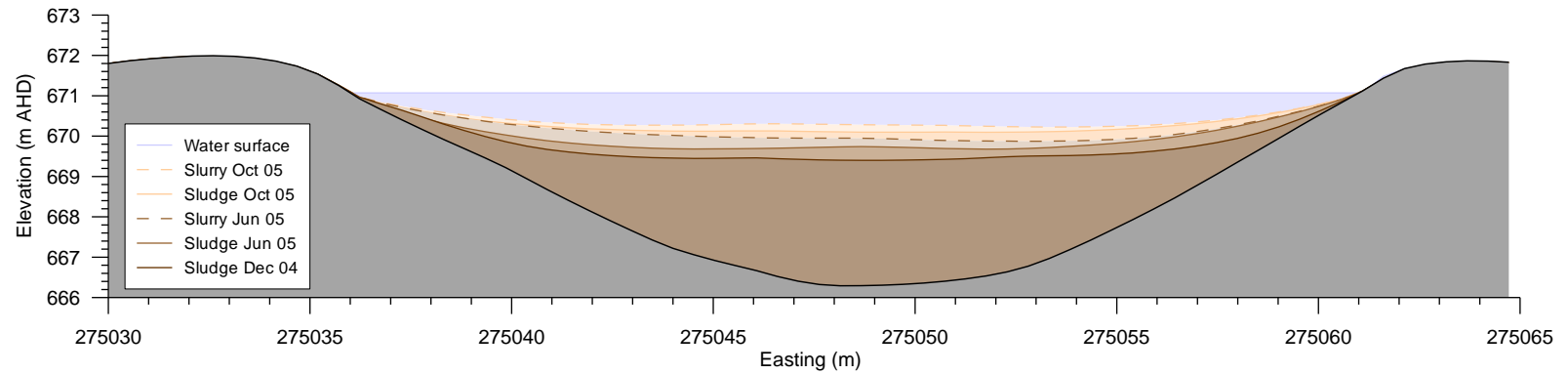
Table 6-2 Sludge volume estimates, associated active treatment volumes and theoretical HRTs and average slurry layer depths (standard deviations given in parentheses).

<i>Date</i>	<i>Sludge volume</i>		<i>Active supernatant treatment volume m^3</i>	<i>Theoretical HRT <i>d</i></i>	<i>Average depth of active slurry layer <i>m</i></i>	
	m^3	%*				
Pre-desludging						
8/12/2004	630	49%	655	23	-	
9/06/2005	724	56%	561	20	0.16	(0.10)
19/10/2005	848	66%	437	16	0.15	(0.09)
Post-desludging						
31/10/2005*	196	15	1089	39	-	
1/03/2006	504	39	781	28	0.23	(0.07)
22/05/2006	567	44	717	26	0.17	(0.05)
21/08/2006	507	39	777	28	0.16	(0.09)
12/01/2007	590	46	695	25	0.09	(0.06)

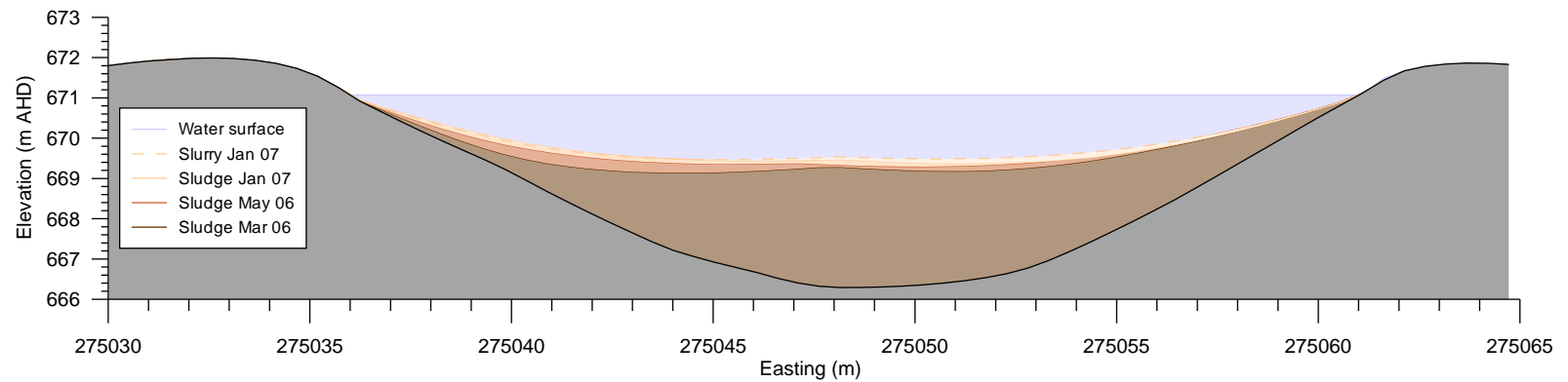
* Calculated as a fraction of total pond capacity.

* Estimated from the volume of sludge removed during desludging (see section 6.3.4).

Figure 6-2 depicts an east-to-west cross-section of the anaerobic pond and sludge levels measured prior to and after desludging. The position and view of the pond cross-section is shown in Figure 6-3, overlain on contour plots of the first set of the sludge measurements made in December 2004 and the last measurements made in January 2007. It is evident in both figures that sludge was reasonably evenly distributed through the pond. Sludge depth measurements performed on 8 December 2004 and 9 June 2005 were of a sufficient resolution to discern peaks and depressions in the sludge surface. The sludge blanket exhibited a shallow concave shape with a thinning layer of sludge remaining high on the embankment faces near the water surface. Otherwise there were no distinct features that could be attributed to preferential deposition close to the inlet, scouring by inflow, concentrated biogas activity or other processes that might deform the sludge blanket. Whilst not of the same resolution, subsequent sludge depth measurements confirmed that sludge was not accumulating more rapidly in any particular region of the pond. The contour plot of the January 2007 sludge measurements given in Figure 6-3 shows a similar concave pattern to the December 2004 plot, with perhaps a slight shift in the location of the apex, most likely related to the altered inlet configuration.



(a) Pre-desludging



(b) Post-desludging

Figure 6-2 Sludge and slurry levels in the anaerobic pond (a) over the period 8 December 2004 and 19 October 2005 prior to desludging and (b) over the period 30 October 2005 and 12 January 2007 following desludging.

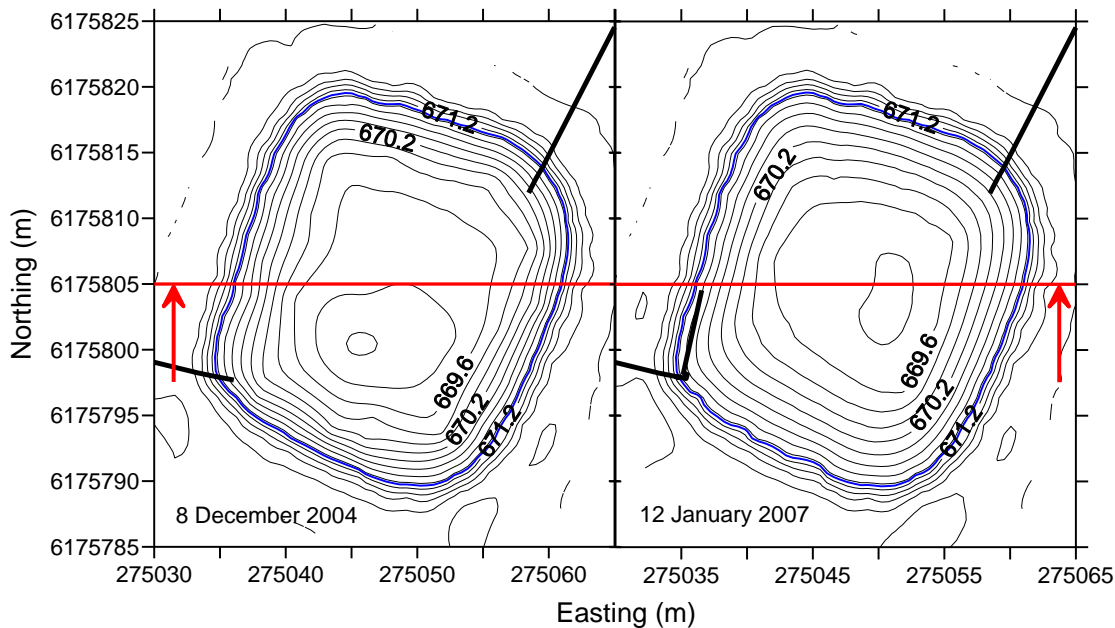


Figure 6-3 Sludge surfaces mapped on 8 December 2004 and 12 January 2007. The red line and arrows indicate the cross-section used in Figure 6-2.

Overall it seems that, contrary to the observations of sludge peaks and valleys in urban anaerobic ponds reported by Nelson & Jimenez (2000), sludge appeared to settle more evenly across the pond. The concave shape is similar to the ‘funnel’ shape of a second sludge blanket observed by Pena, Mara & Sanchez (2000) in a pond of similar length to width ratio, but with a far less exaggerated central depression, and accords with the sludge deposition model proposed by Smith (1980). A number of factors could contribute to the uniform sludge surface including:

- the ‘roiling’ action caused by biogas from anaerobic digestion (Smith 1980; Barth & Kroes 1985);
- settlement and consolidation promoted by the steep pond embankments;
- rapid and extensive distribution of influent solids (Barth & Kroes 1985).

The uniform sludge surface would suggest that at workable sludge volumes (less than 70%), flow through the pond is less likely to be ‘channelled’ by accumulating sludge as observed in longer, square-bottomed ponds through dispersion studies by Pena, Mara & Sanchez (2000) and CFD modelling by Vega et al. (2003). Nonetheless the sludge blanket significantly reduces the HRT of the pond, causing influent to ‘sheet’ across the sludge surface more directly towards the outlet.

6.3.3 Active Sludge or Slurry Layer

Physiochemical profiling of the anaerobic pond supernatant revealed that atop the more solids-laden sludge blanket sits a layer of quasi-suspended sediment. Coined the 'active sludge' or 'slurry' layer, this stratum of unsettled and presumably undigested material has previously been observed in dairy waste stabilisation ponds by Nordstedt & Baldwin (1975), Barth & Kroes (1985), Dawson (2003) and Mukhtar et al. (2004). The presence of this surficial slurry layer was detected by drops in both pH and EC immediately above the measured sludge surface and confirmed through visual inspection of column samples. While contact with the underlying sludge would also cause pH and EC readings to drop, the difference between slurry and supernatant pH and EC levels was not as pronounced as that between sludge and supernatant levels, thus allowing the slurry layer to be identified without the need to extract a sample.

The depth of the slurry layer varied between 0 and 30 cm and generally averaged close to 0.15 m (refer to Table 6-2). The slurry layer observed on the June and October 2005 profiling runs prior to desludging is shown in Figure 6-2 (a). The December 2004 survey did not incorporate physiochemical profiling, thus the slurry layer was not measured. The slurry layer was detected on all subsequent profiling runs, however for clarity it has not been plotted for March and August 2006 in Figure 6-2 (b).

6.3.4 Accumulation Rate

Figure 6-4 plots accumulated sludge against time, with days elapsed measured from pond start-up or desludging. The unfilled data points indicate sludge measurements made in March, May and August 2006 following desludging of the pond. Desludging was performed between 26 and 30 October 2005 using a 7000-L tractor-driven slurry tanker. The operator reported extracting 100 loads, equating to 700 m³ sludge removed. However, an estimate based on a water balance puts the figure closer to 660 m³, which would appear reasonable given that it is likely that the tanker would often have been filled to just below capacity. A desludging volume of 660 m³ equates to approximately 196 m³ remaining in the pond. 196 m³ was thus subtracted from the observed post-desludging volumes to determine accumulated sludge presented in Figure 6-4.

The slope of the fitted line gives a long-term average sludge accumulation rate of 0.73 m³ d⁻¹ with a 95% confidence interval of ± 0.07 m³ d⁻¹. It is recognised that this simple linear model does not reflect the non-linear accumulation process described by Barth & Kroes (1985), but has been applied to 'average out' temporal variability in the absence

of a non-linear model equation against which to fit the data. This long-term average provides the basis for the specific accumulation rates given below in section 6.3.4.1 as well as the sludge reactor hydraulics used in the anaerobic pond model described in Chapters 8 and 9.

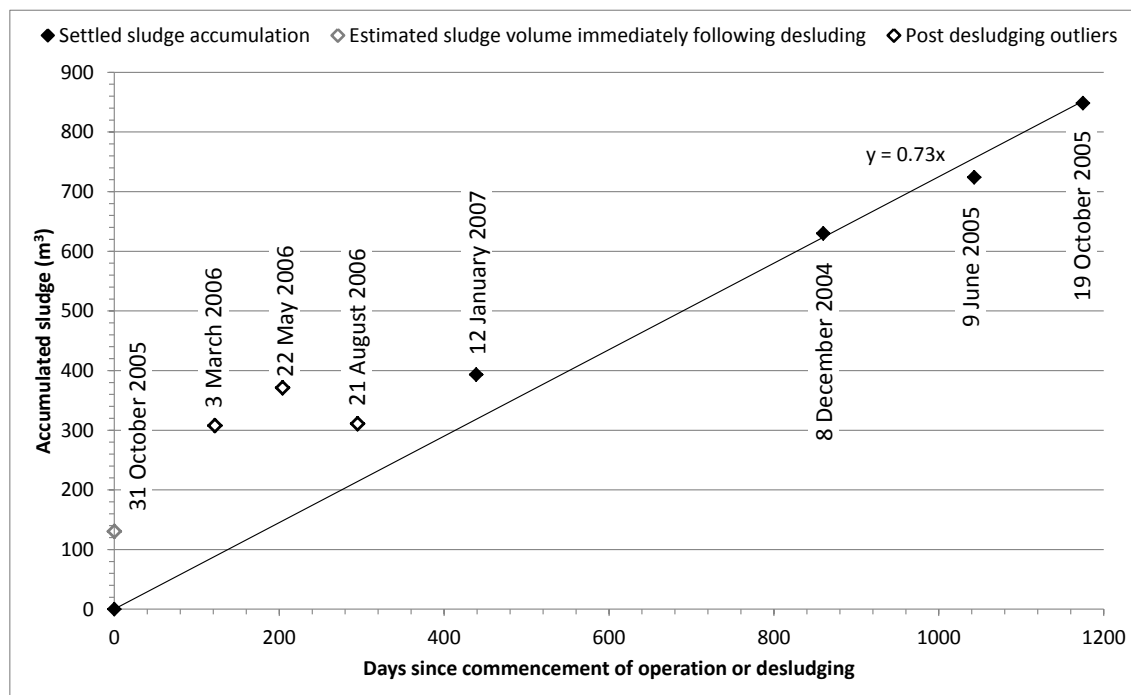


Figure 6-4 Sludge accumulation in the anaerobic pond plotted against time. The unfilled points were considered outliers and have not been included in the linear fit.

The unfilled points have been omitted from the main trend line fit because they are thought to reflect abnormal conditions. Samples of the sludge collected on those dates contained significantly lower solids concentrations than sludge samples collected immediately before desludging (19 October 2005) and 15 months later in January 2007 (refer to Chapter 7). The low solids concentrations, together with the elevated sludge depths, are believed to be related to sludge bulking caused by aeration. On approximately every tenth load, the operator would reverse the flow on the vacuum pump to mix the sludge before extracting the next load. This mixing is thought to have resuspended fine sludge particles, forming an exaggerated hindered settling zone above a heavier sludge layer at the bottom (from which the slurry tanker continued to extract the sludge). Following the completion of desludging, upward force exerted by rising biogas bubbles is thought to have slowed the resettling of the fine suspended sludge particles, causing the sludge level to remain artificially high until at least May 2006. By August, the temperature of the sludge had dropped below 10°C, slowing

biogas production and the sludge appeared to be consolidating, although the solids concentrations were still low.

Before desludging was undertaken, the pond had been operating for just over three years, providing ample time for sludge to undergo compaction and consolidation (Barth & Kroes 1985) arising from the stress imparted by overlying sludge and supernatant and the realignment of sludge particles (Abusam & Keesman 2009). The total solids content immediately prior to desludging was 7.7%. After desludging, sludge solids content varied between 4.6% and 5.2%. By January 2007, almost 15 months after desludging, the solids content had returned to 7.4%. Figure 6-4 also presents an estimate for the volume of the bulked sludge immediately after desludging (indicated by the square grey point). The estimate was produced by applying the fixed solids concentration from the March 2006 sample to the load contained in the remaining 196 m³ of sludge left after desludging (based on the solids concentration before desludging). Given that the solids concentration was probably higher March in 2006 than immediately after desludging (due to settlement), accumulation of sludge relative to the bulked sludge estimate of 327 m³ is comparable to the long-term average until the sludge begins to consolidate in winter. Analysis of the changes in sludge constituent loads after desludging show that mass accumulation in the sludge was similar to pre-desludging rates (see Figure 7-6 in Chapter 7), lending further support to the bulking hypothesis.

Table 6-3 gives the long-term average sludge accumulation rate expressed on a per cow basis and in terms of the fraction of the total pond capacity. The per cow accumulation rate is considerably higher than the rates of 0.18 and 0.25 m³ per cow per year measured by Sweeten & Wolfe (1994) in two similarly-loaded 12 year-old primary anaerobic ponds, although Sweeten & Wolfe (1994) did acknowledge that the observed sludge volumes were “surprisingly low”. The per cow rates were an order of magnitude lower than figures produced by Barth & Kroes (1985), presumably because the systems they observed received all the waste from permanently housed herds.

Table 6-3 Volumetric sludge accumulation rates

<i>Units</i>	<i>Rate</i>
m ³ d ⁻¹	0.73
m ³ cow ⁻¹ y ⁻¹	0.88
% y ⁻¹	21%

6.3.4.1 Specific accumulation rates

Sludge accumulation is typically benchmarked in terms of solids or organic loading. The specific accumulation rates presented in Table 6-4 are based on the anaerobic pond influent loading rates presented in section 3.3.1 of Chapter 7 and are compared with the limited data available in the literature. The TS specific accumulation rate is similar to the US ASAE (2004) standard that was originally measured by Barth & Kroes (1985) and has been adopted here in Australia. The observed TVS specific accumulation rate also agrees with the corresponding range reported by Barth & Kroes (1985). The TVS rates calculated from data presented by Hill et al. (1980) are considerably lower, presumably due to lower settling efficiency in their laboratory-scale pond. Since sludge is formed by particulate material, specific accumulation rates are also given for TSS, TVSS and particulate COD, which are more commonly-used parameters in wastewater treatment reporting and modelling.

Table 6-4 Specific sludge accumulation rates measured in this study and reported elsewhere.

<i>Reference</i>	<i>Basis</i>	<i>m³ kg⁻¹ of TS added</i>	<i>m³ kg⁻¹ TVS added</i>	<i>m³ kg⁻¹ TSS added</i>	<i>m³ kg⁻¹ TVSS added</i>	<i>m³ kg⁻¹ particulate COD added</i>
This study	Field observations	0.0043	0.0067	0.0085	0.0100	0.0066
Nordstedt & Baldwin (1975)	Field observations	0.0033	0.0038			
Hill et al. (1981)	Laboratory tests		0.0019 - 0.0029			
Barth & Kroes (1985)	Field observations	0.0037 - 0.0056	0.0049 - 0.0074			
ASAE (2004); Skerman (2004a) and Birchall et al. (2008)	Recommended design estimate	0.0045				

6.4 WATER QUALITY INDICATORS OF MIXING

This section revisits the data presented in Chapter 5 to examine hydrodynamic behaviours that may be discerned from water quality data.

6.4.1 Transverse Dispersion

As a gross measure of dissolved inorganic constituents, it is proposed that electrical conductivity (EC) can be used to examine dispersion when measured at multiple locations within a reactor. A large fraction of the dissolved salts that constitute EC in dairy shed wastewater including chloride, K and Na are largely unaffected by the

dominant natural treatment processes in stabilisation ponds. Concentrations of other major ionic species, including bicarbonate, Ca, Mg, ammonium and phosphate, however, are subject to changes over time caused by physical, chemical and biological processes. The presence of spatial EC gradients should therefore indicate a lack of dispersion associated with plug flow mass transfer as opposed to complete mixing. For example, a consistent EC gradient in the supernatant ranging from influent to effluent levels following the direction of flow would indicate conditions approximating plug flow. A lack of gradient combined with very different influent and effluent EC levels would indicate extensive dispersion and conditions approximating a completely mixed reactor. The data from which the following analyses are drawn are presented in Appendix G.

6.4.1.1 Anaerobic pond

Influent EC levels were generally lower than EC levels both within the anaerobic pond and in the effluent throughout the monitoring period, but particularly over the autumn-winter period of 2006 (see Chapter 4). This would indicate increases in bicarbonate ions caused by the response of the bicarbonate equilibrium to production of CO₂, dissolution of precipitates such as Ca carbonate or phosphate minerals and/or that anaerobic decomposition of organic material was releasing inorganic species (for example mineralisation of organic N releasing ammonium). As such, low rates of dispersion should be indicated by rising gradients in EC radiating from the inlet, particularly at the surface as more dilute and less dense plugs of influent wastewater remain close to the surface and move towards the outlet unless wind, biogas or some other forcing causes it to mix with surrounding fluid.

Figure 6-5 and Figure 6-6 show EC contours produced from data collected during each profiling event at the surface (5 cm) where the most variation in supernatant physicochemical parameters was observed, and immediately above the sludge blanket (the depth of which varies over time). Note that the perimeters of the contour plots at depth are smaller than the surface plots on account of the tapered shape of the pond basin. Influent EC from the most recent flood wash was estimated to be 1.05 times the conductivity of effluent released in the flood wash to account for salts added by fresh manure and cleaning chemicals (see Chapter 7).

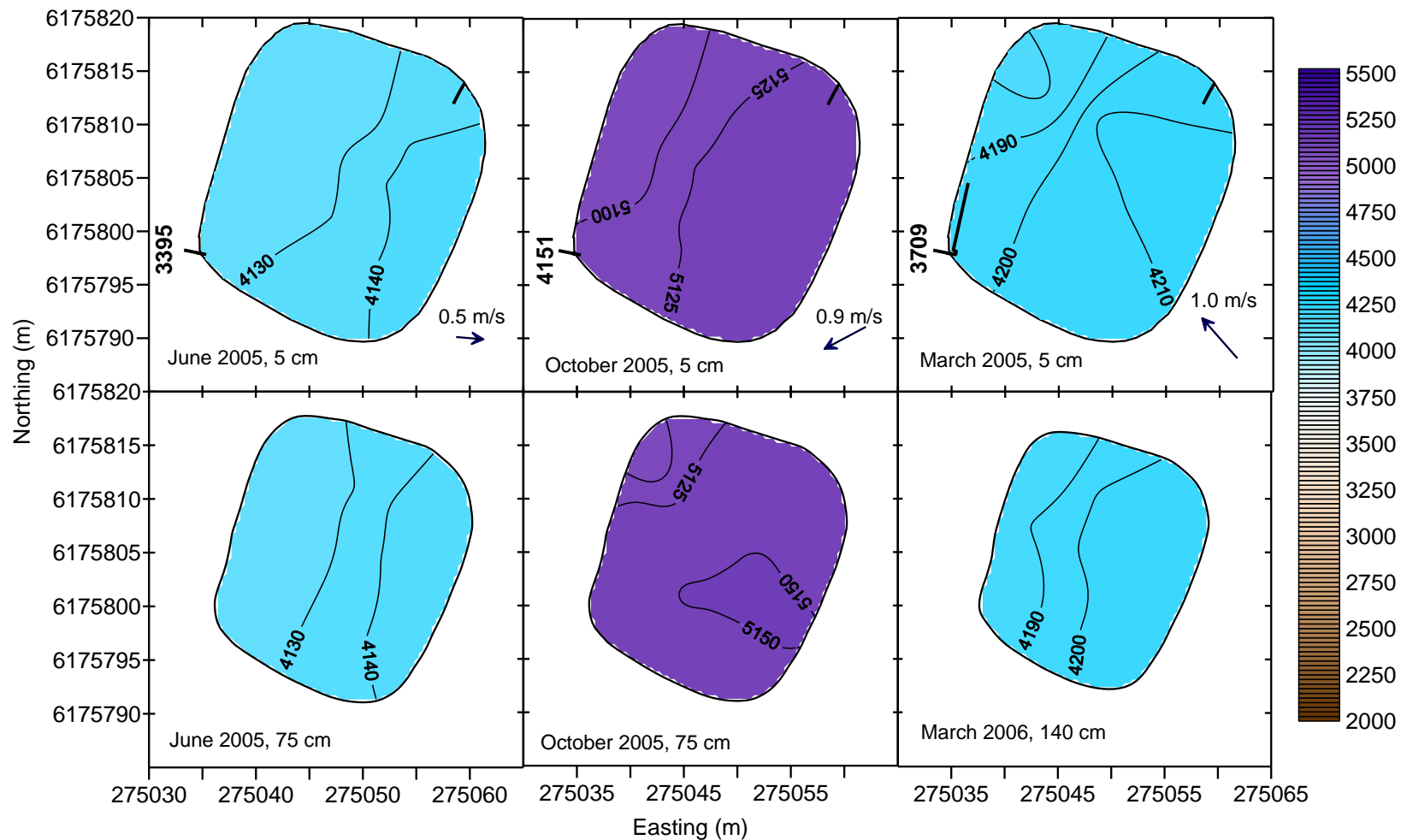


Figure 6-5 Conductivity contours ($\mu\text{S cm}^{-1}$) at the surface (top) and at depth (bottom) in the anaerobic pond for June, October 2005 and March 2006. Inlet EC is given adjacent to the inlet on the left hand side of the surface contour plots. Average wind speed and direction are given in the bottom right corner of the surface plots. Note the change in inlet configuration after the October 2005 profiling event.

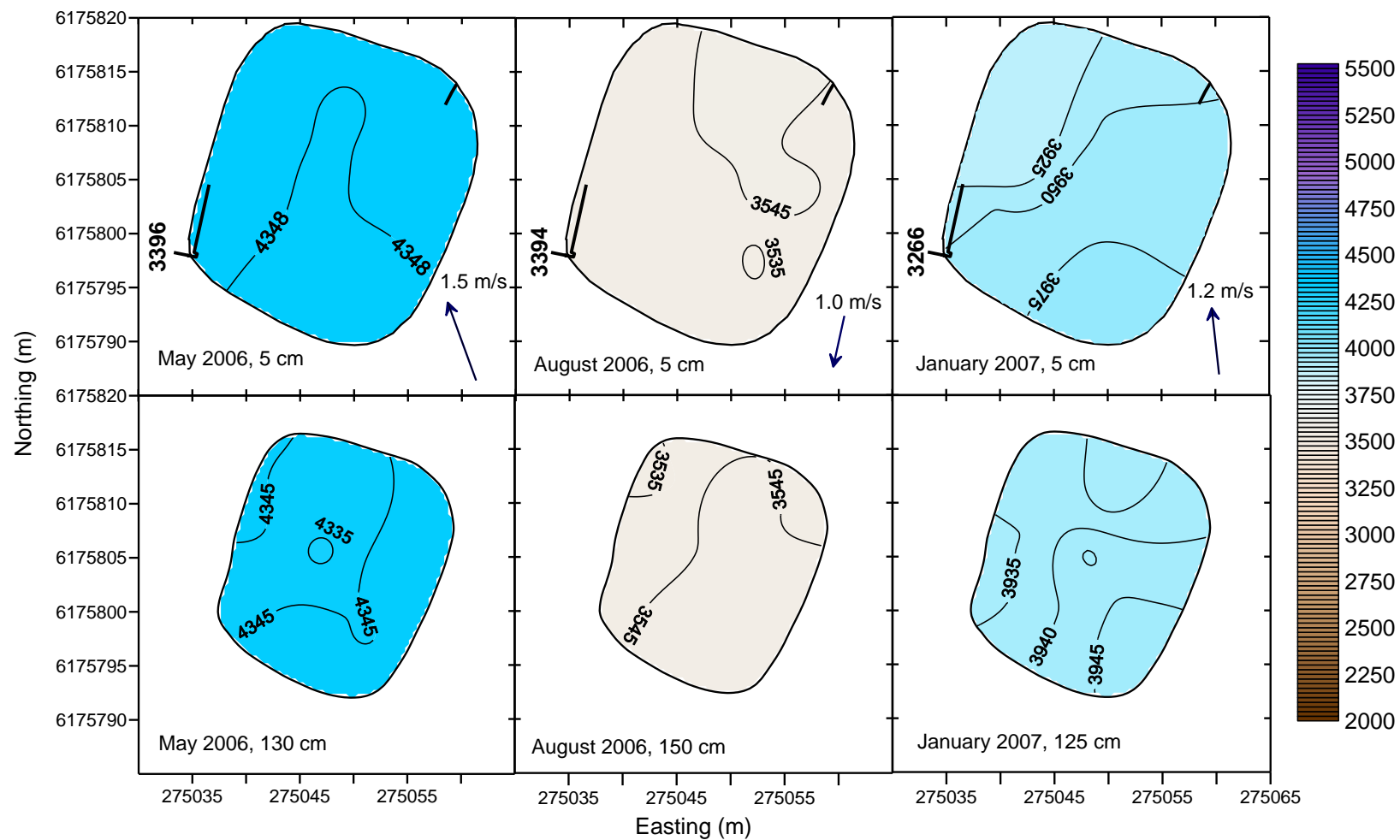


Figure 6-6 Conductivity contours ($\mu\text{S cm}^{-1}$) at the surface (top) and at depth (bottom) in the anaerobic pond for May, August 2006 and January 2007.

Four of the six contour plots (June, October, March 2005 and January 2007) exhibit gradients moving from the inlet to the outlet that could reflect plug flow at the pond surface. Importantly, however, the gradients are only very slight (between 0.5% and 2% across the pond - only just above the 0.5% accuracy limit of the probe), despite larger differentials between the influent EC and levels closest to the inlet (3-20%). In May and August 2006 when the differences between influent and effluent levels had been consistently high (Chapter 4), the gradients are marginal at most. This would suggest that transverse dispersion is significant, causing the supernatant to tend towards a well-mixed state. Transverse dispersion in the anaerobic pond may be caused by the turbulence generated by the inflow jet and wind-induced advection, the effects of which are explored further in section 6.5.

EC contours just above the sludge tended to mimic those at the surface, except on the January 2007 profiling event, when a strong gradient observed at the surface was almost non-existent at depth. Given the timing, this gradient appears to be related to the constrained mixing at the inlet identified in Chapter 4. At the peak of summer the pond becomes mildly stratified due to the very high ambient temperature, which would limit vertical mixing. This would cause slightly less saline (and therefore less dense) influent from the flood wash, which had been released not long before the profiling commenced, to displace supernatant rather than mix with it and as a result remain close to the surface. The confinement of the influent slug to the region just north of the inlet created localised vertical and horizontal EC gradients where inflow would have slowed as its momentum was diminished (refer to section 6.6). Meanwhile supernatant just above the sludge line appears largely unaffected by the inflow, exhibiting an EC gradient similar to that in the corresponding August 2006 contour plot.

6.4.1.2 Facultative pond

Contour plots of EC levels in the facultative pond at the surface (5 cm), at mid-depth (75 or 100 cm) and just above the bottom of the pond (varying depths) are presented in Figure 6-7, Figure 6-8 and Figure 6-9. As with the anaerobic pond plots, wind direction and velocity and influent EC are given in the surface plots. Influent EC was drawn from the in-pond EC data, which given the lack of EC gradients revealed in the previous section, may be considered to closely resemble EC levels in effluent leaving the pond.

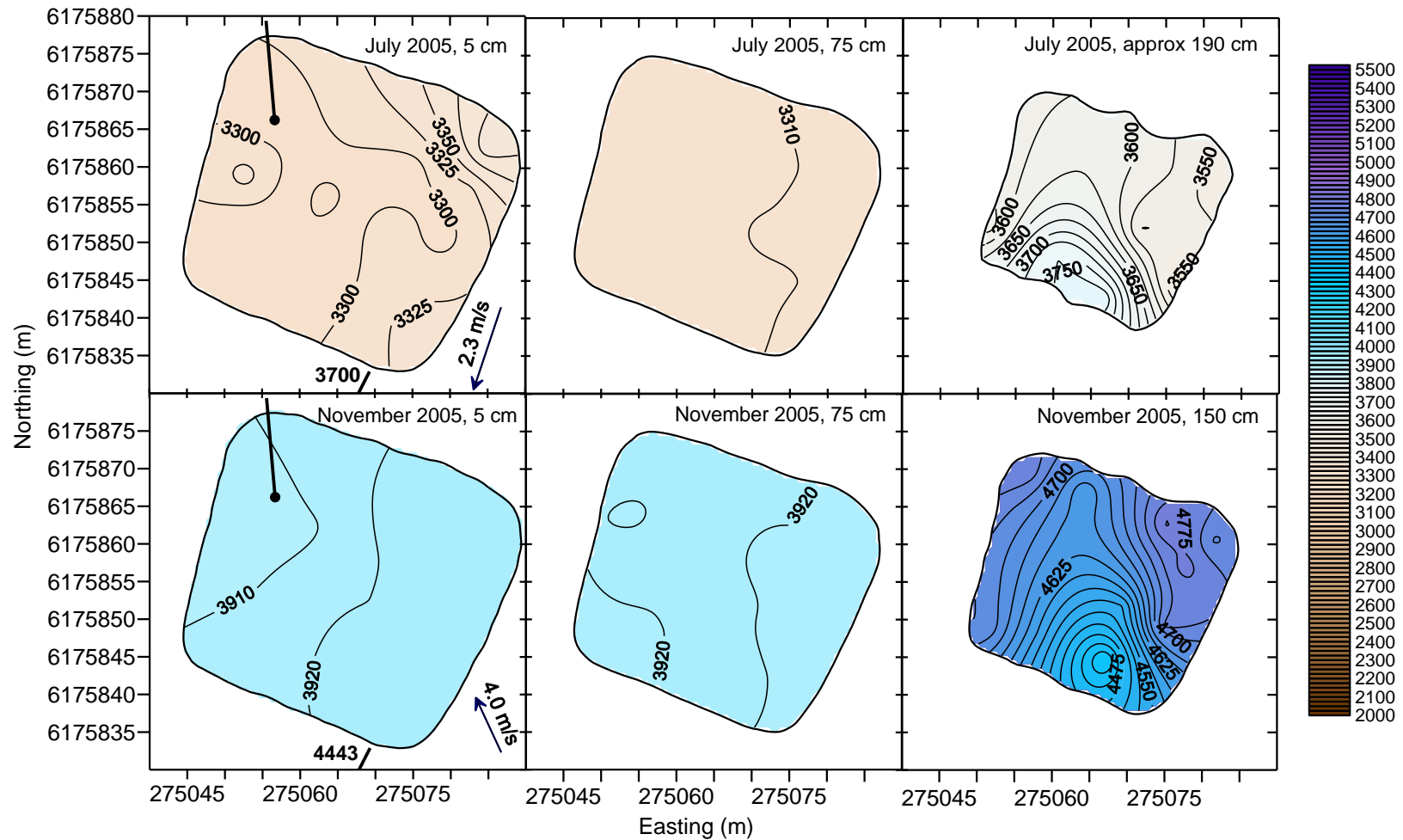


Figure 6-7 Conductivity contours ($\mu\text{S cm}^{-1}$) at the surface, mid-depth and the bottom of the facultative pond for July (top) and November 2005. Inlet EC is given adjacent to the inlet on the bottom right of the surface contour plots. Average wind speed and direction are given in the bottom right corner of the surface plots.

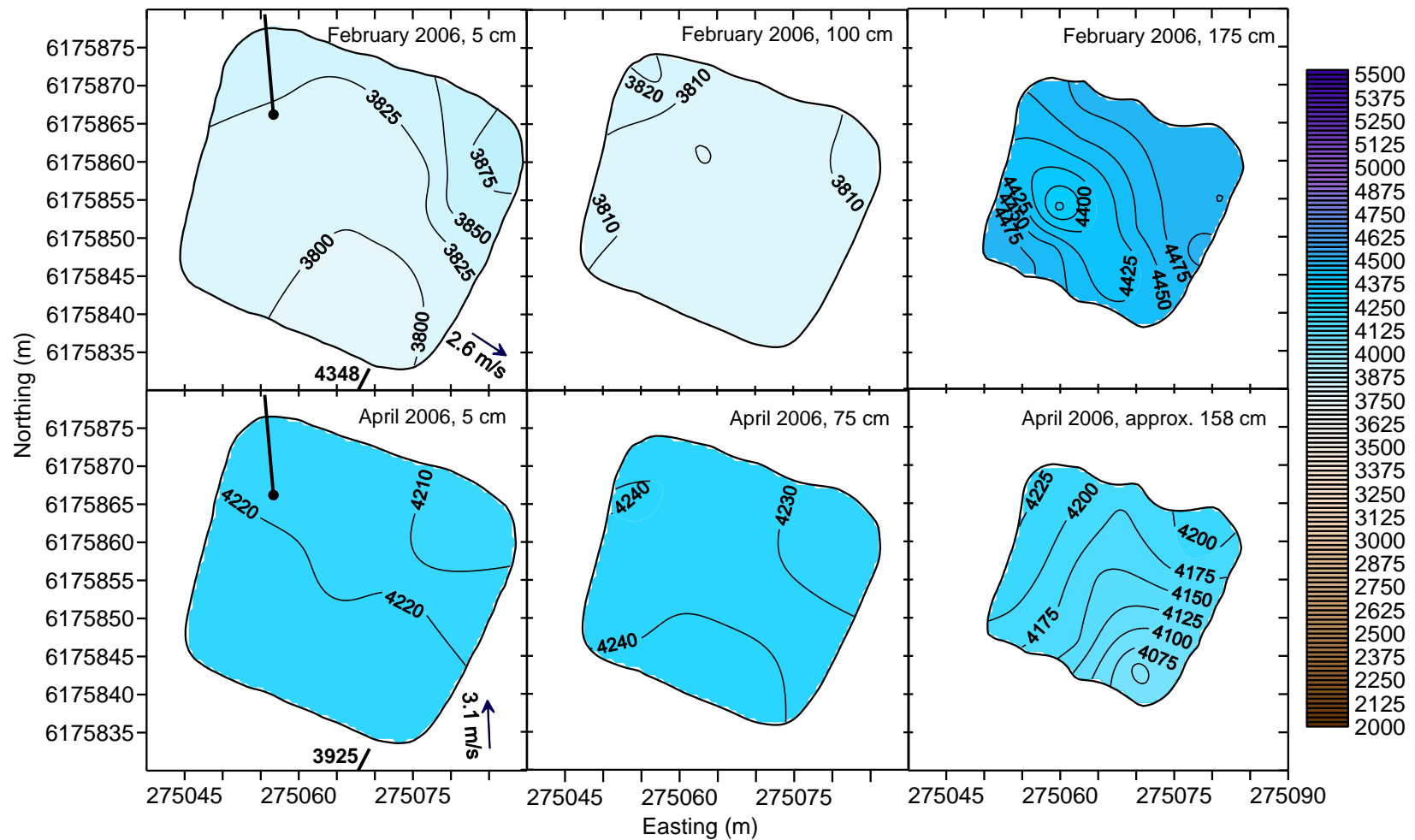


Figure 6-8 Conductivity contours ($\mu\text{S cm}^{-1}$) at the surface, mid-depth and the bottom of the facultative pond for February (top) and April (bottom) 2006.

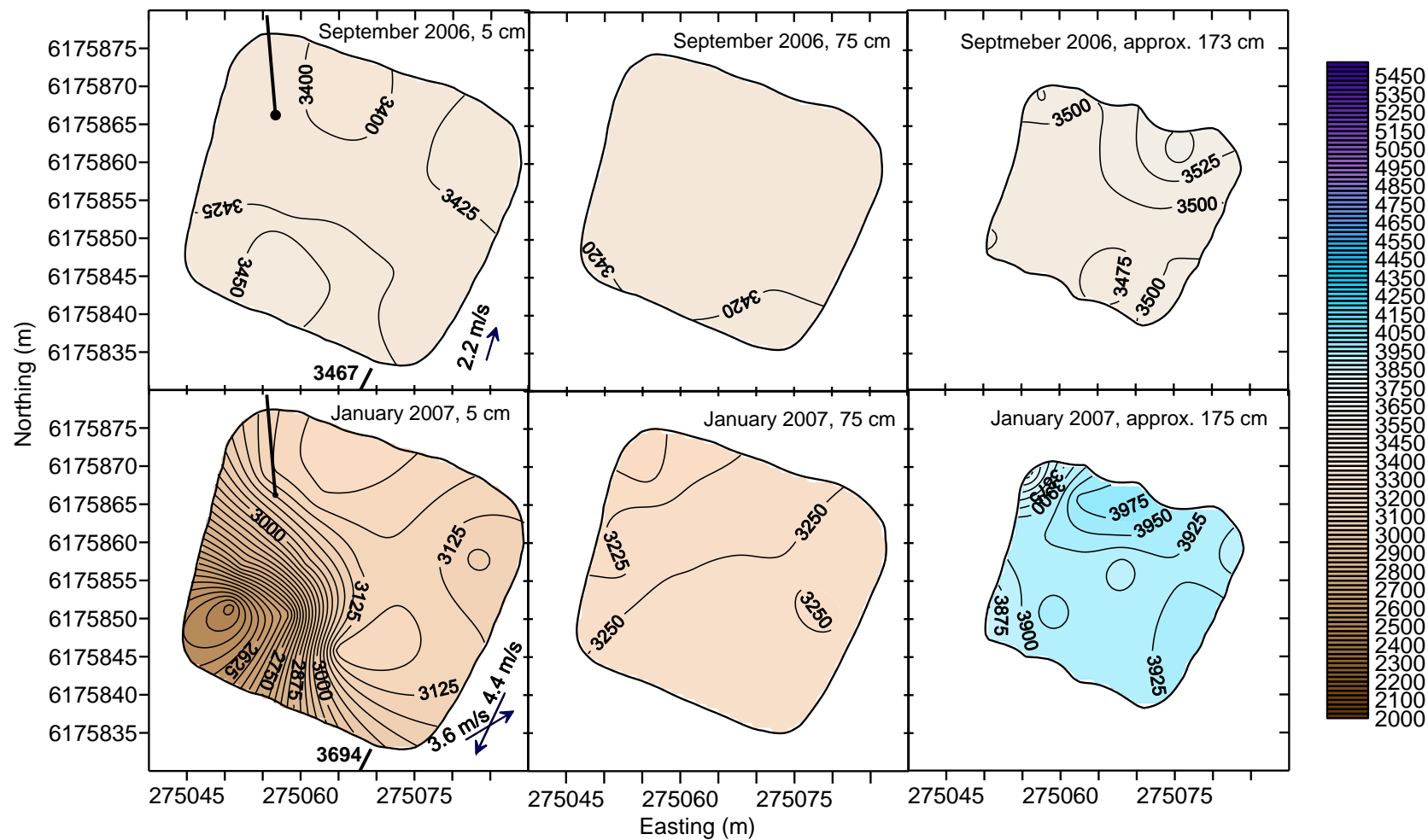


Figure 6-9 Conductivity contours ($\mu\text{S cm}^{-1}$) at the surface, mid-depth and the bottom of the facultative pond for September 2006 (top) and January 2007 (bottom) 2006.

A clear observation arising from the contour plots is that the largest gradients in EC appear to occur vertically rather than transversally. EC levels at the bottom of the pond are very similar to influent levels and are generally higher than levels at the surface and mid-depth. As identified in Chapter 4 (section 3.2.3), the vertical gradient is due to the contrasting biological and chemical conditions between the surface and the bottom of the pond, but may also be related to more saline and denser influent - and potentially infiltrating seepage (Chapter 5) - from the anaerobic pond sinking to the bottom upon entry to the pond. Transverse gradients at the bottom of the pond are mild ($<7\%$), especially when compared with the vertical gradients that approach 20%. However, on four of the six profiling events, EC levels at the bottom of the pond showed the greatest similarity to influent EC levels in the region closest to the inlet location, both when surrounding EC levels (at the bottom) were lower (November 2005) and higher (July 2005 and April, September 2006) than the influent EC. Regardless of whether these patterns are related to changing influent EC or treatment processes, they suggest that the hydraulic regime in the quiescent conditions at the bottom of the pond tend towards plug flow. However as evidenced by the other two bottom layer contour plots, dispersion can at times be significant. It is difficult to identify what is behind the apparent dispersion in February 2006 and January 2007 with just the two sets of observations, although it may be significant that both incidences occurred in summer under conditions of strong thermal and biochemical stratification. Whatever the cause, the two differing states highlight the transient nature of hydraulics and dispersion in the pond.

All six mid-depth plots show a marked absence of transversal gradient in EC, suggesting that the region between the top 10-25 cm and the bottom 50 cm can be considered to be completely mixed. Transverse gradients at the surface are generally very slight and exhibit no clear pattern in relation to the inlet, outlet or the wind. The notable exception is seen in the plot for January 2007 which shows a relatively steep EC gradient had formed in the south-western quarter of the pond. The gradient was also evident at 10 cm depth, but had dissipated by 25 cm (data not shown). The cause of this depression is not clear, but it may have been a result of the combined effects of intense algal activity and wind. In the morning wind blew from the north-east at 4.4 m s^{-1} , causing algal biomass to be concentrated in the corner of the pond having been carried there by the wind-induced surface currents. Indeed a distinctive bright green plume was visible in that corner of the pond at the time. Intense algal photosynthesis driven by high levels of solar radiation may have resulted in unusually high uptake of dissolved nutrients, causing the localised depression in EC. Whether or not this is the

case, it would appear that the surface layer comprises essentially the same mixed supernatant as the layer below, but is altered by the effects of environmental forcing including heating, algal photosynthesis and associated aeration caused by insolation, re-aeration and circulation from wind, dilution and aeration from rain, concentration from evaporation, and heat exchange with the air.

The contour plots for April 2006 provide a good example of the breakdown of stratification by 'turnover' caused by thermal instability, where cooling surface water plunges to the bottom causing vertical mixing. The surface and mid-depth plots have almost identical EC levels and a similar degree of transverse homogeneity. The bottom layer also has very similar EC levels across much of the pond, but the contours show a slight depression around the inlet zone caused by the slightly more dilute influent. Evidently the gradient has been established since a turnover event homogenised the pond supernatant, or if turnover is ongoing it is not rapid enough to effect immediate mixing of the influent and surrounding supernatant.

6.4.2 Thermal Stratification and Hydraulic Efficiency

Thermal stratification can inhibit or even prevent vertical mixing in a pond and is indicated by steep temperature gradients from warmer water at the surface to cooler, more dense water at the bottom. Stratification can also be a contributing factor to short-circuiting (Shilton & Sweeney 2005) and reduced HRT and treatment efficiency (Kellner & Pires 2002). Profiling of the anaerobic pond water column (Chapter 4) revealed only mild temperature gradients forming in the upper 25-50 cm on days when the air temperature was significantly higher than the supernatant temperature, but an overriding pattern of almost constant temperature between the surface and the sludge blanket. Moreover, rising biogas from the digestion activity would aid in breaking down stratification (see section 6.5.3 below).

The facultative pond, on the other hand, showed significant temperature gradients during the day when the air temperature was higher than the temperature of the supernatant at depth as shown in Chapter 4. Presumably due to the high turbidity, the mixed layer appears to have been very shallow (< 5 cm). The underlying thermocline typically extended down to 25 or so cm, below which the gradient tended to ease. At the bottom of the pond conditions are heavily reducing and as shown in the previous section the supernatant is more saline and dense. Data presented in Chapter 4 indicated that when the differential between air and supernatant temperature was small, the thermocline would not form.

Figure 6-10 presents examples of variation in vertical temperature gradients with time in the facultative pond in each of the four seasons. The gradients were calculated using surface temperature data from the Facultative East probe and temperature recorded at depth by the Facultative West probe (see Chapter 4 and Appendix G) assuming transverse variability was low, as was shown in section 6.4.1 above. In the summer plot (Figure 6-10 a), a positive gradient is present day and night, although the data shows that sequential days of low temperatures can lead to a complete breakdown of stratification. The plot for autumn (Figure 6-10 b) is an example of the transition from extended periods of limited vertical mixing to regular (nightly) disintegration of the temperature gradient formed over the course of the day. The gradient starts to reverse (become negative) overnight, which would eventually result in overturn and mixing of the entire supernatant column as noted in section 0. In winter (Figure 6-10 c), the vertical gradient rarely rises above 5 and consistently breaks down at night. Interestingly however, consecutive days of relatively high minimum temperatures resulted in positive temperature gradients persisting overnight. The spring example (Figure 6-10 d) shows the transition from predominantly unstratified conditions to increasingly stratified conditions in the daytime and fewer incidences of zero gradients at night.

As evident in the temperature profiles presented in Chapter 4, temperature gradients under stratified conditions are non-linear. The estimates presented in Figure 6-10 were calculated between the liquid surface and a depth of between 0.7 and 1.0 m depending on the depth of supernatant above the fixed Facultative West probe. The variability in the length over which the gradients were calculated means that the magnitudes of the peaks are not directly comparable between seasons. Nonetheless they provide a good indication of the extent of daily stratification.

Following the lead of Abis & Mara (2006), Table 6-5 summarises the number of days in each season that stratification in the facultative pond could be classified as type I, II or III as defined by Gu & Stefan (1995). Type I stratification is defined as the absence of a temperature gradient (vertically mixed) for consecutive day and night. Type II is daytime stratification preceded or followed by destratification at night and type III is continuous stratification over day and night. Abis & Mara (2006) considered a temperature gradient of $1\text{ }^{\circ}\text{C m}^{-1}$ between the surface and mid-depth as being indicative of stratification. They also defined a fourth stratification state – that of inversion when the surface temperature drops below that at depth. In this instance, inversion was defined as a temperature gradient less than $-0.6\text{ }^{\circ}\text{C m}^{-1}$.

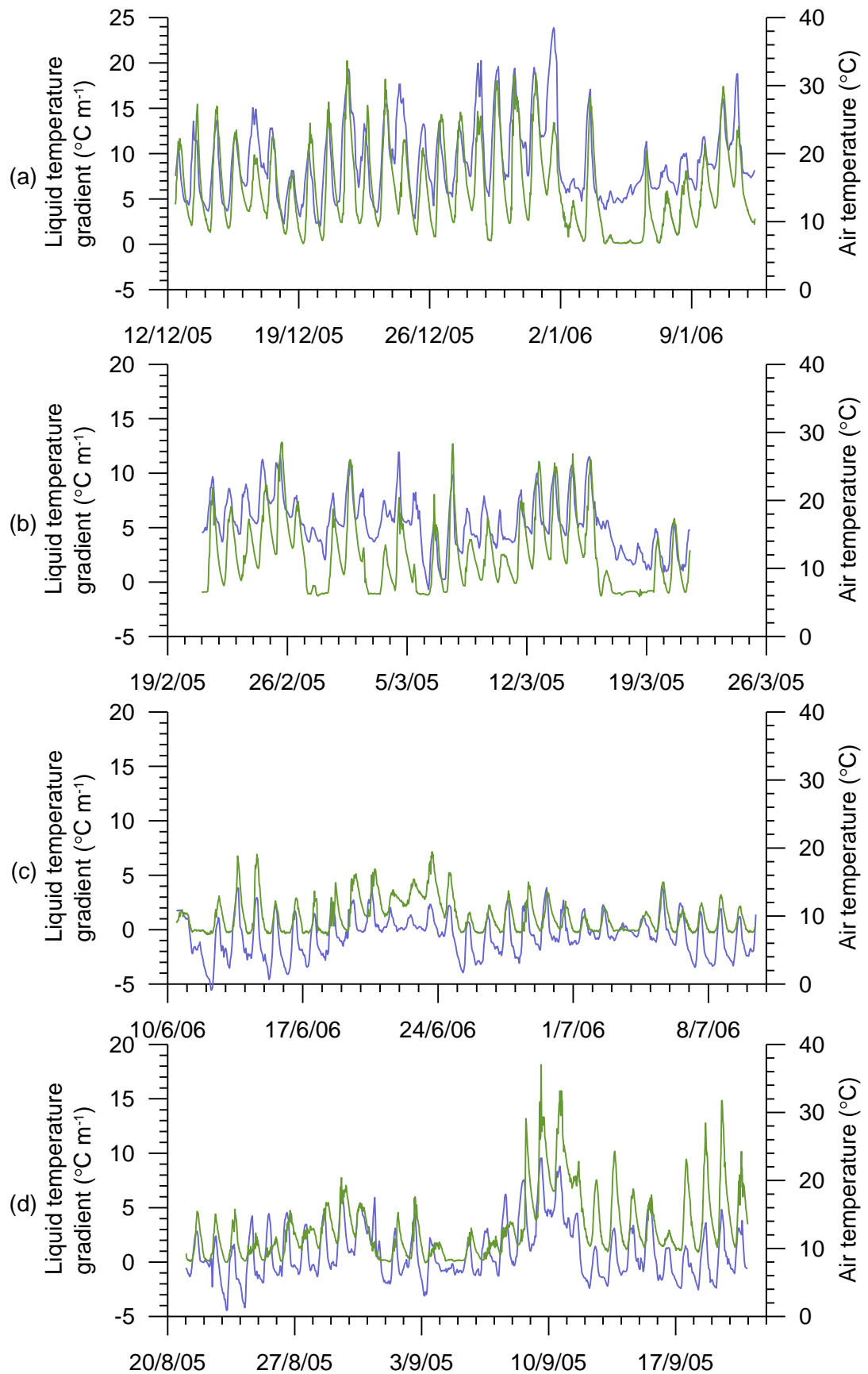


Figure 6-10 Vertical temperature gradients in the facultative pond (green lines) and air temperature (blue lines) in (a) summer, (b) autumn, (c) winter and (d) spring.

The data presented in Table 6-5 shows that the facultative pond was stratified for some portion of the day on 92% of the days where there was sufficient temperature data recorded both at the surface and at depth (637 days). Mixed conditions occurred in all seasons but as expected predominantly in winter. The pond was under continuous type III stratification for at least half the time over the summer and even occasionally in winter, presumably when the minimum air temperature was unusually high on consecutive days. But the most common condition (58% of days over the course of the year) was the diurnal shift between stratified and mixed states (type II stratification). The pond was most prone to overturn by temperature inversion during autumn as ambient temperatures dropped faster than the liquid temperature, although it would appear that unusually low temperatures can lead to inversion even in summer.

Table 6-5 Occurrence of different forms of stratification as defined by Gu & Stefan (1995) in the facultative pond.

<i>Season</i>	<i>Number of days monitored</i>	<i>Type I</i>	<i>Type II</i>	<i>Type III</i>	<i>Inversion</i>	
		%	%	%	Days	%
Summer	155	5	43	52	13	8
Autumn	159	9	76	14	87	55
Winter	142	14	76	10	9	6
Spring	181	4	40	56	1	1
TOTAL	637	8	58	34	110	17

6.5 THEORETICAL ANALYSIS OF ADVECTIVE MIXING INPUTS

Shilton and Sweeney (2005) outlined a theoretical approach to determining the relative influence of wind shear and influent momentum on mixing in stabilisation ponds. The following sections describe a similar analysis together with an estimation of biogas mixing power in the anaerobic pond. Also presented is an analysis of the impact these mixing forces have on vertical mixing and stratification, and by inference, the residual effect on transverse mixing.

6.5.1 Inflow Power

The calculation of inflow power presented by Shilton and Sweeney (2005) assumes a submerged inlet and accordingly considers only the energy of the pipe flow. The inlets to both ponds in this study were raised above the water level, hence the energy of the inflow to each is estimated as the sum of the kinetic energy leaving the inlet pipe and

the energy gained from the fall. Discounting minor exit and drag losses, inflow power input can be shown to be

$$P_i = \frac{1}{2} \rho A_i \alpha_i v_i^3 + \rho A_i v_i g h_i \quad (6-4)$$

where

P_i = Inflow power (W);

ρ = density of in the influent (kg m^{-3});

A_i = cross-sectional area of the inlet (m^2);

α_i = kinetic energy correction factor;

= 1.05 for an outlet under fully developed turbulent flow;

v_i = Inflow velocity (m s^{-1});

h_i = height of the inlet above the pond surface (m).

Mixing power calculations were performed using 5-minute flow data (incorporating flow rate and stage) and binned to daily figures that are summarised in Table 6-6. Average power input to the anaerobic pond was low at just 0.2 W. On account of the diurnal variability in inflow (defined by two sharp daily peaks and virtually zero flow for more than half the day), instantaneous power displayed a lognormal distribution causing the median to be lower than the average and the standard deviation to be high. Inlet power at peak flow was more substantial, averaging 3.3 W and exceeding 2.7 W 50% of the time. However, this level of power input was typically sustained only very briefly (usually less than five minutes) following the release of the flood wash.

The facultative pond inflow mostly impacted on the embankment rather than the supernatant surface causing inflow power to be virtually zero for 390 out of 415 days monitored. On the few days that influent did pour directly into the supernatant, average (non-zero) power input was about 2.2 W with an average daily peak of almost 8 W. Since the influent impact zone sits above the pond high water mark, it would be very rare for inflow to pour into the supernatant. As such, inflow power to the facultative pond may be considered to be negligible under normal operating conditions.

Table 6-6 Inflow power input statistics for the anaerobic and facultative ponds between 10 October 2005 and 5 December 2006. Figures in italics were calculated from non-zero data only.

	<i>Anaerobic pond</i> n = 119552	<i>Facultative pond</i> n = 114723 (5844)
	<i>Power (W)</i>	
Average	0.2	0.1 (2.2)
Standard deviation	0.5	0.8
Median	0.05	0.00
Maximum	13	19
Average daily peak	3.3	7.9
Daily peak standard deviation	2.2	3.6
Median daily peak	2.7	7.5

To obtain a better appreciation of the net impact of the intermittent hydraulic loading to the anaerobic pond, total energy was calculated for each discrete wash down peak. Figure 6-11 shows that analysing inflow energy as discrete events produces a much less skewed distribution. The maximum observed inflow energy amongst the 737 peaks identified was 64.5 kJ (not plotted in Figure 6-11). Average energy was 9.2 kJ while the median was 8.4 kJ. Milking occurs twice a day, indicating the peak flow energy estimates correspond well with the daily average of 17.3 kJ calculated from average power input.

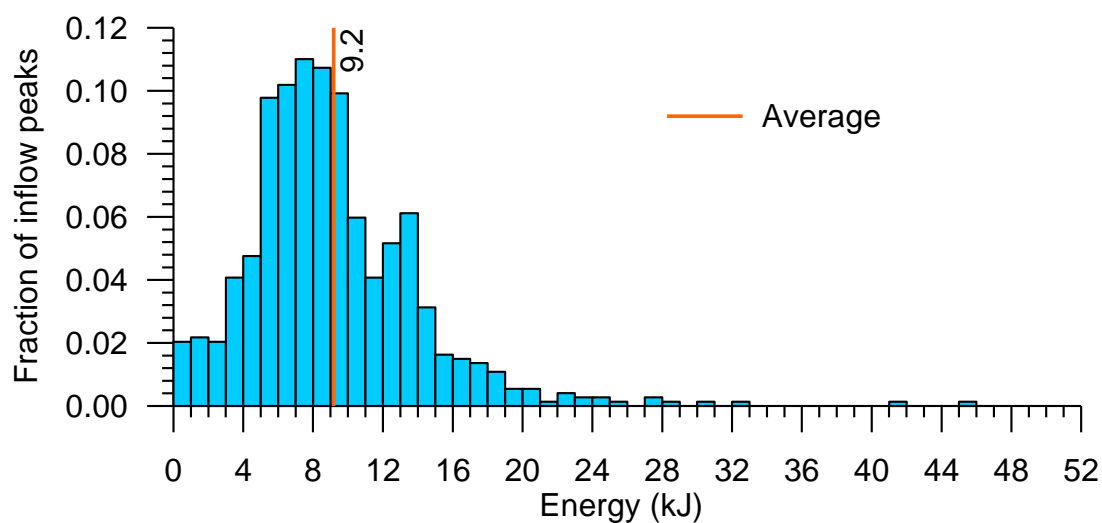


Figure 6-11 Histogram of energy imparted to the anaerobic pond by wash down inflow peaks (10 October 2005 to 5 December 2006).

6.5.2 Wind Shear Power

Wind shear has been shown to have considerable impact on the hydrodynamics and treatment efficiency of stabilisation ponds by inducing surface currents and associated circulation and underflows, which in turn promote short-circuiting and dispersion (Shilton 2001; Sweeney et al. 2003; Shilton & Sweeney 2005; Banda, Sleigh & Mara 2006). Power input from wind shear (P_w) in watts may be expressed as (Shilton & Sweeney 2005)

$$P_w = u_s \tau_w A \quad (6-5)$$

where

u_s = surface water velocity (m s^{-1}),

τ_w = wind shear stress ($\text{kg m}^{-1} \text{s}^{-2}$) and

A = pond surface area (m^2).

Wind shear stress is the product of the square of wind velocity at height z (u_z), the corresponding drag coefficient (C_{D_z}) and air density (ρ_a) (Fitzgerald 1963; Brutsaert 2005):

$$\tau_w = C_{D_z} \rho_a u_z^2 \quad (6-6)$$

Under neutral atmospheric conditions, the value of the drag coefficient may be expressed as a function of surface roughness and depends on the height of the wind speed measurement (z) (Sethuraman & Raynor 1975; Wiernga 1993):

$$C_{D_z} = \left[\frac{\kappa}{\ln(z/z_{0m})} \right]^2 \quad (6-7)$$

where

κ = universal Von Karman constant = 0.41;

z_{0m} = momentum roughness height (m) = 0.0001 m (see Chapter 4).

Surface water (friction) velocity is similarly approximated from the logarithmic wind profile. (Brutsaert 2005):

$$u_s = u_z \frac{\kappa}{\ln(z/z_{0m})} \quad (6-8)$$

It should be noted that the transition from the land terrain over which the wind speed measurements were made and the water surfaces of the pond would create an internal boundary layer. However, the effect of this boundary layer on the wind shear stress calculations is considered to be minimal based on data presented by Condie and Webster (1997).

Wind forcing power was calculated for each pond at an hourly time step. Summary statistics are presented in Table 6-7. Average daily wind power input is much higher than that from the inflow to the ponds. At peak flow, the power imparted by the inflow to the anaerobic pond is comparable to that of the peak wind shear, and unless coincident wind shear is particularly high, inflow energy should dominate flow patterns for the brief periods of each day during which flow peaks. Critically, however, wind power input is sustained for much longer periods over the day, which means that daily energy input (averaging 146 kJ) is almost an order of magnitude greater than that from the inflow. Wind is therefore likely to dominate flow patterns in the anaerobic pond the majority of the time. Histograms of daily wind shear energy for both ponds are presented in Figure 6-12.

Table 6-7 Wind power input statistics for the anaerobic and facultative ponds between 10 October 2005 and 5 December 2006.

	<i>Anaerobic pond</i> n = 10104	<i>Facultative pond</i> n = 10104
	<i>W</i>	
Average	1.7	3.1
Standard deviation	3.5	6.4
Median	0.6	1.2
Maximum	85	161
Average daily peak	5.9	11
Daily peak standard deviation	7.5	14
Median daily peak	3.6	6.9

Average wind power and energy imparted to the facultative pond is almost twice that of the anaerobic pond due to the larger surface area of the former and would certainly be the dominant force driving internal fluid motion. The variability of wind speed (and

direction), however, means that the mixing effect of wind would be inconsistent. Yet the wind power inputs at the upper end of the spectrum demonstrate the potential for wind to radically change the hydrodynamics of the pond. In the facultative pond wind direction could at times be as influential as speed since there are likely to be sheltering effects from the anaerobic pond embankment.

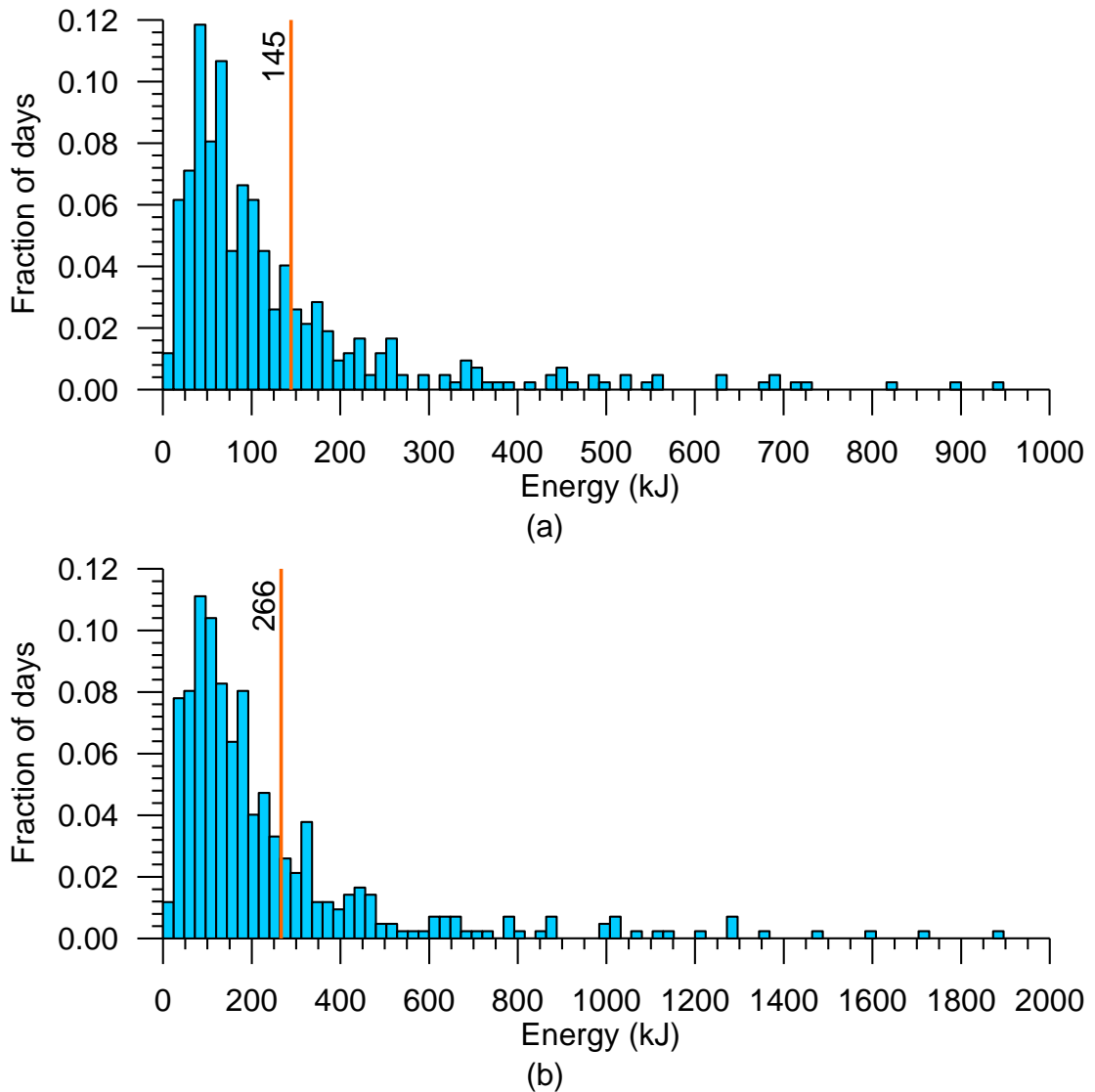


Figure 6-12 Histograms of daily wind shear energy inputs: (a) anaerobic pond; (b) facultative pond (10 October 2005 to 5 December 2006).

6.5.3 Power Exerted by Rising Biogas Bubbles (Anaerobic Pond)

It was clear from visual observation of bubbles and sludge clouds at the surface of the anaerobic pond that significant quantities of biogas were being generated through the anaerobic digestion of the sediments. The rising biogas bubbles would impart some degree of mixing to both the sludge and the supernatant (Pena, Mara & Sanchez 2000) in a similar manner to artificial (pneumatic) destratification using bubble plumes (Stefan

& Gu 1991). The work done by a bubble moving through a water column may be expressed:

$$E_b = D_b z \quad (6-9)$$

where

z = average depth of the supernatant (m);

D_b = drag force (N).

Assuming the bubble quickly reaches terminal velocity, drag force is expressed

$$D_b = \frac{1}{2} C_{D_b} \rho_w A_b U_{b_T}^2 \quad (6-10)$$

where

C_{D_b} = bubble drag coefficient;

A_b = bubble surface area (m²);

ρ_w = supernatant density (kg m⁻³)

= 1000 kg m⁻³;

U_{b_T} = bubble terminal velocity (m s⁻¹).

The drag coefficient at terminal (steady) velocity is given by Zhang, Yang & Mao (2008):

$$C_{D_b} = \frac{4}{3} d_b \frac{(\rho_w - \rho_g)g}{\rho_w U_{b_T}^2} \quad (6-11)$$

where

d_b = effective diameter of the bubble (m);

ρ_g = density of the gas in the bubble (kg m⁻³).

Total energy expended by rising biogas in a day is simply E_b multiplied by the number of bubbles generated per day (N), which is estimated:

$$N = \frac{Q_{biogas}}{V_b} \quad (6-12)$$

where

Q_{biogas} =volumetric biogas production ($\text{m}^3 \text{d}^{-1}$);

V_b = bubble volume (m^3)

$$\approx \frac{1}{6} \pi d^3$$

Power in watts then becomes a function of gas flow and liquid depth:

$$\begin{aligned} P_{biogas} = NE_b &= \frac{1}{86400} \cdot \frac{6Q_{biogas}}{\pi d^3} \cdot \frac{4}{3} d_b \frac{(\rho_w - \rho_g)g}{\rho_w U_{bt}^2} \cdot \frac{1}{2} \rho_w A_b U_{bt}^2 \\ &= \frac{Q_{biogas} g z (\rho_w - \rho_g)}{21600} \end{aligned} \quad (6-13)$$

The total gas production from the digesting sludge may be approximated using the methane (CH_4) equivalent of COD converted under anaerobic conditions and the methane concentration of pond biogas. Long-term COD conversion in the anaerobic pond was found by mass balance (accounting for sludge COD) to be approximately 64.4 kg d^{-1} (see Chapter 7). Under standard conditions the theoretical conversion factor for methane produced from conversion of COD is $0.35 \text{ m}^3 \text{CH}_4 \text{ kg}^{-1} \text{ COD}$ (Lesteur et al. 2010), translating to a base methane production rate of $22.5 \text{ m}^3 \text{d}^{-1}$. When expressed in terms of observed VS destruction in the pond, this amounts to $0.50 \text{ m}^3 \text{CH}_4 \text{ kg}^{-1} \text{ VS}$ destroyed, which agrees well with the specific methane productivity of $0.53 \text{ m}^3 \text{CH}_4 \text{ kg}^{-1} \text{ VS}$ removed reported by Safley & Westerman (1992b) who monitored biogas from a pond operating at a similar loading rate and temperature range. It is higher than methane productivity observed on a lightly loaded DSE pond in NZ by Craggs, Park & Heubeck (2008); however their figure, like Safley & Westerman's (1992b), was calculated from VS removal that did not appear to allow for VS remaining in the sludge and would thus be an underestimation of yield. Expressed in terms of VS loading ($0.21 \text{ m}^3 \text{CH}_4 \text{ kg}^{-1} \text{ VS}$ added), the gas production rate agrees well with Craggs, Park & Heubeck's (2008) data (average $0.211 \text{ m}^3 \text{CH}_4 \text{ kg}^{-1} \text{ VS}$ added).

An Arrhenius temperature adjustment was applied to the base methane production rate to approximate variation associated with temperature fluctuations, thus daily methane production was calculated:

$$Q_{CH_4} = 22.2 \cdot \theta^{(T-T_{REF})} \quad (6-14)$$

where

Q_{CH_4} = volumetric methane production ($\text{m}^3 \text{d}^{-1}$)

θ = Arrhenius temperature adjustment constant = 1.029

T = pond temperature ($^{\circ}\text{C}$)

T_{REF} = reference temperature = 16.0°C

The reference temperature was taken as the average pond temperature over the period from which COD conversion was determined.

The concentration of methane in biogas from DSE ponds is typically higher than from other types of digesters at around 70-80% (Safley & Westerman 1988; Safley & Westerman 1992a; Craggs, Park & Heubeck 2008). Hence total biogas flow was estimated to be

$$Q_{biogas} = \frac{Q_{CH_4}}{0.7} \quad (6-15)$$

Over the course of the monitoring period sludge occupied around 50 percent or so of the pond volume, equating to an average liquid depth of approximately 1.1 m. Under the ideal gas law, the density of biogas containing 70% methane at mid-depth in the pond would be about 1.07 kg m^{-3} .

Average power input from biogas bubbling was calculated to be 16 W. Allowing for diurnal and seasonal variation, this corresponded to an average daily energy input of 1.41 MJ over the same period the other power inputs were modelled. This figure is an order of magnitude greater than wind power inputs and nearly two orders of magnitude greater than inlet power, in part due to the day-to-day consistency of biogas generation. Since biogas motion is vertical, its contribution to mixing would mostly be towards breaking down stratification. Importantly, since stratification and anaerobic digestion are both temperature-driven, peaks in biogas-induced mixing should coincide with times when the potential for stratification is greatest.

6.5.4 Comparative Power Input

Figure 6-13 plots frequency curves of inflow, wind shear and biogas power (on a logarithmic scale) over the period commencing when flow out of the anaerobic pond

was re-established following desludging to the end of the monitoring period (391 days). Biogas bubbles clearly provide the highest and most consistent power input at levels comparable to the power inputs required to destratify reservoirs (0.001 – 0.07 W (H.D.R. Engineering 2001). Power exerted by wind and inflow forcing are far more variable and are only likely to have material impact on mixing for brief periods.

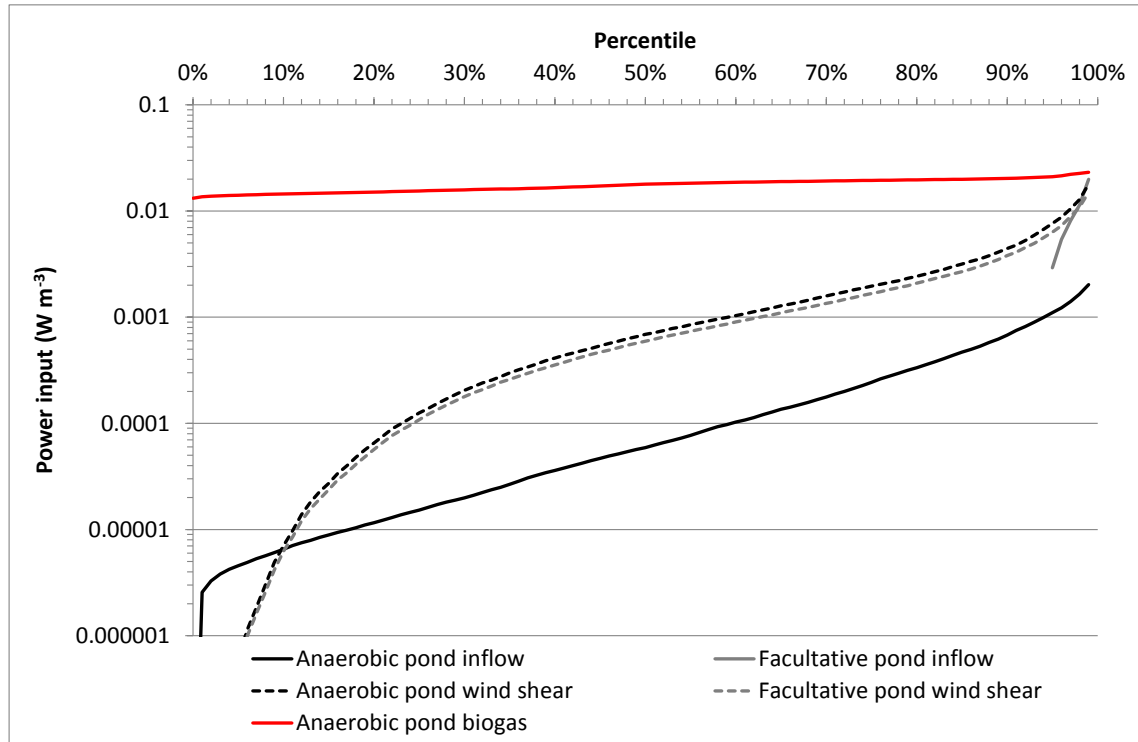


Figure 6-13 Comparison of power exerted by natural mixing forces ranked by frequency.

6.5.5 Energy Required for Effective Vertical Mixing

Pearson, Mara & Arridge (1995) suggested that stratification can be more influential to stabilisation pond treatment efficiency than the degree of axial dispersion. The energy required to achieve a mixed water column may be considered equivalent to the difference in potential energy of a water body in stratified and destratified states (Stefan & Gu 1991). Potential energy of the pond liquid may be expressed (Stephens & Imberger 1993)

$$PE = \int_0^h A(z)\rho(z)gzdz \quad (6-16)$$

where

$A(z)$ = function describing the surface area at depth z (m^2);

$\rho(z)$ = function describing the liquid density at depth z (kg m^{-3});

g = acceleration due to gravity (9.81 m s^{-2});

h = total liquid depth (m).

Polynomial functions for $A(z)$ for both ponds were given in Chapter 3. Density functions under stratified conditions were derived by fitting the following equation to density profiles constructed from the temperature and salinity data collected on the profiling runs:

$$\rho(z) = (1 - e^{at+b}) + cx + d \quad (6-17)$$

where a, b, c, d are fitted coefficients.

When the pond is destratified, $\rho(z)$ becomes constant. It was assumed that destratification would result in the homogeneous liquid column having a density equivalent to the average density (ρ_{ave}) of the stratified liquid column calculated as

$$\rho_{ave} = \frac{\int_0^h \rho(z) dz}{h} \quad (6-18)$$

The energy required for destratification ΔPE is thus expressed:

$$\Delta PE = g\rho_{ave} \int_0^h A(z)z dz - g \int_0^h A(z)\rho(z)z dz \quad (6-19)$$

While an analytical solution to equation 6-19 may be found, for expediency the analysis was performed by discretising the supernatant column into 0.02-m layers. Estimates for the change in potential energy required to achieve vertical mixing on the days where stratification was observed during physicochemical profiling are presented in Table 6-8. Since stratification was rarely observed in the anaerobic pond and was very mild when it did occur, a hypothetical extreme based on the January 2007 facultative pond density profile is also presented. Table 6-8 also gives estimates of energy input from wind shear and biogas motion. Inflow power data for the anaerobic pond analysis have not been included because data collection ceased in December 2006. Note, however, that the morning inflow peak had largely subsided before profiling was commenced, which meant that inlet power to the anaerobic pond was very low during profiling. Influent to the facultative pond was not pouring directly into the supernatant to contribute to mixing during any of the profiling events.

Table 6-8 Estimated energy inputs and energy required to break down stratification observed during pond profiling.

	Units	Anaerobic pond		Facultative pond			
		12 Jan 2007	Hypothetical stratification	21 Jul 2005	1 Feb 2006	4 Sep 2006	11 Jan 2007
Thermocline gradient	$^{\circ}\text{C m}^{-1}$	9	60	31	27	22	60
ρ_{ave}	kg m^{-3}	997.5	998.2	999.8	998.3	999.4	998.4
Temperature gradient to mid-depth	$^{\circ}\text{C m}^{-1}$	3.0	25	8.8	11	8.3	20
ΔPE	kJ	0.4	1.8	1.0	7.9	2.9	9.0
Wind energy during profiling	kJ	58	54	17	19	21	100
Biogas energy during profiling	kJ	245	322	-	-	-	-
Theoretical time to de-stratify after sunset [‡]	hr	<1	<1	1-2	3-4	>12*	<1
Minimum overnight temperature gradient	hr	No data	No data	No data	6	0	6
Observed time to destratify	$^{\circ}\text{C m}^{-1}$	No data	No data	No data	9	4	11

[‡] Based on observed night time conditions.

* Wind energy input after sunset was not sufficient to break down stratification before following sunrise.

The potential energy associated with thermal stratification is essentially the change in the sensible heat response to insolation with depth. Compared with overall sensible heat of the pond liquid (and sludge) and the insolation that drives it, ΔPE is very small (several orders of magnitude lower). The gradient in sensible heat arises through the absorption of incoming radiation in the upper region of the liquid column which limits the penetration and absorption of the same radiation at depth. Accordingly it is most likely to occur when vertical advection is constrained and is exacerbated by suspended particles that absorb heat more readily than water.

The small temperature gradients observed during the day in the anaerobic pond during all profiling events indicate that advection and eddy currents caused by rising biogas help to maintain an even distribution of sensible heat down the liquid column. In January 2007 when heavy stratification was observed in the facultative pond, ΔPE in the anaerobic pond was kept to just 0.4 kJ by the 245 kJ kinetic energy imparted by biogas whilst profiling was being undertaken (Table 6-8). The analysis of hypothetical

stratified conditions based on the density profile of the facultative pond on 11 January 2007 shows that in the unlikely event that the anaerobic pond should become (heavily) stratified, biogas energy should rapidly break down the density gradient once solar radiation subsides. What is more, peak biogas generation would generally coincide with high temperatures, counteracting stratification when it is most likely to occur.

Energy imparted to the anaerobic pond by wind was also higher than the potential energy of stratification; however data from the facultative pond indicates that the destratifying effect of wind appears to be minimal. Wind shear was the only effective mixing force in the facultative pond and theoretically should have been sufficient to cause rapid destratification after sunset following three of the four profiling events. However, observed overnight temperature gradients reveal that the pond remained stratified overnight following the two summer profiling events despite wind-induced energy being greater than ΔPE . Conversely, when overnight wind energy should not have been enough to break down stratification on 4 September 2006 (totalling just 1.9 kJ), the pond did destratify, which suggests that radiation and conduction play a more significant role in determining the night-time stratification state of the facultative pond than does wind. These observations support Shilton's (2001) assertion that wind-induced advection lends itself more to horizontal circulation than vertical circulation and would therefore be more influential to transverse dispersion than destratification.

6.6 FIELD STUDY OF ANAEROBIC POND HYDRODYNAMICS

As explained in section 6.2, the design of the anaerobic pond was liable to make it prone to short-circuiting and the formation of dead zones. This section examines the net impact of the geometry, inlet-outlet arrangement and hydraulic loading on in-pond hydrodynamics. It describes a series of experiments undertaken in the preliminary stages of the field work that involved tracking the direction and velocity of in-pond wastewater movement with the aid of 'drogues' – purpose-built devices designed to follow currents in water bodies.

Drogue tracking was favoured over the more established tracer dispersion method of hydraulic analysis (e.g. Torres et al. 1997; Pena, Mara & Sanchez 2000; Torres et al. 2000) on account of its simplicity and low cost, as well as technical complications alluded to earlier. Drogue tracking has been successfully employed in the study of in-pond flow velocities in stabilisation ponds by Shilton and Kerr (1999) and Barter (2003). Primarily it has been applied to determine predominant flow paths and estimate in-pond flow velocities. Limitations of the method include the two-dimensional nature of drogue movement, the potential interference of wind and the inability to extrapolate the results

of drogue tracking to determine actual residence times. Nonetheless, drogue tracking can provide useful insight into the two-dimensional (horizontal) mixing pattern within a pond, and also the incidence and extent of short-circuiting and the presence of dead zones. It also offers the advantages of a Lagrangian approach to investigating the flow regime that dispersion studies do not.

A similar experiment was not performed on facultative pond simply on account of the lack of fluid motion. The absence of inflow momentum (refer to section 6.5.1) meant that under still wind conditions, drogues placed near the inlet in the pond moved at a pace too slow to facilitate tracking, if at all. The quiescent conditions are also due to the fact that the pond does not have an outfall and therefore does not experience continuous flow. In the absence of wind, measurable fluid motion would therefore be confined to a small radius surrounding the pump intake when the pump is operational. Under windy conditions, drogues still moved very slowly and tended to become trapped at the edges of the pond. Thus drogue tracking was not viable in the facultative pond and the focus of this section lies exclusively with the anaerobic pond.

6.6.1 Methodology

The drogue experiments involved tracking by survey triangulation the movement through the ponds of strategically placed drogues during peak hydraulic loading. The drogues (pictured in Figure 6-14) were based on the Shilton and Kerr (1999) design and were developed through lab testing and subsequent trials in the field. They comprised a submerged 'sail' suspended from polystyrene floats fitted with coloured markers to enable quick visual identification through a theodolite sight. The floats were kept as small as feasibly possible and were weighed down using small lead weights to limit wind-induced movement. The drogue sails were fabricated from lightweight plastic board and were attached to the floats with nylon fishing line and stabilised beneath the float using small lead weights. The fishing line was threaded through lengths of polyethylene irrigation tube that ensured that the line could not become entangled with obstacles such as kikuyu grass overgrowth and other drogues in the pond.

The depth to which the sails were suspended was chosen based on the depth of sludge. Whilst in the middle region of the pond there was up to two metres of water above the sludge blanket, around the edges of the pond the sludge level came within 1 m of the water surface. Thus a total sail length of about 0.5 m was considered appropriate, particularly in light of the findings of Shilton and Kerr (1999) that flow velocities were reasonably uniform through different depths.

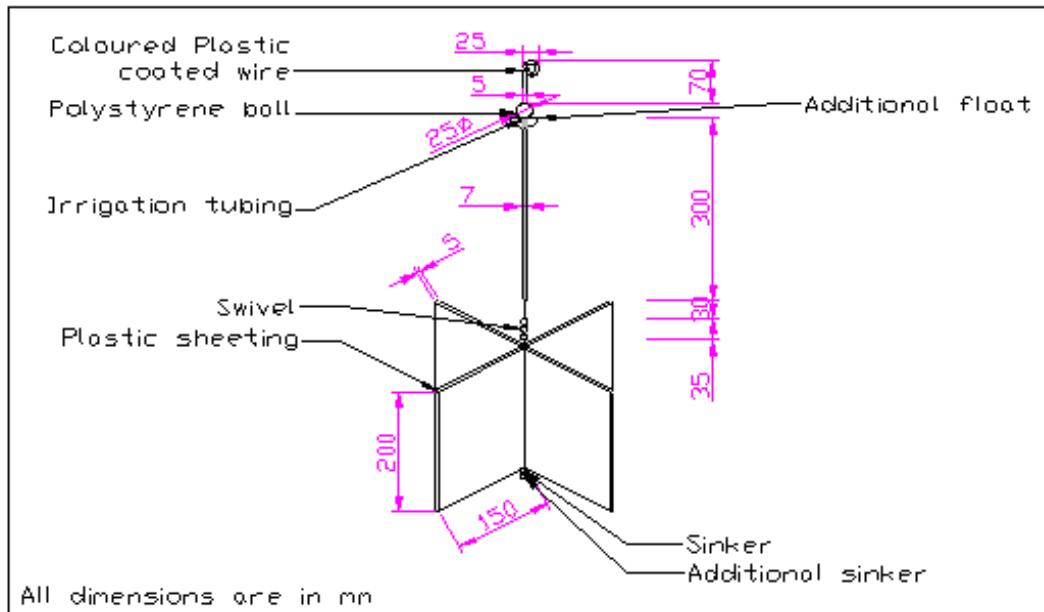


Figure 6-14 Drogue design used in field experiments.

Peak inflow conditions were generated by releasing a flood wash at the dairy holding yard for each experimental run. The quantity of water released in the flood wash depended on the operator and the level of cleaning required (of the yard) and was measured using a Greenspan CTD300 pressure sensor depth gauge deployed in the holding tank. To ensure maximum flow through to the pond, the screen in the solids trap was manually cleared prior to the commencement of the run. Flow into and out of the pond was gauged through the rated flumes described in Chapter 4. Scum on the pond surface that could potentially interfere with the movement of the drogue floats was removed by dragging a rope across the water surface.

For the majority of the experimental runs, the drogues were placed directly in the path of the incoming flow, within a few metres of the inlet. Two additional runs were conducted with the drogues placed several metres to the north of the inlet beyond the immediate influence of the inflow trajectory. Timing of the run and drogue tracking commenced with the release of the flood wash. Drogue locations were surveyed at varying intervals, depending on the rapidity of their movement. They were sighted from two stations, one equipped with a Leica TN400N total station, the other with a Leica T100 theodolite.

6.6.2 Results

The experiment was undertaken in February and March 2005 when the original inlet configuration was still in place. Being a field-based activity, the conditions of the experiment were difficult to control, placing significant constraints on the successful

execution of the experiments. The successful runs were carried out on clear days with light wind; however a number of attempts had to be abandoned due to poor weather conditions. In the end a total of eight successful runs were conducted over four days. Each run comprised tracking the movement of two drogues, producing a total of sixteen drogue trails labelled A through P in the results described below. The data generated from the experiments are given in Appendix J.

6.6.2.1 Flow paths

Figure 6-15 shows the velocity vectors and flow pathways recorded during the drogue runs (except runs C, E and J). Immediately apparent from the velocity field is an overall vortex pattern similar to that observed by Shilton and Kerr (1999). The vortex is characterised by faster velocities following the south-eastern perimeter of the pond from the inlet to the outlet (Drogues A, B, D, I, K and L), and slower velocities associated with movement in the centre of the pond (Drogues F, G and H). The faster outer pathway follows the direction of the inflow trajectory and is reflective of the 'advective zone' of the pond described by Thackston, Shields & Schroeder (1987) and also a potential short-circuiting route. If influent were to move from the inlet to the outlet along this pathway (approximate total distance of 38 m) at the average velocity of drogue A, it would reach the outlet within 45 minutes.

Similar flow pathways around the perimeter of the pond have been previously identified (with the aid of drogues) on a pond of much greater size but similar retention time by Barter (2003). It would appear that at peak flow the inlet jet mimics the effects of the paddle mixer that promoted the 'racetrack' flow pattern observed by Barter (2003). Wood et al. (1995) described inflow-driven short-circuiting around the perimeter of a 2D CFD model of a 5000-m² square-shaped pond with a similar inlet-outlet arrangement. The HRT of the model pond, however, was only two days as the pond received constant inflow. The intermittent hydraulic loading of this pond would limit the fraction of the influent slug moving in the advective flow zone actually leaving the pond. Short-circuiting is most likely to occur when the influent plume is warmer and less dense than the supernatant, causing it to remain close to the liquid surface rather than plunge to the bottom (Agunwamba 2006). Temperature monitoring of the anaerobic pond and the flood wash holding tank (Chapter 4) indicated that the effluent used in flood washing was generally colder than the pond supernatant, except in winter when the differential approached zero. Also, as suggested earlier, the submerged outlet structure would limit the escape of a buoyant plume.

Drogues D and G meandered at a moderate pace following the predominant path along the southern bank, with G making some movement towards the centre near the end of its run. Whilst the 'racetrack' flow pattern may cause a degree of short-circuiting, it would also facilitate recirculation, which, together with the transfer of kinetic energy from the advective flow to surrounding supernatant, would push the pond towards a complete mix flow regime. The tendency of some of the drogues to move towards the centre of the pond is suggestive of a central mixed zone similar to that described by Thackston, Shields & Schroeder (1987).

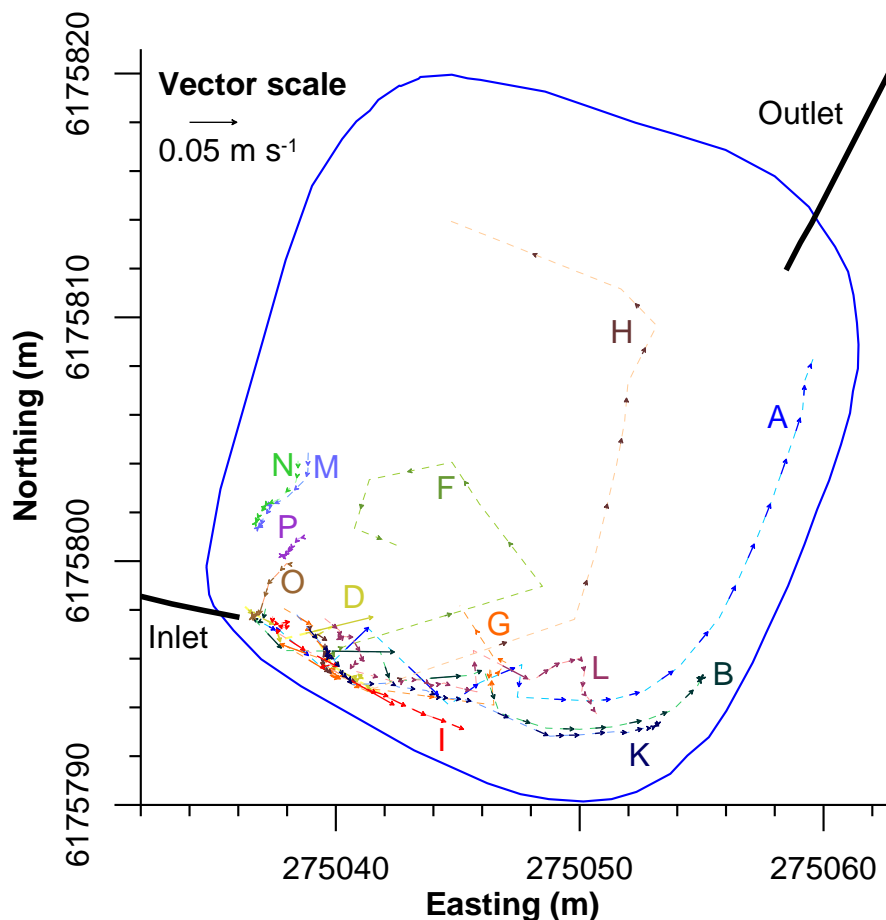


Figure 6-15 Velocity field incorporating drogue trails from 13 of 16 experimental runs.

Drogues M, N, O and P were placed several metres to the north of the inlet away from the trajectory of the inflow in a region that would potentially be prone to stagnancy. The motion of all four drogues was very similar, each drifting at a slow pace towards the inlet seemingly as part of the greater vortex mixing pattern of the pond. The movement of these drogues, however slow, would suggest that this part of the pond was not entirely dissociated from the rest of the pond. Only drogue trail H reached the northern corner of the pond where stagnancy may also have been a problem. Since the observation occurred at the tail end of the run when inflow had dropped substantially, it

is difficult to say whether its deceleration was related to the presence of a dead zone. However the fact that it entered that region of the pond suggests that there must be some fluid movement into, and by extension out of, the area.

A number of drogues (C, E and J – not included in the velocity field diagram) did not follow a flow path but rather oscillated within the immediate vicinity of the inlet for the entire run. This behaviour implied the formation of small eddies around where the influent pours into the supernatant from the inlet pipe which sits about 5 cm above the water surface. The effect of these eddies was to effectively trap the drogues in their region of influence, and sometimes pull drogues back towards the inlet (Drogue G). This form of flow pattern could be likened to the “back-eddy” observed by Shilton and Kerr (1999) and would enhance mixing in the influent impact zone.

Wind effects

It is important at this point to consider the role of wind in determining the pathways of the drogues. Several studies have shown wind shear to be influential to flow paths and a contributing factor to short-circuiting including Barter (2003), Frederick & Lloyd (1996), Pena, Mara & Sanchez (2000) and Salter et al. (2000). In this case the apparent short-circuiting pathway followed by drogue A may have been aided by the prevailing wind which was blowing at 3.9 m s^{-1} almost due north (refer to Table 6-9). The (localised) influence of wind shear tends to be moderate compared with that of inflow momentum (Vega et al. 2003; Shilton 2001). As such, Drogue A would have been most prone to wind-induced supernatant movement as it moved further away from the inlet and as the inflow peak subsided – that is, as it moved along the eastern bank. Drogue B, which was released at the same time as A, became trapped in the sludge near the eastern bank before wind-induced motion could carry it towards the outlet. Drogues C and D were subject to a slightly stronger southerly wind but did not track northwards. C was trapped in the back eddy zone, while D travelled along the southern bank. The spiral flow paths followed by Drogues F, G and H appear to have been assisted by the wind that was consistently blowing from the south-east at the time. Drogue H, however, maintained a northerly direction for much of its run, only moving in the same direction as the wind towards the end of its run. Drogue F's motion at the end of its run was in the opposite direction to the wind. Drogue I resisted the south-easterly wind to follow a steady path along the southern bank.

Overall it may be said that inflow momentum dominated the movement of the drogues within the advective zone, but there were indications that wind influenced fluid flow north of the inlet line of trajectory. Wind effects were, however, inconsistent and

therefore difficult to distinguish from inlet-related hydrodynamics. Vertical velocity profiles associated with wind-induced currents in enclosed water bodies typically follow a logarithmic curve, declining rapidly to zero just above mid-depth and becoming negative due to reverse flow below (Spillane & Hess 1978; Koçyigit & Falconer 2004). The centroids of the drogues were situated approximately 0.6 m below the water surface. At the time of the drogues study, the free water surface would have been less than 1.2 m outside the central region of the pond. Hence drogues travelling near the pond banks may have been affected by reverse currents, which could help explain the apparent contradictions in the responses (or lack thereof) of Drogues D, F and I to wind forcing.

6.6.2.2 In-pond velocities

Table 6-9 provides a summary of the data from each of the drogue tracking runs. The velocities observed in this study were of similar magnitude measured in the study by Shilton and Kerr (1999) on a facultative pond ten times the surface area, suggesting the potential for more turbulent flow and associated mixing in this anaerobic pond. Unfortunately however, Shilton and Kerr (1999) did not provide information on pond loading or retention time that could be used as a basis for further comparison. In-pond velocities also varied substantially, a characteristic of ponds with low length to width ratios predicted by Wood et al. (1995). Inflow velocities tended to be between one and two orders of magnitude greater than in-pond velocities. The ratios between inlet and in-pond velocities are comparable to but generally lower than the singular order of magnitude (0.1 m s^{-1} inlet velocity compared with in-pond velocities of $\sim 0.01 \text{ m s}^{-1}$) predicted by the 2-D modelling performed by Wood et al. (1995), which supports the assertion that the intermittently loaded pond is less prone to short-circuiting than a pond under constant loading.

Figure 6-16 presents plots of inflow and drogue velocity against time. Cross referencing with Figure 6-15 reveals that drogues tended to reach their maximum velocity within the immediate vicinity of influence of the inflow jet. Drogues A, B, D and G exhibited particularly close correlations between proximity to the inlet, inlet flow and drogues velocity. Interestingly the direction of drogue motion at peak velocities often did not align with the inlet orientation, indicating turbulent flow that would promote dispersion of wastewater constituents. Most drogues tended to travel at a much slower, more consistent velocity once they moved beyond the direct influence of the jet, some drifting towards the centre of the pond in the vortex pattern. Drogue A, however, driven by the momentum of a particularly high peak flow rate, retained an elevated velocity (0.01 -

0.02 m s⁻¹). When its velocity began to dissipate it had almost reached the outlet, which does suggest that some degree of short-circuiting is likely to occur with rapid inflows. Agunwamba (2006) observed a similar connection between inflow, in-pond velocity and short-circuiting. Importantly though, peak flows are brief and occur only twice a day, which would help to limit the fraction of the inflow that would actually reach the outlet.

Drogues G and H reached peak velocity almost simultaneously with peak inflow, yet quickly slowed down once they moved away from the inlet despite the inflow remaining relatively high. Moreover, they were unaffected by a second inflow surge released during their run, both having moved north of the influent jet line of trajectory. Drogue G would have been less than 2 m north of the inlet trajectory when the second surge hit, indicating that the advective route to the outlet is narrow relative to the dimensions of the pond. Drogues K and L moved at moderate pace with a slight initial peak when situated closest to the inlet. They continued more slowly to a point about 6 m away from the inlet before being swept into motion again by an inflow surge caused by clearing the solids trap screen later in the run. Then, when a second flood wash was released for Drogues O and P, Drogues K and L showed no acceleration. At almost 18 m west of the inlet they appear to have been beyond the direct influence of the inflow jet.

The placement of Drogues M, N, O and P drew very limited response to the inflow surge. Only Drogue O, which was initially positioned closest to the inlet, produced measurable acceleration as it was drawn towards the inlet by advection currents generated by the inflow. The average velocities of Drogues M, N, O and P were lower than those of most other drogues by up to an order of magnitude. They were also lower than the velocities of Drogues H and F as they moved towards the centre of the pond and beyond. Peak velocities for M, N, O and P were comparable to velocities of drogues moving within the main advective zone after the initial peak had subsided, but these were fleeting.

Table 6-9 Summary of drogue motion, pond inlet flow and wind conditions for each drogue run.

<i>Drogue</i>	<i>Tracking duration</i>	<i>Total distance travelled</i>	<i>Average velocity</i>	<i>Peak velocity</i>	<i>Average wind speed</i>	<i>Wind direction</i>	<i>Flood wash volume</i>	<i>Total inflow</i> *	<i>Peak inlet flowrate</i>	<i>Average inlet velocity</i>	<i>Peak inlet velocity</i>
	<i>Minutes</i>	<i>m</i>	<i>m s⁻¹</i>	<i>m s⁻¹</i>	<i>m s⁻¹</i>	<i>Degrees from North</i>	<i>m³</i>	<i>m³</i>	<i>L s⁻¹</i>	<i>m s⁻¹</i>	<i>m s⁻¹</i>
10 February 2005											
A	51.5	36.2	0.0117	0.0437	3.9	175	5.9	6.4	10.1	0.35	0.65
B	42.5	23.4	0.0092	0.0661				6.0		0.37	
29 March 2005											
C	37.0	0.6	0.0003	0.0015	5.0	179	5.0	4.0	13.6	0.33	0.75
D	38.0	11.0	0.0048	0.0734							
E	104.0	2.4	0.0004	0.0124	2.8	159	2.1	4.5	4.3	0.21	0.50
F	103.0	23.9	0.0039	0.0073							
30 March 2005											
G	150.0	25.8	0.0029	0.0359	2.8	145	23.2	20.6	12.1	0.35	0.71
H	150.0	35.4	0.0039	0.0119							
I	15.0	10.8	0.0120	0.0600	3.2	154	11.7	6.0	9.0	0.48	0.63
J	25.0	3.0	0.0020	0.0139				7.8			
31 March 2005											
K	123.0	16.9	0.0023	0.0139	3.7	50	12.5	16.2	9.4	0.36	0.64
L	123.5	18.0	0.0024	0.0301							
M	59.5	4.4	0.0012	0.0039	1.3	60	10.1	9.4	9.4	0.38	

<i>Drogue</i>	<i>Tracking duration</i>	<i>Total distance travelled</i>	<i>Average velocity</i>	<i>Peak velocity</i>	<i>Average wind speed</i>	<i>Wind direction</i>	<i>Flood wash volume</i>	<i>Total inflow[*]</i>	<i>Peak inlet flowrate</i>	<i>Average inlet velocity</i>	<i>Peak inlet velocity</i>
	<i>Minutes</i>	<i>m</i>	<i>m s⁻¹</i>	<i>m s⁻¹</i>	<i>m s⁻¹</i>	<i>Degrees from North</i>	<i>m³</i>	<i>m³</i>	<i>L s⁻¹</i>	<i>m s⁻¹</i>	<i>m s⁻¹</i>
N	59.0	3.6	0.0010	0.0031							
O	41.0	2.9	0.0012	0.0124	1.4	69	2.3	4.2	8.4	0.31	0.61
P	40.5	1.6	0.0006	0.0032							

^{*} Inflow volumes lower than corresponding flood wash volumes are an artefact of flow equalisation occurring in the solids trap.

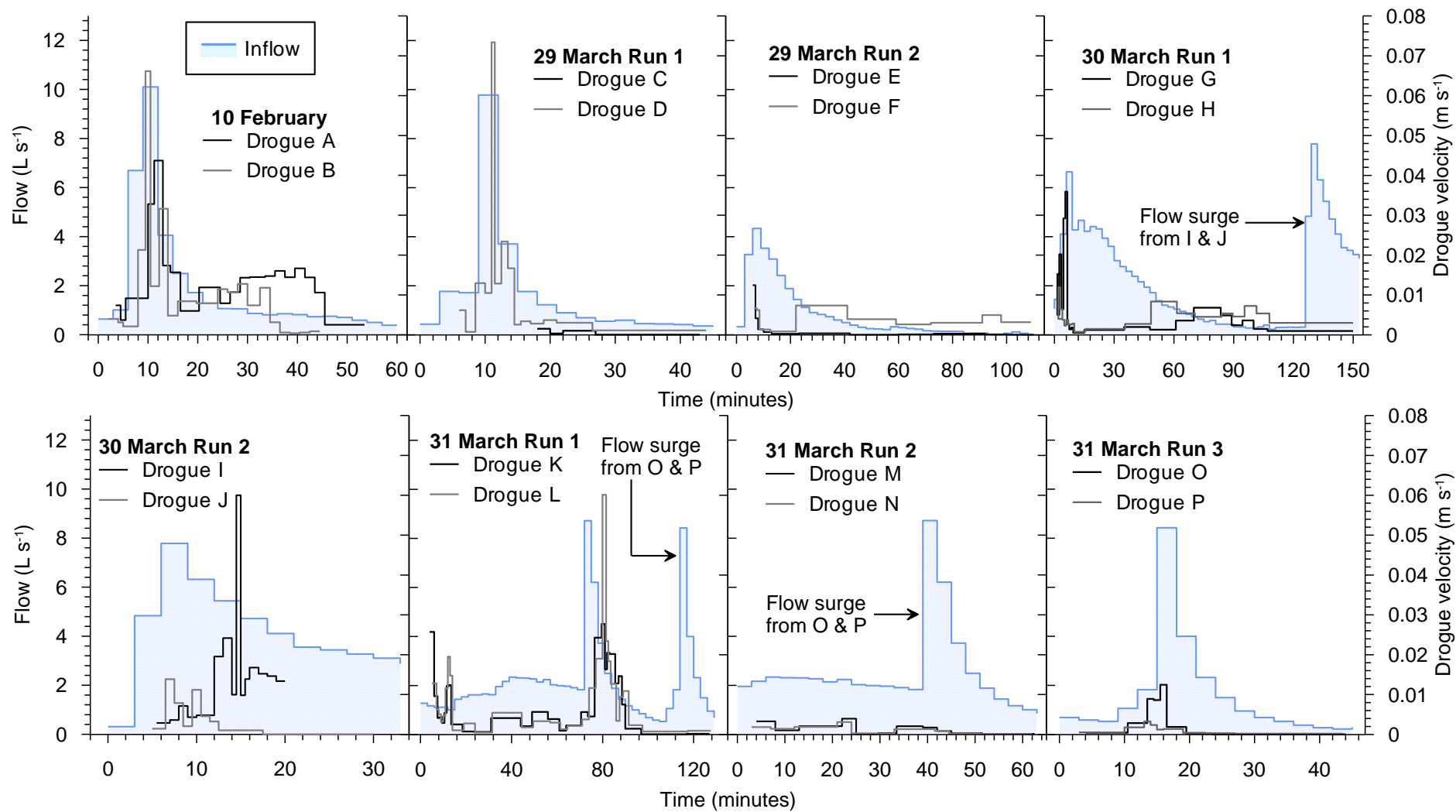


Figure 6-16 Plots of flow and drogue velocity with time for all experimental runs.

6.6.3 Discussion

The combined drogue pathways suggest a circulating flow pattern at a depth of between 0.3 and 0.6 m that tracks around the perimeter of the pond and comprises an advective zone following the southern and eastern embankments between the inlet and outlet, a central mixed zone and a region of low flow to the north of the inlet. The low flow region was not completely stagnant but exhibited much slower velocities than elsewhere in the pond. Diminution of the inflow kinetic energy will inevitably result in lower velocities beyond the advective zone, but the dampened velocities may also reflect the low flux of a dead zone (Shilton & Sweeney 2005) which would reduce the effective volume as predicted in section 6.2.

The apparent advective zone gives rise to the potential for short-circuiting, which was most clearly indicated by the path of Drogue A. However the brevity and limited range of influence of influent surges and the propensity for drogues to drift away from the main advective zone would suggest that short-circuiting is most likely to occur during inflows with particularly high, sustained peak flows and with assistance from a southerly wind. Such surges would be associated with flood washes entering the solids trap just after the solids trap screen has been cleaned to remove caked-on solids, or when the volume of accumulated solids is large enough to cause overtopping of the screen. The inflow surge that drove Drogue A to the outlet dumped a total of 3.7 m³ wastewater into the pond within 9 minutes. Based on the flow data collected over the water balance period, flows of this magnitude occur on less than 5% of wash down events.

The motion of Drogue A was also potentially assisted by the wind, which based on data collected over more than a year should blow from the south to south south-east less than 15% of the time (refer to Figure 5-9 in Chapter 5). Outside these times, wind should generate circulatory currents which cause dispersion and help to break down dead zones (Thackston, Shields & Schroeder 1987; Banda, Sleight & Mara 2006). Together with the localised mixing and circulatory flow caused by inflow momentum (under normal peak flow surges), this should produce well mixed conditions generally. Short-circuiting is thus thought to have been a relatively isolated occurrence and should not have reduced the effective volume or the treatment efficiency in the anaerobic pond under its original inlet configuration. The reconfiguration of the inlet is thought to have had little effect on the potential for short-circuiting as it simply re-oriented the inflow along the western embankment from the previous alignment with the southern embankment.

6.7 SUMMARY

A characterisation of the hydraulics and hydrodynamic behaviour of the pond system has been developed based on analyses of hydraulic loading and retention times, geometries, inlet-outlet configurations, sludge accumulation, salinity gradients, temperature gradients, mixing energy inputs and the outputs from a field drogue tracking experiment. The anaerobic pond is characterised by rapid accumulation of sludge which compromises the residence time and consequently treatment efficiency, and a high degree of mixing as evidenced by small transversal and vertical salinity (EC) gradients, the absence of thermal stratification, and the constant energy input from rising biogas bubbles. The rate of sludge accumulation was quantified using field measurements and was found to be $0.73 (\pm 0.07) \text{ m}^3 \text{ d}^{-1}$, equivalent to $0.88 \text{ m}^3 \text{ cow}^{-1} \text{ y}^{-1}$ or $0.0043 \text{ m}^3 \text{ kg}^{-1} \text{ TS added}$. The sludge accumulation data generated in this study is the first of its kind in Australia and represents robust validation of US data that have been adopted in current Australian best practice design documentation (Birchall, Dillon & Wrigley 2008).

The shape of the anaerobic pond lends itself to recirculation flows, short-circuiting and the formation of dead zones. Tracking of flow paths and velocities using drogues confirmed the existence of a circular flow pattern moving around a central mixed zone. It also indicated that stagnancy may develop orthogonal to the inlet where advection and turbulence from the inlet jet has much less influence over fluid flow. Liquid in that region did, however, move in response to inflows, albeit slowly, and there was little to no indication of an identifiable dead zone in the salinity contours, thus stagnancy is considered to have little effect on overall pond performance. The potential for short-circuiting via an advective zone was also evident, although the conditions under which it may occur are infrequent enough to discount it as a major source of hydraulic inefficiency.

A simplified representation of the hydrodynamics of the anaerobic pond based on the above findings is presented in Figure 6-17. With respect to biokinetic modelling, the findings suggest that the hydraulic regime of the anaerobic pond supernatant can reasonably be simplified to a complete mix (CM) reactor, although the size of the reactor must decrease in proportion with sludge accumulation. This concurs with the assertion from Pena, Mara & Sanchez (2000), based on findings from a series of dispersion studies, that anaerobic ponds should be treated as CM reactors. Moreover, Mason (1996) reported that a tracer study conducted on a New Zealand DSE

anaerobic pond with a very similar hydraulic loading rate and sludge occupying about 60% of the pond's capacity indicated that the pond was completely mixed.

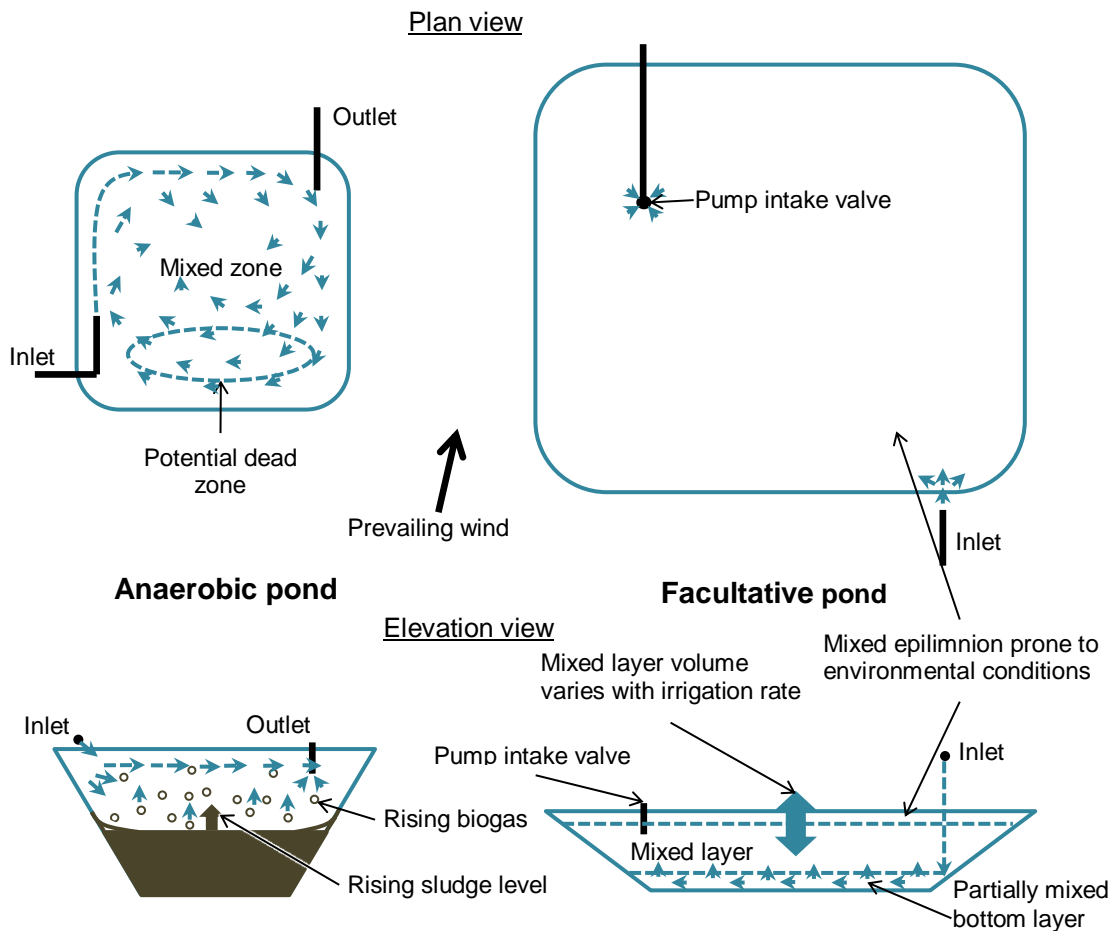


Figure 6-17 Conceptual models of the hydraulics and hydrodynamics of the pond system.

As depicted in Figure 6-17, the facultative pond may be characterised as having very slow advective motion and consisting of two biochemically contrasting and relatively thin layers separated by a layer of largely homogeneous liquid that varies in size with the volume of liquid held in the pond. Being more saline and dense than the bulk of the supernatant, influent sinks to the bottom, creating the heavily reducing anaerobic conditions of the bottom 25-50 cm observed in Chapter 4. The contents of this layer is continually forced upward due to displacement by new influent, or by turnover caused by thermal instability. The uppermost layer is defined by its exposure to environmental forcing rather than the characteristics of the supernatant, which would essentially be the same as that immediately below if not for external factors such as insolation which drives algal photosynthesis, wind, rain, evaporation and air temperature. This forcing generates warm, aerated conditions quite distinct from the layers below. The depth of

the surface layer is relatively constant, being determined by the depth to which solar radiation can penetrate to cause heating and algal photosynthesis, which is a function of the supernatant turbidity. On account of the lack of inflow momentum and a gravity fed outfall, the facultative pond should not be prone to short-circuiting and there are no signs of dead zones in the EC data.

The simulation of the hydraulic regime of the facultative pond needs to be more complex than the anaerobic pond, but can still be based on a configuration of ideal reactors. The liquid body needs to be divided into at least three compartments to reflect the vertical stratification, with CM reactors representing the surface and middle layers. The bottom layer may require additional compartmentalisation using a series of tanks with recirculation flows to represent plug flow with back mixing. Each reactor in the series would also be connected with the middle layer CM reactor. Inflows to the pond would be directed into the first reactor of the bottom layer reactor series. Transfers to the middle layer could be evenly distributed among the reactors in the series under the assumption that vertical flux is uniform across the pond. Exchanges between the middle and surface layers would have to be controlled according to the extent of thermal stratification, with unconstrained exchange occurring when the pond is unstratified and with allowances for zero or very small diffusion exchanges under stratified conditions. The stratification status would need to be a dynamic input to the model or simulated using a one dimensional thermal sub-model.

Chapter 7

WASTEWATER CONSTITUENT MONITORING AND MASS BALANCES

7.1 INTRODUCTION

A central component of this research work was the establishment of a wastewater monitoring and sampling system capable of collecting flow-weighted samples that could be used to determine wastewater constituent loads moving through the pond system. The data thus collected was used to establish material balance across the pond system, which would then inform the development and calibration of the dynamic model of the anaerobic pond described in Chapters 8 and 9. This chapter first describes in detail the approach taken to sampling and analysis of wastewater and sludge samples, in part to demonstrate the robustness of the data. The results of the wastewater characterisation are presented with reference to existing published data on DSE. Constituent concentrations are then combined with flow data (Chapter 5) to quantify constituent load transfers occurring within the system. More in-depth analyses are then presented, including examination of the major trends in the data, correlations between constituents, load data distributions and constituent fractions and ratios within the context of wastewater treatment processes. The culmination of the chapter is the formulation of a mass balance for the various constituents analysed that sheds greater light on partitioning and treatment occurring in the system. The outputs from this are then used to examine in more detail the occurrence and impacts of struvite precipitation and the implications of pond system management for nutrient recovery.

7.2 MATERIALS AND METHODS

Following the principles of stabilisation pond performance evaluation outlined in Pearson et al. (1987), a sampling program was devised to monitor the treatment efficiency of the pond system. Flow-weighted samples were collected on a regular basis for the analysis of standard wastewater constituents including solids, chemical and BOD, nutrients and salts. To facilitate collection of samples from the remote site, an automated sampling system integrated with the flow measurement system described in Chapter 5 was installed. Depth-averaged samples of anaerobic pond sludge were collected on a seasonal basis and analysed for solids, carbon, nutrients and cations.

7.2.1 Sampling Regime

The sampling regime was primarily designed to provide representative flow-weighted composite samples of the wastewater passing through the pond system for characterisation and quantification of wastewater constituent loads. Samples were collected from the three main wastewater transfer points - the inlet pipe to the anaerobic pond, the outlet pipe from the anaerobic pond (inlet to the facultative pond), and the effluent recycling line from the facultative pond – which are shown in Figure 3.8 in Chapter 3. To complement the facultative pond (recycled) effluent samples, depth-averaged samples of the pond supernatant were collected manually at each sampling event. To quantify partitioning of wastewater constituents by sedimentation in the anaerobic pond, depth-averaged sludge samples were collected during water quality profiling of the pond (see section 2.2 of Chapter 4).

7.2.1.1 Flow weighted sampling of anaerobic pond influent and effluent

Wastewater samples taken from the inlet and outlet of the anaerobic pond comprised discrete flow-weighted sub-samples collected by two ISCO 3700 (Teledyne Isco, Inc., U.S.A.) portable (auto-)samplers over a 24-hour sampling window starting at 11 am. The auto-samplers were integrated with the flow measurement system, such that pumping of an influent or effluent sample was triggered (independently) by a pulse signal from the datalogger following the passing of a specified volume of wastewater through the inlet or outlet, respectively. This approach does not eliminate the potential for unbalanced samples of the influent, which is likely to dramatically change in composition over time (refer to section 1.2 in Chapter 2), but with presence of the solids trap upstream was considered to provide sufficient equalisation and mixing to limit sampling bias.

The auto-samplers were programmed and calibrated to collect 600 mL of sample in a separate clean (acid-washed) bottle with each pulse received from the logger. At the completion of the sampling event, the sub-samples were manually combined to form composite flow-weighted samples of the respective sampling locations. The 11:00 am start time was chosen to allow enough time to gather and mix the sub-samples in the morning before transporting them to the laboratory for preliminary processing and analysis on the same day. It also ensured that the samples collected were as fresh as possible given that the first sub-samples to be collected would be from the evening wash down on the day the sequence was initiated, and the second half of the samples (approximately) would come from the wash down on the following morning. The trigger volume for collecting a sub-sample varied over the course of the monitoring to adjust to

changing conditions. Typically though, sub-samples were collected following the passing of each 2000-3000 L of wastewater. Further details on the sampling equipment is presented in Appendix A, while the sampling algorithm may be viewed in the data logger program presented in Appendix E.

It is important to consider here the impact on wastewater sampling of the flow measurement signal drop out problem flagged in Chapter 5 (section 2.1.1). Intermittent loss of flow signal during sampling events may have resulted in the collection of too few sub-samples to constitute representative composite samples. Analysis of the flow data affected by signal drop outs showed that of the 28 complete sampling events (refer to section 7.2.1.4), eight events were potentially compromised by incomplete flow data, affecting seven influent samples and four effluent samples. As detailed in Appendix B, since the signal losses predominantly occurred during overnight lulls in flow, influent (Flume 1) sub-sample losses were mostly less than 10% and are considered to have had relatively minor effect on the respective composite samples. The results from one influent sampling event (5 January 2006) however, did need to be omitted from the final data in part due to high flow signal and sample losses (~25%), but also due to a blockage of the sampling line that further reduced the number of sub-samples collected. Estimated effluent (Flume 2) sample losses were higher due to overnight flow lulls not being as low as in Flume 1. On one event sub-sample loss was estimated to be 40% (22 March 2006), but was assumed to have had limited effect on the composite sample based on the greater compositional consistency over time of anaerobic pond effluent.

7.2.1.2 Facultative pond effluent and supernatant sampling

Accurate flow-weighting of facultative pond effluent samples was not considered necessary since flow out of pond occurred predominantly in discrete and fairly consistent blocks of pumping to refill the flood wash tank. Effluent samples were thus pumped from the flood wash tank as it was refilled following a flood wash. Sampling was initiated according to a time schedule programmed into the stand-alone auto-sampler that followed the typical timing of evening and morning post-milking flood washes occurring within the 24-hour sampling window. Under the assumption that the effluent held in the tank was well mixed by the fall from the pump line outlet at the top of the 4-m high tank to the liquid surface, the sampling hose intake was suspended mid-depth in the flood wash tank. A total of 8 discrete 600-mL sub-samples were collected in two 20-minute blocks over the course of each sampling event - four following the evening flood wash and four following the morning flood wash. Collection

was timed to occur soon after the tank was refilled to ensure fresh effluent samples. The sub-samples from the morning and evening collections were then mixed to form a composite sample.

In addition to the effluent samples, samples of the supernatant from the facultative pond were collected each sampling event using the column sampling method described in Pearson et al. (1987) and Pearson et al. (1988). Manoeuvring across the pond in a dinghy with the aid of a rope strung across the northeast-southwest diagonal of the pond (supporting the pump for the MA), sub-samples were collected from the north-east and south-west quadrants, and at the pond centre (as depicted in Figure 3.11) using the column sampler described in Appendix A. The three sub-samples were combined to form a depth-averaged composite sample of the facultative pond supernatant.

7.2.1.3 Sludge sampling

Sludge samples were collected from the anaerobic pond during five of the six profiling runs described in Chapter 4. Depth-averaged sub-samples of the entire sludge depth were collected at each of the nine profiling locations using the column sampler described in Appendix A and transferred to a bucket for mixing to form a composite sample.

7.2.1.4 Schedule

Sampling of the pond influent and effluents was initiated in January 2005; however extensive technical difficulties with field equipment limited the number of sampling events over the nine months to the end of October to just seven, two of which did not adequately capture anaerobic pond influent samples. Equipment reliability issues were largely resolved by the completion of desludging of the anaerobic pond (31 October 2005), after which time sample events were held at least every three weeks, but mostly on a fortnightly or weekly basis, depending on availability of vehicles and support staff.

In total 31 wastewater sampling events were conducted, the last occurring on 14 September 2006. Of these 28 of were successful in obtaining samples from all the effluent streams. Facultative pond supernatant sampling, however, was not incorporated into the sampling regime until the 5th event in August 2005. Data from all 31 sampling events were used in the wastewater characterisation (section 7.3.1). Analysis of mass flows and balances were performed using data from the 24 sampling events that occurred within the water balance period (29 October 2005 – 14 September 2006), one of which did not include a representative AI sample due to a blockage and

the under-sampling issue raised in section 7.2.1.1. Sludge samples were collected on 5 of the six anaerobic pond profiling events – 1 immediately prior to desludging, 3 during the water balance period and a fifth in January 2007 after the flow measurement equipment had been removed. Sample numbers are summarised in Table 7-1.

Table 7-1 Numbers of influent, effluent, supernatant and sludge samples collected over the course of the study.

<i>Sample</i>	<i>Anaerobic pond influent</i>	<i>Anaerobic pond effluent</i>	<i>Facultative pond effluent</i>	<i>Facultative pond supernatant</i>	<i>Sludge</i>
<i>Abbreviation</i>	<i>AI</i>	<i>AE</i>	<i>FE</i>	<i>FS</i>	<i>AS</i>
12 January – 12 October 2005	5	7	7	3	1
16 November 2005 – 14 September 2006 [‡]	23	24	24	24	3
Total	28	31	31	27	5*

[‡] Within the water balance period.

* The fifth sludge sample was collected in January 2007.

7.2.2 In-field Sample Handling

Sets of sub-samples from the three auto-samplers were first combined in washed, acid-rinsed buckets and mixed using a clean drill-powered paddle mixer to form a composite sample. Measurements of pH and EC were taken (see section 7.2.4.1) before the composite sample was mixed again and transferred into four acid-washed 1-L bottles with the aid of a funnel. Having been collected in buckets and not requiring physico-chemical analysis, composite samples of supernatant from the facultative pond and sludge from the anaerobic pond only required paddle mixing before being transferred to bottles/containers for transport. Prior to transferral, however, aliquots of the facultative pond supernatant sample were pipetted from the sampling bucket to be filtered for chlorophyll-a analysis (see section 7.2.4.1).

Bottled samples were transported in a container packed with ice to the University laboratories. The container was chilled overnight with freezer blocks. All buckets, used auto-sampler bottles, mixers, funnels, filtration apparatus and other sampling gear were washed with detergent and rinsed with 10% hydrochloric acid and then distilled water on-site. Where necessary, items were returned to the laboratory for more intensive cleaning.

7.2.3 Laboratory Sample Preparation

Upon return from the field site, samples of pond influent and effluent and sludge were immediately prepared for in-house laboratory analyses and for shipping to an external laboratory for additional analyses. Pond influent/effluent samples were divided into separate portions to be filtered and homogenised for differentiation of soluble analytic fractions and improved solids entrainment (for analysis of total fractions), respectively. Portions of the filtered and homogenised samples were refrigerated at 4°C for in-house analysis, and the remainder put into frozen storage (<-18°C) for subsequent shipping to the NATA-accredited Environmental Analysis Laboratory (EAL) at Southern Cross University. Two bottles of unprocessed influent/effluent samples were refrigerated for subsequent in-house solids analyses. All sludge samples were frozen immediately upon return from the field. One container of each frozen sludge sample was set aside for shipping to EAL, and a second retained for in-house analyses.

Filtration

Well-mixed portions of pond influent/effluent sample were first centrifuged in 100-mL acid-washed glass tubes at 4075 g for 10-15 minutes to remove particulate material. Centrifuged samples were then pre-filtered through Advantec GC-50 glass fibre filters before final filtration through Advantec MFS 0.45-µm mixed cellulose ester (sterile) membranes. Filtration was performed under vacuum using a 47-mm diameter fritted glass support with a 300-mL cup and 500-mL buchner flask receptacles (all acid-washed). Glass fibre filters were preconditioned by rinsing through with distilled-deionised water while membrane filters had been soaked overnight in distilled-deionised water.

Homogenisation

Well-mixed portions of pond influent/effluent sample were transferred to an acid-washed plastic cup for homogenisation with a domestic kitchen hand blender for at least 30 seconds and until the size of the particulates in the sample were visibly reduced and their distribution reasonably uniform.

Acidification and freezing

Filtered samples were divided between two 125-mL bottles for acid preservation. One bottle would be preserved with concentrated H₂SO₄ for analysis of TDP and NH₄, and the second with HNO₃ for determination of soluble cations, Cl and SO₄. Homogenised samples designated for analysis of TP, TKN and TN were acidified with 0.4 mL H₂SO₄ per 100 mL sample as recommended for dairy shed wastewater samples by Ulery et al.

(2004). HNO_3 was added at 0.6 mL per 100 mL filtered sample as per APHA (1998). Allowing time for equilibration, the pH of all acidified samples was checked with test papers to ensure pH was below 2 before samples were frozen.

7.2.4 Sample Analysis

The wastewater and sludge samples were subject to analyses performed in the field, in-house at the University laboratories and at the external EAL facility. The analyses applied to the various samples collected are summarised in Table 7-2.

Table 7-2 Analyses performed on samples collected in the field.

<i>Sample</i>	<i>Field analyses</i>	<i>In-house analyses</i>	<i>EAL analyses</i>
R	-	Settleable solids	-
AI	pH, EC	BOD ₅ , COD, sCOD, settleable solids, turbidity, TS, TSS, TDS, TVS, TVSS, TVDS, DRP	TP, TDP, TN, TKN, $\text{NH}_3\text{-N}$, soluble cations (Ca, Mg, Na, K), Cl, SO_4
AE	As above	As above	As above
FE	As above	As above	As above
FS	Temperature, pH, EC, DO and ORP [*]	As above Chlorophyll-a	As above
AS	As above [*]	-	TS, TVS, TP, TN, TC, Na, K, Mg, Ca

^{*} In-pond measurements

7.2.4.1 Field analyses

Analyses of standard water quality parameters including temperature, pH, EC, DO and ORP were performed on site using a YSI 556 Multi Probe System (MPS). AI, AE and FE samples were analysed for pH and EC by suspending the MPS sensor in the buckets in which the composite samples were mixed. The MPS was allowed to stabilise over several minutes following paddle mixing of the sample, and the readings recorded on the MPS on-board logger. Physico-chemical parameter measurements for the FS sample were taken in the pond during sampling. At each of the three sub-sampling points, the MPS sensor was lowered to between 5 and 25 cm depth, depending on the gradient of oxygen from the surface, and the readings recorded once the MPS had stabilised. Physico-chemical parameter measurements for sludge were also made in the field while collecting the samples. The MPS was calibrated regularly and the calibration of the MPS was checked prior to every sampling event using YSI 5580 Confidence Solution®.

7.2.4.2 In-house laboratory analyses

Sample preparations, analytical procedures and turnaround times for analyses performed at the University of Wollongong Environmental Engineering Laboratories are summarised in Table 7-3. BOD₅ analysis initially incorporated a range of dilutions for each sample, which were gradually refined and narrowed down as familiarity with sample BOD₅ levels was developed. All tests were run on the day of sampling in at least triplicate on homogenised portions of sample. DO measurement was performed using a YSI Model 59 dissolved oxygen meter with a YSI 5730 BOD bottle probe. Analysis of COD and FCOD was performed on homogenised and filtered samples, respectively, using a dichromate digestion method with Chemetrics COD vials. Digestion was commenced on the day of sampling with determination being completed the after the digested vials were allowed to cool in the dark. Digestion was performed in a Hach COD reactor and subsequent determination was made using a Hach DR/2000 spectrophotometer.

Settleable solids tests were conducted on well-mixed unprocessed samples using 1-L imhoff cones to produce results in volumetric terms. To obtain an indication of the effect of settling time on the outcome, settling was allowed to continue for up to an additional 3 hours beyond the first hour, with readings being recorded every hour. Turbidity analyses were performed nephelometrically using a Hach 2100N turbidimeter. On account of the high solids content of the AI samples, dilutions (factor 5-10) of subsamples transferred from beakers mixed using magnetic beads into measuring cylinders were prepared for turbidity, TS and TSS analyses. Evaporation of samples for TS was conducted in 75-mL dishes and drying was performed at 103°C for at least 24 hours. After cooling and weighing, the residue was then ignited at 550°C for at least 16 hours for determination of TVS. Advantec GC-50 glass fibre filter papers (0.5 µm nominal rating) were used to perform TSS analyses. The filters were then ignited at 550°C for at least four hours for TVSS determination. TDS and TVDS were calculated as the difference between total and suspended solids for each fraction. Total and suspended solids analyses were conducted in at least triplicate on well-mixed (using a magnetic stirrer) portions of sample and were initiated within seven days of sample collection together with settleable solids and turbidity tests.

The procedure for analysing DRP was a manual ascorbic acid colorimetric technique adapted from APHA (1998) and Kuo (1996). A UV-1700 Pharmaspec UV-visible spectrophotometer (Shimadzu Corporation, Japan) was used for measuring absorbance of coloured samples. Alkalinity was not included as a routine analysis;

however a small number of samples were analysed towards the end of the monitoring period in accordance with the APHA (1998) titrimetric method to obtain indicative figures.

Table 7-3 Analyses performed at the University of Wollongong laboratories.

<i>Parameter</i>	<i>Abbreviation</i>	<i>Sample preparation</i>	<i>Reference method</i>	<i>Proximity of analysis to sampling day</i>
Biochemical oxygen demand (5-day)	BOD ₅	Homogenised	APHA (1998) 5210 B	Same day
Chemical oxygen demand	COD	Homogenised	(CHEMetrics n.d.)	Same day
Filterable chemical oxygen demand	FCOD	Filtered	(CHEMetrics n.d.)	Same day
Settleable solids	SS	Mixing to ensure suspension of particulates	APHA (1998) 2540 F	Within 5 days
Turbidity		As above	APHA (1998) 2130 B	Within 5 days
Total solids	TS	As above	APHA (1998) 2540 B	Within 5 days
Total suspended solids	TSS	As above	APHA (1998) 2540 D	Within 5 days
Total dissolved solids	TDS	As above	Calculation: TS - TSS	
Total volatile solids	TVS	As above	APHA (1998) 2540 E	Within 5 days of TS analysis
Total volatile suspended solids	TVSS	As above	APHA (1998) 2540 E	Within 5 days of TSS analysis
Total volatile dissolved solids	TVDS	As above	Calculation: TVS - TVSS	
Dissolved reactive phosphorus	DRP	Filtered	Adapted from APHA (1998) 4500 P-J and Kuo (1996)	Within 48 hours
Alkalinity*			APHA (1998) 2320 B	Delayed analysis of frozen samples
Chlorophyll- <i>a</i> *	Chl- <i>a</i>	Filtered on site	Pearson <i>et al.</i> (1987)	Within 4 weeks

* Not part of routine analyses - performed on a small subset of samples.

* Performed on FS samples only.

For chlorophyll-*a* analysis the methanol extraction and spectrophotometric determination technique recommended for stabilisation pond samples by Pearson *et al.* (1987) was employed. FS samples were filtered on site in triplicate using Advantec GC-50 glass fibre filters. The filters containing the residue were placed in sterile plastic pour plates (with lids) which were in turn wrapped in foil to protect the residue against

light. The enclosed filters were transported from the field site in an ice cooler to then be stored at 4°C until the determination was performed.

7.2.4.3 External laboratory analyses

Analysis of pond influent/effluent nutrients and metals and all sludge physical and chemical properties was outsourced to EAL. All methods employed to analyse the liquid samples conformed to APHA (1998) and are summarised together with sample preparation and preservation in Table 7-4. The methods used by EAL to analyse the sludge samples are listed in Table 7-5.

Table 7-4 Analyses of pond liquid samples performed by EAL.

Constituent	Abbreviation	Sample processing	Acid preservation	Reference method (APHA 1998)
Total dissolved phosphorus	TDP	Filtered	H ₂ SO ₄	APHA 4500 P-H
Total phosphorus	TP	Homogenised	H ₂ SO ₄	APHA 4500 P-H
Total nitrogen	TN	Homogenised	H ₂ SO ₄	APHA 4500 N-C
Total oxidised nitrogen (nitrate + nitrite)	TON	Filtered	H ₂ SO ₄	APHA 4500 NO ₃ ⁻ -F
Total kjeldahl nitrogen	TKN			CALCULATION: TN - NO _x
Ammonia nitrogen	NH ₃ -N	Filtered	H ₂ SO ₄	APHA 4500 NH ₃ -H
Soluble calcium	Ca ²⁺	Filtered	HNO ₃	APHA 3120 ICPOES ⁺
Soluble magnesium	Mg ²⁺	Filtered	HNO ₃	APHA 3120 ICPOES ⁺
Soluble sodium	Na ⁺	Filtered	HNO ₃	APHA 3120 ICPOES ⁺
Soluble potassium	K ⁺	Filtered	HNO ₃	APHA 3120 ICPOES ⁺
Chloride	Cl ⁻	Filtered	HNO ₃	APHA 4500-Cl-
Sulphate	SO ₄ ²⁻	Filtered	HNO ₃	APHA 3120 ICPOES ⁺

⁺Inductively Coupled Plasma - Optical Emission Spectrometry

7.2.4.4 Quality control

As a check on the results coming from EAL, selected samples were analysed for TDP, TP and soluble Ca, Mg, Na and K at the University of Wollongong laboratories. P tests were performed using the sulphuric-nitric acid digestion (APHA 4500-P.B.4) and the manual ascorbic acid determination used for DRP analysis. For analysis of soluble cations, filtered samples were digested with nitric acid (APHA method 3030 G) in preparation for determination by atomic absorption spectroscopy using a Varian SpectrAA. Lanthanum was used as an ionisation suppressant in the AAS determinations, which were run in accordance with Varian procedures (Varian, 1989).

Table 7-5 Analyses of sludge samples performed by EAL.

Constituent	Abbreviation	Reference method
Moisture (%)		Rayment and Higgins 4A1
Total Solids (%)	TS	Calculation
Total volatile Solids (%)	TVS	@550°C
Total Phosphorus (% P)	TP	Rayment and Higgins
Total Nitrogen (%N)	TN	LECO CNS2000 Analyser
Total Carbon (%C)	TC	LECO CNS2000 Analyser
Total Sodium (%)	Na	APHA 3120 ICPOES*note 11
Total Potassium (%)	K	APHA 3120 ICPOES*note 11
Total Calcium (%)	Ca	APHA 3120 ICPOES*note 11
Total Magnesium (%)	Mg	APHA 3120 ICPOES*note 11

7.3 RESULTS

7.3.1 Wastewater Characteristics

7.3.1.1 Anaerobic pond influent and effluent

Table 7-6 summarises the data for physical properties and aggregate solids and organic constituent data collected from sampling of the anaerobic pond influent and effluent waste streams (AI and AE). The complete data are available in Appendix K. As is typical of dairy shed wastewaters, the influent to the system exhibited considerable variability and was heavily laden with solids and organic material. Total incoming solids were evenly split between particulate and dissolved forms. Eighty-six percent of suspended material was organic while organic compounds made up only 39% of dissolved solids. The larger portion of variability in the total solids concentration appears to come from variability in the suspended fraction, which would be a function of the amount of manure deposited on the yard, the volume of water and effluent used in the wash down, and the state of the solids trap (accumulated solids and screen blockages). COD was mostly in particulate form (66%), which also contributed most of the variability in COD, while the filterable component was present in concentrations similar to BOD₅.

Table 7-6 Average physical and aggregate solids and organic constituent concentrations for the anaerobic pond influent (AI) and effluent (AE).

<i>Constituent</i>	<i>Units</i>	<i>Influent</i>						<i>Effluent</i>					
		<i>n</i>	<i>Mean</i>	<i>Standard deviation</i>	<i>Median</i>	<i>5th percentile</i>	<i>95th percentile</i>	<i>n</i>	<i>Mean</i>	<i>Standard deviation</i>	<i>Median</i>	<i>5th percentile</i>	<i>95th percentile</i>
pH		28	8.06	0.22	8.06	7.73	8.42	31	7.87	0.10	7.87	7.74	7.97
EC	mS cm ⁻¹	28	3571	706	3499	2405	4554	30	3902	471	3916	3330	4601
SS	mL L ⁻¹	28	45.5	29.2	34.0	14.7	90.7	31	2.8	1.7	2.4	1.1	6.2
Turbidity	ntu	27	2735	984	2272	1676	4313	30	581	195	568	460	919
TS	mg L ⁻¹	27	6048	1821	5747	3920	8484	31	3012	399	2982	2528	3747
TVS	mg L ⁻¹	27	3797	1371	3353	2359	6167	31	1222	165	1213	1043	1535
TSS	mg L ⁻¹	28	2996	1245	2541	1599	4621	31	700	181	663	520	1097
TVSS	mg L ⁻¹	28	2570	1079	2185	1404	3966	31	562	129	538	419	863
Alkalinity	mg CaCO ₃ L ⁻¹	3	1371	135	1443	1238	1454	3	1580	31	1594	1549	1600
BOD ₅	mg L ⁻¹	28	1111	389	1133	585	1632	30	225	54	233	146	313
COD	mg L ⁻¹	28	5044	1702	4285	3155	7517	31	1412	323	1337	1114	2140
FCOD	mg L ⁻¹	28	1210	350	1287	722	1803	31	485	126	470	370	690

Descriptive statistics for concentrations of nutrients and major cations and anions are presented in Table 7-7. Influent P was dominated by particulate forms (64%); however the majority of influent N was ammoniacal (56%). The small difference between DRP and TDP indicates an inconsequential fraction of soluble organic P. TP variability mostly lay with the particulate fraction, but variability in TN was shared evenly between ammonia and organic N (Org-N). Oxidised N concentrations were negligible. K was the most abundant cation, approaching 500 mg L⁻¹, followed by Na at around 150 mg L⁻¹, while Ca and Mg concentrations both averaged close to 80 mg L⁻¹.

The influent data are comparable to characteristics reported by Tie & Sivakumar (2007b) and (2008b) who collected samples from the same wastewater stream on the same farm site. Comparisons with other published DSE characterisation data are made difficult by the fact that farm and waste management practices are so variable not only geographically but also between farms within a single region. However, settled/screened DSE characteristics of similar magnitude and variability have been reported both in Australia and overseas (refer to Chapter 2). Importantly, the relativities between constituents, particularly solids and organic material, also show good agreement with the published data. As would be expected, raw dairy shed wastewater characteristics are generally more concentrated than those observed here. Raw wastewater data presented by Wrigley (1994) are widely reproduced in Australian best practice documentation; however the concentrations are relatively low on account of the data being collected in the 1990s when dairy farming in Australia was considerably less intensive.

Anaerobic pond effluent is best characterised by its reduced levels of particulate material, with concentrations of SS, turbidity, TSS, TVSS and COD all considerably lower than corresponding influent concentrations. There is also a significant reduction in variability observed in the concentrations of both the particulate and soluble fractions of most constituents. There is evidence of biological activity, with reductions in FCOD (59%) and BOD₅ (80%) concentrations and decreases in the volatile fraction of total and suspended solids (62% to 41% and 86% to 80%, respectively). The pH of the effluent is notably higher than in-pond pH as the liquid is no longer exposed to the acidogenesis and carbon dioxide formation occurring in the pond (refer to Chapter 4).

Table 7-7 Major nutrient, cation and anion composition of the anaerobic pond influent (AI) and effluent (AE).

<i>Constituent</i>	<i>Units</i>	<i>Influent</i>						<i>Effluent</i>					
		<i>n</i>	<i>Mean</i>	<i>Standard deviation</i>	<i>Median</i>	<i>5th percentile</i>	<i>95th percentile</i>	<i>n</i>	<i>Mean</i>	<i>Standard deviation</i>	<i>Median</i>	<i>5th percentile</i>	<i>95th percentile</i>
TP	mg P L ⁻¹	28	64.9	16.9	66.3	40.0	86.7	31	52.6	6.2	52.9	40.4	60.9
TDP	mg P L ⁻¹	28	23.2	6.0	22.6	15.4	33.7	31	29.9	2.7	30.7	25.2	33.2
DRP	mg P L ⁻¹	28	19.1	4.7	19.0	12.8	27.2	31	25.2	2.6	25.7	21.4	28.5
TN	mg N L ⁻¹	26	235	47	235	176	326	29	215	28	217	169	254
NH ₃ -N	mg N L ⁻¹	27	131	35	120	88	203	30	151	25	148	117	193
TON	mg N L ⁻¹	26	0.11	0.06	0.10	0.04	0.22	27	2.5	2.7	1.3	0.05	7.0
Na ⁺	mg L ⁻¹	26	155	28	150	117	208	29	152	15	153	128	172
K ⁺	mg L ⁻¹	26	469	90	466	312	588	29	463	63	459	366	554
Ca ²⁺	mg L ⁻¹	28	87	25	84	52	137	31	99	12	99	76	115
Mg ²⁺	mg L ⁻¹	28	77	17	77	49	101	31	81	11	82	63	100
Cl ⁻	mg L ⁻¹	26	300	60	306	190	375	27	285	33	277	243	325
SO ₄ ²⁻	mg L ⁻²	26	39.2	10.3	36.8	28.0	57.9	27	19.2	2.3	18.9	15.8	22.4

Total N hardly changed through the pond while effluent TP concentrations were generally lower than influent concentrations. $\text{NH}_3\text{-N}$, TDP and DRP concentrations all increased, suggesting the hydrolysis of organically bound fractions and dissolution of inorganic precipitates in the sludge, and possibly in the supernatant as well. The small concentration of soluble organic P (about 4 mg L^{-1}) remains unchanged from the influent, indicating this fraction is associated with non-biodegradable material. Increased soluble Ca and Mg concentrations in the effluent also suggest dissolution of precipitates. Interestingly EC was also slightly higher in the pond effluent, yet TDS was lower. Considering the variance in the data, influent and effluent TDFS concentrations are essentially the same. The ten analyses of nitrate and nitrite concentrations were highly variable, but show that oxidised N constitutes a very small fraction of TN leaving the pond.

Effluent nutrient levels are within the ranges of N, P and K reported by Skerman, Kunde & Biggs (2006) for single (anaerobic) DSE ponds of varying sizes and loading rates (but similar overall design) sampled in southeast Queensland. Interestingly, nutrient and cation concentrations were lower than concentrations measured in anaerobic ponds that were part of systems on Victorian farms, both larger and smaller in terms of herd size, that recycled effluent (Kane 2004, pers. comm. 7 October; McDonald 2013, pers. comm. 18 January). Solids, N and P concentrations reported for various anaerobic ponds in NZ by Longhurst, Roberts & O'Connor (2000) were similar to the present data; however they were not complemented with information about the farm systems making comparisons difficult. Effluent concentrations of COD, BOD_5 and TSS reported by Mason (1996) were slightly lower than those in Table 7-6 despite having a higher specific volume ($\text{m}^3 \text{ cow}^{-1}$). Mason did not report the sludge level in the pond during the study, which if low may have given rise to the stronger performance, but the better effluent quality may also have been due to lower VS production from the herd and the absence of effluent recycling. COD and BOD_5 concentrations in anaerobic ponds of similar specific volumes sampled by Sukias et al. (2001) were also similar to those presented here.

7.3.1.2 Facultative pond supernatant and effluent

Summary statistics for the facultative pond supernatant and effluent monitoring data are presented in Table 7-8 and Table 7-9 below, while the full data are provided in Appendix K. The facultative pond may be characterised by the fact that settleable solids are all but gone and dissolved inorganic solids dominate, making up around 63% of TS. The effluent and supernatant still, however, contain TSS concentrations upwards

of 350 mg L⁻¹. As with the anaerobic pond effluent, much of the suspended material remains organic (81-84%), indicating that the nature of the solids removed is similar to the residual material. BOD₅ concentrations in the pond are more than halved to around 100 mg L⁻¹; however the reduction in COD is not as large, again indicating the refractory nature of the organic material. N and P concentrations are markedly lower in the facultative pond, while cation and anion concentrations remain largely unchanged.

Most of the change in N appears to have come from NH₃-N reductions, although the NH₃-N fraction of total N had increased to 70%. Nitrate and nitrite concentrations were negligible in both the supernatant and the effluent, indicating either very little nitrification was taking place in the pond, or that denitrification was very effective in removing nitrate. Conditions in the pond are not overtly inhibitory to nitrification-denitrification (slightly alkaline, plenty of alkalinity and carbon, temperature above 15°C outside winter) and it is possible that nitrification occurred in the upper layer when algae were actively producing oxygen and for denitrification to have occurred below, or overnight when algal photosynthesis ceased and reducing conditions took hold at the surface. However, observations reported by Craggs et al. (2000) and Sukias et al. (2003) suggest that nitrification would be unlikely to occur due to the lack of attached growth sites exposed to aerobic conditions that could support and sustain an effective nitrifier population.

Compared with much of the data available in the literature, the effluent and supernatant constituent concentrations were relatively high. Nutrient concentrations in facultative ponds in southeast Queensland reported by Skerman et al. (2006) were consistently lower than measured in this system. The two-pond system monitored by Mason (1996) was very similar in design, manure loading and primary pond sludge accumulation to this one, yet effluent from both the anaerobic and facultative ponds had lower average concentrations for all constituents except FCOD. Differences were more exaggerated for suspended solids and constituents incorporating particulate fractions. A later study monitoring effluent on what appears to be the same pond system recorded similar if not even lower nutrient concentrations (Houlbrooke, Horne, Hedley, Hanly, Scotter, et al. 2004) to the Mason (1996) study. Facultative pond concentrations of all constituents monitored on six NZ dairy farms by Sukias et al. (2001) were also markedly lower than observed here. The study by Hickey, Quinn & Davies-Colley (1989) that was the direct precedent to the Sukias et al. (2001) study also reported lower concentrations for all constituents measured. Similarly, data on nutrient concentrations collated by Longhurst, Roberts & O'Connor (2000) from various NZ data sets are consistently lower.

Table 7-8 Average physical and aggregate solids and organic constituent concentrations for the facultative pond supernatant (FS) and effluent (FE).

Constituent	Units	Facultative pond supernatant						Facultative pond effluent					
		n	Mean	Standard deviation	Median	5th percentile	95th percentile	n	Mean	Standard deviation	Median	5th percentile	95th percentile
pH		27	8.11	0.09	8.12	7.94	8.23	31	8.18	0.08	8.17	8.09	8.26
EC	mS cm ⁻¹	27	3749	281	3795	3379	4200	30	3637	325	3700	3064	4100
SS	mL L ⁻¹	27	0.2	0.3	0.1	0.0	0.9	31	0.1	0.1	0.0	0.0	0.3
Turbidity	ntu	26	384	73	365	317	523	29	349	52	326	296	449
TS	mg L ⁻¹	27	2665	255	2608	2305	3041	31	2568	246	2537	2249	2964
TVS	mg L ⁻¹	27	923	114	913	781	1098	31	891	100	880	735	1061
TSS	mg L ⁻¹	27	411	111	402	275	617	31	351	67	347	280	498
TVSS	mg L ⁻¹	27	335	85	316	243	473	31	295	56	272	239	399
BOD ₅	mg L ⁻¹	27	106	22	110	74	142	30	113	26	120	65	142
COD	mg L ⁻¹	26	981	216	914	808	1476	31	906	158	860	758	1288
FCOD	mg L ⁻¹	27	393	54	387	333	493	31	383	72	380	288	512

Table 7-9 Major nutrient, cation and anion composition of the facultative pond supernatant (FS) and effluent (FE).

<i>Constituent</i>	<i>Units</i>	<i>Facultative pond supernatant</i>						<i>Facultative pond effluent</i>					
		<i>n</i>	<i>Mean</i>	<i>Standard deviation</i>	<i>Median</i>	<i>5th percentile</i>	<i>95th percentile</i>	<i>n</i>	<i>Mean</i>	<i>Standard deviation</i>	<i>Median</i>	<i>5th percentile</i>	<i>95th percentile</i>
TP	mg P L ⁻¹	27	39.0	5.2	37.8	33.1	46.6	31	35.3	4.2	35.3	28.8	42.3
TDP	mg P L ⁻¹	27	19.6	3.1	18.5	16.0	25.7	31	18.0	2.7	17.1	14.8	22.7
DRP	mg P L ⁻¹	27	16.8	2.6	16.2	14.0	22.2	31	16.1	2.5	15.3	12.7	20.2
TN	mg N L ⁻¹	27	171	30	171	128	210	29	167	31	170	120	208
NH ₃ -N	mg N L ⁻¹	27	122	10	123	109	134	30	115	11	117	98	135
TON	mg N L ⁻¹	27	0.08	0.10	0.04	0.01	0.35	27	0.57	0.48	0.40	0.03	1.28
Na ⁺	mg L ⁻¹	27	158	14	158	136	178	29	155	14	153	136	175
K ⁺	mg L ⁻¹	27	480	59	471	389	577	29	467	68	463	349	569
Ca ²⁺	mg L ⁻¹	27	98	8	97	87	110	31	94	14	97	64	112
Mg ²⁺	mg L ⁻¹	27	85	11	85	68	101	31	82	11	82	65	101
Cl ⁻	mg L ⁻¹	27	290	23	294	254	320	27	295	19	294	271	324
SO ₄ ²⁻	mg L ⁻²	27	17.3	1.8	17.5	14.3	20.2	27	18.0	1.3	18.2	15.5	19.9

The most contemporary Australian data available for comparison are the facultative pond effluent concentrations reported by the Victorian Department of Primary Industries (DPI) research group that examined the effects of applying facultative pond effluent to land. Collecting data over several years, they reported TN, $\text{NH}_3\text{-N}$, TP and K concentrations very similar to those observed here (Jacobs & Ward 2007a; Jacobs, Ward & Kearney 2008; Jacobs & Ward 2008). EC, Na^+ , Ca^{2+} and Mg^{2+} concentrations, however, were almost double corresponding levels in this study, primarily due to the use of groundwater as a fresh water source (Ward 2012, pers. comm. 5 June).

A key difference between this system and those producing better quality effluents is the recycling of effluent as flush water. The studies mentioned above made no mention of effluent recycling, but it is fair to assume that very few, if any, of the dairies used reclaimed effluent. It has been confirmed, however, that the DemoDAIRY site at which the DPI group conducted their research was recycling effluent for flood washing the holding yard (DemoDAIRY Co-operative Ltd. 2012). Unpublished data on secondary (facultative) pond effluent nutrient and cation concentrations from other pond systems in Victoria does appear to confirm the concentrating effect and/or reduced treatment performance associated with effluent recycling (Kane 2004, pers. comm. 7 October). Systems that incorporated effluent recycling for flush water averaged significantly higher concentrations of all forms of N and P, cations and EC than those that did not recycle effluent. Indeed the averages for the systems using reclaimed effluent were very similar to those recorded in this study.

The purpose of sampling both the effluent and the supernatant (as described in section 7.2.1) was to gauge whether the point of effluent extraction made any difference to its characteristics. The results show that the supernatant and effluent generally had similar concentrations of all constituents; however there are subtle differences between the two forms of sample. Figure 7-1 shows average percentage differences in concentrations of most soluble species including the four major cations and all forms of aggregate dissolved solids are indistinguishable from zero as indicated by the confidence intervals bounding zero. However, for all constituents incorporating a particulate fraction, except BOD_5 , TN and Org-N, recycled effluent samples have consistently lower concentrations. This would be due to the concentration of algal biomass within the euphotic zone that Sukias et al. (2001) showed to extend 0.1-0.2 m below the liquid surface. The depth-averaged samples of the supernatant should have captured biomass from this part of the water column whereas the foot valve on the effluent pumping line is suspended about 0.5 m below the surface and would draw in biomass in much lower concentrations. The large positive apparent differences

between sample Org-N and BOD₅ concentrations, as well as the smaller negative difference in COD concentrations, appear to be related to seasonality. Hydrolysis of soluble organic material and associated ammonification is more effective in the aerated epilimnion during warmer months, causing Org-N and BOD₅ concentrations to be lower in the supernatant samples.

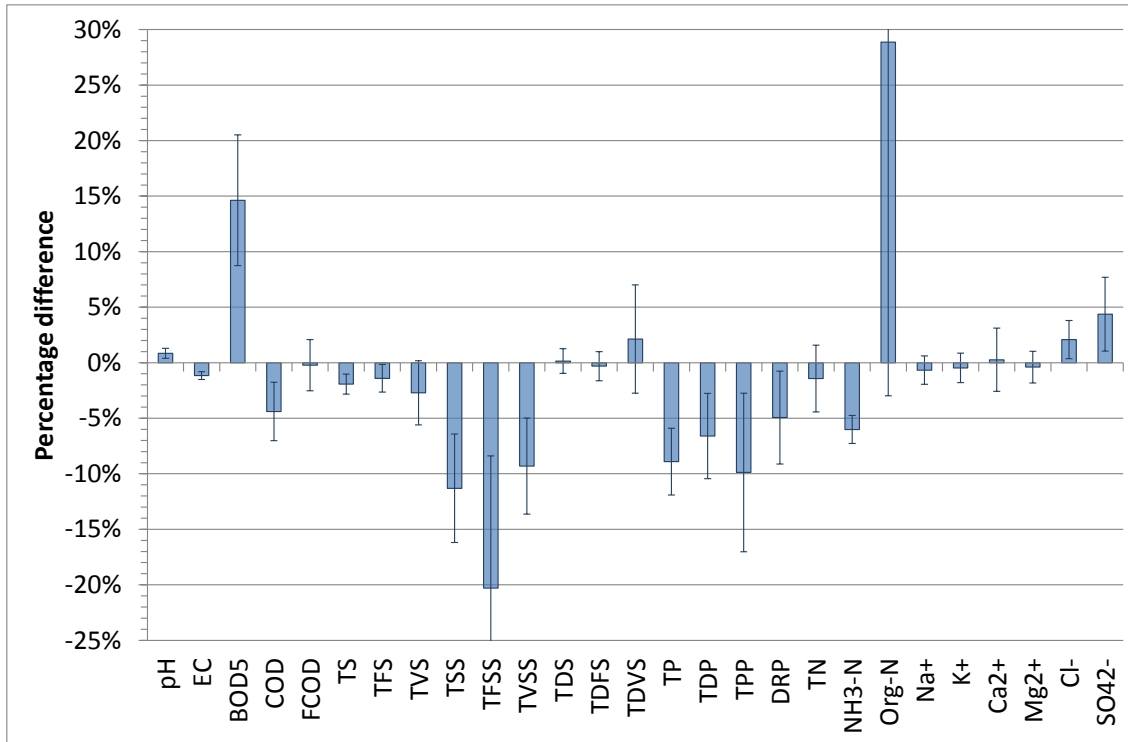


Figure 7-1 Percentage differences between facultative pond supernatant (reference) and recycled effluent. Error bars are 95% confidence intervals.

Supernatant algal biomass

The presence of algae in the facultative pond was measured by chlorophyll-*a* ($(Chl - a)_{ze}$) concentration in samples of the full water column. Although algal growth was likely to be confined to the euphotic zone, sampling the entire water column ensured that no supernatant containing algal biomass was left un-sampled. Figure 7-2 plots the raw chlorophyll-*a* data against time together with estimated chlorophyll-*a* and algal biomass concentrations for the euphotic zone. To estimate the euphotic depth, the light attenuation coefficient k_d was first estimated using an equation quoted by Stefan et al. (1983):

$$k_d = \frac{1.7}{z_s} \quad (7-1)$$

where z_s = Secchi depth (m).

Light attenuation was then used to calculate euphotic depth, taken as the depth at which 99% of downward irradiance is extinguished (Sukias et al. 2001), according to the Beer-Lambert law (Stefan et al. 1983).

$$z_e = \frac{\ln(0.01)}{k_d} \quad (7-2)$$

Measurements of secchi depth were recorded at each sampling event during collection of FS samples, averaging 0.022 m with a standard deviation of 0.008 m. Euphotic zone chlorophyll-a was then back calculated from the full depth concentration:

$$(Chl - a)_{z_e} = \frac{z}{z_e} (Chl - a)_z \quad (7-3)$$

where z = full liquid depth (m);

z_e = euphotic depth (m).

Chlorophyll-a was assumed to constitute approximately 1.5% of algal biomass (APHA 1998), thus biomass concentrations were calculated by multiplying chlorophyll-a by 67. The results plotted in Figure 7-2 show a distinct seasonality to algal growth, peaking in October through December and then declining to a low in June before beginning to rise again as spring commences in September. Ranging from close to zero in winter to almost 100 mg L⁻¹ in summer, full depth biomass concentrations are much lower than supernatant TSS concentrations, indicating that live biomass makes up only a small fraction of suspended material. However, they are of a similar magnitude to the difference between supernatant and effluent TSS concentrations (average 56 mg L⁻¹), which would suggest that algae is the reason for the higher particulate load in depth-averaged samples.

The approach adopted to estimate the light attenuation coefficient was verified against an empirical light attenuation model for dairy shed waste facultative ponds in New Zealand derived by Sukias et al. (2001).

$$\log K_d = 0.411 + 0.443 \log (Turbidity) + 0.191 \log (g_{440}) \quad (7-4)$$

where g_{440} = absorption at 440 nm.

Very similar estimates of k_d to those produced by equation 7-4 are produced when a value of 85 m⁻¹ is adopted for g_{440} , which is within reason given the substantially higher BOD observed in this pond relative to BOD levels recorded in the Sukias et al. (2001)

study. As a check on the Chl-a concentrations, full depth Chl-a data were scaled using equation 7-3 to a depth of 0.4 m, which was the sampling depth adopted by Sukias et al. (2001). The range of the adjusted concentrations was 297 and 6133 $\mu\text{g L}^{-1}$, which is comparable to the Chl-a data collected from dairy facultative ponds in NZ by Sukias et al. (2001). Again, the large range in the data is related to the seasonality of algal growth.

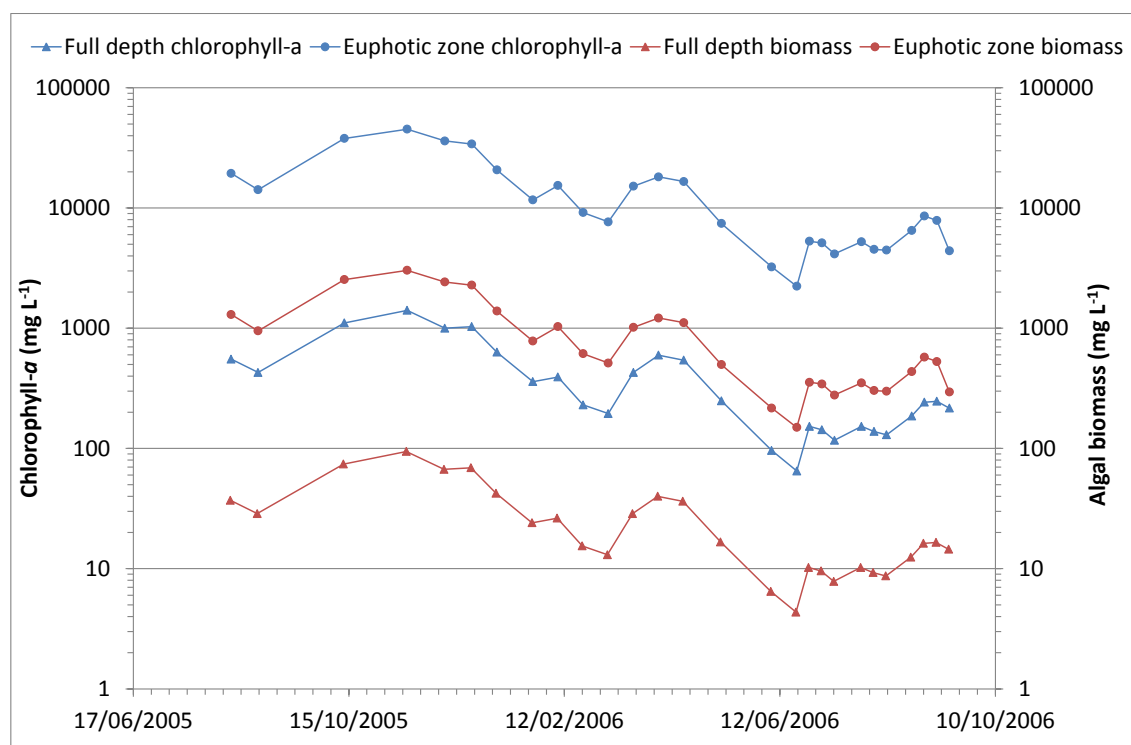


Figure 7-2 Chlorophyll-a concentration measured across the full depth of the supernatant and chlorophyll-a and algal biomass concentrations estimated for the euphotic zone.

7.3.2 Anaerobic Pond Sludge Characteristics

Sludge samples were collected during all anaerobic pond profiling runs except on 9 June 2005, producing a total of five composite samples. The composition of the sludge is presented in Table 7-10. Analytical results were reported on a dry weight basis but for the sake of making comparisons with published data have been converted to mg L^{-1} using bulk density estimates based on moisture content and solids density calculated from fixed to volatile solids content as per the equation derived by Bohnhoff & Converse (1987). Also reported are the constituent concentrations of a single sample collected from the active slurry layer just above the sludge layer (see Chapter 6 for an explanation of the slurry layer) in March 2006, which are discussed later in this chapter. The full sludge composition data are available in Appendix K.

Mean nutrient concentrations are similar to data reported in the literature for DSE anaerobic pond sludges (Barth & Kroes 1985; Cameron et al. 1996; Zaman et al. 1998; Longhurst, Roberts & O'Connor 2000). Importantly both the magnitudes and relativities of the concentrations are very close to those reported by Ward & Jacobs and (2008a) Ward & Jacobs (2008b) who characterised the sludge of an anaerobic pond servicing a milking herd of around 250 heifers (DemoDAIRY Co-operative Ltd. 2007) and designed according to Australian best practice principles. Although the slurry figures are derived from just the one sample, they indicate that P and the major cations are found in higher concentrations in 'fresh', undigested particulate material than in (partially) digested sludge solids.

Table 7-10 Composition of sludge and slurry samples.

<i>Constituent</i>	<i>Sludge (n=5)</i>				<i>Slurry (n=1)</i>	<i>Sludge Slurry</i> <i>mg L⁻¹</i>	
	<i>Min</i>	<i>Max</i>	<i>Mean</i>	<i>Standard deviation</i>			
	<i>% wet weight</i>						
TS	4.64	7.70	5.96	1.45	0.36	61216	11230
	<i>% TS (dry weight)</i>						
TFS	44.0	47.3	45.6	1.28	48.0	27968	5350
TVS	52.7	56.0	54.4	1.28	52.0	33249	5880
TC	25.3	27.9	27.0	1.02	25.8	16600	2898
TP	0.58	0.62	0.60	0.02	0.79	366	88
TN	2.26	2.60	2.45	0.13	2.40	1517	270
Na	0.20	0.27	0.23	0.04	0.93	138	104
K	0.77	1.13	0.90	0.16	3.40	543	382
Ca	1.80	2.04	1.91	0.09	2.40	1183	270
Mg	0.46	0.55	0.51	0.04	1.04	316	117

Comprising five seasonal samples, the sludge data provide unique insight into the dynamics of pond sludge. Figure 7-3 shows solids and carbon content of the five samples in terms of wet weight. A plot for nutrients and cations is given in Figure 7-4. There is notable constancy in the proportionality between constituents over time, but substantial variability between sampling events in absolute terms. All constituents exhibit a significant drop in concentrations following desludging in late October 2005, followed by a gradual rise in concentrations after desludging. This pattern is suggestive of gradual settlement and consolidation of the sludge over time, which was previously

noted in Chapter 6. The first sludge sample (19/10/2005) was taken after 3 years of operation and just before desludging, while collection of the last sludge sample (12/1/2007), which has similar concentrations to the first, occurred 15 months after desludging. Sludge compaction and consolidation are recognised processes in wastewater clarification, but were only recently incorporated into the well-established double exponential settling model for conventional secondary settling tanks (Abusam & Keesman 2009). Nelson & Jimenez (2000) observed correlations between sludge TS concentrations and sludge depth in sewage stabilisation ponds and attributed them in part to sludge 'compression'. They did not, however, examine the temporal aspect of this relationship, nor the effect of desludging.

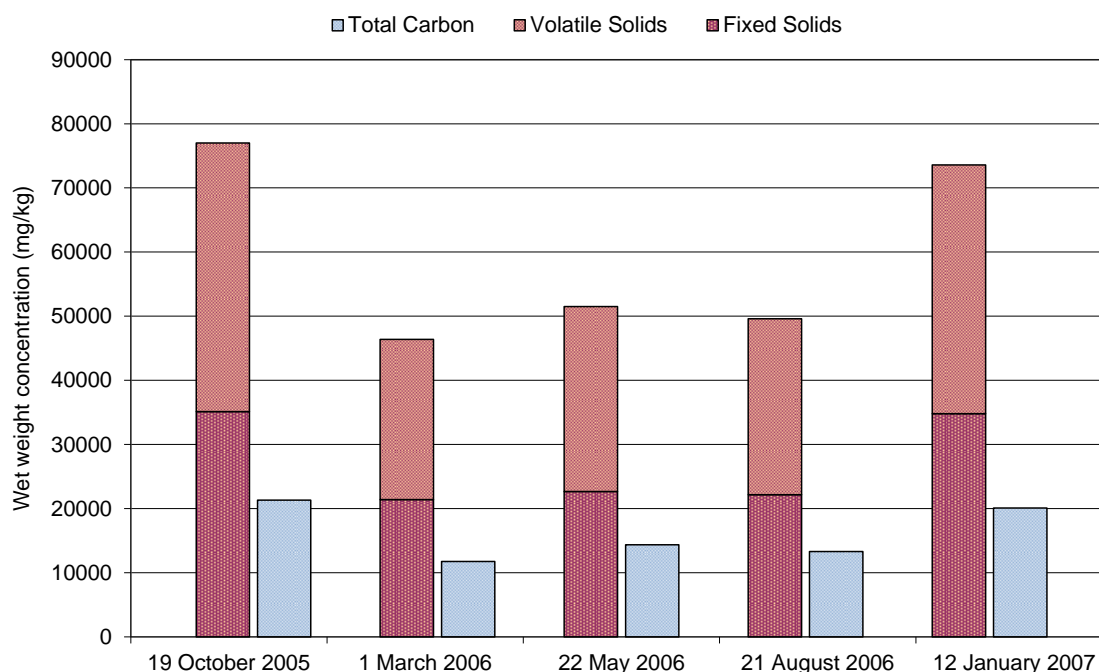


Figure 7-3 Sludge solids and organic carbon by wet weight.

7.3.3 Mass Flows

Wastewater and sludge constituent concentrations were combined with data from the water balance (Chapter 5 and Appendix I) and sludge accumulation analysis (section 3, Chapter 6) to quantify constituent loads entering, accumulating within and leaving the pond system. Load estimates were derived for the year commencing 13 November 2005 (recommencement of flow out of the anaerobic pond following desludging), encompassing 24 of the 31 sampling events.

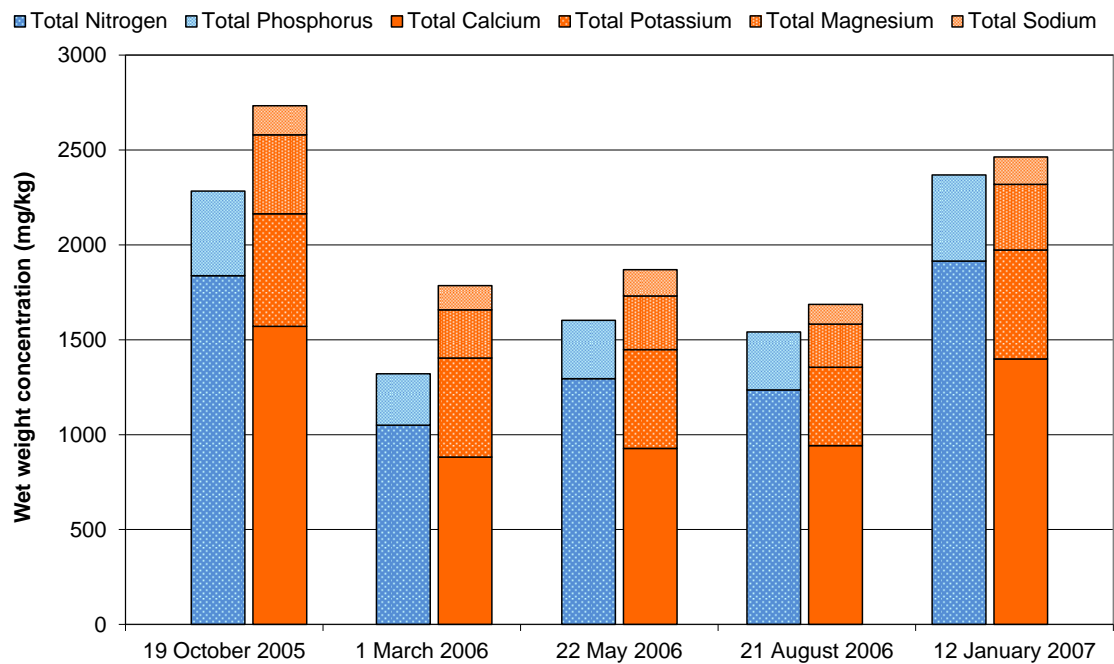


Figure 7-4 Sludge nutrient and cation composition by wet weight.

7.3.3.1 Pond influent and effluent loads

Constituent loads in the wastewaters entering and leaving the two ponds were calculated for each sampling event by multiplying the 24-hour flow by the sample concentration. Average loads and corresponding standard deviations are presented in Table 7-11. To avoid bias from inaccurate anaerobic pond effluent flow measurements identified in Chapter 5, data from two sampling events (16 November 2005 and 5 January 2006) were excluded from the facultative pond loading calculations. The average anaerobic pond loadings are based on data from 23 of 24 sampling events due to autosampler failure on the 5 January 2006 sampling event.

Constituent loads to the anaerobic pond were highly variable, with coefficients of variation (CVs) reaching 48% (TVSS). Passage through the anaerobic pond dramatically reduces variability with the facultative pond influent CVs being in the low to mid-twenties. Relative variability actually rises in the facultative pond (recycled) effluent with CVs around 30%, although this is mostly related to variability in flows as constituent concentrations in recycled effluent are lower and more consistent than anaerobic pond effluent (refer to section 7.3.1).

Table 7-11 Average constituent loading rates to the anaerobic and facultative ponds and in effluent recycled to flood washing over the year commencing 31 October 2005. Error bounds are 95% confidence intervals.

Constituent	Anaerobic pond (n=23)		Facultative pond (n=22)		Recycled effluent	
	kg d^{-1}	$\text{g cow}^{-1} \text{d}^{-1}$	kg d^{-1}	$\text{g cow}^{-1} \text{d}^{-1}$	kg d^{-1}	$\text{g cow}^{-1} \text{d}^{-1}$
TS	169±26	565	73 ± 15	244	49 ± 6	162
TVS	108±20	359	30 ± 5	98	17 ± 2	55
TSS	85±17	283	16 ± 3	54	6.7 ± 1.1	21
TVSS	73±15	242	13 ± 3	43	5.6 ± 0.9	19
TDS	85±11	282	57 ± 12	190	42 ± 5	140
TDVS	35±7	116	17 ± 2	55	11 ± 1	37
BOD ₅	33±4	109	5.7 ± 0.9	19	2.2 ± 0.4	7
COD	143±24	476	33 ± 7	111	17 ± 2.3	56
FCOD	33±4	111	12 ± 3	39	7.1 ± 1.1	24
TP	1.9±0.2	6	1.3 ± 0.2	4	0.6 ± 0.1	2
TDP	0.7±0.1	2	0.8 ± 0.1	3	0.3 ± 0.0	1
DRP	0.6±0.1	2	0.6 ± 0.1	2	0.3 ± 0.0	1
TN	6.7±0.8	22	5.4 ± 0.9	18	3.2 ± 0.5	11
Org-N	3.0±0.5	10	1.7 ± 0.3	6	1.0 ± 0.3	3
NH ₃ -N	3.6±0.5	12	3.7 ± 0.9	12	2.2 ± 0.3	7
Na ⁺	4.3±0.4	14	3.9 ± 0.7	13	2.9 ± 0.4	10
K ⁺	14±0.4	45	12 ± 2	40	9.0 ± 1.2	30
Ca ²⁺	2.3±1.5	8	2.5 ± 0.4	8	1.8 ± 0.2	6
Mg ²⁺	2.1±0.2	7	2.1 ± 0.3	7	1.6 ± 0.2	5
Cl ⁻	8.5±0.3	28	7.1 ± 1.4	24	5.5 ± 0.7	18
SO ₄ ²⁻	1.1±0.2	4	0.5 ± 0.1	2	0.3 ± 0.0	1

Volatile solids (TVS) loading per cow is lower than the estimate of 0.41 kg d^{-1} calculated using the method suggested in the NSW DSE management guidelines (NSW Agriculture 1999) and assuming the herd spends 2.75 hours a day at the dairy (Maloney 2007, pers. comm. 19 February). The volumetric VS loading rate to the anaerobic pond based on the total pond capacity is $0.084 \text{ kg m}^{-3} \text{ d}^{-1}$. At this loading sludge would only have to occupy 30% of the pond before the design loading recommended for the climate zone ($\sim 0.12 \text{ kg VS m}^{-3} \text{ d}^{-1}$) in Birchall, Dillon & Wrigley (2008) is exceeded. The BOD₅ load to the facultative pond expressed on a per cow basis is identical to the loading anticipated by the NSW guidelines. The areal BOD₅

loading to the facultative pond based on the surface area at the 50th percentile of observed liquid depths is 40 kg BOD₅ ha⁻¹ d⁻¹, which is below both the 50 kg BOD₅ ha⁻¹ d⁻¹ upper limit recommended for Australian systems (Birchall, Dillon & Wrigley 2008) and the NZ design loading of 84 kg BOD₅ ha⁻¹ d⁻¹ (DEC 2006).

7.3.3.2 Irrigation loads

There were 19 irrigation events over the year starting 31 October 2005, totalling 256 hours of pumping time. Most effluent irrigation was conducted in summer 2005/06 and autumn 2006. Two irrigations occurred in winter 2006 and three more in the following spring. Total constituent loads and application rates over the monitoring period are presented in Table 7-12. Samples of actual irrigated effluent were not collected, hence loads for individual irrigation events were estimated from linear interpolation between pond effluent sample concentrations recorded closest (either side of) to a given event. Land application rates were simply the total load converted to an annual rate divided by area of the dedicated effluent irrigation paddock (3.2 ha). TN, TP and K⁺ loads amounted to approximately 2%, 3% and 27% of total annual fertiliser use on the farm (at the time of sampling), respectively.

Table 7-12 Constituent loads applied to land over the year commencing 31 October 2005.

<i>Aggregate solids or organic constituent</i>	<i>Total load</i> kg	<i>Application rate</i> kg ha ⁻¹ yr ⁻¹	<i>Nutrient fraction, cation or anion</i>	<i>Total load</i> kg	<i>Application rate</i> kg ha ⁻¹ yr ⁻¹
TS	6904	2132	TP	96	30
TVS	2390	738	TDP	48	15
TSS	940	290	DRP	42	13
TVSS	780	241	TN	447	138
TDS	5964	1842	Org-N	147	45
TDVS	1610	497	NH ₃ -N	298	92
BOD ₅	308	95	Na ⁺	417	129
COD	2330	720	K ⁺	1280	395
FCOD	993	307	Ca ²⁺	252	78
			Mg ²⁺	227	70
			Cl ⁻	777	240
			SO ₄ ²⁻		

7.3.3.3 Anaerobic pond sludge loads

Sludge loads at each profiling event were estimated from the sample concentrations and sludge volume estimated as described in Chapter 6. Total constituent loads accumulated up to the day of desludging and between desludging and the last sampling date are given in Table 7-13. Long term mass accumulation rates were estimated as the slope of the regression (with zero intercept) of cumulative mass against time as per the example for solids loads given in Figure 7-5. Plots for other sludge constituents are presented in Appendix K. In order to combine pre- and post-desludging data, the load of each constituent remaining after desludging (calculated as volume of sludge remaining multiplied by the constituent concentration on 19 October 2005) was added to the corresponding pre-desludging constituent loads. Regression slopes for all constituents were statistically significant, all R^2 values were greater than 0.9 and F-tests indicated that the model fits were sound at the 95% level. Loads removed by desludging were estimated using the sludge composition from 19 October 2005 and the total volume of sludge removed. TN, TP and K loads removed were the accumulation of three years of sedimentation and amounted to 9%, 9% and 8% of total annual fertiliser use, respectively. The average annual accumulation rates, however, represent 3%, 4% and 3% of N, P and K fertiliser demand.

Table 7-13 Accumulated anaerobic pond sludge constituent loads and long term accumulation rates. Error bounds given for accumulation rates are 95% confidence intervals.

Constituent	Total accumulated load		Load removed by desludging	Average accumulation rate	
	Before desludging	After desludging			
	1 August 2002 - 19 October 2005 kg	1 November 2005 - 12 January 2007 kg		kg d ⁻¹	kg cow ⁻¹ yr ⁻¹
TS	67535	29190	52554	58 ± 12	70
TFS	30796	14072	23965	26 ± 6	32
TVS	36739	15117	28589	31 ± 6	38
TP	392	185	305	0.33 ± 0.08	0.4
C	18707	7906	14557	16 ± 4	19
TN	1611	795	1254	1.4 ± 0.4	1.7
*Na	135	57	105	0.11 ± 0.04	0.1
*K	520	230	405	0.40 ± 0.17	0.6
*Ca	1378	534	1072	1.2 ± 0.2	1.4
*Mg	365	126	284	0.31 ± 0.09	0.4

* Total constituent fraction (as opposed to the soluble fraction analysed in wastewater samples).

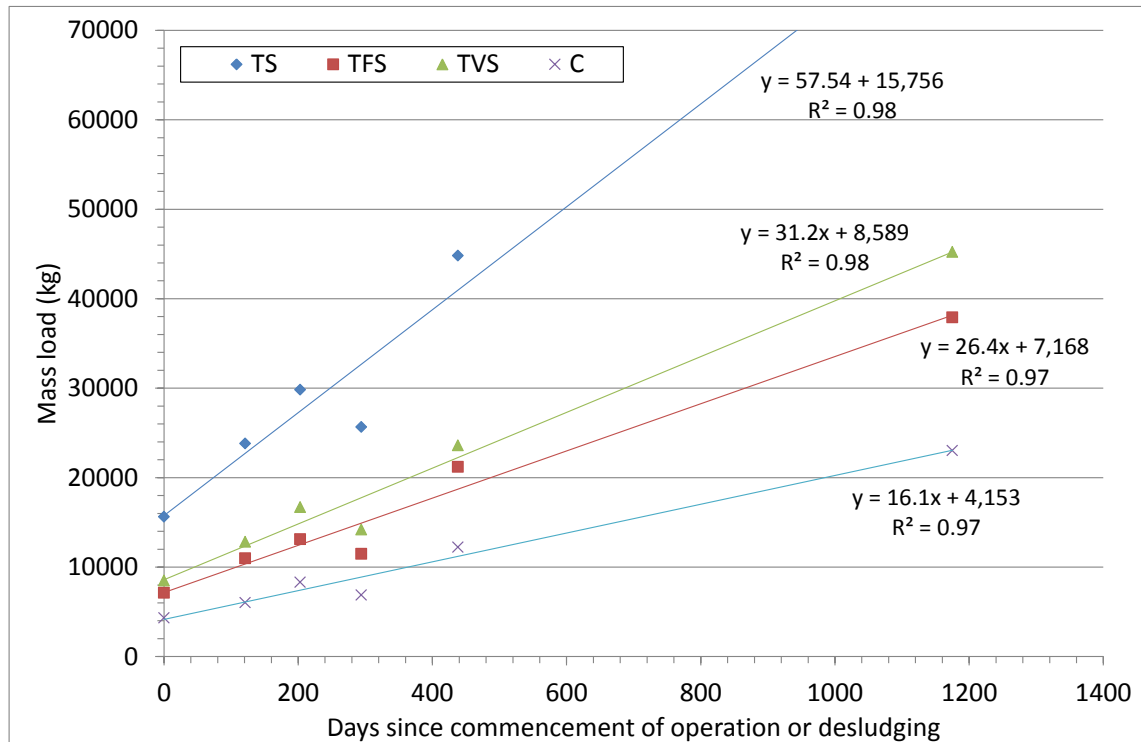


Figure 7-5 Example of linear regressions used to estimate sludge constituent (total, total fixed, and total volatile solids and carbon) mass loading rates.

7.3.3.4 Seepage losses

Leaching of soluble wastewater constituents from the pond basins was estimated under the assumption that concentrations in seepage leaving the pond were equivalent to supernatant concentrations, which in the case of the anaerobic pond were in turn assumed to be the same as effluent concentrations under a complete mix (liquid) flow regime. In the anaerobic pond, leachate is likely to have been drawn through the sludge blanket, but soluble fractions were not analysed for the sludge samples. Data presented by Ward & Jacobs (2008a), however, indicate that concentrations of soluble components are in fact similar to effluent/supernatant concentrations, providing the basis for using effluent concentrations in leachate calculations. Supernatant profiling of the facultative pond suggest that soluble components may be more concentrated at the bottom of the pond from where leachate would be drawn (see section 3.2.3 in Chapter 4). Nonetheless, the composite samples of the water column are thought to provide a reasonable surrogate, especially given the very small seepage flows from the pond.

Table 7-14 presents the estimates of the constituent loads leaving the pond via seepage over the year commencing 31 October 2005. Loads were calculated using average constituent concentrations and total seepage losses over the monitoring period while loss rates were calculated as average seepage multiplied by average

supernatant concentration. Note that the calculation of uncertainty bounds was not feasible as there is no means by which the standard error of the seepage estimates can be determined for the full year.

Apparent seepage losses from the facultative pond were negligible, but nutrient and cation losses from the anaerobic pond were as high as 10% of influent loads. The large differences between the losses from the two ponds are due to the much higher seepage flow from the anaerobic pond (refer to Chapter 5). It is possible that exports of wastewater constituents via seepage are much higher if intrusion of seepage from the anaerobic pond is in fact masking seepage losses as suggested may be the case in Chapter 5. However, in the absence of groundwater flow and quality data we can only base estimates of seepage losses/gains on apparent net hydrogeological fluxes.

Table 7-14 Estimated seepage loads of soluble constituents for the year commencing 30 October 2005.

<i>Constituent</i>	<i>Anaerobic pond</i>		<i>Facultative pond</i>	
	<i>Load</i>	<i>Loss rate</i>	<i>Load</i>	<i>Loss rate</i>
	<i>kg</i>	<i>g d⁻¹</i>	<i>kg</i>	<i>g d⁻¹</i>
TDS	2189	5996	41.0	112
FCOD	448	1226	6.9	19
TDP	29	80	0.4	1
DRP	24	66	0.3	1
NH ₃ -N	140	385	2.2	6
TON	3	7	0	0
Na ⁺	147	402	2.9	8
K ⁺	456	1248	8.9	24
Ca ²⁺	96	262	1.8	5
Mg ²⁺	78	215	1.6	4
Cl ⁻	271	743	5.3	15
SO ₄ ²⁻	18	50	0.3	1

7.4 ANALYSIS AND DISCUSSION

7.4.1 Effects of Sludge Accumulation

Analysis of wastewater constituent time series data reveals peak concentrations for particulate constituents generally coincided with the sludge level in the anaerobic pond reaching its peak before the pond was desludged. Figure 7-6 shows elevated COD,

TSS, TVSS and BOD₅ concentrations in the anaerobic and facultative pond effluents in the 2-3 months prior to desludging. Impaired settling due to the reduced HRT and/or re-suspension of solids from the rising sludge blanket caused elevated effluent solids concentrations, which in turn increased the solids concentration in the facultative pond supernatant and effluent. Higher solids concentrations in recycled effluent would also have increased the solids loading to the solids trap, although the additional load did not appear to be passed on through to the influent to the anaerobic pond. The peaks leading up to desludging are more dramatic in the anaerobic pond. Dilution and additional treatment evidently dampened and/or delayed the effect in the facultative pond. TP (also in Figure 7-6) showed a similar, albeit not so distinctive pattern in the anaerobic pond with concentrations declining less markedly following desludging. The impact of high sludge levels on pond system performance was also noted by Sukias et al. (2001), who observed strong negative correlations between facultative pond effluent BOD₅, turbidity, EC, TSS, TVSS and TN concentrations and free-water depth in the anaerobic pond. Contrary to the findings of Sukias et al. (2001), however, TN concentrations in this study showed no signs of sludge-related increases in either pond.

The soluble fraction of COD also peaked in both ponds in the lead-up to desludging (Figure 7-6), although FCOD concentrations had dropped again before desludging was commenced. It would appear that the reduced HRT caused by the sludge blanket had its greatest effect on removal of soluble biodegradable material when temperature was low. The increased biological activity fostered by the increasing temperature over spring may have been enough to offset the efficiency lost to sludge accumulation. This inference is not verified by the TDVS data which exhibits no distinguishable peak at all, hence it can at best be considered speculative.

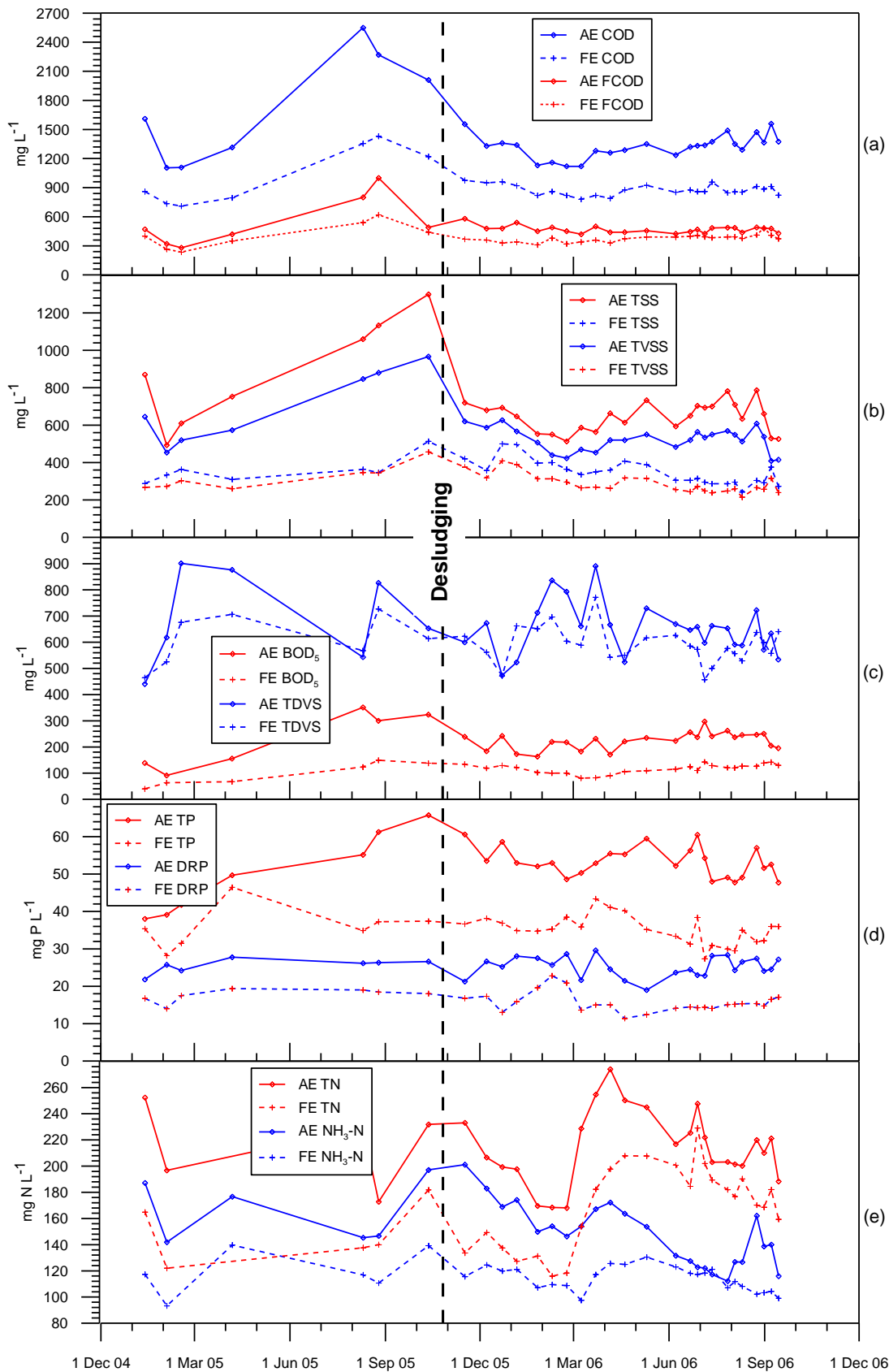


Figure 7-6 Anaerobic (AE) and facultative (FE) pond effluent constituent concentrations over time
(a) COD and FCOD; (b) TSS and TVSS; (c) TVDS and BOD₅; (d) TP and DRP; (e) TN and NH₃-N.

The effects on other soluble constituents were varied. Figure 7-7 shows inert dissolved solids (TDFS) peaking around desludging in the anaerobic pond as did EC (see Chapter 4); however, in the facultative pond EC peaked around June 2006 after exhibiting a smaller peak around the time of desludging. The delayed peak in the facultative pond would be related to prolonged mass transfer between the ponds and to dilution by the existing supernatant and rainfall. This is somewhat contradicted by K^+ and Na^+ concentrations peaking in May/June 2006 in both ponds, whereas Ca^{2+} and Mg^{2+} show peaks of similar magnitude around both October 2005 and June 2006 in both ponds. Cl^- peaks in October 2005 in the anaerobic pond and in June 2006 in the facultative pond. SO_4^{2-} exhibited no distinctive peaks in either pond while oxidised N concentrations were too low to discern peaks (data not shown). Returning to Figure 7-6, NH_3-N concentrations in both ponds exhibit a mild peak immediately prior to desludging while the rising sludge appears to have had no bearing on DRP concentrations.

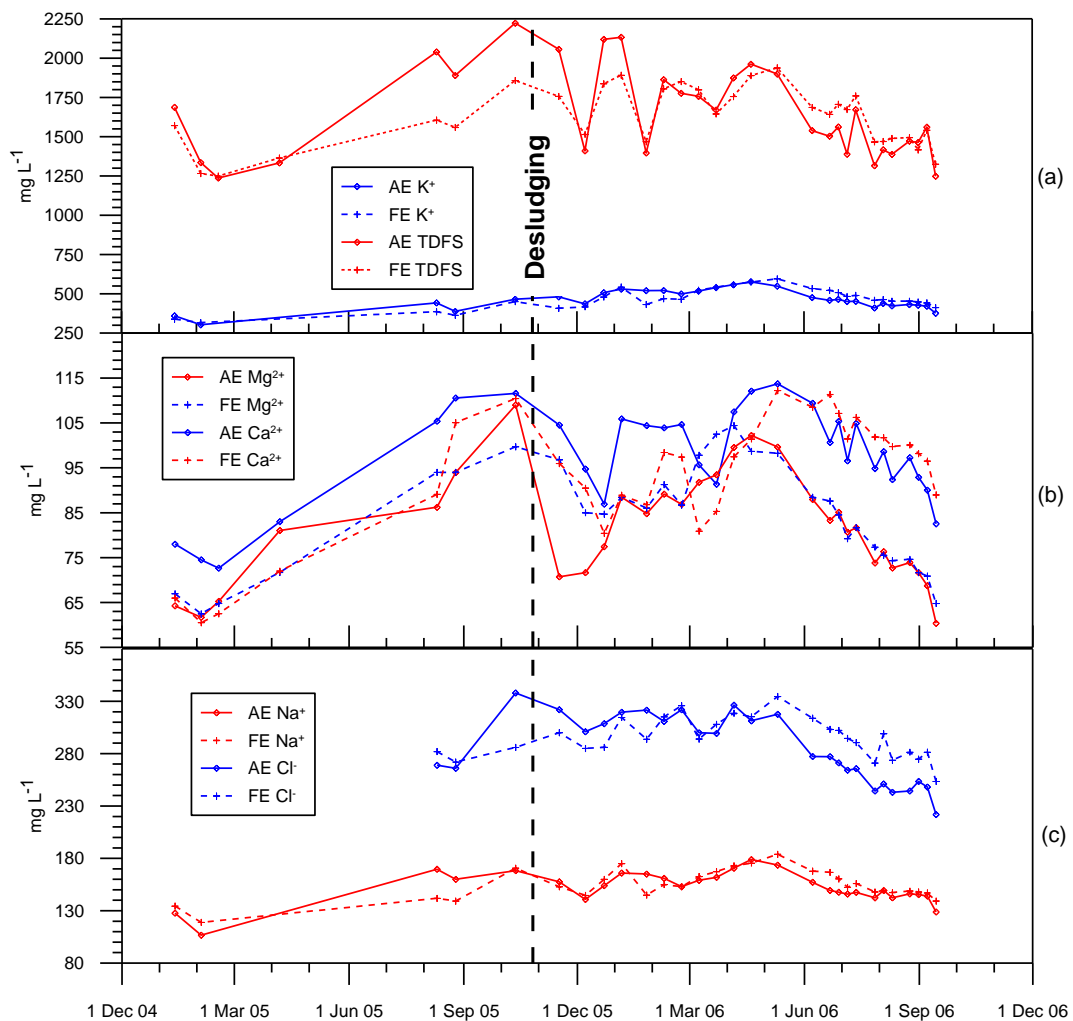


Figure 7-7 Anaerobic (AE) and facultative (FE) pond effluent constituent concentrations over time
(a) TDFS and K^+ ; (b) Ca^{2+} and Mg^{2+} ; (c) Na^+ and Cl^- .

The fact that only three of the eight major ionic species monitored peaked in the anaerobic pond at the same time as EC/TDS/TDFS suggests that other ionic species were behind the increasing concentration of dissolved solids. Anaerobic digestion in the sludge generates carbon dioxide at a rate that increases with rising temperature. This carbon dioxide causes the carbonate buffering system to produce carbonate and bicarbonate ions. Alkalinity was not part of the routine laboratory analyses; however, analyses performed on 3 sets of influent/effluent samples indicated that alkalinity did increase through the anaerobic pond. And as noted in Chapter 4, pH was suppressed in the anaerobic pond, plus it is unlikely that iron, aluminium, manganese or other common ionic species would be present in the concentrations required to push TDS to the levels observed in the pond system. Thus it is suggested that as the liquid volume of the pond declined with increasing sludge, the carbonate/bicarbonate contributions from the sludge became increasingly concentrated, effectively raising aggregate dissolved salt levels.

Another factor that would have contributed to mineral salts peaking in the anaerobic pond prior to desludging would be contributions of soluble cations from digesting sludge. Increases over time in the dissolved fraction of solids have previously been observed in cattle manure held in storage for as little as two weeks (Møller, Sommer & Ahring 2002). The study did not examine specific ionic species, but the changes were attributed to hydrolysis of organic particulate matter. Total Ca and Mg levels in the pond sludge of the present study (averaging 1172 and 313 mg L⁻¹, respectively) were much higher than concentrations of the corresponding soluble forms in the effluent (98 and 82 mg L⁻¹, respectively), suggesting that there is a large bank of organically complexed or precipitated forms of these cations in the sludge that could be subject to solubilisation. K and Na concentrations in the sludge (537 and 137 mg L⁻¹, respectively), on the other hand, were very similar to effluent concentrations (463 and 152 mg L⁻¹, respectively). These cations mainly come from the urine in manure (Safley, Westerman & Barker 1986; Meyer, Ristow & Lie 2007) and being highly soluble, are not likely to be retained in particulate material either in complexed or precipitate forms (Hjorth et al. 2010).

The potential for mineral salts to be released from pond sludge is supported by the higher total cation concentrations (in terms of % dry solids) observed in active slurry compared with digested sludge concentrations (section 7.3.2). Similarly, when expressed as percentage dry solids, the soluble fractions of cations, as well as total P and N in the anaerobic pond influent are in higher concentrations than corresponding sludge fractions. The combined contributions of cations, ammonium and free

orthophosphate from the sludge would also aid in causing aggregate salt levels to rise at high sludge levels as the increasingly smaller supernatant volume has to accommodate the same rate of release of ionic species from the sludge.

7.4.2 Constituent Correlations

In instances where data for a particular constituent are not available, it is helpful to be able to draw on other available data to make estimates to substitute for the missing data. Figure 7-8 presents scatter plots of conductivity against total dissolved solids and fixed dissolved solids. There is a clear distinction in both plots between the system influent and the pond effluents in that the TDS and TDFS content are higher relative to EC in the influent. The steeper slope of the influent EC-TDS plot is a function of both a higher content of dissolved organic compounds in the influent and differing dominant ions between the influent (settled raw wastewater) and the biologically stabilised effluent (Burden et al. 2002). The smaller difference between the influent and effluent EC-TDFS slopes should be solely due to the different ionic make-up. Soluble cation and Cl^- concentrations were very similar between the influent and effluents, hence the ionic species differentiating EC-TDFS relations are most likely carbonate and bicarbonate.

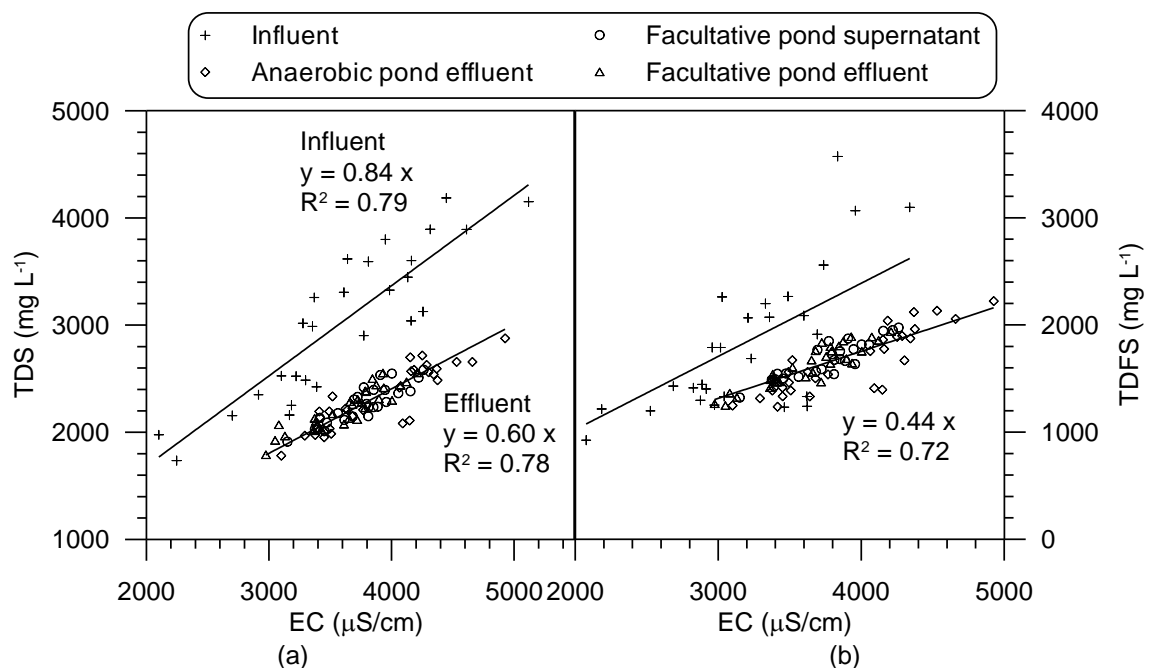


Figure 7-8 Wastewater constituent correlations: (a) EC vs TDS; (b) EC vs TDFS

Figure 7-9 presents correlations between wastewater constituents that are often related in wastewater treatment modelling. The purpose of this plot is to test veracity of the assumption often made in wastewater treatment modelling of constancy in influent

fractionation (see Henze 1992; Melcer et al. 2003). The relationships between fractions of organic material (COD, FCOD and TVSS) show strong consistency; however the relativities of nutrient fractions are not so stable. This suggests that a 'typical' fractionation for COD and influent N (not effluents) may be applicable to DSE, but is not advisable for P. Constituent fractionation for wastewater modelling is elaborated on in Chapter 8.

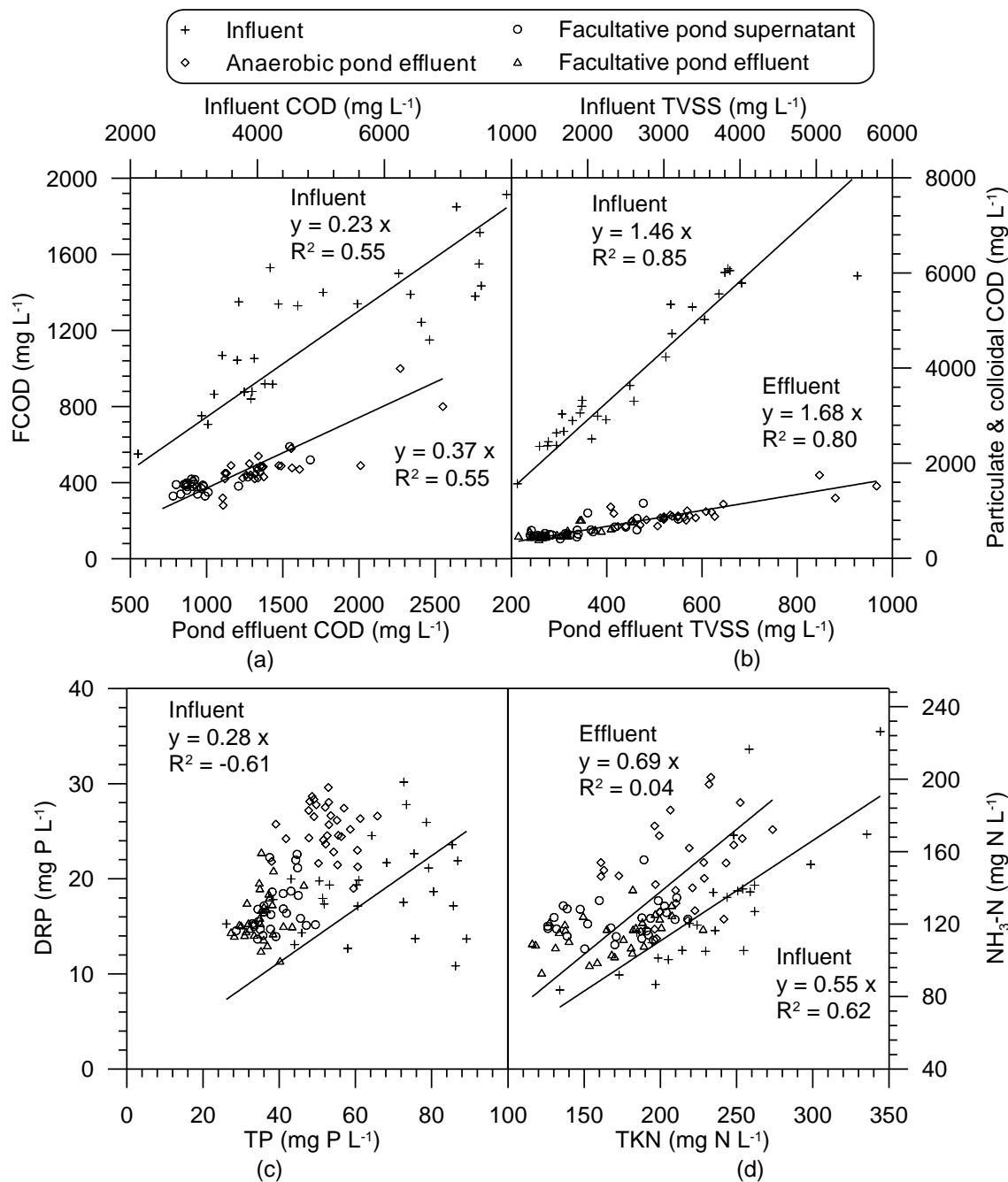


Figure 7-9 Wastewater constituent correlations: (a) COD vs FCOD; (b) TVSS vs particulate and colloidal COD; (c) TP vs DRP; (d) TKN vs NH₃-N.

The plots in Figure 7-10 show that turbidity and TSS are reasonable indicators of algal biomass (as indicated by chlorophyll-*a*). The fits are not particularly strong, although this is due to the presence of residual suspended solids from the influent (as well as data noise). The similarity of the two plots is testament to the close correlation between TSS and turbidity.

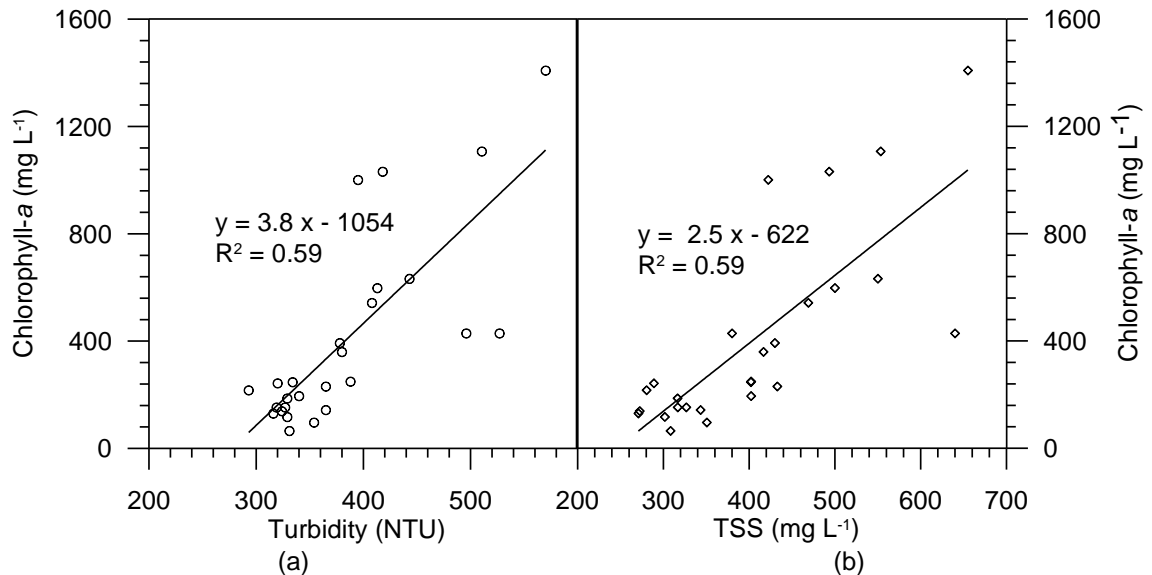


Figure 7-10 Correlations between turbidity, TSS and chlorophyll-*a* in the facultative pond.

7.4.3 Load Distributions

Figure 7-11 presents histograms of particulate/organic wastewater constituent loads in the anaerobic pond influent and effluent (AI and AE) and the facultative pond effluent (FE). It is immediately clear that treatment in both ponds not only reduces the size of the loads leaving the ponds, but also significantly dampens their variability. Critically, however, the effect is much less marked on the nutrients than the measures of solids and organic matter (TSS and COD, respectively). Not only do TN and TP influent loads show much less variability to start with, but the reductions in averages and variability of the loads are not nearly as dramatic. This indicates that the link between particulate (organic) content and particulate/organic N and P fractions is tenuous and that removal of suspended (organic) matter by sedimentation is not likely to translate directly to removal of particulate/organic fractions of N and P. It should also be noted that the distributions of the AI loads are non-normal, particularly those of TSS and COD which exhibit long tails in the positive direction.

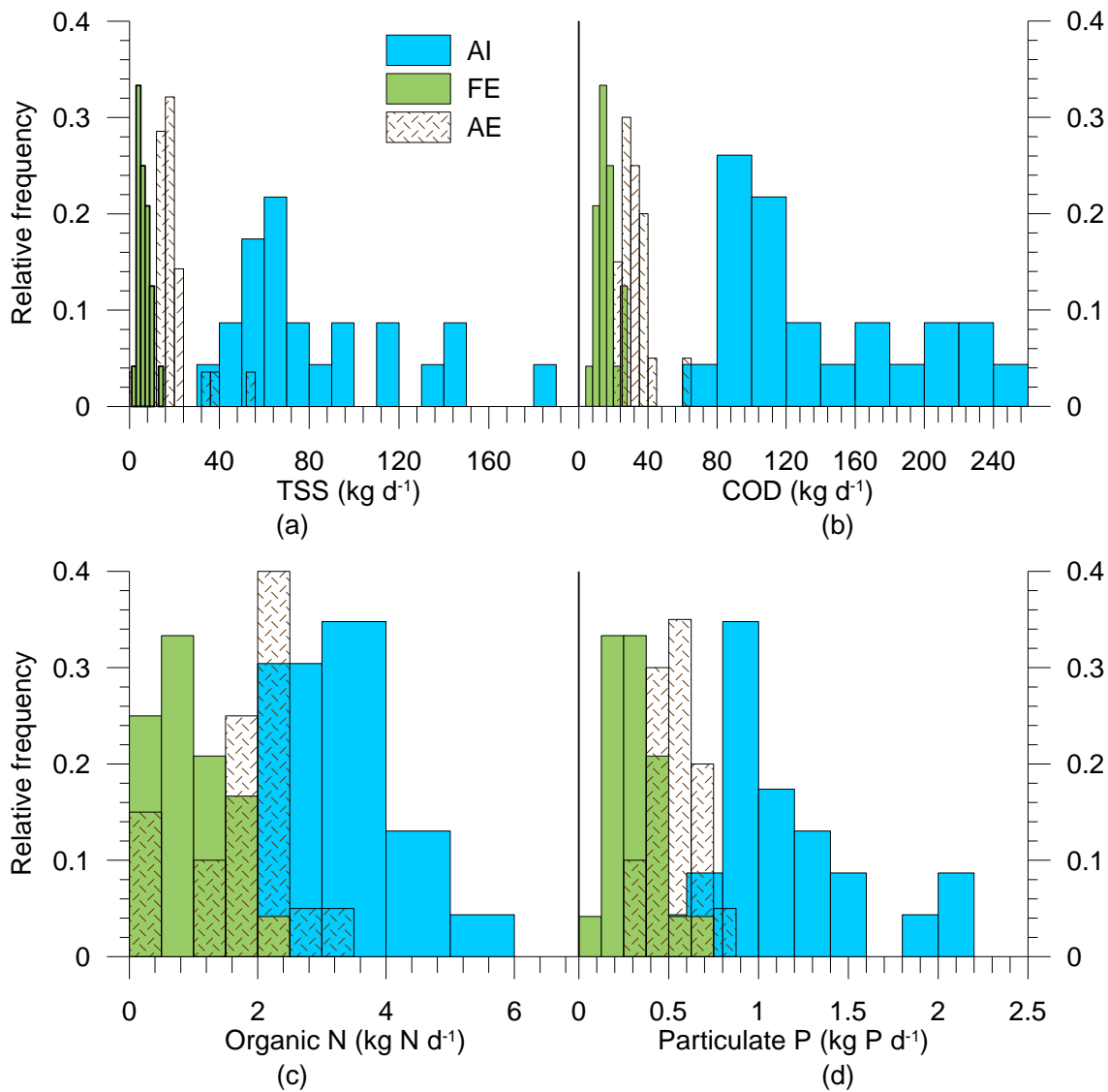


Figure 7-11 Histograms of constituent loads: (a) TSS; (b) COD; (c) Organic N; (d) Particulate P.

Histograms for soluble wastewater constituents are presented in Figure 7-12. Of note is that AI loads are not as widely distributed, and are more resemblant of a normal distribution. Also, it is clear that the majority of variability in DSE comes from the particulate organic matter, which the state of the solids trap would play a significant role in determining, along with variability in manure loads related to herd size and management. The solids trap, however, has less influence on nutrient loads, both particulate and soluble, since nutrients do not appear to be closely associated with settleable particulate matter. This supports the findings of Meyer, Ristow & Lie (2007) who found that more than 80% of N and P are contained in particles smaller than 125 μm that are not readily settleable. Also clear is the distinction between reactive and inert species, with (inert) TDFS and K^+ showing very little change in the size or distribution of loads through the ponds. Inert species loads of a given wastewater still

show considerable variability however, most likely due to varying rates of land application and recycling of effluent.

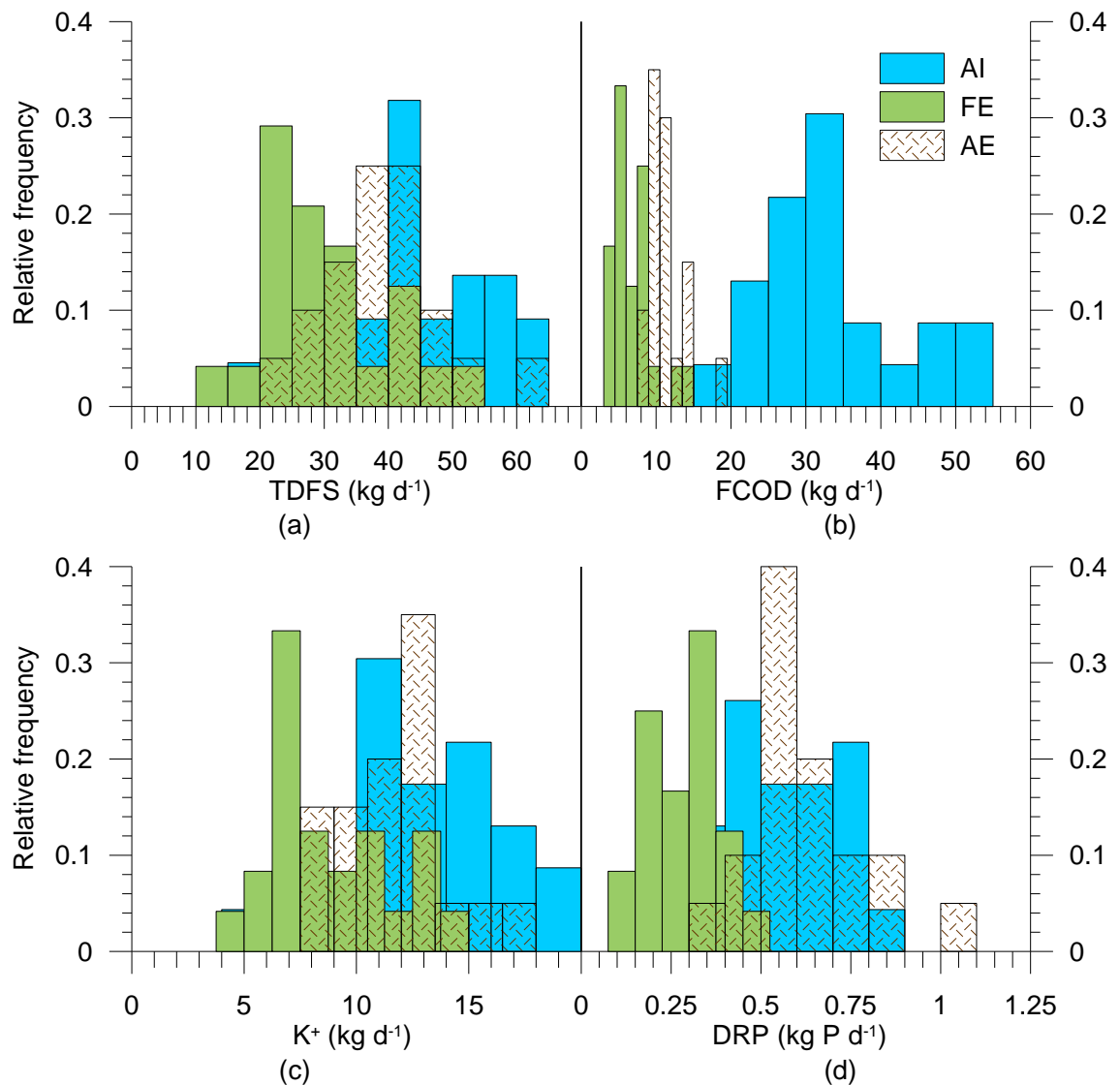


Figure 7-12 Histograms of soluble constituent loads: (a) TDFS; (b) FCOD; (c) K^+ ; (d) DRP.

7.4.4 Constituent Fractions and Wastewater Treatment Processes

Table 7-15 presents ratios of wastewater constituents that provide insight into the treatment performance of the system. Suspended solids made up the main portion of the solids removed in the system, with TSS:TS decreasing significantly through the system. The volatile fraction of suspended solids underwent no change through the system suggesting that organic solids are not greatly affected by hydrolysis whilst in suspension. The COD:TS and TVS:TS ratios show that a large fraction of the material entering the anaerobic pond was oxidisable. Both ratios declined with each treatment stage as the degradable fraction was settled out or metabolised by bacteria. The

influent COD:TS was lower than levels recorded by Sweeten & Wolfe (1994) and Wilkie et al. (2004), which may be indicative of accumulation of inert material through effluent recycling. The high COD in the facultative pond effluent, however, meant that the COD:TS ratio was higher than corresponding values observed by Sweeten & Wolfe (1994), suggesting this system was not as biologically effective as the larger US ponds.

Indeed the ratio of particulate and colloidal COD (PCOD – calculated as the difference between COD and FCOD) to TVSS was relatively steady between the two ponds, indicating most COD reductions involved settling as a precursor to oxidation, while total COD:TVSS increased indicating a large pool of soluble non-biodegradable COD. Perhaps unexpectedly given that manure characteristics can be so variable, the PCOD:VSS ratio of the influent was very similar to the value of 1.55 calculated from data presented by Wilkie et al. (2004). The dominance of settling and the lack of biological treatment was also evidenced by the small change in the TDVS:TDS ratio through the system and the increase in the soluble COD fraction relative to total COD. Interestingly the oxygen demand of influent soluble organic material was low compared with that observed by Wilkie et al. (2004) and continued to decrease through the system. The material leaving the facultative pond was mostly inert, as the ratio TVS:TS was only 35%. Of the organic fraction, less than 30% was readily degradable as indicated by the BOD₅:FCOD ratio.

The FCOD:COD and BOD₅:COD ratios show that only about a quarter or less of the influent organic material is readily biodegradable. The influent FCOD:COD ratio is lower than the figure of 0.38 reported by Wilkie et al. (2004) for settled DSE, most likely on account of lower efficiency of solids separation in this study. It is also lower than the ratio observed by Ellwood & Mason (2003) (0.41); however this is more likely to be related to their analytical method, which employed centrifugation only (no filtration) for determining 'soluble' COD. Initially BOD₅ and FCOD appear to measure a similar fraction of organic matter, but as the wastewater moves through the system, BOD₅ makes up a smaller fraction of FCOD and COD while FCOD:COD increases. This suggests two things. First, BOD₅ actually includes some readily biodegradable, settleable particulate and/or colloidal material. Indeed the influent BOD₅:COD is low compared to data from Ellwood & Mason (2003) and Cumby et al. (1999) for raw dairy shed wastewater, possibly on account of more effective removal of BOD₅ in the solids trap than COD removal. Second, as Sukias et al. (2001) pointed out, some of the large pool of slowly biodegradable COD is hydrolysed (mostly in the sediments as observed above), adding to the refractory soluble fraction of COD as well as the readily degradable fraction.

Table 7-15 Average wastewater constituent ratios

<i>Constituent ratio</i>	<i>Basis</i>	<i>Influent</i>	<i>Anaerobic pond effluent</i>	<i>Facultative pond effluent</i>
TVS:TS	Mass	0.62	0.41	0.35
TDVS:TDS	Mass	0.40	0.29	0.27
TSS:TS	Mass	0.49	0.23	0.14
TVSS:TSS	Mass	0.85	0.81	0.84
COD:TS	Mass	0.84	0.47	0.35
COD:TVSS	Mass	2.05	2.53	3.12
PCOD:TVSS	Mass	1.52	1.66	1.79
FCOD:TDVS	Mass	1.12	0.76	0.65
BOD ₅ :COD	Mass	0.23	0.16	0.12
BOD ₅ :FCOD	Mass	0.95	0.46	0.29
FCOD:COD	Mass	0.25	0.34	0.42
DRP:TP	Mass	0.31	0.48	0.48
DRP:TDP	Mass	0.83	0.85	0.89
NH ₃ -N:TN	Mass	0.55	0.70	0.70
BOD ₅ :TP	Mass	17.3	4.24	3.41
BOD ₅ :TN	Mass	4.89	1.07	0.70
NH ₃ -N:DRP	Molar	16.4	13.9	7.36
Mg ²⁺ :DRP	Molar	5.44	4.42	5.36
Ca ²⁺ :DRP	Molar	3.88	3.18	4.63
SAR	Molar	2.92	2.74	2.77
PAR	Molar	5.22	4.89	4.92

Mineralisation of (settled) organically bound P and/or dissolution of phosphate precipitates appears to be contributing orthophosphate to the effluent, with DRP:TP increasing through the anaerobic pond. Most dissolved P is in the inorganic reactive (orthophosphate) form, with the fraction increasing through the system. The anaerobic pond is also increasing the fraction of ammonium in the wastewater through the mineralisation of organic N, while in the facultative pond removal of ammoniacal N appears to keep pace with mineralisation of organic N. Influent BOD₅:TP and BOD₅:TN ratios are lower than figures determined by Ellwood & Mason (2003) for raw wastewater, but could be high enough to sustain biological N and P removal with adequate hydrolysis and fermentation in the anaerobic pond (Beck et al. 2007). In the ponds, however, the ratios drop to levels unviable for P removal by phosphate accumulating organisms and denitrification.

The molar ratios of ammonium and Mg to DRP (assumed to be equivalent to orthophosphate) in all three wastewaters indicate phosphate is the limiting component

for precipitation of struvite, which requires a 1:1:1 ratio between the three constituents. This is unusual since Mg is often identified as the limiting component in livestock wastes (Hjorth et al. 2010). Molar Ca:P ratios required for precipitation of Ca dihydrogen phosphate ($\text{Ca}(\text{H}_2\text{PO}_4)_2$), tricalcium phosphate ($\text{Ca}_3(\text{PO}_4)_2$) and hydroxyapatite ($\text{Ca}_5\text{OF}(\text{PO}_4)_3$) are 0.5, 1.5 and 1.67, respectively (Hjorth et al. 2010). Again phosphate also appears to be the limiting component for precipitation with Ca in all three wastewaters.

The sodium adsorption ratios (SAR) for all wastewaters were low compared to values reported by Jacobs & Ward (2007a; 2008) and Jacobs, Ward & Kearney (2008) who observed no appreciable impact on soil Na levels resulting from effluent application. They are also well below 6, the level that it is advised will cause rises in the exchangeable sodium percentage (ESP) of non-sodic soils and associated problems with soil structure and permeability in Australia (NSW DEC 2004). Potassium adsorption ratios (PAR) were almost double SARs, but well below the threshold of 10 above which reductions in soil Ca^{2+} and Mg^{2+} will occur under sustained effluent irrigation (Smiles & Smith 2004). The high molar concentration of K^+ relative to that of Na^+ (12.3 to 6.9 mol L^{-1}) may actually suppress the sodicity of the soil because of the preferential affinity of soils for K^+ over Na^+ (Laurenson et al. 2011).

7.4.5 Mass Balances and Pond Treatment Effects

There are three hydraulic pathways by which wastewater constituents may leave the active liquid volume of the pond – deposition to the sludge, in the seepage through the pond floor or in the effluent. Hence the balance for a given constituent, which for conservative species should amount to zero and for reactive species represents the quantity transformed or lost by active treatment processes, is expressed:

$$R_j = L_{inf,j} - L_{eff,j} - L_{seep,j} - \Delta M_j - \Delta S_j \quad (7-5)$$

where all terms are in kg d^{-1} and:

R_j = net mass converted, removed or added through physical, biological or chemical processes;

ΔM_j = change in the stored (liquid) load of constituent j ;

ΔS_j = change in the sludge load of constituent j ;

$L_{inf,j}$, $L_{eff,j}$ and $L_{seep,j}$ are the mass loadings in the influent, effluent and net seepage, respectively.

The sludge accumulation term was only applied to the anaerobic pond since sludge levels in the facultative pond were too low to measure. This meant that the R_j term for the facultative pond incorporated constituent loads held in the sediment. The liquid storage term only applies to the facultative pond in which excess effluent is accumulated over time. While changes (reductions) to the active liquid volume of the anaerobic pond occur as a result of sludge accumulation, the associated constituent loads are captured in the sludge or effluent. The analysis was applied to the year commencing 13 November 2005 to coincide with the recommencement of effluent flow from the anaerobic pond.

It should be emphasised from the outset that developing a static mass balance for a dynamic system is an exercise fraught with potential bias, primarily because imbalances are likely to arise due to the timing of sample collection in relation to trends in constituent concentrations associated with effluent recycling and changing hydraulic and hydrological conditions. Various checks and adjustments have been made to understand and accommodate temporal bias. For example, trend analyses indicated that averages of influent and anaerobic pond effluent loads were reasonably unbiased by temporal variability, but recycled effluent loads based on averages of individual loads calculated from each of the sampling events were biased by a disproportionately high volume of effluent pumped directly onto the yard on many of the sampling events. Accordingly, average recycled effluent loads were instead calculated from average recycled effluent flow and constituent concentrations over the mass balance period. Nevertheless, in considering the outputs presented below it is important to recognise the limitations of the analysis, which also include a lack of an error measure for load estimates due to the diversity of the methods employed to generate those estimates.

7.4.5.1 Anaerobic pond

Figure 7-13 presents partitioning and losses of aggregate solids and organic constituents in the anaerobic pond. Mass loads are plotted as percentages of the influent load. Bars above the x-axis represent constituent loads leaving or accumulating in the pond as well as generation of additional load (the R term in equation 7-5) from biological or chemical processes (blue bars). The blue bars below the x-axis represent reductions in a constituent caused by treatment processes (also the R term in equation 7-5). Net treatment efficiency incorporating sedimentation is the sum of the blue and

brown (representing sludge) bars. The same plot for the major nutrients, cations and anions is presented in Figure 7-14.

Note that dissolved solids fractions were inferred from EC measurements based on the EC-TDS and EC-TDFS relations defined in 7.4.2. Sludge COD was estimated from the carbon content based on the manure particulate organic matter composition reported by Rico et al (2007) and the carbon to oxygen ratio of each component according to its theoretical oxidation equation. Sludge concentrations of soluble sludge constituents that were not analysed in the lab including FCOD, TDP, DRP, $\text{NH}_3\text{-N}$, Ca^{2+} and Mg^{2+} were assumed to be equal to the supernatant concentrations based on data presented by Ward (2010), Zaman et al. (1998) and Cameron et al. (1996) that indicate that soluble species do not accumulate in pond sludge. Lab analyses of sludge Na and K were for total fractions; however since only a very small fraction of these highly soluble species will be particulate bound, total and soluble loads were assumed to be interchangeable. Seepage BOD_5 loads for both ponds were estimated assuming 100% of BOD_5 is soluble. This would not be the case in reality, but the corresponding treatment efficiency estimates are conservative as a result. Balances were not performed for TON due to the relatively low concentrations that would be more susceptible to any error already present in the analysis.

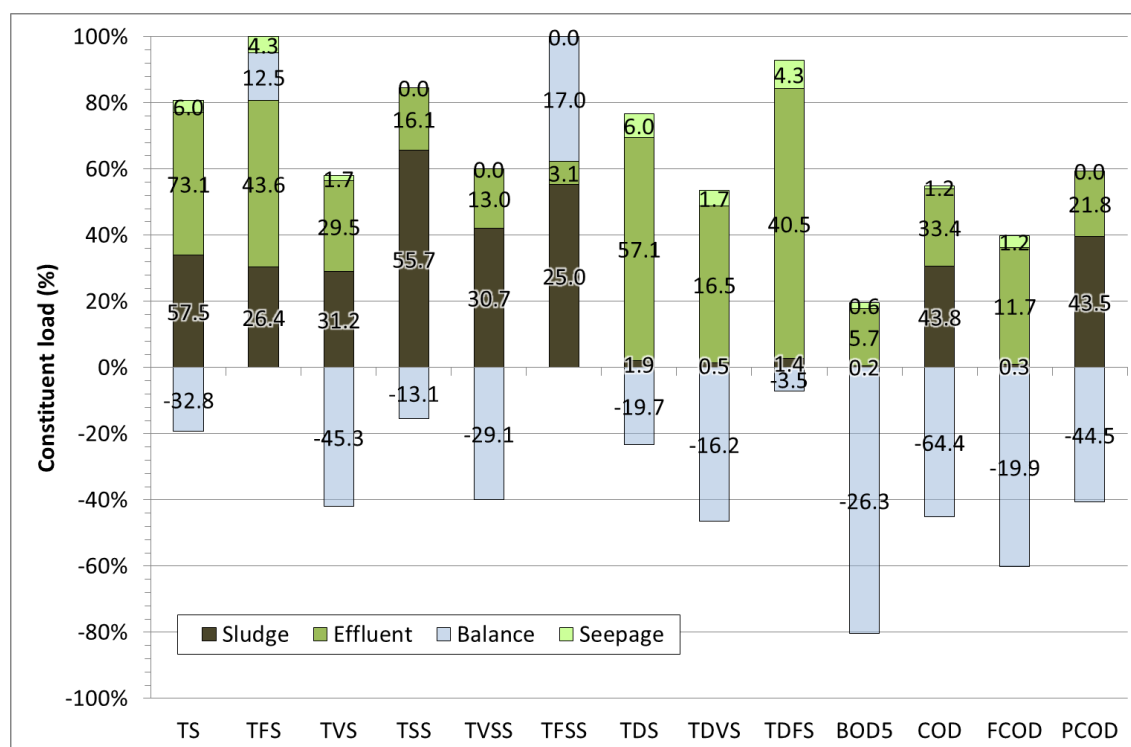


Figure 7-13 Mass balances for aggregate solids and organic constituents in the anaerobic pond.
Data labels are absolute values in kg d^{-1} .

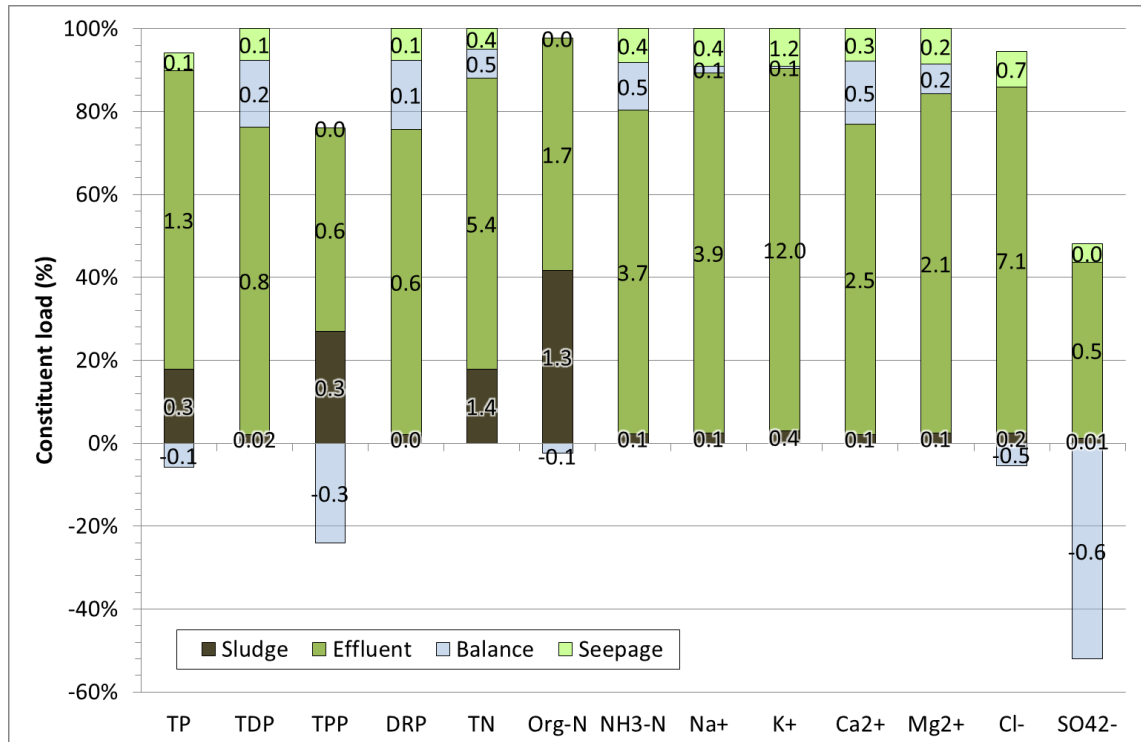


Figure 7-14 Mass balances for the major nutrients, cations and anions in the anaerobic pond.

The first observation to be made is that the mass balances of conservative species mostly produced removal/generation estimates close to zero as expected. In particular, the *R* terms for TP, Na⁺, K⁺ and Cl⁻ are all under 10% with TDFS being the highest at 7%, indicating that bias introduced by sampling is relatively minor. The mass balances for TFS and TFSS, however, are not as reliable. Apparent generation of 12.5 kg d⁻¹ TFS and corresponding net generation of 13.5 kg d⁻¹ TFSS (allowing for precipitation: TFSS generation - TDFS removal), indicates that there is an imbalance of fixed suspended solids in the analysis. A portion of this error is likely to stem from the estimation of sludge TDS and TDFS using EC measurements and the relationships defined 7.4.2. However this approximation unlikely to be the sole source given the magnitude of the error and the apparent balance in the TDFS loads.

Error in sludge load estimates could also arise from sampling bias, analytical error or discrepancies between methods (influent samples were analysed at the University while sludge samples were analysed externally), or the inaccuracy of sludge volume estimates. The influence of sampling bias should be relatively small based on the effective mass accounting seen with the other conservative constituents. Sludge volume estimation has a high degree of uncertainty due to the abstraction of the method and could also explain the imbalance in Org-N discussed below. However it should affect all constituents close to equally, yet the imbalance in TN is not as

dramatic as the TFS imbalance, while for TP there is little sign of any imbalance. In the lab, it is possible that overestimation of TFS occurred due to the hygroscopic nature of the solids causing drying to be incomplete. Inaccurate determination of TVS by incomplete ignition could only result in underestimation of TFS, hence it is unlikely that TVS is inaccurate by association. The problem could also be an artefact of desludging whereby heavier inorganic precipitates that had settled to the bottom of the sludge were not removed by the vacuum hose that could not extend to the very bottom in the middle of the pond and would have preferentially extracted the lighter, less viscous organic sediments. The residual pool of TFSS would have been picked up in the sludge sampling, causing an over-representation of fixed solids that had accumulated since the desludging.

The balances for TVS, TVSS, TDVS, COD, FCOD and PCOD show that there was effective biological breakdown of organic material, although sedimentation accounted for up to 50% of total removal. The 70% removal of TVS came mostly from settling and destruction of TVSS (~ 31 and 29 kg d^{-1} , respectively) with destruction of dissolved volatile solids making up the remaining 16 kg d^{-1} . TVS destruction totalled 42%, which is slightly lower than the mass balanced based estimates of TVS destruction reported by Nordstedt & Baldwin (1975) and Barth & Kroes (1985). Overall VS removal (71% not including seepage losses), however, is comparable to removal efficiencies reported by Safley & Westerman (1992b) and Craggs, Park & Heubeck (2008) (69% and 68%, respectively). Removal of particulate/colloidal COD was significantly higher than FCOD removal, with hydrolysis followed by fermentation and/or oxidation accounting for almost 70% of total COD removal. The production of readily biodegradable material from hydrolysis reduces apparent FCOD removal, although it is likely that a significant fraction of remaining FCOD is non-biodegradable (Mason 1996; Mason & Mulcahy 2003).

Nutrient removal, including that related to sedimentation is low as anticipated by Bolan et al. (2009). At 24% TP reduction in particular was considerably lower than portioning fractions used in the Dairy Pond (50%) and Effluent Toolkit (60%) calculators (Skerman 2004a; McDowell & Birchall 2010) and MEDLI (90%) (Casey & Atzeni 1998). This agrees, however, with the observations of Meyer, Ristow & Lie (2007) that nutrients are concentrated in finer manure particles. TN removal was only 13%, while flux actually came out positive (generation of 8%), which indicates an imbalance between influent, effluent and sludge loads. Given the neutral pH of the pond, it is possible that the main loss pathway, volatilisation, was actually very small and that aside from sedimentation, N removal is very low. The imbalance in TN may be related to bias introduced by

unrepresentative sampling in relation to seasonal variation or an issue related to the laboratory analysis of the wastewater (most likely influent) or sludge samples. Regardless, the results suggest that the main removal pathway for N in the anaerobic pond is sedimentation, not volatilisation, which is also commonly cited as a major pathway for N reduction in DSE ponds (e.g. Van Horn et al. 1994; Bolan et al. 2009). Volatilisation losses have been shown elsewhere to be significant by Rumburg et al. (2008) who estimated $\text{NH}_3\text{-N}$ volatilisation losses from a DSE pond system to be 24% of influent TN. That figure, however, was based on a secondary pond and incorporated losses from all four large (surface area) ponds that were treating/storing effluent with a high N loading from a permanently confined herd.

Critically, $\text{NH}_3\text{-N}$, TDP and DRP loads all increase through the pond. The concomitant reduction in TPP clearly shows that inorganic P is being liberated through mineralisation/hydrolysis of organically bound fractions and dissolution of inorganic precipitate forms. While there is not the corresponding reduction in Org-N, this is likely related to the release of N and P from sediments causing higher effluent concentrations of soluble N and P which has previously been reported by Banks, Heaven & Zotova (2005) in lab-scale facultative ponds. Dawson (2003) also observed substantial rises in ammonia-N occurring in an anaerobic pond treating DSE. Longhurst et al. (2000) identified hydrolysis of urea as being a significant source of $\text{NH}_3\text{-N}$ in DSE ponds. Solubilised amino acids may also be a source of $\text{NH}_3\text{-N}$. Release of organically-bound P is potentially more complex, but is most likely to occur in the sludge, which was the subject of research conducted by Ortuno et al. (2000). They attributed P release to hydrolysis of organic P, but also desorption of P bound to iron (Fe) and aluminium (Al) compounds, particularly under reducing conditions. The only likely source of Fe or Al in the ponds would be the clay, which would already be in a steady state with the P in the overlying sludge and wastewater. P removal in the anaerobic pond is explored further in Chapter 9.

The only major ion species affected by anaerobic treatment was SO_4^{2-} , the loading of which was reduced by 52% presumably by reduction to hydrogen sulphide gas. Balances for Ca^{2+} and Mg^{2+} indicated net generation for both cations, which is related to release of organically bound or complexed forms by hydrolysis of particulate material or dissolution of precipitates as discussed in section 7.4.1. However the 7% net removal of TDFS would suggest that conditions produce net precipitation rather than dissolution. Indeed elevated concentrations of bicarbonate (HCO_3^-) from CO_2 production would lead to precipitation of calcite (CaCO_3) (Hjorth et al. 2010), suggesting that the increases in Ca^{2+} are related to complexed Ca rather than

dissolution of precipitates. The changes to these constituent loads sit within the margin of error for the analysis so it cannot be determined categorically which processes dominate.

7.4.5.2 Facultative pond

Unaccounted for balances of TSS, TVSS and TFSS (47%, 45% and 52%) shown in Figure 7-15 show that settling is still a dominant process at the secondary stage of treatment, although treatment efficiencies for aggregate solids and organic constituents are generally lower than corresponding efficiencies in the anaerobic pond on account of much of the settleable material having been removed in the primary stage. If the sediments can be assumed to have similar solids concentrations to that measured in anaerobic pond sludge just prior to desludging, the volume of sludge theoretically deposited in the pond would be between 32 and 147 m³. The lower estimate represents the case where only inert fixed solids (TFSS) remain in the sludge while the higher figure assumes settled solids are in a similar state of degradation to those in the anaerobic pond and corresponds to a maximum sludge depth of up to 0.15 m. However it is more than likely that much of the sediment load would be hydrolysed and biologically degraded, leaving behind a load closer to that from TFSS loading; hence the absence of measurable sludge observed during the monitoring.

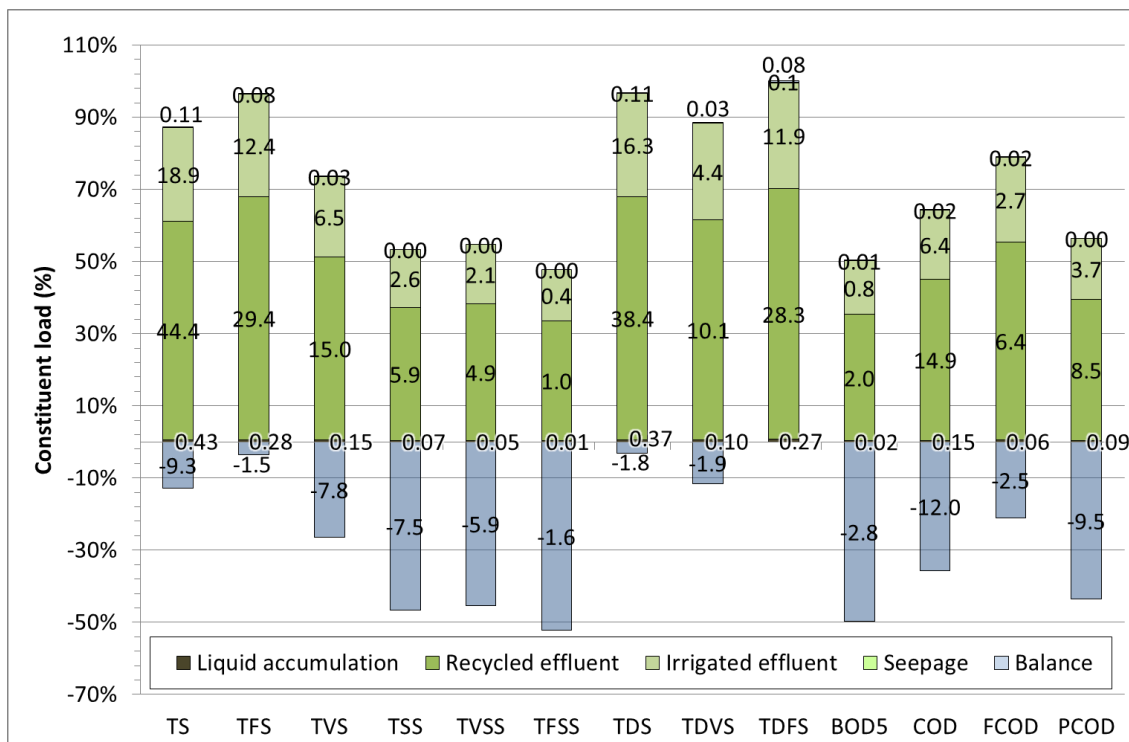


Figure 7-15 Mass balances for aggregate solids and organic constituents in the facultative pond.

Data labels are absolute values in kg d⁻¹.

Removal of COD and TVS amounted to 36% and 26% of the anaerobic pond effluent load, or just 8% and 7% of the total loading to the system. Removal of FCOD is even lower at 21% or 7% of the system loading, although this is again partly due to hydrolysis of PCOD, which constitutes up to 80% of COD removal, depending on the extent of hydrolysis effected on settled organic material. Accordingly, TDVS removal makes up a similarly low fraction of TVDS removal. That only 50% of the incoming BOD₅ load is removed in the pond is also testament to the hydrolysis of slowly biodegradable particulate material. The difference between the effluent (recycled, irrigated and accumulated) COD and BOD₅ loads indicates that some 20% of anaerobic pond effluent, or 5% of system loading is non-biodegradable.

As seen in Figure 7-16 the most notable differences in the treatment effects to those observed in the anaerobic pond were related to the reduction of soluble nutrient fractions, with DRP, TDP and NH₃-N reduced by 39%, 43% and 23%, respectively. In light of the visual observations of struvite formation in the pond and in the recycled effluent holding tank (Chapter 4) and the prevailing supernatant conditions that would promote precipitation, DRP and NH₃-N reductions would at least in part be due to precipitation of struvite. The balance of Mg²⁺ in the pond was negligible, which would contradict the struvite precipitation hypothesis. However the estimate of the struvite precipitation rate derived later in section 7.4.6.1 (2.5 kg d⁻¹) corresponds to a Mg²⁺ removal rate of 0.2 kg d⁻¹ which only occurred for part of the year and would be within the error margins of the analysis. Mg²⁺ removal may also have been masked by unaccounted for Mg²⁺ coming from infiltrating seepage from the anaerobic pond. The same would be the case for the apparent generation of TDFS. The apparent reduction in Ca²⁺ may be related to precipitation of calcite, and possibly Ca phosphates or apatite (Hjorth et al. 2010), again though the negative balance is within the analysis error bounds.

Conditions in the pond (elevated pH, wind agitation) are also conducive to ammoniacal N losses through volatilisation. Net removal of NH₃-N would be suppressed by contributions from mineralisation of Org-N which amount to 12% of the pond effluent load. Expressed in terms of pond surface area, TN removal was 0.9 g m⁻² d⁻¹, which is similar to an estimate for a NZ facultative pond of 0.75 g m⁻² d⁻¹ from Mason (1996). Even without allowing for struvite-related losses, the areal N removal rate is considerably lower than the average ammonia gas flux from a large (5900 m²) secondary pond measured by Rumburg et al. (2008) (2.3 g m⁻² d⁻¹), although the concentrations of TKN and NH₃-N in that pond were very high at 900-1000 and 600-700 mg N L⁻¹, respectively (Rumburg et al. 2004). Assuming proportionality between

ammonia gas flux and in-pond concentrations, the N removal rate observed in this study appears to be applicable to volatilisation.

Nitrification-denitrification is also a potential N removal pathway in summer when the epilimnion is oxygenated by algal respiration. However, as mentioned earlier, work by Sukias et al. (2003) and Craggs et al. (2000) showed that it is difficult to sustain a viable population of nitrifiers to effect nitrification. It is also possible that the lower DO levels immediately below the epilimnion allowed ammonia oxidising biomass to convert ammonia to nitrite (nitrification) (Beck et al. 2007), which would then be denitrified under the anoxic conditions below. Oxidised forms of N rarely exceeded 1 mg L⁻¹ in the effluent or supernatant, but this could have been due to rapid denitrification subsequent to oxidation of NH₃-N. In the absence of N gas flux measurements, it cannot be determined categorically whether or not the combined processes of nitrification-denitrification or nitrification-denitrification played some role in N removal.

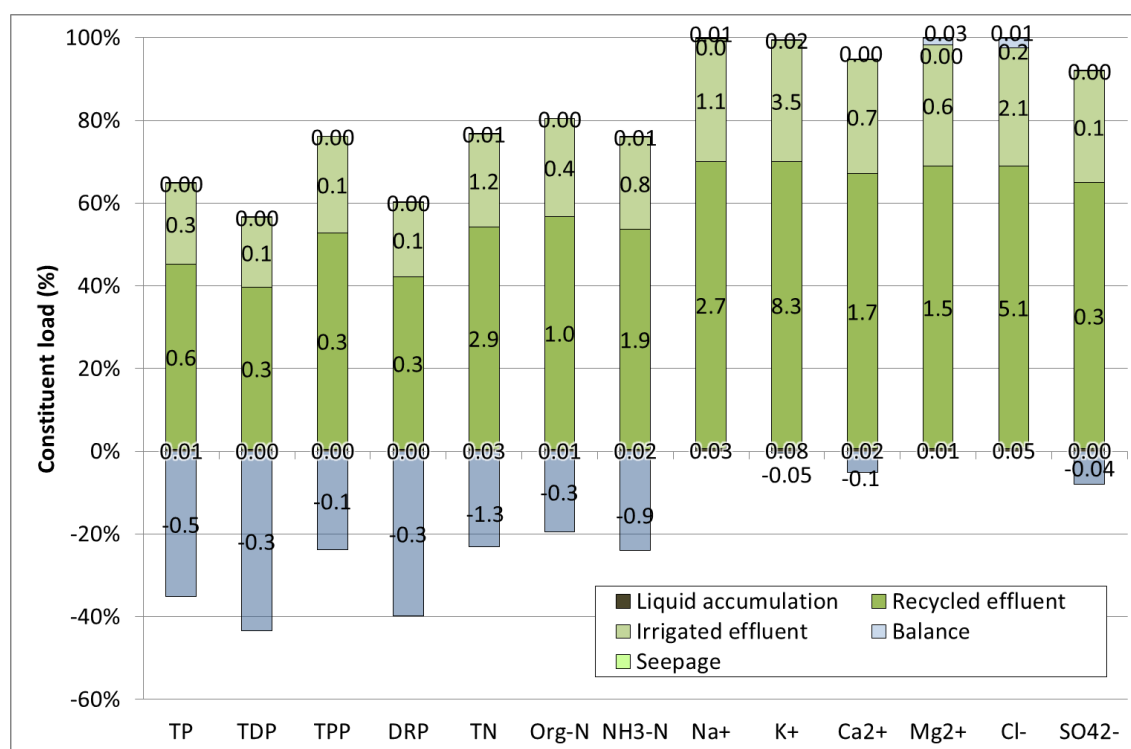


Figure 7-16 Mass balances for the major nutrients, cations and anions in the facultative pond.

7.4.5.3 System

Treatment efficiencies (incorporating sludge partitioning) for the pond system as a whole are presented in Table 7-16. Removal of solids and organic matter is in line with the anticipated degree of treatment stated in the Dairy Australia guidelines (Birchall, Dillon & Wrigley 2008). The system's performance is better than that of other two-stage

DSE pond systems reported by Sweeten & Wolfe (1994), Fyfe (2004) and Bolan, Wong & Adriano (2004). The majority of the removal and conversion of organic material occurs in the anaerobic pond, primarily due to sedimentation of manure solids and subsequent hydrolysis and biological degradation. Rates of partitioning to the sludge in the anaerobic pond and removal of soluble nutrient fractions in the facultative ponds are, in mass terms, very similar, producing overall TP and TN reductions of 49% and 31%, respectively. As expected, highly soluble K^+ , Na^+ and Cl^- are largely unaffected by the pond system; however dissolution or liberation of precipitated or complexed Ca and Mg in the anaerobic pond results in net generation of the corresponding soluble forms. Sulfate removal occurred entirely in the anaerobic pond through reduction to sulphide gas.

Table 7-16 Pond system treatment efficiencies.

<i>Aggregate solids or organic constituent</i>	<i>Treatment efficiency (%)</i>	<i>Nutrient, cation or anion</i>	<i>Treatment efficiency (%)</i>
TS	59	TP	49
TFS	25	TDP	27
TVS	78	TPP	63
TSS	90	DRP	22
TVSS	90	TN	31
TFSS	87	Org-N	55
TDS	27	NH ₃ -N	12
TDVS	53	Na ⁺	1
TDFS	9	K ⁺	3
BOD ₅	89	Ca ²⁺	-14
COD	84	Mg ²⁺	-8
FCOD	68	Cl ⁻	6
PCOD	89	SO ₄ ²⁻	57

7.4.6 Struvite Precipitation

Figure 7-6 (section 7.4.1) shows that DRP concentrations were relatively consistent in the effluent from both ponds over the monitoring period when other soluble conservative species such as K exhibited distinct trends. In the primary pond where the pH is neutral, this could be related to an equilibrium between soluble P released from the sludge and soluble P in the supernatant. In the more alkaline facultative pond, it may be an artefact of phosphate concentrations being regulated by chemical equilibria with various Ca- and Mg-compounds as suggested by Booram, Smith & Hazen (1975).

To gauge the potential for struvite precipitation in each of the ponds, calculations were performed to estimate the supersaturation index of the effluent/supernatant. The index relates the activity of the relevant ionic constituents in solution to the minimum solubility product and is expressed:

$$SI = \log \frac{IAP}{K_{SO}} \quad (7-6)$$

where

SI = saturation index;

IAP = ion activity product;

K_{SO} = minimum solubility product for struvite

= $10^{13.26}$ (Ohlinger, Young & Schroeder 1998).

SI values above zero indicate supersaturation conditions which cause spontaneous precipitation. The ion activity product is expressed

$$IAP = \{Mg^{2+}\}\{NH_4^+\}\{PO_4^{3-}\} \quad (7-7)$$

where braces denote the activity of ion species i , which is determined as follows (Galbraith & Schneider 2009; Metcalf & Eddy et al. 2003):

$$\{i\} = \gamma_i C_i \quad (7-8)$$

$$\log \gamma_i = -0.509 Z_i^2 \left(\frac{\sqrt{I}}{1 + \sqrt{I}} - 0.3I \right) \quad (7-9)$$

$$I = 2.5 \times 10^{-5} \times TDS \quad (7-10)$$

where

γ_i = activity coefficient of ion species i ;

C_i = concentration (M);

Z_i = valency;

I = ionic strength of the solution;

TDS = total dissolved solids (mg L^{-1}) in solution.

Figure 7-17 shows that facultative pond effluent and supernatant were supersaturated throughout the monitoring period. There is considerable noise in the data, but it is clear that supersaturation declines over autumn and winter. Referring back to the water quality data presented in Chapter 4, the triggers for precipitation to start appear to have been EC approaching $4000 \mu\text{S cm}^{-1}$, corresponding to a saturation index of about 4.4, combined with a rise in pH in the flood wash tank of between 0.1 and 0.2 units and temperature dropping below 20°C .

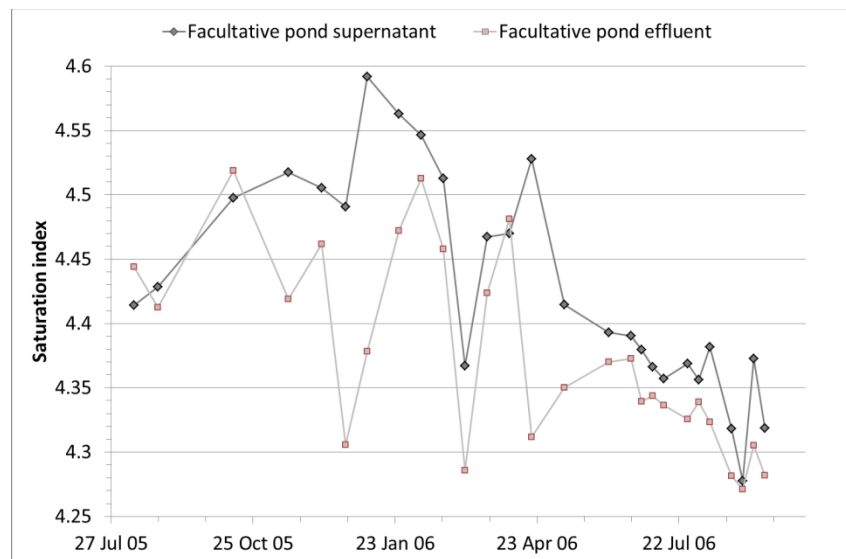


Figure 7-17 Struvite supersaturation indices over time.

As detailed in Chapter 4, both ponds experienced a decline in EC levels between May and September 2006 that could not be attributed to dilution by rainfall or export of salts by effluent irrigation alone. A similar trend is also evident in the supersaturation index plot (Figure 7-17). The decline was preceded by the pump and monitoring equipment problems caused by crystalline deposits. Attempts made to quantify crystal formation in the facultative pond experimentally were unsuccessful so it is uncertain whether spontaneous precipitation could account for the fall in supernatant salinity. Thus to test this supposition, a salt mass balance model adapted from the model formulated by Mason & Flowerday (2005) model was formulated as described in the following section.

7.4.6.1 Dissolved salt accumulation model

In order to simulate dissolved salt (including inert and reactive species) accumulation in the present pond system, the model of a partially closed DSE recycling system developed by Mason & Flowerday (2005) and described in Chapter 2 was extended by adding a second pond, terms for rainfall, runoff evaporation and seepage, and a term

for loss of pond volume to sludge. The mass balance equation for the anaerobic pond was expressed:

$$V_{An(n)}C_{An(n)} = V_{An(n-1)}C_{An(n-1)} + L_M + W_{r(n)}C_{Fac(n-1)} - W_{e(n)}C_{An(n-1)} - S_{An(n)}C_{An(n-1)} \quad (4.1)$$

where

V_{An} = Volume of the anaerobic pond (m^3);

C_{An} = Concentration of total dissolved solids (TDS) in the anaerobic pond supernatant ($g\ m^{-3}$);

L_M = Mass of TDS from manure deposited and chemicals used at the dairy (g)

W_r = Recycled effluent used to wash down the dairy (m^3);

C_{Fac} = Concentration of total dissolved solids (TDS) in the facultative pond supernatant ($g\ m^{-3}$);

W_e = Effluent leaving the anaerobic pond (m^3);

S_{An} = Seepage leaving the anaerobic pond (m^3); and

n = cycle (d).

V_{P1} was re-calculated at each cycle to allow for dilution and concentration from rainfall and evaporation and volume lost to sludge:

$$V_{An(n)} = V_{An(n-1)} + P_{An(n)} + R_{e,An(n)} - E_{An(n)} - S_{An(n)} + W_{0(n)} - W_{e(n)} - S_{An(n)} - SA \quad (4.2)$$

where

P_{An} = Rainfall entering the anaerobic pond (m^3);

$R_{e,An}$ = Embankment runoff entering the anaerobic pond (m^3);

E_{An} = Evaporation from the anaerobic pond (m^3);

W_0 = Influent to the anaerobic pond (including wastewater from flushing with fresh and recycled water and yard and solids trap runoff) (m^3); and

SA = Sludge accumulation

$$= 0.72 \text{ (m}^3 \text{ d}^{-1}\text{) (from Chapter 6).}$$

The mass balance for the facultative pond was expressed:

$$\begin{aligned} V_{Fac(n)} C_{Fac(n)} = & V_{Fac(n-1)} C_{Fac(n-1)} + W_{e(n)} C_{An(n-1)} \\ & - (W_{r(n)} + W_{i(n)}) C_{Fac(n-1)} - S_{Fac(n)} C_{Fac(n-1)} \end{aligned} \quad (4.3)$$

where

V_{Fac} = Volume of the facultative pond (m^3);

C_{Fac} = Concentration of total dissolved solids (TDS) in the facultative pond supernatant (g m^{-3});

W_i = Effluent irrigated to land (m^3); and

S_{Fac} = Seepage leaving the facultative pond (m^3).

The liquid balance for the pond was expressed:

$$\begin{aligned} V_{Fac(n)} = & V_{Fac(n-1)} + P_{Fac(n)} + R_{e,Fac(n)} - E_{Fac(n)} - S_{Fac(n)} + W_{e(n)} \\ & - W_{r(n)} - W_{i(n)} - S_{Fac(n)} \end{aligned} \quad (4.4)$$

where

P_{Fac} = Rainfall entering the facultative pond (m^3);

$R_{e,Fac}$ = Embankment runoff entering the facultative pond (m^3);

E_{Fac} = Evaporation from the facultative pond (m^3);

Hydrological data were sourced from the water balance detailed in Chapter 5 (available in Appendix I), while SA was taken from Chapter 6 (section 3.4). EC data presented in Chapter 4 (given in Appendix G) provided the basis for the initial concentration of TDS in each pond. EC values at the first cycle were multiplied by 0.6 to convert to TDS (refer to section 7.4.2). The only unknown parameter in the model was the salt load from manure (the chemical salt load was determined from the dose and concentration of active ingredients). The combined load from chemicals and manure (L_M) was thus used as a fitting parameter in the model. Whilst likely to vary stochastically, L_M was treated as a constant under the assumption that manure salt loads would not exhibit trending change over time. Strictly speaking, L_M should be regarded as a net term that lumps the loss or gain of dissolved species from dissolution and precipitation reactions

that occur in the anaerobic pond together with the load coming from the dairy. Predicted supernatant TDS concentrations were fitted to observed data (multiplied by 0.6) by adjusting L_M to minimise the squares of the residuals. This provided an empirical basis to estimating salt loading to the system.

Figure 7-18 plots the model predictions of TDS in both ponds against observed data for the period 1 April and 20 September 2006. Note that observed data for the facultative pond was drawn from spot readings of the supernatant (refer to section 7.2.4.1) since all in-pond probes conductivity sensors were compromised by struvite fouling. The model fit produced a value of $18.3 \text{ kg TDS d}^{-1}$ for L_M , which corresponds to a manure EC of approximately 17 mS cm^{-1} when adopting manure generation and density figures from (ASAE 2003) and assuming the herd spends 10% of the day at the dairy. This corresponds well with the average of 16.1 mS cm^{-1} derived from 38 samples of manure reported by (Marino, De Ferrari & Bechini 2008) (note that the literature offers very little in the way of electrical conductivity measurements made on manure samples). The fit produced good agreement between observed and predicted TDS concentrations in the anaerobic pond ($R^2 = 0.93$), with a standard error of an mean absolute percentage error of less than 3%.

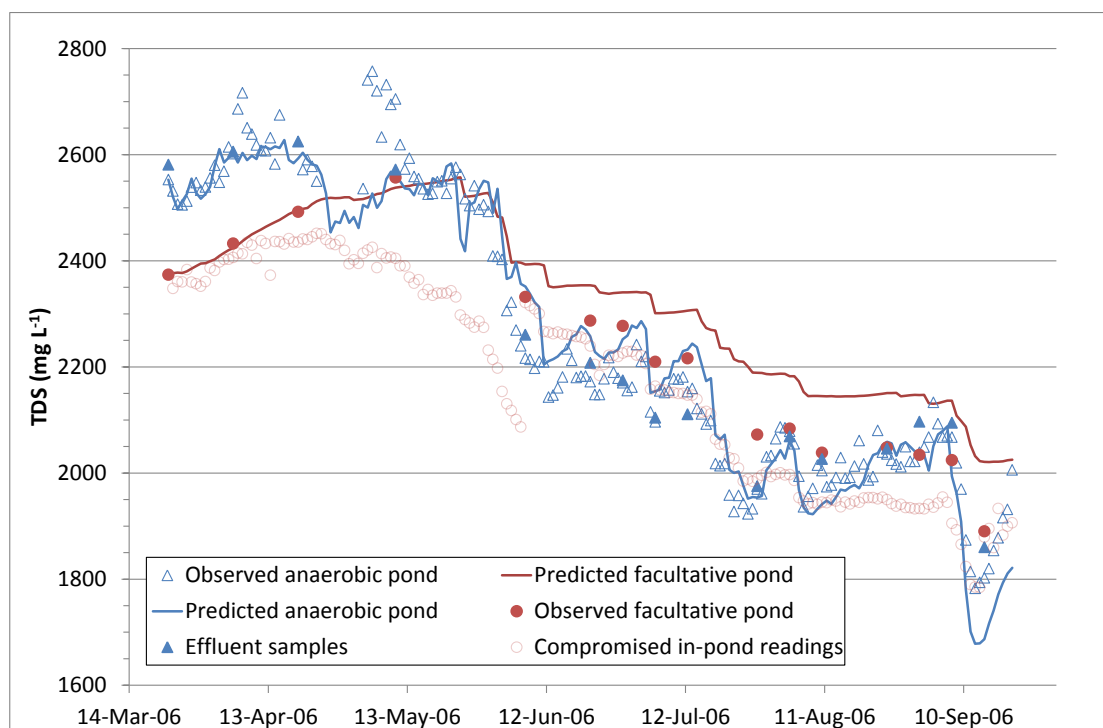


Figure 7-18 Predicted and observed TDS concentrations in the anaerobic and facultative ponds.

There is a distinct difference, however, between predicted and observed TDS concentrations in the facultative pond. The shape of the curves are very similar, but the

observed TDS levels drop substantially faster. This is clear evidence that reactive dissolved inorganic species are coming out of solution either by precipitation or some other process. Given the positive identification of struvite crystals above, it is reasoned that precipitation of struvite and possibly Ca phosphates is the most likely cause. The slope of the differences between observed and predicted salt levels over time gives an average precipitation rate $2.5 \text{ kg TDS d}^{-1}$. This amounts to about 450 kg of precipitate over the 183-day modelling period, which corresponds well to the volume of crystals found in the flood wash tank assuming a crystal bulk density greater than 1000 kg m^{-3} .

The salt removal rate equates to P, N and Mg^{2+} removal rates of 0.3, 0.2 and 0.2 kg d^{-1} , respectively. The P removal rate sits between the average removal rates for DRP and TP estimated in section 7.4.5.2, providing further evidence that struvite precipitation was the main removal mechanism for P in facultative pond effluent (assuming that mineralised particulate P is also prone to precipitation). Based on the coarse estimate of the quantity crystals found in the bottom of the tank, it would appear that most precipitation actually occurred in the flood wash tank. The mixing energy imparted by the fall from the inlet to the liquid surface, and possibly that from the rapid draining of the tank when releasing the flood wash, seems to have turned the tank into a crystallisation reactor. The struvite N removal rate equates to about 20% of the average TN removal rate, although because struvite precipitation occurred for only part of the year its contribution at the time would actually be higher. The mass balance for Mg^{2+} was close to zero, although the struvite removal rate amounts to 12% of the influent Mg^{2+} load, which could very well be lost to error.

7.4.7 Land Application and Nutrient Recovery

Together with water efficiency through recycling, the main operational and economic benefit associated with handling DSE in stabilisation pond systems is the ability to strategically manage nutrient recovery via land application. The disadvantage is the loss of valuable nutrients through the treatment process, and if recycling is employed, the accumulation of salts. Figure 7-19 shows the fate of the three main nutrients in the pond system relative to total fertiliser demand of the improved pasture. Fertiliser demand was based on a strategic approach to nutrient management that considers the fertility of the soil. Soil tests conducted in October 2009 on samples gathered from the main grazed paddocks indicated that Colwell P concentrations were well above critical levels at all locations despite the high P sorption capacity of the soils (based on the soil test interpretation of Gourley et al. (2007)). With soil pH at around 5 helping to ensure applied P is more readily available to plants, a maintenance application of up to 20 kg

P ha⁻¹ yr⁻¹ was considered sufficient based on guidance given in Havilah et al. (2005). K levels were also very high (> 0.6 meq kg⁻¹) in most paddocks, particularly the effluent application area (an artefact of K accumulation from effluent recycling discussed in Chapter 7). Thus K applications should be avoided in those areas, with other areas receiving a maximum of 20 kg K ha⁻¹ yr⁻¹. Strategic N fertiliser use on pastures is defined by Havilah et al. (2005) to be around 100 kg N ha⁻¹ yr⁻¹. Dairy farms, however, typically operate closer to the high use category (400 kg N ha⁻¹ yr⁻¹) to maintain productivity. The fertiliser regime in place at the time of the site monitoring used between (approximately) 170 to 340 kg N ha⁻¹ yr⁻¹ depending on the needs of each paddock. A value of 250 kg N ha⁻¹ yr⁻¹ was adopted to reflect a balance between high, strategic and past fertiliser use.

According to this reference case, the N and P contained in the effluent handled in the pond system could supply 10% and 27% of total demand after accounting for losses from seepage and treatment, respectively. 52% of the N is immediately plant available (soluble form) while 33% of the P is plant available. However around 50% of the total sludge/effluent load is captive to effluent recycling, reducing the recovered fractions of N and P to 5% and 14%, respectively, including the contributions from sludge. By contrast, the total K load is way in excess of fertiliser demand. Just the recoverable fraction could supply 91% of total pasture demand. This is reflective of accumulation through effluent recycling over time and a farm that is effectively saturated with K. Large K surpluses in excess of agronomic needs have been found to be common amongst Australian dairy farms and are a result of K from fertiliser and imported feed inputs remaining on the farm since K is mostly deposited in manure rather than being exported in milk (Gourley et al. 2010). Both the N and P and the K situations demonstrate that the effluent and sludge in the pond system could be managed more effectively to maximise the nutrient recovery potential. This could be achieved by renewing the system water more frequently, which essentially involves adding more fresh water to the system to 'push out' accumulated stocks of nutrients to irrigation.

Water renewal would naturally occur to some extent when drought conditions ease; however it could be accelerated by allowing more stormwater from the dairy to enter the pond, provided at the time there was ample storage capacity to avoid over-filling the system. Connecting the dairy roof gutters to the effluent drainage system would maximise the water available for system renewal. Over the course of the mass balance period, 789 mm of rain fell at the farm, producing up to 911 m³ stormwater which could have been used to replace about 50% of the system water that was present in the facultative pond at the end of the period and increase nutrient recovery

correspondingly. While substantially higher falls would occur outside of drought, there appears to be sufficient capacity in the system to allow stormwater entry if at the start of each annual cycle the facultative pond is pumped out sufficiently. System water renewal could also be promoted through increasing the ratio of fresh to recycled water used to wash down the holding yard in the lead up to and during irrigation periods. However, close attention would have to be paid to determining how much additional fresh water to use as this measure presents a trade-off between nutrient recovery and water efficiency.

The higher volumes of fresh water entering the system would require that the effluent application area be expanded to other parts of the farm since the current irrigation area is already likely to be saturated with P. This would be quite straight forward as it would simply involve tapping into the fresh water irrigation line and shandying the effluent with fresh water. Opening up more of the farm to effluent irrigation could offset the demand for K fertiliser entirely, at least until soil K levels return to less saturated levels. Moreover it allows the pond system to be used as a stormwater harvesting system, which makes more efficient and sustainable use of the large storage capacity of the system. A further benefit of this management approach is to reduce salt accumulation and thereby avoid struvite crystallisation and associated plumbing failures and P and N losses.

The overall strategy would be to run down the volume of the facultative pond over spring and summer, distributing the effluent as broadly as possible through the main irrigation line but avoiding irrigation during wet weather periods. Then by the time the rainfall starts to trend upwards in February, the pond level should be low enough to receive stormwater inflows over the coming year (but not too low so as to avoid degrading the soil liner). A combined water and mass balance could be used to determine the limits and allowances required to implement the strategy. Stormwater diversion would remain an option, if not the default arrangement, to ensure that stormwater only enters the pond system when there is capacity available. It would also be preferable to connect stormwater lines directly to the facultative pond to avoid hydraulic shock loading to the anaerobic pond and associated disturbance of treatment processes. Sludge would still need to be removed from the anaerobic pond every two to three years (or less) to maintain pond function, but also to recover the organic/particulate nutrient fractions.

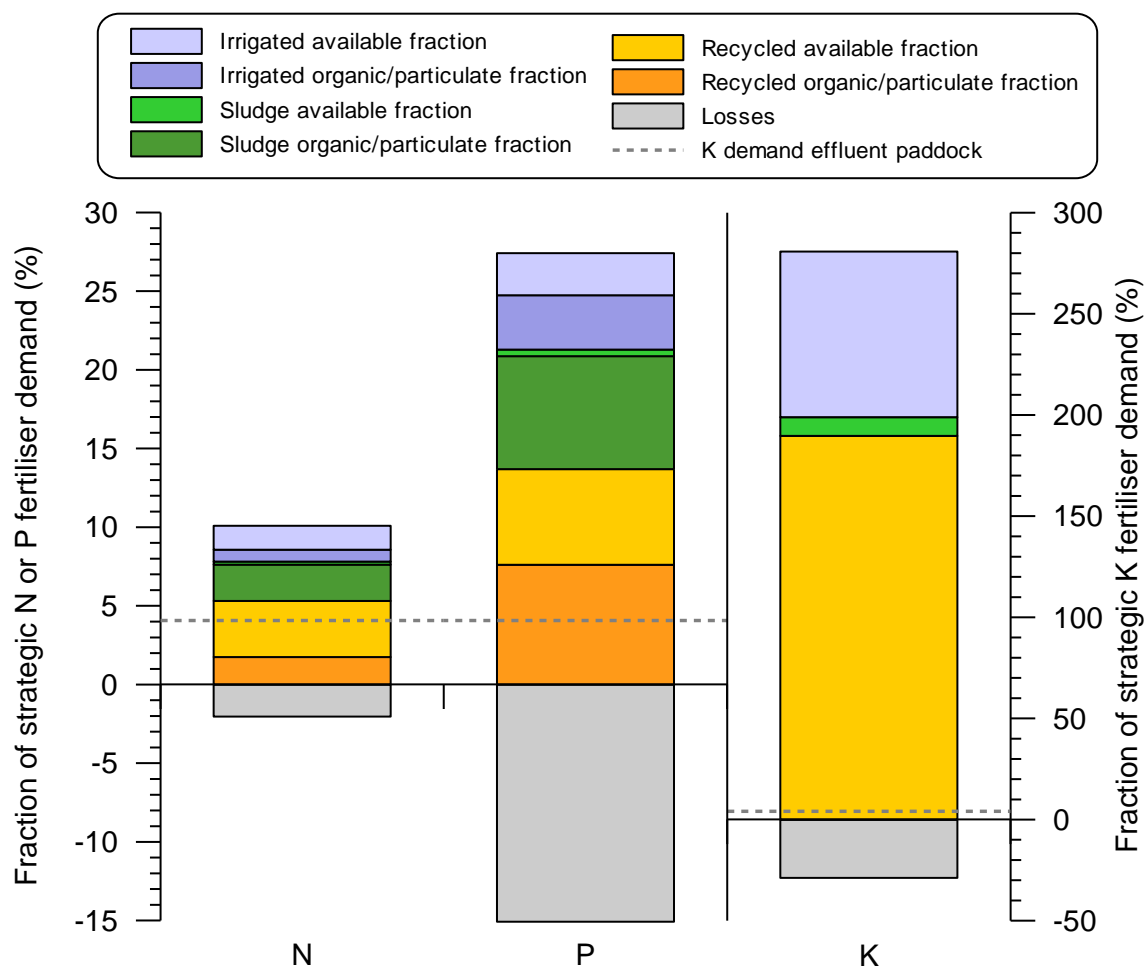


Figure 7-19 Available (soluble) and organic/particulate N, P and K loads plotted as percentages of strategic pasture fertiliser demand. Fertiliser demand for the dedicated effluent application area is also expressed as a fraction of total pasture fertiliser demand.

7.5 SUMMARY

The purpose of the research described in this Chapter was twofold: to produce a robust and detailed data set that could inform a biokinetic model and to examine that data to understand and quantify the partitioning and processes that define DSE stabilisation pond performance. The data set produced was built on best practice field sampling methods that captured representative flow- and volume-weighted samples of system influent, effluent and sludge. The samples were analysed for a comprehensive suite of wastewater constituents that together with the water quality data from Chapter 4 and the flow data from Chapter 5 provide a solid foundation upon which to build a biokinetic model of the system.

Comparisons of wastewater and sludge characteristics with published data showed that the system was similar in nature to other Australian and NZ DSE pond systems and that the data set produced from the monitoring may be considered reasonably

representative of a typical DSE pond system. Influent (raw wastewater pre-treated by a trafficable solids trap) composition exhibited considerable variability, but may be characterised by a large pool of mostly particulate poorly biodegradable organic matter, with average TS, TSS, COD and BOD₅ concentrations of 6048, 2996, 5044 and 1111 mg L⁻¹, respectively. N is evenly split between inorganic (56% ammonia-N) and organic fractions, while P is predominantly in particulate form (~65%). Importantly the particulate fractions of N and P appear to be mostly associated with poorly settleable material, which has ramifications for nutrient removal and recovery. Analysis of correlations between constituents showed that a constant (typical) fractionation for modelling purposes of the influent organic substrate and N content is reasonable, but not necessarily appropriate for P.

The stabilisation pond system was shown to meet BMP design criteria in terms of organic loading (to both ponds) and was functioning well, adequately renovating the wastewater stream to a standard that is acceptable for reuse and recycling. Compared with other ponds systems, the quality of the effluent from the facultative pond appears to be impaired by the concentrating effect of effluent recirculation. Nonetheless, the biological treatment processes of the ponds were working as intended, reducing the variability as well as the loading of aggregate solids and organic constituents. The anaerobic pond achieved TVS and COD destruction rates of 42% and 45% and net removal rates (incorporating sludge partitioning) of 71% and 76%, respectively, while the facultative pond brought the system removal efficiency to 78% and 84%, respectively. System TSS and BOD₅ removal rates were even higher at 90% each. Removal rates would likely be higher if not for the poor biodegradability of the influent, which makes settling an important precursor to breakdown of a large fraction of the influent loading.

Suspended and dissolved material leaving the pond system were mostly inert (65%), while the residual organic content is poorly or non-biodegradable. Nutrient loads in irrigated effluent and accumulating sludge together amounted to about 6% of the total farm fertiliser budget at the time of the study. Seepage losses of soluble nutrients were as high as 10% of influent loads, mostly coming from the anaerobic pond, unless underground transfers from the anaerobic pond to the facultative pond are in fact artificially lowering apparent seepage from the facultative pond.

Sludge was found to play two critical roles in anaerobic pond function, namely the storage and digestion of particulate organic material and the associated release of solubilised organic compounds, nutrients (N and P) and cations (Ca²⁺ and Mg²⁺) into

the supernatant. CO₂ generated by digestions causes the carbonate system to shift towards carbonic acid, which pushes down pH and increases aggregate salt levels. The solubilisation of organic N and P causes an increase in the bio-available fractions of the nutrients, which when considered together with subsequent losses from those same fractions in the facultative pond, makes a case for pumping to irrigation from the anaerobic pond instead of the facultative pond wherever possible. Anaerobic pond sludge also has a dramatic impact on pond performance when allowed to accumulate beyond a certain threshold. The associated reduction in supernatant volume curtails treatment efficiency and concentrates dissolved salts including carbonate/bicarbonate ions formed by CO₂ generation and Ca and Mg liberated from organic complexes in the sediments. The resulting reduction in effluent quality has flow-on effects through the system which are compounded by the effluent recycling feedback loop.

Relatively low removal rates of organic/particulate N and P compared with suspended solids removal showed that the relationship between these constituents is not as close as DSE pond design guidelines would suggest and that settling is not necessarily an effective nutrient removal pathway. Accordingly, TP and TN removal in the anaerobic pond was much lower than typically assumed in design guidelines and tools. Other than a relatively small fraction going to seepage, N and P losses (not sedimentation) in the anaerobic pond were negligible. There appears to be an imbalance in the TN data, the source of which is unclear but could be related to sampling bias and/or inconsistencies in laboratory analyses. However, the implications are most likely to amount to slight underestimation of Org-N mineralisation rate or over-estimation of the sludge N load.

Together with evidence of struvite deposition from Chapter 4, N and P removal rates and calculations of the struvite supersaturation index pointed to struvite precipitation being the primary removal mechanism for P in the facultative pond. A dynamic model incorporating the salt loading and hydrology of the system was used to demonstrate that struvite precipitation reduced soluble salts in the facultative pond at a rate of approximately 2.5 kg d⁻¹, which corresponds to 0.3 kg P d⁻¹, 0.2 kg N d⁻¹ and 0.2 kg Mg d⁻¹. These values were, however, specific to the period March to December 2006 as precipitation is a temporal phenomenon that will only occur under conditions of supersaturation (index values of 4.4 and above, corresponding to EC levels around 4000 µS cm⁻¹) and elevated pH (above 8), and with stimuli for nucleation and crystal growth such as rough submerged surfaces, mixing energy, and low temperatures.

The balance of salts entering and leaving the anaerobic pond was estimated by the salt accumulation model to be 18.3 kg TDS d⁻¹. Assuming that the lower pH of the anaerobic pond, particularly in the sludge, keeps struvite and other mineral salts in solution and that dissolution of precipitants in the influent is negligible, this quantity may be equated to the combined salt load from manure and chemicals captured in the dairy wastewater stream. Based on this loading, struvite precipitation accounted for just under 13% of new salts added to the system. This represents the first known attempt to quantify the amount of struvite precipitated in a manure flush water recycling system.

Ammonia-N removal that was not associated with struvite precipitation was of a comparable rate to volatilisation losses observed/estimated elsewhere, but overall was relatively low. Nitrification, nitritation and denitrification may also contribute to N removal. The extent of biological N removal could not be confirmed without data on ammonia or N gas emissions, but under the prevailing conditions of low oxygen and limited attachment surfaces (particularly within the aerated euphotic zone) it would likely be marginal. Algae was found to be present in numbers that were comparable to populations reported in other DSE ponds and appear to contribute to TSS concentrations, but there were no indications that algae played a significant role in nutrient cycling.

An analysis of nutrient partitioning and losses within the system in the context of nutrient recovery showed that while the total loads of N and P (after treatment and seepage losses) could make significant contributions to the farm nutrient budget, effluent recycling was effectively trapping 50% of this potential in the system. On the other hand, high K use over the years appears to have resulted in high soil K levels which have been transferred to pasture and to the effluent entering the pond system, resulting in a load of K circulating in the pond system that is well in excess of strategic fertiliser needs. Moreover, the distribution of nutrients held in treated effluent (not sludge) is limited to a small area that is likely to be saturated with K and P.

A recommended strategy to overcome these issues and improve nutrient recovery rates would be to add more fresh water to the system through capturing stormwater runoff from the dairy. Harvesting stormwater in this way would make better use of a large water storage facility and would facilitate greater nutrient recovery by effectively forcing more frequent renewal of the system water. To enable such a strategy the effluent irrigation line would have to be fed into the main fresh water irrigation line to allow sufficient distribution of accumulated K. If possible the stormwater line would be connected directly to the facultative pond to avoid hydraulic over-loading of the

anaerobic pond. An annual cycle would then be initiated in which the pond is pumped out almost entirely over spring and early summer to allow stormwater harvesting over the autumn and winter. To provide a quantitative approach to developing such a strategy, the mass balance model described in section 7.4.6.1 could be adapted to predict salt levels and simulate system renewal by stormwater additions and irrigation using long-term historical rainfall and evaporation data.

Chapter 8

FORMULATION AND INITIALISATION OF A DYNAMIC MODEL OF THE ANAEROBIC POND

This is the first of two chapters dedicated to describing the development of a dynamic, biokinetic model of an anaerobic pond treating DSE. It describes the selection of the modelling environment, and the formulation, specification and initialisation of the model, including the input data pre-processing required for dynamic simulation. The next chapter covers calibration of the model, sensitivity analysis and the use of the model to simulate various pond design and operation scenarios.

8.1 INTRODUCTION

Current modelling of DSE treatment in stabilisation ponds in the Australian context is focused on nutrient removal, using static partitioning constants to account for sludge deposition and ammonia volatilisation. It does not discern between different forms of nutrients and makes no links between nutrient dynamics and other key processes such as organic loading and destruction, sludge accumulation and digestion and environmental forcing. Advanced biokinetic (activated sludge) models have been applied to other forms of DSE treatment, namely biological nutrient removal (BNR) in sequencing batch reactors (SBRs) by overseas researchers. Biokinetic models have also been developed for stabilisation ponds treating other types of wastewater. There is no precedent, however, for applying a biokinetic model to DSE stabilisation ponds.

The research described in this and the following chapter seeks to integrate the extensive knowledge and research behind wastewater treatment (activated sludge) modelling with the design principles and operational characteristics of DSE management systems and in doing so establish a modelling platform for the dynamic simulation of DSE (and, by extension, other livestock waste) management ponds. The central aim is to build a mathematical model that could adequately describe the behaviour, treatment performance and nutrient partitioning, conversions and losses that occur within a typical DSE *anaerobic* pond. The original intention of this PhD was to also produce a facultative pond model; however the complexity and scope associated with modelling just the one pond proved to be a considerable task on its own, effectively ruling out the possibility of modelling both within the one thesis project. This chapter describes the formulation of a model based on the anaerobic pond located at Sugarloaf Holsteins farm and incorporating the dynamic hydraulics, hydrology,

wastewater loading and treatment processes that characterise DSE pond systems. It brings together the data and the findings of the preceding chapters to inform the model concept, design and initialisation. The calibration, sensitivity testing and application of the model are described in the following chapter (Chapter 9).

The reason model formulation and initialisation has been allocated a dedicated chapter is that it involved bridging the gap between the high level of sophistication of wastewater treatment modelling and the unknowns and complexities of DSE systems, which on its own required significant review and analysis. Hence, beyond describing the conceptual basis of the anaerobic pond model, this chapter covers considerable territory. Section 8.3 covers the selection and description of the modelling environment. The configuration of the model within the chosen environment to reflect the prevailing conditions and hydraulics of the pond is described in section 8.4. Producing sensible outputs from a wastewater treatment model is entirely dependent on an accurate and detailed characterisation of the influent, which is addressed in section 8.5. Section 8.6 describes the additional process equations with which the base activated sludge model was augmented to accommodate the specific nature of dairy manure characteristics and the extended solids retention time of stabilisation ponds. Finally, section 8.7 explains the process behind building the contiguous daily time step data set that was fed into the model.

8.2 KEY MODEL FEATURES

The research described in the preceding chapters has revealed a number of characteristics that are crucial to generating appropriate modelling outcomes and that the model should accommodate or be capable of simulating, namely:

- dynamic hydrology and hydraulics (in terms of quantities of liquid entering, leaving and being held in the pond);
- considerable seepage losses (approaching 10% of inflow) and associated export of soluble constituents;
- sludge accumulating at a rate of approximately $0.73 \text{ m}^3 \text{ d}^{-1}$ and dynamically interacting with the supernatant by releasing organic acids, soluble waste constituents (cations and nutrients) and biogas;
- neutral in-pond conditions despite alkaline influent;
- sludge accumulation beyond a certain threshold causing deterioration of effluent quality;
- low total n and p reductions;

- average concentrations and loads of soluble nutrient fractions leaving the anaerobic pond being higher than corresponding influent concentrations and loads;
- a consistent (although at times interrupted) pattern of accumulating inert salts (including K) related to effluent recirculation.

8.3 MODELLING PLATFORM

As detailed in the literature review (Chapter 2), there are numerous precedents that may be drawn on in developing a model of the anaerobic pond, including:

- developing or adapting a biokinetic model specific to anaerobic stabilisation ponds based on an idealised mixing regime (such as Fritz, Middleton & Meredith 1979; Colomer & Rico 1993; Dochain et al. 2003) or a series of compartmentalised ideal mixing regimes (such as Soler et al. 2000; Rajbhandari, Annachhatre & Vasel 2007);
- adapting an existing process-based activated sludge type model by applying a compartmental approach to simulating pond hydraulics and hydrodynamics and where necessary, augmenting the process equations with pond-specific processes as done by Houweling et al. (2008), Gehring et al. (2010) and Alvarado et al. (2012);
- developing a mass transport type model that considers dispersion and pond-specific biological and physical-chemical processes under known fluid (not simulated) flow similar to the Moreno-Grau et al. (1996) and Beran & Kargi (2005) models;
- integrating cfd and biokinetic models as pioneered by Sah et al. (2011).

The following considerations were critical to the selection of a particular modelling approach:

- prioritising leveraging existing knowledge in dynamic wastewater modelling;
- recognising that DSE has different characteristics from municipal wastewater, meaning process models and model parameters from other biokinetic stabilisation pond models are not necessarily directly transferable;
- the limited quantitative data available on the hydrodynamics of the ponds with which to calibrate a CFD-based model;
- minimising the complexity of numerical methods and programming required.

Melcer et al. (2003) suggest that with appropriate waste characterisation, activated sludge models such as the Activated Sludge Model family (see Henze 2000) may be applied directly to some industrial wastewaters such as those from food processing. Indeed Whichard (2001) found that the measured values for a number of the critical parameters were in fact within the typical ranges found for municipal wastes. Adapting an activated sludge model presents the option of using an “off-the-shelf” simulation package which has the key advantage of providing a user-friendly simulation environment. To run a uniquely formulated physical-biological-chemical process-based model, a numerical method must be implemented in a programming environment to solve the complex set of differential equations. This is made more complex by applying the process model to combinations of reactors to reflect mixing patterns or having to simultaneously solve mass transport or fluid flow equations. A simulation package alleviates this need as the hydrodynamics of the pond system, including short circuiting, dead zones and stratification, can be approximated, albeit not dynamically, by routing flows and recycle streams through a network of different types of reactors. In addition, most simulation packages allow the user to augment built-in models or even build their own process models. The combined benefits of being able to leverage the extensive experience that has gone into developing the activated sludge models and the flexibility offered by commercial simulation packages presents a reasonable compromise between rigour and pragmatic considerations.

There are numerous simulation packages available in the market including ASIM (Activated Sludge SIMulation Program) (EAWAG 2010), GPS-X using the Mantis2 biological model or the ASM family (Hydromantis 2012), SIMBA® and STOAT based on the ASM family, and BioWin which uses the General ASDM (Activated Sludge Digestion Model) described in Barker & Dold (1997). There is also a freely accessible online simulation environment called JASS (Java based Activated Sludge process Simulator) based on ASM1 and ASM2d developed by Department of Systems and Control, Uppsala University (Department of Systems and Control, Uppsala University 2004), although it does not appear to have the inter-reactor flow routing flexibility of the commercial packages. Based on a range of considerations including accessibility, availability of technical support, flexibility, adaptability and precedents of applications to DSE treatment, as well as technical features including its integrated sludge and wastewater process models and its ability to model wastewater chemistry including pH and precipitation of P, the BioWin package was selected to perform the wastewater treatment modelling.

8.3.1 BioWin Wastewater Treatment Process Models

BioWin is capable of simulating the full range of processes that drive biological treatment including hydrolysis and mineralisation, colloid flocculation, growth and decay of heterotrophic (including phosphate accumulating) organisms, anaerobic fermentation and methanogenesis, ammonia and nitrite oxidation by growth of autotrophs, and denitrification. Moreover, it has the ability to simulate various modes of solids separation or settling, alkalinity and pH fluctuations, mass transfer of gases to the atmosphere, and spontaneous precipitation of struvite, hydroxy-dicalcium-phosphate. It incorporates models for the abovementioned processes into an integrated simulation environment to facilitate modelling of a range of wastewater treatment modes and configurations including activated sludge, biological nutrient removal, sequencing batch reactors, bioreactors, anaerobic digestion, chemical precipitation, settling and dewatering. The main processes of concern in modelling the pond system are those which occur naturally. Table 8-1 links the key processes that were required to simulate anaerobic pond processes to the corresponding process models that are available in BioWin and the BioWin elements that incorporate the process models. All process models are described in the BioWin user manual (EnviroSim Associates Ltd. n.d.), but where available/applicable, published references for process models are also given in the table.

8.3.2 Adjusting Model Parameters for Simulation of DSE Treatment

The default process model parameters used in BioWin have been drawn from studies on municipal wastewaters and may not be directly applicable to DSE. Very little research has been undertaken to quantify wastewater treatment modelling parameters for DSE. Whichard (2001) undertook the only known research designed to experimentally determine a number of standard kinetic and stoichiometric parameters. Using diluted, screened manure collected from scraped yards in an active dairy farm, Whichard (2001) generated estimates for heterotrophic yield, autotrophic/nitrifier maximum specific growth rate and heterotrophic decay rate and found they were all within typical ranges for municipal wastewaters. He also produced estimates for the maximum specific growth rate and half-saturation constant for heterotrophic biomass (1.84 d^{-1} and $234 \text{ mg COD L}^{-1}$, respectively); however these were considered to be unrealistically low on account of a low substrate concentration in the batch reactor that would have artificially limited the growth rate. Whichard (2001) suggested that the growth rate for dairy wastewater was most likely to be comparable to rates observed in municipal wastewater treatment and recommended adopting a maximum specific growth rate of between 2 and 3 d^{-1} for the design of sequencing batch reactors treating

DSE. The measured saturation constant was considerably higher than typical municipal wastewater values and the actual value would likely be even higher. The main impact of a high constant was found to be slower degradation of soluble COD, which is particularly pertinent to a pond system with very high HRTs. Whichard (2001) suggested a value of 200 mg COD L⁻¹ may be most appropriate for DSE.

Other than the work of Whichard (2001), the only investigations of modelling parameters for DSE have been sensitivity analyses of modelling outputs. In modelling DSE treatment in a sequencing batch reactor (SBR), Yanosek et al. (2003) largely adopted parameter values based on the work of Whichard (2001). Using sensitivity analysis, they identified ranges for a number of parameters related to PAOs within which enhanced biological P removal could be achieved, none of which were confirmed experimentally. Beck (2007) found that reducing the default BioWin hydrolysis rate constant by 50% produced much better agreement between simulated and observed data when using BioWin to model biological N removal from dairy manure wastewater in an SBR. This could well have reflected the high content of slowly degradable material in dairy manure, but Beck (2007) suggested that it was an artifact of inhibition of ammonia oxidising bacteria (AOB) by CuSO₄ from a cattle foot bath. Beck (2007) identified the AOB maximum specific growth rate and substrate half saturation coefficient as the most sensitive kinetic parameters of the model.

Melcer et al. (2003) state that activated sludge models may be directly applied to industrial wastewaters provided the wastewater can be appropriately characterised to fit the modelling framework and if oxygen and nitrate are the only significant electron acceptors present. Both these conditions are met with respect to DSE, thus aside from the parameters listed in Table 8-2, default values were retained for model initialisation. Appendix L lists the initial values of all BioWin parameters used in the model calibration process. Whilst it is advised that caution be exercised in adjusting model parameters without an empirical basis, parameters that were targeted for adjustment to achieve closer agreement between observed and predicted effluent constituent concentrations are also given in Table 8-2.

Table 8-1 Stabilisation pond treatment processes and corresponding BioWin process models. Process models and elements used in the final model are identified in bold text.

<i>Process</i>	<i>Process models</i>	<i>Model basis</i>	<i>BioWin element</i>	<i>References</i>
Settling of particulate material	Point separation and ideal settling	Simple mass partitioning (dimensionless)	Dewatering units , point clarifier	Takács, Patry & Nolasco (1991); Vitasovic (1989)
	Ideal separation	Mass partitioning between liquid and sludge volumes	Ideal primary tank, ideal clarifier	
	Modified Vesilind (single exponential) or double exponential models	1-dimensional zone settling based on solids flux theory	Model clarifier	
Biological treatment	BioWin General activated sludge/anaerobic digestion model (ASDM)			
Breakdown of organic material by suspended growth	Activated sludge model	Hydrolysis mediated by ordinary heterotrophic organisms (OHOs) Growth and decay of OHOs	Suspended growth bioreactors (diffused air, variable volume , brush aerator or surface aerator), sequencing batch reactor (SBR), media bioreactor, aerobic digester.	Barker & Dold (1997)
Biological N removal		Hydrolysis, ammonification, growth and decay of ammonia oxidising biomass, nitrite oxidising biomass and anaerobic ammonia oxidisers		
Biological P removal		Hydrolysis, growth and decay of PAOs		
Anaerobic digestion in the sludge	Anaerobic digestion model	Hydrolysis (anaerobic) Heterotrophic growth through fermentation Growth and decay of propionic acetogens Growth and decay of methanogens	Anaerobic digester	
Spontaneous chemical precipitation	Chemical precipitation model	Struvite and Ca phosphates precipitation kinetics	Can be activated in all elements	Musvoto, Wentzel & Ekama (2000); Musvoto et al. (2000); Maurer &

<i>Process</i>	<i>Process models</i>	<i>Model basis</i>	<i>BioWin element</i>	<i>References</i>
Gaseous losses pH	Gas transfer model	Gas-liquid mass transfer	Active in all reactors types	Boller (1999)
		Chemical equilibrium, ionic activity, mass transfer and biological fluxes	Can be activated in all elements	Fairlamb et al. (2003)

Table 8-2 Parameter values adopted at model initialisation and parameters identified as candidates for adjustment during calibration.

<i>Parameter</i>	<i>Symbol</i>	<i>Initial value or likely change</i>	<i>Rational and/or reference</i>
<i>Substitutes for default parameters</i>			
Heterotroph maximum specific growth rate	$\mu_{\max,H}$	2.5 d ⁻¹	Range of 2 to 3 recommended by Whichard (2001)
Heterotroph half-saturation constant	$k_{S,H}$	250 mg COD L ⁻¹	Range of 200 to 300 recommended by Whichard (2001)
AOB maximum specific growth rate	$\mu_{\max,A}$	0.75 d ⁻¹	Measured by Whichard (2001)
Heterotroph aerobic decay rate	b_H	0.25 d ⁻¹	Measured by Whichard (2001)
Heterotroph anoxic/anaerobic decay rate	$b_{H,An}$	0.125 d ⁻¹	Approximately half the aerobic rate as per BioWin default
Heterotroph yield	Y_H	0.42 mg COD mg ⁻¹ COD	Measured by Whichard (2001)
<i>Parameters considered for adjustment</i>			
AOB and NOB growth rates	$\mu_{\max,A}$ and $\mu_{\max,N}$	Lower	Account for inhibition effects of the wastewater (Fairlamb 2010)
Hydrolysis rate	K_H	Adjust to refine model outputs	Experience of Beck (2007) and recommendation from Fairlamb (2010)
Heterotrophic switching function parameter	$K_{O,H}$	Adjust where conditions likely to vary between aerobic, anoxic and anaerobic.	Fairlamb (2010)

8.3.3 New Evaporation Element

A key aspect of the modelling that a standard issue of BioWin could not accommodate was evaporation losses. To address this, the developers of BioWin were commissioned to create a means of removing clean water from model reactors. The resulting custom-built 'Evaporation Unit' acts in a similar fashion to a standard dewatering unit in BioWin, but returns all traces of any constituents present in the effluent from a reactor back to the reactor as a concentrate stream.

8.4 MODEL CONFIGURATION AND FLOW ROUTING

Using BioWin to simulate the various physical, chemical and biological processes acting in the pond system required taking a compartmental modelling approach (see section 4.3 of Chapter 2). BioWin treatment 'elements' representing particular functional aspects of each pond were arranged in a network so as to approximate the overall behaviour of the ponds. Pond loading and hydrology were simulated using influent and effluent elements while pond hydraulics were simulated using pipe elements that transferred wastewater and sludge between treatment elements. The configurations of treatment, influent, effluent and pipe elements were developed based on the findings reported in Chapters 4, 5 and 6 and are depicted in Figure 8-1.

Borrowing from the approaches taken by Rajbhandari, Annachhatre & Vasei (2007) and Houweling et al. (2008), the anaerobic pond was divided into discrete liquid and sludge elements by using separate reactors for each. As demonstrated in Chapter 6, the supernatant in the anaerobic pond appears to be well mixed vertically, primarily due to rising biogas bubbles, while dispersion caused by recirculation and turbulence promotes transversal mixing. Accordingly, the liquid volume of the pond was treated as one large continuous stirred tank reactor (CSTR) using a single 'bioreactor' element. BioWin has a dedicated 'anaerobic digester' element that was used to represent the sludge blanket. The sludge blanket was also treated as a CSTR under the assumptions that sediments were evenly distributed across the pond and that variation in sludge age with depth would not greatly impact the modelling outcomes since sludge did not leave the pond save for the one desludging event. Deposition of sediments to the sludge blanket was simulated using the underflow of a dewatering element preceding the supernatant bioreactor (flow *SA* in Figure 8-1). In their model of a facultative pond, Houweling et al. (2008) placed the dewatering unit after the supernatant reactor. However given that particulate material in the influent tended to settle within 1 hour (based on laboratory settleable solids tests) and the HRT of the pond would typically exceed 20 days, it was deemed more appropriate to direct incoming settleable solids immediately to the digester reactor.

Liquid from the sludge digester was reintroduced to the supernatant via a recirculation flow (*SE*) to facilitate sludge-supernatant transfers while a flow split from the supernatant reactor effluent balanced incoming and outgoing flows. This link between the supernatant and sludge reactors was critical to simulating the transfer of organic compounds and nutrients from the sludge to the supernatant shown by Banks et al. (2005), Hough and Gloyna (1984) and others to be an active process in stabilisation

ponds. Simulating such exchanges using a recycle flow has been shown to be successful in predicting increases in supernatant ammonia N loads caused by hydrolysis of organic N in the sludge (Houweling et al. 2008). An additional dewatering unit was imposed on the SE flow to provide control over particulate transfers, which allowed simulation of declining treatment efficiency related to sludge accumulation.

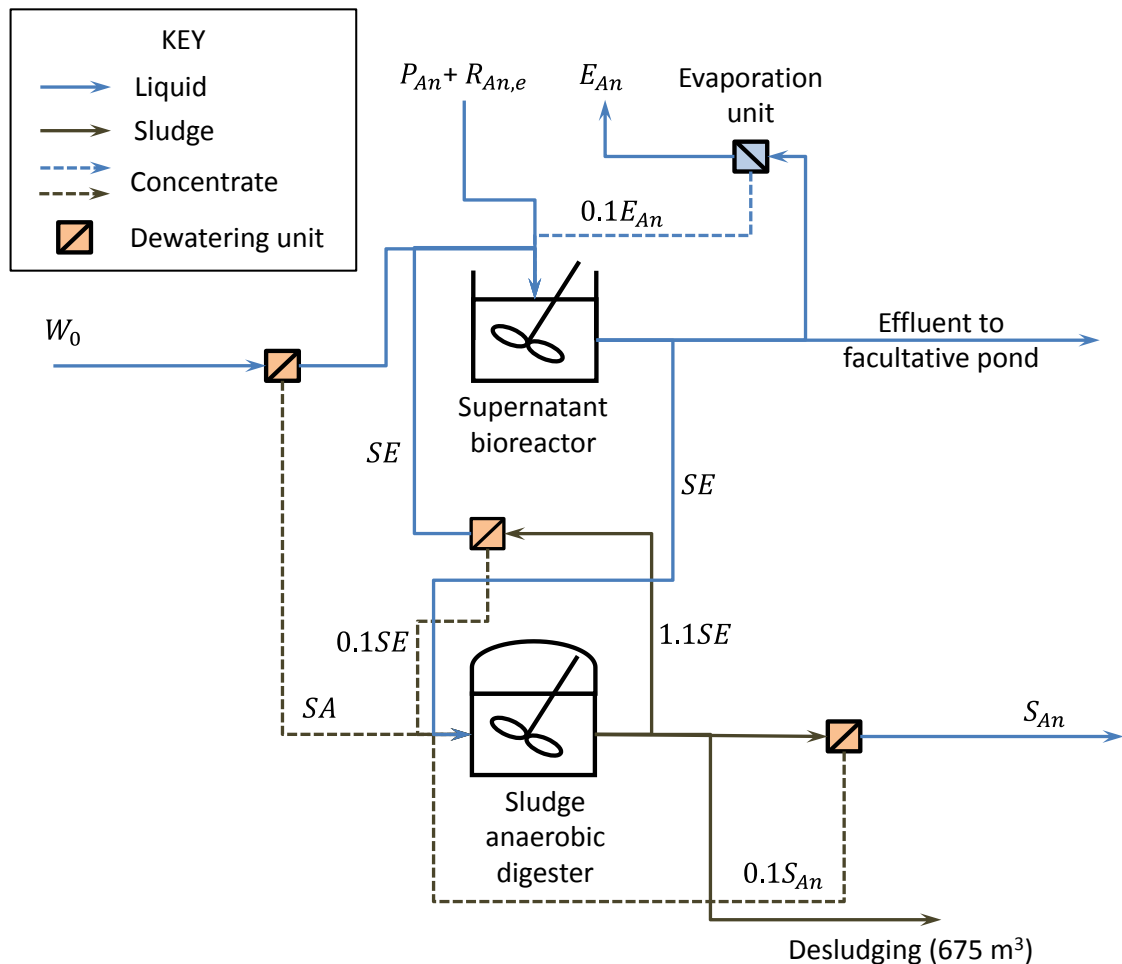


Figure 8-1 BioWin element configuration for the anaerobic pond model.

Wastewater and contaminated runoff from the dairy and solids trap (W_0) were introduced to the system using an 'SV' (state variable) influent element, which allowed all constituent concentrations to be entered as dynamic inputs. Rainfall and embankment runoff ($P_{AN} + R_{An,e}$) were also added as a combined stream using an SV element, but with all constituents set to zero. Evaporation (E_{An}) was extracted using the evaporator element described above together with an effluent element. Seepage losses (S_{An}) were simulated with an effluent element fed by the sludge anaerobic digestion reactor and preceded by a dewatering unit that removed 100% of particulate

constituents. Digestate was also extracted from the digester element via a sludge effluent element to simulate desludging of the pond.

To simulate the reduction in pond liquid capacity caused by sludge accumulation, a variable volume form of bioreactor element was used to model the supernatant. The volume of liquid held in the reactor was reduced by extracting effluent additional to gravity overflow from the reactor at a rate commensurate with the sludge accumulation rate (SA). The volume of sludge held in the anaerobic digester element was allowed to increase at the corresponding rate by ensuring the feed from the recycle line to the sludge allowed for SA in addition to seepage losses and recirculation back to the supernatant. The supernatant reactor was initially assigned a capacity equivalent to the total capacity of the pond. The anaerobic digester element was also sized to pond capacity so that it would be possible to 'fill' the pond with sludge if required. Each dewatering and evaporation unit had to have a return flow back to its source in order to return separated material. All return flows were assigned a nominal ratio of 10% of the element's outflow. A summary of the key features of each element is provided in Table 8-3.

8.5 INFLUENT WASTEWATER CHARACTERISATION

Influent wastewater characteristics are more influential on effluent quality than internal processing in stabilisation ponds (Colomer & Rico 1993). The physical and chemical properties of the wastewater, along with the nature and relative concentrations of substrates and nutrients determine which processes are dominant in a biological system. Accordingly, problems encountered with calibrating process models are often related to inaccurate characterisation of the influent rather than the model equations or parameters (Melcer et al. 2003). This vulnerability to wastewater characteristics is heightened in pond systems that are also prone to environmental conditions, making characterisation critical to effective modelling.

Initialisation of wastewater treatment process models in the BioWin simulator requires a detailed breakdown of the constituents in the influent wastewater as depicted in Figure 8-2. Melcer et al. (2003) assert that the most critical wastewater characteristics to wastewater treatment are readily biodegradable COD and non-biodegradable particulate COD. In BioWin a distinction is made between particulate and non-settleable colloidal fractions in slowly biodegradable influent COD. This division is not always accounted for in modelling biological processes as colloidal material is readily adsorbed onto sludge. However, when considering organics removal through

sedimentation - a key process in stabilisation ponds - distinguishing the colloidal fraction takes on greater importance.

Table 8-3 Summary of BioWin elements used in the anaerobic pond model.

<i>Component</i>	<i>BioWin Element type</i>	<i>Maximum Capacity (m³)</i>	<i>Maximum Depth (m)</i>	<i>Outflow</i>	<i>Underflow</i>
Influent wastewater	State variable (SV) influent	-	-	W_0	
Rainfall and embankment runoff	State variable (SV) influent	-	-	$P_{An} + R_{An,e}$	
Settling of influent particulate material	Dewatering unit	-	-	$W_0 - SA$	SA
Supernatant	Variable volume bioreactor	1284	4.8	$Incoming + SA$	
Sludge	Anaerobic digester	1284	4.8	$Incoming - SA$	
Evaporation	Evaporation unit	-	-	E_{An}	$0.1E_{An}$
	Effluent	-	-	E_{An}	
Sludge recycle	Dewatering unit	-	-	SE	$0.1SE$
Seepage	Dewatering unit	-	-	S_{An}	$0.1S_{An}$
	Effluent	-	-	S_{An}	
Effluent	Effluent	-	-	$W_0 + P_{An} + R_{An,e} - S_{An} - E_{An}$	
Desludging	Sludge	-	-	675 m^3*	

* Divided over a period of 6 days to reflect the actual time taken to desludge the pond.

Dairy shed waste is essentially water contaminated with manure and trace amounts of other organic and inorganic substances. Manure comprises a range of soluble and particulate organic compounds including:

- readily degradable volatile fatty acids (VFAs), non-structural carbohydrates including sugars and starches, and amino acids;
- particulate and colloidal structural carbohydrates that are slow to biodegrade, or potentially inert;
- biologically inert lignin; and
- other insoluble and slowly degradable organic compounds including proteins and lipids.

A theoretical alignment between the BioWin fractionation and DSE organic matter constituents is presented in Figure 8-2. Note that while DSE is likely to contain microbial biomass sloughed from the cows' digestive tracts, the viable population is assumed to be negligible.

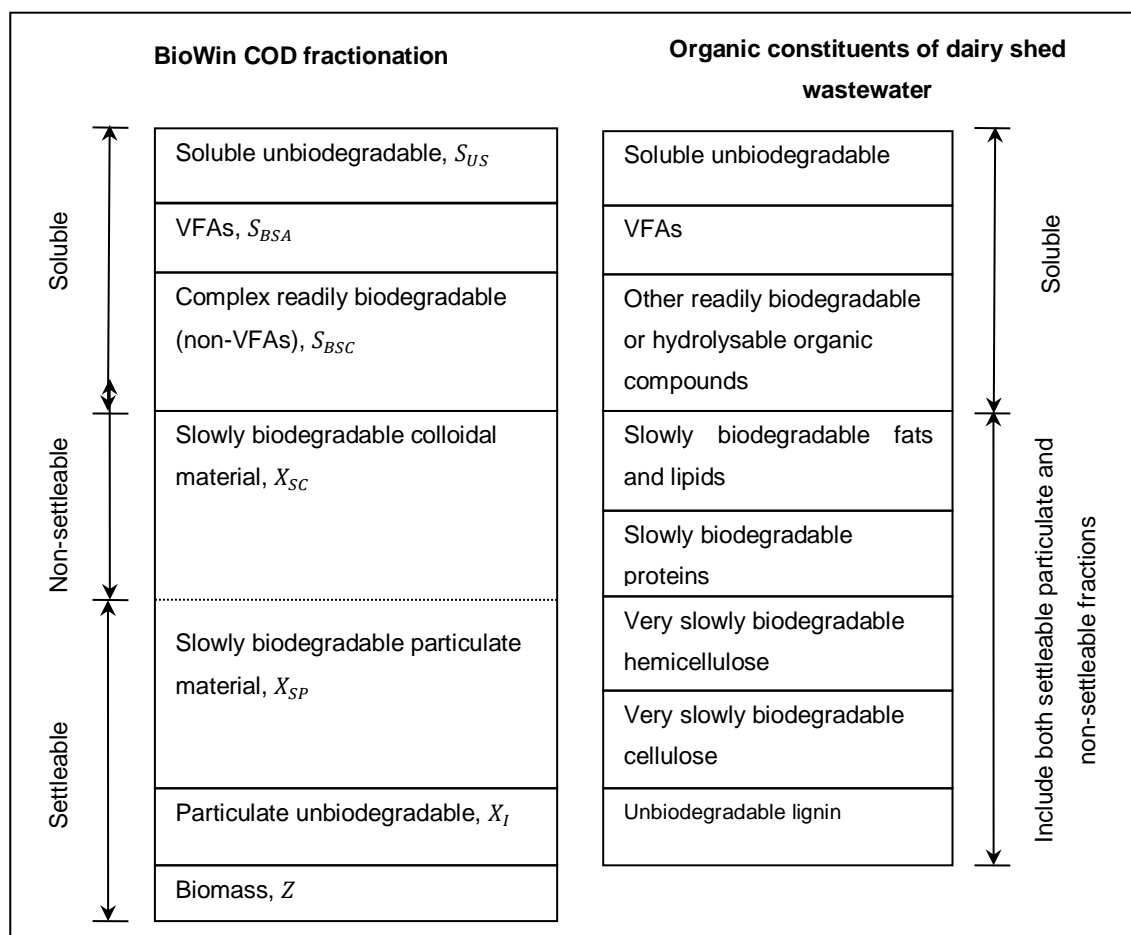


Figure 8-2 Fractionation of organic matter (COD) in the BioWin activated sludge and anaerobic digestion models and dairy shed wastewater organic constituents (adapted from Melcer et al. (2003) and Henze (1992)).

In activated sludge modelling, organic matter is generally quantified using COD or BOD. COD fractions may be determined in the laboratory using physicochemical and batch test methods. Input data available to the modelling comprised only the standard wastewater parameters presented in Chapter 7. Consequently, many of the fractions required for modelling in BioWin had to be estimated or drawn from the literature as described in the following sections. Theoretical oxygen demand (ThOD) was the basis for estimating a number of COD fractions under the assumption that ThOD and COD are generally equivalent. The ThOD values used for the main dairy shed waste components are presented in Table 8-4. Note that the value for lignin was chosen based on the assumption that lignin present in manure would be undigested feed;

hence a ThOD for oat and straw was adopted. All wastewater and sludge constituent concentrations data used in calculations to estimate fractions were drawn from the monitoring data presented in Chapter 7 and Appendix K.

Table 8-4 Chemical formulae and theoretical oxygen demand for key organic components of manure.

<i>Organic matter component</i>	<i>Chemical formula</i>	<i>ThOD (mg COD mg⁻¹ VS)</i>	<i>References</i>	<i>Adopted ThOD (mg COD mg⁻¹ VS)</i>
Acetic acid	C ₂ H ₄ O ₂	1.07	Mason & Mulcahy (2003); Huete et al. (2006)	1.10
Propionic acid	C ₃ H ₆ O ₂	1.51	Mason & Mulcahy (2003); Huete et al. (2006)	1.50
Butyric acid	C ₄ H ₈ O ₂	1.82	Mason & Mulcahy (2003); Huete et al. (2006)	1.80
Valeric acid	C ₅ H ₁₀ O ₂	2.04	Mason & Mulcahy (2003); Huete et al. (2006)	2.00
Carbohydrates	(C ₆ H ₁₀ O ₅) _x	1.19	Møller et al.(2004); Huete et al. (2006)	1.20
Amino acids	C ₄ H _{6.1} O _{1.2} N	1.53	Huete et al. (2006)	1.50
Proteins	(C ₄ H _{6.1} O _{1.2} N) _x	1.53	Huete et al. (2006)	1.50
	C ₅ H ₇ O ₂ N	1.42	Møller et al.(2004)	
	CH _{1.58} O _{0.3} ON _{0.28} S _{0.01}	1.46	Torabizadeh (2011)	
Lipids	C ₅₁ H ₉₈ O ₆	2.88	Huete et al. (2006)	2.90
	C ₅₇ H ₁₀₄ O ₆	2.90	Møller et al.(2004)	
Lignin	C ₄₀ H ₄₈ O ₁₅	1.85	Phillips & Goss (1934) [‡]	1.80
	C ₄₀ H ₄₂ O ₁₆	1.75		
	C ₆ H ₁₀ O ₅	1.19	Møller et al.(2004) (same as carbohydrates, no reference given)	

[‡] Analysis of lignin content of oat and straw.

It is important to note here that soluble components in this study have been isolated using centrifugation and filtration. The division between suspended and dissolved solids according to standard methods (APHA 2005) is made using a 1.3 µm pore size glass fibre filter. When differentiating soluble components of COD, P, and metals, APHA (2005) prescribe the use of a 0.45 µm membrane filter. It is widely accepted, however, that some colloidal material, particularly in untreated wastewaters, is likely to pass through 0.45 µm pores and that 0.1 µm filters and/or flocculation are required to adequately isolate soluble components (Roeleveld & van Loosdrecht 2002; Melcer et

al. 2003). Hence, whilst some colloidal material would have been removed through attachment to centrifuged or filtered particulates, the ‘soluble’ fractions referred to herein most likely over-estimate the true dissolved fractions of their respective constituents. Conversely, calculated or estimated fractions of particulate and colloidal COD are likely to be slightly lower than they should be.

8.5.1 Readily Biodegradable and Non-Biodegradable Soluble COD

Readily biodegradable COD (S_{BS}) comprises simple dissolved organic compounds including volatile fatty acids (VFAs), alcohols, lower amino acids and simple carbohydrates (simple sugars - monosaccharides) (Henze 1992). S_{BS} may be estimated by bioassay batch experiments or physical-chemical analyses, but in the absence of data from such laboratory tests it is generally estimated as the difference between influent soluble COD (FCOD) and non-biodegradable soluble COD (S_{US}) (Melcer et al. 2003). S_{US} is generally regarded as the residue that remains after effective biological treatment in a system with a sludge age of the treatment system of greater than 3 days (Melcer et al. 2003). Considering that the DSE pond system provides only passive treatment and is heavily loaded with organics (relative to sewage treatment plants), allowance should be made for residual biodegradable material, which is indicated by the biochemical oxygen demand (BOD) of the effluent from the secondary pond (Roeleveld & van Loosdrecht 2002). Thus soluble non-biodegradable COD may be estimated as:

$$S_{US} = 0.9 \cdot FCOD_{eff} - FCBOD_{ult,eff} \quad (8-1)$$

where

$FCOD_{eff}$ = filterable COD of the facultative pond effluent (mg L^{-1});

$FCBOD_{ult,eff}$ = ultimate soluble carbonaceous BOD of the facultative pond effluent (mg L^{-1})

$$\cong 1.5 \cdot FCBOD_{5,effluent};$$

$FCBOD_{5,eff}$ = soluble 5-day BOD of the facultative pond effluent (mg L^{-1}).

Total five-day BOD was the only form of BOD analysed during the wastewater monitoring, thus to approximate ultimate FCBOD it was assumed that nitrogenous demand is not exerted within 5 days (Mason 1996) and that soluble BOD makes up approximately 25% of total BOD ($BOD_{5,effluent}$) (see Appendix D and Mason (1996)):

$$FCBOD_{5,eff} = 0.25 \cdot BOD_{5,eff} \quad (8-2)$$

A plot of S_{US} estimates from each wastewater sampling event against time (Figure 8-3 below) indicates that aside from a peak related to excess biodegradable FCOD carried over from the anaerobic pond when sludge levels were high, S_{US} is a relatively constant parameter with perhaps a minor element of accumulation associated with recirculation of effluent.

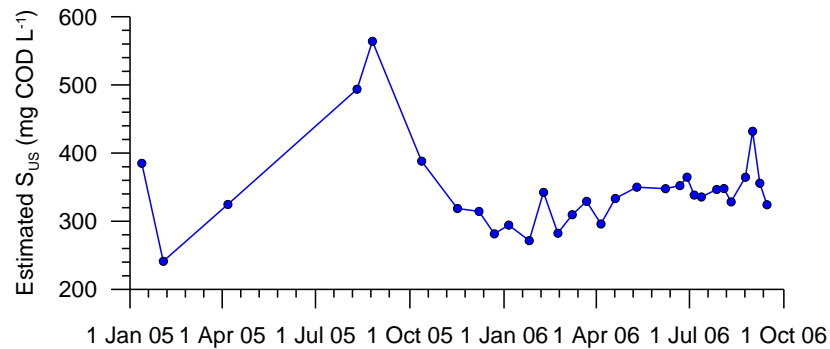


Figure 8-3 Estimated non-biodegradable soluble COD (S_{US}) over time.

Taking S_{BS} as the difference between influent FCOD and S_{US} , the plot presented in Figure 8-4 shows that variability in influent FCOD is almost entirely attributable to readily degradable COD.

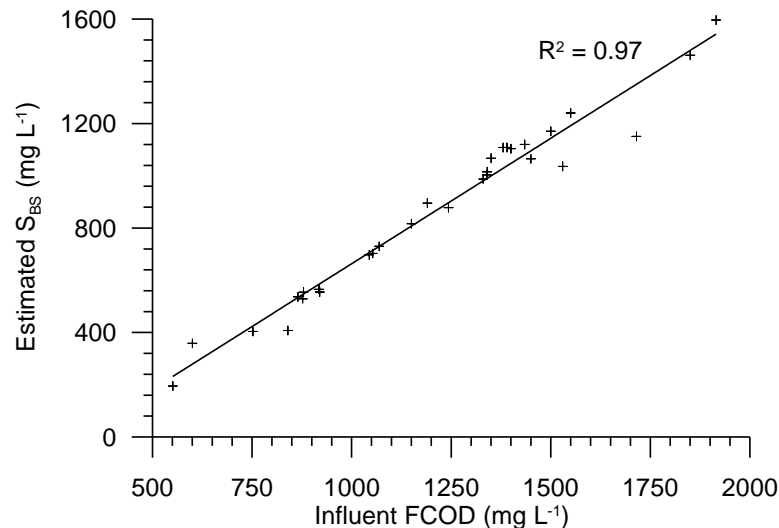


Figure 8-4 Estimated influent S_{BS} plotted against measured influent FCOD

Accordingly, S_{BS} was defined by the linear fit:

$$S_{BS} = 0.96 \cdot FCOD - 297.8 \quad (8-3)$$

Using this approach, average S_{BS} equated to about 17% of influent total COD, which is close to the 10-15% typical range for municipal wastewaters (Melcer et al. 2003). Where data were available, S_{US} was estimated as per equation 8-1. Otherwise S_{US} was calculated as the difference between FCOD and S_{BS} from equation 8-3. Overall estimated S_{US} corresponded to about 6.7% of influent total COD, which is slightly lower than the figure of 8.5% reported by Whichard (2001) for non-biodegradable soluble COD in diluted screened dairy manure.

8.5.1.1 Volatile fatty acids

BioWin further divides soluble readily biodegradable material into a complex fraction and two of the four main volatile fatty acids (VFAs) typically measured in wastewaters¹, namely acetic and propionic acids:

$$\begin{aligned} S_{BS} &= S_{BSC} + S_{BSA} + S_{BSP} \\ &= f_{BSC}S_{BS} + f_{BSA}S_{BS} + f_{BSP}S_{BS} \end{aligned} \quad (8-4)$$

where

S_{BSC} = complex readily biodegradable COD (mg L⁻¹);

S_{BSA} = acetic acid COD (mg L⁻¹);

S_{BSP} = propionic acid COD (mg L⁻¹);

f_{BSC} = complex fraction of readily biodegradable COD (g COD g⁻¹ S_{BS});

f_{BSA} = acetic acid fraction of readily biodegradable COD (g COD g⁻¹ S_{BS});

f_{BSP} = propionic acid fraction of readily biodegradable COD (g COD g⁻¹ S_{BS}).

VFAs play an important role in biological phosphate removal and denitrification processes (Mason & Mulcahy 2003). Acetic acid also acts as the terminal electron acceptor in the methanogenesis step of anaerobic digestion. VFAs are not typically found in high concentrations in municipal wastewaters, but in the case of dairy manure wastewaters, they can constitute more than 10% of volatile solids due to the fermentation of fibre that occurs in cows' ruminant digestive process (Batstone, Pind & Angelidaki 2003). There are numerous studies that have analysed VFA content of dairy

¹ Acetic, propionic, butyric and valeric acids.

manure and wastewater, including those listed in Table 8-5. There is considerable variability in the data; however, as would be expected, removal of particulate COD through screening/settling of manure/wastewater increases the relative VFA COD fraction. Dairy shed wastewater samples analysed by Tie & Sivakumar (2007a) and (2008a) were drawn from the same dairy farm as is the subject of this study and hence are considered the best indicator of COD fractions for this study. Hence the contribution of VFAs to total COD after coarse solids separation is assumed to be $0.05 \text{ g COD g}^{-1} \text{ total COD}$, which corresponds to approximately 30% of S_{BS} and is higher than the VFA content of raw wastewaters and manures, but lower than concentrations in screened wastewater/manure.

Given the retention times of the ponds, the division of the VFA component into acetic and propionic acids is likely to be immaterial to the modelling outcomes. Nonetheless, based on the data in Table 8-5, acetic acid was assumed to make up 60% of VFA COD, which translates to a value of $0.18 \text{ g COD g}^{-1} S_{BS} \text{ COD}$ for f_{BSA} . Since propionic, butyric and valeric acids are all by-products of fermentation and intermediates in the anaerobic digestion process, the remaining 40% of VFA was lumped into the propionic acid fraction ($f_{BSP} = 0.12 \text{ g COD g}^{-1} S_{BS} \text{ COD}$). Complex readily biodegradable COD could then be calculated from the difference between S_{BS} and VFA COD.

8.5.2 Particulate and Colloidal COD

Particulate matter in raw dairy shed wastewater largely comes from manure solids - organic matter that comprises structural carbohydrates cellulose and hemi-cellulose, lignin, proteins and lipids (fats, oils, grease and long chain fatty acids). On account of the grazing-based diet of Australian milking herds, a large fraction of manure solids comprises undigested plant material or lignocellulosic biofibres (Hill, McCaskey & Hamilton 1981). Biofibres constitute the structural material of plants and are resistant to enzymatic hydrolysis due to the barrier formed by slowly degradable hemicellulose knitting with biologically intractable lignin (Angelidaki & Ahring 2000). The crystalline structure of the cellulose in the biofibres also impairs hydrolysis, as does the lack of surface area for microorganisms to attack the fibres (Angelidaki & Ahring 2000).

The apparent biodegradability of particulate and colloidal COD depends, therefore, on the solids retention time of the treatment system in question. The lignin content of the biofibres is completely non-biodegradable, but the structural carbohydrates will eventually be degraded where sufficient time is allowed for hydrolysis to run its course. Table 8-6 summarises data on manure solids composition drawn from the literature.

Particulate COD and COD:VSS figures were calculated where all particulate components could be accounted for using VS and ThOD from Table 8-4.

Table 8-5 VFA characterisation of dairy shed wastewaters and manures.

Source - country	Parameter	Total COD	Total VFA			Acetic acid fraction	Propionic acid fraction
	Units	mg L ⁻¹	mg L ⁻¹	mg COD L ⁻¹	% total COD	% total VFA COD	% total VFA COD
Tie & Sivakumar (2007a) - AUS	Raw wastewater	5400	83	104	2	61	19
	Solids separated wastewater	5150	168	214	4	54	28
	Screened wastewater	5300	226	284	5	57	26
Tie & Sivakumar(2008b) - AUS	Screened wastewater	6370	503	634	10	58	24
Ellwood & Mason (2003) - NZ	Raw wastewater	9616	297	338	4	82	15
Mason & Mulcahy (2003) - NZ	Raw wastewater		240	305		57	18
Safley & Westerman (1992a) - US	Settled and screened wastewater	151323	3932	4916	3		
Møller, Sommer & Ahring (2004) - Denmark	Raw manure	48026	4629	5786	12		
Rico et al. (2007) - Spain	Screened manure	83550	3350	4188	5		
	Raw manure	5400	83	104	2		

BioWin divides particulate COD into slowly biodegradable (X_{SP}) and non-biodegradable fractions (X_I). Non-settleable colloidal COD is prescribed its own slowly biodegradable pool (X_{SC}). This fractionation was slightly modified to accommodate the lignocellulosic content of DSE as described in the following sections.

8.5.2.1 Non-biodegradable and very slowly biodegradable particulate COD

The bulk of the truly non-biodegradable particulate material in dairy shed wastewater should comprise lignin (Mason 1996). Since pond systems are typically desludged at intervals of several years, a relatively high proportion of the incoming structural carbohydrates (cellulose and hemicellulose) should be degraded in the system. As such, the high COD:BOD ratio of the influent, which is normally an indicator of a high proportion of non/slowly-biodegradable particulate material for municipal wastewaters

(Melcer et al. 2003), in this case indicates a high proportion of cellulosic particulate matter that is very slow to degrade rather than being totally intractable.

Melcer et al. (2003) present an iterative method for estimating the non-biodegradable (also termed 'inert' in BioWin) particulate fraction of (total) COD (f_{XI}) for organics-based (non-industrial) wastewaters that makes use of influent COD, cBOD₅ and TVSS data. To apply this method to the influent wastewater data, it was assumed that minimal nitrogenous oxygen demand would be exerted within 5 days, thus rendering BOD₅ a reasonable indicator of cBOD₅. Results from an investigation of BOD exertion in dairy shed wastewaters suggest that this is a reasonable assumption for raw and solids-separated wastewater (see Appendix D). The resulting estimate for the fraction of *conventionally* non-biodegradable particulate COD was 0.57 g COD g⁻¹ total COD, which is comparable to combined lignin, cellulose and hemicellulose fractions listed in Table 8-6. It is also similar to the 0.46 g COD g⁻¹ total COD adopted by (Beck 2007) when modelling biological N removal from pre-fermented DSE in BioWin.

Using this estimate in the BioWin model, however, would result in an underestimation of volatile solids destruction as the extended solids retention time of the anaerobic pond would facilitate hydrolysis of cellulose and hemicellulose that would largely go untreated in a conventional activated sludge plant. Myint et al. (2007) examined the breakdown of cellulose and hemicellulose using a two-phase model of anaerobic hydrolysis of a similar form as that used in BioWin. The two components, which were of almost identical concentration, produced considerably different rate constants with hemicellulose hydrolysed more rapidly than cellulose. The hemicellulose hydrolysis rate constant of 1.4 d⁻¹ was not dissimilar to the default constant used in BioWin adjusted for anaerobic conditions (1.05 d⁻¹), but the cellulose rate constant was substantially lower at 0.09 d⁻¹. Both half saturation constants measured by Myint et al. (2007), 28 for hemicellulose and 1.5 for cellulose, were much higher than the corresponding value of 0.15 used in BioWin. So while these structural carbohydrates are indeed biodegradable, they are clearly not hydrolysed at a rate commensurate with that of slowly biodegradable particulate matter as defined for conventional treatment of municipal wastewater.

Table 8-6 Manure solids composition reported in the literature.

<i>Units</i>		<i>Stafford (1980)</i>	<i>Van Horn et al. (1994)</i>		<i>Møller, Sommer & Ahring (2004)</i>	<i>Rico et al. (2007)</i>		<i>Liao et al. (2004; 2006)</i>	<i>Liao et al. (2007)</i>
Country		US	US		Denmark	Spain		US	
Sample		Dairy cattle manure	Dairy cattle manure	Screened dairy manure solids	Dairy cattle feces	Dairy cattle manure	Screened (1 mm) dairy cattle manure	Dairy cattle manure	
TS	% dry matter		12	25	12	8	4	16	13
VS	% TS	83	83	87-93	90	79	71		
Particulate COD	mg kg ⁻¹		93184 [‡]			87458	67929		
Particulate COD:VSS			1.48 [‡]			1.48	1.73		
Hemicellulose	% TS	12	19	24-28	17	21	3	12	11
Cellulose	% TS	31	27	37-45		24	4	22	23
Lignin	% TS	12		13-15	11	13	13	14	12
Proteins	% TS	13	3		13	15	13	16	18
Lipids	% TS		3		6	6	5		

[‡] Estimate based on lumped cellulose and lignin VS.

Accordingly the BioWin (conventionally) non-biodegradable particulate COD fraction was further divided into fractions of (actual) non-degradable lignin and very slowly degradable cellulosic material.

$$X_I = f_{XI} \cdot COD = X_{IL} + X_{BC} \quad (8-5)$$

where

$$\begin{aligned} f_{XI} &= \text{fraction of conventionally non-biodegradable particulate COD (mg L}^{-1}\text{)} \\ &= 0.57 \text{ g COD g}^{-1} \text{ total COD;} \end{aligned}$$

$$COD = \text{total COD (mg L}^{-1}\text{);}$$

$$X_{IL} = \text{non-biodegradable lignin (g COD g}^{-1} \text{ total COD);}$$

$$X_{BC} = \text{very slowly biodegradable cellulosic material (g COD g}^{-1} \text{ total COD).}$$

In characterising dairy manure wastewater for modelling purposes, Whichard (2001) estimated the non-biodegradable component by assuming that the fraction of fixed suspended material relative to total suspended solids was reflective of the proportion of non-biodegradable COD, producing a figure of 11% which appears to correspond to lignin content based on Table 8-6. Taking a similar approach in characterising DSE for anaerobic digestion modelling, Tie & Sivakumar (2008a) assumed fixed suspended solids to correspond directly to non-biodegradable particulate COD, which together with an assumed ThOD of 1.38 (from Huete et al. 2006) for inert material, produced a non-biodegradable COD fraction of 20%. The balance with total particulate COD was assumed to constitute carbohydrates, which amounted to 23% of total COD. Tie & Sivakumar (2008a) also proposed the inverse approach of using ThOD to calculate carbohydrates from volatile suspended solids and assuming the balance of this with particulate COD to be equivalent to particulate non-biodegradable COD. This produced a slowly degradable carbohydrate fraction of 40% and a particulate non-biodegradable fraction of 3.6%, which would appear patently wrong when compared with the data in Table 8-6.

The above approaches, however, both make the mistake of equating inert inorganic particulate material (expressed as total fixed suspended solids - TFSS) with non-biodegradable organic matter. In the absence of a credible estimation method, X_{IL} was defined as a fraction of total particulate and colloidal COD based on the data presented in Table 8-6. A VS lignin content of 12% TS corresponds to about 695 mg COD L⁻¹ or 18% of average particulate/colloidal COD. Thus lignin COD was calculated

$$X_{IL} = f_{XIL}(COD - FCOD) \quad (8-6)$$

where

$$\begin{aligned} f_{XIL} &= \text{fraction of lignin COD relative to particulate/colloidal COD} \\ &= 0.18 \text{ g COD g}^{-1} \text{ COD} \end{aligned}$$

The cellulosic fraction (f_{XBC}) was then estimated from average influent conventionally inert COD (\bar{X}_I), the typical lignin COD and average particulate/colloidal COD:

$$\begin{aligned} f_{XBC} &= \frac{\bar{X}_{BC}}{\bar{X}_I} \\ &= \frac{f_{XI} \cdot \overline{COD} - \bar{X}_{IL}}{\overline{COD} - \overline{FCOD}} \\ &= \frac{2815 - 695}{2815} \\ &= 0.56 \text{ g COD g}^{-1} \end{aligned} \quad (8-7)$$

where \overline{COD} and \overline{FCOD} are average observed COD and FCOD, respectively (refer to Chapter 7).

This allowed X_{BC} to be calculated at each time step using particulate/colloidal COD:

$$X_{BC} = f_{XBC}(COD - FCOD) \quad (8-8)$$

In order to accommodate these two COD fractions in BioWin, an additional state variable was incorporated into the model to represent the truly non-biodegradable lignin fraction and a new process equation was defined in the BioWin 'Model Builder' as described in section 8.6.1. Hence the BioWin state variable for non-biodegradable particulate COD was re-classified as very slowly degradable (cellulosic) COD ($X_{BC} = f_{XBC} \cdot COD_{influent}$) and the truly non-biodegradable lignin component of COD ($X_{IL} = f_{XIL} \cdot COD_{influent}$) was represented with a user defined state variable (UD3):

$$UD3 = \frac{X_{IL}}{ThOD_L} \quad (8-9)$$

where

$UD3$ = user defined variable (mg VSS L⁻¹);

$ThOD_L$ = theoretical oxygen demand for lignin = 1.8 g COD g⁻¹ TSS.

This reclassification meant that particulate COD outputs from the BioWin model had to be adjusted to account for X_{IL} when comparing with observed data.

8.5.2.2 Slowly biodegradable particulate and colloidal COD

Slowly degradable material is that which requires extracellular enzymatic breakdown prior to being metabolised by bacteria. Given that cellulose and hemicellulose are considered to be largely 'non-biodegradable' in conventional terms, the slowly degradable fraction is likely to consist of proteins, lipids and some complex soluble compounds with large molecular weights including amino acids and sugars. The protein-based COD content can be coarsely estimated by multiplying the particulate organic N concentration by 6.25 and then multiplying this figure by the stoichiometric ratio of oxygen to N for the aerobic decomposition of protein/amino acid (1.5). Assuming a particulate organic N fraction of 30% (see section 8.5.4.2), this produces a fraction of about 6% of total COD. Reported lipids fractions of organic particulates vary between 10 to 18% COD (see Table 8-6), giving an expected range for slowly degradable material of 16 to 24% COD.

Slowly biodegradable COD was estimated by taking the difference between total COD and the COD components determined in the previous sections (Melcer et al. 2003):

$$X_S = COD - S_{US} - S_{BS} - X_{BC} - X_{IL} \quad (8-10)$$

Average X_S calculated this way sits at 956 mg L⁻¹, or about 20% total COD which is within the expected range based on typical lipid and protein content. An alternative method of estimating X_S is to subtract readily biodegradable COD from ultimate CBOD corrected for non-biodegradable COD generated in biomass lysis (Roeleveld & van Loosdrecht 2002).

$$X_S = \left(\frac{1}{1 - f_{BOD}} \right) CBOD_{ult} - S_{BS} \quad (8-11)$$

where

f_{BOD} = correction for non-biodegradable biomass lysis COD

= 0.15;

$CBOD_{ult}$ = ultimate CBOD (mg L⁻¹).

In this case BOD_{ult} was calculated from BOD₅ using a BOD rate constant derived from fitting a BOD curve to measured data. Using the modified BOD exertion model

described in Appendix D with rate and delay constants of 0.18 d^{-1} and 1.7 d , respectively, average ultimate total BOD for the influent was calculated to be 2463 mg L^{-1} . Subtracting 914 mg L^{-1} theoretical nitrogenous oxygen demand (assuming 4.57 mg oxygen demand per mg soluble organic N and $\text{NH}_3\text{-N}$), ultimate CBOD is then 1549 mg L^{-1} . Using the suggested correction factor of 0.15 , X_S is calculated to be 1052 mg L^{-1} , which is equivalent to 21% of total COD and shows good agreement with the primary estimate for f_S .

Slowly biodegradable COD is further divided into colloidal and particulate fractions. The particulate fraction was derived as part of estimating non-biodegradable particulate matter using the Melcer et al. (2003) method and was approximated to be 57% of slowly biodegradable COD. That is

$$f_{XSP} = 0.57 \text{ g COD g}^{-1} X_S \quad (8-12)$$

The colloidal fraction was then simply the balance of slowly biodegradable COD, or

$$f_{XSC} = 1 - f_{SP} \quad (8-13)$$

8.5.3 COD:VSS

Two key parameters in BioWin are the ratios of COD to volatile suspended solids (VSS) for biodegradable and non-biodegradable particulate material. This ratio is generally determined from analysis of COD and TVSS of composite samples, making no distinction between the different components that make up total COD. The data presented in Chapter 7 produced an influent PCOD:TVSS ratio of 1.5 . As demonstrated in Table 8-4 however, DSE comprises a variety of organic compounds with varying theoretical oxygen demands. Hence rather than adopt the coarse estimate from Chapter 7, it was instead decided to base the ratios on the particulate COD breakdown described above.

Since non-biodegradable particulate COD had been reclassified as very slowly degradable cellulosic material, the COD:VSS ratio for this fraction was simply the ThOD for structural carbohydrates ($1.2:1$). Taking the same approach for non-biodegradable lignin COD (ThOD:VSS = COD:VSS = $1.8:1$), the VSS concentration associated with the non-biodegradable fraction could be estimated. The balance of very slowly biodegradable and non-biodegradable VSS with total VSS (TVSS) was then taken to represent VSS of slowly degradable particulate material, which in turn produced a COD:VSS for slowly degradable material (particulate substrate) of 1.26 .

8.5.4 Nitrogen

N is primarily divided into free (gaseous) ammonia and saline ammonia (ammonium) and organic N fractions. The organic fraction is then broken up into biodegradable and non-biodegradable fractions, which are in turn apportioned between soluble and particulate fractions. Both the organic and ammonium fractions in manure are variable as they are prone to mineralisation to ammonium and volatilisation, respectively. Accordingly, while manure can remain on the floor of the dairy or in the yard for up to several hours, it is best to draw on data for fresh manure characteristics rather than stockpiled, land applied or otherwise treated manure. More than 60% of total N is organically bound (Van Horn et al. 1994; Hawke & Summers 2006). A significant fraction of N in manure originates from urine, predominantly as the soluble organic compound urea ($\text{CO}(\text{NH}_2)_2$) (Eghball et al. 2002; Meyer, Ristow & Lie 2007). Urea is rapidly hydrolysed to ammonium carbonate, which can then lead to volatilisation losses when moisture is low and pH is greater than eight (Hjorth et al. 2010). Most particulate N comprises slowly or non-biodegradable undigested protein, microbial tissue and cells sloughed off the animal's digestive tract, with only a fraction being readily degradable proteins, peptides and amino acids (Dahlberg, Lindley & Giles 1988; Hill, McCaskey & Hamilton 1981; He & Honeycutt 2011).

8.5.4.1 Ammonia

The wastewater constituent ammonia ($\text{NH}_3\text{-N}$) referred to in Chapter 7 incorporates both free and saline forms of ammoniacal N, as does the corresponding state variable in BioWin. The balance between the two ammonia phases depends on the equilibrium governed by pH and temperature, which BioWin handles internally without the need for separate state variables. The quantity of (net) ammonia relative to total N can vary greatly between different types of wastewater and also between different sources of the same type of wastewater. Over the course of the monitoring period, the influent ammonia to TKN ratio (f_{NA}) varied between 0.41 and 0.84. On account of this variability, and despite the reasonable correlation between $\text{NH}_3\text{-N}$ and TKN shown in Chapter 7 (section 4.2), $\text{NH}_3\text{-N}$ was considered as an independent constituent rather than calculated from TKN.

8.5.4.2 Organically bound nitrogen

It is not possible to distinguish between biodegradable and non-biodegradable components of soluble organic N through direct measurements; hence the fractionation relies on assumed (or potentially calibrated) non-biodegradable fractions. The only fraction that can be deduced from the data available in this study is that of particulate

non-biodegradable N (f_{XIN}) which in BioWin is expressed relative to particulate non-biodegradable COD. If it is assumed that the majority of biodegradable COD and N partitioned to the sludge is hydrolysed, the particulate non-biodegradable N fraction of influent COD may be approximated as

$$f_{XIN} \approx \varepsilon_X \left(\frac{TN_{sludge} - (NH_3 - N)_{eff}}{COD_{sludge}} \right) \quad (8-14)$$

where

ε_X = particulate COD destruction in the pond (fraction); and

TN_{sludge} , $(NH_3 - N)_{eff}$, COD_{sludge} are the sludge TN, effluent ammonia and sludge COD concentrations, respectively.

Using the mass balance presented in Chapter 7, particulate COD destruction in the sludge was about 39%. Allowing for complete destruction of the (approximately) 26 kg d⁻¹ incoming slowly degradable particulate and colloidal material, destruction of very slowly degradable COD amounts to about 19%. Using effluent $NH_3 - N$ as a proxy for sludge $NH_3 - N$ and the sludge COD concentration from October 2005 (60,009 mg L⁻¹) produces an f_{XIN} of 0.024 g N g⁻¹ COD.

It is important to recognise that with the limited number of user-defined variables available in BioWin, this fraction must incorporate N associated with very slowly biodegradable cellulosic material as well as actual non-biodegradable particulate N. By lumping the two components, it is assumed that N is present at the same concentration in both forms of organic matter. The concentration of particulate non-biodegradable N was thus calculated:

$$X_{IN} = f_{XIN}(X_{IL} + X_{BC}) \quad (8-15)$$

Some 50-70% of N in manure slurries is in dissolved forms including ammonia, urea and amino acids (Liao et al. 2004; Hjorth et al. 2010). Data presented by Tie & Sivakumar (2007b) and Whichard (2001) suggest the percentage is higher for solids-separated DSE. The particulate fraction comprises proteins from indigestible forage (or pasture) and rumen bacteria (Liao et al. 2004) that may be considered poorly degradable. Since average particulate inert N calculated as per equation 8-15 amounts to 24% of TKN, biodegradable particulate N (X_{ON}) was considered zero.

The remaining organic N was then assigned to soluble organic N (N_S):

$$N_S = TKN - (NH_3 - N) - X_{IN} \quad (8-16)$$

Soluble organic N would comprise mostly urea and amino acids. Urea has been found to make up 10-20% of total manure N as excreted (He & Honeycutt 2011); however it is prone to rapid hydrolysis and was thus assumed to be accounted for in the ammonium fraction. Water labile amino acid content in stockpiled manures has been observed to be around 0.7% of total dry matter (He & Olk 2011). Applying this percentage to the TS concentration of the influent produces an average amino acid content of 41 mg N L⁻¹ or about 80% of soluble organic N. The other 20% was assumed to be non-biodegradable, giving a soluble non-biodegradable N fraction f_{NUS} of 0.2 g N g⁻¹ N_S . The concentration of soluble biodegradable N (N_{OS}) was then calculated as the balance of TKN after accounting for the other fractions:

$$N_{OS} = TKN - X_{IN} - f_{NUS}TKN \quad (8-17)$$

8.5.4.3 Oxidised nitrogen

Both forms of oxidised N (nitrite and nitrate) were detected at very low concentrations in the influent wastewater (<0.3 mg L⁻¹). When the two forms were initially determined separately, it was clear that nitrate was the dominant species. Subsequent analyses of oxidised N lumped the two forms as total oxidised N (TON). With nitrite assumed to be zero, daily nitrate concentrations were then defined by the average TON load divided by flow.

8.5.5 Phosphorus

Fractionation of influent P in BioWin accommodates three primary forms of P, including soluble and metal-complexed (inorganic) orthophosphate, particulate biodegradable organic P and particulate non-biodegradable P. BioWin also includes state variables for releasable and fixed stored polyphosphates, hydroxyapatite, hydroxy-dicalcium-apatite and struvite. These P forms, however, tend not to be present in influent streams, so the state variables are more used to quantify the microbial and mineral P by-products of wastewater treatment. Biodegradable soluble organic P is assumed to be rapidly hydrolysed to orthophosphate while non-biodegradable soluble and colloidal organic P fractions are considered to be zero.

DRP measured in the wastewater monitoring was assumed to translate directly to soluble orthophosphate, and metal-complexed orthophosphates (PO₄-P) were assumed to be negligible (metal-complexed P in BioWin is designed to quantify P complexation with iron and aluminium addition, not for other cation-complexed forms).

It was shown in Chapter 7 that DRP did not exhibit a strong correlation with TP. Hence rather than multiply TP by a fraction to calculate the daily soluble orthophosphate concentration, DRP was treated as an independent constituent. As with the N fractionation, particulate very slowly biodegradable and non-biodegradable P (X_{IP}) was defined:

$$X_{IP} = f_{XIP}(X_{IL} + X_{BC}) \quad (8-18)$$

where

f_{XIP} = P fraction of particulate non-biodegradable and very slowly degradable COD.

f_{XIP} was estimated using sludge concentrations in the same manner as X_{IN} , producing a figure of 0.0058 g P per g of particulate non-biodegradable and very slowly degradable COD. The remaining fraction of total P was allotted to particulate biodegradable organic P (X_{OP}).

8.5.6 Cations and Anions

BioWin has state variables specifically assigned to soluble magnesium (Mg^{2+}) and calcium (Ca^{2+}), allowing data collected in the wastewater monitoring to be entered directly into the model. Soluble potassium (K^+) and chloride (Cl^-) were assigned to the 'Other Cations (strong bases)' and 'Other Anion (strong acids)' state variables respectively and their molecular weights nominated in the corresponding BioWin parameters.

8.5.7 Summary of Wastewater Constituent Fractions

The final wastewater constituent fractions estimated or derived for input into the BioWin simulator are summarised in Table 8-7.

8.6 ADDITIONAL TREATMENT PROCESSES

By virtue of their extended solids retention times, DSE anaerobic ponds can degrade organic material that would be classified non-biodegradable in a conventional activated sludge system. To account for this, additional process models had to be incorporated into the standard ASDM model through the 'model builder' component of BioWin. This section describes the custom equations that were added to BioWin to simulate the breakdown of very slowly biodegradable particulate material and biomass endogenous products.

Table 8-7 Summary of wastewater constituent fractions adopted for modelling.

Constituent or parameter	Calculation or value	Coefficients	Estimation method or source
Soluble non-biodegradable COD	$S_{US} = 0.9 \cdot FCOD_{eff} - FCBOD_{ult,eff}$ OR $S_{US} = FCOD - S_{BS}$		Roeleveld & Van Loosdrecht (2002), Melcer et al. (2003)
Readily biodegradable COD	$S_{BS} = 0.96FCOD - 297.8$		Linear regression ($FCOD - S_{US}$) vs FCOD
Acetic acid COD	$S_{BSA} = f_{BSA}S_{BS}$	$f_{BSA} = 0.60$	Table 8-5
Propanoic acid COD	$S_{BSP} = f_{BSP}S_{BS}$	$f_{BSP} = 0.40$	Table 8-5
Complex readily biodegradable COD	$S_{BSC} = S_{BS} - S_{BSA} - S_{BSP}$		$1 - f_{BSA}$
Non-biodegradable and very slowly degradable particulate COD	$X_I = f_{XI}COD$	$f_{XI} = 0.57$	Melcer et al. (2003)
Non-biodegradable lignin COD	$X_{IL} = f_{XIL}(COD - FCOD)$	$f_{XI} = 0.18$	Table 8-6
Very slowly biodegradable cellulose and hemicellulose	$X_{BC} = f_{BC}(COD - FCOD)$	$f_{XI} = 0.56$	Table 8-6
Slowly biodegradable particulate and colloidal COD	$X_S = COD - S_{US} - S_{BS} - X_{BC} - X_{IL}$		
Colloidal slowly biodegradable COD	$X_{SC} = f_{XSC}X_S$	$f_{XSC} = 0.43$	Melcer et al. (2003)
Non-colloidal slowly biodegradable COD	$X_{SP} = f_{XSP}X_S$	$f_{XSP} = 0.57$	Melcer et al. (2003)
COD:VSS substrate		1.26	Calculated
COD:VSS very slowly biodegradable COD		1.20	Table 8-4
Free and saline ammonia	$NH_3 - N$	0.54	Measured in this study
Unbiodegradable particulate N	$X_{IN} = f_{XIN}X_I$	$f_{XIN} = 0.024$	Sludge N:COD
Particulate biodegradable organic N	$X_{ON} = 0$		Particulate N content from Hjorth et al. (2010) and Tie & Sivakumar (2007b)
Soluble unbiodegradable organic N	$N_{US} = f_{NUS}N_S$	$f_{NUS} = 0.042$	Estimated amino acid content (He & Olk 2011)
Soluble biodegradable organic N	$N_{OS} = (1 - f_{NUS})N_S$		
Orthophosphate	PO4-P (incl. MeP)		Measured in this study
Unbiodegradable particulate P	$X_{IP} = f_{XIP}X_I$	$f_{XIP} = 0.0058$	Sludge P:COD
Molecular weight of other cations	39.1		Molecular weight of K
Molecular weight of other anions	35.5		Molecular weight of chloride

8.6.1 Degradation of ‘Non-Biodegradable’ Particulate COD

While BioWin includes a process model for hydrolysis of particulate COD, it is intended for material that is more readily degradable than that found in DSE. To address this short-coming, the BioWin biokinetic model was augmented with an additional process equation to represent the conversion of very slowly degradable particulate COD to soluble COD. However, instead of using a first order equation as per Houweling et al. (2008), a hydrolysis model specific to the cellulose and hemicellulose fractions in manure formulated by Myint, Nirmalakhandan & Speece (2007) was adapted. The model considers hydrolysis as a surface limited reaction involving ordinary heterotrophic organisms (OHO) and PAO biomass and is expressed as (Myint, Nirmalakhandan & Speece 2007):

$$\frac{dX_{BC}}{dt} = k_{HBC}(Z_{OHO} + Z_{PAO}) \frac{X_{BC}/(Z_{OHO} + Z_{PAO})}{K_{BC} + X_{BC}/(Z_{OHO} + Z_{PAO})} \quad (8-19)$$

where

X_{BC} = very slowly degradable cellulosic COD (mg L⁻¹)

$= f_{BC} \cdot COD$;

k_{HBC} = maximum specific hydrolysis rate for cellulosic material (d⁻¹)

$= k_{HBC,37} \theta^{T-37}$;

θ = temperature adjustment coefficient;

T = pond temperature (°C);

Z_{OHO} = concentration of OHO biomass (mg COD L⁻¹);

Z_{PAO} = concentration of PAO biomass (mg COD L⁻¹);

K_{BC} = half saturation coefficient for hydrolysis of cellulosic material (g COD g⁻¹ COD).

The original Myint, Nirmalakhandan & Speece (2007) model uses two equations – one each for cellulose and hemicellulose substrates. Data presented in Table 8-6 suggest that cellulose and hemicellulose in DSE given above are approximately evenly split. To limit the additional state variables required in the model, the model was reduced to the one equation with the rate constant being the harmonic mean of the two rate constants

derived by Myint, Nirmalakhandan & Speece (2007). Similarly the saturation constant was taken as the harmonic mean of the saturation constants. An Arrhenius temperature dependency function was added to the original model to account for the fact that the experiments Myint, Nirmalakhandan & Speece (2007) used to derive the model parameters were conducted at 37 °C. The value for the temperature adjustment coefficient was adopted from the Barker & Dold (1997) hydrolysis rate temperature dependency function.

The degradation of very slowly degradable material would also cause the release of organically bound nutrients from the sludge, thereby contributing to the transferral of nutrients to the supernatant. Two additional process equations were introduced to the model to simulate the breakdown of very slowly biodegradable N and P. Both took the form of equation 8-19, but were adjusted by the (current) ratios of very slowly degradable N/P to very slowly biodegradable material. Since X_{IN} and X_{IP} incorporated very slowly biodegradable and non-biodegradable fractions, both were scaled to reflect the very slowly biodegradable fractions only. The equation for degradation of very slowly degradable N was:

$$\begin{aligned} \frac{dX_{IN}}{dt} &= \frac{X_{BC}X_{IN}}{(X_{BC} + X_{IL})} \cdot \frac{1}{X_{BC}} \cdot k_{HBC}Z_{OHO} \frac{X_{BC}/(Z_{OHO} + Z_{PAO})}{K_{BC} + X_{BC}/(Z_{OHO} + Z_{PAO})} \\ &= \frac{X_{IN}}{(X_{BC} + X_{IL})} \cdot k_{HBC}Z_{OHO} \frac{X_{BC}/(Z_{OHO} + Z_{PAO})}{K_{BC} + X_{BC}/(Z_{OHO} + Z_{PAO})} \end{aligned} \quad (8-20)$$

Similarly, the equation for degradation of very slowly biodegradable P was:

$$\frac{dX_{IP}}{dt} = \frac{X_{IP}}{(X_{BC} + X_{IL})} \cdot k_{HBC}Z_{OHO} \frac{X_{BC}/(Z_{OHO} + Z_{PAO})}{K_{BC} + X_{BC}/(Z_{OHO} + Z_{PAO})} \quad (8-21)$$

Hydrolysis was assumed to convert very slowly degradable material into complex (non-acetate) readily biodegradable material. Ramdani et al. (2010) showed that the dominant by-products from anaerobic digestion of poorly degradable sludges were soluble and colloidal proteins. The degradation product of very slowly degradable N was therefore set to soluble organic N. In the absence of a corresponding P state variable, the by-product from degradation of very slowly degradable P was assigned to phosphate under the assumption that soluble organic P would be rapidly hydrolysed. The stoichiometry of the processes is summarised in Table 8-8.

Table 8-8 Stoichiometry of the process models for the biodegradation of very slowly degradable (hemicellulose and cellulose) COD and associated particulate bound N and P.

<i>Process</i>	<i>State variable</i>	<i>Value</i>
Break down of very slowly biodegradable COD to complex readily biodegradable COD	X_{BC}	-1
	S_{BSC}	1
Release of organically bound N content of particulate very slowly degradable COD	X_{XP}	-1
	$PO_4 - P$	1
Release of organically bound P content of particulate very slowly degradable COD	X_{IN}	-1
	N_{OS}	1

8.6.2 Decay of Endogenous Products

Prolonged SRTs (greater than 40 days) have also been shown to lead to decay of endogenous products (Jones et al. 2008). Ramdani et al. (2010) characterised the degradability of endogenous products by performing 90-day laboratory batch experiments on mixed liquor from a membrane bioreactor. Using a first order decay function to model the process, they derived a first order decay constant of 0.005 d^{-1} for anaerobic conditions. Based on these findings the following process model was incorporated into BioWin using the model builder:

$$\frac{dX_e}{dt} = b_{Xe} X_e IN_{yes} IP_{yes} \quad (8-22)$$

where

b_{Xe} = decay rate = 0.005 d^{-1} ;

X_e = endogenous products (mg COD L^{-1});

$$IN_{yes} = \frac{X_{IN}}{k_{IN} + X_{IN}}$$

$$k_{IN} = 0.1 \text{ mg N L}^{-1}$$

$$IP_{yes} = \frac{X_{IP}}{k_{IP} + X_{IP}}$$

$$k_{IP} = 0.1 \text{ mg P L}^{-1}$$

The IN_{yes} and IP_{yes} switching functions were applied to limit the process under low nutrient conditions. Following the modelling approach of Ramdani et al. (2010), X_e was converted into slowly biodegradable particulate matter (X_{sp}). The stoichiometry is presented in Table 8-9.

Table 8-9 Stoichiometry of the model for decay of endogenous products.

<i>Process</i>	<i>State variable</i>	<i>Value</i>
Break down of endogenous products	Z_E	-1
	X_{SP}	1
Conversion of P content of endogenous products	X_{IP}	$-f_{PZE} = -0.07$
	X_{OP}	f_{PZE}
Conversion of N content of endogenous products	X_{IN}	$-f_{NZE} = -0.022$
	N_{ON}	f_{NZE}

8.7 DATA PRE-PROCESSING

On account of the temporal variability of the system, particularly the seasonality of temperature, rainfall and evaporation, and the gradual accumulation of sludge and salts, simulations were set up to run dynamically. Steady state simulations were only performed to test initial model configurations in the preliminary stages of model development. In order to ‘establish’ the models such that conditions at the commencement of the calibration period adequately reflected the state of the ponds, simulations were run from the inception of the pond system in 2002 as per Houweling et al. (2008). Dynamic simulations were run on a daily time step and required data inputs and flow routing to be entered as time series.

Monitoring at the site commenced in November 2004, although not all components of the monitoring system came on line at the time and technical difficulties resulted in data collection failure or losses at various times. Table 8-10 summarises the data available from the monitoring that was used in the modelling of the pond system. Data inputs for missing days and the period before monitoring commenced were generated as described in the following sections. The resulting contiguous input data are provided in Appendix L.

Table 8-10 Summary of data available for use in modelling.

<i>Data</i>	<i>Collection commenced</i>	<i>Collection ceased</i>	<i>Usable data</i>	<i>Appendix</i>
Wastewater flows				
Anaerobic pond inflows	20 November 2004	5 December 2006	598 of 747 days	I
Anaerobic pond outflows	15 September 2005	5 December 2006	438 of 446 days	I
Meteorology				
Rainfall	24 November 2004	5 December 2006	708 of 741 days	H
Evaporation	24 November 2004	5 December 2006	707 of 741 days	H
Air temperature	24 November 2004	5 December 2006	708 of 741 days	H
Stormwater runoff (estimated from rainfall)	24 November 2004	5 December 2006	708 of 741 days	I
Seepage (estimated)	29 October 2005	5 December 2006	All	I
Anaerobic pond supernatant temperature	25 November 2004	19 February 2007	802 of 816 days	G
Wastewater characteristics	12 January 2005	14 September 2006	31 sampling events	K

8.7.1 Wastewater Flows

Monitoring of the wastewater flow entering the anaerobic pond from the solids trap commenced in November 2004; however the flume monitoring flow leaving the pond did not start collecting reliable data until September the following year. Monitoring of flows leaving the facultative pond also started in November 2004, but the flow meter was configured to capture direct pumping to the dairy only in October 2005. To generate synthetic inflows to the anaerobic pond outside the monitoring period and to substitute for missing data in the monitoring period, the wastewater stream was divided into three separate streams including:

1. Wastewater from fresh water used to hose down the dairy parlour and clean the milking machine and milk vat (W_f);
2. Wastewater from the flood wash ($W_{r,f}$); and
3. Wastewater from direct pumping of recycled effluent ($W_{r,y}$).

Daily flows for each stream were formulated using a monte carlo method that involved applying randomly generated probabilities to normal distributions defined by their respective means and standard deviations observed during the water balance period.

8.7.2 Meteorology and Hydrology

Hourly site-specific meteorological data (temperature, rainfall, relative humidity, wind speed and direction, solar radiation) were available for most days from 24 November 2004. Missing data points from 5 May 2005 onwards (total were filled using hourly data from an SCA weather station located 6.7 km from the site at Wingecarribee reservoir (station number 568113). The hourly SCA data also allowed evaporation to be estimated using the model described in Chapter 5 where on-site meteorological data were not available.

Missing rainfall and evaporation pre-dating 5 May 2005 were drawn from a range of sources in the order of preference given in Table 8-11, depending on availability. These alternative sources provided daily records, which meant that missing hourly data required the substitution of all hourly data from that day with the single corresponding record from an alternative source. To account for methodological and other differences between pond evaporation and evaporation estimates from the alternative sources, replacement data were multiplied by the empirical adjustment factors given in Table 8-11 that were derived by regressing 9am daily evaporation data generated against corresponding data from the alternative source (see Appendix H for regression plots).

Table 8-11 Alternative meteorological data sources and adjustment factors derived from regression analysis.

<i>Preference</i>	<i>Rainfall</i>	<i>Evaporation</i>		
	<i>Source</i>	<i>Source</i>	<i>Anaerobic pond adjustment factor</i>	<i>Facultative pond adjustment factor</i>
1	Farm records	SCA weather station 568113 Penman-Monteith estimates*	1.27	0.99
2	SCA weather station 568113	SCA weather station 568113 – US Class A pan data	0.82	0.66
3	SCA rainfall station 568070	SILO FAO Penman-Monteith estimates (Allen et al. 1998)	1.14	0.93

* Estimation method unknown

8.7.2.1 Stormwater runoff

Stormwater runoff was estimated for three catchments draining to the ponds including the pond embankments (R_e), the solids trap (R_s) and the holding yard at the dairy (R_y). Runoff from the pond embankments was estimated using measured and externally sourced rainfall data in the soil moisture model used in the water balance (Chapter 5, section 3.2) adapted to a daily time step. Estimates of runoff from the solids trap were required for the periods when inflow to the anaerobic pond was not measured. Since the solids trap was concrete-lined, and drained directly to the pond, runoff was assumed to occur with every rainfall event and was calculated by multiplying the plan area of the drive-in bay, the sump and the adjacent solids storage facility by rainfall. Runoff from the holding yard also had to be estimated in the absence of anaerobic pond inflow data, although an added complexity was that it would only occur when the farmer neglected to put the stormwater diversion in place. Since there was no means of predicting the timing or frequency of yard runoff, its occurrence was determined under the condition:

$$W_0 - W_f - W_{r,f} - W_{r,y} - R_s \geq A_y P \quad (8-23)$$

where wastewater flows were generated using monte carlo simulation and

R_s = Runoff from the solids trap

$= A_s P$;

A_s = plan area of the solids trap;

P = rainfall;

A_y = plan area of the holding yard.

8.7.2.2 Seepage

The same model fitted to the water balance data in Chapter 5 was used to generate the full time series for seepage flows from both ponds, requiring no selection or replacement of field data.

8.7.3 Pond Temperatures

Average daily temperatures in the anaerobic pond were calculated from hourly data where 22 or more hourly data points were available. Data presented in Chapter 4 shows that temperatures in both ponds varied widely between and within seasons, but

did not exhibit the extreme fluctuations that air temperature does. Hence rather than use static averages or air temperatures as proxies, pond temperatures outside the monitoring period were modelled by combining a simple moving average and linear regression with air temperature data as the independent variable:

$$T_P = \beta_0 + \beta_1 \cdot (SMA_{AT,n}) \quad (8-24)$$

where

T_P = Average daily pond temperature (°C);

β_0, β_1 = Regression coefficients;

$SMA_{AT,n}$ = Mean of the current and previous $n - 1$ daily air temperature records (°C);

The period of the air temperature moving average n was determined together with the regression coefficients by minimising the sum of the squares of the errors. Table 8-11 presents the parameters determined for the anaerobic pond temperature model together with coefficients of determination (Adjusted R^2). The same model was used to in-fill missing data.

Table 8-12 Anaerobic pond temperature model parameters and coefficients of determination.

n	β_0	β_1	Adjusted R^2
14	-1.23	1.29	0.93

8.7.4 Influent Characteristics

While daily flow and hydrological data were available for the monitoring period, influent characteristics data were limited to those generated from the 31 sampling events. As noted earlier, influent loading is a primary determinant of effluent characteristics; hence the shortage of influent characteristics data presented a significant barrier to undertaking dynamic modelling of the system. Influent characteristics, however, may be expressed as functions of a number of independent factors including the manure load deposited at the dairy and the volume of water/effluent used to remove it, constituent loads contained in reclaimed effluent, and the state of the solids trap in terms of accumulated solids and the extent of clogging of the screen; all of which can be inferred from other data that is available between sampling events. Loads from cleaning chemicals were assumed constant while soil and other debris brought into the

dairy by the herd were assumed to constitute a relatively small fraction of constituent loads.

Given that dairy operators manually hose down the dairy and determine the volume of the flood wash when opening and closing the release valve, it is reasonable to assume that water/effluent usage and resulting wastewater flows are functions of the manure load and therefore are likely to be proportional to wastewater constituent loading. As such, the concentration of the influent wastewater should theoretically be similar from day to day. Day-to-day variability in concentrations should arise from stochastic factors that affect the amount of water/effluent used per quantity of manure such as the quantity and location of manure deposits, the time elapsed between deposition and washing, and human response and performance. Trends and very large deviations from average influent wastewater characteristics should be related to changes in the quality of the recycled effluent, changes to dairy wash down procedures, the state and performance of the solids trap, and dilution by stormwater runoff.

The chief objective of this aspect of the modelling was to mimic trends in influent wastewater constituent concentrations related to accumulation of non-biodegradable and inert species within the system caused by effluent recycling. The volume and electrical conductivity of recycled effluent used in the flood wash may be considered reasonable indicators of non-reactive constituent loads contributed by effluent recycling, which should comprise mainly inert inorganic material and recalcitrant forms of COD and organically bound constituents. The main change to the management of the system during the wastewater sampling period was made in late March 2006 when the farmers shifted from an ad hoc approach to cleaning out the solids trap to a weekly regime. More regular emptying of the trap would have reduced or eliminated the incidence of influent overtopping the solids trap screen, but increased the frequency of elevated peak flows related to clearing blockages from the screen. Both effects, together with day-to-day variation in the state of the solids trap, should have been picked up in the anaerobic pond inflow data, with high peak flows indicating when the screen was overtopped or had been recently cleaned. Finally, stormwater runoff flows were estimated as described in section 8.7.2.1, allowing wastewater flow to be isolated from the total inflow to the pond.

The above rationale was used in constructing linear regression models of wastewater constituent loading. A base model was specified to describe constituent loads as functions of the combined fresh water and pumped effluent volumes and the flood wash volume (explaining variance associated with the manure load), the recycled

effluent salinity load (explaining variance associated with the recycled effluent) and peak daily flow (explaining variance associated with the performance of the solids trap). Equation 8-25 below was thus fitted to observed data to produce a predictive model for the wastewater constituents listed in Table 8-13.

$$L_x = \alpha_0 + \alpha_1(W_f + W_{r,y}) + \alpha_2 W_{r,f} + \alpha_3(W_{r,f} EC_{r,f}/1000) + \alpha_4 PW_0 \quad (8-25)$$

where

L_x = daily load of constituent x (kg);

$\alpha_0, \dots, \alpha_5$ = regression coefficients;

W_f = fresh water used for hosing and cleaning (m^3);

$W_{r,y}$ = effluent pumped directly onto the holding yard (m^3);

$W_{r,f}$ = flood wash volume (m^3);

$EC_{r,f}$ = electrical conductivity of the recycled effluent used in the flood wash ($mS\ cm^{-1}$);

R_y = daily stormwater runoff from the holding yard entering the pond (no diverted) (m^3);

PW_0 = peak daily inflow ($L\ s^{-1}$);

Table 8-13 summarises the regression coefficients and statistics from each of the wastewater constituent models. Detailed model outputs including data plots of predictions and residuals are presented in Appendix L. Models were constructed using a stepwise process. Variables with t test p -values up to 0.05 were entered into the model, then in order to maximise the explanatory power of each model, only variables with p -values greater than 0.2 were removed. Improvement to the model was gauged by the change to adjusted R^2 – variables that did not increase the statistic were not retained. Peak flow and runoff volume were found not to add explanatory power to any of the models. Due to collinearity, the effluent salinity load ($W_{r,f} EC_{r,f}/1000$) and floodwash volume ($W_{r,f}$) tended to be mutually exclusive. All variables produced positive correlations with dependent variables except for $W_{r,f}$ in the DRP and TFSS models, which were also the weakest models in terms of predictive power.

The regression equations were used to provide a basis for estimating loads and then concentrations of each constituent on days between sampling events and outside the monitoring period. Where real conductivity data were not available, interpolated or average $EC_{r,f}$ values were inserted into the regression model, while synthesised data (section 8.7.1) were used in the absence of real flow data. All other sub-constituents were estimated from the observed or predicted constituent data according to the fractionations described in section 8.5.

8.8 SUMMARY

An approach to modelling an anaerobic pond treating DSE has been established through:

- selection of an appropriate biokinetic modelling platform;
- formulation of a reactor configuration that reflects the dominant mass transport pathways in the pond;
- devising a detailed characterisation of the influent to the pond, drawing from the data presented in Chapter 7 in combination with various published data and estimation methods;
- identification and specification of additional process models to complement the BioWin Activated Sludge/Anaerobic Digestion Model, including equations for hydrolysis of very slowly biodegradable COD, N and P and conversion of endogenous products to biodegradable material;
- preparation of a comprehensive data set to be used as dynamic inputs for model calibration and scenario simulations.

Table 8-13 Wastewater constituent linear regression model coefficients and statistics.

Wastewater constituent	Regression coefficients					Model statistics				
	α_0	α_1	α_2	α_4	α_6	R^2	Standard error of the estimate	F-test		Durbin-Watson test
								F	Significance	
COD	-56.081	3.290	2.968	NS	NS	0.73	44.274	33.00	0.000	1.63
FCOD	-19.658	1.393	0.666	NS	NS	0.80	9.587	48.76	0.000	1.13
TFSS	-4.678	0.131	-0.086	1.249	NS	0.68	4.532	16.17	0.000	2.04
Alkalinity	-12.974	1.079	0.634	NS	NS	0.87	6.443	76.99	0.000	1.16
TKN	-2.119	0.287	0.094	NS	NS	0.86	1.295	68.78	0.000	1.33
NH ₃ -N	-1.918	0.149	0.069	NS	NS	0.78	1.075	42.20	0.000	1.36
TP	-0.611	0.050	0.035	NS	NS	0.86	0.357	76.31	0.000	1.69
DRP	0.253	0.007	-0.012	0.055	NS	0.62	0.141	8.55	0.001	1.94
Ca ²⁺	-1.819	0.085	0.058	NS	NS	0.85	0.641	67.35	0.000	1.06
Mg ²⁺	-1.090	0.080	0.042	NS	NS	0.92	0.357	129.90	0.000	1.22
K ⁺	-1.303	0.380	0.184	NS	NS	0.84	2.238	61.37	0.000	1.42
Cl ⁻	-2.872	0.293	0.142	NS	NS	0.90	1.321	104.67	0.000	1.03

* NS = Not significant at the (initial) 95% confidence level.

The work has bridged a significant gap between the well-established, well-documented and complex field of activated sludge modelling, and the relatively poorly quantified field of DSE stabilisation pond performance and modelling. In doing so it has also revealed significant knowledge gaps in relation to DSE characterisation, particularly in terms of biodegradability and the different forms and fractions of N and P. The initialisation of the model described in this Chapter proceeds to model calibration, sensitivity analysis and application in the following chapter.

Chapter 9

ANAEROBIC POND MODEL CALIBRATION, SENSITIVITY ANALYSIS AND SCENARIO SIMULATIONS

Following on from the initialisation of the model of the anaerobic pond detailed in Chapter 8, this chapter details the process of and the outcomes from the calibration of the model against data collected in the field. Also presented is a sensitivity analysis that explores the relative influence of key model parameters on simulation outcomes, as well as the results from using the model to simulate a number of different operational scenarios for DSE anaerobic ponds. The outcomes of the modelling exercise are then reflected upon within the context of seeking to improve modelling, design and operation of DSE and other livestock waste stabilisation pond systems.

9.1 INTRODUCTION

The central concern in developing a dynamic model of the anaerobic pond was to attempt to account for all the physical, chemical and biological processes known to be influential to DSE stabilisation ponds performance. The BioWin simulation package provides a comprehensive suite of well-established biological and chemical process models as well as the ability to incorporate additional user-defined process models. However, inability to simulate hydrodynamics and other modes of mass transport in BioWin necessitated simplification and approximation for some physical processes, most notably sedimentation and transfer of constituents from the sludge to the supernatant via advection and diffusion. The refinement of the model described in sections 9.2.1 to 9.2.5, therefore, focused primarily on establishing sound rationale and identifying appropriate data to inform these aspects of the modelling.

It was resolved at the outset to avoid changing BioWin parameters to calibrate the model and to focus on adjusting parameters that were either added to the model either in the data-pre-processing stage (particularly influent characterisation and flow routing) or through the BioWin Model Builder. The process of arriving at final parameter values is described in section 9.2.6. The basis of the calibration was the sludge and effluent constituent concentration data reported in Chapter 7 and the pond pH data from Chapter 5. Model outputs are compared with these data in section 9.2.7. Quantification of the calibration error is presented in 9.2.7, while the calibrated model parameter values are given in section 9.2.8.

Models of this kind are often calibrated to one set of data and then validated against another. This can be done by dividing the data from the one site into calibration and validation sets, or by applying the model to data from a different site. However, on account of the nature of the data set that was collected from the one site and contained a broad suite of variables but a limited number of samples, the decision was made to calibrate the model to all the available data. Not being able to validate the model meant that sensitivity analysis was critical to understanding the limitations of the model. Described in 9.3, the sensitivity analysis examined the relative influence of model parameters that were either based on assumptions drawn from the literature, or were adjusted specifically to calibrate the model. The main concerns related to DSE pond performance are the ability to produce effluent of a quality suitable to its destination/use and the partitioning and forms of nutrients. As such, the measures of model sensitivity were based on COD and suspended solids removal efficiencies, COD, solids and nutrient loads in the sludge, and effluent nutrient loads divided into total and bioavailable fractions.

The same basis was used for evaluating the outputs from the scenario simulations described in section 9.4. These simulations were run to investigate the implications for pond performance of three design, construction and management scenarios that reflect desirable yet practical changes that could be made to the anaerobic pond. A fourth scenario considered the effect that ignoring the potential dead zone identified in Chapter 6 had on the model calibration.

Section 9.5 looks at the outcomes from the modelling in terms of

- the suitability of the adopted modelling approach,
- identifying means to improve modelling of DSE and other livestock waste stabilisation ponds,
- implications for best practice design and management of DSE systems, and
- the potential for building a dynamic model of a full DSE management system incorporating facultative pond, effluent recirculation and multiple effluent and sludge extraction points.

9.2 MODEL REFINEMENTS AND CALIBRATION

The creators of BioWin assert that adjustment of kinetic rate and stoichiometric constants should be avoided and focus placed upon properly characterising the influent wastewater. In addition, Alvarado et al. (2012) clearly stated that biokinetic models based on simplified pond hydraulics should not be optimised by manipulating biokinetic

parameters. As such, apart from adopting experimentally derived parameters specific to dairy shed waste reported in the literature, adjustment of kinetic parameters to improve the agreement between observed and predicted effluent quality was avoided. Indeed Houweling et al. (2008) calibrated a similar model of a facultative pond by adjusting the specific growth rate for nitrifying biomass, but acknowledged that the same effect could have been achieved by adjusting the active volume of the water column or the temperature dependency coefficient of the growth rate. With the exception of adjustments made to a parameter related to mass transfer of gaseous components (see section 9.2.1 below), the main alterations made to the initial model described in Chapter 8 were related to flow routing, dewatering unit solids separation efficiencies, the addition and refinement of new process equations, and the characterisation of the influent.

9.2.1 Controlling Gaseous Carbon Dioxide and Ammonia Losses

The only change made to an internal BioWin parameter, other than those identified in Chapter 8, was a necessary precursor to progressing the calibration using additional/external parameters. Using BioWin's default aeration and mass transfer parameters resulted in significant losses of carbon dioxide that caused the pH of the supernatant to rise above eight, which in turn resulted in excessive losses of gaseous ammonia via volatilisation. Data presented in Chapter 5 showed that despite the pH of the influent averaging around eight, pH in the anaerobic pond supernatant and sludge consistently remained around seven on account of production of VFAs and carbon dioxide from anaerobic digestion. The mass balance of N in the anaerobic pond (Chapter 7) suggested that ammonia losses were minimal. BioWin simulates gaseous losses using mass transfer equations with specific mass transfer coefficient for each of the main gases. It also uses a 'surface turbulence factor' (herein abbreviated to f_T) to scale losses according to the liquid surface conditions. The more turbulence expected at the surface from mechanic mixing or aeration the higher the factor.

Model outputs plotted in Figure 9-1 show that a preliminary² reduction in this factor from the default of 2 to 0.04 produced much better agreement between observed and predicted data for both supernatant pH and effluent ammonia. This better reflects the quiescent conditions at the pond surface as compared with the highly turbulent conditions that would occur in an activated sludge tank. Figure 9-1 also shows the reduction in gaseous CO₂ losses resulting from the parameter change. Note the drop in

² The factor was adjusted again later in the iterative calibration process.

ammonia-N concentrations in October-November 2005 are due to the cessation of outflow caused by desludging. The same effect is seen wherever effluent stops flowing in all the time series plots presented herein.

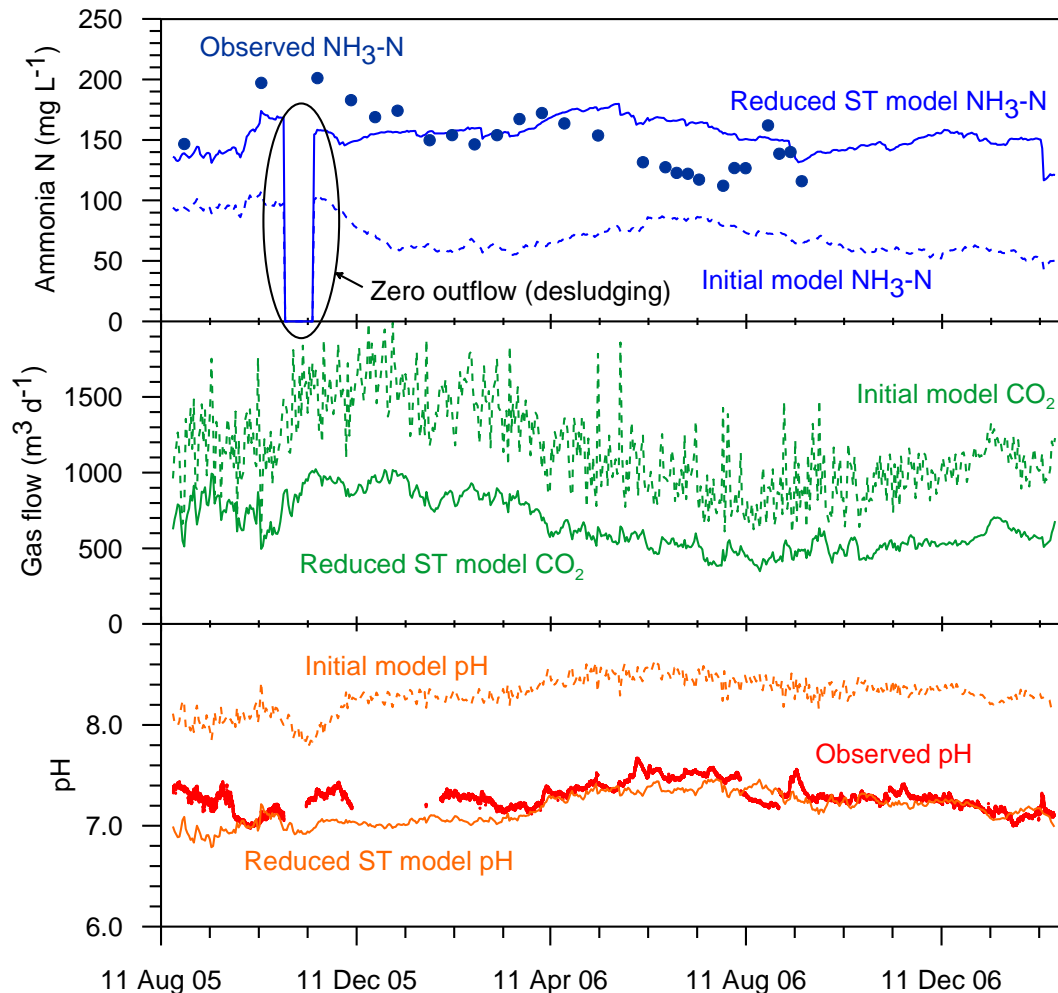


Figure 9-1 Predicted anaerobic pond supernatant pH, CO₂ gas and effluent NH₃-N levels plotted with corresponding observed data.

9.2.2 Settling and Sludge-Supernatant Flux

Sedimentation and the return of constituents from the sediments to the supernatant are critical processes in primary ponds with high solids loading. Sedimentation not only removes suspended material from the effluent but also creates the sludge blanket which effectively becomes an anaerobic digester. Sedimentation may be handled in a number of ways in BioWin, but in the absence of particle size and density data to inform the parameters of a settler model, a mass partitioning approach using point separation was a necessary simplification. Exchanges between the sludge and the supernatant caused by diffusion, rising biogas bubbles and re-suspension of sediments, however, are not readily accommodated in BioWin. The dynamic

settler/clarifier models in BioWin are capable of simulating sludge compaction and re-suspension of solids related to excessively high sludge levels. Being 1-dimensional, however, they can at best only approximate the variability associated with the irregular shape of the pond. Neither can they simulate diffusion and biogas-induced dispersion of soluble sludge constituents into the supernatant. Settling and sludge-supernatant flux were therefore handled using three components:

- partitioning of solids from the influent to the sludge using a dewatering unit (A in Figure 8-1 in Chapter 8) to simulate initial settling of coarse material;
- transfer of soluble sludge constituents to the supernatant through a flow connection regulated by a second dewatering element (unit B in Figure 8-1);
- a return flow from the supernatant to the sludge to make up liquid losses from sludge-supernatant transfers.

The primary (influent) dewatering unit was designed to simulate the rapid settling rate of the coarse influent settleable solids and was assigned a constant removal efficiency of 72% through obtaining alignment between observed and predicted TSS concentrations (after desludging). The second unit provided control over the load of particulate material returned to the supernatant and was operated at 100% efficiency except at high sludge levels (see below). Under the assumption that biogas-induced advection dominates over diffusion-driven mass transport, the rate of flux between sludge and supernatant was defined as a linear function of biogas flow.

$$SE = f_s Q_{biogas} \quad (1.2)$$

where

SE = sludge-supernatant flux ($\text{m}^3 \text{d}^{-1}$);

f_s = sludge-supernatant flux coefficient ($\text{m}^3 \text{filtrate m}^{-3} \text{biogas}$);

Q_{biogas} = volumetric biogas production ($\text{m}^3 \text{d}^{-1}$).

This approach is similar to that taken by Houweling et al. (2008) in linking sludge-supernatant flux in an aerated pond to the rate of air flow. The temperature-adjusted biogas flow rate was estimated in data pre-processing as per the method employed to estimate mechanical power exerted by rising biogas described in Chapter 6. This is likely to be an over-estimation of biogas originating from the sludge as it is based on total VS destruction. Accordingly the flux coefficient is specific to the input biogas flow data and effectively acts as a scaling factor that would need to be readjusted if applied

to a pond system with differing influent characteristics or VS destruction. Ideally the sludge-supernatant flux would be tied to the sludge biogas flow rate calculated internally by BioWin, making the flux coefficient more generalisable. However this requires the use of the BioWin Controller module which was not available to this project³.

The arrangement of dewatering units and circulating flows described above required the fitting of two key parameters – the removal efficiency of the primary dewatering unit and the sludge-supernatant flux coefficient. Two additional parameters were required to simulate the declining performance of the pond caused by excessive sludge levels as described below.

9.2.2.1 Declining settling performance

Operating the second dewatering unit at 100% efficiency assumes that all particulate material re-suspended by biogas resettles before reaching the outlet. In reality this will not be the case as some fraction of sediments re-suspended close to the outlet will inevitably leave the pond. Effectively the assumption of complete resettling transfers the control of actual reduction in settling efficiency related to re-suspension to the first dewatering unit. Under quasi-steady state conditions when the pond has low to moderate sludge build-up, this arrangement is satisfactory. However effluent suspended solids concentrations were observed to increase once the sludge rose to within 1.2 m of the liquid surface (equivalent to 3.6 m depth over the deepest point in the pond and about 70 cm below the outlet pipe intake) and occupied about 52% of the pond. The rise was arrested when the pond was desludged, after which TSS dropped back to relatively stable concentrations. Evidently as sludge edged closer to the liquid surface, settled solids were increasingly being re-entrained into the water column near the outlet and/or the incidence of short-circuiting was becoming more frequent. Judging, however, by the observed particle sizes of the suspended material, the former option was more likely.

To account for the increasing entrainment of settled material, a simple declining linear trend was applied to the solids partitioning factor of the recycle route dewatering unit as shown in Figure 9-2. The parameters of the linear function are given in Table 9-3. It is believed that the reduction in performance would more likely follow some form of exponential decline similar to the idealised curve plotted on the same graph, but for the

³ The specialised evaporator unit developed for this model caused the BioWin simulation environment to be incompatible with the standard Controller module.

purposes of this modeling the trajectory to complete failure did not need to be accurately defined. Nonetheless, the effect of the slope of the linear model was tested in the sensitivity analysis below.

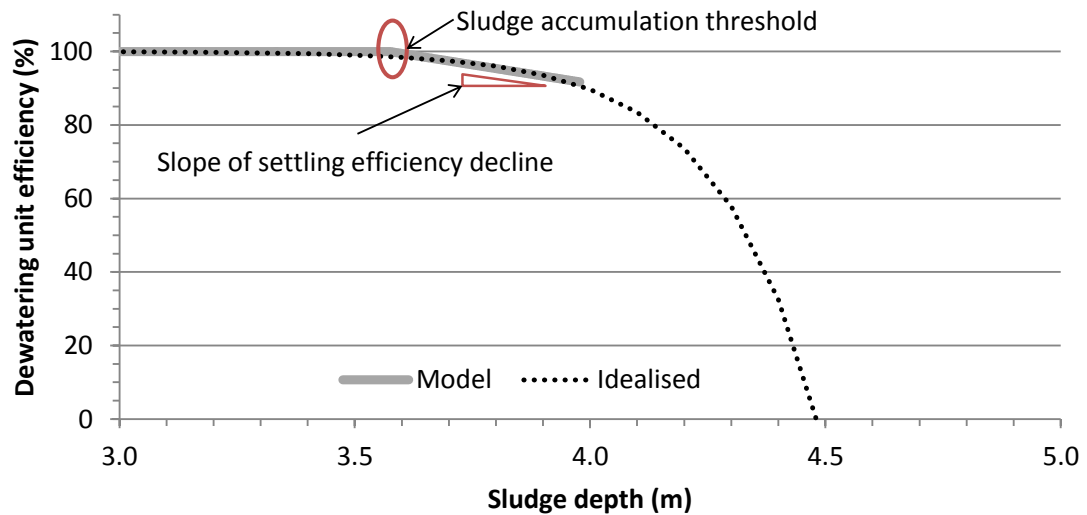


Figure 9-2 Model and idealised sludge dewatering unit solids removal efficiency curves.

9.2.2.2 Accumulation of acetate

Simulations run at low seepage rates revealed that acetic acid accumulated in the sludge reactor when flow exchanges between the sludge and supernatant were also low. Where f_s was set below 0.075, acetic acid concentrations exceeding $10,000 \text{ mg L}^{-1}$ would cause the pH to drop below 4.3. The high acetic acid concentration and the low pH both caused inhibition growth of heterotrophic organisms, which in turn impaired the hydrolysis of particulate COD in the sludge and drastically reduced the production of biogas to well below the production rate estimated in Chapter 6. Published data on sludge pH in DSE ponds indicate that sludge pH tends to neutral across a range of loading and seepage rates (see Cameron et al. 1996; Zaman et al. 1998; Mukhtar et al. 2004; Ullman & Mukhtar 2007; Ward & Jacobs 2008b; Ward & Jacobs 2008a). This would suggest that transfers of acetic acid from the sludge to the supernatant (and also losses to seepage) are an important feature of DSE anaerobic ponds.

Figure 9-3 plots the number of days from commencement of operation that pH remained inhibitory to biological growth⁴ in the digester reactor at different sludge-supernatant fluxes under conditions of negligible seepage. The time required for pH to reach non-inhibitory levels increases exponentially at f_s values below 0.15. Below $f_s =$

⁴ Defined as reducing the growth rate by 50%.

0.09 the sludge never recovers from becoming acidic. However, while exchange coefficients above 0.15 appeared to have little bearing on effluent COD concentrations, they do result in the transfer of excessive soluble P and N loads to the supernatant. These constraints provided boundaries for the fitting process.

Further guidance in identifying an appropriate rate of sludge-supernatant flux was sought from the literature. In tying sludge-supernatant flux to aeration air-flow rates, Houweling et al. (2008) simulated fluxes of up to $2.4 \times 10^{-3} \text{ m}^3 \text{ d}^{-1}$ per m^3 pond volume. Applying this figure to the anaerobic pond volume translates to a flux of $3.1 \text{ m}^3 \text{ d}^{-1}$. This corresponds to a value of $0.1 \text{ m}^3 \text{ m}^{-3}$ for f_s at average biogas flow, which sits at the low end of the feasible range identified in Figure 9-3.

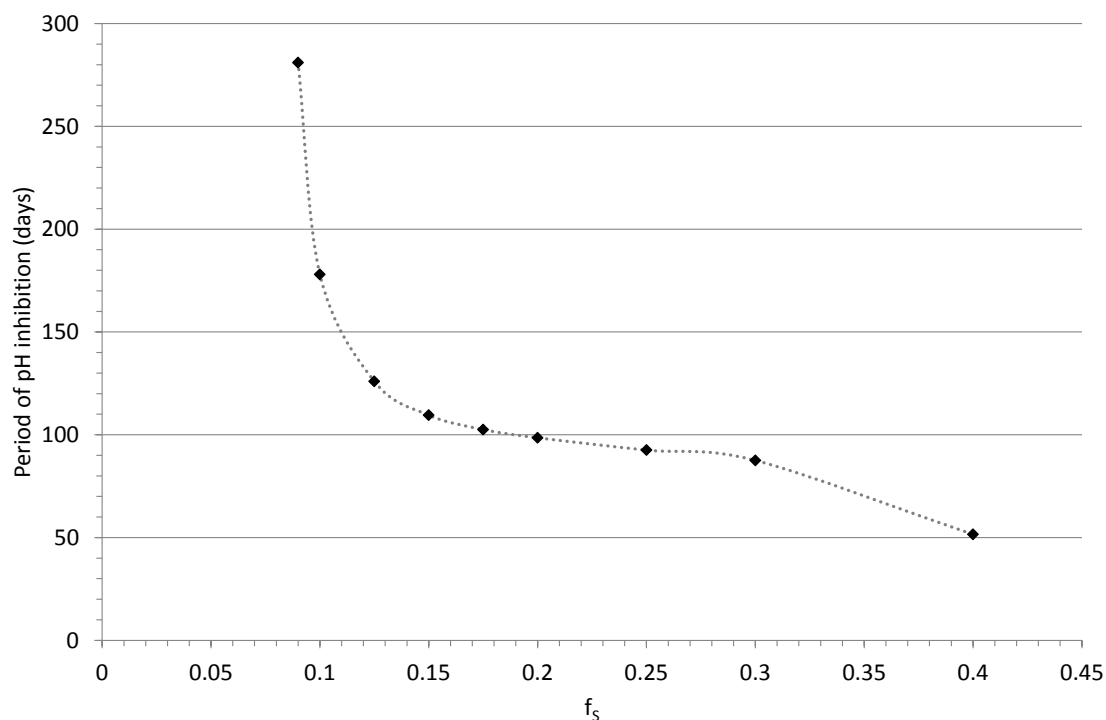


Figure 9-3 Number of days anaerobic digestion in the sludge is inhibited by low pH plotted against the sludge-supernatant exchange areal flux rate f_s .

9.2.3 Hydrolysis of Very Slowly Biodegradable Material

Taking the harmonic mean of the kinetic parameters derived by Myint, Nirmalakhandan & Speece. (2007) for use in the lumped process model of hydrolysis of cellulosic material assumed a certain division between hemicellulose and cellulose in the influent organic material. Early simulations of sludge solids and COD concentrations revealed that the initial values for the maximum specific hydrolysis rate and the half saturation coefficient were too low. In other words, the harmonic mean weighted the parameters too heavily towards the slower-degrading cellulose. The parameters were therefore

adjusted by weighting the harmonic mean more towards hemicellulose. Figure 9-4 shows that using weighted harmonic means ensured that the model curve retained a shape similar to that of the curves derived by Myint, Nirmalakhandan & Speece (2007) and remained within the envelope demarked by the cellulose and hemicellulose curves.

Note that the influence of the Arrhenius temperature adjustment coefficient (θ) was also explored, but it was found that even removing the temperature dependence altogether by assigning θ to unity could not make up the differences between observed and predicted sludge COD and TVSS produced by the initial kinetic parameters. Hence it was assumed that the temperature dependency function held true, leaving the kinetic parameters subject to refinement.

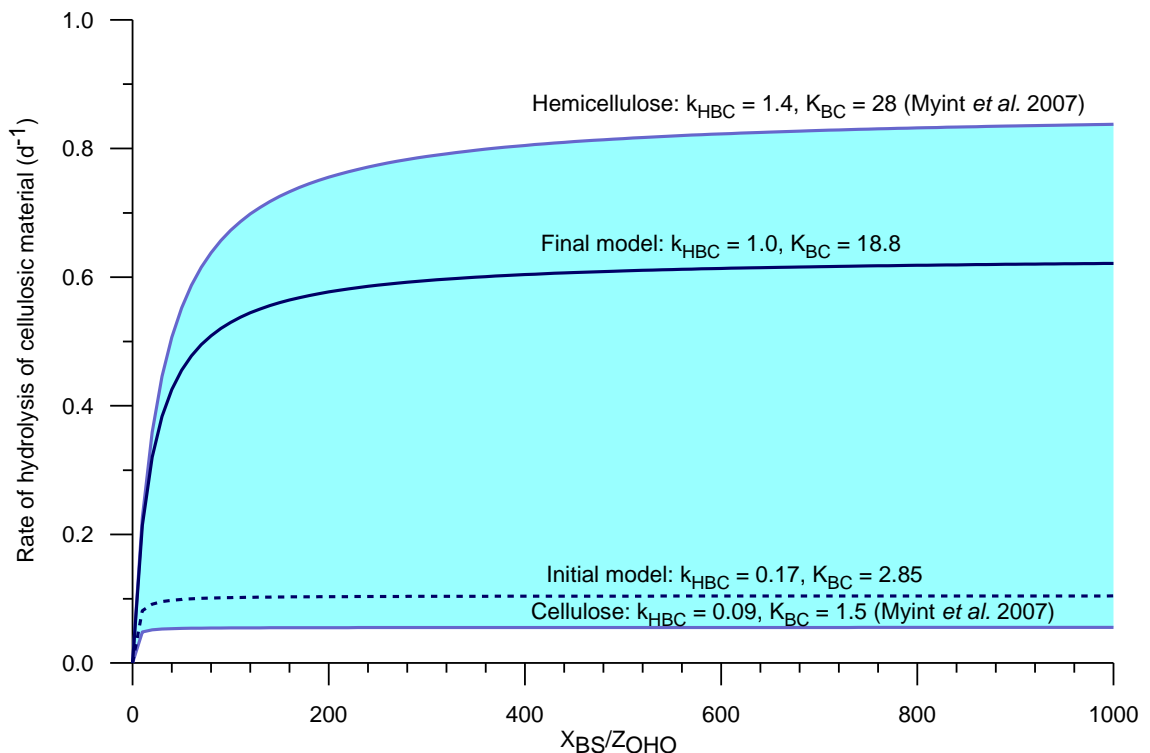


Figure 9-4 Process model curves for hydrolysis of cellulosic material.

9.2.3.1 Release of soluble calcium and magnesium

While sludge concentrations of Na and K were similar to effluent concentrations, total Ca and Mg concentrations in the sludge were significantly higher than effluent levels, indicating the presence of large pools of particulate forms of the cations, either complexed with the organic material or in precipitate form. Initial simulation runs produced predictions of effluent Ca^{2+} and Mg^{2+} that were consistently lower than observed concentrations, which agreed with the indications from the mass balance for

the pond (Chapter 7) that both cations were being generated in the pond. Accordingly, two stoichiometric parameters were added to the hydrolysis of X_{BC} that enabled the process to yield soluble (ionic) Ca and Mg. The parameters were defined in the same manner as the fractions of inert N and P using the ratio of sludge Ca and Mg to sludge COD:

$$f_{XICa} = \varepsilon_X \cdot \frac{Ca_{sludge} - Ca^{2+}_{effluent}}{COD_{sludge}} = 0.021 \quad (1.3)$$

$$f_{XIMg} = \varepsilon_X \cdot \frac{Mg_{sludge} - Mg^{2+}_{effluent}}{COD_{sludge}} = 0.005 \quad (1.4)$$

where

f_{XICa} = Ca fraction of particulate non-biodegradable and very slowly degradable COD;

f_{XIMg} = Mg fraction of particulate non-biodegradable and very slowly degradable COD;

ε_X = particulate COD destruction in the pond (fraction).

9.2.4 Organic Nitrogen Fractionation

Low predictions of effluent TKN suggested that either the initial fractionation of organic N was resulting in too much N being partitioned to the sludge or mineralised to ammonium. Improvements made to effluent TKN predictions by adjusting the fraction of particulate non-biodegradable N were countered by poorer sludge TN predictions. Moreover the long retention time of the pond caused complete mineralisation of incoming biodegradable organic N, suggesting that the problem lay with the influent fraction of mineralisable N. Increasing fraction of soluble non-biodegradable N (f_{NUS}) from 0.2 to 1.0 slightly reduced effluent ammonia-N concentrations and increased effluent TKN predictions, which improved overall relative error of both. The implications of assigning all soluble organic N to the non-biodegradable fraction are discussed in section 9.5.

9.2.5 Non-Settleable Particulate P

Of all the constituents tracked in the simulations, P exhibited the poorest agreement between observed and predicted concentrations under the initial fractionation and model specification. Figure 9-5 shows that predicted effluent TP concentrations were

around 35% below observed levels while predicted sludge concentrations were some 65% too high. Evidently too much P was being partitioned to the sludge by the dewatering units, indicating that the settleable fractions of COD and P were not proportional. The problem could not be resolved using the existing BioWin P fractionation, which only provided for varying the biodegradable and non-biodegradable fractions of settleable particulate P. Moreover, dissolved P averaged less than 40% of total P and more than 80% of this soluble fraction was inorganic (DRP) (Chapter 7), which suggests that P was more concentrated in the remaining suspended (poorly settleable) particulate material than in the pond sediments.

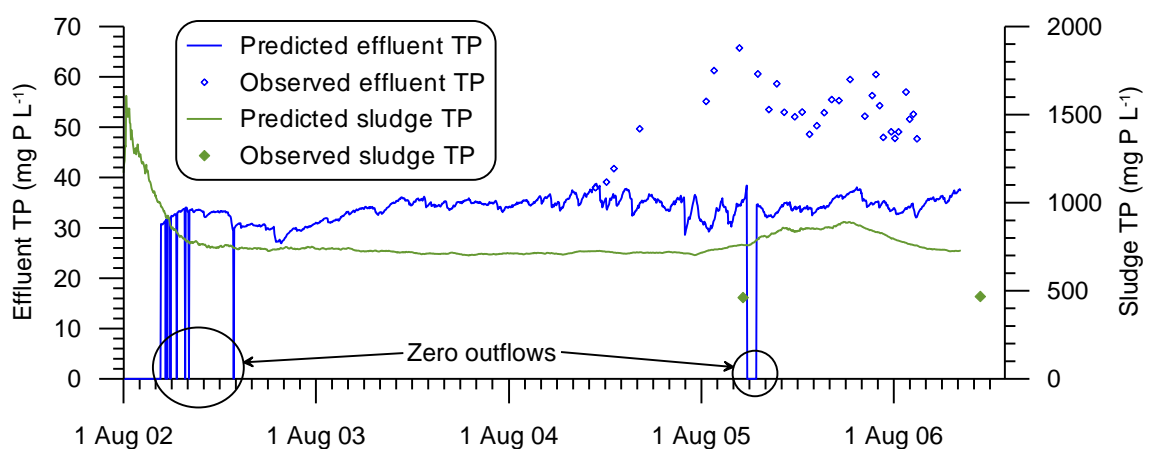


Figure 9-5 Observed and predicted total P concentrations from a simulation run based on the conventional BioWin P fractionation. Note again the zero concentrations resulting from zero outflow.

Similar observations were made by Meyer et al. (2007) who found that 87% of total dairy (lactating cow) manure P was contained in the 40% of faecal solids (35% of total solids) that were less than 125 μm in size. Another 9% of manure P was held in the coarsest particulate fraction measured ($>2000 \mu\text{m}$), while the remaining 4-5% was evenly distributed amongst the particle sizes in between. Meyer et al. (2007) did not analyse the soluble fraction of manure P but did find that close to 100% of P was associated with faecal material (as opposed to urine). Van Horn et al. (1994) and Eghball et al. (2002) also reported faecal P making up more than 90% of total manure P.

P in manure originates from undigested feed, animal metabolites or associated microflora (He & Honeycutt 2011). Most P in dairy manure is in mineral form, in part due to the presence of the enzyme phytase in the rumen that can hydrolyse organic ingested phytate P. Data on the total organic P in manure vary, but reported concentrations are consistently well below 50%. Some 20-40% of TP in dairy manure is

water extractable (Dao et al. 2006; Toth, Dou & He 2011), which appears to be reflected in the observed influent TDP and DRP concentrations. The small differences between DRP and TDP in the influent reflect the low soluble organic P content of dairy manure, which typically constitutes as little as 5% of TP (Hjorth et al. 2010). Much of the balance of total and soluble organic P would likely constitute the particulate organic P that is settling out in the pond.

A large fraction of manure P may be classified as labile adsorbed P, comprising (mostly) inorganic as well as organic forms of P that are loosely bound to particulate material. Using EDTA as an extractant in a P fractionation procedure, Dao et al. (2006) found that around 15% of dairy manure P was derived from insoluble Ca and Mg phosphates complexed with organic matter in manure. The EDTA effected ligand exchange by taking the place of phosphate anion in cation-phosphate pairs complexed on manure particles. Similarly, Zhang et al. (2010) found that sequestering Ca from 'calcium-phosphorus solids' in anaerobically digested dairy manure with an EDTA chelating agent released 91% of total P and 93% total Ca into solution.

Extraction with EDTA or other organic ligands also increases recovery of phytate P, which has been linked to the presence of complexed Ca and Mg forms of the phosphomonoester (Dao 2004; Dao et al. 2006). Phytate P is the dominant form of organic P found in dairy manure and has a high affinity to polyvalent cations. Together they can form insoluble, colloidal complexes with organic matter that inhibit precipitation of inorganic phosphates and are resistant to enzymatic hydrolysis, particularly at pH above 8 (Dao 2003; Dao 2004). Toor et al. (2005) found that reductions in phytate from feed to faeces to manure indicated the effects of hydrolysis occurring in the rumen and then in manure storage, and attributed the resistance to hydrolysis of the remaining phytate in stored manure to complexation with polyvalent cations. While not classified as such, the 'poorly soluble' inorganic and organic P that was largely associated with Ca and Mg P and extractable with NaOH-EDTA solution reported by Turner & Leytem (2004) is also likely to have been complexed forms of P released by ligand exchange with the EDTA.

Preliminary analyses of raw and treated DSE samples indicated that the majority of particulate P was acid-hydrolysable, which would indicate that tightly organically bound P makes up only a small portion of the insoluble P fraction and is likely to correspond to the poorly biodegradable P fraction f_{XIP} defined in Chapter 8. Total reactive phosphate analysis of the same samples indicated that only a small fraction of non-filterable P was readily solubilised. The non-reactive, hydrolysable P fraction that is similar in size to the

apparently non-settleable fraction in the influent could well be (soluble) phosphate and phytate complexed with organic particulate matter. Its poor settleability may be related to smaller organic matter particles having a greater propensity for P complexation on account of having greater surface area per unit mass, which would also help explain the disproportionate concentration of P in small particles observed by Meyer et al. (2007).

The true nature of this non-settleable particulate bound P cannot be determined without further research. For the immediate purposes of this modelling, a new P fraction was defined in BioWin with a user-defined state variable (*UD1*) that is not prone to settling. The concentration of influent *UD1* was calculated as a fraction of the remaining P after accounting for orthophosphate (as *DRP*) and particulate very slowly biodegradable and non-biodegradable P.

$$UD1 = f_{NSP}(TP - DRP - X_{IP}) \quad (1.5)$$

In the absence of an understanding of this P fraction, no process equations that act on *UD1* were defined in the model. However, if the fraction was to be confirmed to be complexed P, some form of isotherm equation similar to those used to describe P sorption equilibria could be used to describe complexation with particulate COD. If the fraction is simply organically bound P, some form of hydrolysis equation should be added to simulate its conversion to orthophosphate. Consideration should also be given to whether this fraction should in fact be prone to some degree of settling, particularly in a secondary pond. This could be achieved using a process equation that converts it to one of the existing particulate forms of P.

9.2.6 Calibration Process

Calibrating the model was an iterative process involving preliminary trial-and-error simulation runs to identify appropriate ranges for the key parameters described above, followed by systematically making incremental adjustments to parameters within those ranges and re-running simulations to determine the optimum values. The process was guided by comparison of observed and predicted effluent and sludge constituent concentrations through examination of the error terms and mean absolute percentage errors as well as visual inspection of time series plots. Since parameter adjustments often resulted in improvement in the predictions of one constituent and poorer predictions of another, the ultimate selection of parameter values was based on judgment rather than a unifying quantitative error measure. The process was expansive in its exploration of parameter specifications, but it was not exhaustive in determining

optimum values on account of the time required to run a simulation (typically around 1.5 hours for the final model configuration). Thus while parameter values adopted in the calibration are believed to be close to their optimum, a slightly different combination may produce a better overall result than that reported here.

9.2.7 Model Outputs

9.2.7.1 Effluent quality

Figure 9-6 and Figure 9-7 plot observed and predicted effluent concentrations for the key constituents monitored in the wastewater sampling. The full output data from BioWin that the plots are drawn from are presented in Appendix L. Note that soluble orthophosphate predictions from BioWin were assumed to correspond to (observed) DRP concentrations from wastewater analysis. The plots show that reasonable agreement between observed and predicted data in terms of magnitude was achieved for all parameters. The model is also dynamically responsive, producing reasonable predictions of temporal shifts and trends in concentrations for most parameters.

Figure 9-6 shows that the model produces reasonable predictions of COD, TVSS and TSS concentrations in the lead-up to and in the months following desludging, although predicted TSS concentrations do not rise as rapidly as they should suggesting that the ratio of fixed to volatile solids in the sludge-supernatant flux is too low. The model fails, however, to predict the gradual rise in total COD and TVSS between June and September 2006. The cause of the observed rise is not clear. However, consistently low influent COD concentrations observed over this period appear to have exerted excessive leverage on the regression model used to predict influent COD (see Chapter 8), which resulted in the particulate organic loading to the pond over the period to be lower than it should have been.

Predictions of FCOD are also reasonably close to observed values, including when sludge encroachment was undermining the performance of the pond, but are generally 10% too high. Simulations run at the default (higher) OHO growth rate or a lower half saturation constant did not improve the result. Lowering the OHO decay rate did not have significant impact, and neither did lowering the sludge-supernatant flux coefficient. Results from sensitivity analysis (see section 9.3 below) indicated that the problem actually lies with the estimation method for non-biodegradable soluble COD. It would appear that despite the extended HRT and partially aerobic treatment of the facultative pond, treated effluent still contains a sizeable fraction of biodegradable

soluble COD. Experimental laboratory work is required to more accurately characterise soluble COD in DSE.

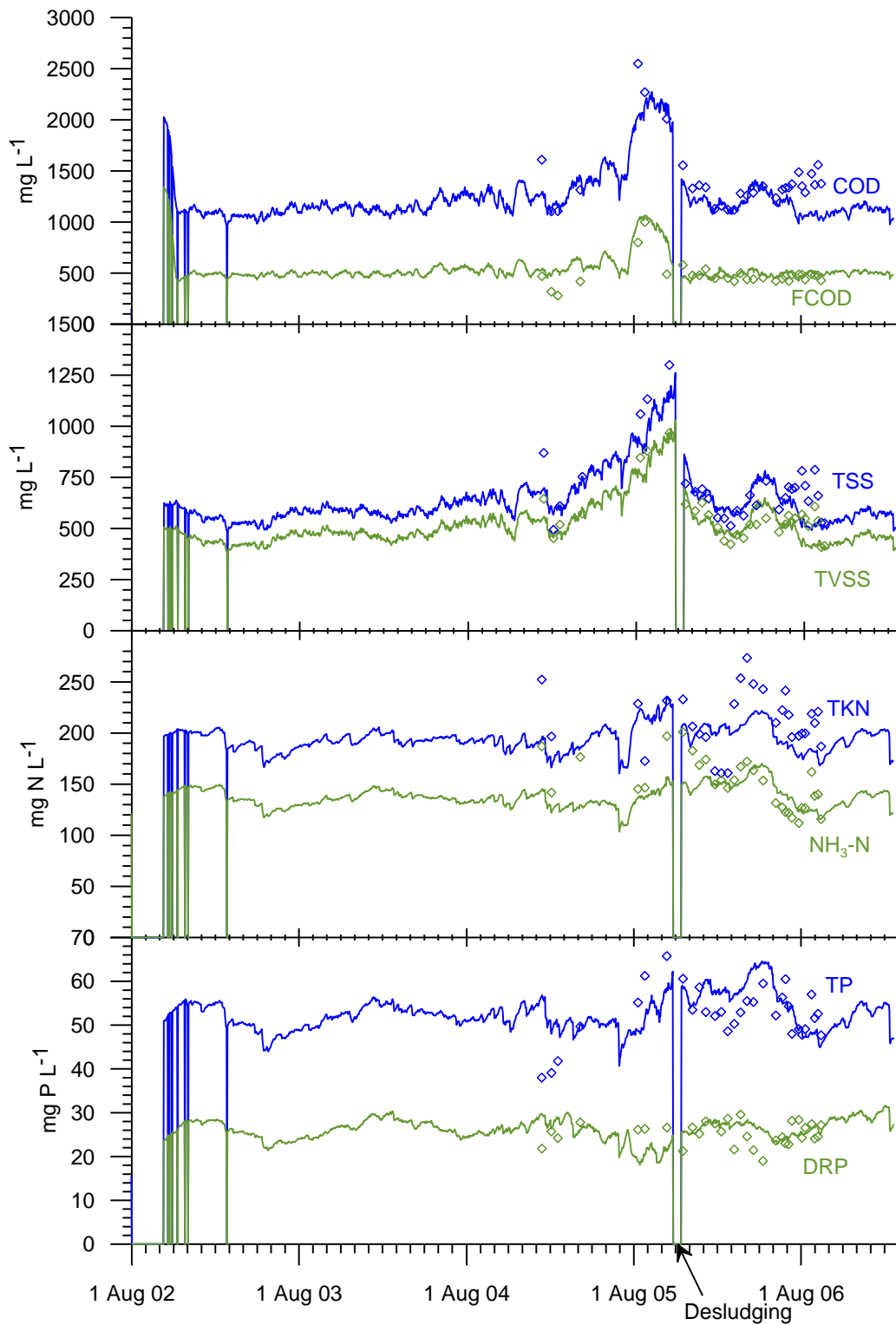


Figure 9-6 Predicted and observed anaerobic pond effluent COD and FCOD (top), TSS and TVSS (upper middle), TKN and NH₃-N (lower middle), and TP and DRP concentrations (bottom). Predicted data are represented by lines while discrete points represent observed data. Each is colour coded in accordance with their corresponding labels.

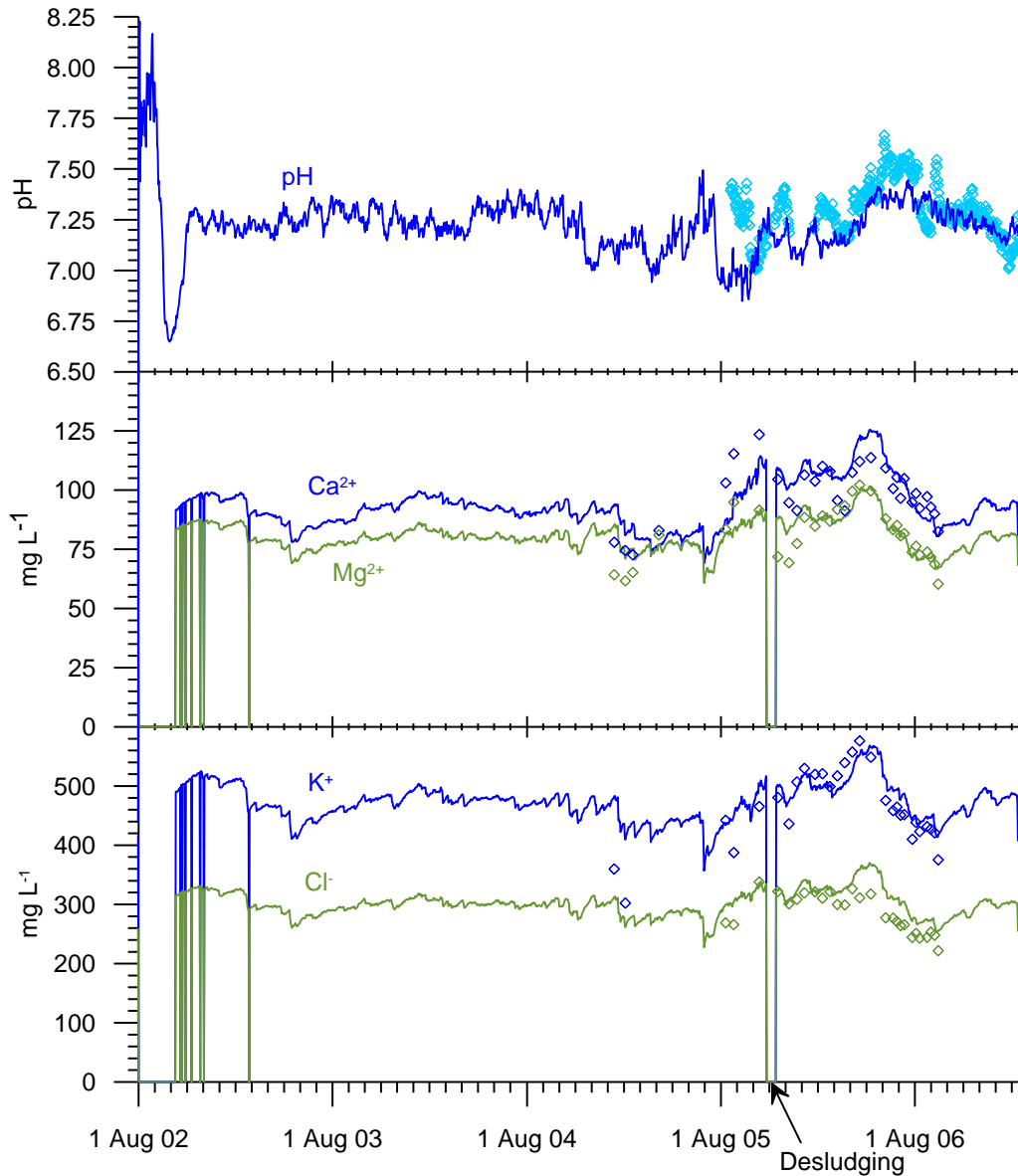


Figure 9-7 Predicted and observed anaerobic pond supernatant pH (top) and effluent Ca^{2+} and Mg^{2+} (middle), and K^{+} and Cl^{-} (bottom) concentrations. Predicted data are represented by lines while diamond points represent observed data. Each is colour coded in accordance with their corresponding labels, except for observed pH data which have been coloured light blue for visibility.

Effluent TKN predictions (Figure 9-6) are perhaps the least convincing of all the model outputs. The model seems to pick up the approximate trends in the observed data, but the predicted concentrations are consistently low. The same problem afflicts the sludge TN concentrations, suggesting that the organic N loading to the model is low. This reflects similar observations made in formulating the mass balance for N in the pond (Chapter 7). Ammonia-N predictions (Figure 9-6) are reasonably good after desludging, but the model fails to predict the rise and fall in ammonia N caused by high sludge levels and subsequent desludging. That effluent DRP (orthophosphate) concentrations

do not exhibit the same response to sludge levels suggests that there is some relationship between re-suspended particulate matter and ammonia that the model does not reproduce. The fluctuations in predicted total P largely follow observed movements, while predicted DRP steadily sits around 25 mg L^{-1} in the same manner as the observed data.

Strong agreement between predicted and observed pH levels (Figure 9-7) indicates that the surface turbulence and sludge-supernatant flux coefficients are appropriately balanced. Predictions of effluent cation concentrations are also strong (Figure 9-7). This is to be expected for K and Na since they are untouched by any process models. Ca^{2+} and Mg^{2+} , however, are prone to spontaneous chemical precipitation reactions as well as receiving contributions from hydrolysis of sludge. Predicted concentrations were negligible for all modeled precipitates but struvite, which was produced in the supernatant for a brief period over the winter of 2006. Thus it is inferred that the yields of Ca^{2+} and Mg^{2+} from hydrolysis of cellulosic material may be considered reasonable augmentations to the model, confirming the finding of the mass balance in Chapter 7 that the cations are indeed being liberated from the sludge.

Error measures for the model predictions including the root-mean-square error (RMSE), the coefficient of variation of the RMSE (CV (RMSE)) and the mean absolute percentage error (MAPE) are presented in Table 9-1. Values for CV (RMSE) were mostly around 0.1-0.15 indicating that model predictions of effluent quality are reasonably robust. Similarly, MAPEs were generally less than 15%. FCOD predictions exhibited the highest relative error when considering all data points. The MAPE and CV (RMSE) reduce to less than 9% and 0.11, respectively, when the errors associated with the unusually low FCOD concentrations recorded in early 2005 and the exaggerated errors of the pre-desludging period are excluded from the calculations.

9.2.7.2 Sludge characteristics

Figure 9-8 plots predicted and observed sludge concentrations for COD, TVSS, TP, TN and pH. Predicted sludge pH levels were slightly lower than observed; however this is likely due to pH measurements being made only at the surface of the sludge where a diffusion-related concentration gradient is likely to exist for soluble constituents including hydronium and VFAs. The five other constituent curves all exhibit the same pattern of a steep decline in constituent concentrations in the first four or so months followed by a more gentle decline until the disruption caused by desludging. The initial decline is caused by the more rapid hydrolysis of conventionally slowly biodegradable particulate COD and organic N and P and hydrolysis of cellulosic material associated

with an initial bloom of OHOs. As the OHO population stabilises, the rate of hydrolysis slows to the steady rate dictated by the poor degradability and relatively low temperature (compared with mesophilic digesters) of the sludge.

Table 9-1 Error measures for the model predictions of effluent quality.

<i>Constituent</i>	<i>n</i>	<i>RMSE</i>	<i>CV (RMSE)</i>	<i>MAPE</i>
COD	31	227	0.16	11
FCOD	31	107	0.22	16
TVSS	31	71	0.13	9
TSS	31	111	0.16	11
TN	29	33	0.15	14
NH ₃ -N	30	22	0.15	11
TP	31	6.5	0.12	10
DRP	31	3.6	0.14	12
Ca ²⁺	31	8.6	0.09	7
Mg ²⁺	31	7.2	0.09	7
K ⁺	29	40	0.09	7
Cl ⁻	27	28	0.10	9
pH	485	0.15	0.02	2

The long-term average concentrations represented by the observed data are well-matched by the model predictions for all constituents except TSS concentrations, which are dramatically under-predicted. This is related to the imbalance of fixed solids identified in Chapter 7, and confirms that the loading of TFSS to the pond is simply not sufficient to produce the apparent sludge TFS loads. Fixed solids are unaffected by the model since predicted precipitation in the pond is minimal, hence there is no question that the issue is related to the input data rather than the model itself. The implications of the data discrepancy for the model calibration lie with the kinetic parameters for the hydrolysis of very slowly biodegradable material and the sludge-supernatant flux coefficient. If the error extends to TVS, then the fitted hydrolysis rate would be inaccurate, causing f_s to also be inaccurate since it is related to the transfer of volatile solids breakdown products. Based on the mass balance figures for TVS given in Chapter 7 and the results of the sensitivity analysis of the hydrolysis parameters presented in section 9.3, it is estimated that the reduction in the hydrolysis parameters would be 20% at most and the associated reduction in f_s would be even less. If the problem is in fact confined to TFS data as is likely the case (see Chapter 7), then the consequence of the discrepancy is immaterial to the model.

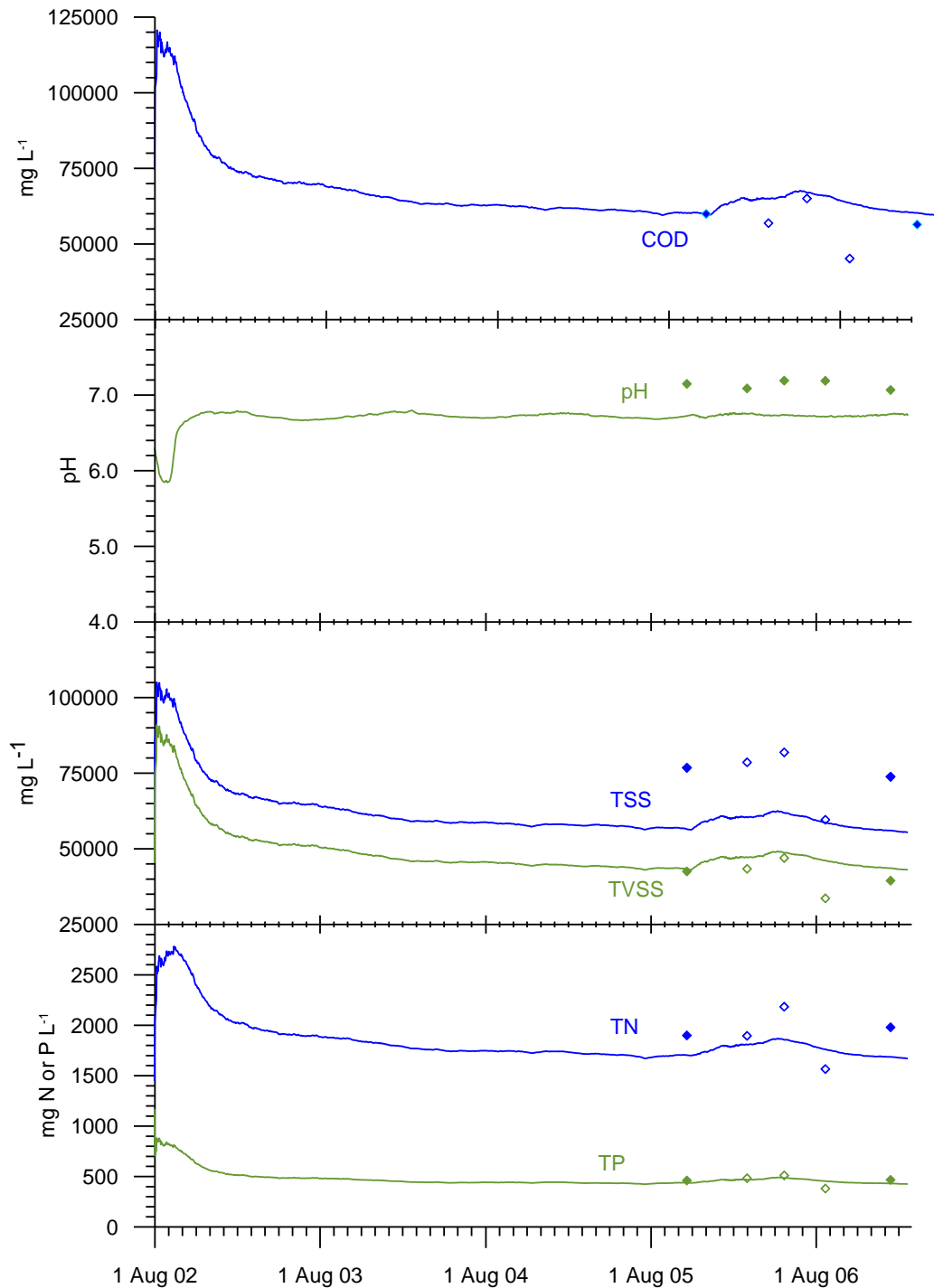


Figure 9-8 Predicted and observed anaerobic pond sludge COD (top), pH (upper middle), TSS and TVSS (lower middle), TN and TP (bottom) concentrations. Predicted data are represented by lines while diamond points represent observed data. Each are colour coded in accordance with their corresponding labels.

Note that the three middle ‘observed’ data points (1 March, 22 May and 21 August 2006) in each plot (denoted by their lack of fill) have been adjusted to account for the bulking of the sludge material caused by desludging (refer to Chapter 6). As such these points have been included for comparative purposes only and were not used in the

error calculations described in the following section. Importantly, however, there is reasonable agreement between these data points, the reliable observed data points and the predicted data. The prediction errors for sludge constituent concentrations are presented in Table 9-2. Predictions of four of the six constituents produced MAPEs of less than 10% and similarly small CV (RMSE) values. The large error associated with TSS is related to the issue with fixed solids mentioned above. The errors reported for TN predictions are also related to an imbalance in the observed data identified through the mass balance presented in Chapter 7.

Table 9-2 Error measures for the model predictions of sludge composition.

<i>Constituent</i>	<i>n</i>	<i>RMSE</i>	<i>CV (RMSE)</i>	<i>MAPE</i>
COD	2	1958	0.03	3
TVSS	2	2426	0.06	6
TSS	2	19050	0.25	25
TN	2	245	0.13	13
TP	2	10.3	0.02	2
pH	5	0.40	0.06	6

9.2.7.3 Biogas production

One particular benefit that this calibrated model provides is the ability to gauge emissions of methane (CH_4) and carbon dioxide (CO_2) from the pond. Figure 9-9 plots predicted biogas production and composition over time, which exhibits notable day-to-day variability and strong seasonality. The simulation reveals that while methane production is greatest in the sludge, similar quantities are produced in the supernatant, presumably because a large fraction of long chain fatty acids and VFAs produced from hydrolysis of the sludge is transferred to the supernatant where they are broken down together with influent biodegradable soluble COD. Simulated average methane production from the sludge and supernatant combined was $26.8 \text{ m}^3 \text{ d}^{-1}$, which is higher than the estimate based on COD conversion of $22.5 \text{ m}^3 \text{ d}^{-1}$ presented in Chapter 4 most likely due to the estimate for COD conversion being biased by the greater number of samples taken in winter and due to the fact that the estimate was based on a conservative (low temperature) conversion factor (Metcalf & Eddy et al. 2003). Volumetric methane production was $0.02 \text{ m}^3 \text{ m}^{-3} \text{ d}^{-1}$, which is twice that observed by Craggs et al. (2008) due to the volumetric loading rate being proportionally higher (0.083 compared with $0.046 \text{ kg VS m}^{-3} \text{ d}^{-1}$ based on total pond volume). In terms of COD added, methane yield was $0.17 \text{ m}^3 \text{ kg}^{-1} \text{ COD d}^{-1}$, or on a per cow basis 32.7 m^3

cow⁻¹ yr⁻¹. Total biogas production is higher in the supernatant than the sludge due to generation of greater volumes of CO₂. Also worth noting is the impact on biogas production of the October 2005 desludging event. Biogas production in the sludge dropped dramatically, but recovered within 2 months while supernatant production was largely unaffected.

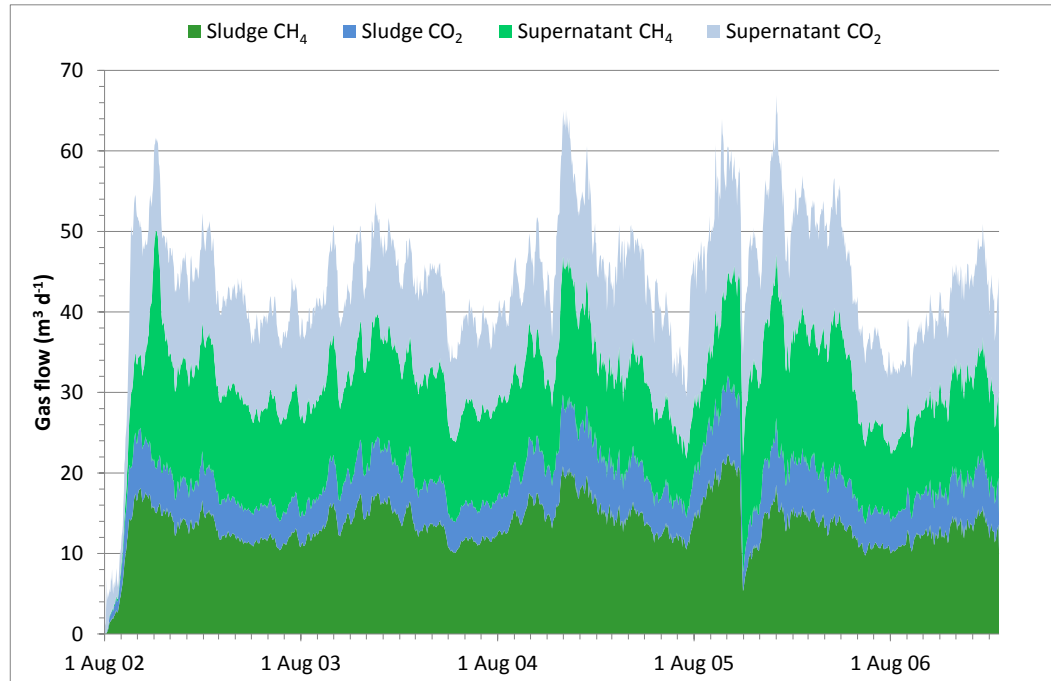


Figure 9-9 Predicted biogas emissions from the sludge and supernatant.

9.2.8 Final Model Parameter Values

Table 9-3 summarises the values adopted in the calibrated model for parameters related to pond hydraulics, influent characterisation parameters that were changed from initial values given in Chapter 8, additional process model parameters and BioWin parameters that were changed from their default values. All other parameter values used in the model remained as per the model initialisation.

Table 9-3 Final adopted model parameters.

Name	Abbreviation	Role	Value	Units
Surface turbulence factor	f_T	Scales mass transfer losses by altering the intensity of mixing at the liquid surface	0.06	-
Influent dewatering unit (A) efficiency		Settles a constant fraction of incoming particulate material to the sludge	72	%
Sludge-supernatant flux coefficient	f_S	Scales the exchange of sludge and supernatant according to biogas flow	0.1	m ³ sludge m ⁻³ biogas
Sludge accumulation threshold		Defines the sludge depth above which pond settling efficiency starts to decline	3.58	m
Slope of settling efficiency decline		Sets the rate at which settling efficiency declines once the sludge accumulation threshold has been exceeded	-20.5	% m ⁻¹
Maximum cellulosic material hydrolysis rate	k_{HBC}	Sets the upper limit to the rate of hydrolysis of very slowly biodegradable (cellulosic) material	1.03	d ⁻¹
Cellulosic material hydrolysis half saturation constant	K_{BC}	Monod half saturation constant for regulation of the hydrolysis rate of cellulosic material	19.6	mg X_{SBC} per mg OHO biomass COD
Particulate very slowly biodegradable and non-biodegradable Ca fraction	f_{XICa}	Stoichiometric constant defining the amount of soluble Ca released by hydrolysis of very slowly biodegradable material	0.021	mg Ca ²⁺ per mg ($X_{SBC} + X_{IL}$)
Particulate very slowly biodegradable and non-biodegradable Mg fraction	f_{XIMg}	As above for Mg	0.005	mg Mg ²⁺ per mg ($X_{SBC} + X_{IL}$)
Soluble non-biodegradable N fraction	f_{NUS}	Fraction of soluble organic N that is non-biodegradable	1	mg N mg ⁻¹ N_S
Non-settleable particulate P fraction	f_{NSP}	Fraction of the difference between total and very slowly biodegradable P that is non-settleable	0.7	mg P mg ⁻¹ ($TP - DRP - X_{IP}$)

9.3 SENSITIVITY ANALYSIS

To explore the model sensitivity to and relative influence of key model parameters a one-factor-at-a-time approach was taken to undertaking a sensitivity analysis. This involved re-running the calibrated model after changing the value of a single model parameter while keeping all other parameters at their calibration value and quantifying consequent changes to key model outputs. The process was repeated for each parameter that was either fitted in the calibration process or has a high degree of uncertainty in its assigned value. The analysis focused on parameters associated with the influent characterisation, hydraulics and settling and additional process equations entered into the BioWin model builder. It also examined the influence of those BioWin parameters that were changed to values specific to DSE treatment and ponds (refer to Chapter 8).

The stability function defined in Chapter 5 (equation 5-46) was used to gauge the relative sensitivity of selected indices to varying the key parameters in the model. All parameters selected for the analysis were adjusted by $\pm 20\%$. Table 9-4 summarises the parameters tested and their adjusted values used in the sensitivity analysis. Ammonia oxidising biomass (AOB) maximum specific growth rate was the only BioWin parameter that was changed from its default value but not included in the sensitivity analysis on account of simulated biomass concentrations being close to zero.

Sensitivity indices adopted for the analysis included COD, FCOD, TVSS and TSS removal rates (incorporating partitioning to sludge – that is average difference between influent and effluent loads), sludge COD, TVSS, TN and TP loads, and total effluent nutrient and cation loads. Recognising that the periods before and after desludging were defined by quite distinct operating conditions, which some parameters were specifically designed to address, two values were calculated for each sensitivity index - one from the year before desludging commenced and the second from the year after flow was re-established in the anaerobic pond outlet. The results for indices based on removal rates are presented in Table 9-5. Only those parameters that displayed relative sensitivities of more than ± 0.25 (those that produced a change in an index of more than $\pm 5\%$ when the parameter was changed by $\pm 20\%$) for any given sensitivity index are presented. Similarly selected results for the effluent and sludge loads are presented in Table 9-6 and Table 9-7, respectively.

Table 9-4 Model parameters and their adjusted values included in the sensitivity analysis.

Parameter	Abbreviation	Adjusted values	
		80%	120%
Influent characterisation parameters			
COD Fraction of non-biodegradable lignin COD	f_{XIL}	0.15	0.22
COD Fraction of very slowly biodegradable (cellulosic) material	f_{XBC}	0.45	0.67
RBCOD equation intercept [‡]		-238	-357
Fraction of soluble non-biodegradable organic N	f_{NUS}	0.8	-
Fraction of non-settleable particulate P	f_{NSP}	0.56	0.84
Hydraulic and settling parameters			
Sludge-supernatant flux coefficient	f_S	0.08	0.12
Sludge accumulation threshold		9.14	10.56
Settling decline slope		-16.4	-24.6
Model builder parameters			
Maximum rate and half saturation constant for hydrolysis of very slowly biodegradable material*	k_{HBC}, K_{BC}	0.97, 18.2	1.08, 20.6
Endogenous product decay rate	b_{Xe}	0.004	0.006
BioWin model parameters			
Surface turbulence factor	f_T	0.048	0.072
Maximum OHO growth rate	$\mu_{max,H}$	2.0	3.0
OHO half-saturation constant	$k_{S,H}$	200	300
OHO anoxic/anaerobic decay rate	$b_{H,An}$	0.1	0.15
OHO yield	Y_H	0.336	0.504

[‡] Equation 8.3 in Chapter 8.

^{*} The rate and half saturation constants for hydrolysis of cellulosic material were adjusted in tandem based on the relative weighting of their harmonic means since this was the approach taken to determining their optimum calibration values.

The most dramatic changes to indices were those associated with sludge loads responding to changes in concentrations or the rate of biodegradation of particulate material, which is to be expected given that sludge accumulates over time. The parameters that caused the largest changes to sludge loads were the influent fraction of very slowly biodegradable material (f_{XBC}) and the OHO anaerobic decay rate ($b_{H,An}$), with both producing relative sensitivities greater than 1. These parameters would have profound effects on the model calibration, particularly on the parameters for hydrolysis of very slowly biodegradable material and the fraction of inert lignin in the influent, both

of which exhibited relative sensitivities above/below ± 0.25 . There is clearly a high degree of interaction between these four parameters that can only be disambiguated through experimental work.

The fraction of very slowly biodegradable material is also particularly influential to FCOD removal efficiencies and effluent P (and to a lesser extent N) loads, emphasising the need to determine its true value through laboratory characterisation. FCOD removal was sensitive to the intercept for the equation used to estimate RBCOD, which relates back to the over-prediction of effluent FCOD concentrations identified in section 9.2.7.1. The threshold for the decline in settling efficiency is also a critical parameter when sludge levels are high, having greatest impact on the removal and sludge loads of particulate COD and suspended solids, particularly when reduced below its calibration value. Being a fitted parameter, however, it is essentially empirical and cannot be verified by any other means. Changes to effluent nutrient and cation loads caused by parameter adjustments were mostly relatively minor, except those caused by f_{XBC} , the non-biodegradable soluble N fraction and the non-settleable particulate P fraction. As would be expected the effects of the changing N and P fractions were largely confined to $\text{NH}_3\text{-N}$ and TP and DRP, respectively, suggesting that the parameters are less critical to the behaviour of the overall model.

Table 9-5 Relative sensitivities for COD, FCOD, TVSS and TSS removal efficiencies. Relative sensitivities exceeding ± 0.25 are identified with shaded cells.

<i>Parameter</i>	$\Delta P_j / P_j$	<i>Pre-desludging</i>				<i>Post-desludging</i>			
		<i>COD</i>	<i>FCOD</i>	<i>TVSS</i>	<i>TSS</i>	<i>COD</i>	<i>FCOD</i>	<i>TVSS</i>	<i>TSS</i>
f_{XBC}	-20%	-0.01	-0.33	0.07	0.07	-0.06	-0.19	-0.05	-0.04
	20%	-0.12	-0.33	-0.09	-0.07	-0.10	-0.22	-0.08	-0.07
RBCOD equation intercept	-20%	-0.08	-0.28	-0.01	-0.01	-0.05	-0.21	0.00	0.00
	20%	-0.08	-0.22	0.00	0.00	-0.06	-0.19	0.00	0.00
Sludge accumulation threshold	-20%	0.46	-0.06	0.59	0.70	0.02	-0.01	0.02	0.02
	20%	0.18	0.02	0.24	0.28	0.00	0.01	0.01	0.02

Table 9-6 Relative sensitivities for effluent nutrient and cation loads. Relative sensitivities exceeding ± 0.25 are identified with shaded cells

<i>Parameter</i>	$\Delta P_j / P_j$	<i>Pre-desludging</i>							<i>Post-desludging</i>						
		<i>NH₃-N</i>	<i>TN</i>	<i>DRP</i>	<i>TP</i>	<i>Ca²⁺</i>	<i>Mg²⁺</i>	<i>K⁺</i>	<i>NH₃-N</i>	<i>TN</i>	<i>DRP</i>	<i>TP</i>	<i>Ca²⁺</i>	<i>Mg²⁺</i>	<i>K⁺</i>
f_{XBC}	-20%	0.01	-0.19	0.48	-0.34	-0.06	-0.02	0.00	0.01	-0.22	0.49	-0.34	-0.03	-0.02	0.00
	20%	-0.04	-0.20	-0.08	-0.17	-0.11	-0.03	0.01	-0.06	-0.22	-0.18	-0.21	-0.10	-0.04	0.01
f_{NUS}	-20%	-0.27	0.00	0.00	0.00	0.00	0.00	0.00	-0.22	0.00	0.03	0.00	0.00	0.01	0.00
f_{NSP}	-20%	0.00	0.00	-0.45	0.16	0.00	0.00	0.00	0.00	0.00	-0.52	0.14	0.00	0.01	0.00
	20%	0.00	0.00	-0.44	0.16	0.00	0.00	0.00	0.00	0.00	-0.52	0.14	0.00	0.01	0.00

Table 9-7 Relative sensitivities for sludge COD, FCOD, TVSS and TSS loads.

<i>Parameter</i>	$\Delta P_j / P_j$	<i>Pre-desludging</i>				<i>Post-desludging</i>			
		<i>COD</i>	<i>TVSS</i>	<i>TN</i>	<i>TP</i>	<i>COD</i>	<i>TVSS</i>	<i>TN</i>	<i>TP</i>
f_{XIL}	-20%	0.61	0.56	0.46	0.42	0.60	0.55	0.45	0.42
	20%	0.62	0.57	0.46	0.42	0.61	0.57	0.45	0.43
f_{XBC}	-20%	1.55	1.79	1.19	1.32	1.51	1.74	1.16	1.25
	20%	1.87	2.16	1.37	1.30	1.87	2.16	1.34	1.36
Sludge accumulation threshold	-20%	0.54	0.54	0.45	0.41	0.21	0.21	0.18	0.15
	20%	0.18	0.18	0.16	0.15	0.06	0.06	0.06	0.07
Hydrolysis of very slowly biodegradable material	-20%	-0.27	-0.31	-0.19	-0.17	-0.27	-0.31	-0.20	-0.20
	20%	-0.24	-0.28	-0.17	-0.15	-0.23	-0.27	-0.16	-0.13
OHO anoxic/anaerobic decay rate	-20%	1.32	1.52	0.93	0.77	1.21	1.40	0.87	0.73
	20%	0.73	0.84	0.52	0.48	0.72	0.83	0.53	0.50

9.4 SCENARIO SIMULATIONS

The benefit of a mathematical model calibrated to a real world system is that it can be used to explore alternative designs, modes of operation and management regimes. This section describes the reconfiguration of the model to run simulations representing four different scenarios:

2. The presence of a hydraulic dead zone
3. Operating the pond at a higher organic loading rate
4. Regular (annual) desludging
5. Lining the pond to meet best practice seepage prevention standards

The first scenario was effectively testing a fundamental assumption made in building the model and could be considered akin to a sensitivity analysis except that it involved a significant change to flow routing calculations performed in the data pre-processing as opposed to adjustment to a single parameter. The second scenario considers the potential for revising a fundamental design parameter used in sizing DSE anaerobic ponds. The third examines the impact on pond performance of a regimented pond maintenance regime in which pond sludge is removed on an annual basis rather than reactively. It considers three different approaches to desludging distinguished by whether or not supernatant is also removed and whether the sludge is mixed with the supernatant. The fourth scenario looks at the effect on pond performance of the only aspect of best practice that the anaerobic pond does not adhere to – maintaining low

seepage flows. The method and results for each scenario are presented in the following sections. The output data from each scenario are given in Appendix L.

9.4.1 Presence of a Dead Zone

The first scenario considered the impact of a large dead zone on pond performance. The potential for the formation of a dead zone in the corner of the pond perpendicular to the inlet pipe (north-western corner under the original inlet configuration or the south-eastern corner under the reconfigured inlet) was indicated by results from theoretical analysis of pond hydraulics and drogue tracking experiments presented in Chapter 6. The findings were not, however, conclusive and without a means to quantify the size of a dead zone or its effect on the pond's hydraulic retention time (HRT), the supernatant reactor in the calibrated model was sized to reflect the full liquid capacity of the pond. This scenario simulation was designed to gauge how the pond would be affected if its active volume was reduced by the establishment of a permanent dead zone occupying one quarter of the total liquid volume.

9.4.1.1 Model modifications

To perform the simulation, the volume of the supernatant was scaled dynamically according to the sludge level so that as the liquid capacity shrank due to sludge accumulation, so did the volume of the dead zone. The shape of the pond, the sludge accumulation rate and the trigger for compromised settling efficiency (sludge proximity to the outlet) were kept the same as the calibrated model, ensuring that the change only affected the biokinetics of the pond. The scenario also retained the desludging timing and volume and the influent flows and characteristics of the calibrated model.

Sludge return flows were also kept the same under the assumption that soluble components emanating from the sludge into the dead zone would ultimately enter the active zone through diffusion. Any bias introduced to the model from this assumption should result in higher effluent concentrations of soluble constituents. The removal efficiency of the influent dewatering unit was kept at 72% based on the assumption that settling of most particulate material occurs within hours, if not minutes, of entering the pond and would largely be unaffected while the HRT remains in the order of days. This contention was founded on observations made during laboratory settleable solids tests and is supported by the findings of Skerman et al. (2008) who reported that solids removal in small piggery manure anaerobic ponds under exceptionally high loading rates was comparable to that of conventionally loaded systems.

9.4.1.2 Results

Figure 9-10 shows the difference over time between the supernatant active liquid volumes of the calibrated model and dead zone scenario simulations. Despite the reduction in HRT, the reduction in COD and suspended solids removal efficiencies was mostly less than 3% (see Figure 9-11). The difference was slightly more exaggerated for FCOD before desludging (6%) when the volume of supernatant in the dead zone scenario had dropped to 320 m³. To check whether this reduction in FCOD removal was related to the fact that the model does not allow for the breakdown of soluble biodegradable COD transferred from the sludge into the dead zone, the simulation was rerun with the sludge-supernatant flux reduced by 25%. This made no difference to the outcome, suggesting that a dead zone can contribute to impaired breakdown of organic material when the total supernatant volume is significantly reduced by accumulated sludge.

Average effluent nutrient and cation loads before and after desludging were all within $\pm 1\%$ of the calibrated model predictions with the exception of the pre-desludging DRP load which was 2% higher than the calibrated model value. The effect on sludge COD, TVSS, TN and TP loads was also marginal at 1% and 0.8% reductions, respectively. The results indicate that DSE anaerobic ponds designed according to current loading recommendations have significant treatment buffer such that the loss of 25% of the active pond supernatant volume to a dead zone should not materially affect the performance of the pond.

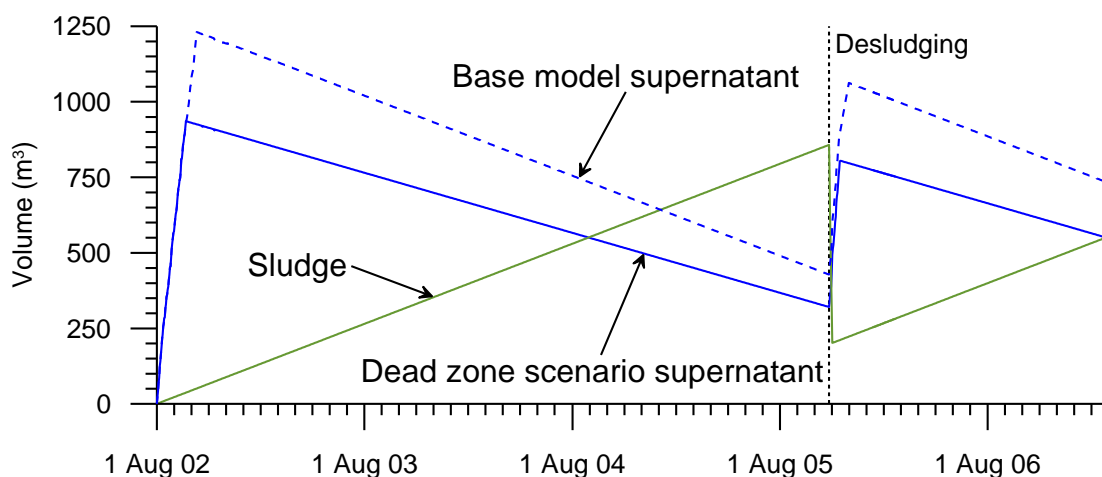


Figure 9-10 Supernatant and sludge reactor liquid volumes over time in the calibrated model simulation and the dead scenario simulation. Sludge volume was the same in both simulations.

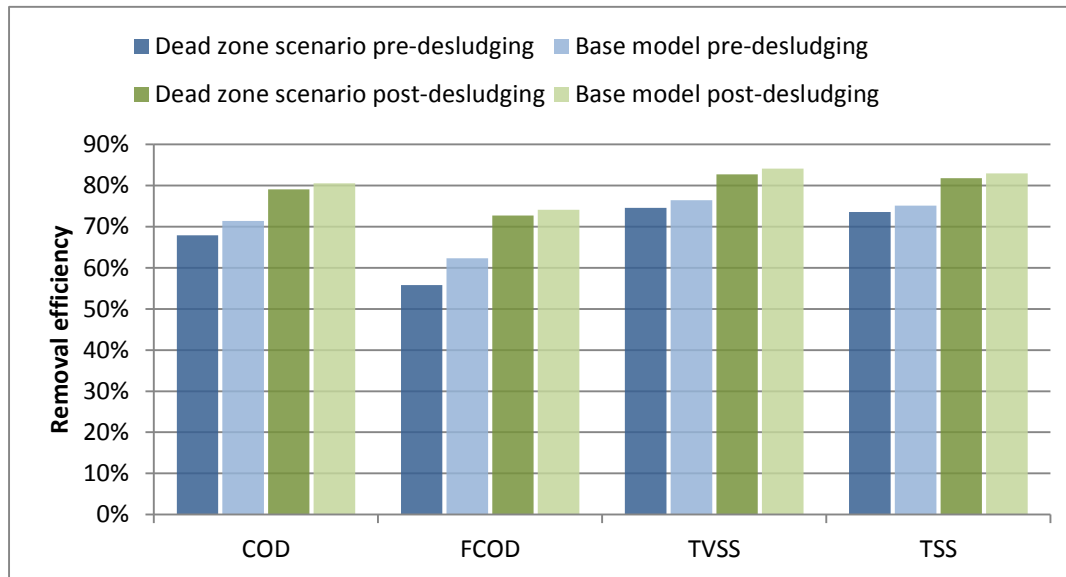


Figure 9-11 Removal efficiencies before and after desludging from the calibrated model and dead zone scenario simulations.

9.4.2 High Organic Loading Rate

Birchall, Dillon & Wrigley (2008) questioned the need to adhere to the anaerobic pond organic loading rate recommended by ASAE (2004) for sizing ponds in Australia, suggesting that it may be reasonable to construct smaller ponds that take up less land and are easier to desludge. Skerman et al. (2008) investigated this proposition for ponds treating piggery wastewaters, finding that acceptable VS removal and destruction (67% and 46%, respectively) could be achieved at loading rates between 0.5 and 0.9 kg VS m⁻³ d⁻¹. To test the effect of increasing the organic loading rate on the present pond, simulations were run with a reduced pond size but with a similar depth. This was fundamentally different from the dead zone scenario, however, in that the total capacity of both the sludge and supernatant reactors was smaller and the supernatant reactor only reduced in size in direct proportion with sludge growth. In addition, since the geometry of the smaller pond was different, the rate of increase in the sludge depth in relation to sludge volume had to be adjusted. The simulated pond total capacity (sludge and supernatant) was set to 666 m³ - about 52% of the real pond capacity – which results in an organic loading rate based on total volumetric capacity of 0.16 kg VS m⁻³ d⁻¹. Allowing for a maximum 60% sludge accumulation (3.75 m or 400 m³), this corresponds to a peak VS loading rate of 0.4 kg m⁻³ d⁻¹, more than twice the current recommended limit of 0.17 kg m⁻³ d⁻¹.

9.4.2.1 Modifications to pond geometry and seepage

The pond bathymetry was simplified to a rhomboidal shape as per Figure 9-12. With batter slopes of 2:1 and a square surface area of 400 m². The dimensions of the pond at a given depth were calculated as

$$L = W = 2 + 4H \quad (5.1)$$

where

L =pond length at the liquid or sludge surface = 20 m;

W =pond width at the liquid or sludge surface (m);

H = depth of liquid or sludge (m).

Sludge or combined liquid and sludge volume was expressed

$$V = \frac{1}{3}(2 + 4H)^2 \left(\frac{1}{2} + H \right) - \frac{2}{3} \quad (5.2)$$

With hydraulic loading in m³, liquid and sludge depth had to be calculated from the accumulated volume:

$$H = \frac{(3V + 2)^{\frac{1}{3}}}{2^{\frac{4}{3}}} - \frac{1}{2} \quad (1.1)$$

Evaporation and rainfall inputs taken from the calibrated model were adjusted to reflect the smaller liquid surface area. Adjustments to the embankment runoff calculations were also made to allow for the reduced catchment area. The model for seepage described in Chapter 4 had to be modified to reflect the different shape of the pond. The wetted area of the pond, $A_{w,An}$, was expressed

$$A_{w,An} = 8\sqrt{5}(H + H^2) + 4 \quad (5.3)$$

Seepage could then be expressed as an integral of wetted area:

$$\int dS_{An} = \sqrt{\frac{k_s}{2tv}} \int_0^H h^{\frac{1}{2}} \left(\frac{dA_{w,An}}{dH} \right) dH$$

$$S_{An} = \sqrt{\frac{k_s}{2tv}} \cdot \frac{2}{15} \cdot H^{\frac{3}{2}} (40\sqrt{5} + 48\sqrt{5}H) \quad (5.4)$$

where k_s , t and v are as defined in Chapter 4.

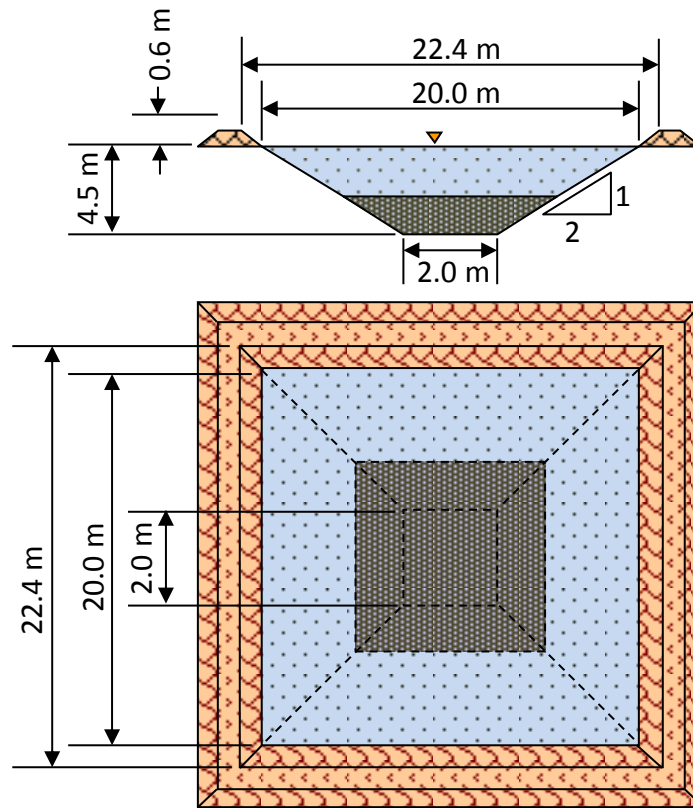


Figure 9-12 Pond geometry used to simulate high loading scenario.

9.4.2.2 Modified influent loading and the ‘base model’

Unlike in the previous scenario that was intended to replicate historical conditions, this simulation sought to reflect average conditions that were independent of changes to the quality of recycled effluent occurring over time. The regression model used for predicting influent loads was explicitly designed to account for recycled effluent quality, which is a function of anaerobic pond effluent quality. To negate the influence of this feedback loop, daily hydraulic loading was drawn entirely from synthetic inflow data calculated as described in the ‘data pre-processing’ section of Chapter 8 while influent constituent loads were based on the average loading rates presented in Chapter 7. To provide baseline data for comparison, the original calibrated model was rerun with the same time-independent input data. This modified version of the calibrated model will herein be referred to as the ‘base model’.

9.4.2.3 Desludging

Desludging was scheduled to occur when the sludge depth reached 3.75 m, which meant that sludge exceeded the settling efficiency decline threshold after about 13

months. The threshold was kept the same as the calibrated model in keeping with the assumption that compromised performance is defined by the proximity of the sludge to the outlet. The removal efficiency of the primary dewatering unit was also kept the same based on the same rationale applied in the dead zone scenario. Sludge-supernatant flux was left unchanged on the assumption that sediments should accumulate and digest at the same rate and therefore gas production from the sludge will be the same.

9.4.2.4 Results

Figure 9-13 compares predicted effluent COD and FCOD and sludge COD concentrations from the high loading rate scenario and the base model simulations. Effluent COD and FCOD were similar between the two models, although as expected, the faster rise in the sludge level of the highly loaded pond causes treatment efficiency to decline sooner and generally more rapidly than in a larger pond. Despite the shorter periods between desludging events, stabilisation of the sludge (as indicated by sludge COD concentrations) was as effective under the high loading scenario as it was in the base model. Average removal efficiencies at times when the sludge level was below the threshold for declining settling efficiency were 75% and 67% for COD and FCOD, respectively. Table 9-8 shows that corresponding removal efficiencies from the base model (when the sludge level was below the threshold) were 6% higher. TVSS, TSS, TN and TP removal efficiencies during periods of low sludge were also lower under the high loading scenario. Compared, however, with the 50% reduction in reactor size, the reductions in treatment efficiency are small.

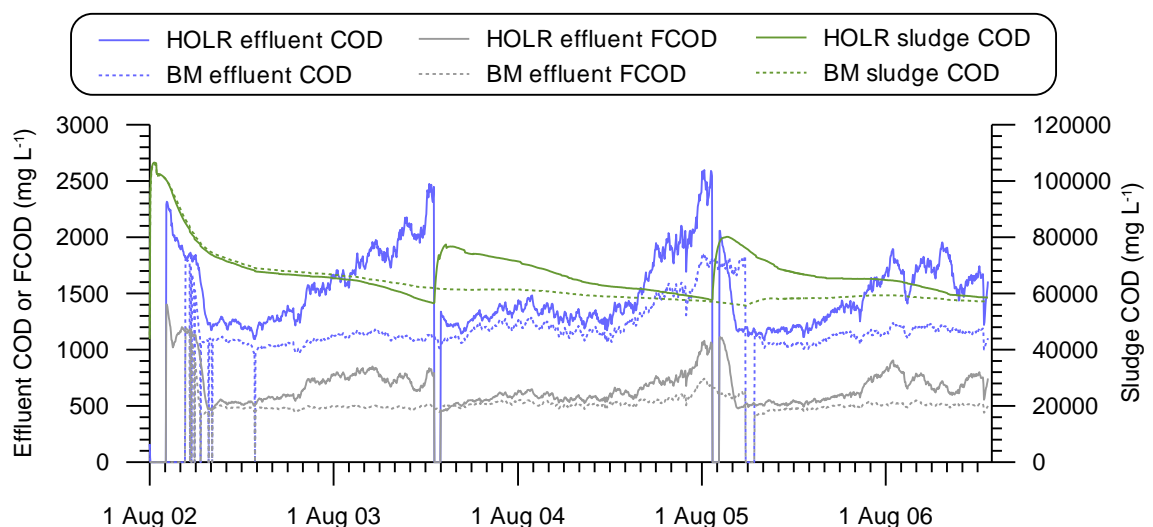


Figure 9-13 Predicted COD concentrations in the high organic loading rate scenario model (HOLR) and the base model (BM).

Table 9-8 Average simulated effluent concentrations, effluent loads and removal efficiencies during periods when sludge accumulation was below the threshold for compromised settling efficiency.

<i>Parameter</i>	<i>High loading rate</i>			<i>Base model</i>		
	<i>Effluent concentration (mg L⁻¹)</i>	<i>Effluent load (kg d⁻¹)</i>	<i>Removal efficiency</i>	<i>Effluent concentration (mg L⁻¹)</i>	<i>Effluent load</i>	<i>Removal efficiency</i>
COD	1379	35	75%	1133	27	81%
FCOD	637	16	67%	505	12	73%
TVSS	555	14	81%	463	11	85%
TSS	659	17	80%	568	14	84%
TN	0	4.6	29%	184	4.4	31%
NH ₃ -N	0	3.2	11%	130	3.1	11%
TP	0	1.2	31%	50	1.2	34%
DRP	0	0.62	-10%	26	0.62	-11%

Figure 9-14 compares the make-up of COD in the sludge and effluent between the scenario simulation and the base model. Sludge values were based on concentrations on the day before desludging while the effluent values are from average concentrations across days when sludge was not reducing settling efficiency. Simulated sludge COD from both models is almost entirely made up of very slowly biodegradable and non-biodegradable particulate COD, with small fractions of slowly degradable, soluble inert and endogenous products COD. The base model has a higher concentration of non-biodegradable COD only because it accumulated sludge over a longer period. The main differences between the highly loaded pond and the full size pond, however, are evident in the effluent COD fractions. Where the base model effectively achieves complete hydrolysis of slowly biodegradable material, the shorter retention time of the smaller pond causes there to be more residual slowly biodegradable COD. Similarly, the hydrolysis of cellulosic (very slowly biodegradable) material is less effective in the smaller pond. Effluent complex readily biodegradable COD concentrations were negligible under both simulations, but it would also appear that acetoclastic methanogens fare better with the longer retention time – effluent acetate concentrations are lower while the biomass concentration is higher in the full size pond (see Figure 9-15).

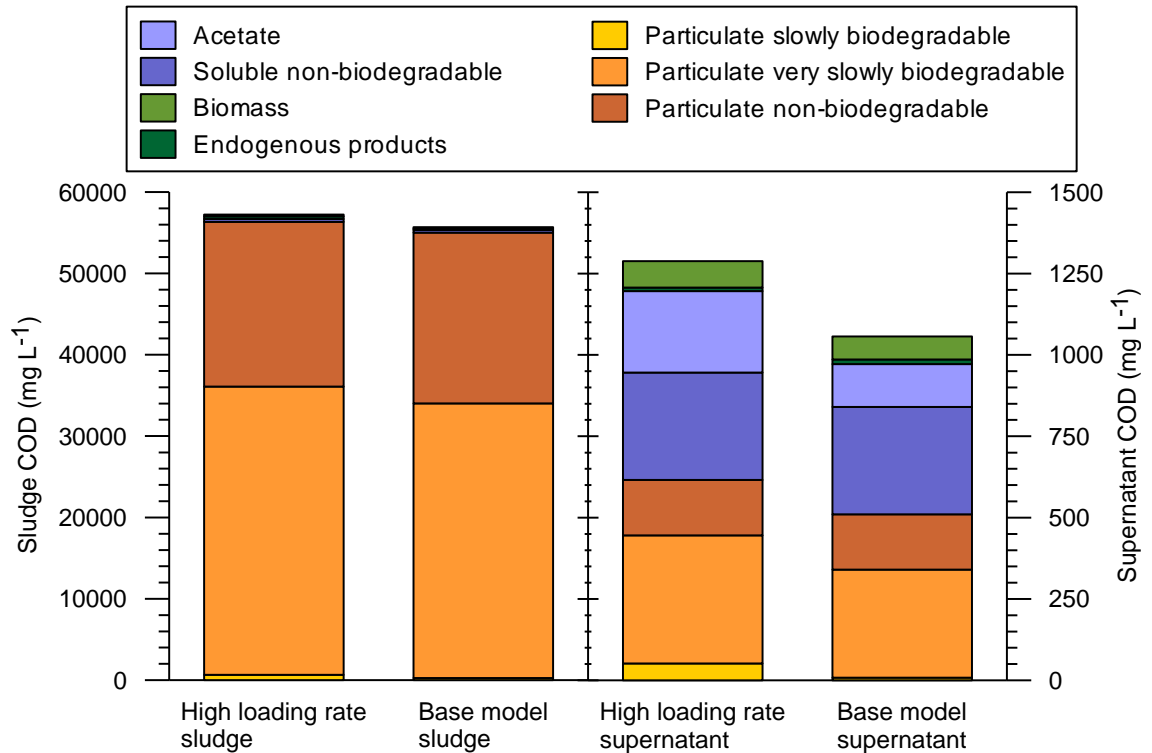


Figure 9-14 Comparison of sludge and effluent COD fractions between the high loading rate scenario and the base model outputs.

The effect of the reduced retention time can also be seen in the biomass concentrations presented in Figure 9-15. COD from endogenous decay products is clearly higher in the supernatant of the base model due to the longer retention time allowing a larger fraction of biomass to die off before settling out or leaving in the effluent. Concentrations of the main live organism populations, OHOs and (acetoclastic and hydrogenotrophic) methanogens, are not substantially higher in the smaller pond despite the higher substrate concentration, which confirms that growth is limited by environmental conditions (as opposed to substrate availability), resulting in the lower reductions in COD.

Finally, consideration needs to be given to the effect on the simulation outputs of the uncertainty surrounding the sludge fixed and volatile solids data used to calibrate the model. A 20% lower hydrolysis rate would result in proportionally lower increases in concentrations of very slowly biodegradable material in the effluent since the rate is already slow and therefore has limited effect on suspended material. The rise in effluent particulate COD would partly be offset by lower acetate COD concentrations stemming from the reduced hydrolysis and the lower sludge-supernatant flux coefficient. Thus the net effect of a misinformed calibration on the outcomes of this scenario analysis would be minimal.

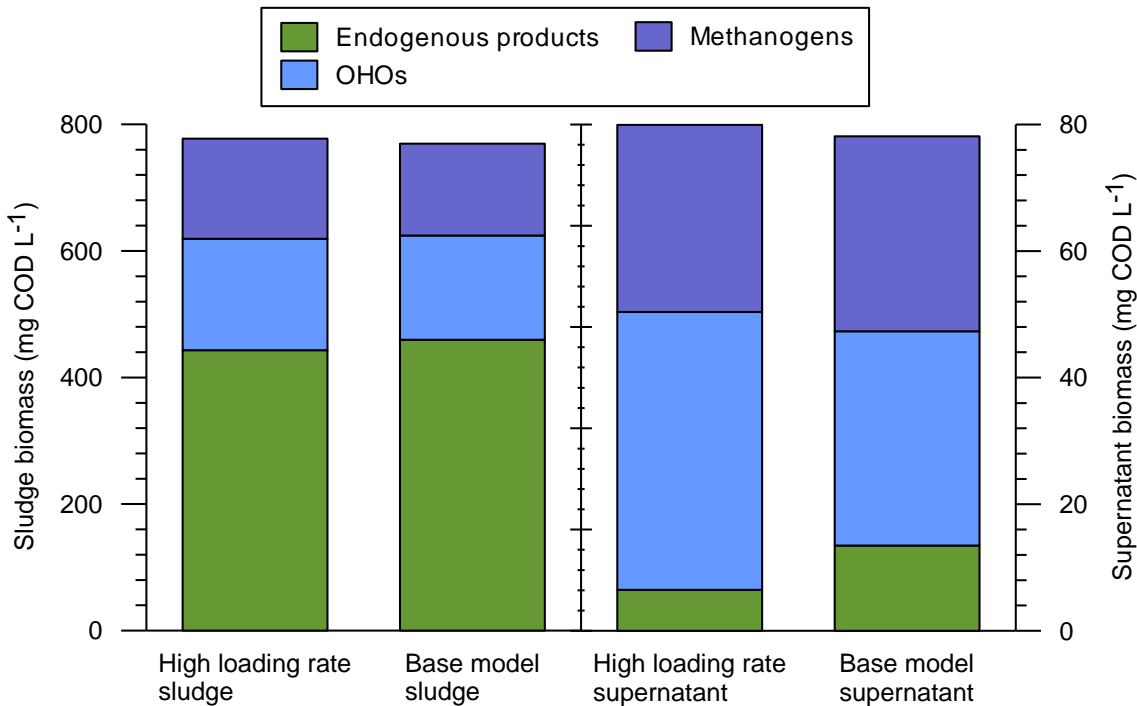


Figure 9-15 Simulated average sludge and supernatant biomass concentrations from the high loading rate scenario and base models.

9.4.3 Regular Desludging

Desludging is often performed reactively when the pond shows signs of failure rather than according to a schedule. Regular desludging offers the benefits of minimising the risk of pond failure and access to the valuable nutrients and organic matter. Frequent desludging, however, runs the risk of washing out the bacterial populations that effect treatment and interrupting the digestion process before it can effectively stabilise the sludge. To examine the impact of regular (annual) desludging, a total of three scenarios simulations were run. The first, desludging scenario A, tested the effects of removing just the accumulated sludge once each year, which in practical terms would involve pumping out from the bottom of the pond to a vacuum tanker or similar without any mixing with the supernatant. The second scenario (B) considered the impact of independently removing sludge and supernatant once a year, again without mixing, to obtain the maximum nutrient benefit and allow rejuvenation of recycled effluent. Sludge would be pumped out using a vacuum tanker from below the sludge line while effluent would be extracted via a suction line close to the liquid surface to feed a travelling irrigator. Alternatively the process could occur sequentially using just the vacuum tanker. The third scenario (C) simulated mixing of the sludge with the supernatant before extraction, an approach often used to homogenise the product spread to land with an agitator and either a heavy duty slurry pump or a vacuum tanker.

9.4.3.1 Desludging timing and volumes

Desludging was performed at the beginning of the month of November when evaporation is typically higher than rainfall. Table 9-9 summarises the volumes of sludge and supernatant extracted and the time allocated to each desludging event under the three scenarios. A and B scenarios removed all accumulated sludge from the pond. Only two days were allocated to desludging under the sludge only (A) scenario as the volume of sludge accumulated over the period of a year was around only 265 m³. Under the mixed scenario C, all accumulated sludge is mixed into the supernatant and a total of 700 m³ of the mixture is removed, leaving a residual (resuspended) sludge volume that increases with each event. The total sludge-effluent volume of 700 m³ was chosen for the B and C desludging scenarios as a practical quantity to extract using a vacuum tanker (similar to that extracted in the actual recorded desludging event) and represents about 54% of the pond capacity.

Table 9-9 Volumes of sludge and effluent removed under the three regular desludging scenarios.

	<i>A</i> <i>Sludge only</i>	<i>B</i> <i>Sludge + effluent</i>	<i>C</i> <i>Mixed sludge + effluent</i>
Sludge (m ³)	Sludge volume at commencement of desludging	Sludge volume at commencement of desludging	180-254 m ³
Effluent (m ³)	0	700 – sludge removed	700 – sludge removed
Desludging period (d)	2	5	5

9.4.3.2 Model modifications

Influent loading for all three desludging scenarios was the same as used for the high loading rate scenario. Accordingly the outputs from the scenarios were compared with the ‘base model’ described in 9.4.2.2. Under the A and B desludging scenarios, the base model sludge-supernatant flux was retained. This is likely to over-estimate transferral of soluble constituents to the supernatant in the initial period after desludging, but the effect on the overall model outputs should be minor given the low sensitivity to the parameter observed in the sensitivity analysis. For the C scenario, sludge-supernatant flux was essentially substituted with a complete transferral of total sludge contents into the supernatant reactor during each desludging event. Note that the C scenario provides at best an approximation of resettling of resuspended sediments following desludging as the artificial division into sludge and supernatant reactors prevents simulation of the zone settling that would take place following the

event. Nonetheless, to simulate the reformation of the sludge blanket, the fraction of the sludge blanket that remained in the supernatant after desludging was gradually returned to the sludge reactor at the same rate of accumulation as settleable influent solids ($0.73 \text{ m}^3 \text{ d}^{-1}$). The top-most plot in Figure 9-16 shows supernatant reactor liquid volumes over time under each scenario while sludge volumes are plotted in Figure 9-17. The resettling of sludge under the mixing scenario is apparent in the steeper slopes of the C scenario sludge volume.

9.4.3.3 Results

Figure 9-16 shows that regular desludging prevents rising effluent COD and FCOD concentrations associated with accumulating sludge that was observed in the actual pond. The same is the case for all particulate constituents. Average COD, FCOD TVSS and TSS removal under scenarios A and B presented in Figure 9-17 were almost identical to the base model when its sludge level was below 3.75 m. The plots of effluent COD and FCOD concentrations for scenarios A and B were almost indistinguishable (Figure 9-16), indicating that removing effluent as well as sludge has no material impact on pond function. However, under the C scenario, mixing the sludge with the supernatant causes a period of very high (particulate) COD levels, reducing its average treatment efficiency (Figure 9-17). FCOD levels are unaffected on account of sludge and supernatant concentrations being very similar. The resulting increased particulate loading to the facultative pond could also potentially compromise its treatment efficiency and the quality of effluent recycled to the dairy. The model predicts that the pond recovers reasonably quickly from the shock of desludging mixing, returning to steady COD and FCOD removal within about five months. The true rate of recovery of the anaerobic pond following desludging cannot, however, be accurately deduced from the model as the physical process of settling is modelled with essentially empirical parameters.

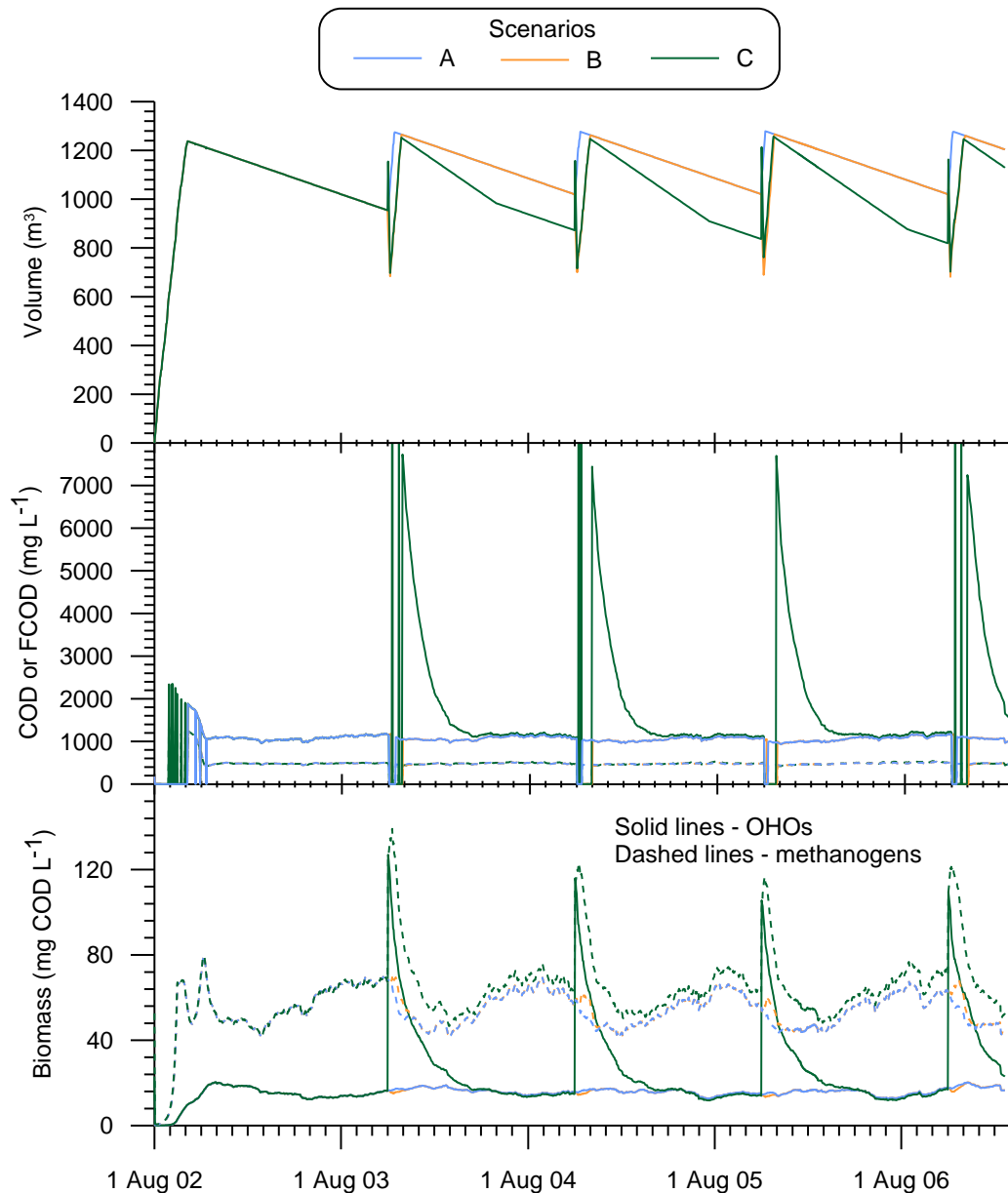


Figure 9-16 Predicted supernatant volumes (top), effluent COD and FCOD concentrations (middle) and supernatant biomass concentrations (bottom) from the three desludging scenario simulations.

Under all scenarios, sludge COD and TVSS concentrations rise sharply following each desludging event as fresh incoming manure solids take the place of the evacuated partially digested solids (see Figure 9-16). In scenarios A and B both constituents quickly return to pre-desludging levels in concert with associated peaks in OHO and methanogen biomass populations (also shown in Figure 9-16). Sludge COD and TVSS under scenario C, however, fail to return to the levels recorded before the first desludging event. This would appear to be related to the over-simplification of the resettling process after mixing and desludging whereby particulate material is simply returned to the sludge by the sludge-supernatant flux recycle flow, and the sludge

regains its volume through additional flow into the reactor. Perhaps most importantly, the complete removal of sludge under scenarios A and B does not cause biomass populations to drop below critical levels (wash out). Seeding by supernatant biomass and the influx of fresh substrate helps to stimulate biomass populations immediately following desludging such that biomass concentrations peak over 1000 mg COD L⁻¹ before declining over the following months as the sludge ages. Under scenario C mixing ensures that biomass is always retained in the pond.

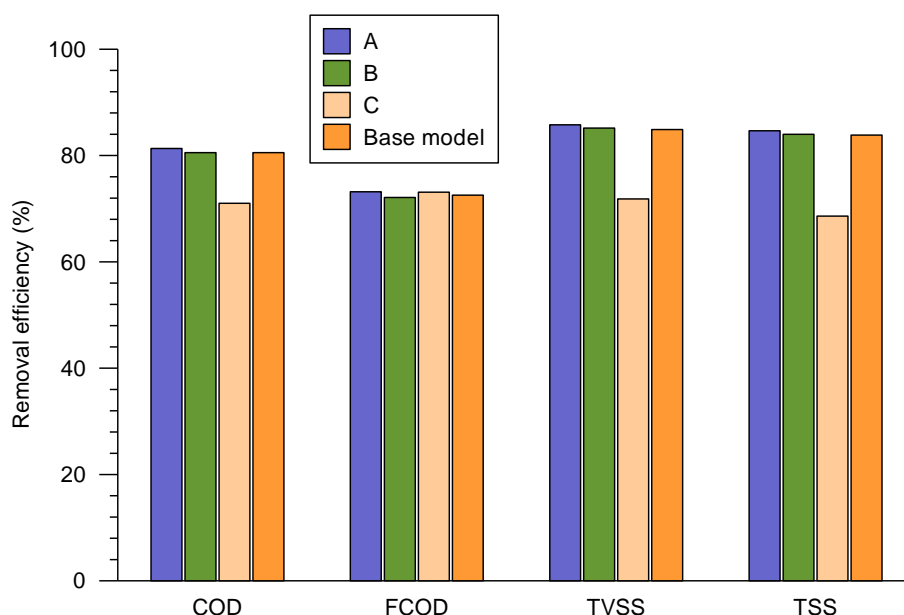


Figure 9-17 Removal efficiencies under the desludging scenarios A, B and C compared with those of the base model.

Figure 9-19 compares the nutrient loads extracted from the model pond on the last desludging event of each of the three scenarios. Despite extracting sludge only, scenario A provides slightly smaller total N and P loads than scenario B but higher than scenario C. The advantages of extracting both supernatant and sludge are higher K loads as well as higher proportions of NH₃-N and DRP, all of which should help to provide more immediate response from pasture or crops to which the effluent and sludge are applied. However, whilst mixing sludge with supernatant provides the additional benefit of a homogeneous product, it inevitably results in less sludge being extracted than when extracting sludge and supernatant separately. This is the reason for the lower TN and TP loads under scenario C.

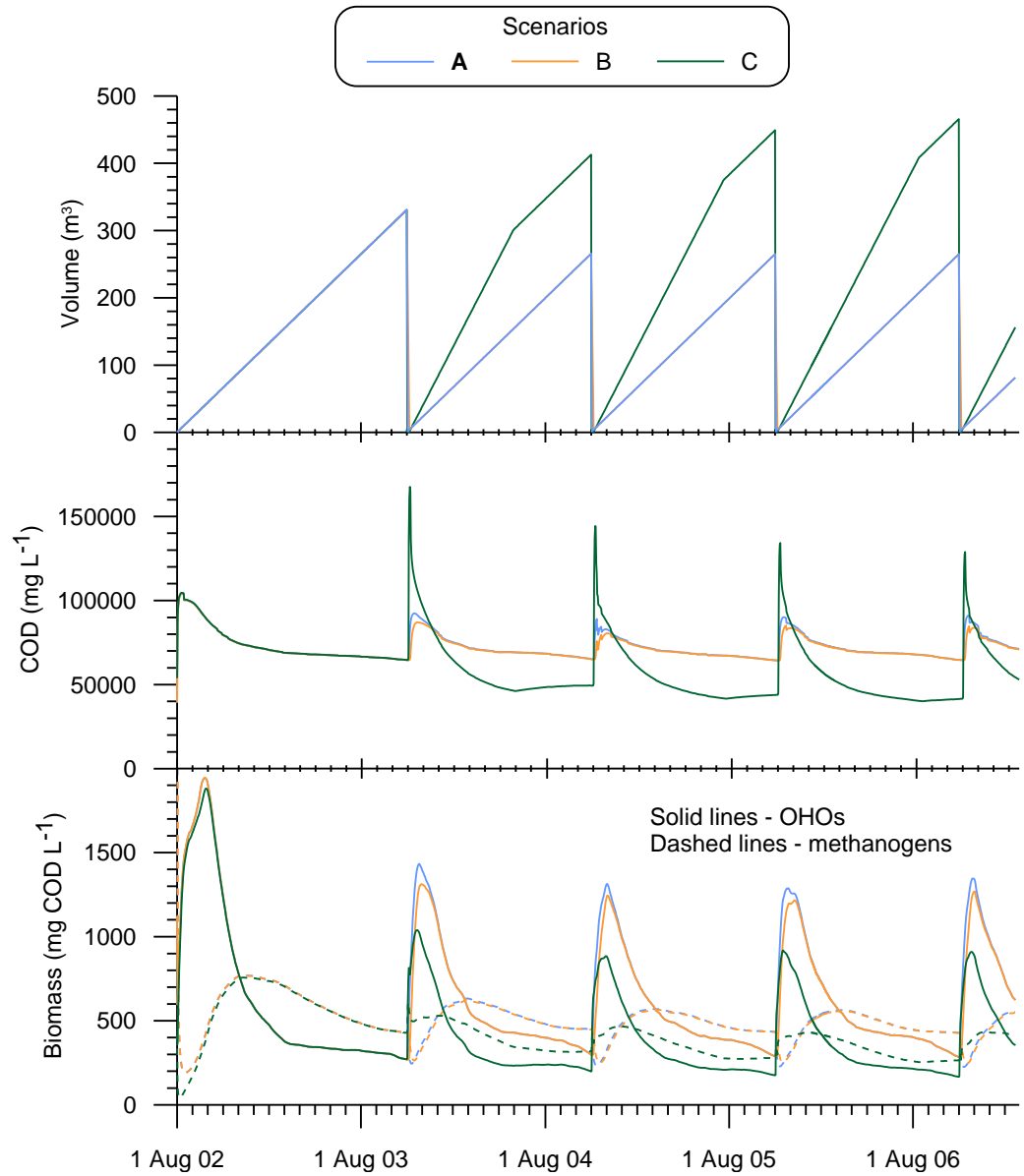


Figure 9-18 Predicted sludge volumes (top), COD and FCOD concentrations (middle) and biomass concentrations (bottom) from the three desludging scenario simulations.

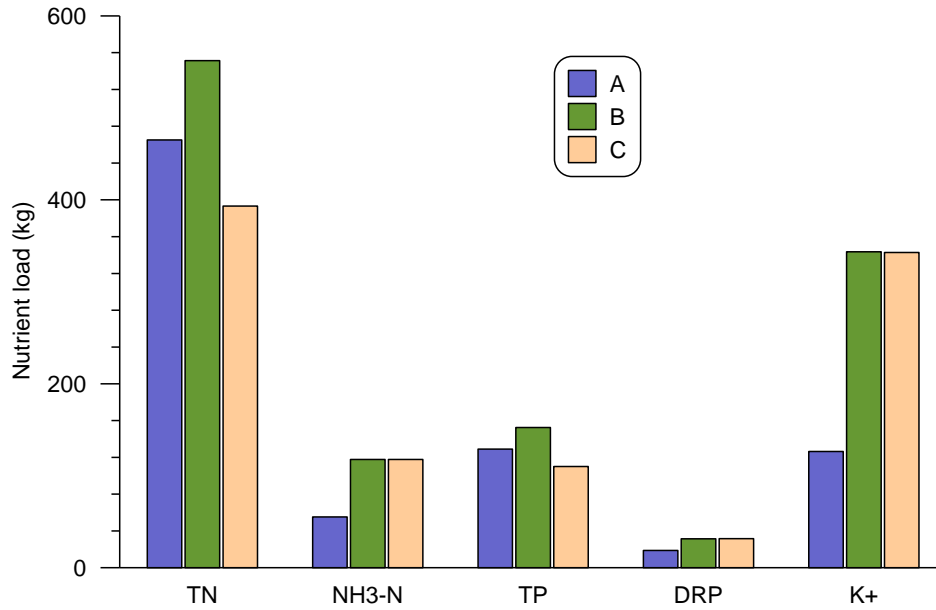


Figure 9-19 Nutrient loads extracted during the final desludging events of scenarios A, B and C.

9.4.4 Low Seepage Losses

The pond system at the centre of this study satisfies best practice standards in most respects, but as the system water balance (Chapter 5) revealed, the anaerobic pond was losing up to 10% of wastewater inflow to seepage. Clearly the in-situ clay liner was not adequately compacted, or was not a suitable liner material to start with. This scenario considered the extent to which a liner that met the recommended hydraulic conductivity of 10^{-9} m s^{-1} (Birchall, Dillon & Wrigley 2008) would alter the performance of the pond, particularly with regard to effluent nutrient loads.

9.4.4.1 Model modifications

The main modification to the model required to run this scenario was applied in the flow routing pre-processing, where the basis of the seepage calculations were changed from the Cihan et al. (2006) seal formation model to the standard Darcy equation used to model seepage from the facultative pond. Wetted area is a function of liquid depth, thus the Darcy equation may be expressed as an integral:

$$\begin{aligned} \int dS_{An} &= \int k_l \left(\frac{H}{L_l} + 1 \right) dA_{w,An} \\ &= \frac{k_l}{L_l} \int_{h_B}^h (h - h_B + L_l)(3\beta_3 h^2 + 2\beta_2 h + \beta_1 c) dh \end{aligned} \quad (4.5)$$

where

k_l = pond liner hydraulic conductivity

$$= 1 \times 10^{-9} \text{ m s}^{-1}$$

$$= 8.64 \times 10^{-5} \text{ m d}^{-1};$$

L_1 = liner thickness (m);

H = liquid depth

$$= h - h_B;$$

h = liquid elevation – 660 (m);

h_B = elevation of the lowest point of the pond floor – 660 (m);

$$\beta_3 = 8.01985291207075 \times 10^{-1};$$

$$\beta_2 = -1.09909301601711 \times 10^{-1};$$

$$\beta_1 = 1.41166181229088 \times 10^2.$$

Integrating yields:

$$S_{An} = \frac{3}{4}\beta_3 h^4 + \frac{2}{3}\beta_2 h^3 + \frac{1}{2}\beta_1 h^2 + (L_1 - h_F)(\beta_3 h^3 + \beta_2 h^2 + \beta_1 h) \quad (5.5)$$

Aside from the wastewater loading, which was again based on average loading, all other aspects of the base model were unchanged, including the desludging timing and volume.

9.4.4.2 Results

The simulation revealed that the main effect on pond performance of having very low seepage losses is the accumulation of acetate in the pond during the early stages of operation alluded to in section 9.2.2.2. Figure 9-20 shows that pH in the sludge stays below five for several months as production of acetate by fermentation of complex readily biodegradable COD outpaces methanogenesis while the population of acetoclastic methanogens becomes established. The low pH over this period would inhibit the growth of methanogens, but eventually a critical mass is achieved in the supernatant at around the three month mark, causing supernatant acetate to drop dramatically (note the logarithmic scale on the acetate plot in Figure 9-20). The flow on effect is a spike in methanogen biomass in the sludge which breaks down the accumulated acetic acid, allowing pH to rise to a non-inhibitory range of around 6.6 - 6.8. In the base model, conveyance of acetate out of the sludge reactor via seepage keeps pH from dropping much below six and limits the period with suppressed pH to less than two months.

With close to no seepage removing soluble constituents from the sludge reactor, those constituents end up in the pond effluent. Accordingly, the effluent FCOD load is

increased by 16%, causing FCOD removal, and consequently COD removal, to be slightly lower in this scenario than in the base model at 67% and 77%, respectively. Table 9-10 presents soluble COD and nutrient seepage and effluent loads under the ideal seepage scenario simulation and the base model simulation. Under the ideal seepage scenario, the low seepage flow results in reductions of an order of magnitude to soluble constituents. This is a considerable gain in regard to preventing groundwater contamination, but it also presents an important nutrient recovery benefit, with around 10% or more increases in the nutrients retained in the effluent.

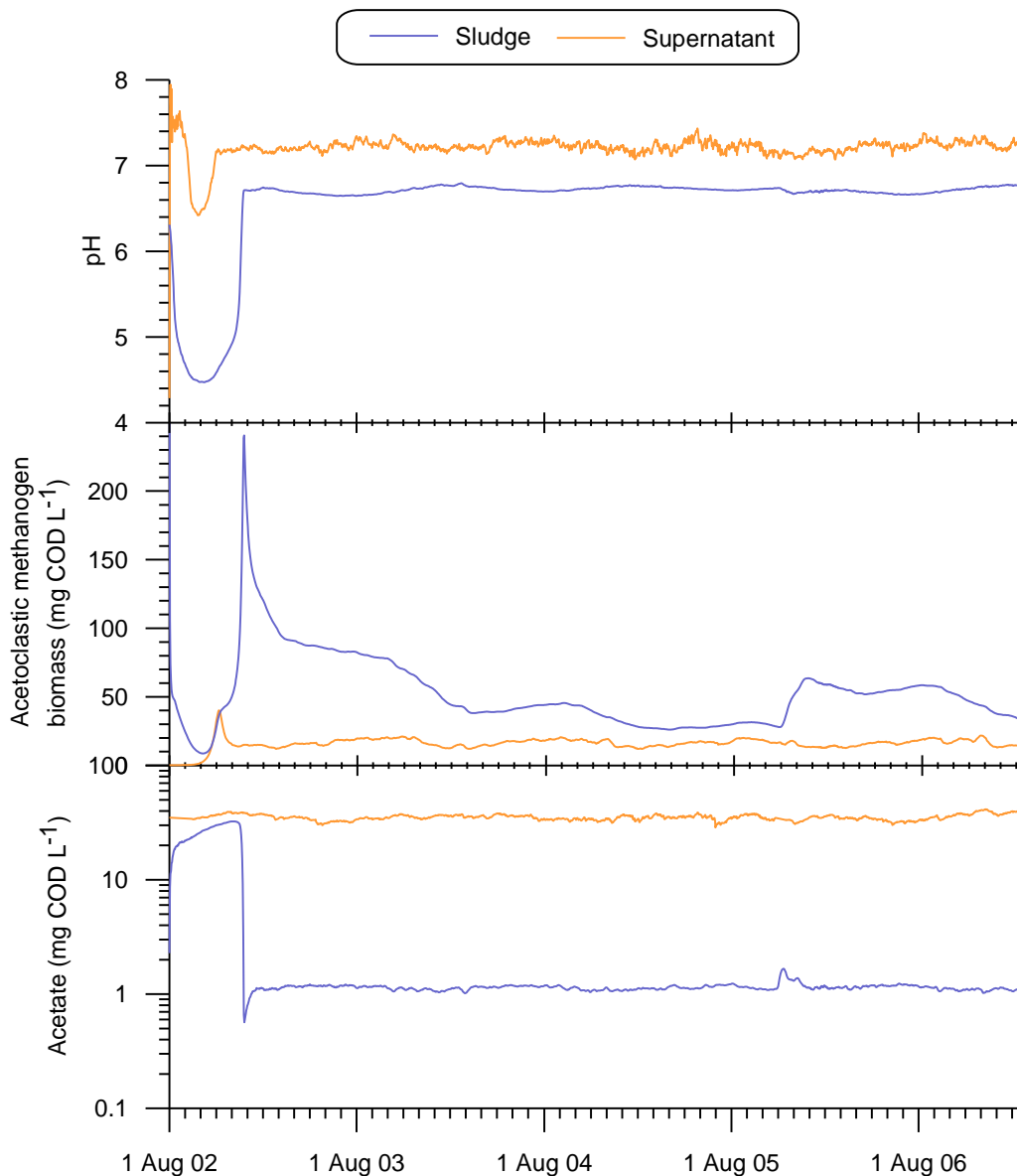


Figure 9-20 pH and acetoclastic methanogen biomass and acetate concentrations in the sludge and supernatant under the low seepage scenario.

Table 9-10 Average yearly soluble COD and nutrient loads contained in seepage and effluent from the ideal seepage scenario and the base model simulations.

<i>Constituent</i>	<i>Ideal seepage scenario</i>		<i>Base model</i>		<i>Nutrient recovery benefit</i> <i>% of influent load</i>
	<i>Seepage load</i>	<i>Effluent load</i>	<i>Seepage load</i>	<i>Effluent load</i>	
	<i>kg yr⁻¹</i>		<i>kg yr⁻¹</i>		
FCOD	135	5285	760	4446	
NH ₃ -N	45	1292	282	1086	10
Soluble inert N	7	343	54	296	2
DRP	18	273	89	214	11
K ⁺	90	4442	703	3830	12
Ca ²⁺	36	921	212	766	21
Mg ²⁺	19	747	134	638	15

9.5 DISCUSSION

This model represents an initial but important step towards dynamic biokinetic modelling of livestock waste stabilisation ponds. It constitutes a shift from static empirical models that at best provide very approximate estimates of effluent quality to a dynamic modelling approach capable of predicting effluent and sludge characteristics in response to nuanced influent wastewater variations and to changes in design characteristics and management practices. In taking an approach previously used to model facultative stabilisation ponds treating urban wastewater (see Gehring et al. 2010; Houweling et al. 2008), the model incorporates a comprehensive array of chemical and biological processes by leveraging the knowledge developed in activated sludge and anaerobic digestion modelling, in this case by using the BioWin simulation package. Running dynamic simulations allows the temperature-dependence of pond performance to be properly accounted for as well as the variable hydrology of the pond including the effects of dilution and concentration caused by rainfall and evaporation, respectively, and the export of wastewater constituents via seepage losses. The model also considers the different forms of nutrients that are present in manure wastewaters rather than just the total quanta, which presents the opportunity to better understand the response from pasture or crops receiving pond effluent when examining nutrient recovery options.

In expanding on the BioWin General Activated Sludge/Anaerobic Digestion Model (ASDM), this modelling approach has addressed critical differences between mechanised systems treating urban wastewater and stabilisation ponds treating DSE.

In particular it handles the slower rates of hydrolysis noted by Beck (2007) and anticipated by the designers of BioWin (Fairlamb 2010) through including an additional particulate component (very slowly biodegradable COD) in the characterisation of influent organic material and an additional process equation for the hydrolysis of the new component. It also accommodates the long-term retention of solids within the system through a novel approach to managing flow routing through and between the reactors representing the sludge and supernatant. Providing for extended solids retention times allows the slower hydrolysis process to take effect as well as a second additional process model used to simulate decomposition of endogenous products.

Despite settling in the pond being handled with simple mass partitioning, the model is capable of simulating the declining performance associated with sludge accumulation. The model does not appear to be constrained by the hydraulic simplification necessitated by the implementation in BioWin, although it no doubt would benefit from a more sophisticated approach to pond hydraulics. Importantly, the model simulates the shock impacts associated with desludging of the pond reasonably well, which would indicate a degree of robustness. Moreover, sensitivity analysis showed that model predictions of effluent quality and removal efficiencies were not greatly affected by adjustments to singular parameters, which is appropriately reflective of the real pond's resilience but is also a sign of the robustness of the model itself.

9.5.1 Insights into DSE Characteristics, Treatment and Modelling

9.5.1.1 Poorly biodegradable material

The process of characterising the influent (see Chapter 8) and subsequent modelling revealed that DSE contains large fractions of poorly biodegradable organic material as well as sizeable fractions of non-biodegradable nutrients, in both soluble and particulate forms. This affects the standard to which DSE can be expected to be treated with conventional pond technology, but also has implications for the recycling of effluent for wash down purposes since non-biodegradable material will inevitably accumulate within a system over time. As shown by the scenario simulations, desludging is an effective means of renewal for anaerobic ponds that should be regularly used in concert with irrigation from the secondary pond to maintain workable and safe effluent quality for recycling. With regard to developing this model further, and in particular expanding it to facultative ponds and effluent recycling, these fractions need to be quantified through laboratory analyses to validate or revise the numbers derived in Chapter 8.

The importance of accurately quantifying poorly biodegradable constituent fractions was demonstrated in the sensitivity analysis. Sludge concentration predictions were highly sensitive to the fraction of non-biodegradable COD and even more so to the fraction of very slowly biodegradable COD. Laboratory quantification of these COD components is essential to reducing the uncertainty associated with the interactive effects with the two other model parameters that greatly influenced sludge predictions, namely the endogenous decay rate and the two parameters that define hydrolysis of very slowly biodegradable COD. The insights gained from the sensitivity analysis also demonstrate the value of calibrating to sludge data as well as effluent data, which is a practice that has not been widely adopted in the development of other stabilisation pond models.

9.5.1.2 Mobility of soluble constituents

The ideal seepage scenario quantified the benefits associated with lining the anaerobic pond to the recommended standard, but perhaps its most useful insight was that related to the importance of modelling transport of soluble constituents, in particular acetate, from the sludge to the supernatant. When simulating low seepage with an under-estimated sludge-supernatant flux coefficient, the associated limited avenues of escape from the sludge for (soluble) constituents resulted in acetate accumulating in the sludge, causing high acidity and impairing biomass growth to the point where anaerobic digestion in the sludge all but ceases entirely. This suggests that exchanges between the sludge and supernatant, particularly the transfer of intermediate organic acids noted previously by Pescod (1996), are fundamental to pond functionality. Conversely, if sludge-supernatant flux was set too high under normal seepage conditions, the model would over-predict effluent concentrations of $\text{NH}_3\text{-N}$ and DRP , which shows the importance of modelling this behaviour with some accuracy. Simulating the connection between sludge and supernatant with a uni-directional advective flow linked to biogas flow is a considerable simplification, the limitations of which are discussed in section 9.5.2.3. However in the absence of data to inform a more appropriate model, the approach has provided an adequate approximation of reality both in this instance and in at least one other model of a stabilisation pond (Houweling et al. 2008).

9.5.1.3 Greenhouse gas emissions

Model predictions of methane and carbon dioxide emissions were used to determine average yearly greenhouse gas emissions from the anaerobic pond. Table 9-11 presents average biogas production and composition over the modelling period

(excluding the first month and a half of operation and the two months following desludging when pond biological processes were becoming (re-)established) in total volumetric terms and in terms of mass yield per milking cow. Applying a global warming potential factor of 21 for methane emissions (DCCEE 2009), total greenhouse gas (GHG) emissions from the pond amount to 441 kg CO₂e cow⁻¹ yr⁻¹. This makes up 7% of the total GHG emissions estimated by Christie et al. (2012) to be generated from the average Australian dairy farm (6340 kg CO₂e cow⁻¹ yr⁻¹). Despite the manure load to the pond being around 10% of daily excretion, the methane component (427 kg CO₂e cow⁻¹ yr⁻¹ or 6.7% total farm GHG emissions) is actually higher than Christie et al.'s (2012) estimate for the methane contribution from all excreted manure through the day (5.1% for NSW farms, 4.7% Australia-wide average). With more than 80% of farms using pond systems (Watson & Watson 2012), this result suggests that one of the parameters used to estimate methane emissions from managed manure under the National Greenhouse Gas Inventory method (DCCEE 2009) such as fraction of total manure load or the methane conversion factor may be too low.

Table 9-11 Average predicted sludge and supernatant biogas production and GHG emissions.

	<i>Total biogas</i> <i>m³ d⁻¹</i>	<i>CH₄</i> <i>%</i>	<i>CO₂</i> <i>%</i>	<i>CH₄ yield per cow</i> <i>kg cow⁻¹ yr⁻¹</i>	<i>CO₂ yield per cow</i> <i>kg cow⁻¹ yr⁻¹</i>	<i>Total GHG emissions</i> <i>kg CO₂e cow⁻¹ yr⁻¹</i>
Sludge	20	71	28	10.5	4.2	225
Supernatant	25	51	49	9.8	9.4	215
Total	45			20.3	13.6	441

9.5.1.4 System implications of scenarios

The results from the high organic loading rate scenario indicate that an anaerobic pond operated at loading rates up to 0.4 kg VS m⁻³ will produce slightly lower COD removal efficiencies, but should produce effluent of reasonable quality and should not become overloaded provided the allocated sludge volume is not exceeded. Average effluent FCOD loading from the heavily loaded pond when sludge was below the threshold that triggers declining settling performance was 16 kg d⁻¹. Assuming BOD₅ loading to be about half that of FCOD based on the data presented in Chapter 7, this corresponds to an areal loading rate of 57 kg ha⁻¹ d⁻¹ (at the median recorded liquid depth), which exceeds the Australian recommended limit for DSE ponds (50 kg ha⁻¹ d⁻¹) but is within the workable range for facultative ponds. Given the high content of poorly degradable material, however, the elevated loading to the facultative pond could pose a problem

for effluent recycling for yard washing, particularly when the loading starts to rise as sludge nears the outlet, or after an extended period without sufficient effluent renewal. It is therefore recommended that a 10-20% buffer is allowed for in the sizing of facultative ponds supporting heavily loaded anaerobic ponds in systems that recycle effluent for yard washing. Alternatively (or additionally) heavily anaerobic ponds should be desludged annually to avoid compromised performance.

It is important to note here that this model considers influent wastewater that has passed through a solids trap before entering the pond. Raw DSE will contain higher concentrations of non-biodegradable and very slowly degradable particulate material that is likely to further reduce pond performance and shorten the time before the pond requires desludging. Research into raw wastewater characteristics and the impacts of solids traps on the various COD fractions is required to properly understand how anaerobic ponds would respond to different loadings associated with changes upstream.

Of the other scenarios only mixed annual desludging should have broader impacts on the pond and recycling system. Elevated effluent constituent concentrations may not persist for as long as indicated in the simulation and will depend on the settleability of the partially digested sludge. Nonetheless the results point to the potential for re-suspended particulate matter to be transferred to the facultative pond, impairing treatment and also potentially resulting in accumulation of sludge in the secondary pond. In the low seepage scenario, 40% of the additional FCOD retained in the effluent is non-biodegradable, which would cause a slight reduction in recycled effluent quality. Otherwise the higher load of (available) nutrients retained in the effluent should improve irrigation nutrient recovery rates unless lost to volatilisation (N) or precipitation (N and P). Changes in effluent loads caused by the presence of dead zones were very low and should have no bearing on the secondary pond or effluent recycling.

9.5.1.5 Desludging and nutrient recovery

The results from the first two desludging scenarios demonstrate the advantages of regular desludging in relation to maintaining effluent quality and accessing the nutrients contained in the sludge. Extracting just the sludge from the pond captures the bulk of particulate-bound nutrients and involves hauling fewer tanker loads. Removing supernatant in addition to the sludge promotes renewal of recirculated effluent and in doing so reduces nutrient losses that would otherwise occur in the facultative pond. It also captures larger loads of soluble nutrients, which in the case of N and P should

provide more immediate benefits to the pasture or crop it is applied to, but in the case of K may ultimately result in over-application.

Figure 9-21 compares the nutrient ratios of the sludge, supernatant and mixed sludge and supernatant pasture with that of the tailored fertiliser regime described in Chapter 7. Note that urea fertiliser (that rapidly hydrolyses to ammonium) and sludge/supernatant $\text{NH}_3\text{-N}$ were classified as available N, while fertiliser superphosphate and sludge/supernatant soluble orthophosphate were classified as available P. Sludge on its own provides the most directly transferrable mix of nutrients for strategic N fertiliser use, but would still require additional N if applied at rates appropriate to P or K demand. Supernatant has a similar N:P ratio and higher available N and P fractions but has a very large excess of K. The mix of sludge and supernatant also has an over-abundance of K, albeit less exaggerated than the supernatant ratio. The critical difference between the separately and mixed sludge-supernatant scenarios is that under scenario B supernatant can be pumped or hauled to different parts of the farm and applied at different rates, whereas under the mixing scenario, the land application rate would be set by the K content, which would cause both N and P to be under-supplied. Thus while mixing the pond contents before desludging provides a more homogeneous product and simplifies the process, it limits control over application rates and nutrient recovery.

The other disadvantage of scenario C is the very poor effluent quality that follows each desludging event. Average effluent FCOD loading for the scenario (including days with no flow) was 12 kg d^{-1} , which corresponds to a very manageable facultative pond BOD loading of approximately $38 \text{ kg ha}^{-1} \text{ d}^{-1}$. However, as reported in Chapter 7, even the mild impairment of anaerobic pond performance associated with a high sludge level caused a measurable decline in facultative pond effluent quality. Hence the elevated load of poorly degradable particulate material from sludge mixing would still likely result in higher particulate COD concentrations in facultative pond effluent. The impact would be mitigated with desludging occurring in spring and the increasingly warm temperatures ensuring the facultative pond performs at its peak. Nonetheless, close attention should be paid to the quality of recycled effluent following desludging of the anaerobic pond if mixing is employed.

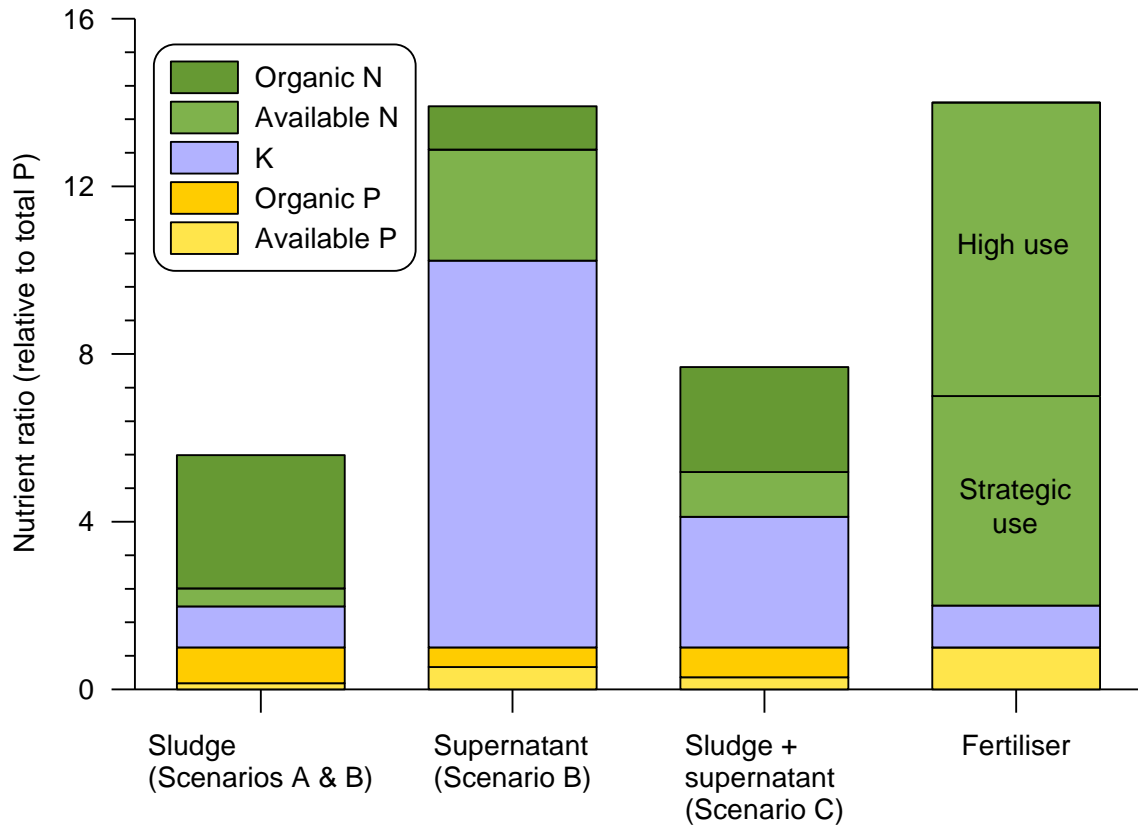


Figure 9-21 Nutrient ratios in the sludge, supernatant, mixed sludge and supernatant compared with a fertiliser regime appropriate to recent soil nutrient levels. The denominator of all ratios is total P.

9.5.2 Model Limitations

There are a number of limitations associated with the robustness and generalisability that limit (but do not preclude) its utility outside the detailed observations and data confines of this study. The first is that the model has not been subjected to validation, which means the various assumptions and fitted parameters have not been tested outside the calibration domain. Since there was insufficient data in the time series to allow it to be divided into discrete calibration and validation periods, validation will require the acquisition of a data set that includes influent, effluent and sludge characteristics as well as some measurements or estimates of inflows and outflows, as well as seepage. The focus of any validation would primarily lie with testing those parameters that were identified as being highly influential in the sensitivity analysis (including the characterisation parameters that are also discussed below), but should also extend to testing the more empirical parameters including the sludge-supernatant flux coefficient and the settling parameters.

9.5.2.1 Influent COD characterisation and related model parameters

Another critical limitation is the fact that model relies on a largely theoretical break down of the sub-components of COD. On account of the long retention time of the pond, influent acetic and propanoic acid fractions of readily biodegradable COD are relatively inconsequential as evidenced by high rates of acetate formation by fermentation of complex readily biodegradable COD and propionate conversion, and of acetate destruction. The adjustment of the non-biodegradable soluble COD fraction f_{US} in the sensitivity analysis showed that despite the extended retention time of the system, effluent from the facultative pond contains residual biodegradable soluble COD, causing the method adopted for estimating f_{US} to overestimate the fraction. Experimental quantification of this fraction could involve simple batch tests performed on seeded facultative pond effluent (to minimise the time requirement).

The greatest uncertainty in relation to COD loading, however, is associated with the biodegradability of the particulate fraction, which as mentioned earlier exerts significant influence on predictions of sludge constituent concentrations. While the COD fraction of combined very slowly biodegradable and non-biodegradable material was estimated using actual data, the division between the two sub-components was based on data reported in the literature. The uncertainty surrounding sludge predictions based on assumed fractionation parameters is compounded by their interaction with the two parameters related to the hydrolysis of very slowly biodegradable material (the rate and half saturation constants). The higher the assumed non-biodegradable content, the higher the hydrolysis rate needs to be to destroy enough COD and VSS to achieve calibration with the sludge data. Conversely, a lower non-biodegradable fraction means a larger pool of cellulosic material that is susceptible to hydrolysis, which leads to a lower hydrolysis rate. The OHO decay rate constant also interacts with the hydrolysis of very slowly biodegradable material. Higher decay rates push up the sludge COD by increasing endogenous decay products that settle out to the sludge, which would force a higher hydrolysis rate to achieve calibration.

The balance found in the model calibration among these four intertwined parameters appears sound given the sensitivity of the model to parameter adjustments and the performance of the model in the scenario simulations. However, this is no guarantee of accuracy. The only way to reduce the uncertainty surrounding this aspect of the model is to conduct laboratory experiments. The cellulose and hemicellulose fraction (f_{XBC}) and lignin COD fraction (f_{XIL}) should be verified first since the initial values have been drawn from raw manure analyses as opposed to wastewater that has been through

solids separation. The OHO decay rate ($b_{H,An}$) was drawn from Whichard's (2001) laboratory work with sequencing batch reactors treating solids separated DSE, which could be adapted to reflect the conditions of stabilisation ponds. Whichard's measured $b_{H,An}$ was 67% lower than the BioWin default. If it is in fact inaccurate, it is likely that it would be even lower as the cellulosic material hydrolysis rate is already high within the range between experimentally determined values for cellulose and hemicellulose. The two hydrolysis parameters were initially based on an amalgam of corresponding discrete values derived for cellulose and hemicellulose by Myint, Nirmalakhandan & Speece (2007) using a heated laboratory scale reactor. Again an adaptation of the experimental approach could be used to verify the final fitted values.

9.5.2.2 P fractionation

The process of model calibration revealed that the conventional BioWin fractionation of P does not adequately describe the forms of P found in DSE. A reasonably high level of confidence can be maintained for the P data against which this model was calibrated since analyses of effluent concentrations of 32 effluent samples were verified by in-house analyses. Moreover, the mass balance for the period (Chapter 7) produced a relatively low error of 5%. The influent soluble orthophosphate content is well-defined using DRP, while poorly biodegradable particulate P could be estimated from the sludge P concentration. However it is clear from the dramatic improvement to the model made by adding a fourth P state variable that DSE contains a significant P fraction that is neither soluble nor settleable.

The presence of this fraction that also appears to be poorly biodegradable, or rapidly replenished from another P fraction could be verified by analysing particulate P in liquid decanted from settled influent samples. The inference was made that the unknown fraction could comprise P complexed with polyvalent cations (primarily Ca) to organic matter. Determining the true chemical nature of this fraction will require more involved analyses such as ligand exchange extraction of non-settleable manure solids, enzymatic hydrolysis and nuclear magnetic resonance spectroscopy. Examination of this form of P should also consider the relationship with Ca^{2+} and Mg^{2+} . The modelling suggested that Ca^{2+} was one of the by-products of sludge hydrolysis. Known to be closely associated with P in dairy manure (Turner & Leytem 2004), it is also possible that release of complexed P may also liberate Ca^{2+} .

9.5.2.3 Settling and sludge-supernatant flux

While settling under low sludge conditions based solely on mass partitioning is similar to the first order removal approach taken in other biokinetic stabilisation pond models (see Chapter 2), the empirical handling of the deterioration in settling efficiency caused by elevated sludge levels limits the generalisability of the model. To incorporate a dynamic settling model capable of simulating re-suspension of sediments would add considerable complexity to the model and would be difficult to verify experimentally. It may be preferable, then, to attempt to validate the approach taken here on an independent data set and test whether the approach can be applied more generally.

As discussed in section 9.5.1.2, the transfer of soluble constituents appeared to be reasonably represented by a hydraulic flow that was a function of biogas flow coupled with a dewatering unit to return particulate material to the sludge. The fitted sludge-supernatant flux coefficient largely ultimately determines the scale of the flow, which means that changing the basis of the flow function would not dramatically affect the model outputs provided the new model also contained a fitted parameter. However, for the purpose of making the pond model generalisable the assumption that the flow is driven by biogas flow needs to be tested experimentally or using detailed modelling.

Pescod (1996) stated that transferral of sludge constituents is aided by biogas, but also suggested that pond performance may be a function of the sludge surface area. While biogas distribution may be a function of surface area, production remains a function of sludge volume, hence relating performance to sludge area also infers a diffusion based mass transport process. Colomer & Rico (1993) modelled flux from the sludge as the product of sludge mass quantified on an areal (per m^2) basis and its rate of fermentation. Transport of N and P were directly proportional to these variables (adjusting for liquid depth), but BOD transport was scaled to account for 'drag of the mud by biogas' (p. 679). Rajbhandari et al. (2007) took a diffusion approach to simulating sludge-supernatant exchanges. Interestingly their mass transfer coefficients were very high (0.8 m d^{-1} for soluble COD), suggesting that the equation described dispersion assisted by biogas flow. It would seem that it is reasonable to assume biogas is the main driver behind sludge-supernatant flux, but the form of the equation used to describe the process needs further examination.

Assuming that the biogas function is in fact a sound basis for modelling sludge-supernatant flux, the flow equation needs to draw directly on BioWin's off-gas flow rate prediction rather than estimates of biogas flow generated in data pre-processing, which requires making the implementation of BioWin used for this model compatible with the

BioWin Controller module. Average biogas production (from the sludge and supernatant) as predicted by BioWin was $45 \text{ m}^3 \text{ d}^{-1}$, which is substantially higher than the $32 \text{ m}^3 \text{ d}^{-1}$ average used as the basis for the pre-processing estimates of total biogas production. The difference is in part related to the high CO_2 content of supernatant biogas but would also be related to the inaccuracy of the mass balance underpinning the pre-processing estimation method. The biogas flow used to predict sludge-supernatant flux should actually be that coming from the sludge only, which was predicted to average around $20 \text{ m}^3 \text{ d}^{-1}$.

Figure 9-22 is a plot of total biogas flow estimated in the data pre-processing together with BioWin's predictions of sludge biogas production. As alluded to above, adjusting the calibrated model to use BioWin biogas predictions would not cause a radical change to the outputs since the flux coefficient would be raised to account for the offset that clearly exists between pre-processing estimates and the BioWin predictions. The changes to the model outputs would therefore be more subtle. The pre-processing estimates reasonably approximate the seasonality of biogas flow, leaving the largest deviations from the current model outputs to arise from day-to-day differences between estimated and predicted flows and differences arising from pond establishment and desludging. This would suggest that while the current calibration may not accurately predict the minutiae of daily fluctuations in effluent concentrations, it may be considered reasonably robust and appropriate to predicting trends and gauging the effects of the scenarios explored above. However, further research is required to better understand the roles of diffusion and biogas-driven advection in sludge-supernatant mass transfers and their effect on different constituents.

9.5.2.4 Nitrogen imbalance and non-biodegradable soluble N

The strongest fit to observed effluent and sludge N concentrations arose from assigning 100% of soluble organic N to the non-biodegradable pool. This essentially assumes that any biodegradable N present in raw manure is mineralised before it reaches the pond and that the remaining soluble organic N is made up of non-biodegradable amino acids. The need for this assumption in part arises from an imbalance in effluent and sludge data. The mass balance given in Chapter 7 shows that there was either an excess of N partitioned to the sludge or a shortage of incoming N, which would indicate that the analyses of influent or sludge TN may not have been accurate. No in-house verification of N analysis was performed, so the source of the error could not be traced. The model was not particularly sensitive to f_{NUS} , making its verification a relatively low priority to the ongoing development of the current model,

although it may become more of a priority in expanding the model to the facultative pond and effluent recycling.

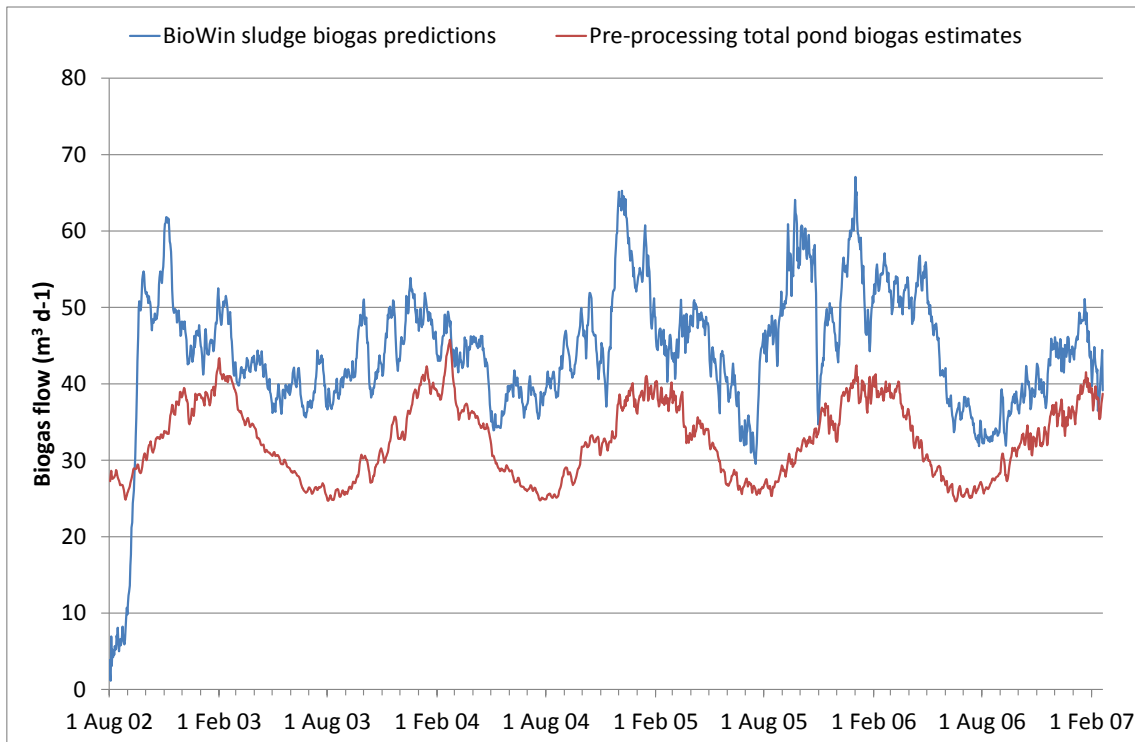


Figure 9-22 Biogas flows estimated in the data pre-processing and predicted in BioWin.

9.5.3 Model Expansion

Developing a complete model of the two-pond system was beyond the scope of this thesis, but remains an important next phase in producing a model that can be used to simulate and optimise effluent recycling, nutrient recovery and other DSE management strategies. A model of the facultative pond could be used to better understand the partitioning of nutrients in the pond and develop strategies to maximise nutrient recovery. It could also be used to understand how fluctuations in the liquid volume impact on the treatment performance of the pond. Introducing a recycle connection between the facultative pond and the anaerobic pond models would provide a more powerful means of understanding the relationships between accumulation of different inert and non-biodegradable constituents, pond performance, struvite precipitation and pond hydrology.

The preceding chapters have laid the groundwork for formulating a model of the facultative pond of a similar form to the anaerobic pond model. In addition, the effluent predictions from the anaerobic pond model should simplify the process of characterising the influent to the pond. The present anaerobic pond model uses

regression equations to predict the effect of recycled effluent on influent characteristics (between sampling events). Linking the facultative pond model to the anaerobic pond model via a recycle connection would eliminate the need for the regression models. However, it would also require the development of a means to simulate the manure load from the dairy and the effect of the solids trap on raw wastewater.

9.6 SUMMARY

The model of the anaerobic pond formulated in BioWin as described in Chapter 8 was calibrated through an iterative process of adjusting critical parameters related to:

- internal hydrodynamics (sludge-supernatant flux coefficient);
- mass transfer (surface turbulence coefficient);
- settling (influent dewatering unit efficiency, sludge accumulation threshold, slope of the linear decline in the secondary dewatering unit efficiency);
- kinetics of the hydrolysis of very slowly biodegradable COD (maximum cellulosic material hydrolysis rate, cellulosic material hydrolysis half saturation constant);
- stoichiometry of the hydrolysis of very slowly biodegradable COD (particulate very slowly biodegradable and non-biodegradable Ca and Mg fractions);
- influent characteristics (soluble non-biodegradable N fraction, non-settleable particulate P fraction);

In the light of the findings of Whichard (2001) that most kinetic and stoichiometric parameters used in conventional activated sludge models are transferrable to DSE treatment, and following the recommendation from Alvarado et al. (2012), adjustments to BioWin default parameters beyond the changes made in the initialisation of the model, were avoided. The calibrated model produced predictions of effluent and sludge characteristics with relative errors generally between 5 and 15%. Predicted effluent concentrations exhibited appropriate responses to the gradual accumulation and relatively sudden removal of sludge based on a linear decline in solids removal efficiency. The calibration process showed that characterisation of DSE requires further research to quantify the poorly settleable fractions of particulate, organically-bound P and N and to validate the assumptions made in relation to non-biodegradable and very slowly degradable fractions of COD. It also demonstrated the important role played by biogas-assisted flows between the sludge and supernatant in transporting hydrolysis and fermentation products including VFAs, ammonia-N and orthophosphate.

The model produced predictions of biogas emissions comparable to estimates made in Chapter 6 and to published data. Methane production in terms of COD loading to the pond is $0.17 \text{ m}^3 \text{ kg}^{-1} \text{ COD d}^{-1}$ and corresponds to a herd production rate of $32.7 \text{ m}^3 \text{ cow}^{-1} \text{ yr}^{-1}$ and a volumetric production rate of $0.02 \text{ m}^3 \text{ m}^{-3} \text{ d}^{-1}$. The GHG equivalent of these emissions is $427 \text{ kg CO}_2\text{e cow}^{-1} \text{ yr}^{-1}$, which is higher than published estimates for the methane GHG contribution from the entire manure load of a cow on a typical Australian dairy and shows the multiplying effect of digestion in anaerobic ponds.

Sensitivity analysis showed that the most critical model parameters were related to sludge loading and biodegradation including the influent fractions of non-biodegradable and very slowly biodegradable COD, the threshold beyond which settling efficiency starts to decline, the kinetic parameters for hydrolysis of very slowly biodegradable material and the OHO anaerobic decay rate. The effects of adjusting these parameters were mostly confined to sludge predictions, but the assumed values for f_{XBC} and $b_{H,An}$ would nonetheless have significant influence on the calibration of the model due to the close interactions between the parameters. With regards to effluent predictions, the model was most sensitive to f_{XBC} , the assumed fractions of soluble non-biodegradable N and non-settleable P and the calculation of soluble non-biodegradable COD. It is worth noting that five of the eight most sensitive parameters were influent characterisation parameters, highlighting again the need for more detailed characterisation of DSE.

The calibrated model was used to run a series of simulations designed to test various design and operation scenarios including the existence of a dead zone causing hydraulic inefficiency, increasing the loading rate to the pond, performing different forms of desludging on a regular basis and the proper sealing of the pond floor to prevent seepage losses. The first scenario simulation demonstrated that the performance of anaerobic ponds designed according to current conventions should not be affected by the formation of a dead zone occupying up to 25% of the total pond capacity, except at very high sludge levels.

Increasing the peak organic loading rate to the pond to $0.4 \text{ kg VS m}^{-3} \text{ d}^{-1}$ mildly reduces treatment performance under normal operating conditions, but also accelerates the decline in effluent quality caused by sludge accumulation since sludge accumulates more rapidly. Stabilisation of the sludge was found to be unchanged by the additional loading, but more frequent desludging is required to avoid pond failure. Heterotrophic and methanogen biomass populations were largely unaffected by the higher loading

rate and more frequent desludging, indicating that the slow growth rates of microorganisms in ponds are not related to substrate availability.

The regular (annual) desludging scenario modelling incorporated three approaches to desludging – removal of sludge only, sludge and supernatant extracted separately, and mixing of sludge and supernatant before extraction. The first two scenarios had much the same impact on pond performance in preventing the rise of constituent concentrations associated with high sludge levels. Under the mixing scenario, effluent concentrations of particulate constituents remain very high until the re-suspended material eventually settles out, which would have implications for treatment efficiency and potentially sludge accumulation in the secondary pond. Critically annual desludging did not result in biomass washout under any of the scenarios. Nutrient recovery potential is highest using separate extraction of sludge and supernatant. Applications of effluent would be constrained by K^+ levels, although segregated effluent and sludge provides some additional flexibility in satisfying agronomic nutrient application rates, helping avoid over-application of K. Extracting sludge alone provides a good balance of nutrients but does not access the larger pool of plant available (soluble) nutrient forms held in the supernatant. Mixing sludge and supernatant taps into the available nutrient pool but is bound to applications set according to K^+ requirement and causes more particulate forms to remain in the pond, which would likely compromise recycled effluent quality.

Sealing the pond to meet best practice standards in relation to preventing seepage increases nutrient recovery potential by around 10%. The corresponding increase in the soluble COD load to the facultative pond should have only a minor impact on the quality of recycled effluent as it is mostly made up of readily biodegradable COD.

The sheer number and complexity of the various processes at play, as well as their interactions, means that the model as it stands will almost certainly require further refinement and perhaps some more radical changes to specific elements. Many of the model parameters will need to be revisited should more detailed characterisation of DSE be undertaken and data relating to chemical and biological kinetic parameters from lab and field based experiments become available. In addition, the model needs to be validated outside the data domain of the calibration to test the various parameters that have been tailored to suit the conditions of this particular anaerobic pond, particularly the empirical sludge-supernatant flux and compromised settling parameters. Nonetheless the development of this model represents a significant progression in understanding and predicting the behaviour of DSE ponds.

Chapter 10

CONCLUSIONS AND RECOMMENDATIONS

The research presented in this thesis was formulated with the aim of addressing four research gaps in the field of DSE management and treatment using pond systems:

- lack of data on DSE pond systems, particularly within Australia;
- simplistic understanding of treatment processes, nutrient partitioning and losses in DSE pond systems and their effects on nutrient recovery;
- lack of data on the impacts of effluent recycling on pond system performance and nutrient recovery;
- application of dynamic biokinetic modelling to DSE ponds.

All four aspects necessitated the collection of a comprehensive data set that encompassed pond loading and conditions, environmental forcing, pond hydrology and hydraulics and effluent constituent loads. The data generated for this thesis thus constitutes an unprecedented data collection effort both in Australia and overseas in terms of scope, rigour and detail. In addition, the data collection was undertaken on a commercial dairy farm otherwise entirely separate from research activities, which not only added a level of practical difficulty to the activity, but also ensures that the data are a true reflection of real world operations. Many of the outcomes of this research are related to characterisation of the pond system and its performance. Findings specific to the anaerobic pond were then translated into a dynamic, biokinetic model, which on account of the detailed data backdrop, performed well at predicting pond performance not only under normal operating conditions, but also in the compromised state of high sludge levels.

10.1 POND SYSTEM CHARACTERISTICS

10.1.1 Water Quality

Real-time measurement of water quality parameters and seasonal profiling of the water column in each pond unveiled the complexity of DSE ponds, demonstrating the nature and extent of spatial and temporal variability of temperature, pH, EC, DO, ORP and turbidity. The anaerobic pond was characterised by relatively constant physico-chemical conditions, dominated by heavily reducing conditions created by the high organic load that kept pH close to neutral and DO at zero throughout the year. The water column was similarly consistent with vertical mixing from rising biogas bubbles

ensuring that gradients in water quality parameters, including temperature, were practically non-existent. The only form of stratification in the pond was physical, caused by the ever-growing bank of sediments or sludge, identifiable by a sudden drop in pH and EC at the interface with the overlying supernatant.

The facultative pond exhibited a more complex profile, characterised by gradients in most water quality parameters forming between a heated, aerated, alkaline surface layer (epilimnion) and cooler, anaerobic, and more neutral and saline conditions at the bottom. Gradients were steepest during summer when solar radiation heated the water and stimulated algal photosynthesis at the surface, producing dramatic diurnal peaks in DO (at times reaching supersaturation with concentrations above 20 mg L^{-1}), ORP, pH (approaching 9.0) and turbidity. Under very hot conditions in summer, pH and EC gradients were observed to extend right to the bottom of the pond as heightened temperatures exaggerated the contrast between anaerobic and aerobic treatment processes occurring at depth and at the surface, respectively.

Stabilisation ponds are classified according to their aeration status and redox potential; however the two ponds were also distinguished by their temperature and pH, with the sludge blanket effectively regulating both in the anaerobic pond while the facultative pond was defined by thermal and biochemical stratification. EC on the other hand, followed a persistent rising trend in both ponds that was caused by effluent recycling and associated accumulation of salts. The trend was periodically interrupted by large rainfall events and desludging of the anaerobic pond. It was also reversed for a period primarily by the combination of higher rainfall and regular effluent irrigation, although precipitation of mineral struvite from the facultative pond effluent was shown to contribute significantly to the reduction in EC levels.

10.1.2 Hydrology

A system water balance was developed to provide full accounting of the hydrology of the pond system for subsequent wastewater treatment modelling. It also provided some valuable insights, most notably the likely infiltration of seepage from the anaerobic pond directly into the facultative pond. While this modelling-derived observation could not be verified with field measurements, the stark contrast between the very low estimates of (net) seepage losses from the facultative pond and the much higher losses from the anaerobic pond and other earthen ponds reported in the literature, as well as the very low apparent (fitted) hydraulic conductivity, present a strong case that such infiltration is occurring. The water balance also showed that evaporation losses from the ponds are higher than what would be predicted for other

water bodies using a conventional combination method approach. This is related to elevated liquid temperatures, the formation of an internal boundary layer over the water surface, and in the anaerobic pond, turbulence at the liquid surface caused by escaping biogas bubbles. The standard error of the calibration and sensitivity analysis of the seepage and evaporation models indicated that there is significant uncertainty in the apportionment of the water balance residual between the two components. Confidence may be drawn, however, from the rigour applied in the calibration process, the reasonable agreement between the model predictions and similar data published elsewhere, and the strong correlation between observed and predicted data in the validation of the models.

10.1.3 Hydraulic Regimes

The hydraulics and hydrodynamics of the pond system were also characterised to provide a basis for deciding how to handle the same when modelling wastewater treatment. The anaerobic pond was well mixed both vertically and transversally as evidenced by lack of temperature and EC gradients. Analysis of mixing energy inputs including inflows, wind and rising biogas bubbles showed that mixing would be dominated by biogas flux except during brief periods of high wind or inflow and that these inputs would be more than sufficient to prevent or break down thermal stratification. The HRT of the anaerobic pond, however, is compromised by sludge accumulation, which occurs at a rate of $0.73 \text{ m}^3 \text{ d}^{-1}$ or $0.88 \text{ m}^3 \text{ cow}^{-1} \text{ yr}^{-1}$, increasing the potential for poor biological treatment performance, particularly under high flow conditions. The active treatment volume of the pond can also be compromised by hydraulic inefficiencies which were explored in a series of drogue tracking experiments. The results indicated that there is potential for short-circuiting to occur but only under conditions of very high peak flow, which occur less than 5% of the time. The drogue experiments did not completely rule out the potential for stagnancy, but flows towards and away from the hydraulically sheltered region orthogonal to the inlet, plus a lack of EC gradient suggested that advective mixing did occur in this part of the pond. Based on the above findings it was determined that the hydraulic regime of the supernatant of the anaerobic pond could be reasonably approximated by a complete mix reactor.

The hydraulic regime of the facultative pond was found to be decidedly more complex. Data were not collected on the internal hydrodynamics of the facultative pond on account of prevailing quiescent conditions; however transverse EC gradients indicated that influent to the pond was sinking to the bottom and moving radially from the inlet in a semi-plug flow fashion. Displacement and diffusion, or thermal upwelling in autumn,

convey suspended and soluble constituents upwards into a well-mixed middle layer that varies in volume with the rate of effluent pumping to irrigation. On more than 90% of days and around 35% of nights, thermal stratification defines an overlying, hydraulically discrete surface layer (epilimnion) that is prone to environmental forcing and biochemical gradients. When thermal stratification is in force exchanges between the hypolimnion and epilimnion would be limited to diffusion and particulate settling. Outside stratified periods, the middle and upper two layers appear to merge, with mixing driven by diffusion, and convection and wind-induced currents. However, contradictions between the theoretical ability for wind to break down thermal stratification overnight and observed lack of destratification suggested that energy imparted by wind shear is directed more into horizontal circulation currents than vertical mixing.

10.2 DEVELOPING A DYNAMIC BIOKINETIC MODEL OF THE ANAEROBIC POND

In developing a dynamic biokinetic model of the anaerobic pond, the approach pioneered by Houweling et al. (2005) and (2008) and Gehring et al. (2010) of adapting an existing activated sludge model was adopted. This was a pragmatic decision that recognised that sufficient data could not be collected to calibrate a computation fluid dynamics model and that the scope of the research did not allow for development of a computer program or environment in which to implement a full biokinetic model, with or without mass transfer or fluid dynamics equations. The other benefit of the approach was to be able to leverage the significant existing stock of knowledge in biological wastewater treatment modelling that has been compiled in contemporary activated sludge models.

10.2.1 Formulation and Initialisation

The model was thus implemented using the Activated Sludge/Anaerobic Digestion (ADSM) model in the BioWin simulation environment (EnviroSim Associates Ltd. 2007) which incorporates a comprehensive suite of process models directly applicable to anaerobic stabilisation ponds. It also provides a means of incorporating additional process models and state variables into the simulation platform, which allowed the modelling to accommodate the prolonged hydrolysis of poorly biodegradable cellulosic material and the conversion of endogenous products, both of which occur with the very long solids retention time of the sludge. A simple reactor configuration was devised to represent the hydraulic regime of the pond. The pond was divided into an anaerobic digestion reactor representing the sludge and, based on the findings from Chapter 6, a single complete mix reactor representing the supernatant. Flux between the reactors

was quantified as a (constant) fraction of biogas flow. Settling under normal conditions was simulated using simple mass partitioning applied to the influent while sludge-supernatant flux was subject to 100% removal of particulate material. When sludge came within 1.2 m of the liquid surface, the removal efficiency applied to the sludge-supernatant flux followed a linear decline.

With mostly aggregate constituent data available from the wastewater sampling and analysis, an extensive literature review was undertaken to inform a more detailed breakdown of influent composition. Key kinetic and stoichiometric parameters specific to DSE were also drawn from the literature. Model initialisation required pre-processing of input data including hydrologic, temperature and influent constituent concentrations in preparation for dynamic simulations at a daily time step. Wastewater sampling had been conducted every few weeks, thus it was necessary to synthesise influent characteristics on the days between sampling events using multiple regression models based on constituent loads.

10.2.2 Calibration and Sensitivity Analysis

Model calibration was a non-linear, iterative process that involved fitting 11 parameters using various aspects of the calibration data set. Model predictions were generally close to observed data and followed the large trends associated with sludge accumulation. Mean absolute percentage errors for sludge and effluent predictions generally lay between 5% and 15%. The largest error margin was related to sludge TSS predictions being 25% too low; however this was attributed to an issue with analysis of sludge fixed solids rather than a flaw in the model.

The calibration process revealed shortcomings with applying the conventional fractionation of P to DSE. Organically bound P in DSE appears to be held mostly in non-settleable colloidal material. An expedient but ultimately unsatisfactory fix was to add a non-settling state variable representing this fraction of P. The same issue probably applies to organically bound N, since a large fraction of organic N had to be designated as soluble to achieve agreement. Another modification was to add stoichiometric parameters that yielded Ca^{2+} and Mg^{2+} from hydrolysis of very slowly biodegradable material.

Sensitivity analysis showed that the model parameters that wielded the largest influence on model (sludge) predictions were influent fractions of non-biodegradable and very slowly biodegradable material ($f_{SBC,i}$), the kinetic parameters for hydrolysis of very slowly biodegradable material, the threshold for compromised settling, and the

heterotroph decay rate. Interactions between these parameters would mean that an inaccurate assumed value for one of these parameters would have significant influence on the calibration of the fitted parameters. Effluent predictions were less sensitive to the main assumed and fitted parameters, although f_{SBC} , the assumed fractions of soluble non-biodegradable N and non-settleable P and the calculation of soluble non-biodegradable COD all had relative sensitivities of over 25% with at least one sensitivity index. Five of the eight most sensitive parameters were influent characterisation parameters, emphasising the need for more detailed characterisation of DSE.

10.2.3 Limitations

The main limitations of the model relate to its generalisability outside the calibration data domain and include:

- lack of validation;
- dependence on empiricisms for the decline in settling performance caused by rising sludge and sludge-supernatant flux;
- simplistic handling of the poorly settleable P fraction;
- influent COD fractionation based on inferences from other data sources.

10.3 POND TREATMENT PROCESSES AND PERFORMANCE

10.3.1 The Role of Sludge

Analysis of wastewater and sludge sampling data together with the biokinetic modelling demonstrated the critical role played by the sludge accumulating in the anaerobic pond. Continuously receiving fresh particulate organic material but without an outflow, the sludge effectively behaves like a batch digester with a solids retention time of several years. The combined effect of settling and digestion produces TVSS and particulate COD removal rates of about 80%, with actual destruction/conversion rates of around 40%. Conversely, mineralisation of particulate-bound N and P results in increases to loads of ammonia-N and orthophosphate in the effluent of 15% and 25%, respectively. Hydrolysis of particulate organic matter also liberates complexed forms of Ca and Mg, producing net increases in effluent Ca^{2+} and Mg^{2+} loads. Sludge digestion influences pH and dissolved salt levels by converting organic material to carbon dioxide (and methane) and thereby pushing the carbonate system equilibrium towards carbonic acid. Modelling showed that VFA production in the sludge was also important to pH levels, so much so that if not for hydraulic or diffusion flux to the supernatant,

accumulation of VFAs can result in very low pH and inhibition of fermentation and methanogenesis.

The physical level of sludge accumulation is also a fundamental determinant of anaerobic pond effluent quality, and can have flow on effects on facultative pond effluent quality. When allowed to come within 1.2 m of the liquid surface or about 0.7 m of the outlet intake, rising sludge was observed to cause an approximately linear decline in settling efficiency, resulting in rising effluent COD, BOD₅, TSS, TVSS and TP concentrations. Effluent concentrations of dissolved salts (EC, TDS and TDFS) were also correlated with sludge level due to the continued production and concentration of bicarbonate, Ca²⁺, Mg²⁺, ammonium and orthophosphate ions by the rising sludge. The declining anaerobic pond effluent quality caused facultative pond effluent COD, TSS, TVSS concentrations to peak just before the anaerobic pond was desludged, and contributed to other constituents peaking soon after.

10.3.2 Anaerobic Pond Performance

Hydrolysis of particulate material is the rate limiting step in biological treatment in the anaerobic pond as evidenced by the high conversion rates for soluble COD (60%) and BOD₅ (80%) despite the continual contributions of solubilised organic material from the sludge. Based on this level of COD removal, predicted methane production rates in terms of COD added, yield per cow and pond volume are 0.17 m³ kg⁻¹ COD d⁻¹, 32.7 m³ cow⁻¹ yr⁻¹ and 0.02 m³ m⁻³ d⁻¹, respectively, which amounts to 427 kg CO₂e yr⁻¹ or about 7% of the emissions from a typical dairy farm in NSW.

In terms of nutrient removal, the pond has very limited impact on TN or TP loads. Sedimentation removes 50% of particulate P, about half of which is returned to the supernatant as soluble P, resulting in a net TP removal of just 24%. N removal is similarly low; however, there is uncertainty surrounding the exact values as there appeared to be an imbalance in the various mass flows. Settling was estimated to remove over 40% of organic N; yet apparent ammonia-N generation was higher than apparent mineralisation, causing TN removal to be only 13%. The imbalance also prevented close agreement between predicted and observed N effluent and sludge concentrations in the modelling, and is thought to have arisen from either sampling bias or an inconsistency between laboratory analysis of influent and sludge N. The imbalance is small and does not alter the finding that volatilisation losses from the pond are low, presumably due to the neutral pH. The low particulate nutrient removal rates also show that organic forms of N and P are concentrated in fine, non-settleable particles, which concurs with findings elsewhere (Meyer, Ristow & Lie 2007). This, and

the contributions of soluble forms from the sludge, challenge the commonly-held notion that DSE nutrients readily 'drop out' in pond systems.

Simulations run with the biokinetic model showed how the pond recovers rapidly from the shock of desludging. Even annual desludging that removes the majority of sludge and effluent should not cause wash out of critical heterotrophic, acetogenic or methanogenic organisms that would lead to compromised treatment performance. The presence of a dead zone occupying up to 25% of the supernatant volume should also have little bearing on the treatment performance of the pond. Lining the pond to achieve a seal that meets current BMP standards would cause a small rise in effluent COD concentrations, a fraction of which would be passed on to recycled effluent from the facultative pond. It would also, however, increase potential nutrient recovery by around 10% and increase the fraction of plant available nutrients in the effluent. In general, the modelling results showed that except under conditions of high sludge, the pond is resilient to hydraulic perturbations.

10.3.3 Facultative Pond Processes and Performance

Treatment processes are fundamentally different in the facultative pond. Due to the dramatically reduced solids load, settled solids are hydrolysed fast enough to prevent sludge accumulation. Destruction/conversion of organic material is effective but limited by the high percentage of non-biodegradable particulate and soluble material, resulting in TVS and COD removals of 26% and 36%, respectively. Apparent removal by sedimentation is also not as effective (47% and 52% for TSS and TFSS, respectively) due to the fact that the suspended matter remaining in the effluent from the anaerobic pond is poorly settleable. As such, nutrient removal is mostly associated with reductions in soluble forms, with removal of organic/particulate forms of N and P contributing to 10% or less of the removal of their corresponding total fractions. Ammonia-N removal in the facultative pond is around 24%. The elevated pH in the upper region of the supernatant, and published research on N removal in DSE ponds suggest that this is probably caused by volatilisation. However, in the absence of flux measurements for ammonia or N gas, removal by nitrification and/or nitrification combined with denitrification cannot be categorically ruled out.

A third process that contributes to N removal is struvite precipitation, which was observed to occur over autumn and winter under specific conditions including:

- struvite supersaturation index around 4.4;
- elevated salt levels (around 4000 $\mu\text{S cm}^{-1}$) causing heightened ionic activity;

- pH above 8;
- temperature below 20 °C;
- high mixing energy and/or contact with submerged, rough surfaces.

Despite the facultative pond supernatant being supersaturated at every sampling event, struvite precipitation was observed to be active mainly over the autumn and winter of 2006. pH data from the flood wash tank where most precipitation occurred indicated a subtle rise over the precipitation period, which combined with lower temperatures and possibly a shift in the equilibrium precipitation was estimated to have reduced the salt load of recycled facultative pond effluent by 2.5 kg per day, removing approximately 0.2 kg N per day as well as 0.3 kg P d⁻¹ and 0.2 kg Mg²⁺ d⁻¹. These rates correspond to 3% of pond TN loading or 5 % of NH₃-N loading, 23% of TP loading or 49% of DRP loading, and 12% of Mg²⁺ loading, respectively.

10.3.4 System Performance

Incorporating sedimentation and accounting for seepage losses, the pond system as a whole achieved effective removal of TS (59%), TVS (78%), TSS (90%), TVSS (90%), COD (84%), FCOD (69%) and BOD₅ (89%). TP removal approached 50%, while TN removal was only 33% (although is likely to be slightly higher if the N imbalance in the anaerobic pond is due to inaccurate influent analysis). Despite contributions from sludge mineralisation in the anaerobic pond, the system produced net reductions in NH₃-N and DRP loads through volatilisation, precipitation and possibly nitrification or nitritation combined with denitrification in the facultative pond. Conversely, Ca²⁺ and Mg²⁺ loads increased through the system due to the contributions from the anaerobic pond sludge being higher than removal (precipitation) in the facultative pond.

10.4 IMPLICATIONS FOR DSE MANAGEMENT

Current understandings of nutrient partitioning and losses in DSE pond systems do not appear to reflect actual conditions, at least in the case of the system that was the subject of this research. Partitioning of N and P to the sludge in the primary anaerobic pond was much lower than generally anticipated in design guidelines and tools. In addition, N losses from volatilisation are much lower than the 40-50% anticipated in guidelines and tools. Assuming that design figures are based on American experience, this may be related to the lower N loading and concentrations in the pond supernatant. Precipitation of struvite from recycled effluent was found to cause P losses that were comparable to sludge accumulation in the anaerobic pond; however precipitation will

only occur under supersaturation conditions so should not be considered a regular loss mechanism.

Seasonal measurements of sludge volume have provided validation of the current design figure for sludge accumulation in primary ponds. Existing best practice guidelines suggest using a rate of $0.0045 \text{ m}^3 \text{ kg}^{-1} \text{ TS}$ in the influent – the estimate from the field data was $0.0043 \text{ m}^3 \text{ kg}^{-1} \text{ TS}$ added, equivalent to $0.88 \text{ m}^3 \text{ cow}^{-1} \text{ yr}^{-1}$.

The data produced in Chapter 4 can be used as a guide to diagnosing the performance of DSE pond systems using simple water quality parameters. EC and pH can be used to gauge the depth of sludge in the anaerobic pond. EC can also be used to track salt accumulation in recycling systems so long as background levels in fresh water supplies are determined concurrently. Large deviations from the pH levels observed in this study can indicate departures from normal biological function related to over- or under-loading, inhibition of biological activity, extreme climate or other factors. Lack of DO production over summer in a facultative pond would also indicate over-loading or wash out of algal biomass during periods of high effluent irrigation rates.

Results from scenario simulations of a highly loaded anaerobic pond indicate that design limits for peak VS loading can be relaxed substantially. An upper limit of $0.3 \text{ kg VS m}^{-3} \text{ d}^{-1}$ is suggested as an alternative to the current limit of $0.17 \text{ kg VS m}^{-3} \text{ d}^{-1}$. The main drawback of increased loading rates is the need to desludge the pond more frequently, and under a highly loaded design, the risk of inadequate treatment due to high sludge levels is amplified. However, frequent desludging was also shown to improve overall performance, so if a farm operator is prepared to undertake regular (annual) desludging, a higher loading rate may be appropriate. High loading rates may be particularly advantageous on farms with larger herds (>500 milking cows) that would benefit from having two parallel anaerobic ponds to allow switching between ponds during desludging.

The ongoing accumulation of salts and associated issues of struvite precipitation causing pump failures and elevated K loads points to the need for design of effluent recycling systems to be based on combined water and mass balance that accounts for hydrology and associated losses/concentration as well as the timing of effluent irrigation events. The mass balance model described in Chapter 3 provides a firm basis for such an approach.

Recycling systems may also be managed in a different fashion to maximise both water and nutrient efficiency. Stormwater from all hard surfaces at and around the dairy may

be directed *into* the pond system, preferably straight to facultative pond to avoid hydraulic over-loading of the anaerobic pond, provided that runoff in a 90th percentile rainfall year does not exceed annual fresh water usage (with an allowance for leaving effluent in the pond to avoid degrading the pond liner) and sufficient effluent is pumped out of the system by the end of the acceptable irrigation period. These preconditions are easily met in the drier dairying regions of Australia, but in high rainfall areas such as Northern NSW and Southeast Queensland the strategy may be impractical. Where applicable though, the strategy would help with limiting the potential for struvite precipitation and mitigating the accumulation of K in the system, which is likely to be a problem on many farms due to widespread K inefficiency and saturation (Gourley et al. 2012). It can also help to maximise nutrient recovery by forcing more regular system water renewal. Harvesting stormwater in this manner represents a departure from recommendations made by practitioners in the past to divert stormwater away from pond systems, but presents the opportunity to utilise pond systems to their full resource recovery potential.

Where pump-out from a two-stage pond system normally goes to an irrigator capable of handling solids, consideration might also be given to pumping from the anaerobic pond to maximise nutrient recovery, at least when it comes time to desludge the pond. The desludging scenario simulations showed that separate extraction of sludge and supernatant recovers a higher proportion of the plant available nutrients in the system and in doing so avoids nutrient losses incurred in the facultative pond. In a recycling system, it would aid in achieving more complete system water renewal. Interestingly from a nutrient recovery perspective, the practice of mixing supernatant and sludge is not advisable as it both reduces nutrient recovery efficiency and in a K-rich system, constrains land application to the agronomic rate for K, leaving P and N demand unmet.

10.5 RECOMMENDED FUTURE RESEARCH

The proposed alternative strategy for managing effluent recycling systems requires testing and verification in the field. The strategy has the potential to provide significant water efficiency and nutrient recovery benefits, hence it is recommended that a trial be initiated on a commercial dairy farm with an effluent recycling system that has sufficient storage capacity. The trial should run for at least two years and commence in winter to encompass two system draw-down periods and the recovery from each. If successful, the approach adopted in the trial could then be documented in best practice guidelines.

The process of fractionating influent COD and the difficulties encountered with the P fractionation in the biokinetic modelling demonstrated the need for more detailed characterisation of DSE, whether it be for the purposes of modelling stabilisation ponds or other forms of biological treatment. Critical fractions to be quantified include non-biodegradable and very slowly biodegradable particulate COD, non-biodegradable soluble COD, colloidal and/or non-settleable COD, P and N, and soluble organic N.

While this study managed to achieve sound estimates of seepage out of the anaerobic pond through a water balance approach, the process was complex and data intensive. Moreover, it could not discern between net seepage flow, and infiltration and exfiltration flows. To provide a more rapid estimation of seepage losses from pond, an in-situ test for determining liner (or waste seal) hydraulic conductivity needs to be developed.

The occurrence of spontaneous precipitation of struvite in the flood wash tank suggests that there may be potential to harvest the mineral as an alternative method of nutrient recovery. Research could be undertaken to examine the comparative costs and benefits of avoiding struvite precipitation versus intentional precipitation for nutrient recovery, particularly in the context of larger farms with greater levels of confinement and manure capture.

Where this research failed to produce any conclusive evidence was in relation to the roles of ammonia volatilisation, nitrification, nitrification and denitrification in the removal of N from the facultative pond. While determining the exact pathways for N losses is not essential to improving best practice in DSE management in terms of its current objectives, the increasing focus on nitrous oxide emissions in relation to global warming and climate change may require that this work is undertaken.

In order for the biokinetic model of the anaerobic pond to be considered generalisable, it requires validation using an independent data set, which could potentially draw on existing data sets, but may best be developed afresh. Lessons from this work may be applied to avoid having to replicate the level of detail achieved in this study. Research might also be directed towards identifying and quantifying the factors that drive sludge-supernatant flux and the decline in settling efficiency caused by sludge accumulation.

Finally, while the potential of the data set has been explored quite extensively, there remains significant opportunity to utilise it further in developing a biokinetic model for the facultative pond. This would perhaps be a more complex task than developing the anaerobic pond model on account of the dynamic internal thermal and hydraulic changes as well as the additional process equations required for simulating algal

growth kinetics and associated nutrient cycling. Such a model, however, could be used to examine N pathways and struvite precipitation more closely and to develop additional strategies for maximising nutrient recovery. It would also facilitate connecting the feedback loop of effluent recycling to the anaerobic pond so that accumulation of refractory COD, P and other salts can be explored.

10.6 CLOSING REMARKS

The research presented in this thesis marks the first detailed, longitudinal study of a DSE pond system undertaken in Australia. The breadth and depth of the data collected is unprecedented amongst published research into DSE ponds and has enabled the development and calibration of a complex dynamic biokinetic model. The model of the anaerobic pond comprises the first known attempt at mechanistic modelling of wastewater treatment in a stabilisation pond treating DSE. Existing models of DSE pond systems have relied on gross simplification of the complex processes that occur in stabilisation ponds and fail to examine their real effects on nutrients and other wastewater constituents. Moreover, they do not adequately predict nutrient loads in sludges and effluents, limiting their utility in planning effluent and sludge applications and farm nutrient budgeting more broadly. The work presented in this thesis thus presents a significant advancement in modelling capability and in providing validation or otherwise of existing models. Finally, the research presents a thorough examination of the long-term performance of best practice systems in terms of nutrient recovery and reuse. It provides insights into improving effluent and sludge handling practices to maximise nutrient and water efficiency within the context of growing resource constraints, which will play increasingly significant roles in shaping the future of the dairy industry and other agriculture in Australia and globally.

REFERENCES

- ABARE & MAF 2006, *Agricultural Economies of Australia and New Zealand: Past, Present, Future*, ABARE, Canberra.
- Abbas, H, Nasr, R & Seif, H 2006, 'Study of waste stabilization pond geometry for the wastewater treatment efficiency'. *Ecological Engineering*, vol.28, no.1, pp25–34.
- Abis, K & Mara, DD 2006, 'Temperature Measurement and Stratification in Facultative Waste Stabilisation Ponds in the UK Climate'. *Environmental Monitoring and Assessment*, vol.114, no.1, pp35–47.
- Abusam, A & Keesman, KJ 2009, 'Dynamic Modeling of Sludge Compaction and Consolidation Processes in Wastewater Secondary Settling Tanks'. *Water Environment Research*, vol.81, no.1, pp51–56.
- Agunwamba, JC 2006, 'Effect of the Location of the Inlet and Outlet Structures on Short-Circuiting: Experimental Investigation'. *Water Environment Research*, vol.78, no.6, pp580–589.
- Allen, RG, Pereira, LS, Raes, D & Smith, M 1998, *Crop evapotranspiration - Guidelines for computing crop water requirements*, FAO - Food and Agriculture Organization of the United Nations, Rome. Available at: <http://www.fao.org/docrep/X0490E/x0490e00.htm#Contents> [Accessed April 9, 2010].
- Alvarado, A, Vedantam, S, Goethals, P & Nopens, I 2012, 'A compartmental model to describe hydraulics in a full-scale waste stabilization pond'. *Water Research*, vol.46, no.2, pp521–530.
- Aneja, V, Bunton, B, Walker, J & Malik, B 2001, 'Measurement and analysis of atmospheric ammonia emissions from anaerobic lagoons'. *Atmospheric Environment*, vol.35, no.11, pp1949–1958.
- Angelidaki, I & Ahring, BK 2000, 'Methods for increasing the biogas potential from the recalcitrant organic matter contained in manure'. *Water Science & Technology*, vol.41, no.3, pp189–194.
- ANZECC & ARMCANZ 2000, *Australian and New Zealand guidelines for fresh and marine water quality*, Australian and New Zealand Environment and Conservation Council and Agriculture and Resource Management Council of Australia and New Zealand. Available at: <http://www.environment.gov.au/water/publications/quality/pubs/nwqms-guidelines-4-vol1.pdf> [Accessed August 30, 2012].
- APHA 2005, *Standard methods for the examination of water and wastewater* AD Eaton, Water Environment Federation., & American Water Works Association., (eds.), American Public Health Association, American Water Works Association, Water Environment Federation (U.S.), Washington, D.C.;
- APHA 1998, *Standard methods for the examination of water and wastewater* 20th ed., American Public Health Association, American Water Works Association and Water Environment Federation (U.S.), Washington, D. C.

- Arthy, R & Biggs, CA 2005, *Dairy effluent management manual*, Queensland Department of Primary Industries and Fisheries, Brisbane.
- ASAE 2004, *Design of anaerobic lagoons for animal waste management*, ASAE Standard EP403.3 FEB04, American Society of Agricultural Engineers, St Joseph, Mich.
- ASAE 2003, 'Manure production and characteristics', in *ASAE Standard*, ASAE Standard D384.1 FEB03, American Society of Agricultural Engineers, St. Joseph, Mich, pp.683–685.
- ASAE 2005, 'Manure production and characteristics', in *ASAE Standard*, ASAE Standard D384.2 MAR05, The Society for engineering in agricultural, food, and biological systems, pp.1–19.
- ASCE 1996, *Hydrology handbook*, American Society of Civil Engineers, New York.
- Atzeni, MG, McGahan, EJ & Casey, KD 1995, 'Modeling sustainable piggery effluent disposal', in *Queensland Pig Research and Development Seminar*, Queensland Pig Consultancy Group, University of Queensland.
- Australian Government 2013, 'Australian Agriculture Assessment 2001 - Nutrient management in Australian agriculture'. *National Land and Water Resources Audit*, 2001. Available at: http://www.anra.gov.au/topics/agriculture/pubs/national/agriculture_nutrient.html [Accessed February 26, 2013].
- Banda, CG, Sleigh, PA & Mara, DD 2006, 'CFD-based design of waste stabilization ponds: significance of wind velocity', in 7th IWA Specialist Conference on Waste Stabilization Ponds, IWA, Bangkok, Thailand.
- Banks, CJ, Heaven, S & Zotova, EA 2005, 'Some observations on the effects of accumulated benthic sludge on the behaviour of waste stabilisation ponds'. *Water Science and Technology*, vol.51, no.12, pp217–226.
- Barker, PS & Dold, PL 1997, 'General model for biological nutrient removal activated-sludge systems: model presentation'. *Water Environment Research*, vol.69, no.5, pp969–984.
- Barth, CL & Kroes, J 1985, 'Livestock waste lagoon sludge characterization', in *Agricultural waste utilization and management*, Fifth International Symposium on Agricultural Wastes, American Society of Agricultural Engineers, Chicago, pp.660 – 671.
- Batstone, DJ, Pind, PF & Angelidaki, I 2003, 'Kinetics of thermophilic, anaerobic oxidation of straight and branched chain butyrate and valerate'. *Biotechnology and Bioengineering*, vol.84, no.2, pp195–204.
- Battistoni, P, De Angelis, A, Pavan, P, Prisciandaro, M & Cecchi, F 2001, 'Phosphorus removal from a real anaerobic supernatant by struvite crystallization'. *Water Research*, vol.35, no.9, pp2167–2178.
- Battistoni, P, Fava, G, Pavan, P, Musacco, A & Cecchi, F 1997, 'Phosphate removal in anaerobic liquors by struvite crystallization without addition of chemicals: Preliminary results'. *Water Research*, vol.31, no.11, pp2925–2929.

- Beal, LJ, Burns, RT & Stalder, KJ 1999, 'Effect of anaerobic digestion on struvite production for nutrient removal from swine waste prior to land application', in ASAE Annual International Meeting, ASAE, Toronto, Canada.
- Beck, JL 2007, *Optimization of biological nitrogen removal from fermented dairy manure using low levels of dissolved oxygen*, Master of science thesis, Virginia Polytechnic Institute and State University, Blacksburg, VA.
- Beck, JL, Gilmore, KR, Love, NG, Knowlton, K & Ogejo, JA 2007, 'Nitrogen Removal from Dairy Waste Using Deammonification Fueled by Fermented Dairy Manure'. *Proceedings of the Water Environment Federation*, vol.2007, no.9, pp8055–8073.
- Beran, B & Kargi, F 2005, 'A dynamic mathematical model for wastewater stabilization ponds'. *Ecological Modelling*, vol.181, no.1, pp39–57.
- Birchall, S, Dillon, C & Wrigley, R 2008, *Dairy Effluent and Manure Management Database*, Dairy Australia.
- Bohnhoff, DR & Converse, JC 1987, 'Engineering properties of separated manure solids'. *Biological Wastes*, vol.19, no.2, pp91–106.
- Bolan, NS, Horne, DJ & Currie, LD 2004, 'Growth and chemical composition of legume-based pasture irrigated with dairy farm effluent'. *New Zealand Journal of Agricultural Research*, vol.47, no.1, pp85–93.
- Bolan, NS, Laurenson, S, Luo, J & Sukias, JPS 2009, 'Integrated treatment of farm effluents in New Zealand's dairy operations'. *Bioresource Technology*, vol.100, no.22, pp5490–5497.
- Bolan, NS, Wong, L & Adriano, DC 2004, 'Nutrient removal from farm effluents'. *Bioresource Technology*, vol.94, no.3, pp251–260.
- Booram, CV, Smith, RJ & Hazen, TE 1975, 'Crystalline Phosphate Precipitation from Anaerobic Animal Waste Treatment Lagoon Liquors'. *Transactions of the ASABE*, vol.18, no.2, pp340–343.
- Bos, MG 1989, *Discharge measurement structures* 3rd rev. ed., International Institute for Land Reclamation and Improvement, Wageningen.
- Brewer, A, Cumby, T & Dimmock, S 1999, 'Dirty water from dairy farms, II: treatment and disposal options'. *Bioresource Technology*, vol.67, no.2, pp161–169.
- Brutsaert, W 2005, *Hydrology: an introduction*, Cambridge University Press, New York.
- Brutsaert, W 1975, 'On a derivable formula for long-wave radiation from clear skies'. *Water Resources Research*, vol.11, no.5, p742.
- Burden, FR, Foerstner, U, McKelvie, ID & Guenther, A 2002, *Environmental monitoring handbook*, McGraw-Hill, New York.
- Calligan, L 2010, *Dairy shed water use in Victoria*, Department of Primary Industries, Victoria, Melbourne. Available at: http://new.dpi.vic.gov.au/__data/assets/pdf_file/0007/27880/Dairy-Shed-Water-Use-in-Victoria-2009-Analysis.pdf [Accessed November 23, 2010].

- Cameron, KC, Rate, AW, Noonan, MJ, Moore, S, Smith, NP & Kerr, LE 1996, 'Lysimeter study of the fate of nutrients following subsurface injection and surface application of dairy pond sludge to pasture'. *Agriculture, Ecosystems & Environment*, vol.58, no.2-3, pp187–197.
- Campbell Scientific 1999, 'On-line estimation of grass reference evapotranspiration with the Campbell Scientific automated weather station'.
- Casey, K & Atzeni, M 1998, 'Pond chemistry and water balance', in *MEDLI Version 1.2 Technical Manual*, Department of Natural Resources, Queensland, Indooroopilly, pp.4–1 – 4–22.
- Charman, PEV & Murphy, BW 1991, *Soils, their properties and management: a soil conservation handbook for New South Wales*, University of Sydney Press, Sydney.
- Chastain, JP, Vanotti, MB & Wingfield, MM 2001, 'Effectiveness of Liquid-Solid Separation for Treatment of Flushed Dairy Manure: A Case Study'. *Applied engineering in agriculture*, vol.17, no.3, pp343–354.
- CHEMetrics 'COD vials for the determination of chemical oxygen demand: Test procedure'. Available at: <http://www.chemetrics.com/products/pdf/icod.pdf> [Accessed March 20, 2012].
- Christie, KM, Gourley, CJP, Rawnsley, RP, Eckard, RJ & Awty, IM 2012, 'Whole-farm systems analysis of Australian dairy farm greenhouse gas emissions'. *Anim. Prod. Sci.* Available at: <http://dx.doi.org/10.1071/AN12061> [Accessed September 10, 2012].
- Cihan, A, Tyner, JS & Wright, WC 2006, 'Seal formation beneath animal waste holding ponds'. *Transactions of the ASABE*, vol.49, no.5, pp1539–1544.
- Cogley, JG 1979, 'The Albedo of Water as a Function of Latitude'. *Monthly Weather Review*, vol.107, no.6, p775.
- Colomer, FL & Rico, DP 1993, 'Mechanistic model for facultative stabilization ponds'. *Water Environment Research*, vol.65, no.5, pp679–685.
- Condie, SA & Webster, IT 1997, 'The Influence of Wind Stress, Temperature, and Humidity Gradients on Evaporation from Reservoirs'. *Water Resources Research*, vol.33, no.12, pp2813–2822.
- Cothren, GM, Chen, S, Rahman, M & Malone, R 2001, 'Hydrologic modeling of aquatic plant treatment systems polishing dairy lagoon effluents'. *Journal of Environmental Science and Health, Part A: Toxic/Hazardous Substances and Environmental Engineering*, vol.36, no.10, p1905.
- Craggs, R, Park, J & Heubeck, S 2008, 'Methane emissions from anaerobic ponds on a piggery and a dairy farm in New Zealand'. *Australian Journal of Experimental Agriculture*, vol.48, no.2, pp142–146.
- Craggs, RJ, Tanner, CC, Sukias, JPS & Davies-Colley, RJ 2000, 'Nitrification potential of attached biofilms in dairy farm waste stabilisation ponds'. *Water Science and Technology*, vol.42, no.10, pp195–202.

- Craig, IP 2006, 'Comparison of precise water depth measurements on agricultural storages with open water evaporation estimates'. *Agricultural Water Management*, vol.85, no.1-2, pp193–200.
- Cumba, HJ & Hamilton, DW 2002, 'Liquid balance model for swine waste management systems using single-stage anaerobic lagoons'. *Transactions of the ASABE*, vol.45, no.4, pp973–981.
- Cumby, T, Brewer, A & Dimmock, S 1999, 'Dirty water from dairy farms, I: biochemical characteristics'. *Bioresource Technology*, vol.67, no.2, pp155–160.
- Cussler, EL 2009, *Diffusion: Mass Transfer in Fluid Systems* 3rd edn., Cambridge University Press, Cambridge.
- Dahlberg, SP, Lindley, JA & Giles, JF 1988, 'Effect of Anaerobic Digestion on Nutrient Availability from Dairy Manure'. *Transactions of the ASABE*, vol.31, no.4, pp1211–1216.
- Dairy Australia 2012, *Australian dairy industry in focus 2012*, Dairy Australia, Southbank. Available at: <http://www.dairyaustralia.com.au/Our-Dairy-Industry/~media/Publications/Australian%20Dairy%20Industry%20in%20Focus/2009/Australian%20Dairy%20Industry%20In%20Focus%202009.ashx?la=en> [Accessed November 15, 2010].
- Dairy Australia 2009, *Background paper: Environment and natural resources August 2009*, Dairy Australia. Available at: <http://www.dairyaustralia.com.au/~media/Documents/Industry-overview/Current-industry-issues/ADIC%20basin%20plan%20response/LMDB%20inquiry/LMDB%20Environment%20%20Natural%20Resources.ashx>.
- Dairy Australia 2013, 'Dairy Facts at a glance'. *Dairy Australia*. Available at: <http://www.dairyaustralia.com.au/Statistics-and-markets/Farm-facts/Dairy-at-a-glance.aspx> [Accessed February 26, 2013].
- Dairy Effluent Guidelines Steering Committee 2006, 'SA Murray Darling Basin Dairy Effluent Guidelines'. Available at: <http://www.dairyingfortomorrow.com/index.php?id=52> [Accessed November 22, 2010].
- DairyCatch 2006, *Environmental Best Management Practice Guidelines*, Department of Agriculture and Food Western Australia, Bunbury.
- DairySA 2008, 'Resource Not Waste – SA dairy effluent project'. Available at: <http://www.dairysa.com.au/OnFarmAction/HandyTipsandTools/NaturalResourceManagement.aspx> [Accessed November 23, 2010].
- Dao, TH 2004, 'Organic Ligand Effects on Enzymatic Dephosphorylation of myo-Inositol Hexakis Dihydrogenphosphate in Dairy Wastewater'. *Journal of Environmental Quality*, vol.33, no.1, pp349–357.
- Dao, TH 2003, 'Polyvalent cation effects on myo-inositol hexakis dihydrogenphosphate enzymatic dephosphorylation in dairy wastewater'. *Journal of Environmental Quality*, vol.32, no.2, p694.

- Dao, TH, Lugo-Ospina, A, Reeves, JB & Zhang, H 2006, 'Wastewater Chemistry and Fractionation of Bioactive Phosphorus in Dairy Manure'. *Communications in Soil Science and Plant Analysis*, vol.37, no.7-8, pp907–924.
- Davison, T & Andrews, J 1997, *Feed pads down under*, The State of Queensland, Department of Primary Industries. Available at: <http://www.dairyinfo.biz/default.asp?PageID=120&n=Feedpads+Downunder> [Accessed April 14, 2010].
- Dawson, M 2003, *Evaluation of Dairy Shed Waste Storage and Treatment Systems*, Honours thesis, University of Wollongong, Faculty of Engineering.
- DCCEE 2009, *National Inventory Report 2007 – Volume 1. The Australian Government Submission to the UN Framework Convention on Climate Change May 2009*, Department of Climate Change and Energy Efficiency, Canberra. Available at: <http://www.climatechange.gov.au/~media/publications/greenhouse-acctg/nationalinventory-report-2008-vol1.ashx> [Accessed October 12, 2012].
- DEC 2006, *Managing Farm Dairy Effluent Manual* 3rd edn., Dairying and the Environment Committee. Available at: <http://www.dairynz.co.nz/page/pageid/2145838774>.
- DemoDAIRY Co-operative Ltd. 2007, *Annual report 2006-2007*, DemoDAIRY Co-operative Limited Research and Development Farm, Warrnambool.
- DemoDAIRY Co-operative Ltd. 2012, interview, 'Effluent recycling at DEMODairy', 2012
- Department of Systems and Control, Uppsala University 2004, 'JASS - a Java based Activated Sludge process Simulator'. Available at: <http://www.it.uu.se/research/project/jass/> [Accessed July 10, 2012].
- Di, HJ & Cameron, KC 2000, 'Calculating nitrogen leaching losses and critical nitrogen application rates in dairy pasture systems using a semi-empirical model'. *New Zealand Journal of Agricultural Research*, vol.43, no.1, p139.
- Di, HJ, Cameron, KC, Moore, S & Smith, NP 1998, 'Nitrate leaching and pasture yields following the application of dairy shed effluent or ammonium fertilizer under spray or flood irrigation: results of a lysimeter study'. *Soil Use and Management*, vol.14, no.4, pp209–214.
- Dingman, SL 1994, *Physical Hydrology*, Prentice Hall, New Jersey.
- Dochain, D, Gregoire, S, Pauss, A & Schaeffer, M 2003, 'Dynamical modelling of a waste stabilisation pond'. *Bioprocess and Biosystems Engineering*, vol.26, no.1, pp19–26.
- Dodds, PE, Meyer, WS & Barton, A 2005, *A Review of Methods to Estimate Irrigated Reference Crop Evapotranspiration across Australia*, Cooperative Research Centre for Irrigation Futures. Available at: <http://www.irrigationfutures.org.au/default.asp>.
- Dougherty, W & Stein, B 2009, *Optimising nutrient productivity on dairy farms – (FNLI risk assessments)*, NSW Department of Primary Industries.

- Doyle, JD, Oldring, K, Churchley, J & Parsons, SA 2002, 'Struvite formation and the fouling propensity of different materials'. *Water Research*, vol.36, no.16, pp3971–3978.
- Doyle, JD & Parsons, SA 2002, 'Struvite formation, control and recovery'. *Water Research*, vol.36, no.16, pp3925–3940.
- DPI 2009, 'Dairy shed water: How much do you use? A comprehensive guide to calculating water use in the dairy shed'. Available at: [http://www.dpi.vic.gov.au/DPI/nrenfa.nsf/LinkView/FAAE1DA19F3437AACA257635001A58B073F4ECDB559620FBCA2574FD0011EE69/\\$file/Dairy%20shed%20water.pdf](http://www.dpi.vic.gov.au/DPI/nrenfa.nsf/LinkView/FAAE1DA19F3437AACA257635001A58B073F4ECDB559620FBCA2574FD0011EE69/$file/Dairy%20shed%20water.pdf) [Accessed March 2, 2010].
- EAWAG 2010, 'ASIM 4.0 for university institutes (research & teaching)'. Available at: <http://shop.eawag.ch/en/asim-40-university-institutes-research-teaching> [Accessed July 10, 2012].
- Eghball, B, Wienhold, BJ, Gilley, JE & Eigenberg, RA 2002, 'Mineralization of manure nutrients'. *Journal of Soil and Water Conservation*, vol.57, no.6, pp470–473.
- Ellis, KV & Rodrigues, PC 1995a, 'Developments to the first-order, complete-mix design approach for stabilisation ponds'. *Water Research*, vol.29, no.5, pp1343–1351.
- Ellis, KV & Rodrigues, PC 1995b, 'Multiple regression design equations for stabilization ponds'. *Water Research*, vol.29, no.11, pp2509–2519.
- Ellwood, BN & Mason, IG 2003, 'Characteristics of farm dairy yard wastewater related to biological nutrient removal'. *Transactions of the ASAE*, vol.46, no.3, pp825–827.
- EnviroSim Associates Ltd. 2007, *BioWin 3 Process Simulator*, EnviroSim Associates Ltd., Ontario.
- EnviroSim Associates Ltd. 'User manual for BioWin 3'.
- Escalas-Cañellas, A, Ábrego-Góngora, CJ, Barajas-López, MG, Houweling, D & Comeau, Y 2008, 'A time series model for influent temperature estimation: Application to dynamic temperature modelling of an aerated lagoon'. *Water Research*, vol.42, no.10-11, pp2551–2562.
- Fairlamb, M 2010, *BioWin Training Course*, EnviroSim Associates Ltd., Sydney.
- Fairlamb, M, Jones, R, Takács, I & Bye, C 2003, 'Formulation of a general model for simulation of pH in wastewater treatment processes'. *Proceedings of the Water Environment Federation*, vol.2003, no.7, pp511–528.
- Ferrara, RA & Harleman, DRF 1980, 'Dynamic nutrient cycle model for waste stabilization ponds'. *Journal of the Environmental Engineering Division*, vol.106, no., pp37–54.
- Ferrara, RA & Harleman, DRF 1981, 'Hydraulic Modeling for Waste Stabilization Ponds'. *Journal of the Environmental Engineering Division*, vol.107, no.4, pp817–830.

- Fischer, HB 1967, 'The mechanics of dispersion in natural streams'. *Journal of the Hydraulics Division, Proceedings of the ASCE*, vol.93, no.6, pp187–216.
- Fitzgerald, L 1963, 'Wind-induced Stresses on Water Surfaces: A Wind-tunnel Study'. *Australian Journal of Physics*, vol.16, no.4, pp475–489.
- Flemmer, CL & Flemmer, RC 2008, 'Water effluent from New Zealand dairy farms from 1997 to 2000'. *New Zealand Journal of Agricultural Research*, vol.51, no.2, p181.
- Frederick, GL & Lloyd, BJ 1996, 'An evaluation of retention time and short-circuiting in waste stabilisation ponds using *Serratia marcescens* bacteriophage as a tracer'. *Water Science and Technology*, vol.33, no.7, pp49–56.
- Fritz, JJ, Meredith, DD & Middleton, AC 1980, 'Non-steady state bulk temperature determination for stabilization ponds'. *Water Research*, vol.14, no.5, pp413–420.
- Fritz, JJ, Middleton, AC & Meredith, DD 1979, 'Dynamic Process Modeling of Wastewater Stabilization Ponds'. *Journal Water Pollution Control Federation*, vol.51, no.11, pp2724–2743.
- Fyfe, J 1999, *Dairy shed waste management and biogas recovery*, Honours thesis, University of Wollongong, Department of Civil, Mining and Environmental Engineering.
- Fyfe, J 2004, *Performance Evaluation of Two Dairy Shed Waste Management Systems in The Southern Highlands of NSW*, Masters thesis, University of Wollongong, Faculty of Engineering.
- Galbraith, SC & Schneider, PA 2009, 'A review of struvite nucleation studies', in *International Conference on Nutrient Recovery from Wastewater Streams.*, International Water Assn, p.69.
- Gardner, T, Vieritz, A, Atzeni, M, Beecham, RE, et al. 1998, *MEDLI*, software, version 1.3, CRC for Waste Management & Pollution Control Ltd., Department of Natural Resources, Mines and Water, Department of Primary Industries, Queensland.
- Gardner, T, Vieritz, A, Atzeni, M, Beecham, RE, et al. 1996, 'MEDLI: a computer based design model for sustainable effluent disposal from intensive rural industries using land irrigation', in *Land Application of Wastes in Australia and New Zealand: Research and Practice, NZ Land Treatment Collective Annual Conference*, pp.114–124.
- Geary, PM & Moore, JA 1999, 'Suitability of a treatment wetland for dairy wastewaters'. *Water Sci. Technol.*, vol.40, no.3, pp179–185.
- Gehring, T, Silva, JD, Kehl, O, Castilhos, AB, Costa, RHR, Uhlenhut, F, Alex, J, Horn, H & Wichern, M 2010, 'Modelling waste stabilisation ponds with an extended version of ASM3'. *Water Science & Technology*, vol.61, no.3, p713.
- Georgacakis, D & Samantouros, K 1986, 'Effect of effluent recycling and chloride salts on a simulated anaerobic swine lagoon'. *Agricultural Wastes*, vol.15, no.2, pp97–111.

- Glanville, TD, Baker, JL, Melvin, SW & Agua, MM 2001, 'Measurement of leakage from earthen manure structures in Iowa'. *Transactions of the ASAE*, vol.44, no.6, pp1609–1616.
- Golden Software, Inc. 2007, *Grapher*, Golden Software, Inc., Golden.
- Golden Software, Inc. 2008, *Surfer*, Golden Software, Inc., Golden.
- Gourley, C 2012, 'Milking the best possible value from fertiliser nitrogen'. *The Fertilizer*, vol.no.14, pp6–8.
- Gourley, CJP, Dougherty, WJ, Aarons, SR & Hannah, MC 2010, *Accounting for Nutrients on Australian Dairy Farms - Final report*, Dairy Australia.
- Gourley, CJP, Dougherty, WJ, Weaver, DM, Aarons, SR, Awty, IM, Gibson, DM, Hannah, MC, Smith, AP & Peverill, KI 2012, 'Farm-scale nitrogen, phosphorus, potassium and sulfur balances and use efficiencies on Australian dairy farms'. *Animal Production Science*, vol.52, no.10, pp929–944.
- Gourley, CJP, Melland, AR, Waller, RA, Awty, IW, Smith, AP, Peverill, KI & Hannah, MC 2007, 'Making Better Fertiliser Decisions for Grazed Pastures in Australia'. Available at: <http://www.asris.csiro.au/downloads/BFD/Making%20Better%20Fertiliser%20Decisions%20for%20Grazed%20Pastures%20in%20Australia.pdf> [Accessed December 11, 2012].
- Gourley, CJP, Powell, JM, Dougherty, WJ & Weaver, DM 2007, 'Nutrient budgeting as an approach to improving nutrient management on Australian dairy farms'. *Australian Journal of Experimental Agriculture*, vol.47, no.9, pp1064–1074.
- Grayson, RB 1996, *Hydrological recipes: estimation techniques in Australian hydrology*, Cooperative Research Centre for Catchment Hydrology, Clayton.
- Gu, R & Stefan, HG 1995, 'Stratification dynamics in wastewater stabilization ponds'. *Water Research*, vol.29, no.8, pp1909–1923.
- Güngör, K, Müftügil, MB, Ogejo, JA, Knowlton, KF & Love, NG 2009, 'Prefermentation of liquid dairy manure to support biological nutrient removal'. *Bioresource Technology*, vol.100, no.7, pp2124–2129.
- H.D.R. Engineering 2001, *Handbook of Public Water Systems*, John Wiley & Sons.
- Ham, JM 2002a, 'Seepage losses from animal waste lagoons: A summary of a four-year investigation in Kansas'. *Transactions of the ASAE*, vol.45, no.4, pp983–992.
- Ham, JM 2002b, 'Uncertainty analysis of the water balance technique for measuring seepage from animal waste lagoons'. *Journal of Environmental Quality*, vol.31, no.4, p1370.
- Ham, JM & DeSutter, TM 1999, 'Seepage losses and nitrogen export from swine-waste lagoons: A water balance study'. *Journal of Environmental Quality*, vol.28, no.4, pp1090–1099.
- Hanhoun, M, Montastruc, L, Azzaro-Pantel, C, Biscans, B, Frèche, M & Pibouleau, L 2011, 'Temperature impact assessment on struvite solubility product: A

- thermodynamic modeling approach'. *Chemical Engineering Journal*, vol.167, no.1, pp50–58.
- Harris, WG, Wilkie, AC, Cao, X & Sirengo, R 2008, 'Bench-scale recovery of phosphorus from flushed dairy manure wastewater'. *Bioresource Technology*, vol.99, no.8, pp3036–3043.
- Haughton, S 2006, 'Dairy effluent: designing a trafficable solids trap'. *Agriculture Notes*. Available at: [http://www.dpi.vic.gov.au/DPI/nreninf.nsf/v/AF28BE404DE3910CCA25741F0081172C/\\$file/Dairy%20Effluent_Designing_a_Trafficable_Solids_Trap.pdf](http://www.dpi.vic.gov.au/DPI/nreninf.nsf/v/AF28BE404DE3910CCA25741F0081172C/$file/Dairy%20Effluent_Designing_a_Trafficable_Solids_Trap.pdf).
- Havilah, E, Warren, H, Lawrie, R, Senn, A & Milham, P 2005, 'Fertilisers for pastures'. Available at: <http://www.dpi.nsw.gov.au/agriculture/resources/soils/improvement/pastures> [Accessed April 18, 2012].
- Hawke, RM & Summers, SA 2006, 'Effects of land application of farm dairy effluent on soil properties: A literature review'. *New Zealand Journal of Agricultural Research*, vol.49, no.3, p307.
- Hawke, RM & Summers, SA 2003, 'Land application of farm dairy effluent: Results from a case study, Wairarapa, New Zealand'. *New Zealand Journal of Agricultural Research*, vol.46, no.4, p339.
- Hazelton, PA 1992, *Soil landscapes of the Kiama 1:100 000 sheet*, Department of Conservation and Land Management, Sydney.
- He, Z & Honeycutt, CW 2011, 'Enzymatic hydrolysis of organic phosphorus', in Z He, (ed.), *Environmental chemistry of animal manure*, Environmental science, engineering and technology, Nova Science Publishers, New York, pp.253–274.
- He, Z & Olk, DC 2011, 'Manure amino acid compounds and their bioavailability', in *Environmental chemistry of animal manure*, Environmental science, engineering and technology, Nova Science Publishers, New York, pp.179–199.
- Henze, M 2000, *Activated Sludge Models ASM1, ASM2, ASM2d and ASM3*, IWA Publishing, London.
- Henze, M 1992, 'Characterization of Wastewater for Modelling of Activated Sludge Processes'. *Water Science and Technology*, vol.25, no.6, pp1–15.
- Hickey, CW, Quinn, JM & Davies-Colley, RJ 1989, 'Effluent characteristics of dairy shed oxidation ponds and their potential impact on rivers'. *New Zealand Journal of Marine and Freshwater Research*, vol.23, no., pp569–584.
- Hill, DT, Hamilton, HE & McCaskey, TA 1980, 'Operating characteristics of two-cell lagoon systems with recycle treating dairy waste', in *Livestock waste: A renewable Resource*, 4th International Symposium on Livestock Wastes, ASAE, Amarillo, Texas, pp.228–231.
- Hill, DT, McCaskey, TA & Hamilton, HE 1981, 'Lagooning Properties of Flushed' Dairy and Swine Wastes in Multi-Cell Systems Employing Recycle'. *Transactions of the ASAE*, vol.24, no.2, pp459–464.

- Hill, DT, Taylor, SE & Grift, TE 2001, 'Simulation of low temperature anaerobic digestion of dairy and swine manure'. *Bioresource Technology*, vol.78, no.2, pp127–131.
- Hjorth, M, Christensen, K, Christensen, M & Sommer, S 2010, 'Solid—liquid separation of animal slurry in theory and practice. A review'. *Agronomy for Sustainable Development*, vol.30, no.1, pp153–180.
- Holford, ICR, Hird, C & Lawrie, R 1997, 'Effects of animal effluents on the phosphorus sorption characteristics of soils'. *Australian Journal of Soil Research*, vol.35, no., pp365–373.
- Hopkins, D 2002, 'Dairy effluent: Struvite management in dairy effluent systems'. *Notes Information Series*, vol.no.AG1038.
- Houlbrooke, DJ 2008, *Best practice management of Farm Dairy Effluent in the Manawatu- Wanganui region.*, Horizons Regional Council, Hamilton. Available at: <http://www.envirolink.govt.nz/PageFiles/376/421-hzlc43.pdf> [Accessed February 23, 2013].
- Houlbrooke, DJ, Horne, DJ, Hedley, MJ & Hanly, JA 2004, 'The performance of travelling effluent irrigators: Assessment, modification, and implications for nutrient loss in drainage water'. *New Zealand Journal of Agricultural Research*, vol.47, no.4, p587.
- Houlbrooke, DJ, Horne, DJ, Hedley, MJ, Hanly, JA, Scotter, DR & Snow, VO 2004, 'Minimising surface water pollution resulting from farm-dairy effluent application to mole-pipe drained soils. I. An evaluation of the deferred irrigation system for sustainable land treatment in the Manawatu'. *New Zealand Journal of Agricultural Research*, vol.47, no.4, p405.
- Houlbrooke, DJ, Horne, DJ, Hedley, MJ, Hanly, JA & Snow, VO 2004, 'A review of literature on the land treatment of farm-dairy effluent in New Zealand and its impact on water quality'. *N. Z. J. Agric. Res.*, vol.47, no.4, pp499–511.
- Houlbrooke, DJ, Horne, DJ, Hedley, MJ, Snow, VO & Hanly, JA 2008, 'Land application of farm dairy effluent to a mole and pipe drained soil: implications for nutrient enrichment of winter-spring drainage'. *Australian Journal of Soil Research*, vol.46, no.1, pp45–52.
- Houng, HSJ & Gloyna, EF 1984, 'Phosphorus model for waste stabilisation ponds'. *Journal of Environmental Engineering*, vol.110, no.3, pp550–561.
- Houweling, D, Chazarenc, F, Leduc, R & Comeau, Y 2007, 'Effect of baffles on nitrification in aerated facultative lagoons in a cold climate'. *Water Science and Technology*, vol.55, no.11, pp73–79.
- Houweling, D, Kharoune, L, Escalas, A & Comeau, Y 2008, 'Dynamic modelling of nitrification in an aerated facultative lagoon'. *Water Research*, vol.42, no.1-2, pp424–432.
- Houweling, D, Kharoune, L, Escalas, A & Comeau, Y 2005, 'Modeling ammonia removal in aerated facultative lagoons'. *Water science and technology*, vol.51, no.12, pp139–142.

- Hubble, I 2002, *Study Tour Report: Farm Dairy Effluent and Feed Pad Management and Systems in New South Wales*, Department of Primary Industries, Water and Environment, Tasmania.
- Hubble, I & Phillips, R 1999, 'Tasmanian dairy farm effluent management program'. *Journal of Cleaner Production*, vol.7, no.2, pp167–168.
- Huete, E, de Gracia, M, Ayesa, E & Garcia-Heras, JL 2006, 'ADM1-based methodology for the characterisation of the influent sludge in anaerobic reactors'. *Water Science & Technology*, vol.54, no., p157.
- Hydromantis 2012, 'Water & Wastewater Treatment Software & Engineering - GPS-X'. Available at: <http://www.hydromantis.com/GPS-X.html> [Accessed July 10, 2012].
- Idso, SB 1981, 'A set of equations for full spectrum and 8- to 14- μ m and 10.5- to 12.5- μ m thermal radiation from cloudless skies'. *Water Resources Research*, vol.17, no.2, pp295–304.
- Idso, SB & Jackson, RD 1969, 'Thermal radiation from the atmosphere'. *Journal of geophysical research*, vol.74, no.23, pp5397–5403.
- IPNI 2013, 'Fertilizer Use on Australian Dairy Farms'. *International Plant Nutrition Institute*. Available at: <http://anz.ipni.net/article/ANZ-3132> [Accessed February 26, 2013].
- Isbell, RF 2002, *The Australian soil classification*, CSIRO Publishing, Collingwood, Vic.
- Jacobs, AFG, Heusinkveld, BG, Kraai, A & Paaijmans, KP 2008, 'Diurnal temperature fluctuations in an artificial small shallow water body'. *International Journal of Biometeorology*, vol.52, no.4, pp271–280.
- Jacobs, AFG & van Pul, WAJ 1990, 'Seasonal changes in the albedo of a maize crop during two seasons'. *Agricultural and Forest Meteorology*, vol.49, no.4, pp351–360.
- Jacobs, JL & Ward, GN 2007a, 'Effect of second pond dairy effluent applied in spring to silage regrowth of perennial ryegrass based pasture in southern Australia. 1. Dry matter yield and botanical composition changes'. *Aust. J. Agric. Res.*, vol.58, no.2, pp137–143.
- Jacobs, JL & Ward, GN 2007b, 'Effect of second pond dairy effluent applied in spring to silage regrowth of perennial ryegrass based pasture in southern Australia. 2. Changes in nutritive characteristics and mineral content'. *Aust. J. Agric. Res.*, vol.58, no.2, pp145–151.
- Jacobs, JL & Ward, GN 2007c, 'Effect of second-pond dairy effluent on turnip dry matter yield, nutritive characteristics, and mineral content'. *Aust. J. Agric. Res.*, vol.58, no.9, pp884–892.
- Jacobs, JL & Ward, GN 2008, 'Effluent and nitrogen fertiliser effects on dry matter yield, nutritive characteristics, and mineral and nitrate content of turnips'. *Aust. J. Agric. Res.*, vol.59, no.7, pp624–631.
- Jacobs, JL, Ward, GN & Kearney, G 2008, 'The effect of dairy effluent on dry matter yields, nutritive characteristics, and mineral content of summer-active regrowth

- forage crops in southern Australia'. *Aust. J. Agric. Res.*, vol.59, no.6, pp578–588.
- Janzen, JJ & Bishop, JR 1983, 'Bacterial Quality of Recycled Wastewater Used for Flushing Holding Pens'. *Journal of Dairy Science*, vol.66, no.1, pp168–170.
- Jeffrey, SJ, Carter, JO, Moodie, KB & Beswick, AR 2001, 'Using spatial interpolation to construct a comprehensive archive of Australian climate data'. *Environmental Modelling & Software*, vol.16, no.4, pp309–330.
- Jegede, OO, Ogolo, EO & Aregbesola, TO 2006, 'Estimating net radiation using routine meteorological data at a tropical location in Nigeria'. *International Journal of Sustainable Energy*, vol.25, no.2, p107.
- Jensen, ME, Allen, RG & Burman, RD eds. 1990, *Evapotranspiration and irrigation water requirements*, American Society of Civil Engineers, New York.
- Johnson, FM & Sharma, A 2007, 'Estimating Evaporation – Issues and Challenges', in MODSIM 2007 International Congress on Modelling and Simulation, Modelling and Simulation Society of Australia and New Zealand, pp.589–595. Available at: http://www.mssanz.org.au/MODSIM07/papers/10_s61/EstimatingEvaporation_s61_Johnson_.pdf.
- Jones, R, Parker, W, Khan, Z, Murthy, S & Rupke, M 2008, 'Characterization of sludges for predicting anaerobic digester performance'. *Water science and technology*, vol.57, no.5, pp721–726.
- Kane, J 2004, email, 'Unpublished dairy shed effluent data, South-west Victoria, 2001', 7 October 2004
- Kayombo, S, Mbwette, TSA, Mayo, AW, Katima, JHY & Jorgensen, SE 2002, 'Diurnal cycles of variation of physical-chemical parameters in waste stabilization ponds'. *Ecological Engineering*, vol.18, no., pp287–291.
- Kayombo, S, Mbwette, TSA, Mayo, AW, Katima, JHY & Jorgensen, SE 2000, 'Modelling diurnal variation of dissolved oxygen in waste stabilization ponds'. *Ecological Modelling*, vol.127, no.1, pp21–31.
- Kellner, E & Pires, EC 2002, 'The influence of thermal stratification on the hydraulic behavior of waste stabilization ponds'. *Water Science and Technology*, vol.45, no.1, pp41–48.
- Khan, S, Abbas, A, Rana, R & Carroll, J 2010, *Dairy water use in Australian dairy farms: Past trends and future prospects*, CSIRO: Water for a Healthy Country National Research Flagship. Available at: <http://www.clw.csiro.au/publications/waterforahealthycountry/index.html#reports> [Accessed November 22, 2010].
- Koçyigit, MB & Falconer, RA 2004, 'Modelling of wind-induced currents in water basins'. *Proceedings of the ICE - Water Management*, vol.157, no.4, pp197–210.
- Kuo, S 1996, 'Phosphorus', in *Methods of soil analysis; Part 3 Chemical methods*, Soil Science Society of America book series, Soil Science Society of America, Madison, Wis.

- Ladson, AR 2008, *Hydrology: an Australian introduction*, Oxford University Press, South Melbourne.
- Laurenson, S, Smith, E, Bolan, NS & McCarthy, M 2011, 'Effect of K⁺ on Na–Ca exchange and the SAR-ESP relationship'. *Aust. J. Soil Res.*, vol.49, no.6, pp538–546.
- Lawrie, R 1998, 'Soil chemical properties characteristic of areas receiving high strength organic wastes', in *ASSSI National Soils Conference Proceedings*, Brisbane, pp.120–128.
- Le Corre, KS, Valsami-Jones, E, Hobbs, P & Parsons, SA 2009, 'Phosphorus Recovery from Wastewater by Struvite Crystallization: A Review'. *Critical Reviews in Environmental Science and Technology*, vol.39, no.6, pp433–477.
- Lesteur, M, Bellon-Maurel, V, Gonzalez, C, Latrille, E, Roger, JM, Junqua, G & Steyer, JP 2010, 'Alternative methods for determining anaerobic biodegradability: A review'. *Process Biochemistry*, vol.45, no.4, pp431–440.
- Liao, W, Liu, Y, Liu, C & Chen, S 2004, 'Optimizing dilute acid hydrolysis of hemicellulose in a nitrogen-rich cellulosic material—dairy manure'. *Bioresource Technology*, vol.94, no.1, pp33–41.
- Liao, W, Liu, Y, Liu, C, Wen, Z & Chen, S 2006, 'Acid hydrolysis of fibers from dairy manure'. *Bioresource Technology*, vol.97, no.14, pp1687–1695.
- Liao, W, Liu, Y, Wen, Z, Frear, C & Chen, S 2007, 'Studying the effects of reaction conditions on components of dairy manure and cellulose accumulation using dilute acid treatment'. *Bioresource Technology*, vol.98, no.10, pp1992–1999.
- Loehr, RC 1984, *Pollution control for agriculture*, Academic Press, Inc., Orlando.
- Loewenthal, R, Kornmuller, U & van Heerden, E 1994, 'Modelling struvite precipitation in anaerobic treatment systems'. *Water Science and Technology*, vol.30, no.12, pp107–116.
- Longhurst, RD, Roberts, AHC & O'Connor, MB 2000, 'Farm dairy effluent: A review of published data on chemical and physical characteristics in New Zealand'. *New Zealand Journal of Agricultural Research*, vol.43, no.1, pp7–14.
- Maidment, DR 1993, *Handbook of hydrology*, McGraw-Hill, New York.
- Maloney, G 2007, interview, 'Management of Sugarloaf Holsteins Dairy Farm', 19 February 2007
- Mangelson, KA & Watters, GZ 1972, 'Treatment Efficiency of Waste Stabilization Ponds'. *Journal of the Sanitary Engineering Division*, vol.98, no.2, pp407–425.
- Marchand, P 1997, *Hydrodynamic modeling of stabilization ponds*, Masters of Sciences thesis, McGill University, Montreal.
- Marino, P, De Ferrari, G & Bechini, L 2008, 'Description of a sample of liquid dairy manures and relationships between analytical variables'. *Biosystems Engineering*, vol.100, no.2, pp256–265.

- Mashauri, DA & Kayombo, S 2002, 'Application of the two coupled models for water quality management: facultative pond cum constructed wetland models'. *Physics and Chemistry of the Earth, Parts A/B/C*, vol.27, no.11–22, pp773–781.
- Mason, IG 1996, 'Performance of a facultative waste stabilization pond treating dairy shed wastewater'. *Transactions of the ASAE*, vol.40, no.1, pp211–218.
- Mason, IG & Flowerday, MV 2005, 'Simulation of Inert Component Accumulation during the Recycling of Farm Dairy Wastewater'. *Biosystems Engineering*, vol.92, no.2, pp265–273.
- Mason, IG, McLachlan, RI & Gérard, DT 2006, 'A double exponential model for biochemical oxygen demand'. *Bioresource Technology*, vol.97, no.2, pp273–282.
- Mason, IG & Mulcahy, J 2003, 'Volatile fatty acid production from farm dairy wastewater'. *Transactions of the ASAE*, vol.46, no.3, pp819–824.
- Maurer, M & Boller, M 1999, 'Modelling of phosphorus precipitation in wastewater treatment plants with enhanced biological phosphorus removal'. *Water Science and Technology*, vol.39, no.1, pp147–163.
- McDonald, S 2013, email, 'Unpublished dairy shed effluent data, Gippsland region, 2006', 18 January 2013
- McDonald, S 2005, *Water use in dairy sheds*, Department of Primary Industries, Victoria. Available at: http://www.dairyextension.com.au/edit/water_and_climate_change/WATER%20USE%20IN%20DAIRY%20SHEDS%20REPORT%202005.PDF.
- McDowell, A & Birchall, S 2010, *Effluent Toolkit*, software, version 9.0, Department of Primary Industries, Victoria, Victoria.
- McGahan, EJ, Ouellet-Plamondon, C & Watts, PJ 2010, *Estimates of Manure Production from Animals for Methane Generation*, Rural Industries Research and Development Corporation., Barton, ACT.
- McGahan, EJ, van Sliedregt, H, Skerman, AG, Dunlop, M & Redding, MR 2009, *DairyBAL - A Nutrient and Effluent Mass Balance Spreadsheet Model for Dairy Farms*, software, version 3.1, DPI Intensive Livestock Environmental Management Unit, Toowoomba.
- McGarvey, JA, Miller, WG, Sanchez, S, Silva, CJ & Whitehand, LC 2005, 'Comparison of bacterial populations and chemical composition of dairy wastewater held in circulated and stagnant lagoons'. *Journal of Applied Microbiology*, vol.99, no.4, pp867–877.
- McGarvey, JA, Miller, WG, Sanchez, S & Stanker, L 2004, 'Identification of bacterial populations in dairy wastewaters by use of 16S rRNA gene sequences and other genetic markers'. *Applied and Environmental Microbiology*, vol.70, no.7, pp4267–4275.
- McGarvey, JA, Miller, WG, Zhang, R, Ma, Y & Mitloehner, F 2007, 'Bacterial Population Dynamics in Dairy Waste during Aerobic and Anaerobic Treatment and Subsequent Storage'. *Applied and Environmental Microbiology*, vol.73, no.1, pp193–202.

- McGrath, R. & Mason, I. 2004, 'An Observational Method for the Assessment of Biogas Production from an Anaerobic Waste Stabilisation Pond treating Farm Dairy Wastewater'. *Biosystems Engineering*, vol.87, no.4, pp471–478.
- McJannet, DL, Webster, IT, Stenson, MP & Sherman, BS 2008, *Estimating open water evaporation for the Murray-Darling Basin report*, CSIRO. Available at: <http://www.csiro.au/Outcomes/Water/Water-for-the-environment/EstimatingOpenWaterEvaporationMDBSY.aspx> [Accessed January 4, 2012].
- McKenzie, N, Isbell, RF, Brown, K & Jacquier, D 1999, 'Major soils used for agriculture in Australia', in *Soil Analysis: An Interpretation Manual*, CSIRO Australia, Collingwood, pp.71–94.
- McVicar, TR, Van Niel, TG, Li, LT, Hutchinson, MF, Mu, X & Liu, Z 2007, 'Spatially distributing monthly reference evapotranspiration and pan evaporation considering topographic influences'. *Journal of Hydrology*, vol.338, no.3–4, pp196–220.
- Melcer, H, Tam, T, Dold, PL, Jones, RM, et al. 2003, *Methods for wastewater characterization in activated sludge modeling*, Water Environment Federation, Alexandria, VA.
- Metcalf & Eddy, Tchobanoglous, G, Burton, FL & Stensel, HD 2003, *Wastewater engineering: treatment and reuse* 4th edn., McGraw-Hill, Boston.
- Meyer, D, Harner, JP, Tooman, EE & Collar, C 2004, 'Evaluation of weeping wall efficiency of solid liquid separation'. *Applied Engineering in Agriculture*, vol.20, no.3, pp349–354.
- Meyer, D, Ristow, PL & Lie, M 2007, 'Particle size and nutrient distribution in fresh dairy manure'. *Applied Engineering in Agriculture*, vol.23, no.1, pp113–117.
- Meyer, WS, Smith, DJ & Shell, G 1999, *Estimating reference evaporation and crop evapotranspiration from weather data and crop coefficients*, CSIRO Land and Water. Available at: <http://www.clw.csiro.au/publications/technical98/tr34-98.pdf>.
- Møller, H., Lund, I & Sommer, S. 2000, 'Solid–liquid separation of livestock slurry: efficiency and cost'. *Bioresource Technology*, vol.74, no.3, pp223–229.
- Møller, HB, Sommer, SG & Ahring, BK 2004, 'Methane productivity of manure, straw and solid fractions of manure'. *Biomass and Bioenergy*, vol.26, no.5, pp485–495.
- Møller, HB, Sommer, SG & Ahring, BK 2002, 'Separation efficiency and particle size distribution in relation to manure type and storage conditions'. *Bioresource Technology*, vol.85, no.2, pp189–196.
- Monaghan, RM & Smith, LC 2004, 'Minimising surface water pollution resulting from farm-dairy effluent application to mole-pipe drained soils. II. The contribution of preferential flow of effluent to whole-farm pollutant losses in subsurface drainage from a West Otago dairy farm'. *New Zealand Journal of Agricultural Research*, vol.47, no.4, p417.

- Moreno-Grau, S, García-Sánchez, A, Moreno-Clavel, J, Serrano-Aniorte, J & Moreno-Grau, MD 1996, 'A mathematical model for waste water stabilization ponds with macrophytes and microphytes'. *Ecological Modelling*, vol.91, no.1–3, pp77–103.
- Mukhtar, S, Ullman, JL, Auvermann, BW, Feagley, SE & Carpenter, TA 2004, 'Impact of anaerobic lagoon management on sludge accumulation and nutrient content for dairies'. *Transactions of the ASAE*, vol.47, no.1, pp251–257.
- Munch, EV & Barr, K 2001, 'Controlled struvite crystallisation for removing phosphorus from anaerobic digester sidestreams'. *Water Research*, vol.35, no.1, pp151–159.
- Musvoto, EV, Wentzel, MC, Loewenthal, RE & Ekama, GA 2000, 'Integrated chemical–physical processes modelling—I. Development of a kinetic-based model for mixed weak acid/base systems'. *Water Research*, vol.34, no.6, pp1857–1867.
- Myint, M, Nirmalakhandan, N & Speece, RE 2007, 'Anaerobic fermentation of cattle manure: Modeling of hydrolysis and acidogenesis'. *Water Research*, vol.41, no.2, pp323–332.
- Nameche, T & Vassel, JL 1998, 'Hydrodynamic studies and modelization for aerated lagoons and waste stabilization ponds'. *Water Research*, vol.32, no.10, pp3039–3045.
- NCRS 2008, 'Agricultural Waste Characteristics', in *Agricultural Waste Management Field Handbook*, National Engineering Handbook, United States Department of Agriculture.
- Nelson, KL & Jimenez, BC 2000, 'Sludge accumulation, properties and degradation in a waste stabilization pond in Mexico'. Available at: <http://search.proquest.com/docview/17891350?accountid=17095>.
- Nelson, NO, Mikkelsen, RL & Hesterberg, DL 2003, 'Struvite precipitation in anaerobic swine lagoon liquid: effect of pH and Mg:P ratio and determination of rate constant'. *Bioresource Technology*, vol.89, no.3, pp229–236.
- Nennich, TD, Harrison, JH, VanWieringen, LM, Meyer, D, et al. 2005, 'Prediction of Manure and Nutrient Excretion from Dairy Cattle'. *Journal of Dairy Science*, vol.88, no.10, pp3721–3733.
- NLWRA 2008, *Signposts for Australia agriculture - The Australian dairy industry*, National Land and Resources Audit, Canberra.
- Nordstedt, RA & Baldwin, LB 1975, 'Sludge accumulation and stratification in anaerobic dairy waste lagoons'. *Trans. ASAE*, vol.18, no.2, pp312–315.
- NSW Dairy Effluent Subcommittee 1999, *Draft NSW Guidelines for Dairy Effluent Resource Management*, NSW Agriculture, Orange.
- NSW DEC 2004, *Environmental guidelines: use of effluent by irrigation*, Department of Environment and Conservation (NSW), Sydney.
- Nunez, M, Davies, JA & Robinson, PJ 1972, 'Surface albedo at a tower site in Lake Ontario'. *Boundary-Layer Meteorology*, vol.3, no.1, pp77–86.

- Ohlinger, KN, Young, TM & Schroeder, ED 1999, 'Kinetics Effects of Preferential Struvite Accumulation in Wastewater'. *Journal of Environmental Engineering*, vol.125, no.8, p730.
- Ohlinger, KN, Young, TM & Schroeder, ED 1998, 'Predicting struvite formation in digestion'. *Water Research*, vol.32, no.12, pp3607–3614.
- Oke, TR 1992, *Boundary layer climates*, London.
- Ortuno, JF, Saez, J, Llorens, M & Soler, A 2000, 'Phosphorus release from sediments of a deep wastewater stabilization pond'. *Water Science and Technology*, vol.42, no.10-11, pp265–272.
- Page, DI, Hickey, KL, Narula, R, Main, AL & Grimberg, SJ 2008, 'Modeling anaerobic digestion of dairy manure using the IWA Anaerobic Digestion Model no. 1 (ADM1)'. *Water science and technology: a journal of the International Association on Water Pollution Research*, vol.58, no.3, pp689–695.
- Paing, J, Picot, B, Sambuco, JP & Rambaud, A 2000, 'Sludge accumulation and methanogenic activity in an anaerobic lagoon'. *Water Science & Technology*, vol.42, no.10-11, pp247–247–255.
- Parker, DB, Auvermann, BW & Williams, DL 1999, 'Comparison of evaporation rates from feedyard pond effluent and clear water as applied to seepage predictions'. *Transactions of the Asae*, vol.42, no.4, pp981–986.
- Parker, DB, Eisenhauer, DE, Schulte, DD & Martin, DL 1999, 'Modeling seepage from an unlined beef cattle feedlot runoff storage pond'. *Transactions of the Asae*, vol.42, no.5, pp1437–1445.
- Parker, DB, Eisenhauer, DE, Schulte, DD & Nienaber, JA 1999, 'Seepage Characteristics and Hydraulic Properties of a Feedlot Runoff Storage Pond'. *Transactions of the ASAE*, vol.42, no.2, pp369–380.
- Paterson, C & Curtis, T 2005, 'Physical and chemical environments', in *Pond treatment technology*, IWA Publishing, London ; Seattle, pp.49–65.
- Pearson, HW, Mara, DD & Arridge, HA 1995, 'The influence of pond geometry and configuration on facultative and maturation waste stabilisation pond performance and efficiency'. *Water Science and Technology*, vol.31, no.12, pp129–139.
- Pearson, HW, Mara, DD & Bartone, CR 1987, 'Guidelines for the Minimum Evaluation of the Performance of Full-Scale Waste Stabilization Pond Systems'. *Water Research*, vol.21, no.9, pp1067–1075.
- Pearson, HW, Mara, DD, Konig, A, Deoliveira, R, Mills, SW, Smallman, DJ & Silva, SA 1987, 'Water Column Sampling as a Rapid and Efficient Method of Determining Effluent Quality and the Performance of Waste Stabilization Ponds'. *Water Science and Technology*, vol.19, no.12, pp109–113.
- Pena, MR, Mara, DD & Sanchez, A 2000, 'Dispersion studies in anaerobic ponds: Implications for design and operation'. Available at: <http://search.proquest.com/docview/17892244?accountid=17095>.

- Persson, J 2000, 'The hydraulic performance of ponds of various layouts'. *Urban Water*, vol.2, no.3, pp243–250.
- Persson, J & Wittgren, HB 2003, 'How hydrological and hydraulic conditions affect performance of ponds'. *Ecological Engineering*, vol.21, no.4–5, pp259–269.
- Pescod, MB 1996, 'The role and limitations of anaerobic pond systems'. *Water Science and Technology*, vol.33, no.7, pp11–21.
- Peverill, KI, Reuter, DJ & Sparrow, LA 1999, *Soil analysis: an interpretation manual*, CSIRO Publishing, Collingwood, Vic.
- Phillips, M & Goss, MJ 1934, 'The Chemistry of Lignin'. *Chemical Reviews*, vol.14, no.1, pp103–170.
- Pilgrim, DH 1998, *Australian rainfall and runoff: a guide to flood estimation*, Institution of Engineers, Australia, Barton, A.C.T.;
- Polprasert, C & Bhattarai, K 1985, 'Dispersion Model for Waste Stabilization Ponds'. *Journal of Environmental Engineering*, vol.111, no.1, pp45–59.
- Preul, HC & Wagner, RA 1988, 'Waste stabilization pond prediction model'. *Water Science and Technology*, vol.19, no.12, pp205–211.
- Qureshi, A, Lo, KV, Liao, PH & Mavinic, DS 2008, 'Real-time treatment of dairy manure: Implications of oxidation reduction potential regimes to nutrient management strategies'. *Bioresource Technology*, vol.99, no.5, pp1169–1176.
- Qureshi, A, Lo, KV, Mavinic, DS, Liao, PH, Koch, F & Kelly, H 2006, 'Dairy Manure Treatment, Digestion and Nutrient Recovery as a Phosphate Fertilizer'. *Journal of Environmental Science and Health, Part B*, vol.41, no.7, pp1221–1235.
- Rajbhandari, BK, Annachhatre, AP & Vasel, JL 2007, 'Modeling of anaerobic treatment of wastewater in ponds'. *Water Science and Technology: A Journal of the International Association on Water Pollution Research*, vol.55, no.11, pp47–56.
- Ramdani, A, Dold, P, Déléris, S, Lamarre, D, Gadbois, A & Comeau, Y 2010, 'Biodegradation of the endogenous residue of activated sludge'. *Water Research*, vol.44, no.7, pp2179–2188.
- Ramsey, DS & Megehee, DB 1988, 'Evaluation of recycled wastewater for dairy flush systems'. *Biological Wastes*, vol.26, no.1, pp59–64.
- Reichert, P, Borchardt, D, Henze, M, Rauch, W, Shanahan, P, Somlydy, L & Vanrolleghem, P 2001, 'River Water Quality Model no. 1 (RWQM1):II. Biochemical process equations'. *Water Science and Technology*, vol.43, no.5, pp11–30.
- Rico, JL, García, H, Rico, C & Tejero, I 2007, 'Characterisation of solid and liquid fractions of dairy manure with regard to their component distribution and methane production'. *Bioresource Technology*, vol.98, no.5, pp971–979.
- Roberto, JSJ & Sweeten, JM 1985, 'Control of crystal formations in recycle flush systems at caged layer operations', in *Agricultural waste utilization and management*, 5th International Symposium on Agricultural Wastes, American Society of Agricultural Engineers, Chicago, pp.624–631.

- Roeleveld, PJ & van Loosdrecht, M 2002, 'Experience with guidelines for wastewater characterisation in The Netherlands'. *Water Science and Technology*, vol.45, no.6, pp77–87.
- Rogers, G & Alexander, A 2000, *A survey on environmental management of Bonlac dairy farms*, Bonlac Foods. Available at: <http://epanote2.epa.vic.gov.au/EPA%5Cpublications.nsf/PubDocsLU/dairyfarms?OpenDocument> [Accessed March 2, 2010].
- Rowell, JG, Miller, MH & Groenevelt, PH 1985, 'Self-Sealing of Earthen Liquid Manure Storage Ponds: II. Rate and Mechanism of Sealing'. *Journal of Environmental Quality*, vol.14, no.4, pp539–543.
- Rumburg, B, Mount, GH, Yonge, D, Lamb, B, Westberg, H, Neger, M, Filipy, J, Kincaid, R & Johnson, K 2008, 'Measurements and modeling of atmospheric flux of ammonia from an anaerobic dairy waste lagoon'. *Atmospheric Environment*, vol.42, no.14, pp3380–3393.
- Rumburg, B, Neger, M, H. Mount, G, Yonge, D, Filipy, J, Swain, J, Kincaid, R & Johnson, K 2004, 'Liquid and atmospheric ammonia concentrations from a dairy lagoon during an aeration experiment'. *Atmospheric Environment*, vol.38, no.10, pp1523–1533.
- Safley, LMJ & Westerman, PW 1988, 'Biogas production from anaerobic lagoons'. *Biological Wastes*, vol.23, no.3, pp181–193.
- Safley, LMJ & Westerman, PW 1992a, 'Performance of a dairy manure anaerobic lagoon'. *Bioresource Technology*, vol.42, no.1, pp43–52.
- Safley, LMJ & Westerman, PW 1992b, 'Performance of a low temperature lagoon digester'. *Bioresource Technology*, vol.41, no.2, pp167–175.
- Safley, LMJ, Westerman, PW & Barker, JC 1986, 'Fresh dairy manure characteristics and barnlot nutrient losses'. *Agricultural Wastes*, vol.17, no.3, pp203–215.
- Sah, L, Rousseau, D & Hooijmans, C 2012, 'Numerical Modelling of Waste Stabilization Ponds: Where Do We Stand?' *Water, Air, & Soil Pollution*, vol.223, no.6, pp3155–3171.
- Sah, L, Rousseau, DPL, Hooijmans, CM & Lens, PNL 2011, '3D model for a secondary facultative pond'. *Ecological Modelling*, vol.222, no.9, pp1592–1603.
- Salter, HE, Ta, CT, Ouki, SK & Williams, SC 2000, 'Three-dimensional computational fluid dynamic modelling of a facultative lagoon'. *Water Science and Technology*, vol.42, no.10-11, pp335–335–342.
- Senzia, MA, Mayo, AW, Mbvette, TSA, Katima, JHY & Jørgensen, SE 2002, 'Modelling nitrogen transformation and removal in primary facultative ponds'. *Ecological Modelling*, vol.154, no.3, pp207–215.
- Sethuraman, S & Raynor, GS 1975, 'Surface drag coefficient dependence on the aerodynamic roughness of the sea'. *Journal of geophysical research*, vol.80, no.36, pp4983–4988.
- Shilton, A 2001, *Studies into the hydraulics of waste stabilisation ponds*, PhD thesis, Massey University, Palmerston North.

- Shilton, A & Harrison, J 2003a, *Guidelines for the hydraulic design of waste stabilisation ponds*, Institute of Technology and Engineering, Massey University, Palmerston, New Zealand.
- Shilton, A & Harrison, J 2003b, 'Integration of coliform decay within a CFD (computational fluid dynamic) model of a waste stabilisation pond'. *Water Science and Technology*, vol.48, no.2, pp205–210.
- Shilton, A & Sweeney, D 2005, 'Hydraulic design', in *Pond Treatment Technology*, IWA Publishing, London.
- Shuttleworth, WJ 1993, 'Evaporation', in *Handbook of Hydrology*, McGraw-Hill, Inc., New York, pp.4.1 – 4.53.
- SILO 2008, 'Data Drill for Latitude, Longitude: -34.55, 150.55'. Available at: <http://www.longpaddock.qld.gov.au/silo/> [Accessed November 24, 2008].
- Silva, RG, Cameron, KC & Hendry, T 1999, 'A lysimeter study of the impact of cow urine, dairy shed effluent, and nitrogen fertiliser on nitrate leaching'. *Australian Journal of Soil Research*, vol.37, no., pp357–368.
- Silver, B, Whitelaw, H & Malone-McGrath, F 2009, *Results of the DairySAT Evaluation of Dairy Farmers in the Sydney Catchment Authority Region of Southern Highlands, Kangaroo Valley and Camden*, Dairy Farmers and National Foods Farm Services.
- Simpkins, WW, Burkart, MR, Helmke, MF, Twedt, TN, James, DE, Jaquis, RJ & Cole, KJ 2002, 'Potential impact of earthen waste storage structures on water resources in Iowa'. *Journal of the American Water Resources Association*, vol.38, no.3, pp759–771.
- Skerman, AG 2004a, *Dairy Pond*, Department of Primary Industries, Queensland.
- Skerman, AG 2004b, *Dairy Solids trap*, software, version 2.1, Department of Primary Industries, Queensland, Toowoomba, Queensland.
- Skerman, AG 2004c, 'The development and use of dairy effluent calculators'. *Australian Journal of Dairy Technology*, vol.59, no.2, pp182–185.
- Skerman, AG, Collman, G, Duperouzel, D, Sohn, J, Atzeni, MG & Kelly, A 2008, *Improved piggery effluent management systems incorporating highly loaded primary ponds*, Department of Primary Industries and Fisheries, Toowoomba, Queensland.
- Skerman, AG, Kunde, T & Biggs, C 2006, *Nutrient Composition of Dairy Effluent Ponds*, Queensland Department of Primary Industries and Fisheries.
- Smiles, DE & Smith, CJ 2004, 'A survey of the cation content of piggery effluents and some consequences of their use to irrigate soils'. *Soil Res.*, vol.42, no.2, pp231–246.
- Smith, RE 1980, 'Sludge as a condition indicator of anaerobic lagoons', in *Livestock waste: A renewable resource*, Fourth International Symposium on Livestock Wastes, Amarillo, Texas, pp.15–17.

- Soares, SRA & Bernardes, RS 2001, 'Reaction coefficient (K) evaluation for full-scale facultative pond systems'. *Bioresource Technology*, vol.78, no.1, pp99–102.
- Soler, A, Moreno, MD, Saez, J & Moreno, J 2000, 'Kinetic model for deep waste stabilization ponds operating in batch mode'. *Water Science and Technology*, vol.42, no.10-11, pp315–325.
- Sperling, M von & Chernicharo, CA 2005, *Biological Wastewater Treatment in Warm Climate Regions*, IWA Publishing.
- Spillane, KT & Hess, GD 1978, 'Wind-Induced Drift In Contained Bodies of Water'. *Journal of Physical Oceanography*, vol.8, no.5, pp930–935.
- Spitters, CJT, Toussaint, HAJM & Goudriaan, J 1986, 'Separating the diffuse and direct component of global radiation and its implications for modeling canopy photosynthesis Part I. Components of incoming radiation'. *Agricultural and Forest Meteorology*, vol.38, no.1–3, pp217–229.
- Stace, HCT 1968, *A Handbook of Australian Soils*, Rellim Technical Publications, Glenside, S.A.
- Stafford, DA 1980, *Methane production from waste organic matter*, CRC Press, Boca Raton, Fla.
- Stefan, HG, Cardoni, JJ, Schiebe, FR & Cooper, CM 1983, 'Model of light penetration in a turbid lake'. *Water Resources Research*, vol.19, no.1, pp109–120.
- Stefan, HG & Gu, R 1991, 'Conceptual design procedure for hydraulic destratification systems in small ponds, lakes, or reservoirs for water quality improvement'. *Journal of the American Water Resources Association*, vol.27, no.6, pp967–978.
- Stephens, R & Imberger, J 1993, 'Reservoir Destratification via Mechanical Mixers'. *Journal of Hydraulic Engineering*, vol.119, no.4, pp438–457.
- Stumm, W & Morgan, JJ 1981, *Aquatic chemistry: an introduction emphasizing chemical equilibria in natural waters* 2d ed., Wiley, New York.
- Sturman, A & Tapper, N 1996, *The weather and climate of Australia and New Zealand*, Oxford University Press, Melbourne;
- Sukias, JPS, Craggs, RJ, Tanner, CC, Davies-Colley, RJ & Nagels, JW 2003, 'Combined photosynthesis and mechanical aeration for nitrification in dairy waste stabilisation ponds'. *Water Science and Technology*, vol.48, no.2, pp137–144.
- Sukias, JPS, Tanner, CC, Davies-Colley, RJ & Nagels, JW 2001, 'Algal abundance, organic matter, and physico-chemical characteristics of dairy farm facultative ponds: implications for treatment performance'. *New Zealand Journal of Agricultural Research*, vol.44, no., pp279–296.
- Sukias, JPS, Tanner, CC & Nagels, JW 2003, 'Outflow volumes and mass flow impacts on receiving waters from dairy farm pond systems', in *5th International IWA Specialist Group Conference on Waste Stabilisation Ponds*, Auckland, pp.801–808.

- Sund, JL, Evenson, CJ, Strevett, KA, Nairn, RW, Athay, D & Trawinski, E 2001, 'Nutrient Conversions by Photosynthetic Bacteria in a Concentrated Animal Feeding Operation Lagoon System'. *J Environ Qual*, vol.30, no.2, pp648–655.
- Suzuki, K, Tanaka, Y, Osada, T & Waki, M 2002, 'Removal of phosphate, magnesium and calcium from swine wastewater through crystallization enhanced by aeration'. *Water Research*, vol.36, no.12, pp2991–2998.
- Sweeney, DG, Cromar, NJ, Nixon, JB, Ta, CT & Fallowfield, HJ 2003, 'The spatial significance of water quality indicators in waste stabilization ponds--limitations of residence time distribution analysis in predicting treatment efficiency'. *Water science and technology: a journal of the International Association on Water Pollution Research*, vol.48, no.2, pp211–218.
- Sweeney, DG, Nixon, JB, Cromar, NJ & Fallowfield, HJ 2005, 'Profiling and modelling of thermal changes in a large waste stabilisation pond'. *Water Science and Technology*, vol.51, no.12, pp163–172.
- Sweeten, JM & Wolfe, ML 1994, 'Manure and Waste-Water Management-Systems for Open Lot Dairy Operations'. *Transactions of the Asae*, vol.37, no.4, pp1145–1154.
- Sydney Catchment Authority 2010, 'Personal communication'.
- Tadesse, I, Green, FB & Puhakka, JA 2004, 'Seasonal and diurnal variations of temperature, pH and dissolved oxygen in advanced integrated wastewater pond system treating tannery effluent'. *Water Research*, vol.38, no.3, pp645–654.
- Takács, I, Patry, GG & Nolasco, D 1991, 'A dynamic model of the clarification-thickening process'. *Water Research*, vol.25, no.10, pp1263–1271.
- Thackston, E, Shields, F & Schroeder, P 1987, 'Residence Time Distributions of Shallow Basins'. *Journal of Environmental Engineering*, vol.113, no.6, pp1319–1332.
- Thom, AS & Oliver, HR 1977, 'On Penman's equation for estimating regional evaporation'. *Quarterly Journal of the Royal Meteorological Society*, vol.103, no.436, pp345–357.
- Tie, L & Sivakumar, M 2008a, 'Anaerobic Digestion (AD) Modelling of Australian Dairy Shed Wastewater', in *Sustainable Development to Save the Earth: Technologies and Strategies Vision 2050*, Commemorative International Conference of the Occasion of the 4th Cycle Anniversary of KMUTT, Bangkok.
- Tie, L & Sivakumar, M 2008b, 'Bioenergy Recovery by Anaerobic digestion of Australian Dairy Shed Wastewater using CSTR Digesters', in *Sustainable Development to Save the Earth: Technologies and Strategies Vision 2050*, Commemorative International Conference of the Occasion of the 4th Cycle Anniversary of KMUTT, Bangkok.
- Tie, L & Sivakumar, M 2007a, 'Dairy Shed Wastewater Characterisation for ADM1 Modelling', in *OzWater 2007*, AWA, Sydney.
- Tie, L & Sivakumar, M 2007b, 'Dairy shed wastewater treatment and modelling by anaerobic digestion technology'. *International Journal of Environment and Waste Management*, vol.1, no.4, pp321–337.

- Toor, GS, Cade-Menun, BJ & Sims, JT 2005, 'Establishing a Linkage between Phosphorus Forms in Dairy Diets, Feces, and Manures'. *Journal of Environmental Quality*, vol.34, no.4, pp1380–1391.
- Torabizadeh, H 2011, 'All Proteins Have a Basic Molecular Formula'. *World Academy of Science, Engineering and Technology*, vol.no.78, pp961–965.
- Torres, J., Soler, A, Sáez, J & Llorens, M 2000, 'Hydraulic performance of a deep stabilisation pond fed at 3.5 m depth'. *Water Research*, vol.34, no.3, pp1042–1049.
- Torres, JJ, Soler, A, Sáez, J & Ortuño, JF 1997, 'Hydraulic performance of a deep wastewater stabilization pond'. *Water Research*, vol.31, no.4, pp679–688.
- Toth, JD, Dou, Z & He, Z 2011, 'Solubility of manure phosphorus characterized by selective and sequential extractions', in Z He, (ed.), *Environmental chemistry of animal manure*, Environmental science, engineering and technology, Nova Science Publishers, New York, pp.227–251.
- Türker, M & Çelen, I 2007, 'Removal of ammonia as struvite from anaerobic digester effluents and recycling of magnesium and phosphate'. *Bioresource Technology*, vol.98, no.8, pp1529–1534.
- Turner, BL & Leytem, AB 2004, 'Phosphorus Compounds in Sequential Extracts of Animal Manures: Chemical Speciation and a Novel Fractionation Procedure'. *Environmental Science & Technology*, vol.38, no.22, pp6101–6108.
- Tyner, JS & Lee, J 2004, 'Influence of seal and liner hydraulic properties on the seepage rate from animal waste holding ponds and lagoons'. *Transactions of the ASAE*, vol.47, no.5, pp1739–1745.
- Tyner, JS, Wright, WC & Lee, J 2006, 'Lagoon sealing and filter cakes'. *Transactions of the ASAE*, vol.49, no.2, pp527–531.
- Ulery, AL, Flynn, R & Parra, R 2004, 'Appropriate Preservation of Dairy Wastewater Samples for Environmental Analysis'. *Environmental Monitoring and Assessment*, vol.95, no.1-3, pp117–124.
- Ullman, JL & Mukhtar, S 2007, 'Impact of dairy housing practices on lagoon effluent characteristics: Implications for nitrogen dynamics and salt accumulation'. *Bioresource Technology*, vol.98, no.4, pp745–752.
- Uludag-Demirer, S, Demirer, GN & Chen, S 2005, 'Ammonia removal from anaerobically digested dairy manure by struvite precipitation'. *Process Biochemistry*, vol.40, no.12, pp3667–3674.
- Uludag-Demirer, S, Demirer, GN, Frear, C & Chen, S 2008, 'Anaerobic digestion of dairy manure with enhanced ammonia removal'. *Journal of Environmental Management*, vol.86, no.1, pp193–200.
- Valiantzas, JD 2006, 'Simplified versions for the Penman evaporation equation using routine weather data'. *Journal of Hydrology*, vol.331, no.3-4, pp690–702.
- Valsami-Jones, E 2001, 'Mineralogical controls on phosphorus recovery from wastewaters'. *Mineralogical Magazine*, vol.65, no.5, pp611–620.

- Van Horn, HH, Wilkie, AC, Powers, WJ & Nordstedt, RA 1994, 'Components of Dairy Manure Management Systems'. *Journal of Dairy Science*, vol.77, no.7, pp2008–2030.
- Vega, GP, Peña, MR, Ramírez, C & Mara, DD 2003, 'Application of CFD modelling to study the hydrodynamics of various anaerobic pond configurations'. *Water science and technology: a journal of the International Association on Water Pollution Research*, vol.48, no.2, pp163–171.
- Vieritz, AM, Gardner, T, Littleboy, M, Atzeni, MG, Beecham, RE & Casey, KD 1998, 'MEDLI - A model for designing sustainable irrigation systems for the reuse of effluent', in *ASSSI National Soils Conference Proceedings*, ASSSI National Soils Conference, ASSSI, Brisbane, pp.154–161.
- Vitasovic, Z 1989, 'Continuous Settler Operation: A Dynamic Model', in *Dynamic Modeling and Expert Systems in Wastewater Engineering*, Lewis Publishers Inc., Chelsea Michigan, pp.59–81.
- Wang, H, Magesan, GN & Bolan, NS 2004, 'An overview of the environmental effects of land application of farm effluents'. *New Zealand Journal of Agricultural Research*, vol.47, no.4, pp389–403.
- Wang, J, Song, Y, Yuan, P, Peng, J & Fan, M 2006, 'Modeling the crystallization of magnesium ammonium phosphate for phosphorus recovery'. *Chemosphere*, vol.65, no.7, pp1182–1187.
- Ward, AD & Trimble, SW 2004, *Environmental Hydrology* 2nd edn., Lewis Publishers, Boca Raton.
- Ward, GN 2010, *Environmentally sustainable and productive use of dairy pond sludge for forage production on farm*, Department of Primary Industries, Victoria, Warrnambool.
- Ward, GN 2012, interview, 'Land application of dairy effluent and sludge', 5 June 2012
- Ward, GN & Jacobs, JL 2008a, 'Effectiveness of dairy first pond sludge as a nutrient source for forage crop production', in *Proceedings of the 14th Australian Society of Agronomy Conference*, Australian Agronomy Conference, 21-25 September, Australian Society of Agronomy, Adelaide.
- Ward, GN & Jacobs, JL 2008b, 'Effectiveness of dairy first pond sludge as a nutrient source for perennial ryegrass pasture production', in *Proceedings of the 14th Australian Society of Agronomy Conference*, Australian Agronomy Conference, 21-25 September, Australian Society of Agronomy, Adelaide.
- Ward, RC & Robinson, M 2000, *Principles of hydrology*, McGraw-Hill, London.
- Watson, P 2006, *Dairying for Tomorrow: Survey of NRM practices on dairy farms*, Dairy Australia, Frankston. Available at: <http://www.dairyingfortomorrow.com/index.php?id=27> [Accessed November 23, 2010].
- Watson, P & Watson, D 2012, *Survey of Natural Resource Management on Dairy Farms*, Dairy Australia.

- Webster, IT & Sherman, BS 1995, 'Evaporation from fetch-limited water bodies'. *Irrigation Science*, vol.16, no.2, pp53–64.
- Westerman, PW, Safley, LMJ & Barker, JC 1985, 'Crystalline buildup in swine and poultry recycle flush systems', in *Agricultural waste utilization and management*, 5th International Symposium on Agricultural Wastes, American Society of Agricultural Engineers, Chicago, pp.613–623.
- Westerman, PW, Safley, LMJ & Barker, JC 1990, 'Lagoon liquid nutrient variation over four years for lagoons with recycle systems', in *Agriculture and food processing wastes*, 6th international symposium on agricultural and food processing wastes, ASAE, Chicago, pp.41–49.
- Westerman, PW, Safley, LMJ, Barker, JC & Chescheir, GM 1985, 'Available nutrients in livestock waste', in *Agricultural waste utilization and management*, 5th International Symposium on Agricultural Wastes, American Society of Agricultural Engineers, Chicago, pp.295–307.
- Wheeler, DM, Shepherd, M & Power, I 2012, 'Effluent management in OVERSEER® Nutrient Budgets', in *Advanced nutrient management: gains from the past - goals for the future*, Occasional Report, Fertilizer and Lime Research Centre, Massey University, Palmerston North, New Zealand, p.9 pages. Available at: <http://www.overseer.org.nz/OVERSEERModel/Information/References.aspx> [Accessed January 1, 2013].
- Whichard, DP 2001, *Nitrogen removal from dairy manure wastewater using sequencing batch reactors*, Masters thesis, Virginia Polytechnic Institute and State University, Blacksburg. Available at: <http://scholar.lib.vt.edu/theses/available/etd-08082001-103610/> [Accessed November 4, 2011].
- Wiernga, J 1993, 'Representative roughness parameters for homogeneous terrain'. *Boundary-Layer Meteorology*, vol.63, no.4, pp323–363.
- Wilcock, RJ, Nagels, JW, Rodda, HJE, O'Connor, MB, Thorrold, BS & Barnett, JW 1999, 'Water quality of a lowland stream in a New Zealand dairy farming catchment'. *New Zealand Journal of Marine and Freshwater Research*, vol.33, no.4, pp683–696.
- Wilkie, AC, Castro, HF, Cubinski, KR, Owens, JM & Yan, SC 2004, 'Fixed-film Anaerobic Digestion of Flushed Dairy Manure after Primary Treatment: Wastewater Production and Characterisation'. *Biosystems Engineering*, vol.89, no.4, pp457–471.
- Wilkinson, SR 1979, 'Plant nutrient and economic values of animal manures'. *Journal of Animal Science*, vol.48, no.1, pp121–133.
- Wood, J, Fernandez, G, Barker, A, Gregory, J & Cumby, T 2007, 'Efficiency of reed beds in treating dairy wastewater'. *Biosystems Engineering*, vol.98, no.4, pp455–469.
- Wood, MG, Howes, T, Keller, J & Johns, MR 1998, 'Two dimensional computational fluid dynamic models for waste stabilisation ponds'. *Water Research*, vol.32, no.3, pp958–963.

- Wood, MG, Keller, J, Howes, T & Johns, MR 1995, 'hydrodynamic modelling of agro-processing wastewater ponds', in *Proceedings of the 16th annual convention AWWA*, Australian Water & Wastewater Association Incorporated, Sydney, pp.1001–1008.
- Wrigley, R 1994, *Managing Dairy-Shed Wastes*, Dairy Research and Development Corporation, Glen Iris.
- Wrigley, TJ, Webb, KM & Venkitachalm, H 1992, 'A laboratory study of struvite precipitation after anaerobic digestion of piggery wastes'. *Bioresource Technology*, vol.41, no.2, pp117–121.
- Xian-Hua, W, Yi, Q & Xia-Sheng, G 1994, 'Graphical presentation of the transformation of some nutrients in a wastewater stabilization pond system'. *Water Research*, vol.28, no.7, pp1659–1665.
- Yanosek, KA, Wolfe, ML & Love, NG 2003, 'Assessment of enhanced biological phosphorus removal for dairy manure treatment', in *Animal, Agricultural and Food Processing Wastes IX, Proceedings*, 9th International Symposium on Animal, Agricultural and Food Processing Wastes, Raleigh, NC, pp.212–220. Available at: [:/WOS:000224513200026](#).
- Zaman, M, Cameron, KC, Di, HJ & Inubushi, K 2002, 'Changes in mineral N, microbial biomass and enzyme activities in different soil depths after surface applications of dairy shed effluent and chemical fertilizer'. *Nutrient Cycling in Agroecosystems*, vol.63, no.2, pp275–290.
- Zaman, M, Noonan, MJ, Cameron, KC & Di, HJ 1998, 'Nitrogen mineralisation rates from soil amended with dairy pond waste'. *Soil Res.*, vol.36, no.2, pp217–230.
- Zhang, L, Yang, C & Mao, Z 2008, 'An Empirical Correlation of Drag Coefficient for a Single Bubble Rising in Non-Newtonian Liquids'. *Industrial and Engineering Chemistry Research*, vol.47, no.23, pp9767–9772.
- Zhang, RH & Westerman, PW 1997, 'Solid-liquid separation of animal manure for odor control and nutrient management'. *Applied engineering in agriculture*, vol.13, no.5, pp657–664.
- Zhang, T, Bowers, KE, Harrison, J. & Chen, S 2010, 'Releasing Phosphorus from Calcium for Struvite Fertilizer Production from Anaerobically Digested Dairy Effluent'. *Water Environment Research*, vol.82, no.1, pp34–42.

APPENDICES

Appendix A FIELD MONITORING EQUIPMENT AND SAFETY

To satisfy the data requirements identified for the characterisation and modelling objectives of this thesis, an intensive and rigorous monitoring program was devised. The program had to be tailored to suit the conditions and accessibility of the site and the research budget without compromising the research objectives. A combination of loaned, hired and purchased equipment designed for remote site installations was used to support a monitoring program comprising five main components including:

1. monitoring of site meteorological conditions,
2. real-time measurement of effluent flows into and out of the ponds
3. real-time monitoring of in-pond (supernatant) water quality parameters,
4. profiling of pond supernatant water quality and sludge sampling, and
5. regular effluent and sludge sampling and analysis.

Monitoring of meteorological conditions, wastewater flows, and supernatant physiochemical parameters was facilitated by automated equipment installed at the site. Pond supernatant profiling was performed manually at seasonally-based intervals over the monitoring period. Wastewater sampling was conducted using automated equipment linked to the flow monitoring set-up in accordance with recommended pond monitoring methods (Pearson, Mara & Bartone 1987). Effluent samples were processed and analysed at the University of Wollongong Environmental Engineering laboratories and at an external laboratory depending on the type of analysis to be performed.

A.1 MONITORING EQUIPMENT

A.1.1 Meteorological Conditions

Real-time meteorological data were collected using an automated weather station (AWS) erected on the crest of the anaerobic pond. The station consisted of a Campbell Scientific CR-10X data logger recording measurements from the weather sensors listed in TABLE A-1. The logger was housed in an enclosed trailer adjacent to the anaerobic pond to which the weather station sensors were also mounted. Power to the data logger and weather station was supplied by three solar panels connected via regulators to two 6V batteries in series. The logger was also enabled for telemetric control using a CDMA modem.

Weather station readings were scanned continuously in 10-second intervals, and relevant data were recorded hourly and daily at 9:00 am. Rainfall measurements were

made in 0.2-mm increments in real-time and totals reported hourly and daily. Grass reference crop evapotranspiration (ET_0) was calculated on an hourly basis using the Campbell Scientific implementation of the Penman-Monteith equation (Campbell Scientific 1999). Vapour pressure was calculated from relative humidity and saturation vapour pressure. Recording of climate data is summarised in TABLE A-1. The code for the weather station data collection and computation may be viewed in the data logger algorithm given in Appendix E.

A.1.2 Effluent Flows

TABLE A-2 summarises the equipment used to measure flow into and leaving the anaerobic pond and effluent pumped from the facultative pond both to irrigation and for recycling. The two ultrasonic stage measurement devices measuring stage in the flumes were each powered by a 12V battery connected through regulators to two solar panels. The flow meter attached to the facultative pond effluent pumping line was connected to mains power. The ultrasonic probes and the electromagnetic flow meter were connected to the same data logger that supported the AWS. The CTDP300 probe had stand-alone power and logging as described in section A.1.3.

The rating curve of the flumes was verified against flow measurements made over a period of two months with a Mace HVFlo flow meter incorporating Doppler velocity and level measurement sensors. This was operated as a stand-alone device with its own power and logging capability.

A.1.3 Pond Water Quality

Water quality in the ponds was monitored in real time using a collection of eleven Greenspan multi-parameter probes (seven CDTP300 and four CS304 probes). Generally the same type of probe was deployed to the same location as summarised in TABLE A-3. Probes were typically deployed in the field several months at a time. To maintain data quality, they were subjected to repairs and/or laboratory calibration before being redeployed on a rotational basis, often to a different location using the same type of probe. Facultative pond water quality was also monitored using a Greenspan flow injection Mini-Analyser (housed fed by a submersible pump) to provide laboratory grade water quality analyses. The Mini-Analyser was both self-cleaning and self-calibrating, but due to the biologically active and mildly alkaline nature of the effluent as well as its solids content, the mini-analyser was susceptible to frequent periods of malfunction or downtime while sampling pumps and sensors were cleaned and maintained.

TABLE A-1 Automated weather station components and data collection.

Parameter	Sensor type	Sensor make and model	Accuracy	Real-time readings	Hourly data	Daily data
Air temperature	Temperature sensor	Vaisala HMP45A (Pt 1000 IEC 751)	± 0.2 °C	Every 10 seconds	Average (°C)	24-hour maximum and minimum
Relative humidity (RH)	Humidity sensor	Vaisala HMP45A (HUMICAP [®] 180)	$\pm 1\%$ RH	Every 10 seconds	Current value (%)	RH at 24-hour maximum and minimum temperatures
Rainfall	Tipping bucket rain gauge	Hydrological Services TB1 - 0.2	2-3 %	0.2 mm increments	Total (mm)	24-hour total (mm)
Shortwave radiation	Pyanometer	Apogee PYR-P	± 5 %	Every 10 seconds	Average solar flux density (kW/m ²)	24-hour total (MJ)
Wind speed	3-cup anemometer	RM Young Wind Sentry anemometer/vane 03001	± 0.5 m s ⁻¹	Every 10 seconds	Mean (km/hr)	24-hour mean and maximum
Wind direction	Wind vane	RM Young Wind Sentry anemometer/vane 03001	$\pm 5^\circ$	Every 10 seconds	Mean and standard deviation (degrees)	24-hour mean and standard deviation
Vapour pressure	Calculation ⁺			Every 10 seconds	Average (kPa)	-
ET _o	Calculation ⁺			-	Total (mm)	24-hour total (mm)

⁺Using other climate data

TABLE A-2 Flow measurement equipment and data collection.

Flow	Monitoring equipment	Make and model	Accuracy	Real-time readings	Minimum time step data	Daily data
System inflow and anaerobic pond outflow	Long-throated V-notch flume	-		Every 10 seconds	3-5 minute current value and 490totalized flow (24-hour cycle)	24-hour total
	Ultrasonic stage measurement	Probe level monitor PL-511 (Siemens Milltronics Process Instruments Inc., Canada)	$\pm 0.25\%$ of full scale ($\sim \pm 0.0005$ m)			
Facultative pond effluent irrigation pumping	Electromagnetic flow meter	Emflux 2020 (Combined Instrument Systems Pty. Ltd., Australia)	$\pm 1\%$ rate	Every 10 seconds	3-5 minute current value and totalised flow (24-hour cycle)	24-hour total
Facultative pond effluent recycle pumping						
Flood wash	Pressure sensor in flood wash tank	Greenspan CTD300 probe	$\pm 0.02\%$ full scale (~ 0.001 m)	30 seconds or pressure changes of > 0.1 m	Half-hour current value	-
System inflow	Doppler velocity and depth sensors	Mace HVFlo (Measuring & Control Equipment Co. Pty. Ltd., Australia)	$\pm 1\%$ velocity, $\pm 1\%$ depth	Every 2 minutes	Every 2 minutes	-

TABLE A-3 Real time water quality monitoring equipment and data collection.

Pond location	Monitoring equipment	Parameters (accuracy)	Typical logging thresholds	Typical logging period
Anaerobic Central	CTDP300 probe	Temperature (± 0.2 °C), pH (± 0.2 pH), EC (± 1 % full scale, $\sim 100 \mu\text{S cm}^{-1}$)	Changes greater than 1.0 °C temperature, 0.5 pH, or 250-500 $\mu\text{S/cm}$ EC	30 minutes
Anaerobic East	CTDP300 probe	As above	As above	30 minutes
Anaerobic West	CTDP300 probe	As above plus pressure (± 0.12 %, ~ 0.001 m)	As above plus 0.02 m pressure	30 minutes
Facultative Central	Flow injection Mini-Analyser	Temperature, pH (± 0.4 pH), ORP (± 5 % full scale), EC (± 2 % full scale) turbidity (± 2.5 % full scale, ~ 20 NTU) DO (± 0.2 mg L ⁻¹)	-	0.5 - 1 hour
	CS304 probe	Temperature (± 0.2 °C), pH (± 0.2 pH), EC (± 1 % full scale, $\sim 100 \mu\text{S cm}^{-1}$), DO (± 0.3 mg L ⁻¹)	Changes greater than 1.0 °C temperature, 0.5 pH, 250-500 $\mu\text{S/cm}$ EC or 0.5-1.0 mg L ⁻¹ DO	30 minutes
Facultative East	CS304 probe	As above	As above	30 minutes
Facultative West	CTDP300 probe	As above except pressure (± 0.12 %, ~ 0.001 m) instead of DO	Changes greater than 1.0 °C temperature, 0.5 pH, 250-500 $\mu\text{S/cm}$ EC or 0.05-0.1 m pressure	30 minutes
Flood Wash Tank	CTDP300 probe	As above except pressure error ~ 0.01 m	As above except 0.02 m pressure	30 minutes
Dairy Shed Water Supply	CTDP300 probe	As above but without pressure	As above but without pressure	30 minutes

A.1.4 Supernatant Profiling and Sludge Sampling

Water quality profiling of pond supernatant was performed from an aluminium dinghy using a YSI 556 Multi Probe System fitted with the sensors listed in TABLE A-4. The YSI meter had internal memory for recording readings and was fitted with a barometer to assist calibration of the DO probe. Tags were attached to the probe cable to indicate the depth from which the sensors were taking readings. Total liquid and sludge depth measurements and sludge samples were taken using the column sampler described below.

TABLE A-4 YSI 556 multi probe system.

<i>Sensor</i>	<i>Accuracy</i>
Temperature	± 0.15 °C
pH	± 0.2 pH
ORP	± 20 mV
EC	The greater of $\pm 0.5\%$ of reading or ± 0.001 mS/cm
DO	The greater of $\pm 2\%$ of the reading or ± 0.2 mg L ⁻¹ at DO 0 to 20 mg L ⁻¹ , or $\pm 6\%$ of the reading at DO 20 to 50 mg L ⁻¹
Barometer	± 3 mm Hg within $\pm 15^\circ\text{C}$ temperature range from calibration point

A.1.4.1 Column sampler

Measurement of pond liquid and sludge depths and collection of samples of the water/sludge column were conducted using a column sampler similar to that described by Pearson et al. (1987). The sampler (pictured in Plate A-1) consisted of five 1-m lengths of clear, 50-mm diameter polycarbonate tube affixed along their length with measuring tape to indicate depth. Water-tight threaded collars allowed the tubes to be connected end to end for measurement and sampling of water/sludge columns up to 5 m deep. To enable sampling of the sludge/water column, the bottom end of the primary length of the sampler was fitted with a butterfly valve that could be operated with a pull cord. Attached to the number of tubes required for the depth of water/sludge to be sampled, the primary tube would be lowered (vertically oriented) into the water/sludge with the valve open, filling it with an undisturbed sample of the water/sludge column. To remove the sample, the butterfly valve would be closed using the pull cord and a cap fitted with a rubber washer screwed onto the opening of the top-most tube to establish a vacuum. The sampler would then be lifted out of the pond and the sample released into a bucket via the butterfly valve. When collecting sludge samples, water was first decanted from the upper column via bleed tubes fitted at 10- to 50-cm intervals (more

bleed tubes were added to the primary tube subsequent to the photo on the left in PLATE A-1 being taken) or by tilting the column to allow liquid to drain from the top end of the sampler. PLATE A-1 also shows the column sampler being put to use in the anaerobic pond.



PLATE A-1 Column sampler (left) and in use collecting a sample from the anaerobic pond (right).

A.1.5 Effluent sampling

Effluent samples were collected using ISCO 3700 portable samplers powered by solar-charged batteries. The two samplers connected to the anaerobic pond inlet and outlet flumes were triggered by the data logger recording the flow data (code given in electronic Appendix E). The data logger program allowed for user-input values for the time of sampling sequence initiation, the number of days until the sequence is initiated and the quantity of effluent flow allowed to pass between samples. The samplers were housed in the monitoring control trailer and were connected to the inlet and outlet pipes by 12-mm hosing laid underground for protection from roving cattle. To prevent blockages caused by coarse solids settling in the sample line, the intake opening was oriented downstream as depicted in FIGURE A-1. The sampling intake from the pond outlet was attached directly to the bottom of the pipe with the opening facing upward.

The third auto-sampler was a stand-alone installation drawing effluent from the flood wash tank. It ran according to a schedule that collected samples immediately after morning and afternoon flood wash events.

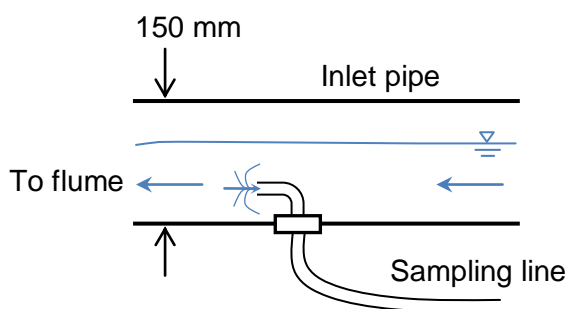


FIGURE A-1 Anaerobic pond inlet sampling intake.

The intake lines to the auto-samplers were purged with air before and after sample collection by reversing the peristaltic pump flow. At the completion of the sampling event, sub-samples from each auto-sampler were transferred to dedicated acid-washed buckets (corresponding to their sampling location) and mixed with a paddle stirrer to form composite samples before being decanted into acid-washed bottles for transport to the laboratory. Different sample bottles were used for transportation to save having to make a special trip to the site just to replace auto-sampler bottles. All auto-sampler sample bottles were washed with hot water and detergent and rinsed with acid then distilled water on site immediately after sample mixing and decanting.

Sampling of supernatant from the facultative pond was performed using the column sampler described earlier. Sample liquid from each of the three sampling locations in the pond was emptied into an acid-washed 25-L bucket for mixing before being decanted into sample bottles.

A.2 OCCUPATION HEALTH AND SAFETY CONSIDERATIONS

A risk assessment of the various field work activities is summarised in TABLE A-5. Operating and maintaining the monitoring program required regular visits to the farm which is not in close proximity to services and often has only limited human presence. The remoteness of the site heightened the risks involved with the research meant that working alone on many activities was not feasible. Tasks that involved any of the hazards outlined in TABLE A-5 were only performed in the presence of a research/technical assistant or a farm operator.

TABLE A-5 Assessment of risks associated with field work activities.

Hazard	Risks	Likelihood of an incident	Consequences	Risk rating	Preventative measures
Weather exposure - heat/sun	Heat stress, dehydration, sunburn	Could occur but only rarely	Minor to moderate	Medium	Protective clothing, hats sunscreen, ready supply of drinking water
Weather exposure – cold and rainfall	Slips and falls, common cold, hypothermia	Could occur at some time	Insignificant to minor	Medium	Avoid site visits during rain, rain jackets, warm clothing, all weather boots or gum boots
Lightning	Electric shock, burns	Could occur, but only rarely or probably never will	Moderate to major	Medium	Leave site or seek shelter during thunder storms
Barbed wire or electric fencing	Cuts, eye injury, electric shock	Could occur but only rarely	Minor to moderate	Medium	Use gates wherever possible, plastic sleeves over barbed wire where regular access required
Pathogen exposure	Contracting disease, parasites	Could occur but probably never will	Moderate to major	Medium	Minimise contact with effluent, avoid splashing effluent, regular and thorough hygiene practices
Working close to or in the ponds	Falling into pond – pathogen and drowning risks	Could occur, but only rarely or probably never will	Moderate	Medium to high	Walk along pond crest wherever possible, slow and deliberate movements when at pond's edge or in boat, tethering to anchor on the crest when wading above knee depth
Handling chemicals	Burns or poisoning	Could occur but only rarely	Minor to moderate	Medium	Protective eyewear and gloves, storage and handling as per MSDS sheets
Manual handling heavy equipment, large samples	Injury	Could occur but only rarely	Minor to moderate	Medium	Lift or move items above 20 kg with assistance or trolley
Using a ladder to access flood wash tank	Injury	Could occur but only rarely	Minor to moderate	Medium	Always have a second person to stabilize the ladder
Snake bite (mostly in spring/summer around the ponds)	Poisoning	Could occur but probably never will	Moderate to major	Medium	Due care when moving around site on foot, Leave area when snake sighted, first aid kit always on hand

Appendix B INFILLING MISSING WASTEWATER FLOW DATA

Between October 2005 and 5 June 2006, an undetected ground loop was causing interference to the signal between the ultrasonic level sensors attached to the flumes and the datalogger, particularly when stage readings fell below 16 mm and the solar power supply was constrained (overnight and overcast days). The resulting loss of usable flow measurements was substantial enough to necessitate developing a method to fill the gaps with synthesised data. The flow into and out of the anaerobic pond generally followed a pattern of two daily peaks of varying magnitude. While the regularity of the peaks was predictable, the size and shape was not. Hence rather than formulating a function to interpolate missing data, data from complete flow peaks of similar size and shape elsewhere in the time series record were inserted into the gaps.

Data used for interpolation were identified by comparing the viable flow data from a day affected by signal drop-outs to corresponding data points from every other day in the record that had a complete complement of flow data (288 5-minute measurements). Since flow through the two flumes was directly related, data from both flumes were used in the comparison in order to strengthen the matching. This helped to maximise the data used in selecting ‘infill’ data and to ensure that infilling of a particularly large gap in one flume was informed by a realistic approximation. The selection of infill data was made according to the lowest sum of squares of the differences result calculated for each comparison day as

$$SS_{x,y} = \sum_{i=1}^n \left(Q1_{x,i} - Q1_{y,i} \right)^2 + \sum_{j=1}^m \left(Q2_{x,j} - Q2_{y,j} \right)^2 \quad (B-1)$$

where:

$SS_{x,y}$ = sum of squares of the differences for day to be interpolated x and comparison day (with complete flow record) y ;

n = number of viable data points in flow record for Flume 1 on day x ;

$Q1_{x,i}$ = stage or flow recorded in Flume 1 at interval i on day x ;

$Q1_{y,i}$ = stage or flow recorded in Flume 1 at interval i on day y ;

m = number of viable data points in flow record for Flume 2 on day x ;

$Q2_{x,j}$ = stage or flow recorded in Flume 2 at interval j on day x ;

$Q2_{y,j}$ = stage or flow recorded in Flume 2 at interval j on day y ;

To align with the prevailing flow pattern, a day was defined as the 24 hours from 7 am. Flow and stage data that were suppressed by signal interference were identified according to a specific set of rules that were devised by analysis of the entire flume data record and may be viewed in TABLE B-1. To allow for day-to-day shifts in the timing of flow peaks, the interval corresponding to i or j in the comparison day could be offset by up to ± 2 hours in the sum of squares calculation. Infilled data are flagged as a 'T' in the 'Synthesised?' field in the flume data presented in Appendix J. An example of the data infilling results is presented in FIGURE B-1, which shows the original data falling below 0.01 m due to signal interference (dashed lines) and the interpolated data (solid lines).

TABLE B-1 Rules for identifying data points affected by signal interference.

<i>Flume</i>	<i>Rule</i>
Inlet (flume 1)	$S1_i \leq 0.005 \text{ m}$ $S1_i \leq 0.016 \text{ m AND MINIMUM}(S1_{i-24}, \dots S1_{i+24}) \leq 0.005 \text{ m}$ $S1_{i-1} - S1_i \leq -0.01 \text{ m AND MINIMUM}(S1_i, \dots S1_{i+24}) \leq 0.005 \text{ m}$
Outlet (flume 2)	$S2_i \leq 0.010 \text{ m}$ $S2_i \leq 0.016 \text{ m AND MINIMUM}(S2_{i-24}, \dots S2_{i+24}) \leq 0.01 \text{ m}$ $ S2_{i-1} - S2_i \geq 0.007 \text{ m AND } S2_i \leq 0.037 \text{ m AND MINIMUM}(S2_{i-24}, \dots S2_{i+24}) \leq 0.016$ $S2_{i-1} = 0 \text{ AND } S2_i \leq 0.037 \text{ m AND MINIMUM}(S2_i, \dots S2_{i+24}) \leq 0.016 \text{ m}$

$S1_i$ = stage recorded in flume 1 at interval i .

$S2_i$ = stage recorded in flume 2 at interval i .

The ground loop issue caused data losses from Flume 1 on a total of 189 days out of the 420-day monitoring period. However only 5% of the Flume 1 data affected fell within typical periods of peak flow (8 to 10 am and 4 to 6 pm), which means that the great majority of signal drop-outs occurred during lulls in flow. Since stage in Flume 2 rarely dropped below 0.02 m, interference with the signal from the flume's stage meter did not occur as frequently as it did with Flume 1. A total of 88 days of Flume 2 data were affected and on only 55 of these was more than 25% of data lost. As a check on the veracity of the infilling method, daily flow on days containing synthesised data was compared with daily flow on days that were unaffected by the ground loop. FIGURE B-2 shows that the distributions are almost identical for both flumes. Applying a student's t-test (equal variances) produced probabilities that the null hypothesis of

equal means holds of 0.87 and 0.39 for Flume 1 and Flume 2, respectively, demonstrating that there is no material difference between the means of the unaffected and infilled data.

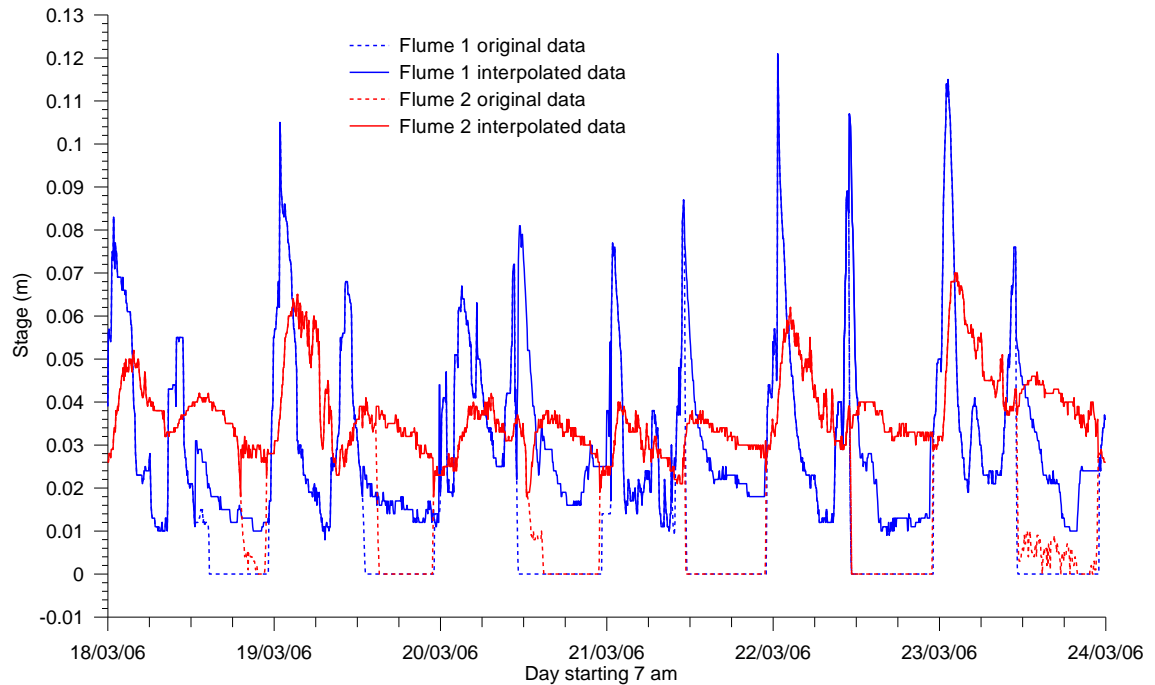


FIGURE B-1 Extract from the flume data interpolation results. Signal drop outs in the original data are indicated by the (mostly flat) sections of zero or very low readings.

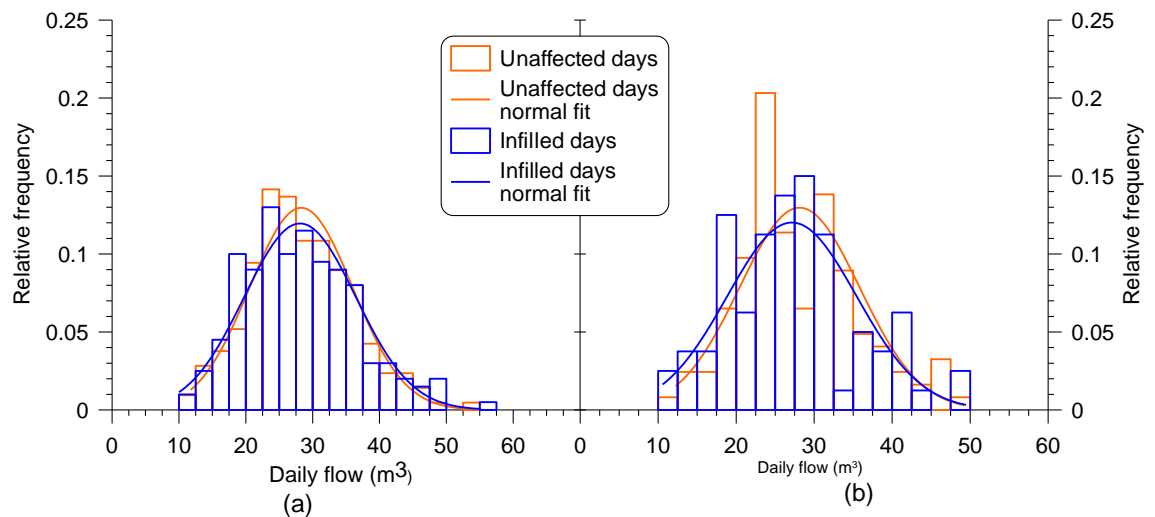


FIGURE B-2 Histograms comparing distributions of daily flow data unaffected by the ground loop and infilled flow data: (a) Flume 1; (b) Flume 2.

An indication of the effect the accuracy of the infilling process would have on the overall water balance may be obtained by comparing the total flow on the affected days with and without the infill data. Infilling added 923 m³ or 21% to the total raw flow data

from Flume 1 while the flow attributed to Flume 2 increases by 581 m³ or 28% with the addition of infill data. Inaccuracy in the method of 10% would therefore cause a 2% change in total estimated flow in Flume 1 for the period and less than 3% in Flume 2. Thus unless the method is wildly inaccurate, which is highly unlikely given that it draws on reliable data from similar times in the day, it should not dramatically increase the uncertainty of analyses incorporating the synthetic data.

B.1 IMPLICATIONS OF MISSING FLOW DATA FOR WASTEWATER SAMPLING

The wastewater constituent monitoring described in Chapter 7 was predicated on a flow-weighted approach whereby samples were collected once a specified volume of effluent had passed through the sampling point. Drop outs in the flow measurement signal could therefore have resulted in under-sampling. TABLE B-2 lists the sampling events affected by the signal drop outs and provides estimates of the likely percentage of sub-samples missed based on a comparison between the raw data with missing flow readings and the infilled data. It also gives the percentage of readings that were missed during the peak flow times for flume 1 (see above). Sub-sample losses were mostly below 20%, with five of the eleven composite samples requiring no additional sub-samples to make up for missed flow. The sampler attached to Flume 1 potentially missed a quarter of the total sub-samples that should have been collected on 5 January 2006, thus it was excluded from the wastewater characterisation and related analyses/modelling.

TABLE B-2 Samples affected by flow signal drop outs.

<i>Date of sampling event date</i>	<i>Influent</i>				<i>Effluent</i>		
	<i>Recorded flow (m³)</i>	<i>Estimated flow (m³)</i>	<i>Data loss from peak flow times (%)</i>	<i>Estimated sample loss (%)</i>	<i>Recorded flow (m³)</i>	<i>Estimated flow (m³)</i>	<i>Estimated sample loss (%)</i>
16/11/2005	20.3	19.5	6	0			
7/12/2005	31.6	30.1	0	0			
22/12/2005					30.3	30.1	0
5/01/2006*	19.5	13.9	44	25	58.9	50.5	13
8/03/2006	27.2	26.9	0	0			
22/03/2006	33.6	28.4	10	15	27.6	15.9	40
5/04/2006	23.2	22.7	17	0			
19/04/2006	28.4	23.0	17	18	26.4	22.4	11

* Flume 1 sample data omitted from wastewater sampling data set.

Appendix C WATER BALANCE MODEL FITTING CONSTRAINTS

TABLE C-1 Fitting constraints used in estimating evaporation and seepage parameters for the facultative pond.

<i>Parameter</i>	<i>Constraint or value</i>
f_{α}	
Lower limit	$\alpha_{min} \geq 0.087 - 6.76 \times 10^{-5} R_{S,in,max} + 0.11[1 - e^{-0.01Turb_{min}}]$ ≥ 0.133
Upper limit	$\alpha_{max} \leq 0.087 - 6.76 \times 10^{-5} R_{S,in,min} + 0.11[1 - e^{-0.01Turb_{max}}]$ ≤ 0.195
	Where: α_{min} is albedo calculated at peak solar noon elevation using the empirical equation from Stefan et al. (1983) and assuming maximum direct radiation and minimum turbidity conditions; α_{max} is albedo calculated at minimum solar noon elevation assuming maximum diffuse radiation and turbidity conditions; $R_{S,in,max}$ and $R_{S,in,min}$ are maximum and minimum observed solar radiation over monitoring period; $Turb_{min}$ and $Turb_{max}$ are minimum and maximum observed turbidity (NTU).
Initial value	0 - no turbidity effect on albedo
f_{EA}	
Lower limit	$\gamma\lambda E_A / (\Delta R_n + \gamma\lambda E_A) \geq 0.15$ } based on the assertion from Brutsaert (2005) $\gamma\lambda E_A / (\Delta R_n + \gamma\lambda E_A) \geq 0.35$ } that this ratio is typically found to be in the range 0.2-0.3.
Upper limit	
Initial value	$f_{EA} = 1$ (no correction)
k_l	
Lower limit	$K_S \geq 0$
Upper limit	$K_S \leq 1.44 \times 10^{-4} \text{ } mh^{-1}$ - highest observed conductivity reported by Ham (2002a)
Initial value	$K_S \leq 5.76 \times 10^{-6} \text{ } mh^{-1}$ - average observed conductivity reported by Ham (2002a)

TABLE C-2 Fitting constraints used in estimating evaporation and seepage parameters for the anaerobic pond.

<i>Parameter</i>	<i>Constraint or value</i>
f_{EA}	
Lower limit	$f_{EA} \geq 0$
Upper limit	$\sum E_{Fac} \leq \sum E_{Pan}$
Initial value	$f_{EA} = 1$ (no correction)
k_s/v	
Lower limit	$k_s/v \geq 7.24 \times 10^{-4} \text{ m h}^{-1}$ – preliminary fit result
Upper limit	-
Initial value	$k_s/v \geq 7.24 \times 10^{-4} \text{ m h}^{-1}$

Appendix D INVESTIGATION OF DSE BIOCHEMICAL OXYGEN DEMAND CHARACTERISTICS

D.1 INTRODUCTION

This study was conducted to develop a better understanding of the nature of biochemical oxygen demand (BOD) exerted by dairy shed waste. In particular it sought to quantify the BOD kinetic rate constant k_{20} and the ultimate BOD (BOD_{ult}) for a range of dairy shed wastewaters. Analyses of BOD were performed over time to generate time series of BOD to which a modified BOD equation was fitted using non-linear regression.

D.2 METHODOLOGY

D.2.1 Sampling

Samples of raw and treated wastewaters were manually collected from three separate dairy farms. Sampling of raw wastewater and screened/settled wastewater from solids traps involved a variety of techniques designed to obtain the most representative sample of a wash down event. Initially grab samples were collected in 1-L bottles or through a pump regularly over the course of the flow, the size and frequency of samples adjusted to roughly reflect the flow rate. Where wastewater was conveyed in an open channel, samples were collected using a 'flow diversion' sampler that comprised a 50-mm length of pipe placed in line with the direction of flow T-junction that transferred a small portion of the flow passing through the main pipe to a 20-L acid-washed container. Grab samples of pond effluent were taken from outfalls, the supernatant immediately adjacent to outfalls, or reclaimed effluent holding tanks. All samples were transported to the laboratory in an ice box and analyses were initiated the same day.

D.2.2 Laboratory analysis

Upon arrival at the laboratory, samples were immediately prepared for BOD analysis. Sub-samples to be analysed for total BOD were first homogenised with a domestic hand blender while sub-samples to be analysed for filterable BOD (FBOD) were filtered through 1.3- μ m glass fibre filters. The homogenised and filtered samples were then diluted to ratios appropriate to the strength of the wastewater with beffered distilled water in accordance with standard methods (APHA 1998). Diluted samples were then transferred to BOD bottles in triplicate and their dissolved oxygen (DO) concentration measured with a YSI 5730 BOD bottle probe. Blanks were prepared measurement

using unseeded buffered dilution water. The diluted samples and blanks were placed in an incubator set at 20°C for up to 30 days and DO readings taken at regular intervals to generate the time series. Samples were not treated to suppress nitrogeous oxygen demand.

Each time a DO reading was taken a small fraction of sample would be lost when removing the DO probe. Hence readings were generally taken every 2-3 days initially and then less frequently beyond 10 days so as to minimise disturbance of the sample. In addition, extra bottles of diluted samples were incubated together with the samples being analysed for use as top-up water when DO measurements were taken.

All samples were also analysed for COD, TS, TVS, TSS and TVSS according to standard methods (APHA 1998). COD analysis was also performed on a subset of filtered samples (1.3 µm glass fibre) to determine filterable COD (FCOD). Non-filterable COD (PCOD) was estimated as the difference between COD and FCOD.

D.2.3 BOD Curve fitting

Time series data generated from the BOD analyses were used to generate BOD curves according to the equation

$$BOD_t = BOD_{ult} [1 - e^{-k_{20}(t-d)}]$$

where

BOD_t = BOD at time t (mg L⁻¹);

BOD_{ult} = Ultimate BOD (mg L⁻¹);

k_{20} = BOD rate constant (d⁻¹);

d = BOD exertion delay (d).

This is a modified version of the conventional model for BOD exertion that is similar to that used by Mason, McLachlan & Gérard (2006). However, rather than superimposing one form of the conventional equation onto another, this approach simply applies a constant time offset to the number of days elapsed to allow for a delay in BOD exertion that was observed in the majority of the BOD time series recorded. Curve fits were generated using non-linear regression in the Grapher (Golden Software, Inc. 2007) plotting software. Initial values for unknown parameters k_{20} , BOD_{ult} and d were generally set below their estimated value and broad, but realistic limits were placed on the potential range for the parameters to minimise the constraints placed upon the potential outcomes.

D.3 RESULTS AND DISCUSSION

Examples of total and filterable BOD exertion curve fits are presented for raw wastewater, solids separated wastewater, anaerobic pond effluent and facultative pond effluent in FIGURE D-1. The modified BOD exertion model was found to generally fit well with the observed data demonstrating that BOD is often not immediately exerted in dairy shed wastewater. Given there should be no shortage of bacteria or nutrients in dairy shed wastewaters, the presence of this delay suggests that the organic material in the wastewater, including filterable fraction, is not as readily degradable as other wastewaters. This could be related to a predominance of complex (fermentable) readily biodegradable material, or of colloidal/fine particulate material that requires extracellular enzymatic breakdown prior to bacterial consumption.

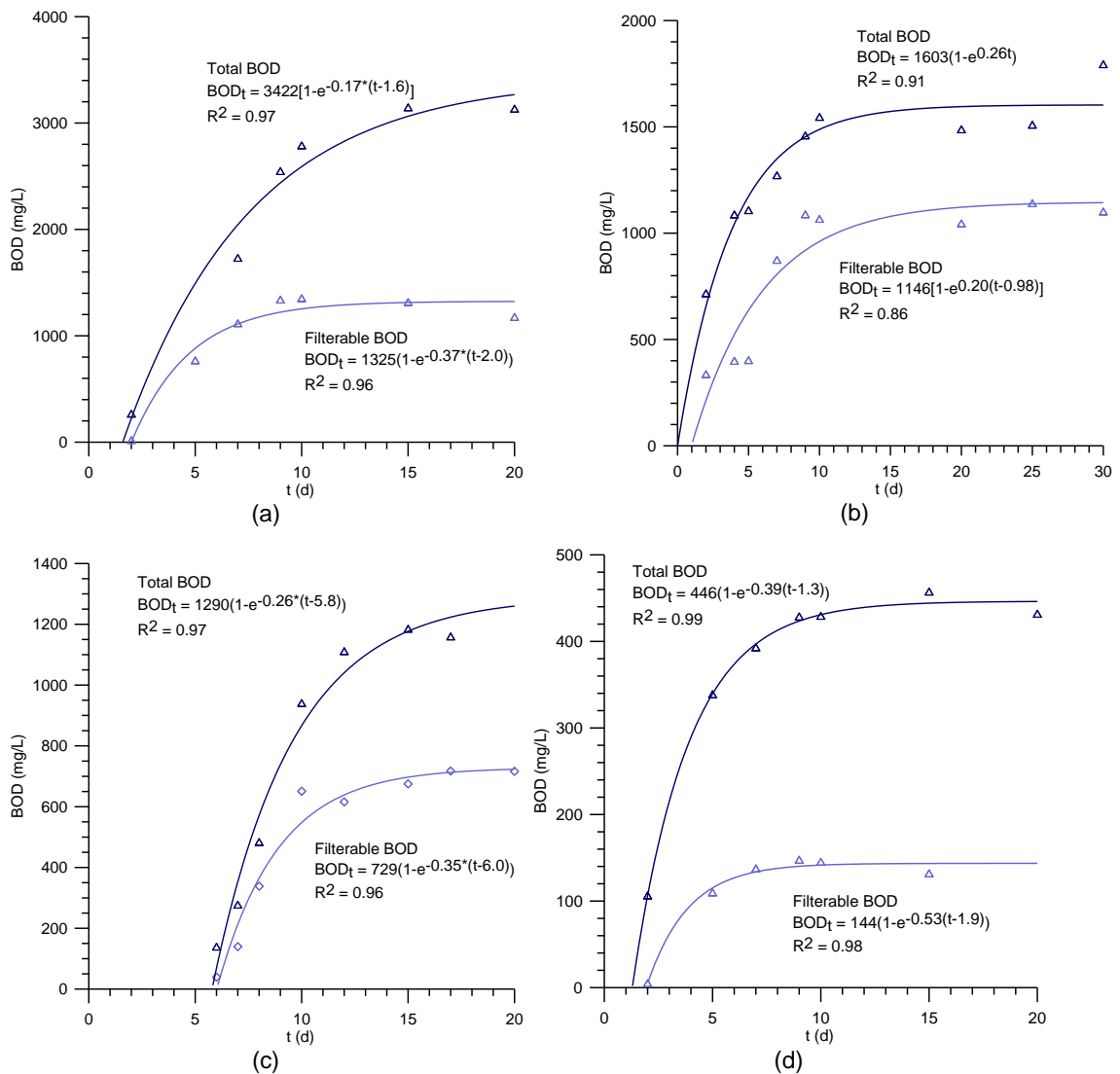


FIGURE D-1 Examples of total and filterable BOD exertion curve fits. (a) Raw wastewater, (b) solids separated wastewater, (c) anaerobic pond effluent and (d) facultative pond effluent.

It should be noted that the glass fibre filters used would not remove all colloidal material. Hence FBOD and FCOD do not represent the soluble fractions of BOD and COD, respectively. Rather they reflect the sum of the entire soluble fraction and a portion of the colloidal fraction.

FIGURE D-2 and FIGURE D-3 show the ultimate BOD estimates derived for the total and filterable fractions. As would be expected, the BOD concentrations of the raw and solids separated wastewaters are much higher and exhibit greater variability than those of the pond effluents. Facultative pond effluent appears to exhibit the most stable BOD, demonstrating the stabilising effects of the pond systems.

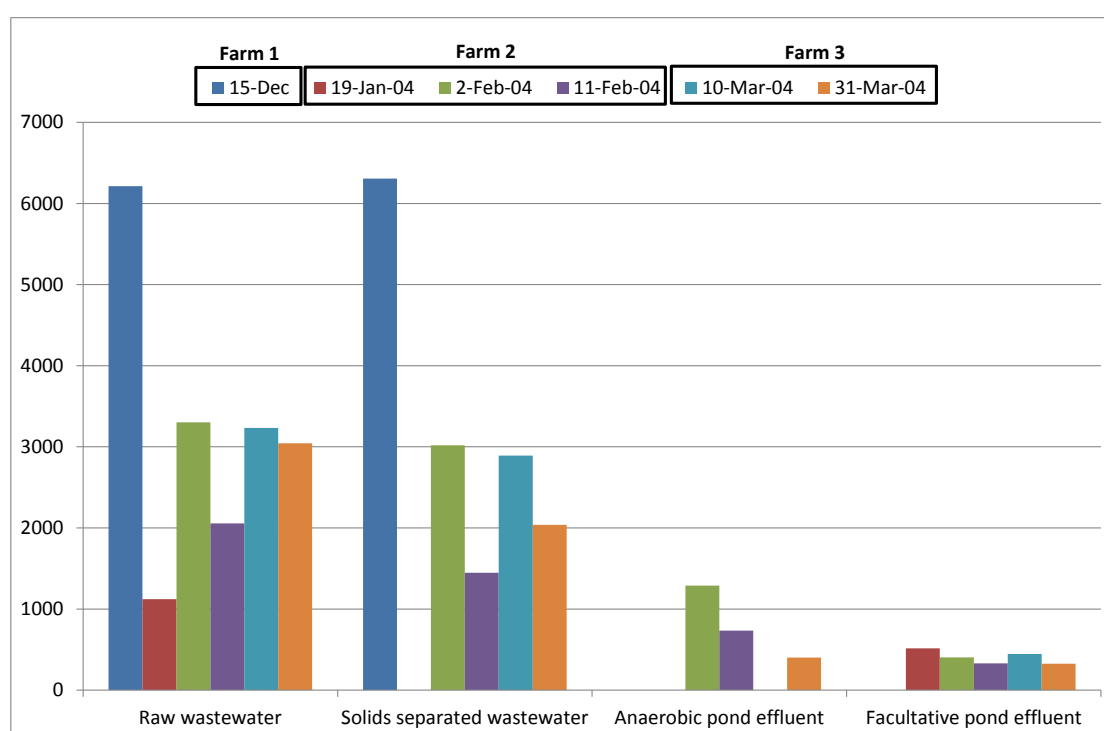


FIGURE D-2 Ultimate BOD estimates for each type of wastewater by sampling date.

Average figures for the modified BOD exertion model parameters are presented in TABLE D-1. Total BOD k_{20} values for raw and solids separated wastewaters were, on average, lower than k_{20} values for pond effluents, suggesting more sustained exertion due to a larger presence of slowly degradable material. This is likely due to the higher proportion of degradable particulate matter in the raw and solids separated wastewaters since corresponding k_{20} values for filterable BOD were about the same as or higher than the pond effluent values. Averages taken across all the wastewaters are very similar between the filterable and total fractions, and are very close to typical values suggested for municipal wastewaters (Metcalf & Eddy et al. 2003).

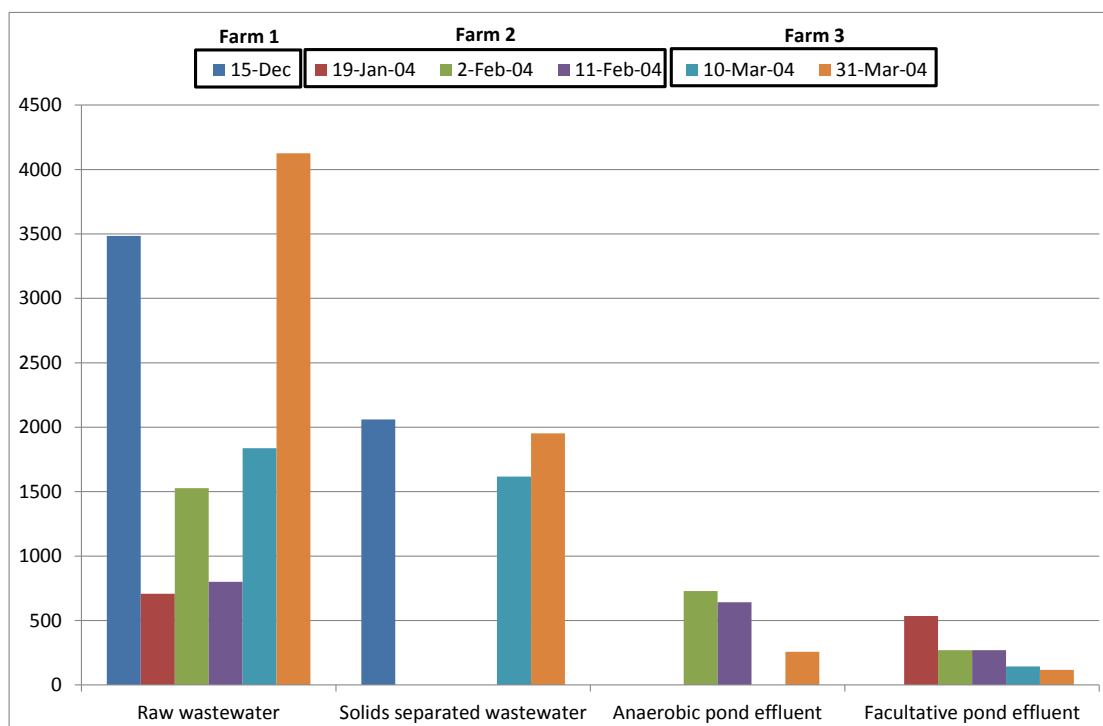


FIGURE D-3 Ultimate filterable BOD estimates for each type of wastewater by sampling date.

TABLE D-1 Parameter estimates for the modified BOD exertion model.

	Total BOD						Filterable BOD				
	k_{20}			d			k_{20}			d	
	n	Mean	S.D.	Mean	S.D.		n	Mean	S.D.	Mean	S.D.
Raw wastewater	8	0.25	0.14	1.2	1.4		8	0.35	0.18	1.4	1.3
Solids separated wastewater	6	0.18	0.07	1.7	1.7		4	0.25	0.09	1.3	0.2
Anaerobic pond effluent	3	0.29	0.16	3.3	2.2		3	0.21	0.09	3.5	2.2
Facultative pond effluent	6	0.38	0.07	2.8	1.6		6	0.27	0.15	3.2	1.7
All wastewaters	23	0.27	0.13	2.0	1.7		21	0.29	0.15	2.2	1.7

The rate and delay constants given in TABLE D-1 incorporate nitrogenous oxygen demand (NOD) and should not be applied to carbonaceous demand. It is believed that the observed delays in BOD exertion were in fact related to the time required to form critical populations of *Nitrosomonas* and *Nitrobacter* bacteria to initiate oxidation of ammonia. As such, low BOD measurements in the first one to five days that necessitated the delay parameter in the BOD exertion model were primarily measuring consumption of readily degradable organic material. As ammonia oxidising bacteria became established, the shape of the exertion curve changed (steepened). This explains the shorter delay apparent in the raw and solids separated wastewaters – carbonaceous BOD was higher relative to NOD, bringing the fitted d parameter closer to zero.

However, it is interesting to note that there was no clear distinction of nitrogenous oxygen demand in the observed BOD data. That is, no dramatic jumps in BOD were observed later in the time series that would reflect the initiation of NOD, which would suggest that NOD exertion coincides with carbonaceous BOD exertion, and/or that total BOD is heavily dominated by one of either carbonaceous BOD or NOD. In the raw and solids separated wastewater, carbonaceous BOD is likely to be dominant given the relativities of COD (carbon) and N typically observed in dairy shed wastewaters. However, the BOD of the pond effluents is more likely to be dominated by NOD as the COD:N ratio is dramatically reduced after anaerobic treatment.

The delay in BOD exertion d appears to increase with degree of treatment, confirming that pond treatment effectively reduces the fraction of readily degradable organic matter. Longer delays in the pond effluent BOD exertion might also suggest that NOD is dominant

The longer delays in filterable fractions of the pond effluents would suggest that the delays are primarily related to the presence of colloidal material as colloids are more likely to be adsorbed onto suspended particulate matter and thus filtered out of the raw and solids separated wastewaters that have very high TSS concentrations (Melcer et al. 2003). And while colloidal material should eventually flocculate and settle out with the particulate matter in the ponds, there is a number of means by which colloidal material may accumulate in the water column including resuspension from the sludge in anaerobic ponds and growth of algae in facultative ponds.

It could also indicate that the observed BOD in pond effluent is dominated by NOD as the longer delay may be related to the time required to form critical populations of *Nitrosomonas* and *Nitrobacter* bacteria to initiate oxidation of ammonia.

TABLE D-2 presents ratios between various measured or estimated wastewater parameters. The ratio of filterable BOD₅ to total BOD₅ reduces with the degree of treatment, confirming that the consumption of degradable soluble and colloidal material is more rapid than consumption of particulate organic material. BOD_{ult}:BOD₅ is also higher in the raw and solids separated wastewaters, suggesting a higher portion of rapidly hydrolysable organic matter. The slightly higher values of the same ratio for the filterable fraction of the pond effluents suggest that there may be a high proportion of fine colloidal material after treatment.

The COD:BOD ratios are high compared with typical values for municipal wastewaters, which concurs with similar observations made by Sukias et al. (2001) and indicates a

high fraction of slowly degradable or inert particulate material. Ratios with filterable COD are based on only 2 to three samples so must be interpreted with caution. The ratio of filterable to total COD is lower than typically observed in municipal wastewaters (Melcer et al. 2003), especially given that the FCOD figures likely comprise some colloidal COD. Ratios between FCOD and BOD_{ult} are all close to one, suggesting that BOD_{ult} is also a reasonable indicator of readily biodegradable organic material.

TVSS:TSS ratios are also high compared to municipal wastewater values, again suggesting a high proportion of inert particulate COD (Melcer et al. 2003). Finally, the ratios of particulate COD to TVSS are lower than those typical of municipal wastewater (1.6 – 1.8 mg COD / mg VSS), which indicates more intractable material may be present in dairy shed wastewater. Again, however, these figures are based on only a handful of samples and may not be representative of typical characteristics.

TABLE D-2 Ratios of standard wastewater parameters.

	<i>Raw wastewater</i>		<i>Solids separated wastewater</i>		<i>Anaerobic pond effluent</i>		<i>Facultative pond effluent</i>	
	<i>Mean</i>	<i>S.D.</i>	<i>Mean</i>	<i>S.D.</i>	<i>Mean</i>	<i>S.D.</i>	<i>Mean</i>	<i>S.D.</i>
FBOD ₅ :BOD ₅	0.8	0.3	0.6	0.3	0.5	0.1	0.3	0.2
BOD _{ult} :BOD ₅	1.7	0.5	2.1	0.5	1.4	0.3	1.2	0.1
FBOD _{ult} :FBOD ₅	1.4	0.3	1.5	0.2	1.7	0.4	1.8	1.0
FBOD _{ult} :BOD _{ult}	0.6	0.3	0.6	0.3	0.7	0.2	0.7	0.4
COD: BOD ₅	4.4	1.4	3.8	1.3	6.0	4.4	2.6	1.1
COD:FBOD ₅	5.8	4.1	3.4	1.4	12.4	12.8	6.0	3.3
COD:BOD _{ult}	2.4	0.9	2.1	0.9	4.8	4.5	2.1	0.8
COD:FBOD _{ult}	4.2	2.1	2.4	0.6	7.5	7.2	4.5	3.4
FCOD:COD	0.3	0.1	0.4	-	0.4	0.3	0.6	0.1
FCOD:BOD ₅	2.0	0.3	2.3	-	1.8	0.2	1.6	0.5
FCOD:FBOD ₅	2.4	2.0	2.1	-	3.2	1.1	3.7	2.0
FCOD:BOD _{ult}	0.9	0.2	1.3	-	1.3	0.3	1.3	0.3
FCOD:FBOD _{ult}	1.5	0.8	1.3	-	1.8	0.8	2.9	1.7
TVSS:TSS	0.9	0.1	0.6	0.2	0.7	0.1	0.8	0.1
PCOD:TVSS	1.0	0.2	0.9	-	1.2	0.8	1.4	0.5